BOWEN BASIN SYMPOSIUM 2005

THE FUTURE FOR COAL – FUEL FOR THOUGHT

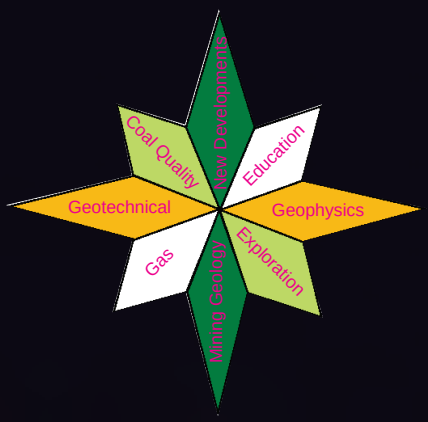

Edited by
JW Beeston

RYDGES CAPRICORN RESORT, YEPPOON, QUEENSLAND

Wednesday 12 to Friday 14 October 2005

BBGG Bowen Basin Geologists Group

COAL GEOLOGY GROUP

GEOLOGICAL SOCIETY OF AUSTRALIA Incorporated

AUSTRALIAN INSTITUTE OF GEOSCIENTISTS AIG

BOWEN BASIN SYMPOSIUM 2005

THE FUTURE FOR COAL — FUEL FOR THOUGHT PROCEEDINGS

JW BEESTON
Editor

ORGANISED BY
THE BOWEN BASIN GEOLOGISTS GROUP
AND
THE GEOLOGICAL SOCIETY OF AUSTRALIA INCORPORATED
COAL GEOLOGY GROUP

YEPPOON, QUEENSLAND 12–14 OCTOBER 2005

Organised by:

Bowen Basin Geologists Group and
GSA Inc Coal Geology Group

Organising Committee:

POSITION	INCUMBENT
President	Doug Dunn
Secretary	Nick Gordon
Treasurer	Renate Sliwa
Trade Displays & Sponsorship Coordinator	Troy Peters & Bill Smith
Venue Organiser & Social Event Convenor	Warwick Smyth
Paper Coordinator & Public Relations/Advertising	Wes Nichols
Proceedings Publisher/Editor	Jim Beeston
Flyer/Registration Brochure	Chris McMahon
Dinner Activities Organiser	Barry Saunders & Glenn Wilson
Satchels Organiser	Simon Brady
Student Assistant Organiser	Kyle Waye
Workshops Organiser	Renate Sliwa

Special Thanks to:

Merryl Peterson, (Secretary, BBGG)
Dianne Sommer (immediate past chair of the BBGG)
Claire Avenell (immediate past secretary of the BBGG)
Paper Review Committee (Basil Beamish, Mark Biggs, Joan Esterle, Nick Gordon, Barry Saunders, Warwick Smyth, Glenn Wilson)
Wes Nichols (Chairman, GSA Coal Geology Group)
Mark Biggs (Secretary, GSA Coal Geology Group)
Peter Crosdale (Treasurer, GSA Coal Geology Group)
John Draper (Immediate Past Treasurer, GSA Coal Geology Group)
Jim Beeston (JOAT, GSA Coal Geology Group)

Thanks to St Brendan's College for providing logistical support

Proceedings prepared by: JW & SA Beeston Scientific/Technical Desktop Publishing Services
Proceedings published by: GSA Coal Geology Group
(This proceedings volume is a peer-reviewed publication of the Coal Geology Group of the Geological Society of Australia Inc)

Issued: October 2005
ISBN: 0 646 45291 6
Printed by: Impulse Digital Printing

Reference guides:

BEESTON, J.W., (Editor), 2005: *Bowen Basin Symposium 2005 — The future for coal — Fuel for thought.* Geological Society of Australia Inc. Coal Geology Group and the Bowen Basin Geologists Group, Yeppoon, October 2005.

ASFAHANI, J., BORSARU, M. & NICHOLS, W., 2005: *In situ* delineation of coal seams in dry blast holes with a low gamma-ray activity logging tool. *In* Beeston, J.W. (Editor): *Bowen Basin Symposium 2005 — The future for coal — Fuel for thought.* Geological Society of Australia Inc. Coal Geology Group and the Bowen Basin Geologists Group, Yeppoon, October 2005, 1–6.

CONTENTS

GEOTECHNICAL

GAS

POSTER PAPERS

GEOTECHNICAL

GOLD SPONSORS

SILVER SPONSORS

BRONZE SPONSORS

AQUILA Resources Limited

McElroy Bryan Geological Services
MBGS
Consulting Geologists

GeoConsult

THE MINSERVE GROUP

QGS

SGRS
Geotechniques - Uncompromised

URRAGH
Mining Since 1983

ABC Products (Rocky) Pty Ltd
Major suppliers of all Drilling
and Mining Consumables
Ph 07 49277276 Rockhampton

TRADE EXHIBITORS

CSIRO

VELSEIS

GEOIMAGE

AUSLOG

CAPRICORN WEST

METECH

MICROMINE

MAPTEK

ALT

SURPAC

DTH

PRECISION ENERGY

TEXCEL

GEOSOFT

GSQ

MITCHELL DRILLING

ACIRL

PREPLAB

SRK

MINCOM

IMC

Jamal Asfahani, Mihai Borsaru and Wes Nichols

In situ *delineation of coal seams in dry blast holes with a low gamma-ray activity logging tool*

This paper describes the application of the spectrometric low activity tool using a ^{137}Cs gamma-ray source of activity-1.8 MBq for delineating the coal/rock interface in dry, large diameter blast holes.

INTRODUCTION

Borehole logging geophysics is widely used in the coal mining industry in the exploration stage and is gradually gaining ground in mine production.

The nonspectrometric (total gamma-rays count) backscattered gamma-gamma technique is routinely used in borehole logging to delineate the coal seams and for *in situ* determination of density and ash content. The ash content is estimated through the correlation that, in general, exists between density and %ash in coal (Samworth, 1974; Reeves, 1976; Lavers & Smits, 1976; Brom & Driedonks, 1981; Daniels & others, 1983).

This technique requires a gamma-ray source and a scintillation detector to record the backscattered gamma-rays. According to the distance chosen between the gamma-ray source and the scintillation detector, the backscattered gamma-gamma technique can be used for bed resolution (BRD), high resolution (HRD) and long-spaced (LSD) density logs. These tools are excentralized and use gamma-rays sources (generally ^{137}Cs) of activity in excess of 1850MBq.

Borsaru & others, 1985 developed a spectrometric backscattered gamma-gamma technique for the determination of ash in coal seams that is not based on the correlation between ash and density. The tool is centralised and is using a ^{137}Cs gamma-ray source of only 40MBq. The fact that this technique is using a gamma-ray source of much lower activity is a plus and makes it more 'user friendly'.

Prompt gamma neutron activation analysis (PGNAA) is a newer technique developed for coal logging. It has been demonstrated that this technique can be used to delineate the coal seams intersected by boreholes and for the determination of density, ash, Fe, Si, Al, Ca and S (Borsaru & others, 2001a; Borsaru & others, 2004a). The technique is also able to determine *in situ* the deformation temperature of coals for which a correlation exists between the deformation temperature and the percentage of Al, Si and Fe present in coal. The technique requires a ^{252}Cf neutron source as the primary source of radiation and a BGO scintillation detector for the detection of the gamma-rays-produced by the interaction of neutrons with the surrounding nuclei.

The three borehole logging techniques mentioned above are all used in the coal mining industry in Australia and overseas. One common hindrance for all these methods is the use of a radioactive source and the extra care required. To overcome this problem, research has been carried out over the past 11 years to develop probes for borehole logging and portable nucleonic instruments that use very low activity gamma-ray sources (below 3.7MBq activity). SCINTREX/AUSLOG Pty Ltd in Brisbane developed a 'microdensity-caliper gamma-gamma tool' using a ^{137}Cs source of 3.66MBq activity to delineate the coal seams in boreholes.

It operates in excentralized mode and records the total scattered gamma-radiation. CSIRO Exploration and Mining also developed a low activity spectrometric gamma-gamma borehole logging tool for the coal mining industry. The tool is centralized and was developed for both delineation of coal seams and coal ash determination (Borsaru &Ceravolo, 1994). The activity of the gamma-ray source used in the tool is 1.8MBq. More recently CSIRO Exploration and Mining developed a low radioactivity portable coal face ash analyser and a stockpile probe for the determination of coal ash on the coal face and in coal stockpiles respectively (Borsaru & others, 2001b; Borsaru & others, 2004b). Both instruments use very low activity gamma-ray sources (1.5MBq).

This paper describes the application of the spectrometric low activity tool using a ^{137}Cs gamma-ray source of activity 1.8MBq for delineating the coal/rock interface in dry, large diameter blast holes.

PRINCIPLE OF SPECTROMETRIC BACKSCATTERED GAMMA-RAY TECHNIQUE

The principle of the spectrometric backscattered gamma-ray technique for the delineation of coal seams in boreholes and determination of ash content in coal was described in previous publications (Borsaru & others, 1985; Borsaru & Ceravolo, 1994). The intensity of a backscattered gamma-ray spectrum at higher energy (>150keV) is determined by density of the scattering medium and at low energies by both the density and its equivalent atomic number (Z_{eq}), a substitute for the atomic number Z for a multi-element medium.

The theory of the gamma-ray absorption shows that the photoelectric absorption cross-section per atom is $\sigma(E) \sim Z^{4.5}/E^n$, where E is the energy of the gamma-ray and $2.5 \leq n \leq 3.5$.

The meaning of this expression is that:

- the count-rate in the low energy region (~ below 80keV) of the backscatter gamma-ray spectrum is lower for a high Z_{eq} scattering medium than for a low Z_{eq} one.
- low-energy gamma-rays are absorbed more readily than high-energy gamma-rays for the same scattering medium.

Consequently, the shape of the backscatter gamma-ray spectrum is a function of the energy of the gamma-ray used as a primary source of radiation and scattering medium.

Due to the fact that coal contains elements with lower atomic number Z than the rock (C, H, O…) and (Si, Ca, Al…) respectively, the shape of the backscatter spectra in coal and rock must be different. The low-energy part of the spectra are mostly affected by the difference between Z_{eq} of coal and rock. The present spectrometric technique records the whole energy spectrum and is therefore-capable of selecting different areas of the spectra which are most sensitive to coal and rock and subsequently increase the sensitivity of coal/rock delineation.

THE PROBE AND EQUIPMENT

The logging probe was fabricated from anodised aluminium of 3mm thickness and 60mm diameter. A 37 dia x 75mm NaI(Tl) scintillation detector is used for the detection of gamma-radiation. The detector was shielded from the gamma-ray source by 30mm of lead of conical shape. This short source-detector spacing allows the use of a low activity source as a primary source of radiation without affecting the counting statistics.

The lead shielding absorbs 85% of the 662keV gamma-radiation produced by the ^{137}Cs gamma-ray source. The remaining 15% of gamma-radiation penetrates the shielding and produces a 662keV peak in the detector. This Gaussian shape peak is used to stabilise the gain. Gain stabilisation is an essential feature in spectrometric measurements when only selected sections of the spectra are considered in data analysis and gain drifts can introduce large errors.

Because the energy of the gamma-rays released by the primary source of radiation plays an important role in the shape of the backscatter spectrum, two sources were tested during the course of this work:

- one test was carried out with one 1.8MBq ^{137}Cs source that emits gamma-rays of 662keV energy, the gain stabilisation is achieved as in the first case by the 662keV gamma-ray peak produced by ^{137}Cs.
- the second test was carried out with two gamma-ray sources: 1.8MBq ^{137}Cs and 1.2MBq ^{133}Ba. The three more intense gamma-rays produced by ^{133}Ba have energies of 80, 300, and 350keV accompanied by a 32keV X-ray. Most of the lower energy gamma-rays produced by ^{133}Ba are stopped by the lead shield and the gain stabilisation is achieved as in the first case by the 662keV gamma-ray peak produced by ^{137}Cs.

The backscattered gamma-ray spectra were recorded every 5cm and stored onto the hard disk of a laptop computer. The logging speed was 2.5m/min. The logging system is a single wire system using a common conductor for communications as well as powering the tool. Pulses produced by the gamma-ray detector are processed by a microprocessor incorporated in the probe and transmitted to the uphole computer.

The system is using a high speed A2D (analog to digital) convertor with the data being processed into 480 channels. The full logging system consists of the probe, winch, a laptop computer and the 18.5 x 18.5 x 6.5cm ‘SWISS’ box. The SWISS box provides the power supply and the interface between the tool and the laptop computer. The logging system is portable and so does not require a dedicated logging truck.

FIELD TESTS

The tool was tested in two blast, dry holes. The holes were drilled through the overburden and a few metres into the coal seam. It is important to know the interface between rock and coal for blast purposes. The field tests were carried out to test the sensitivity of the tool for identifying this interface. The holes were drilled at an angle. For this reason we logged the holes with the tool both centralised and without centraliser. It is easier to just drag the tool up the wall of the borehole than to centralise it when the hole is not vertical. The tests were carried out to see whether the excentralised log could provide a delineation coal/rock comparable to the centralised log.

Figure 1(a) shows the backscattered energy spectra acquired in coal and rock while logging; the tool was not centralized and employed both the ^{137}Cs and ^{133}Ba sources. The figure shows the small peak at 662keV used for gain stabilisation.

Figure 1(b) shows an enlarged image of the energy region below 300keV of the same spectra. Figure 1(b) shows a large variation in the gamma-ray intensity of the two spectra at low energy (<100keV) due to the difference between the average atomic number of coal and rock. The count rate is higher in coal than in rock. The count rates at higher energy, (above 150keV) where the density plays the major part, vary in opposite direction: the higher density rock produces a higher count rate than the coal. This shows how important it is to record the whole gamma-ray energy spectrum, which is achieved in a spectrometric measurement.

By dividing the count rates recorded in two energy windows selected in the low and the high energy regions respectively, the differentiation between coal and rock is enhanced. The total count (non-spectrometric) log employed by commercial logging companies, which records the total number of gamma-rays regardless of their energy, can not provide the same sensitivity for coal/rock delineation because, for coal,

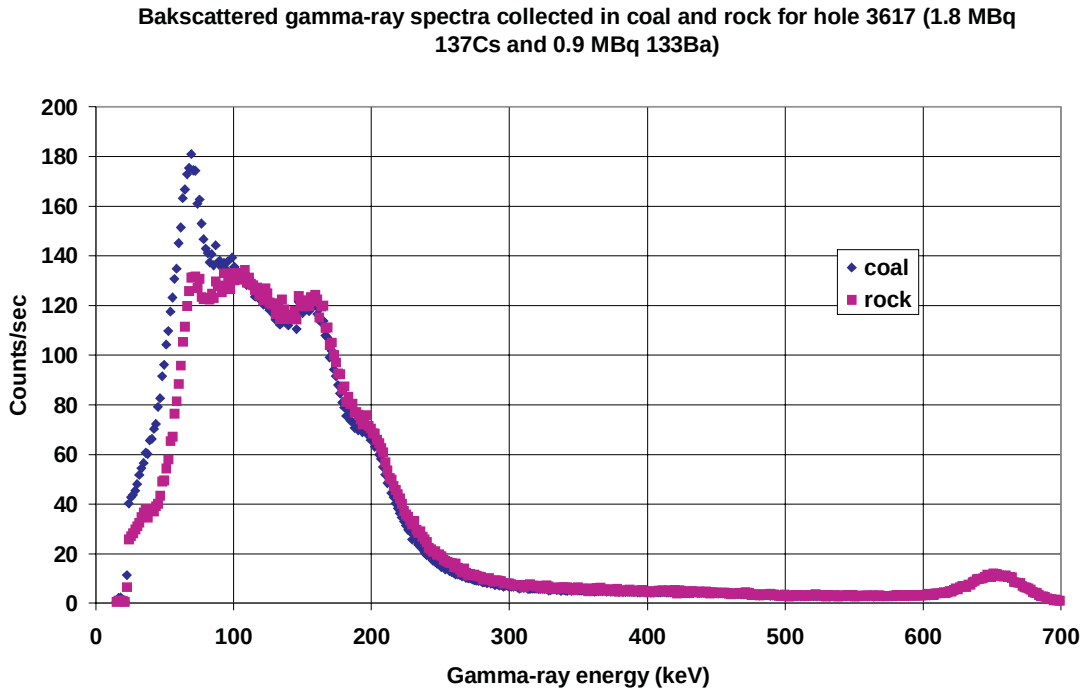

Figure 1(a): Backscattered energy spectra acquired in coal and rock with the excentralised tool employing both the ^{137}Cs and ^{133}Ba sources

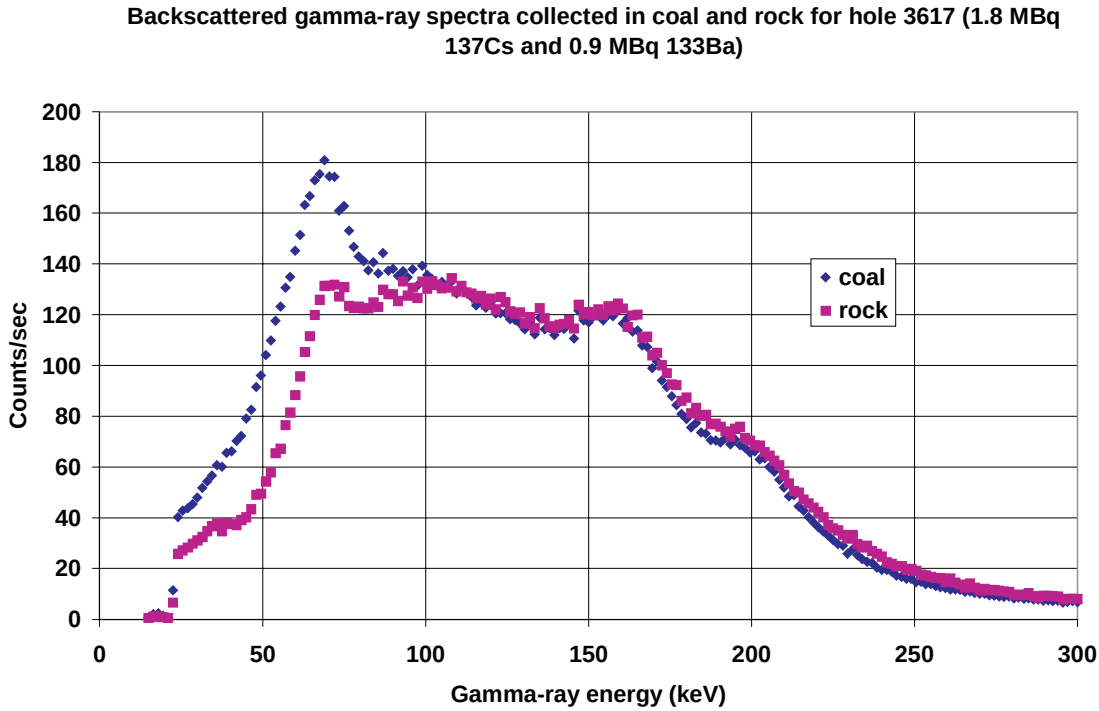

Figure 1(b): Expanded backscattered energy spectra acquired in coal and rock with the excentralised tool employing both the ^{137}Cs and ^{133}Ba sources below 300keV energy

the increase in the count rate in the low energy region corresponds to a decrease in count rate in the high energy region, and the opposite is true for rock.

Figure 2 shows the backscattered spectra recorded in coal and rock when only the ^{137}Cs gamma-ray source was used and; the tool was centralized. The shapes of the spectra shown in Figure 2 are different than the shapes of the spectra shown in Figure 1 due to the difference in the energy of the gamma-rays released by ^{137}Cs and ^{133}Ba. Figure 2 also shows a distinct variation in the count rates in coal and rock. Both Figures 1 and 2 demonstrate that the count rate recorded in an energy window at low energy (~ 25–70keV) is different between coal and rock and therefore can be used to distinguish between the coal and rock in the borehole. The-ratio between the count rates recorded in two energy

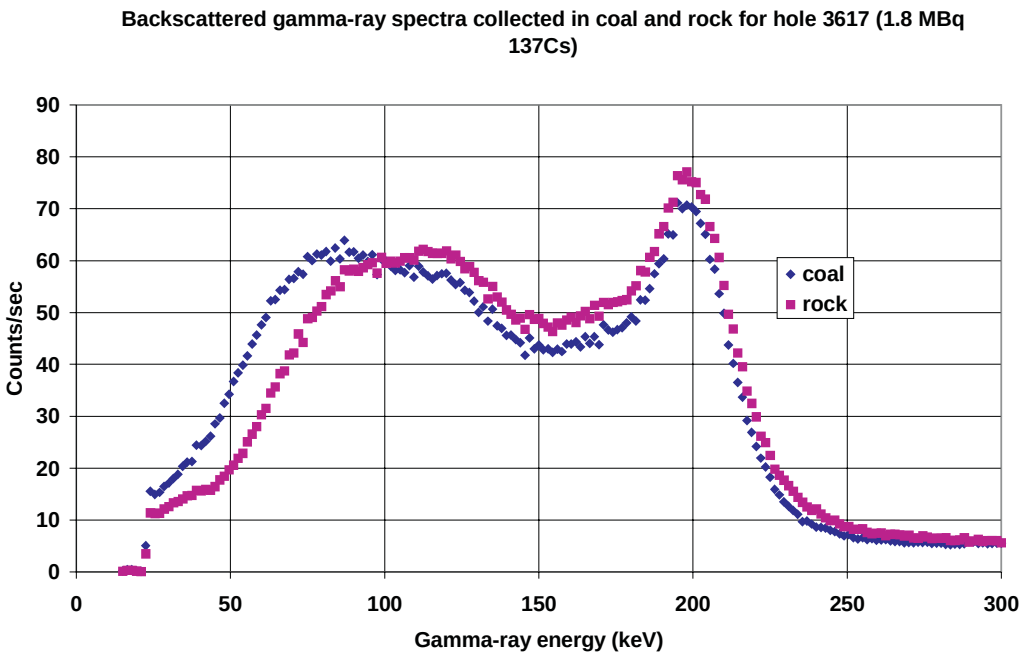

Figure 2: Backscattered energy spectra acquired in coal and rock with the centralised tool employing only one 1.8MBq ^{137}Cs source

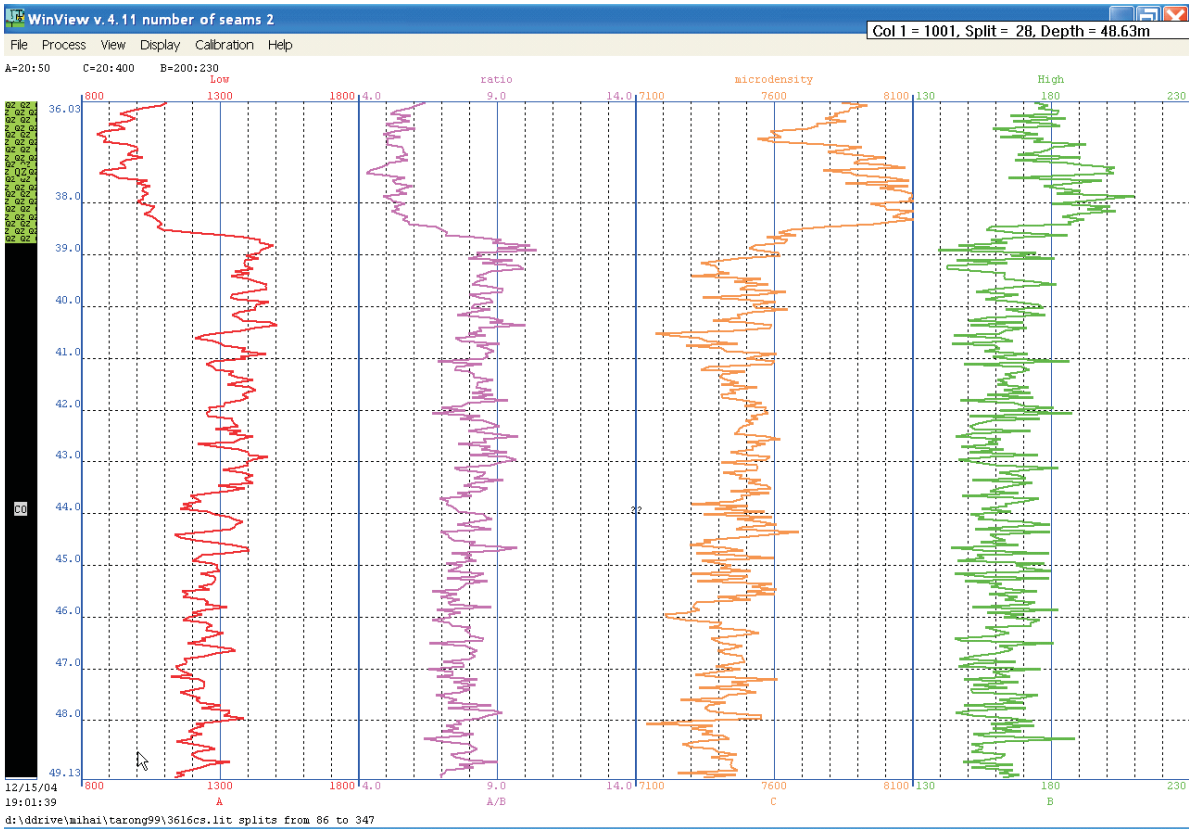

Figure 3: Differentiation of coal and rock given by the spectrometric low activity gamma-ray tool using one ^{137}Cs gamma-ray source (centralised)

windows at low energy (~25–70keV) and higher energy (~120–220keV) would be even more sensitive to differentiate the coal and the rock. This is the basis of this technique to identify the interface between coal and rock in blast holes.

Figure 3 shows the delineation between the coal and the interseam sediment with the spectrometric low radioactivity gamma tool (centralised) using a ^{137}Cs gamma-ray source of activity 1.8MBq. The first column shows the variation in the count rate recorded in the low energy window (30–75keV). The ratio between the average count rate recorded in coal (1400) and rock (900) is 1.55.

The second column shows the variation of the ratio between the count rates recorded in the low energy window

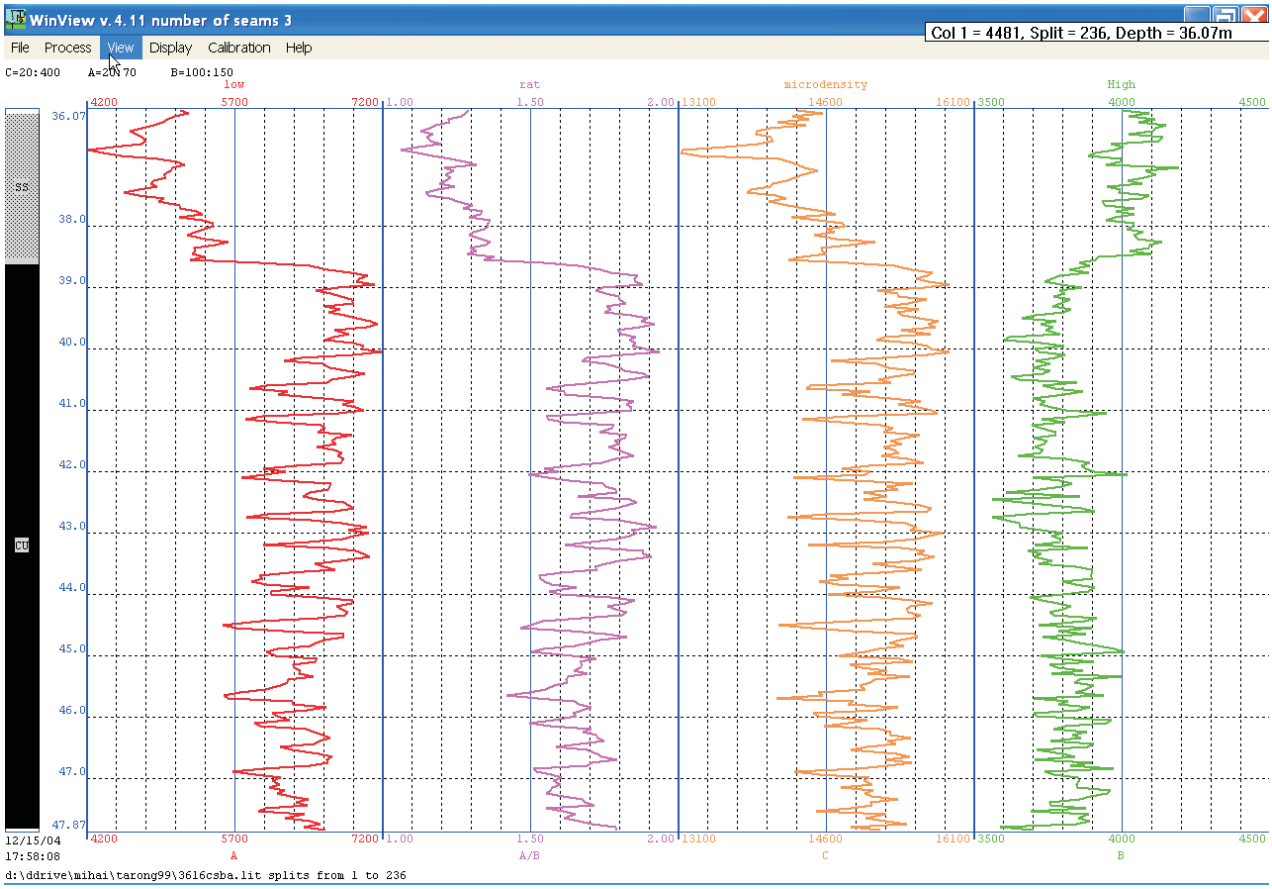

Figure 4: Delineation between coal and rock given by the spectrometric low activity gamma-ray tool using one ^{137}Cs and one ^{133}Ba gamma-ray sources (excentralised)

(30–75keV) and the count rate recorded in a window chosen in the high energy region (300–345keV). The difference between the average ratios recorded in coal (9) and rock (5) is 1.8. This gives better sensitivity to delineate the coal from rock than the first column. The third column shows the count rates recorded in a large energy window (30–600keV).

This simulates a nonspectrometric (total gamma ray counts) measurement where the gamma rays of very low energy can be stopped by some lead shielding and the rest of the spectrum recorded as-total counts regardless of energy. This simulates a measurement with the microdensity (total count) tool, which is not spectrometric. The ratio of the average count rates recorded in rock (8000) and coal (7400) is 1.08. This shows a much lower sensitivity than in the previous (spectrometric) columns. The last column shows the count rate recorded in the high energy window (300–345keV) which is more related to the density of the formation. The ratio between the average count rate in rock (190) and coal (160) is 1.06, which is quite low. This is expected because a tool with short source detector distance, as the present case, is not sensitive for density measurements.

Figure 4 shows logs taken with the tool using both ^{137}Cs and ^{133}Ba and the tool operating without a centraliser. This pattern is much the same as the one shown by Figure 3. The differentiation of coal and rock is best achieved by the ratio between count rates recorded in the low and high energy region (column 2) and is much more sensitive than the simulated total count log (column 3).

SUMMARY AND CONCLUSIONS

The present work demonstrates that the spectrometric low activity tool employing either one ^{137}Cs gamma ray source or two (^{137}Cs and ^{133}Ba) gamma ray sources can be used to delineate coal from rock in large diameter dry blast holes. There is no advantage to use two gamma ray sources or to centralise the tool. The delineation can be achieved with the tool employing one ^{137}Cs gamma ray source and dragged along the wall of the hole drilled at an angle. The gamma ray source is very weak and does not require any shielding. The operator is not exposed to an unacceptable dose of radiation.

The delineation of coal and rock interfaces by a nonspectrometric tool is less pronounced and may not be as useful in achieving accurate differentiation between coal and carbonaceous shale.

The SIROLOG low activity tool is commercially available.

REFERENCES

BORSARU, M., CHARBUCINSKI, J., EISLER, P.L. & YOUL, S.F., 1985: Determination of ash content in coal by borehole logging in dry boreholes using gamma-gamma methods. *Geoexploration*, **23**, 503–518.

BORSARU, M. & CERAVOLO, C., 1994: A low activity spectrometric gamma-gamma borehole logging tool for the coal industry. *Nuclear Geophysics*, **8**(4), 343–350.

BORSARU, M., BIGGS, M.S., NICHOLS, W.J.F. & BOS, F., 2001a: The application of prompt – gamma neutron activation analysis to borehole logging for coal. *Applied Radiation and Isotopes*, **54**, 335–343.

BORSARU, M., DIXON, R., ROJC, A., STEHLE, R. & JECNY, Z. 2001b: Coal face and stockpile ash analyser for the coal mining industry. *Applied Radiation and Isotopes*, **55**, 407–412.

BORSARU, M., BERRY, M., BIGGS, M. & ROJC, A., 2004a: *In situ* determination of sulphur in coal seams and overburden rock by PGNAA. *Nuclear Instruments and methods of physical Research*, **B 213**, 530–534.

BORSARU, M., CHARBUCINSKI, J., ROJC, A., THANH, N.D. & TUY, N.T., 2004b: Probe for the determination of ash in coal stockpiles. *Nuclear Instruments and methods of physical Research*, **B 213**, 422–425.

BROM, R.W.C. & DRIEDONKS, F., 1981: Applications of petrophysical logging in the evaluation of coal deposits. *SPWLA 22nd Annual Logging Symposium*, paper KK.

DANIELS, J.J., SCOTT, J.H. & LIU, J., 1983: Estimation of coal quality parameters from geophysical well logs. *SPWLA 24th Annual Logging Symposium*, paper KK.

LAVERS, B.A. & SMITS, L.J.M., 1976: Recent developments in coal petrophysics. *SPWLA 17th Annual Logging Symposium*, paper S.

REEVES, D.R., 1977: Application of wireline logging techniques to coal exploration. *In* Muir, W.L.G. (Editor): *Proceedings of the first International Coal Exploration Symposium*, London, England, 18-21 May, 112–128.

SAMWORTH, J.R., 1974: The radiation density log applied to the resolution of thin beds in coal measures. *SPWLA 3rd European Symposium*, London, paper R.

J. Asfahani, Geology Department, Atomic Energy Commission, P.O. Box 6091, Damascus, Syria\
M. Borsaru, CSIRO Exploration and Mining, P.O. Box 883, Kenmore, Qld 4069, Australia
W. Nichols, Callide Coalfields, P.O. Box 144, Biloela, Qld 4715, Australia

Basil Beamish and Lucas Hogarth

Hot spot development in stored subbituminous coal from Callide

There is a need for a definitive test to quantify what is a reasonable timeframe for safe coal storage to reduce the risk of coal ignition from spontaneous combustion. A bulk coal, as-received test method has been developed using a 2-metre column apparatus. This paper presents the results from a series of column tests that have been conducted on subbituminous coal at different airflow rates from the same initial start temperature of 30°C. The inherent reactivity of the coal towards oxygen is very high due to the low rank, which is reflected in the R_{70} value of the coal (in excess of 11°C/h). The column tests show that after eight to nine days a hot spot in excess of 150°C is established in the stored coal. However, once this stage is reached, it takes longer for the coal to progress towards an ignition temperature as the airflow rate decreases. The column tests also show that ignition temperatures for the coal are reached within two to three weeks if the coal is stored in a loosely compacted state.

INTRODUCTION

When coal is stored in either stockpiles or large feed bins, there is always the risk of spontaneous combustion if the coal is not moved or used in a 'reasonable timeframe'. This situation is created when the heat generated by oxidation reactions is not dissipated from the coal pile and there is enough air present to sustain the oxidation reaction, which is temperature dependent. Unfortunately, the heterogenous nature of coal and the contributing factors that control whether heat is gained or lost from the coal/oxygen system make it difficult to predict the onset of a heating with any confidence. Hence, defining what is a 'reasonable timeframe' for coal storage before creating an unacceptable risk has been a long-standing question for the coal producers and users.

One possible approach to assess the risk of coal self-heating is to perform bulk coal tests under conditions close to those that exist in operations. Bulk coal self-heating tests have been limited due to the expense and time taken to obtain results. Some success has been obtained with various column-testing arrangements using kilograms rather than tonnes of bulk coal (Li & Skinner, 1986; Stott & Chen, 1992; Akgun & Arisoy, 1994; Arief, 1997), but the equipment used has not gained wide acceptance by the coal industry. This is because there has been a wide variation in the results obtained and no attempt has been made to transfer the information into a form that is readily useable by industry personnel.

A new laboratory has been established within the School of Engineering at The University of Queensland (UQ) that uses a 2-metre column to conduct a practical test capable of providing reliable data on coal self-heating (Beamish & others 2002). This can be used to predict the onset of coal self-heating with acceptable engineering certainty for risk management purposes. Preliminary results from this new work are providing definitive insights into hot spot development (Beamish & Daly, 2004; Beamish & Jabouri, 2005). This paper presents the results of a parametric study on the effects of different airflow rates on hot spot development in stored subbituminous coal from Callide. These results have direct applicability to both the Callide Mine as the coal producer and the Callide Powerstation, which uses the coal.

COLUMN SELF-HEATING ASSESSMENT

Equipment

Beamish & others (2002) describe the basic operation of the UQ 2-metre column, which has a 62L capacity, equating to 40–70kg of coal depending upon the packing density used. The coal self-heating is monitored using eight evenly spaced thermocouples along the length of the column that are inserted into the centre of the coal at each location (Figure 1). Eight independent heaters correspond to each of these thermocouples and are set to switch off at 0.5ºC below the coal temperature at each location so that heat losses are minimised and effectively adiabatic conditions are maintained radially. Therefore, the coal behaves as if it were a much larger mass that is undergoing self-heating. Consequently, the UQ 2-metre column provides a test environment that is closer to reality than small-scale test equipment used for rating the propensity of coal to spontaneously combust.

Supply of samples and preparation for testing

For all of the tests, fresh run-of-mine coal was obtained from the Callide Mine conveyor that feeds the Callide Powerstation. The first two samples (DC5 and DC6) were taken from the same batch of coal delivered in a sealed 200L drum. The third sample (DC7) was supplied in two 20L sealed buckets and six double bags sealed with pull ties. All samples had a top particle size below 75mm and a size distribution of each batch of coal was determined prior to loading into the UQ 2-metre column. The average particle size of the samples was determined using the procedure described by Kunii & Levenspiel (1991) for estimating the

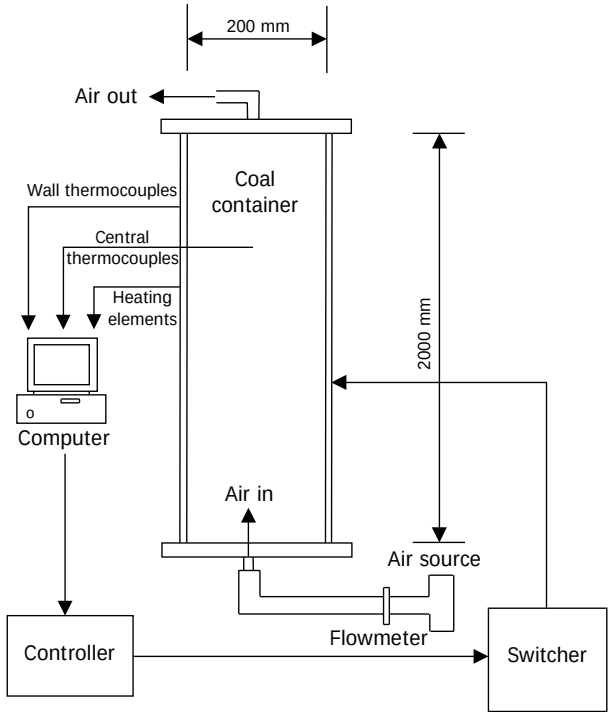

Figure 1: Schematic of UQ 2-metre column self-heating apparatus (modified from Arief, 1997)

surface-volume average particle size from the size distribution of the coal. The results of this analysis showed that the feed coal was reasonably uniform, with the average particle size of the three samples ranging from 3.39–3.47mm.

Three subsamples were taken as each column test was loaded to obtain data on the as-received moisture of the coal. Samples DC5B2, DC5B3, DC7B2 and DC7B3 were also taken at this stage to establish the R_{70} self-heating rate of the coal (Humphreys, Rowlands & Cudmore, 1981; Beamish, Barakat & St George, 2001).

R_{70} test procedure

The R_{70} test procedure essentially involves drying a 150g sample of <212µm crushed coal at 110°C under nitrogen for approximately 16 hours. Whilst still under nitrogen, the coal is cooled to 40°C before being transferred to an adiabatic oven. Once the coal temperature has equilibrated at 40°C under a nitrogen flow in the adiabatic oven, oxygen is passed through the sample at 50mL/min. A data logger records the temperature rise due to the self-heating of the coal. The average rate that the coal temperature rises between 40°C and 70°C is the initial self-heating rate index (R_{70}), which is in units of °C/h and is a good indicator of the inherent coal reactivity towards oxygen.

Column test procedure

A standard test procedure has been developed for UQ 2-metre column coal self-heating tests. The coal was loaded into the column with three 20L plastic buckets. Once all the coal was in the column it was sealed and the heaters used to set the starting coal temperature, which in this case was 30ºC to simulate a typical daytime temperature for the Callide Mine and the Powerstation feed bins. Temperature equilibration was achieved overnight. Air was then introduced to the coal at the desired flow rate for the tests (DC5-DC7). A computer records all data at ten-minute increments. The column has several safety devices including computer-controlled trips on the external heaters and a temperature trip on the air inlet line. These were set to ensure maximum safety during operation of the column.

RESULTS OF R_{70} AND COLUMN TESTING

Sample properties and test conditions

A summary of the coal properties and column test conditions is contained in Table 1. The moisture content of the samples reached a maximum of 14.4%, which is indicative of the subbituminous rank of the coal. The low volatile matter content is a reflection of the high inertinite content of the Callide coal (Biggs & others, 1995). Due to the nature of bulk coal testing, each column test had some differences in average ash content or test moisture content (Table 1). However, these are not considered to have as much impact on the hot spot development as the physical parameter of airflow rate (Schmal, Duyzer & van Heuven, 1985).

Table 1: Coal properties and column test conditions

Column test	DC5	DC6	DC7
Moisture content (%, ar)	13.8	14.4	13.5
Ash content (%, db)	24.5	20.3	26.9
Volatile matter (%, daf)	30.8	30.8	35.5
Specific energy (MJ/kg, daf)	29.77	29.77	31.35
Bulk density (kg/m^3)	1160	1072	1097
Average particle size (mm)	3.39	3.39	3.47
Initial coal temperature (°C)	30	30	30
Air temperature (°C)	23	23	23
Airflow rate (L/min)	0.5	0.25	0.15

R_{70} values of the column samples

Figure 2 shows the self-heating curves obtained in the UQ adiabatic oven for the column samples. The R_{70} values determined from this test show that there is a significant difference in the reactivity of each sample to oxygen. Generally, as the mineral matter content in the coal increases, the R_{70} value decreases (Beamish & Blazak, in press; Beamish & others, 2005)). This is best illustrated by plotting the R_{70} value against the ash content of the coal on a dry basis (Figure 3). The high R_{70} values obtained (in excess of 11ºC/h) are a reflection of the low rank of coal (Beamish, in press) and confirm the coal is very reactive to oxygen. However, the coal is not as reactive as Waikato coals from New Zealand, which have R_{70} values in excess of 16ºC/h (Beamish & others, 2005). Bowen Basin high volatile bituminous coals have R_{70} values around 2ºC/h.

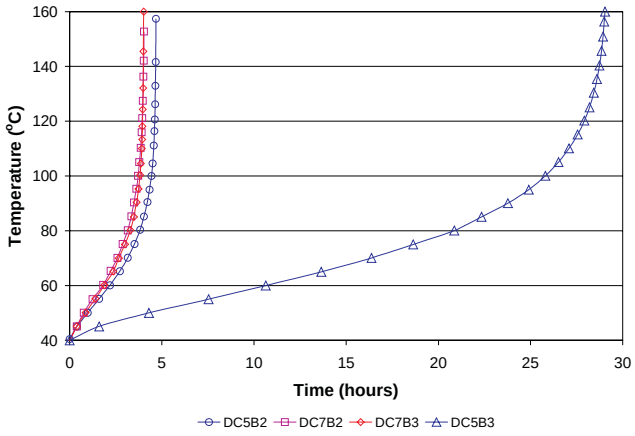

Figure 2: Adiabatic self-heating curves for Callide coal

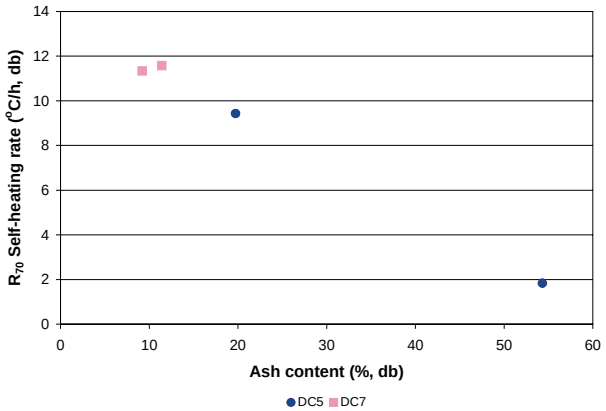

Figure 3: Relationship between R_{70} self-heating rate and ash content of Callide coal

Effect of decreasing airflow rate on hot spot development in as-mined coal

The tests are designed to simulate wind effects on loosely compacted stockpiles. The general pattern of hot spot development is the same for all three tests (Figures 4–6), but the decreasing airflow creates some subtle differences. In the initial stages of self-heating, a warm spot appears at 127–145cm from the air inlet and progresses slightly downwind as the coal temperature continues to rise in this region. At around 80ºC, the rise in the coal temperature begins to slow for DC5 as the coal nearer the inlet dries out. A noticeable hot spot then develops at 127cm from the air inlet before migrating down the column towards the air source and creating a large hot spot 55cm from the air inlet (Figure 4). DC6 shows a small hot spot developing at 127cm (Figure 5), whereas DC7 does not (Figure 6). However, in both cases the hot spot migrates down the column to form a large hot spot 73cm from the air inlet.

Further fundamental differences between the three tests are seen in Figure 7. The lower airflow enables the maximum temperature to increase more rapidly in the column during the early stage of hot spot development. However, the coal

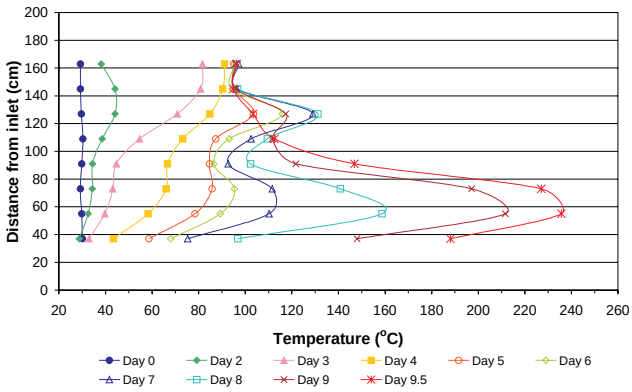

Figure 4: UQ 2-metre column temperature profile for Callide coal, airflow 0.5L/min

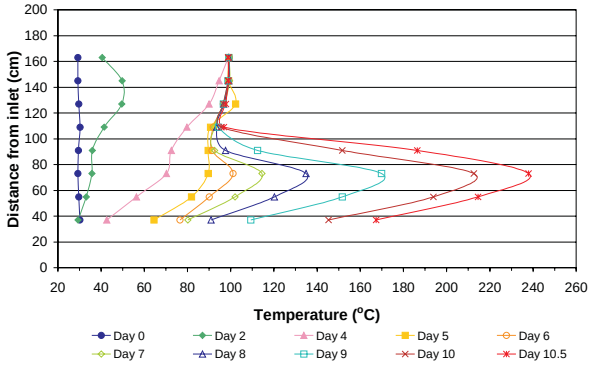

Figure 5: UQ 2-metre column temperature profile for Callide coal, airflow 0.25L/min

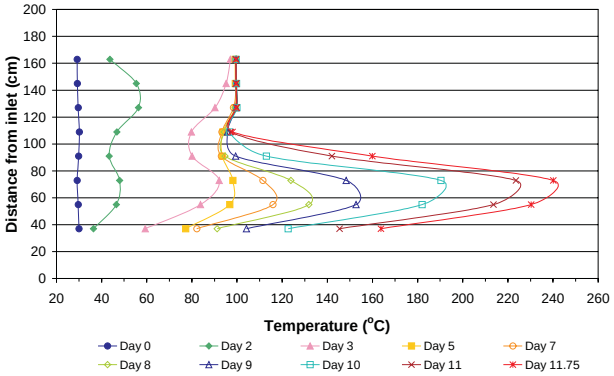

Figure 6: UQ 2-metre column temperature profile for Callide coal, airflow 0.15L/min

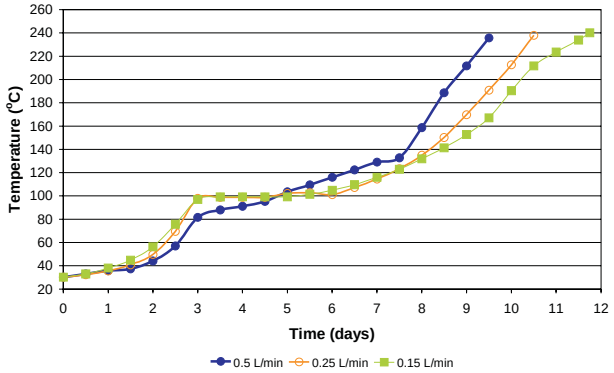

Figure 7: UQ 2-metre column temperature history for Callide coal at different airflow rates

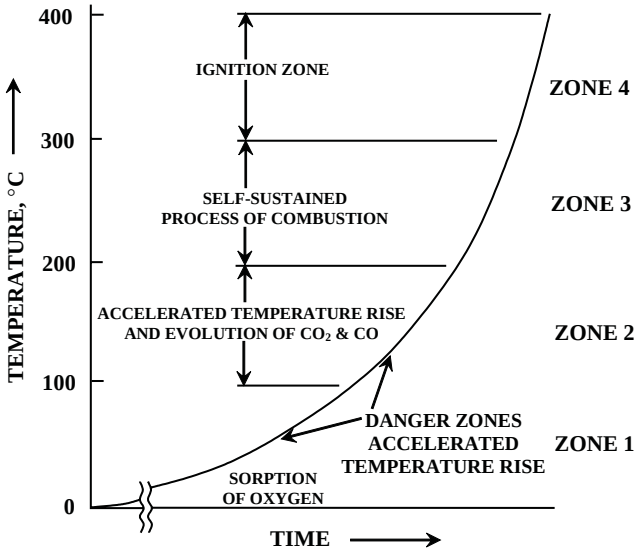

Figure 8: Schematic of coal spontaneous combustion temperature history (modified from Walters (1996) and Barve & Mahadevan, 1994)

temperature then plateaus for several days before the coal dries out sufficiently for the hot spot to continue to increase in temperature and begin to migrate towards the air source. In the higher airflow rate test (DC5, 0.5L/min, Figure 7) the coal temperature increase only slows for a short period before continuing to increase again.

The pattern of hot spot development shown by the column testing is consistent with the moist coal self-heating models of Schmal, Duyzer & van Heuven (1985), Arisoy & Akgun (1994), Portola (1996) and Monazam, Shadle & Shamsi (1998).

In particular, the moist coal model of Schmal, Duyzer & van Heuven (1985) predicts the plateau effect of the initial hot spot development seen in the lower airflow rate tests (Figure 7). They maintain heat effects due to evaporation and condensation of moisture is responsible for the coal reaching a constant maximum temperature of 80–90ºC, which in the case of the Callide coal appears to be 98–99ºC. This level continues until the coal becomes dry locally, after which a steep temperature rise occurs at the dried spot.

Hot spot development in moist coal is therefore not a simple continuous process, which is often conveyed in published schematics of coal spontaneous combustion (eg Walters, 1996; Barve & Mahadevan, 1994). The self-heating curve used in these explanations (Figure 8) is more akin to the dry coal curves obtained from R_{70} adiabatic testing (Figure 2). This simplistic view does not take into consideration the moisture evaporation and condensation effects seen in bulk coal testing (Figure 7), nor does it consider the migrating nature of a hot spot.

The results of the three column tests suggest that in loosely compacted coal, such as that found at the base of the thick seam at Callide due to highwall spalling, the time for a serious hot spot to develop (>150ºC) is between eight to nine days. Extrapolating the results shown in Figure 7 yields a timeframe to reach ignition (temperatures in excess of 400ºC) of two to three weeks. Experience at the mine agrees with these bulk experimental results. Therefore, uncompacted stockpiles of this coal should not be kept for this period of time.

CONCLUSIONS

Coal from the feed belt of the Callide Mine provides a reasonably consistent sample for investigating hot spot development in bulk self-heating tests with a 2-metre column. The coal is subbituminous in rank and is very reactive towards oxygen, as shown by R_{70} values in excess of 11ºC/h.

High levels of moisture in the coal, up to 14.4% as-received, have a significant effect on hot spot development, consistent with moist coal self-heating models that consider evaporation and condensation processes. At low airflow rates, this effect is accentuated causing the coal to reach a plateau temperature of 98–99ºC for several days, before becoming dry locally near the point of air ingress. Once this stage is reached, a major hot spot develops that not only rapidly increases in temperature, but also migrates towards the air source.

From the UQ 2-metre column tests on Callide coal it can be seen that it is possible for the coal to self-heat and proceed to ignition in two to three weeks if the coal is stored in a loosely compacted state. This is quite a short timeframe compared with coals of higher rank, which may take several months to reach ignition when stored under the same conditions.

ACKNOWLEDGEMENTS

ACARP and a University of Queensland Early Career Researcher grant provided financial support for the project. The authors also would like to thank Callide Mine, especially Wes Nichols and Iain Hodge for their continued support of this work.

REFERENCES

AKGUN, F. & ARISOY, A., 1994: Effect of particle size on the spontaneous heating of a coal stockpile, *Combustion and Flame*, **99**, 137–146.

ARIEF, A.S., 1997: Spontaneous combustion of coal with relation to mining storage, transportation and utilisation, PhD Thesis, The University of Queensland, Brisbane, Australia.

ARISOY, A. & AKGUN, F., 1994: Modelling of spontaneous combustion of coal with moisture content included, *Fuel*, **73**, 281–286.

BARVE, S.D. & MAHADEVAN, V., 1994: Prediction of spontaneous heating liability of Indian coals based on proximate constituents. *In*, *Proceedings of 12th International Coal Preparation Congress*, Cracow, Poland, 557–562.

BEAMISH, B.B., in press: Comparison of the R_{70} self-heating rate of New Zealand and Australian coals to Suggate rank parameter, International Journal of Coal Geology.

BEAMISH, B.B. & BLAZAK, D.G., in press: Relationship between ash content and R_{70} self-heating rate of Callide coal, International Journal of Coal Geology.

BEAMISH, B.B. & DALY, M.D., 2004: Self-heating of gas-drained coal. *In*, *Proceedings 2004 CRC Mining Research and Effective Technology Transfer Conference*, Noosa, 15–16 June.

BEAMISH, B.B. & JABOURI, I., 2005: Factors affecting hot spot development in bulk coal and associated gas evolution. *In*, *Proceedings COAL2005 Conference*, The Australasian Institute of Mining and Metallurgy, 187–193.

BEAMISH, B.B., BARAKAT, M.A. & ST GEORGE, J.D., 2001: Spontaneous-combustion propensity of New Zealand coals under adiabatic conditions. *In*, Lindsay, P. & Moore, T.A. (Editors): *Geotechnical and Environmental Issues Related to Coal Mining*, *Special Issue, International Journal of Coal Geology*, **45**(2–3), 217–224.

BEAMISH, B.B., BLAZAK, D.G., HOGARTH, L.C.S. & JABOURI, I., 2005: R_{70} relationships and their interpretation at a mine site. *In*, *Proceedings COAL2005 Conference*, The Australasian Institute of Mining and Metallurgy, 183–185.

BEAMISH, B.B., LAU, A.G., MOODIE, A.L. & VALLANCE, T.A., 2002: Assessing the self-heating behaviour of Callide coal using a 2-metre column, *Journal of Loss Prevention in the Process Industries*, **15**, 385–390.

BIGGS, M.S., BURGESS, A.W. & PATRICK, R.B., 1995: Callide Basin. *In*, Ward, C.R., Harrington, H.J., Mallett, C.W. & Beeston J.W., (Editors): Geology of Australian Coal Basins, *Geological Society of Australia Coal Geology Group, Special Publication* **1**, 471–488.

HUMPHREYS, D., ROWLANDS, D. & CUDMORE, J.F. 1981: Spontaneous combustion of some Queensland coals. *In*, *Proceedings Ignitions, Explosions and Fires in Coal Mines Symposium*, The Australasian Institute of Mining and Metallurgy: Illawarra Branch, 5-1 to 5-19.

KUNII, D. & LEVENSPIEL, O., 1991: *Fluidization Engineering*, Krieger, New York.

LI, Y-H. & SKINNER, J.L., 1986: Deactivation of dried subbituminous coal, *Chemical Engineering Communications*, **49**, 81–98.

MONAZAM, E.R., SHADLE, L.J. & SHAMSI, A., 1998: Spontaneous combustion of char stockpiles. *Energy & Fuels*, **12**, 1305–1312.

PORTOLA, V.A., 1996: Assessment of the effect of some factors on spontaneous coal combustion. *Journal of Mining Science*, **32**(3), 212–218.

SCHMAL, D., DUYZER, J.H. & VAN HEUVEN, J.W., 1985: A model for the spontaneous heating of coal. *Fuel*, **64**, 963–972.

STOTT, J.B. & CHEN, X.D., 1992: Measuring the tendency of coal to fire spontaneously. *Colliery Guardian*, **240**(1), 9–16.

WALTERS, A.D., 1996: Joseph Conrad and the spontaneous combustion of coal - Part 1. *Coal Preparation*, **17**, 147–165.

B Basil Beamish and Lucas CS Hogarth, School of Engineering, The University of Queensland, Brisbane, Q, 4072

Ken Preston

Estimating the In Situ *relative density of coal — old favourites and new developments*

Seam thickness, seam extent (area) and coal density are the three components of an estimate of *in situ* coal tonnes within a seam. Normally a significant effort is made to characterise thickness and extent, but density remains the least well understood and the least well characterised of the three. This is in spite of the fact that inaccurate density values can make a significant difference to tonnage estimates. Until the early 1990s there was little published about the subject and the density 'dark ages' were in full swing.

In 1993, Ken Preston and Richard Sanders presented a method for estimating the *in situ* density of coal and pointed out a number of incorrect methods then commonly in use in the industry. Since that time the problem has attracted the attention of others and three significant papers have been written on estimating the density of coal. The first was by Grant Quinn in 2000 and the second and third were the results of concurrent ACARP projects, firstly by Ian Fletcher and Richard Sanders and secondly by Andrew Meyers, Chris Clarkson, Robert Leach and Terry Wex, both finalised in 2003.

There are now three new methods 'on the market' for estimating the density of coal as well as the established Preston and Sanders method and a number of traditional methods. The question now arises 'which one to use?' This paper reviews each method and offers a view as to their individual strengths and weaknesses. It examines the level of accuracy that is trying to be achieved and offers some advice as to which approach to take. Overall its purpose is to clarify the current state of understanding on the subject.

INTRODUCTION

Preston & Sanders (1993), states that: "The relative density of coal is a fundamental physical parameter which should be understood by geologists, who need to know the *in situ* relative density of coal for use in reserve calculations.*"* This statement is as true today as it was when it was written.

Fortunately, since that paper was written, this fact has gained greater acceptance and geologists and engineers, in the main, recognise that something has to be done to 'get it right' and that getting it right is more than a trivial exercise. The method for estimating the *in situ* relative density of coal proposed by Preston & Sanders (1993) was adopted by many, rejected by some and remained unknown to others. Whilst it served its purpose in jolting the industry into recognising the problem and it did propose a sound solution, it did not purport to be the final word on the subject. The difficulties, both practical and logical, in determining the correct density had not gone away and there was still no single, simple, universally accepted and bullet proof method that could be employed to solve the problem. Fortunately where a problem exists there are always people who are keen to try to solve it and during the last five years there have been three new methods developed and published.

Whilst this has been a good thing, it has led to some confusion about what course of action to take. This paper does not set out to present any new or original research on the subject of determining the *in situ* density of coal. Its nature and purpose is to restate the problem that is inherent in estimating the *in situ* density of coal and then to review each of the methods that are currently available to the practitioner for its estimation. Comments are made about the strengths and weaknesses of each method and recommendations are made with regard to how to proceed.

BACKGROUND

The activity, on which coal geologists spend much of their professional life working, is that of characterising coal seams in terms of their location, disposition, extent, size and quality. At the end of a campaign of data collection, interpretation and spatial modelling, a new resource model is produced and the inevitable question that arises from geologists, engineers and project owners is 'how much coal do we have' or in other words 'what are our coal resources and reserves'?

The answer to this is a relatively simple calculation, namely:

> *in situ* coal tonnes = seam thickness (m) x areal extent of the coal seam (m^2) x *in situ* relative density of the coal

At the exploration and evaluation stage much effort generally goes into defining and measuring seam area and thickness and the technology and methods for doing this are well understood. However this has traditionally not been the case with *in situ* coal density where the parameter cannot be measured directly and the methods and logic for estimating it are often poorly understood.

This was certainly the case prior to the early 1990s when the density 'dark ages' were in full swing. In these times *in situ* coal density was invariably guessed at (…if you have no better value use 1.40…) or estimated incorrectly as a result of either no adjustment from laboratory determined values or

spurious adjustments following dubious logic. In the 1990s two things happened which brought the matter of *in situ* coal density estimation into the spotlight.

Firstly, Preston & Sanders (1993) highlighted the importance of *in situ* coal density estimation, discussed some of the incorrect methods then in use and provided a reasoned and logical method for making the estimate by adjusting laboratory determined density to account for the moisture loss in the test procedure. The remarkable feature of this paper was that it was the first time that anybody had made any reasonable attempt to identify and come to grips with the problem.

Secondly, the mid-1990s saw the rise of the smaller mining companies with limited financial resources and the entry of mining contractors into the coal business who came to service their needs on a 'dollar per tonne' basis rather than the traditional owner operator basis. This sort of mining demanded a more precise system of coal bookkeeping than most of the major companies were happy to live with, and with the demand for a more accurate way of estimating *in situ* coal tonnes, the spotlight fell upon all of the relevant factors, including coal density. For once, with dollars at stake, accurate knowledge of coal density really mattered.

With a greater level of interest in the matter of density estimation it was inevitable that there would be other people who would think about, research and write about the matter. Quinn (2000) offered an alternative view of what is really important in coal resource and reserve estimation and a complementary method for estimating the density of coal. In 2001 two groups of researchers received ACARP funding to investigate the matter of *in situ* coal density estimation and both of these published their final reports (Meyers & others, 2003; Fletcher & Sanders, 2003).

The current position is that there is a number of methods available for estimation of the *in situ* density of coal and these are discussed below.

THE PROBLEM

The density of a substance is a function of the mass and volume of the substance in question. Relative density is density of the substance relative to the density of water under standard conditions. Normally density may be determined using Archimedes Principle which briefly states that "the buoyant force on a submerged object is equal to the weight of the fluid displaced". Hence volume and mass of an object may be determined by measuring the mass in air and the mass when submerged in water.

Unfortunately coal is a porous substance and is characterised by extensive pores, joints, cracks and voids. These are invariably water filled in the natural state. Applying the Archimedes method under these circumstances is therefore very difficult. So to summarise, the problem in its traditional form is to be able to extract samples from the ground and to determine their mass and volume whilst retaining the original void space and contained moisture. Some solutions to the problem attempt to confront this head on; others sidestep it and attempt to estimate relative density indirectly.

METHODS FOR ESTIMATING THE RELATIVE DENSITY OF COAL FOR USE IN TONNAGE CALCULATIONS

The main methods that are either being used or that have been promoted for use around the industry are summarised in Table 1.

Table 1: Methods for estimating the relative density of coal for use in tonnage calculations

Method Number	Short Name	Brief Description	Proponent
1	Laboratory Relative Density (RD)	Use of relative density as determined by AS 1038.21.1.1-2002, without adjustment.	
2	Laboratory Relative Density adjusted incorrectly	Use of relative density values determined according to AS 1038.21.1.1-2002, incorrectly adjusted upwards for *in situ* moisture.	
3	Preston & Sanders method	Use of relative density values determined according to AS 1038.21.1.1-2002, correctly adjusted downwards for *in situ* moisture.	Preston & Sanders, 1993
4	Apparent Relative Density (ARD)	Use of relative density of lump sample (previously "apparent relative density") as determined by AS 1038.21.2-1992, without adjustment.	
5	RD derived from ARD	Use of two alternative methods to derive *in situ* RD when the dataset mainly comprises ARD values.	
6	Quinn method	Use of float-sink data to estimate coal density.	Quinn, 2000
7	Fletcher & Sanders method	Use of multiple linear regression equations to directly estimate *in situ* density from various coal properties. Estimation of *in situ* moisture by simple and multiple linear regression then application of Preston & Sanders method to estimate *in situ* coal density.	Fletcher & Sanders, 2003
8	Meyers method	Use of multiple linear regression equations to directly estimate *in situ* coal density from various coal properties. Estimation of *in situ* moisture by multiple linear regression.	Meyers & others, 2003
9	Wireline log method	Determination by quantitative analysis of wireline log data.	

Method 1, Laboratory Relative Density (RD)

This method uses the unadjusted results of the Australian Standard method for coal density determination in a density bottle (AS 1038.21.1.1-2002). By way of acknowledging the fact that the method is incorrect, those who use it normally state that: 'tonnes (or reserves) are quoted at air dried basis'.

Characteristics

AS 1038.21.1.1-2002 sets out a method by which the mass of water displaced by a known mass of air-dry coal that has been crushed to -212µm is determined in a density or pycnometer bottle.

Crushing removes all of the fissures and voids that exist *in situ* and some of the pores. Partial drying removes much but not all (normally between 60 and 80 percent) of the moisture that would normally exist in the coal in its *in situ* state.

The results of this procedure are then used without adjustment to estimate coal tonnes.

Strengths and Weaknesses

Strengths	Weaknesses
The test procedure is regulated by an Australian Standard	The coal samples tested are in a completely different state to in situ conditions
The determination is direct rather than indirect	The process of grinding and partial air drying reduces volume and mass, but volume is reduced at a greater rate. Thus the relative density of the sample is increased by this process
Reasonable precision can be expected (repeatability if RD <1.6 is ±0.03; =1.6 is ±0.04)	The relative density values reported overestimate *in situ* density of the coal sample
The test is relatively cheap	The associated disclaimer often used with this method …'tonnes are quoted at air dried basis'…is nonsensical
Frequently geologists have large data sets of these density determinations	

Observations

The results of coal density determinations using AS 1038.21.1.1-2002 form a good basis for estimating the *in situ* density of coal. However they cannot be used without adjustment as the method overestimates the true value, typically by 2–5%.

Method 2, Laboratory Relative Density Adjusted Incorrectly

Characteristics

Up to 10 years ago, it was not uncommon to see examples of practitioners recognising that laboratory density was determined at air dried moisture basis (which of course was always lower than *in situ* moisture basis) and then taking steps to 'correct' the density value. Using the apparently self evident but incorrect logic that since coal gets heavier when you add water to it, it follows that adding water increased its density. Adjustments were then made in the following manner:

Air dry coal density	1.45
Air dry coal moisture	2.0%
in situ coal moisture	6.0%
…therefore *in situ* coal density	= 1.45*(100-2)/(100-6) = 1.51

A 4.3% error is introduced to a number that is already 1.8% too high, giving a total error of 6.2%.

The reason that this is incorrect is that water cannot be added to coal in the state that it is in during the test, unless the volume is recreated to receive the moisture.

Observations

There are no strengths to this method; it is just plain wrong.

Method 3, The Preston & Sanders Method

The Preston & Sanders method uses RD as a base and adjusts it to account for the impact of *in situ* moisture. The details are set out in the paper and will only be presented here as a summary.

Characteristics

- The base relative density value is determined using AS 1038.21.1.1-2002, previously described. (strictly speaking the 1993 paper referred to AS 1038.21 Part 4 which was the predecessor of AS 1038.21.1.1-1994, now issued as AS 1038.21.1.1-2002).
- Air dried moisture is determined according to AS 1038.3-2000
- *in situ* moisture must be estimated by the geologist by reference to fundamental coal properties and other moisture test results
- The calculation that follows is:

$$\text{relative density } (\textit{in situ}) = \frac{RD_{ad} * (100 - M_{ad})}{100 + RD_{ad} * (ISM - M_{ad}) - ISM}$$

where:

RD_{ad} relative density, air dry basis

M_{ad} moisture, air dry basis

ISM *in situ* moisture

- *In situ* relative density calculated in this manner will always be lower than the density determined in the

laboratory according to AS 1038.21.1.1-2002, since when voids and pores are recreated and 'refilled' with moisture, volume will increase at a greater rate than mass.

Strengths and Weaknesses

Strengths	Weaknesses
Is based upon the Australian Standard method which is the most reliable method available for the direct determination of the relative density of a coal sample	The estimation of *in situ* moisture is not a simple mechanical process that can be automated. It requires some understanding of coal science together with results of other moisture testwork to arrive at a reasonable estimate of *in situ* moisture
The logic of the process is intuitive and can be readily followed, accepted and explained to others	
The adjustment process is a simple calculation that can be carried out in a spreadsheet or modelling package	

Observations

The method outlined has gained strong acceptance in the industry. It is logical and simple but some knowledge and experience is required to estimate the *in situ* moisture of the coal. The veracity of the method has been demonstrated at many mine sites.

Much has been made of the difficulties of estimating the *in situ* moisture of coal. It is correct to say that there is no standard test or simple solution to this problem. *In situ* moisture of coal is a function of:

- coal rank
- coal type
- mineral matter content and composition.

Examination of data sets of air dry moisture, Moisture Holding Capacity and where available, Water Holding Capacity, and ROM moisture (if an operating mine), together with consideration of the previously mentioned factors, will lead the astute geologist to an estimate of *in situ* moisture within 0.75–1.5 percentage points of the true value (generally higher error for higher moisture coals).

Method 4, Apparent Relative Density (ARD)

This method uses the unadjusted results of the Australian Standard method for coal density determination of lump samples (AS 1038.21.2). This is a direct laboratory based method that uses lump coal in a water bath. It clearly follows what we recognise as the method by which Archimedes is reputed to have found that the loss in weight of an object weighed in water, is equal to the mass hence the volume of water displaced.

Characteristics

- AS 1038.21.2 uses a wire cage, a tank of water and a balance to determine the relative density of air dry lump coal samples by immersion.
- The coal is not crushed, hence it contains all of its pores, but probably few or no cracks or voids of any magnitude. Hence volume is reasonably but not entirely preserved.
- Partial drying to 'air dry' removes some but not all of the moisture that would exist in the coal in its *in situ* state.
- Air dry moisture determined later on milled coal is probably less than the air dry moisture in the lump sample, which itself is likely to be significantly less than *in situ* moisture.

Strengths and Weaknesses

Strengths	Weaknesses
The test procedure is regulated by Australian Standard	The results of the determination are of relatively poor accuracy and typically quite variable. No precision data are quoted in the Standard
The determination is direct rather than indirect	The moisture of the coal sample does not replicate the moisture of *in situ* coal
The test is relatively cheap	Moisture adjustments according to the Preston & Sanders method cannot be made to the results
Frequently geologists have large data sets of these ARD determinations	Only lump coal can be tested, suggesting a possible bias to the more competent durainous components

Observations

This method of estimating *in situ* relative density of coal does not give precise, repeatable values, nor does it give results that are at a moisture basis that matches the *in situ* state.

Method 5, RD Derived from ARD

Where density has historically been determined by AS 1038.21.2-1992 (ARD), but there is a small complementary data set of determinations by AS 1038.21.1.1-2002 (RD), it is often the case that attempts are made to determine a relationship between them. This exercise is done in recognition of the fact that direct use of ARD is not valid, but that there are insufficient RD values to move to fully using that data to map the *in situ* relative density. At least two approaches are known to be in use, namely:

Approach 1

- where ARD and RD pairs exist, derive a relationship between them, with RD as the unknown.

- Apply this relationship to the full ARD dataset to produce a new set of derived RD values.
- Apply the Preston & Sanders method to the resultant dataset.

Approach 2

- Where RD, moisture and ash values exist, convert RD and ash from air dry to dry basis and derive a relationship between them, with RD_{dry} as the unknown.
- Apply this relationship to the full ash dataset to produce a new set of derived RD_{dry} values.
- Apply the Preston & Sanders method to the resultant dataset.

Application of these adjustments shows that the user is at least aware of the limitation of ARD data. Both methods constitute valid attempts to make corrections. Both will always be limited by the statistical nature of the exercise and results will vary in integrity.

Method 6, The Quinn Method

The details of this method were published in the Queensland Government Mining Journal in Quinn (2000). The method uses float-sink data to estimate the density of coal. The details are set out in the paper and only a summary is presented here.

Characteristics

- Quinn stated that it is not necessary to estimate the *in situ* density of coal, since what really matters is "…the weight of coal after mining, on the surface, either as crushed run of mine (ROM) product or beneficiated product…"
- It follows that this method does not seek to estimate *in situ* density or tonnes, but instead a density value that can be applied to the ROM volume to give the weight of coal after mining.
- The method is based upon using normal float sink data to develop a curve of fractional ash vs. inverse RD.
- The equation that describes the (usually linear) relationship can "…then be used to predict the Apparent RDs from raw ash to calculate the reserves expected to be delivered at the surface from a known volume in the ground".
- There are no moisture adjustments applied to this ARD value, although the weight of coal is adjusted to reflect ROM or product moisture.

Strengths and Weaknesses

Strengths	Weaknesses
If float sink data is available but no other density data, then the method may be used to give some indication of coal density	Does not provide any way of estimating *in situ* coal density, hence *in situ* coal mass. This begs the question as to whether it is possible to estimate Coal Resources as these are always *in situ* (not mined and on the surface)
Useful process for checking float-sink data	Since float sink data is based upon air dried coal it is difficult to see how the moisture basis of "the weight of coal on the surface" can be known with any precision and it is not clear how the weight of coal is adjusted from an unknown starting point to an often unknown (for new projects) end point (ROM or product coal moisture)
	Float sink data may not be available for the resource in question
	Fine coal is normally excluded from float-sink processes (either goes to reject or flotation) hence introducing a small bias to float sink data

Observations

The Quinn method does not purport to be a method of estimating the *in situ* density of coal. Rather it is a method for estimating the density of mined coal. Most mine planning systems and most coal accounting systems known to the author commence from a starting point of *in situ* coal tonnes. The proposition that this information is not required is not widely accepted. The accuracy of the proposed method is not known and the uncertainties over moisture basis and moisture adjustments raise concerns.

Method 7, The Fletcher & Sanders Method

The method referred to as the 'Fletcher & Sanders method' embodies the contents of ACARP Project Report C10041. In reality it comprises at least two methods for *in situ* coal density estimation. The report is extensive and detailed and only a summary is presented here.

Characteristics

- Fletcher & Sanders set out to develop a robust, numerical method for the estimation of *in situ* moisture of coal which can be used to complement the Preston & Sanders method for estimating *in situ* coal density.
- The research that went into the project had many lines of investigation, including:
  - » A survey of industry practitioners and their coals to try to develop an understanding of coal moisture contents at different conditions (air dry, MHC, EM, *in situ,* ROM, product etc) and their relationship to other coal properties

  - » Experimentation on a wide range of lump samples, traditional core samples and samples from ACARP Project C10042 representing a good selection of Australian black coals
  - » Data were subject to detailed statistical analysis
- Through analysis and reasoning, it was determined that, for the samples used in this study only, *in situ* moisture could be considered to be approximately equal to the 'as received' moisture of the samples. This provided a baseline against which other moisture values could be compared against *in situ* moisture. Relationships were developed between *in situ* moisture and equilibrium moisture (ASTM D1412) and with moisture holding capacity (AS 1038.17-2000). These are:

  in situ moisture = 1.117 * equilibrium moisture + 0.317

  in situ moisture = 1.1431 * moisture holding capacity + 0.348
- In addition to testing, comparing and considering various moisture values of a range of coal samples, an exhaustive statistical analysis was carried out to examine relationships between a range of coal properties and *in situ* moisture and *in situ* density of coal. This resulted in eighteen multivariate expressions being developed for estimating *in situ* moisture and ten expressions being put forward for estimating *in situ* coal density. These are not replicated here, but are tabulated in the project report.
- The net outcome of the project is that it provided ways to estimate *in situ* coal density either by single or multivariate regression with other coal properties and it provided ways to estimate *in situ* coal moisture so that these values could be used to estimate density via the Preston & Sanders equation.

Strengths and Weaknesses

Strengths	Weaknesses
The study draws upon a large data set representing Australian black coals with a good spread of rank and type	*in situ* moisture has had to be assumed to be approximately equal to the as received moisture of the sample in order to provide a starting point for comparison and ultimate derivation of the equations
The equations recommended for determining moisture and density are readily amenable to numerical manipulation	The study is highly dependent on statistics and hence it is difficult for the practitioner to readily comprehend or to convince others of its logic or validity
	Many of the inputs to the equations are not readily available for raw coal (petrographic and ultimate analyses etc). Some key variables must be input at the difficult to estimate 'organic, mineral matter free' basis
	The number of equations put forward tends to suggest too many possible solutions, so begs the question of which one is best? which one is correct? They do not all give the same or similar results
	The fact that the equations are not identified by name or number creates a referencing problem for any practitioner (but is not a criticism of the method)

Observations

The methods for estimating *in situ* moisture and density were based upon a substantial amount of sound scientific work. However there are some difficulties in the practical application of the method and some questions remain about the conclusions put forward and the accuracy of the final estimates. There may also be some potential difficulties in convincing others (bankers, auditors etc) of the validity of the results. The study report has only been available for two years and it is thought that the methods outlined have not been widely tested.

Method 8, The Meyers Method

The method referred to as the 'Meyers method' (after the principal researcher) embodies the contents of ACARP Project Report C10042. The report is extensive and detailed and only a summary is presented here.

Characteristics

- Meyers and associates took a completely different approach to the estimation of the *in situ* density of coal.
- The approach was based upon the geotechnical method for determination of soil density, set out in AS 1289.5.3.2 – 1993. This involved:
  - » drilling a nest of short cores in exposed coal seams
  - » collecting the coal contained within the hole
  - » determining the volume of the hole using sand of a known density
  - » determining the mass of coal extracted (including adjustments for core bit) and hence its density (the 'sand replacement density')
- Testing was carried out at seven sites covering Permian and Mesozoic black coals over a range of rank and type.
- All samples collected were subjected to a battery of analytical and physical tests, including apparent relative density at as received moisture according to a method, which is claimed to be an improvement upon AS 1038.21.2-1992.
- Cross plotting of RD_{dry} and ARD from the sand replacement method against dry ash and cross

Table 2: Meyers method for estimation of the *in situ* density of coal

	Parameter	Co-efficient	Power	Intercept
Primary Model	Ash, dry basis	$-3.953*10^{-6}$	2	
	Ash, dry basis	$+6.924*10^{-3}$	1	
	Volatile Matter daf basis	$+9.7*10^{-5}$	2	
in situ Relative Density =	Volatile Matter daf basis	$-1.246*10^{-2}$	1	
	Ultimate Carbon daf basis	$-6.518*10^{-4}$	2	
	Ultimate Carbon daf basis	$+9.801*10^{-2}$	-2	
	Relative Density, AS 1038.21.1.1, dry basis	$+5.144*10^{-1}$	2	
	Relative Density, AS 1038.21.1.1, dry basis	-1.404	1	
				-1.104
Secondary Model	Ash, dry basis	$+2.582*10^{-5}$	2	
	Ash, dry basis	$+6.251*10^{-3}$	1	
in situ Relative Density =	Volatile Matter daf basis	$+8.608*10^{-5}$	2	
	Volatile Matter daf basis	$-1.32*10^{-2}$	1	
	Ultimate Carbon daf basis	$-6.447*10^{-4}$	2	
	Ultimate Carbon daf basis	$+9.253*10^{-2}$	1	
				-1.602

plotting ARD_{ad} against RD_{ad} showed that there was a large amount of scatter in the data, indicating (as would be expected) that the methods of determination were affected by substantial experimental error.

- This scatter was ultimately adjusted out using a five step process ending with *in situ* relative density being highly correlated with ARD at as received moisture.
- The newly determined *in situ* relative density values were then evaluated against a raft of other coal properties and two multiple factor polynomial expressions developed. These expressions form the Meyers method for estimation of the *in situ* density of coal (Table 2).

Meyers and associates also put forward a similar style model for estimating *in situ* moisture of coal. Presumably this could be used as an input to the Preston & Sanders method, but the authors did not suggest that procedure.

Strengths and Weaknesses

Strengths	Weaknesses
The study draws upon a sound data set representing Australian black coals with a range of rank and type	The study is highly dependent on statistics and hence it is difficult for the average practitioner to readily comprehend or to convince others of its validity
The equations recommended for determining density are readily amenable to numerical manipulation	Ultimate carbon values are rarely determined on raw coal, suggesting the likely use of a less accurate average product coal value
In certain circumstances the equations provide reliable results	The equations do not provide reliable results across a range of coals

Observations

The methods for estimating *in situ* coal density were based upon a substantial amount of innovative scientific work. However there are some difficulties in the practical application of the method and some questions remain about the conclusions put forward and the accuracy of the final estimates. There may also be some potential difficulties in convincing others (bankers, auditors etc) of the validity of the results. The study report has only been available for two years and it is thought that the methods outlined have not been widely tested.

Method 9, The Wireline Log Method

This method involves the quantitative assessment of wireline log data to estimate *in situ* coal density. It is the only method that measures the *in situ* density of coal directly in the *in situ* state. The probe 'sees' the organic matter, the mineral matter and the water within the coal all together and has the best chance of making an accurate measurement.

Characteristics

- A calibrated and properly zeroed gamma-gamma density/caliper probe is run across a coal seam in a fluid filled hole
- Raw data is collected continuously and aggregated at say 1cm intervals
- Data is suitably processed to determine density from raw counts
- Averaging of all full and partial intervals over the entire coal seam interval is carried out to produce an average *in situ* density for the seam interval.

- A variation on the process might see a relationship being derived between wireline log determined density of coal and that determined by AS 1038.21.1.1-2002. This relationship might then be used to extend the value of the process without the need to carry out wireline log data assessment at every point of observation.

Strengths and Weaknesses

Strengths	Weaknesses
The log should represent a direct determination of *in situ* coal density at *in situ* moisture. Conditions will never get closer to ideal than those applicable to this method	The data is sensitive to hole condition variations, especially caving. It is also sensitive to changes in tool types and tool calibration.
The log data is generally collected for other purposes and little extra cost is incurred	Imprecise zeroing of wireline logs is not uncommon. This can make the use of historical data sets somewhat problematical
	For thin coal seams, boundary effects are likely to have a negative impact on accuracy
	Limited skilled people available to carry out the processing

Observations

At first examination this method appears to be direct and simple and the one that practitioners would choose to use over less direct methods. Despite this, it is not in common use. Perhaps this is because of the difficulties of collecting good consistent log data; perhaps it is because practitioners are uncomfortable with dealing with geophysical signals that they do not fully understand. Perhaps it just requires too much processing and there are easier ways around the problem.

It is considered that this method has potential that has not been realised and that there is scope for its further development into a robust, easy to use tool.

HOW ACCURATE DO ESTIMATES OF *IN SITU* RELATIVE DENSITY HAVE TO BE?

Before moving to discuss the issue of which method is 'best' it is worth discussing what level of accuracy we are trying to achieve.

There is no industry standard that sets out any sort of quantitative accuracy benchmarks that must be met for either coal tonnage estimates or the individual components of coal tonnage estimates. The JORC Code, 2004 refers only to estimates of tonnage as having '…a low level of confidence…', '…a reasonable level of confidence…' and '…a high level of confidence…' to describe Inferred, Indicated and Measured resources respectively. The Coal Guidelines, 2003 restate these comments and add: 'The estimator should ensure that the *in situ* density applied is clearly stated and can be justified on technical grounds'.

All practitioners attempt to estimate seam area and seam thickness as accurately as possible within the constraints of the resources available to them. However each are estimates and are subject to errors related to insufficient data points, inability of modelling routines to accurately represent the data, lack of knowledge of the location and extent of irregularities and discontinuities (faults, washouts, subcrop, pinchouts, splitting, intrusion etc) and the like. Estimating *in situ* coal density is no different. It is an estimate and will be subject to lack of precision due to a number of factors. What is important then is that the method used is technically valid and that it recognises the issues that arise in addressing the problem and successfully accounts for them. It is unlikely that error can ever be eliminated from any single point determination and certainly it will never be eliminated from spatial modelling of a set of data points that is only a small sample of the population (the normal circumstance).

In summary there is no point attempting to achieve pin point accuracy on coal density estimates when the overall tonnage estimate will be affected by estimation error across the full range of variables that make up that estimate. What is important is to achieve a level of accuracy that is in keeping with that of the other key parameters.

ESTIMATING *IN SITU* RD — WHICH METHOD SHOULD I USE: WHICH SHOULD I AVOID?

The nine methods outlined may be considered as being of four distinct types and recommendations for or against their use are discussed as follows, according to these types.

- The first group includes those that use laboratory based, Australian Standard style density determinations, either adjusted or unadjusted (Methods 1–5). Of these, Method 2 produces the most inaccurate and biased estimates of *in situ* density and should not be used under any circumstances. Method 1 is similar in nature except that the error is not so great. Again its use should be avoided. Method 4 is generally considered to be imprecise and biased, but probably does not exhibit the same level of bias exhibited by Method 2. When large ARD datasets exist an effort to carry out some sort of adjustment according to Method 5 is a recommended approach.

  Method 3, the Preston & Sanders method, has established itself as the industry benchmark. It is based upon the most accurate laboratory method available to us for relative density determination, it recognises the influence of *in situ* moisture, executes the adjustment to *in situ* moisture correctly, and it is logically intuitive and easy to understand. Its continued use is recommended.

- The Quinn method sits on its own as being the only one based upon float sink data. It also does not attempt to estimate *in situ* coal density. This method is an innovative and alternative use of a concept

commonly in use for checking float sink data. The logic of the inverse density concept is not questioned. However the extent to which it can be used for estimating *in situ* coal density and hence tonnes is questioned. Deployment of the method hinges upon the availability of washability data, which for some coals, may be entirely lacking. In the view of the author, the claim that it is not necessary to estimate tonnes *in situ* is not supported by normal industry practice. The suggested approach to moisture and moisture adjustment is also considered to be somewhat unconvincing.

No recommendation is made regarding the use or otherwise of this method. However practitioners intending to use this method would need to satisfy themselves that there are happy with the logic and process and can justify it to others.

- The Fletcher & Sanders method and the Meyers method have been established by different experimental methods, but are grouped together as they rely entirely on statistical relationships to establish an estimate of *in situ* coal density and moisture from a range of other coal properties. Both of these methods have practical limitations in terms of availability of the quality parameters required as inputs. Each has complex derivations that are likely to be difficult for the practitioner to understand and accept and to explain and justify to others.

  Again, no recommendation is made regarding the use or otherwise of these methods. However practitioners intending to use these methods will need to satisfy themselves that there are happy with the logic and process that has been used to develop them, they are happy with the highly statistical nature of the relationships and the range of results that they produce and that they can argue and support the case for using them to others.

- The wireline log method also sits on its own as being the only direct method for *in situ* density determination. In theory it appears to hold the most potential but practical (and perhaps imagined) difficulties appear to have held it back from being in widespread use. It is considered that providing the data is well collected, checked and processed, this method is likely to produce reliable estimates of *in situ* coal density. The science behind it is well known and it can readily be understood and accepted by most practitioners. Its further development is recommended.

CONCLUSIONS

In the past 15 years the importance of correctly estimating the *in situ* density of coal for the purpose of accurate tonnage calculations, and the problems inherent in doing this, have achieved due recognition in the Australian black coal industry. Whilst a number of researchers have put forward solutions to the problem, there is still no single, simple, universally accepted and bullet proof method. Nevertheless the debate has been healthy and welcome.

For the industry practitioner the keys to achieving a satisfactory estimate are three fold. Firstly understand the nature of the problem and recognise that there is no simple quick fix solution that can unthinkingly be applied to achieve a sound result. To quote loosely from a popular novel, "…only the worthy will succeed". Sound data and correct thought processes are essential to success. Secondly, in considering the methods available to you, decide which will give you a result of acceptable accuracy, using logic that you yourself can understand and accept and which you can explain and argue a case for when challenged by others. The researchers may well fight for the intellectual high ground, but for the practitioner, the best solution is not necessarily the most complex or the most elegant, but the one that can be accepted as giving sound results and the one that he or she can explain and justify. Finally it is critical that the moisture content of the coal is understood at all stages of any estimation process. Uncertainties in coal moisture content are the bane of accurate coal accounting and unless this fact is properly recognised and considered at all stages, successful coal tonnage estimates and tonnage reconciliations will not occur.

REFERENCES

AS 1038.3-2000. Coal and coke – Analysis and testing. Part 3: Proximate analysis of higher rank coal.

AS 1038.17-2000. Coal and coke – Analysis and testing. Part 17: Higher rank coal - Moisture-holding capacity (equilibrium moisture).

AS 1038.21.1.1-2002. Coal and coke – Analysis and testing. Part 21.1.1: Higher rank coal and coke – Relative density – Analysis sample/density bottle method.

AS 1038.21.2-1992. Coal and coke – Analysis and testing. Part 21.2: Higher rank coal and coke – Relative density - Lump sample.

AS 1289.5.3.2-1993. (now updated as AS 1289.5.3.2-2004) Methods of testing soils for engineering purposes. Method 5.3.2: Soil compaction and density tests.

ASTM D 1412-1999. Standard test method for Equilibrium moisture of coal at 96 to 97 Percent relative humidity and 30°C.

Australasian Code for Reporting of Exploration Results, Mineral Resources and Ore Reserves, (The JORC Code), 2004

Australian Guidelines for the Estimating and Reporting of Inventory Coal, Coal Resources and Coal Reserves, 2003.

CLARKSON, C., LEACH, K.R., MEYERS, A.D. & WEX, T., 2003: Estimation of *in situ* Density of Coal from Apparent Relative Density and Relative Density Analyses, ACARP Project Report C10042.

FLETCHER, I.S. & SANDERS, R.H., 2003: Estimation Of *in situ* moisture of coal seams and product total moisture, ACARP Project Report C10041.

PRESTON, K.B. & SANDERS, R.H., 1993: Estimating the *in situ* Relative Density of Coal, *Australian Coal Geology*, **9**, May 1993.

QUINN, G.W., 2000: A New Method For Estimating the Density of Coal for Resource and Reserve Calculations, *Queensland Government Mining Journal,* January 2000.

Ken Preston, Rio Tinto Coal Australia Pty Limited

Stephen Fraser, Ruth Henwood, Joan Esterle, Colin Ward, Peter Mason and Jon Huntington

Non-destructive mineralogical determinations via spectral reflectance logging of coal and coal measure sediments using HyLogger™

The HyLogger™ system uses spectral reflectance measurements to identify mineralogies from drill-core or drill-chip samples. We have used the HyLogger™ to measure the spectral responses from drill-core of coal and coal measure sediments to see if we can detect and identify mineral matter. Results from a medium rank bituminous coal from Queensland (Goonyella Middle seam) are presented. Hylogger™ was able to identify siderite, ankerite, calcite, illite, Mg-chlorite, jarosite and halloysite within this coal.

The spectral reflectance results were used to control sampling for a parallel program of mineralogical analysis by X-ray diffraction (XRD). However, the results from the two analytical methods tended to be complementary rather than confirmatory, with differences related to the physics of the measured parameters and the chemistry of the materials being measured. If minerals are poorly crystalline and in volumetrically small proportions, they tend not to be detected from the XRD results (at least in our sample set).

The study shows that, despite the low reflectivity of coal and carbonaceous rocks, the HyLogger™/TSG system is capable of making meaningful and spatially consistent mineralogical determinations. In a number of instances the HyLogger™ system could not obtain a meaningful mineralogical response; these poorly responsive areas tended to occur in spatially coherent blocks that corresponded to the darker/shinier coal layers on the linescan image. These areas were commonly associated with lower-ash, bright banded coal types. Hence the HyLogger™ data have the potential to produce coal brightness-profile information in addition to mineralogical assessment.

INTRODUCTION

Over the past decade, spectral reflectance measurements of rocks, soils, minerals, drill core, chips and powders have been shown to provide mineral information that can be used to interpret geology and geotechnical parameters. The majority of this work has been conducted in 'hardrock' deposits in Australia and elsewhere (Huntington & others, 1997; Cudahy, 1997; Cudahy & others, 1997; Scott & others, 1998).

Figure 1: Coal core tray under the HyLogger™. The tray sits on a robotic X-Y table and the tray sections are moved under the spectrometer that sits in the overlying enclosed cabinet.

In the CSIRO HyLogger™ spectral logging system (Huntington & Whitbourn, 2002), core trays are automatically moved, beneath a stationary spectrometer using a robotic X-Y table (Figure 1). The spectrometer operates at visible-to-shortwave infrared wavelengths (400–2500nm), which are ideal for sensing iron oxides, sulphates, hydroxyl-bearing and carbonate minerals.

Calibrated spectra are collected continuously from a window (adjustable between 10mm and 30mm wide) scanning the full length of the core or chip tray. The core is also imaged with a high-resolution (0.1mm), three-colour digital linescan camera.

The measurement rate is adjustable up to 60mm/second, depending on the required spatial resolution and spectral sensitivity. From the spectra, automated and specialized

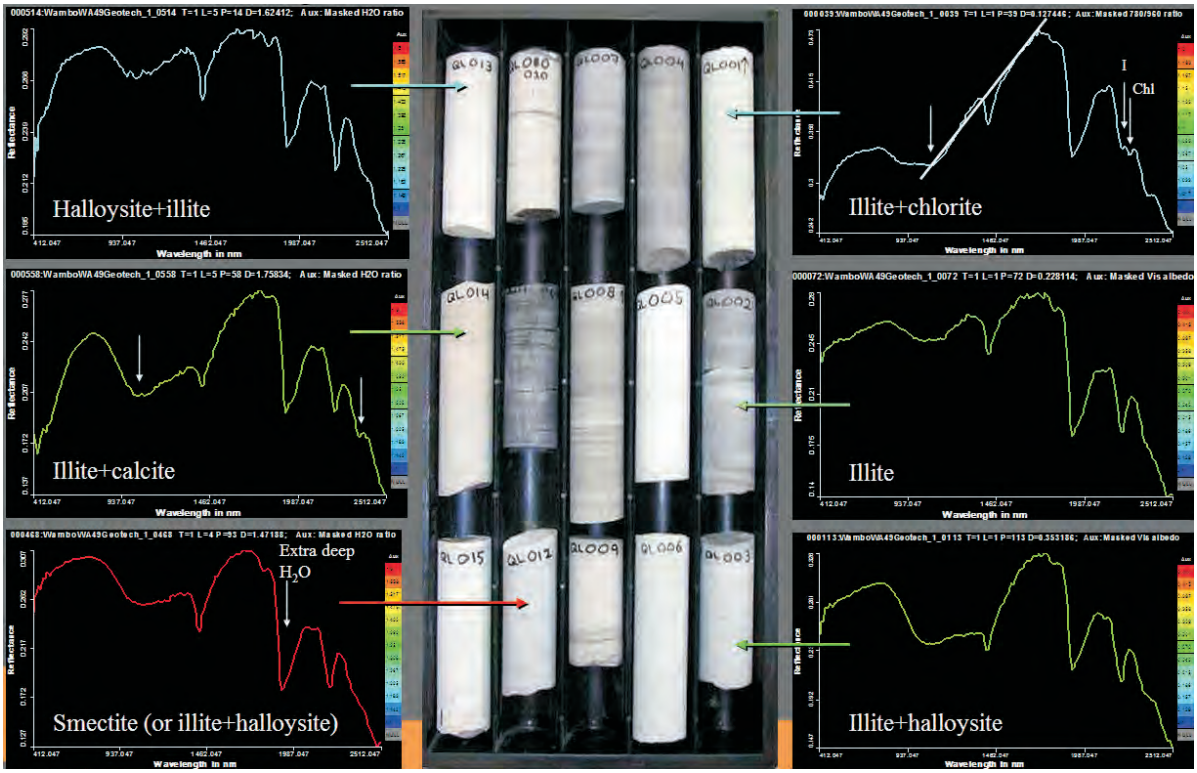

Figure 2: Selected mineral spectra from floor and roof sediments (after Hatherly & others, 2004)

software systems (The Spectral Assistant (TSA) module within The Spectral Geologist (TSG) software package) interpret the contained mineralogy and produce scalars or indices of the relative amount of various mineral phases or their chemical variations as a function of core depth. The advantage of such a semi-automatic system is its ability to rapidly and continuously sample at much greater spatial resolution than previously possible. The interpreted mineralogical logs can then be loaded into existing bore-hole interpretation software packages.

The objective of this study was to determine whether such a system could be applied to coal and coal measures. Preliminary findings from a previous ACARP Project (C11037- Quantitative Geophysical Log Interpretation; Hatherly & others, 2003), demonstrated HyLogger™'s capacity to discriminate iron oxides, chlorites, carbonate and clay minerals, and different micas in roof and floor lithologies for geotechnical assessment (Figure 2). HyLogger™ technology can potentially identify clay, carbonate and sulphate mineral species in coal interburden, and so provide advanced knowledge of potential geotechnical or environmental issues in spoil materials.

Our focus in this paper is the detection of mineral matter species in coal, which represents a substantially increased challenge because of coal's low reflectivity (black in the visible!). The detection level of a particular mineral, using reflectance spectrometry, depends on its host rock type. For example, pure samples of siderite, clay minerals or apatite are easy to measure and identify. Detection limits of these minerals in 'rock-mixtures' are more difficult to quantify because the reflectance properties of the host rocks are essentially dependent on the other mineralogies present. For coal, which hosts very low proportions of mineral matter, the challenge is for detection at any level.

Approach

The approach was first to test coals with known abundances of different minerals, in particular clays, sulphides, and carbonates such as calcite and siderite. Coal core from the Goonyella Middle (GM) seam are presented here. Because of coal's low reflectivity in the visible spectral region, we have concentrated this analysis within the shortwave infrared region (SWIR – 1300–2500nm), where clays, carbonates and sulphates have characteristic absorption features. Samples were taken from critical intervals for quantitative XRD analysis using the Rietveld-based Siroquant™ technique (Ward & others, 1999; Ruan & Ward, 2001) for comparison with the spectral reflectance results.

Results

A 'virtual core tray' produced from the linescan camera via the TSG software from the GM core is shown in Figure 3. The linescan 'core image' is referenced against depth and to the spectral measurements, which provides a ready mechanism to check mineralogical spectral interpretations against the core photo and other logs. The mineral shown on the right-hand end of each tray section is the predominant mineral interpreted by the TSG software for each section.

Example results from the TSG software mineralogical assignments are shown in Figures 4, 5 & 6. Illite and

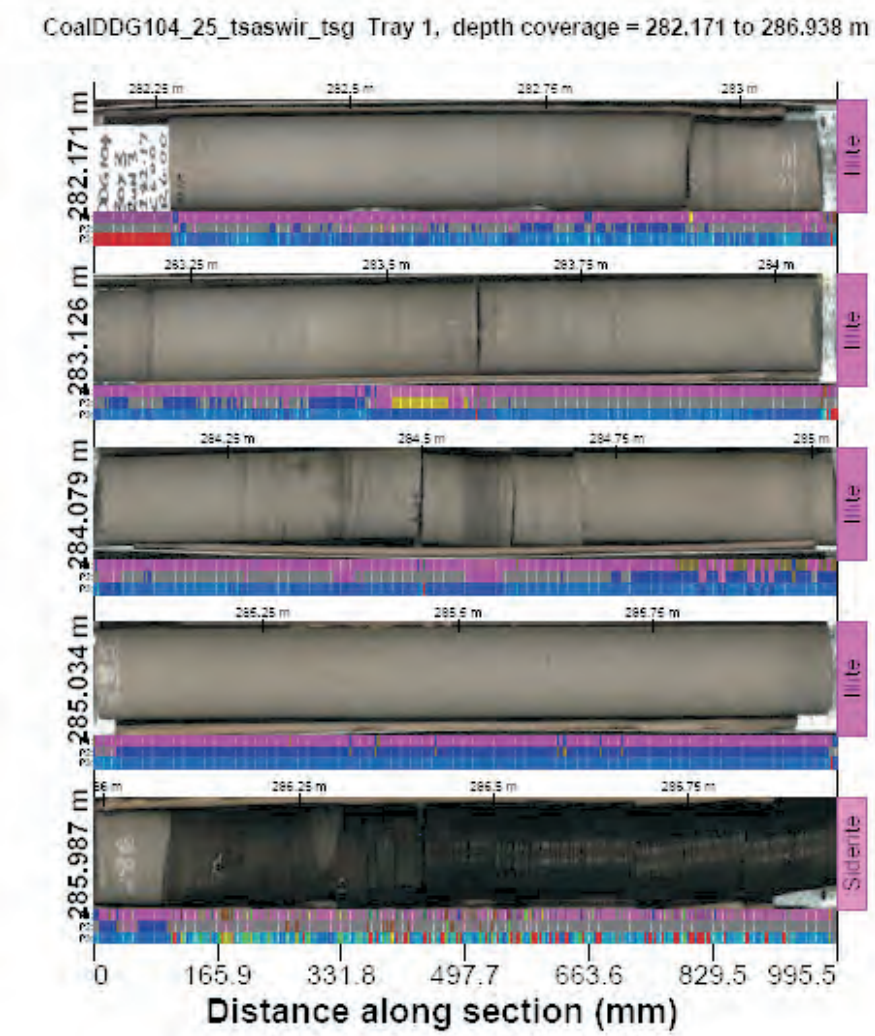

Figure 3: 'Virtual' Core Tray" #1 of the GM drill hole, showing roof sandstones and carbonaceous mudstone.

halloysite[1] are detected in roof sediments (Figure 4); siderite in carbonaceous mudstone (Figure 5); and siderite, Mg-chlorite and 'aspectra' identifications from coal in Figure 6. From left-to-right, the columns of significance in these figures are, 'Depth', 'TSA_AMineral1', and 'TSA_AMineral2'.

In TSG, various parameters or derived scalars can be displayed in columns referenced to depth, and these can be readily changed/reordered by the analyst. The TSG 'Floater' window overlain on Figures 4 and 5 shows the actual spectral measurement at a given depth, along with the TSG interpreted mineralogy considered the 'best fit'.

The 'coal-brightness' column in Figure 6 is an attempt at creating a coal brightness profile using both the spectral and linescan data from the HyLogger™.

Various minerals were detected in the coal sections of the core. These included, siderite, halloysite, ankerite, dolomite, gypsum (the latter, sometimes, but not always, associated with chalk markings on the core), Mg-chlorite, montmorillonite, and illite, in approximate decreasing level of abundance.

In contrast, illite, halloysite and siderite were the main minerals detected in the roof sandstones and siltstones. Figure 7 shows the combined 'Assemblage Histogram' for the data set. In decreasing order of detection the minerals in this core are, illite, halloysite, siderite, gypsum, ankerite, epidote, dolomite, Mg-chlorite and montmorillonite.

The XRD results on the coal showed high percentages of kaolinite and quartz with varying amounts of siderite, ankerite and chlorite. However, quartz is not detectable within HyLogger™'s current spectral range. The XRD results on the sandstones and siltstones show quartz, I/S (interlayered illite/smectite) and kaolinite, with a high proportion of feldspar (albite — also spectrally undetectable with HyLogger™) and minor chlorite.

As a general statement, the spectral reflectance measurements and XRD determinations support each other in approximately 30% of cases, while there were significant differences in the remainder. Table 1 displays the results of

1 Halloysite is a hydrated, low-temperature member of the kaolinite group.

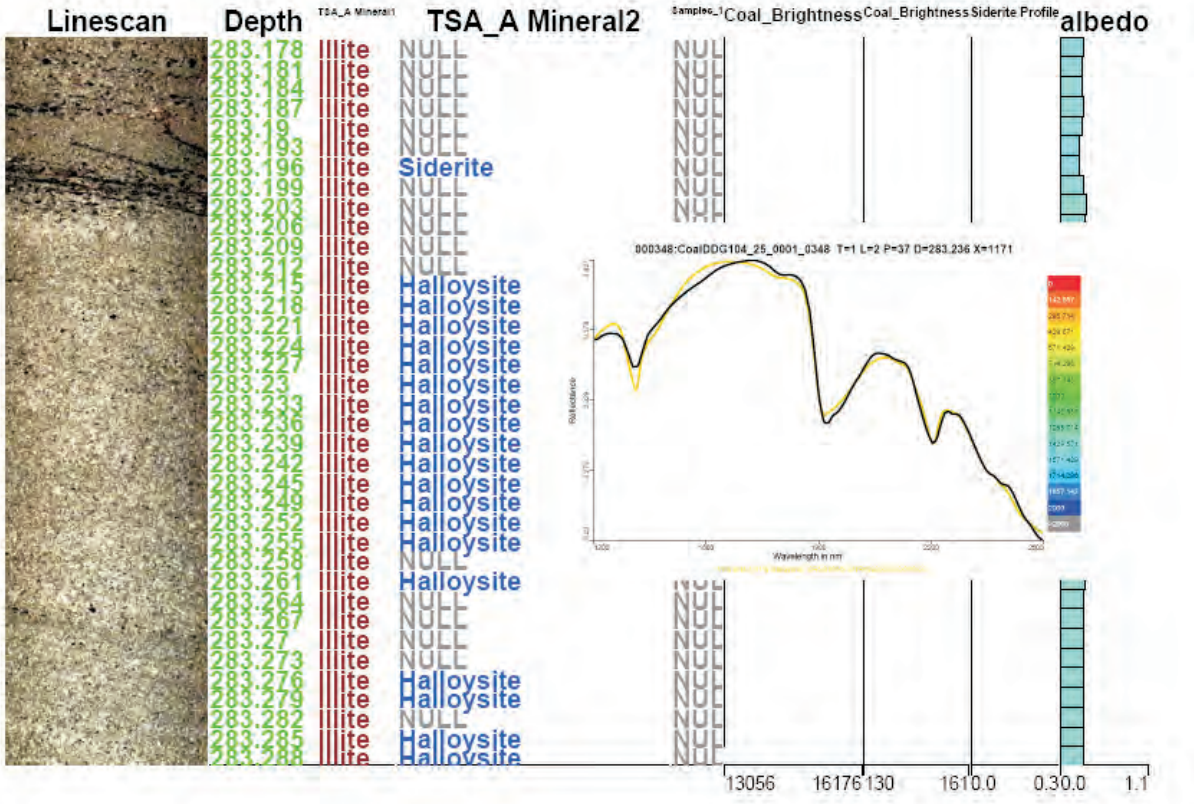

Figure 4: Illite and halloysite spectra from the 'roof' sandstones in drill hole DGG104. The columns are from left-to-right, the linescan image, depth, TSA_AMineral1, and TSA_AMineral2; (the remaining columns can be ignored at this stage.) The 'Floater' window shows the actual spectral measurement at 283.236m, along with the TSA interpreted illite-halloysite 'mixture' considered the 'best fit'.

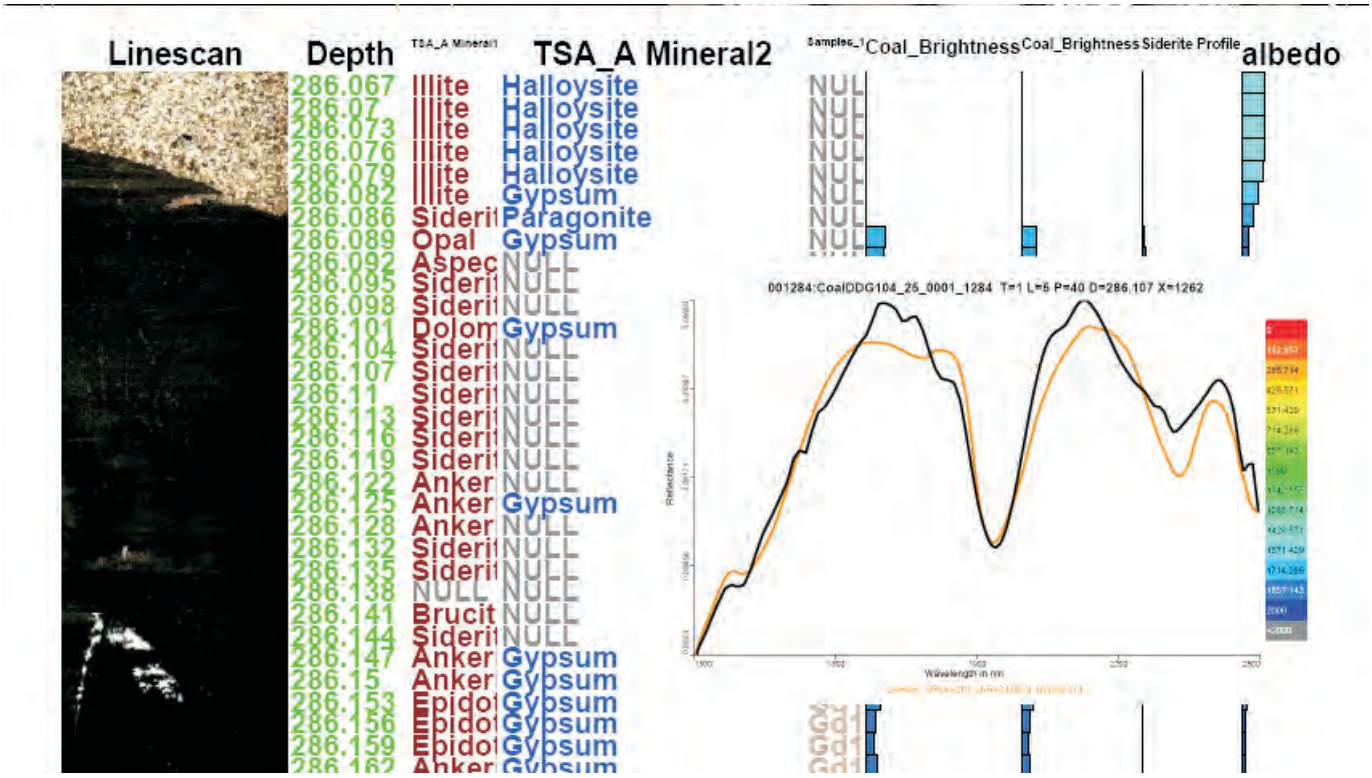

Figure 5: Siderite from the top of the carbonaceous mudstone in the GM core. The 'Floater Window' shows the spectrum measured at 286.107m in white and the library siderite. spectrum in brown.

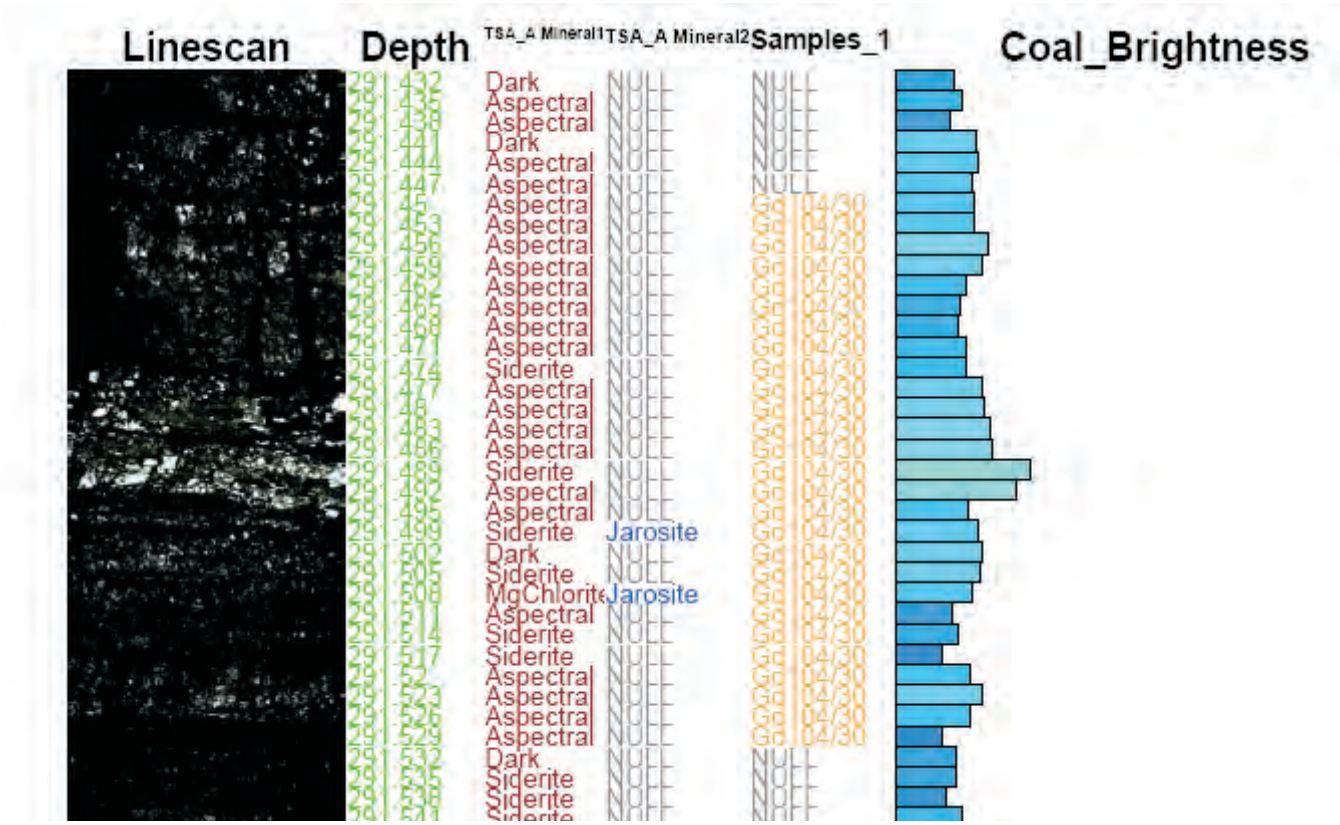

Figure 6: Siderite, Mg-chlorite and jarosite responses from GM data between 291.432 and 291.538m. The 'aspectral' responses tend to correspond to areas of 'bright' coal. The right-side column is an attempt to create a coal 'brightness profile' log for these data.

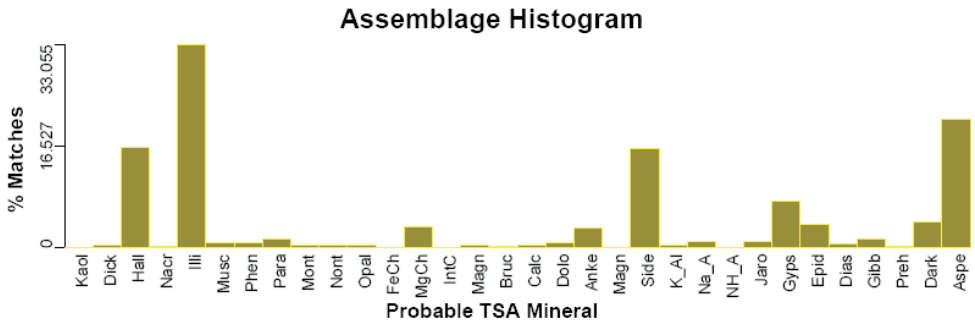

Figure 7: Assemblage Histogram of the TSG/TSA mineralogies detected on the GM core. The mineralogies in decreasing order of detection are, illite, halloysite, siderite, gypsum, ankerite, epidote, dolomite, Mg-chlorite and montmorillonite.

the HyLogger /TSG and XRD Siroquant™ mineralogical determinations (after Henwood, 2004). It is important to note that the 'weightings' for the HyLogger™ /TSG interpretations are qualitative and derived on the basis of the relative amounts of spectrally detectable materials present.

Table 1 shows the varied correspondence between the HyLogger™/TSG and XRD Siroquant™ results. For sample GD104/13a, the HyLogger™/TSG analysis reported siderite, epidote and dolomite, and these compare favourably to the XRD results of siderite and dolomite. However, the mineralogical HyLogger™/TSG (siderite, Mg-chlorite and halloysite) and XRD determinations (interlayered illite-smectite and kaolinite) for sample GD104/27 vary significantly (see Discussion).

Discussion

Detection of mineral matter

At the beginning of this project, our main concern was that we would not be able to sensibly measure or interpret mineralogical spectra from coal and carbonaceous rock because of their inherent low reflectivity. Our findings show that we can see spectral responses belonging to mineral matter in coal; and, that these responses have a meaningful spatial coherence. However, the Hylogger™/TSG system is not able to detect mineralogical responses in all coal pixels measured. There are at least two controls influencing this: (1) whether or not significant levels of mineral matter are actually present in the coal; and (2) how well the sensitivity

Table 1: Comparison of mineralogical determinations using HyLogger™ / TSG and XRD SIROQUANT for samples from drill hole GM. (XRD fields for pyrrhotite, anorthite, albite and microcline were omitted from the table

Sample	Lithology	HyLogger/TSG Spectral Interpretation				XRD SIROQUANT : Mineral percentages of whole rocks and LTA residues											
		TSA_Min_1	Wt Min1	TSA_Min_2	Wt Min2	LTA %	Quartz	I/S	Kaolinite	Illite	Chlorite	Anatase	Dolomite	Ankerite	Siderite	Calcite	Apatite
GD104/3	Sandstone	Illite	1				20.6	17.5	9	2.8	3.9			6	4.5	2.4	
GD104/4	Sandstone	Illite	0.523	Siderite	0.477		35.9	10.7	4.2	6.2			1.1		22.8		
GD104/7A	Sandstone	Illite	0.608	Halloysite	0.392		26.1	32.6	7.8	4.4				6.7	3.2		
GD104/8	Carb S	Siderite	0.767	Ankerite	0.233	90.85	75.5	11.4	13.1								
GD104/9	Sandstone	Siderite	0.839	Gypsum	0.161		15.7	8.7	3.3	4.5					65.8		
GD104/13A	Sandstone	Siderite	0.9	Epidote	0.05		11	4.3	0.8	3.8			12.5		66.3		
GD104/16B	Tuff	Illite	1				1.6	82.4	4.1	10.8		1.1					
GD104/16C	Carb S	Illite	0.02	Gypsum	0.01	83.30	24.2	40.8	9.1	20.6		0.6		3.3	1.5		
GD104/16D	Tuff	Illite	0.95	Montm.	0.05		7.7	59.1	7.4	15.1				1.6			
GD104/18	Mudstone	Halloysite	0.702	Gypsum	0.298	77.44	21.8	24	44.4			1		1.6	1		
GD104/20	Carb S	Ankerite	0.88	Dolomite	0.1	71.82	39	53	2.5				3.1		2.4		
GD104/22	Tuff	Illite	0.8	Siderite	0.2		20.7	47	8.1	13.4		0.9	1.1	2.2	1.3	0.8	4.5
GD104/22A	Carb S	Gibbsite	0.53	Na_Alunite	0.03	61.68	64.3	19.2	15.1				1.5				
GD104/22C	Tuff	Illite	0.95	Halloysite	0.05		5.9	53.9	9.6	27.2	1			0.5	1.9		
GD104/23	Carb S	Siderite	1			54.94	9.9		3.7				45.9			40.5	
GD104/24	Sandstone	Siderite	0.95	Dickite	0.05		16.3	12.9	6.7	5.8				7.4	37.5	5.3	
GD104/25A	Sandstone	Ankerite	0.676	Siderite	0.324		18.8	19.6	23.8		2.3			30	1.9		
GD104/25B	Coal	Siderite	0.75	Ankerite	0.21	17.25	58.7	13	16.7	10.5				1.1			
GD104/27	Coal	Siderite	0.9	MgChlor	0.05	13.37	23.8	34.2	32.3								
GD104/28	Coal	Ankerite	0.87	Calcite	0.05	13.89	31.6	18.5	38		5.7						
GD104/30	Coal	Siderite	0.43	Jarosite	0.04	12.24	16.9	31.2	34.8		7.3		1.3		6.1		
GD104/31A	Coal, dull, silty	Halloysite	0.834	Siderite	0.125	71.74	9.7	19.3	61		8.4	1.6					
GD104/32	Coal	Siderite	0.835	MgChlor	0.124	20.34	18.1	21.2	40.5	3.5	7			0.6	5.4		
GD104/33	Coal	MgChlorite	0.745	Siderite	0.147	23.24	17.1	22.9	56.9		3.1						
GD104/35	Coal	Siderite	0.437	Jarosite	0.146	23.44	36.8	36.1	24.9						2.2		
GD104/36	Coal	Siderite	0.735	MgChlor	0.111	23.12	35.1	17.1	37.9			0.5		3.1	6.3		
GD104/37	Tuff	Illite	0.727	Halloysite	0.134		1.9	51.8	23.3	15.3	0.9				0.8	0.9	
GD104/39	Coal	Siderite	0.432	MgChlor	0.265	22.74	64.5	23.3	12.2								
GD104/40A	Mudstone	Siderite	0.345	Dolomite	0.228		5.5	67.8	4.9	4.6	0.9			2.3	5.8		
GD104/40B	Mudstone	Illite	1				3.6	49.6	7.5	17.4			9.4		7.8		
GD104/41	Coal	Montmorillonit	0.718	Gypsum	0.282	21.07	43.4	26	27.3					0.6	2.8		
GD104/42	Coal	Siderite	0.236	MgChlor	0.159	11.66	81.4		14.8					1.1	2.7		
GD104/43	Tuff	Illite	0.642	Halloysite	0.342		3.8	43	44.2						1.7		
GD104/44	Coal	Siderite	0.749	Hornblende	0.106	14.30	16.4	28	49.8		2.3				3.5		
GD104/46	Coal	Siderite	0.679	MgChlor	0.1162	6.96	52.2	16.3	18.6						12.9		
GD104/47	Sandstone	Illite	0.867	Halloysite	0.149		32.9	25.3	22.5	6.7			0.4		0.6		
GD104/51	Sandstone	Halloysite	0.905	Illite	0.05		30.4	20.8	17	4.1	2.4			4.3	4.1		

and accuracy of the HyLogger™ hardware and the TSG/TSA software permit low reflectance signal levels to be detected and identified.

It is not our intention to enter into an extended discussion on the signal-to-noise capabilities of the HyLogger or the sensitivity of the TSG software; however, these parameters are critical to the performance of the system on materials with low reflectivity. Our observation that 'null', 'aspectral' or 'dark' assignments (henceforth both referred to as 'aspectral') tend to be made in spatially coherent blocks that are typically related to dark and shiny ('bright') coal layers is encouraging (Figure 6). Consequently, we have begun to investigate whether it is feasible to extract brightness-profile logs from the HyLogger data. A first attempt at such a log is shown on the right hand column of Figure 6.

Comparison between Spectral Reflectance and XRD

The XRD and spectral reflectance methods are fundamentally different in terms of the way in which minerals are identified. The XRD method uses incident X-rays to penetrate rock material; these X-rays are diffracted by a material's crystalline structure to yield characteristic diffraction peaks related to that mineral's molecular cell-spacings. The XRD method essentially relies on the crystallinity or long-range ordering within a substance, so that poorly-crystalline or amorphous materials can only be detected and quantified by indirect methods (Ward & French, 2004).

Reflectance spectra are primarily sensitive to the chemistry of the minerals present, and require less crystalline structure for a determination. However, some of the major rock-forming minerals, for example quartz and feldspars, do not have unique or characteristic reflectance spectra in the VNIR-SWIR spectral region. Because of the reliance on low-energy reflected radiation, the spectral reflectance method's depth of penetration is limited to approximately the wavelength of the energy being observed. Consequently, reflectance spectra are strongly influenced by surficial oxidation or weathering effects, and are biased by the tendency of rocks to break or disaggregate along joint planes (foliations, cleats) where some minerals occur preferentially, or as coatings.

Because of the inherent differences between the XRD and spectral reflectance methods, attempts at reconciling the minerals detected and their geological significance are not necessarily intuitive (Camuti & others, 1987; Fraser & Camuti, 1992; Henwood, 2004). The differences between the two techniques are perhaps best illustrated by the discussion on gypsum that follows.

Gypsum occurs regularly in the HyLogger™/TSG interpretations in isolated or small spatial clusters on the HyLogger™ spectral logs, but was not identified in the XRD results. On the linescan core image, those locations where gypsum was noted typically coincide with chalk marks used to annotate the core and assist with logging. This relationship between the chalk markings and the identification of gypsum on the HyLogger™/TSG results tends to confirm that the spectral reflectance measurements are sensitive to gypsum in the surficial chalk markings.

X-ray diffraction analysis failed to identify gypsum in these samples because the source of the gypsum, the chalk mark, was volumetrically too small as a proportion of the whole sample to register. Consequently, because of its limited depth penetration, the HyLogger™ is sensitive to those minerals that occur on the surfaces of samples being scanned. In particular, minerals that occur as coatings on surfaces, or along joint surfaces that have been disaggregated, tend to be seen by the spectral reflectance approach and not identified by XRD. This effect is exacerbated if the surficial minerals are related to oxidation, hydration and/or are poorly crystalline.

In an apparent anomaly, the HyLogger™/TSG system commonly identifies halloysite (a regularly hydrated kaolinite-group mineral; Moore & Reynolds, 1997) in samples where XRD identifies moderately well ordered kaolinite. While dehydrated halloysite has an XRD pattern similar to that of very poorly ordered kaolinite, fully hydrated halloysite should be clearly distinguishable from kaolinite in X-ray diffraction patterns.

Fully hydrated halloysite has not been detected in the XRD data for the present study, and the kaolinite in the samples has the XRD characteristics of well ordered rather than poorly ordered material. The kaolinite in the coals and associated strata, although relatively well ordered by XRD, thus appears to have the infra-red spectral characteristics of halloysite.

Two possible explanations for this anomaly are, (1) that the halloysite is primarily surficial and perhaps related to weathering?/hydration of the kaolinite since it was pulled from the drill-hole; or, (2) that there is a mixture of kaolinitic and halloysitic polymorphs present, and the more abundant and better ordered kaolinite dominates the XRD response. The water-bearing halloysite dominates the spectral-reflectance measurements, however, because the method is more sensitive or responsive to halloysite than kaolinite. Spectral reflectance measurements in the SWIR region are particularly sensitive to bound or free water and hydroxyl vibrations, so the HyLogger™/TSG approach is sensitive to halloysite. There is also the possibility that free water plus kaolinite intimately associated in the materials could spectrally begin to resemble halloysite. Further work is required to resolve some of these issues[2].

Currently we would not be confident in identifying or separating interlayer illite-smectite (I/S) materials using

2 Subsequent investigations indicate that the kaolinite spectra in the TSA training libraries are relatively well-ordered. Hence the TSA does not know about poorly crystalline or disordered kaolinites. Thus if it is given a disordered kaolinite it may tend to report it as halloysite, when commonly it is not. (Inserted June 28, 2005).

reflectance spectroscopy. Our past experience suggests that the spectral reflectance method tends to see the phases present as separate minerals. The HyLogger™/TSG results show significant illite with traces of smectite (montmorillonite) whereas the XRD results tend to identify interlayered illite-smectite (I/S) with minor illite. Samples GD104/16b and /16d illustrate this relationship (Table 1). The HyLogger™/TSG interpretations for both these samples show illite as the dominant mineral; however, I/S is the dominant mineral detected by XRD, with illite itself being detected in significantly lesser proportions. As noted by Henwood (2004) on her work on the GM core, "*the illite component of the I/S in these samples….. appears to have been interpreted by TSA (HyLogger/TSG) as illite*".

Another 'irregularity' that presents itself in these data is that the XRD analyses of some of the carbonaceous shale and coal samples indicate predominately quartz and I/S ± kaolinite, whereas the HyLogger™/TSG identifies siderite, ankerite, calcite ± jarosite, ± Mg-chlorite (see samples DG104/25b, /27, /28 /30, /31a/ 32, on Table 1). This observation may result from the XRD method preferentially identifying crystalline phases, whereas the spectral reflectance method identifies minerals such as the above carbonates and sulphates that may have an amorphous structure when occurring on the surface of coal samples. Because the spectral reflectance method essentially measures surficial mineral responses, when coal fractures or breaks along cleat surfaces, the mineralization present on those surfaces is preferentially detected. However, the XRD method tends not to see these cleat mineral species because in terms of the bulk of the rock these minerals are volumetrically in small proportions and poorly crystalline or amorphous.

CONCLUSIONS

Despite coal and carbonaceous materials having very low reflectivities the HyLogger™/TSG system has been able to identify meaningful and spatially consistent mineralogical interpretations within the coal core studied. The Hylogger™/TSG system was not able to detect meaningful mineral responses from all coal pixels. However, the observation that 'aspectral' assignments tend to occur in spatially coherent blocks that typically correspond to the darker/shinier coal layers (on the linescan image), this suggests that the method may be used to log coal brightness This study indicates that for a high percentage of the coals measured, carbonate and sulphate minerals (siderite, ankerite, calcite and jarosite) exist on the coal surface, possibly as coatings on fractures, joint or cleat surfaces. Because these minerals are poorly crystalline and volumetrically small, these minerals were not detected by XRD.

REFERENCES

CAMUTI, K., FRASER, S.J., HUNTINGTON, J.F., CUFF, C., COOK, R.N., & GARDAVSKY, V., 1987: A study of the surficial clay distribution at Mount Leyshon: Implications for high-spectral resolution remote sensing. *AMIRA Project P231, CSIRO IEER Restricted Investigation Report* **No. 1718R**, Volumes 1 & 2.

CUDAHY, T.J., 1997: Geometry of the spectral-mineralogical alteration halo at Birthday South, Fimiston gold deposit, Western Australia. *CSIRO Exploration and Mining Report* **421R**.

CUDAHY, T.J., YANG, K., MASON, P., GRAY, D., SCOTT, K. & HUNTINGTON, J., 1996: Kalgoorlie field spectral workshop manual. *CSIRO Exploration and Mining Report* **301R**.

FRASER, S.J. & CAMUTI, K., 1992: Mapping surficial alteration clays using XRD and spectral reflectance techniques. *In*, Proceedings of the 'Clays in Exploration Workshop' Townsville, November 18, 1992: James Cook University, *EGRU publication* **44**, 75–80.

HATHERLY, P., SLIWA, R., TURNER, R. & MEDHURST, T., 2003: Quantitative geophysical log interpretation for rock mass characterization. ACARP Project No C11037. *CSIRO Exploration & Mining Report* **1196F**.

HENWOOD, R.E., 2004: Mineral matter variations in the Goonyella Middle Seam, Grosvenor Downs: A comparison with CSIRO's HyLogger**™**. BSc (Honours) thesis, School of Biological, Earth and Environmental Sciences, University of New South Wales.

HUNTINGTON, J., CUDAHY, T., YANG, K., SCOTT, K., MASON, P., GRAY, D., BERMAN, M., BISCHOF, L., RESTON, M., MAUGER, M., KEELING, J. & PHILLIPS, R. 1997: Mineral Mapping with Field Spectroscopy for Exploration. *CSIRO Exploration and Mining Report* **419R**.

HUNTINGTON, J. & WHITBOURN, L., 2002: Automated Mineralogical Logging of Drill Core, Chips, and Powders. Final Report CSIRO/AMIRA Project P685, Automated Mineralogical Logging of Drill Core, Chips and Powders. *CSIRO Exploration and Mining Report* **1021R**.

MOORE, D.M & REYNOLDS, R.C., Jr., 1997: *X-Ray Diffraction and the Identification and Analysis of Clay Minerals, 2nd Edition*. Oxford University Press, New York.

RUAN, C.D. & WARD, C.R., 2002: Quantitative X-ray powder diffraction analysis of clay minerals in Australian coals using Rietveld methods. *Applied Clay Science*, **21**, 227–240.

SCOTT, K.M., YANG, K. & HUNTINGTON, J.F., 1998: The application of spectral reflectance studies of chlorites in exploration. *CSIRO Exploration and Mining Report* **545R**.

WARD, C.R. & FRENCH, D., 2003: Determination of glass content and estimation of glass composition in fly ash using quantitative X-ray diffractometry. *Proceedings of 12th International Conference on Coal Science*, Cairns, Queensland, 2–6 November, (CD publication).

WARD, C.R., TAYLOR, J.C. & COHEN, D.R., 1999: Quantitative mineralogy of sandstones by X-ray diffractometry and normative analysis. *Journal of Sedimentary Research*, **69**, 1050–1062.

S. Fraser, J.Esterle, CSIRO Exploration and Mining, PO Box 883, Kenmore, QLD 4069
C.R. Ward, R. Henwood*, School of Biological, Earth and Environmental Sciences, University of New South Wales, Sydney, NSW 2052,* Present Address: McElroy Bryan Geological Services Pty Limited, PO Box 34, Willoughby, NSW, 2068
P. Mason, J. Huntington, CSIRO Exploration & Mining, PO Box 136 North Ryde, NSW 1670

Colin Ward, Zhongsheng Li and Lila Gurba

Chemical changes in macerals of Bowen Basin coals with rank advance from bituminous coal to anthracite, using electron microprobe techniques

Changes in the elemental composition of the individual macerals in seams from the German Creek, Moranbah and Rangal Coal Measures have been studied over a wide range of rank conditions (bituminous coal to anthracite), using light-element electron microprobe techniques. The objects of the study were to establish the coalification tracks of the key macerals in these and other Australian coals, and to provide an improved basis from which to evaluate the performance of such coals in different utilisation processes.

The microprobe results show that the carbon content of the telocollinite increases dramatically from 66–90% as the vitrinite reflectance of the coals (Rv_{max}) increases from 0.39–1.75%, but increases only slightly, from 90–91%, as Rv_{max} increases from 1.75–3.52%. Oxygen decreases from around 26% to approximately 5% as Rv_{max} increases from 0.39–1.75%, and then decreases only very slightly into the anthracite range. The nitrogen content of the telocollinite in these coals also appears to decrease slightly with rank advance, and appears moreover to display a relatively abrupt drop at around 2% Rv_{max}. This may be associated with the development of ammonium illite in the mineral matter. Organic sulphur in the telocollinite, on the other hand, seems to remain essentially constant with rank advance, at least in this particular succession.

The principal inertinite components in the coals, fusinite and inertodetrinite, have significantly higher but more somewhat constant carbon contents, varying only from around 81–93% C over the rank range studied. Oxygen in these macerals decreases from around 12% to a little over 2% with the same degree of rank advance. Sulphur and nitrogen also appear to be significantly lower in the fusinites and inertodetrinites than in the vitrinites of the same coal samples. Semifusinite is somewhat more variable in composition, with characteristics intermediate between those of the fusinite/inertodetrinite and those of the vitrinite macerals.

INTRODUCTION

A considerable amount of information is available on the chemical composition of Bowen Basin coals based on conventional, whole-coal ultimate analysis data (e.g. Joint Coal Board and Queensland Coal Board, 1987; Maher & others, 1995; Coxhead, 1997). Whole-coal analyses, however, represent aggregated chemical data from a mixture of different types of organic bands and particles (the different coal macerals), together with moisture and mineral matter, and thus whole-coal analysis only provides an overview of the coal's composition. Very little information is available on the composition of the individual organic particles (macerals) within particular coals, even though the composition of components at this scale may be significant in better understanding the coal's behaviour and characteristics, including the dynamics and chemical mechanisms of coking and combustion processes.

It is the individual macerals within the coal that actually characterise the material, and that react, either separately or with each other, when the coal is used in different ways. More specific knowledge of maceral chemistry in particular coals inherently provides a better basis for understanding coal genesis and classification. It may also provide important insights the behaviour of different coals under particular utilisation conditions, with a range of practical applications in coal preparation, marketing and use.

It is, however, inherently difficult to isolate cleanly the individual macerals in a coal for separate chemical analysis, without contamination by minerals or other organic components. The recent development of special techniques for light-element analysis using the electron microprobe (Bustin & others, 1993, 1996; Mastalerz & Gurba, 2001) provides a mechanism for directly determining the elemental composition of the individual macerals in coal polished sections, based on analysing areas only a few microns across. These techniques have been applied to maceral studies in coals of the Sydney and Gunnedah Basins (Ward & Gurba, 1999; Gurba & Ward, 2000; Ward & others, 2003a), but only in a limited way to Bowen Basin coal samples.

The coals of the Bowen Basin range from sub-bituminous to anthracitic in rank, with vitrinite reflectance (Rv_{max}) ranging from 0.35% to over 3.5% due mainly to variations in burial depth (Beeston, 1995). This represents a wider rank variation than that found in other Australian coal basins, and as such provides an opportunity to test the variations in maceral chemistry with rank for coals of a similar geological age and depositional setting. Since the Bowen Basin also provides a large part of Australia's black coal production, better knowledge of the constitution of these coals at the maceral scale is also of considerable economic significance.

SAMPLING AND ANALYTICAL PROGRAM

A series of coal samples from the German Creek and Moranbah Coal Measures was made available for the study by the Queensland Department of Natural Resources and Mines, from boreholes drilled by the Department as part of its regional exploration programs. The samples, taken from sites across the basin, had vitrinite reflectance values ranging from 0.39–3.52% (Table 1), and thus represent coals from two contiguous stratigraphic sequences covering a wide rank range. Petrographic data for the samples, based on conventional optical microscopy, have been published separately by Beeston (1978, 1981, 1995). Several other samples of Bowen Basin coal, mostly grab samples from the overlying Rangal Coal Measures, were also included for comparison in the sample set. A more complete discussion of the geological setting and other aspects of the sample suite is given by Ward & others (2005).

Polished block samples of each coal were prepared in a similar way to samples for conventional optical microscopy, and coated with carbon for electron microprobe analysis as described by Bustin & others (1993). Individual points within the different macerals of each coal were analysed using a Cameca SX-50 electron microprobe equipped with the Windows-based SAMx operating system and interface software. The accelerating voltage for the electron beam was 10kV and the filament current 20nA, with a magnification of 20,000x giving an beam spot size on the sample of around 5ìm in diameter. As discussed by Bustin & others (1993), an independently analysed anthracite sample was used as the standard for carbon in the analysis process. Mineral samples supplied with the instrument were used as standards for the other elements. Further details of microprobe procedures for coal macerals are given by Bustin & others (1993, 1996), Mastalerz & Gurba (2001) and Ward & others (2005).

The percentages of carbon, oxygen, nitrogen, sulphur, silicon, aluminium, calcium and iron were measured for each point, with a note on the type of maceral represented in each case. The results of the individual analyses were tabulated in spreadsheet format. Although care was taken to analyse only ‘clean’ macerals and avoid areas where visible minerals were also present, the area analysed for some points unavoidably included mineral components (e.g. quartz, clay, pyrite) as well as the organic matter. Points that apparently included mineral contaminants (e.g. points with high Si or unexpectedly high Fe and S percentages) were excluded from consideration; so, too, were points that included some of the mounting epoxy resin, indicated by unusual oxygen and high nitrogen contents.

Exclusion of mineral-bearing macerals could not, however, always be achieved. The sample from Central Colliery, for example, was found to contain small (<1%) but roughly equal proportions of Si and Al at many points in apparently ‘clean’ vitrinite and semifusinite (Table 3), suggesting the presence of clay minerals such as kaolinite intimately admixed with the maceral structures. Such information is potentially of significance in preparation and use of this and similar materials. Exclusion of all points with mineral contamination, moreover, would have provided a very limited data set to characterise this particular coal sample.

A summary of the elemental composition for the main maceral groups in each sample, after removal of points that

Table 1: List of coal samples studied

Sample No.	Borehole	Depth interval (m)	Sample details	Rv max %
PS 2302	Consuelo NS 3	17.18-18.39	Bandanna Formation	0.39
PS 1035	Emerald NS 53	334.32-334.65	Ply, German Creek Seam	0.70
PS 1210	Emerald NS 85	176.61-180.05	German Creek Seam F1.60	0.90
PS 1204	Talbot NS 75/76	94.13-97.36	German Creek Seam F1.60	1.10
PS 1128	Talbot NS 40	45.97-49.85	German Creek Seam F1.60	1.31
PS 1115	Talbot NS 30	221.69-224.21	German Creek Seam F1.50	1.52
PS 1134	Cairns County NS 33	265.44-267.43	German Creek Seam F1.60	1.75
PS 6657	Wodehouse NS 1	259.49-260.59	Moranbah Coal Measures	2.14
PS 6674	Wodehouse NS 1	665.34-666.56	Moranbah Coal Measures	2.70
PS 6861	Killarney NS 1	306.59-307.72	Moranbah Coal Measures	3.52
Other coal samples				
Central Colliery		German Creek Coal Measures		1.40
Ensham		Rangal Coal Measures		0.81
Nebo West		Rangal Coal Measures		2.10
Yarrabee		Rangal Coal Measures		2.20
Baralaba (Coolum seam)		Rangal Coal Measures		2.15

included significant mineral or epoxy contaminants, is given in Table 2. The values given represent the average composition of a number of different points on each maceral for each coal sample. Additional information, including the standard deviations associated with the key determinations, is provided by Ward & others (2005). Although a few points on liptinite macerals (sporinite and cutinite) were also analysed in some of the coals at the lower end of the rank range, these macerals change their appearance with rank advance (Taylor & others, 1998), and could not be separately identified in the higher-rank coal samples. Figure 1 shows the variation in organic C, O, N and S for each maceral in each coal, plotted against the respective vitrinite reflectance value.

ELEMENTAL COMPOSITION OF MACERAL GROUPS

As indicated in Table 2 the carbon content of the telocollinite in the coals increases dramatically from 66–90% as the vitrinite (telocollinite) reflectance (Rv_{max}) increases from 0.39–1.75%. This is also shown in Figure 1a. In contrast, carbon in telocollinite increases only slightly, from 90–91%, as Rv_{max} increases over the rest of the rank range. Oxygen in the telocollinite decreases from around 26% to approximately 5% as Rv_{max} increases from 0.39–1.75% (Figure 1b), and then decreases only slightly as rank increases into the anthracite range.

Desmocollinite shows a similar variation in carbon and oxygen content to telocollinite, but has a slightly higher proportion of carbon and slightly lower proportion of oxygen relative to the telocollinite in the same coal samples. The difference is slight, but seems to persist to at least some extent throughout almost the entire rank range, and the two vitrinite types only have similar C and O contents in the highest-rank coal sample (Rv_{max} = 3.5%).

Fusinite and inertodetrinite have significantly higher but more constant carbon contents than the vitrinite macerals, varying respectively from about 81 and 86% to around 93% C over the same rank interval. Oxygen in these macerals decreases respectively from 12% and 9% to a little over 2% with the same degree of rank advance. Inertodetrinite appears to have higher proportions of carbon and lower proportions of oxygen than the fusinite in the same coals over the lower part of the rank range, although the difference becomes insignificant at higher rank levels. Semifusinite has carbon and oxygen contents that are intermediate between those of the fusinite/inertodetrinite and those of the vitrinite in the same coal samples. The carbon and oxygen contents of all the maceral groups converge to the point where they show only slight differences between each other above a vitrinite reflectance of around 1.8%.

Nitrogen and organic sulphur both appear to be significantly lower in the fusinite and inertodetrinite than in the vitrinites of the same coal samples, confirming findings from other coals by Gurba (2001). Semifusinite generally has intermediate nitrogen and sulphur contents. The nitrogen content of both vitrinite macerals decreases slightly with rank (Figure 1c), and seems to display a relatively abrupt drop at around 2% Rv_{max}. This may be associated with the development of ammonium illite in the mineral matter, which has been identified in other Bowen Basin coals at a similar rank level (Ward & Christie, 1994). Nitrogen in the inertinite macerals, however, appears to remain relatively constant with rank advance, and may even show a slight increase with rank in the inertodetrinite component. Differences in nitrogen content between vitrinite and inertinite macerals are therefore most marked in the sub-bituminous and bituminous coals (up to Rv_{max} = 2%), and appear to be less significant in higher rank materials.

Although the macerals, especially the vitrinite macerals, in the lowest rank coal studied have the lowest (organic) sulphur contents, and those of the highest rank coal (with the exception of inertodetrinite) have the highest levels of organic sulphur (Figure 1d), the proportion of organic sulphur in the individual maceral groups of the bulk of the samples does not appear to vary significantly with rank. This is in contrast to some of the results from previous studies (Ghosh, 1971; Harrison, 1991), which have suggested that organic sulphur in coal shows a decrease with rank advance. As with findings reported from other coals by Ward & Gurba (1998), the organic sulphur content of the inertinite macerals, with some exceptions, is typically around half that of the vitrinites in the same coal samples, especially below the 2% vitrinite reflectance level.

DISCUSSION AND CONCLUSION

The data in Figure 1 provide a clear illustration of the coalification tracks, in chemical terms, of the individual macerals in Bowen Basin coals over the rank range from sub-bituminous to anthracite. Although not plotted in Figure 1, the macerals in the samples studied from the Rangal Coal Measures (Table 2) have similar compositions to those in coals of equivalent rank from the German Creek and Moranbah Coal Measures.

The dramatic changes in the elemental composition of the vitrinite from Rv_{max} 0.39–1.75% probably reflect the breakdown of large-molecule organic compounds to smaller compounds, and the associated volatile loss with the rank advance (Taylor & others, 1998). Li & others (2004) have further described a progressive increase in the proportion of aromatic functional groups with rank advance in the vitrinites of these coals, based on complementary micro-FTIR spectrometry techniques applied to the same polished sections. The vitrinite and semifusinite macerals of the lowest-rank coal (Rv_{max} = 0.39%) also show small proportions of calcium in the organic matter, but this is lost, apparently due to similar molecular structure changes, at higher rank levels. Similar occurrences of Ca, along with Al and Fe in some cases, are also noted by Ward & others (2003b) in a number of low-rank coal samples from other sedimentary basins. These mostly disappear as the rank of the coal increases.

Table 2: Elemental analysis of maceral groups in coal samples

Sample + Maceral	No	C%	N%	O%	Al%	Si%	S%	Ca%	Fe%
PS2302 – TC	15	66.38	2.08	26.25	0.06	0.03	0.37	0.18	0.06
PS2302 – DSC	6	69.53	1.65	24.24	0.03	0.06	0.34	0.21	0.02
PS2302 – SF	14	76.80	1.46	16.23	0.01	0.02	0.19	0.18	0.09
PS2302 – FUS	13	81.18	0.77	12.58	0.01	0.02	0.15	0.16	0.02
PS2302 – IND	1	86.01	0.58	9.18	0.03	0.02	0.16	0.21	0.27
PS1035 – TC	12	76.43	1.89	15.76	0.03	0.04	0.74	0.02	0.06
PS1035 – DSC	3	77.38	1.99	14.56	0.03	0.06	0.76	0.01	0.03
PS1035 – SF	8	82.23	1.74	11.10	0.04	0.08	0.50	0.09	0.04
PS1035 – FUS	6	87.85	0.83	6.44	0.04	0.05	0.28	0.19	0.01
PS1035 – IND	3	88.93	0.71	5.81	0.04	0.06	0.33	0.18	0.00
PS1210 – TC	8	78.64	2.42	12.88	0.03	0.02	0.63	0.01	0.10
PS2310 – DSC	13	79.90	2.17	12.15	0.04	0.04	0.64	0.01	0.07
PS1210 – SF	12	82.78	1.30	9.75	0.03	0.03	0.40	0.02	0.02
PS1210 – FUS	10	85.61	1.34	7.90	0.01	0.02	0.37	0.06	0.04
PS1210 – IND	2	88.41	0.27	5.99	0.06	0.04	0.31	0.32	0.06
PS1204 – TC	10	84.41	2.28	8.42	0.02	0.03	0.58	0.01	0.04
PS1204 – DSC	6	85.40	2.05	6.78	0.02	0.04	0.64	0.02	0.01
PS1204 – SF	4	88.89	0.92	5.17	0.03	0.03	0.36	0.01	0.00
PS1204 – FUS	7	89.41	0.99	5.16	0.02	0.05	0.32	0.09	0.07
PS1204 – IND	2	93.57	0.45	2.55	0.00	0.01	0.23	0.08	0.15
PS1128 – TC	8	87.19	2.42	4.66	0.04	0.07	0.68	0.02	0.00
PS1128 – DSC	2	86.95	2.82	5.06	0.05	0.08	0.72	0.00	0.05
PS1128 – SF	8	90.05	1.17	3.90	0.03	0.05	0.48	0.02	0.05
PS1128 – FUS	5	91.62	0.58	3.84	0.02	0.04	0.31	0.15	0.01
PS1128 – IND	2	95.01	0.84	1.37	0.00	0.01	0.15	0.01	0.04
PS1115 – TC	13	87.27	1.88	5.49	0.03	0.03	0.54	0.01	0.06
PS1115 – DSC	6	87.90	1.82	5.05	0.05	0.09	0.51	0.03	0.00
PS1115 – SF	7	90.46	0.95	4.20	0.02	0.04	0.35	0.07	0.01
PS1115 – FUS	2	92.75	0.84	3.56	0.20	0.19	0.26	0.27	0.15
PS1115 – IND	3	91.69	1.12	3.45	0.01	0.02	0.27	0.14	0.00
PS1134 – TC	17	89.84	1.96	5.35	0.03	0.06	0.53	0.02	0.01
PS1134 – DSC	5	90.42	1.82	4.75	0.03	0.05	0.56	0.02	0.02
PS1134 – SF	12	92.33	1.23	3.87	0.02	0.03	0.43	0.07	0.04
PS1134 – FUS	6	92.42	1.26	3.51	0.01	0.02	0.34	0.14	0.07
PS1134 – IND	4	93.07	0.85	3.38	0.02	0.02	0.36	0.14	0.10
PS1134 – TC	17	89.84	1.96	5.35	0.03	0.06	0.53	0.02	0.01
PS1134 – DSC	5	90.42	1.82	4.75	0.03	0.05	0.56	0.02	0.02
PS1134 – SF	12	92.33	1.23	3.87	0.02	0.03	0.43	0.07	0.04
PS1134 – FUS	6	92.42	1.26	3.51	0.01	0.02	0.34	0.14	0.07
PS1134 – IND	4	93.07	0.85	3.38	0.02	0.02	0.36	0.14	0.10

Table 2 (continued)

Sample + Maceral	No	C%	N%	O%	Al%	Si%	S%	Ca%	Fe%
RC6657 – TC	22	90.69	1.49	4.53	0.02	0.05	0.72	0.01	0.04
RC6657 – DSC	3	91.00	1.31	3.94	0.03	0.09	0.75	0.02	0.07
RC6657 – SF	12	92.77	1.08	3.04	0.04	0.06	0.63	0.01	0.02
RC6657 – FUS	2	93.88	1.14	2.71	0.00	0.02	0.47	0.01	0.14
RC6674 – TC	29	91.01	1.49	5.18	0.03	0.05	0.70	0.01	0.04
RC6674 – DSC	6	92.52	1.35	4.30	0.07	0.10	0.69	0.01	0.07
RC6674 – SF	16	93.61	0.83	2.81	0.02	0.03	0.51	0.04	0.02
RC6674 – FUS	6	94.94	0.33	2.36	0.05	0.05	0.36	0.14	0.04
RC6674 – IND	1	94.31	1.26	2.61	0.01	0.02	0.31	0.26	0.21
RC6861 – TC	14	91.05	1.43	5.52	0.02	0.04	0.84	0.01	0.07
RC6861 – SF	8	91.01	1.34	5.10	0.01	0.04	0.87	0.02	0.04
RC6861 – FUS	14	92.95	1.04	3.57	0.02	0.03	0.78	0.01	0.08
RC6861 – IND	1	92.06	1.04	3.61	0.02	0.02	0.28	0.51	0.08
Central – TC	15	87.36	1.82	6.31	0.78	1.03	0.59	0.02	0.04
Central – DSC	5	85.72	2.02	7.23	1.32	1.76	0.54	0.01	0.00
Central – SF	10	90.17	1.31	6.24	0.83	1.00	0.38	0.07	0.06
Central – FUS	8	92.37	1.07	3.35	0.24	0.27	0.27	0.07	0.08
Central – IND	3	93.98	0.24	1.71	0.01	0.03	0.15	0.13	0.06
Ensham – TC	15	80.69	2.57	12.32	0.01	0.03	0.30	0.02	0.08
Ensham – DSC	3	81.48	2.28	10.66	0.06	0.06	0.43	0.00	0.06
Ensham – SF	13	85.50	1.90	8.05	0.03	0.04	0.22	0.24	0.04
Ensham – FUS	5	87.24	1.33	6.52	0.04	0.05	0.23	0.05	0.04
Ensham – IND	4	92.85	0.90	2.61	0.01	0.02	0.10	0.02	0.00
Nebo West – TC	20	90.51	1.49	6.17	0.02	0.03	0.64	0.01	0.05
Nebo West – DSC	5	91.28	1.42	5.07	0.07	0.09	0.63	0.01	0.05
Nebo West – SF	11	92.65	0.97	3.49	0.05	0.05	0.48	0.06	0.02
Nebo West – IND	4	94.72	0.54	2.52	0.01	0.00	0.21	0.18	0.05
Yar 1 – TC	19	89.81	1.57	4.97	0.01	0.01	0.54	0.02	0.02
Yar 1 – DSC	3	91.95	1.63	3.11	0.02	0.00	0.68	0.01	0.02
Yar 1 – SF	6	91.72	1.05	3.29	0.03	0.04	0.51	0.02	0.02
Yar 1 – FUS	8	93.14	0.73	2.71	0.03	0.04	0.39	0.04	0.02
Yar 1 – IND	3	93.27	1.05	2.73	0.01	0.02	0.43	0.04	0.00
Coolum – TC	17	89.84	1.97	4.99	0.01	0.04	0.44	0.02	0.03
Coolum – DSC	4	90.22	1.68	4.39	0.05	0.07	0.47	0.02	0.08
Coolum – SF	16	90.05	1.47	4.05	0.03	0.04	0.38	0.02	0.05
Coolum – FUS	4	91.86	0.54	3.38	0.01	0.01	0.41	0.03	0.01
Coolum – IND	7	93.90	0.51	2.94	0.02	0.01	0.25	0.15	0.02

TC = telocollinite DSC = desmocollinite SF = semifusinite FUS = fusinite IND = inertodetrinite
No = number of points analysed for individual maceral in each sample

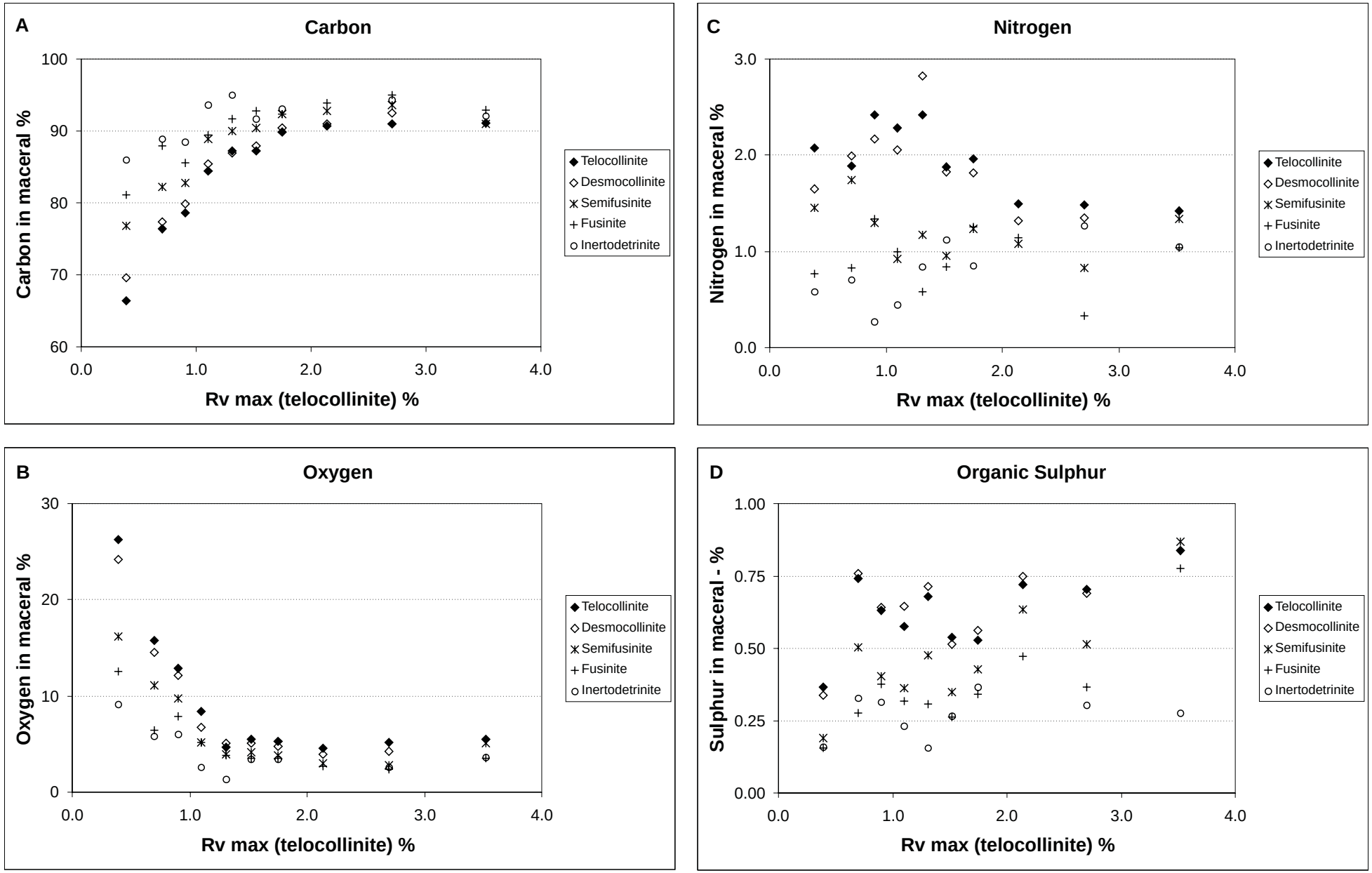

Figure 1: Variations in C, O, N and S contents (wt% by microprobe) in the different macerals of the German Creek Coal Measures with rank advance. Each data point represents the average concentration of the respective element for a number of such macerals in each coal sample.

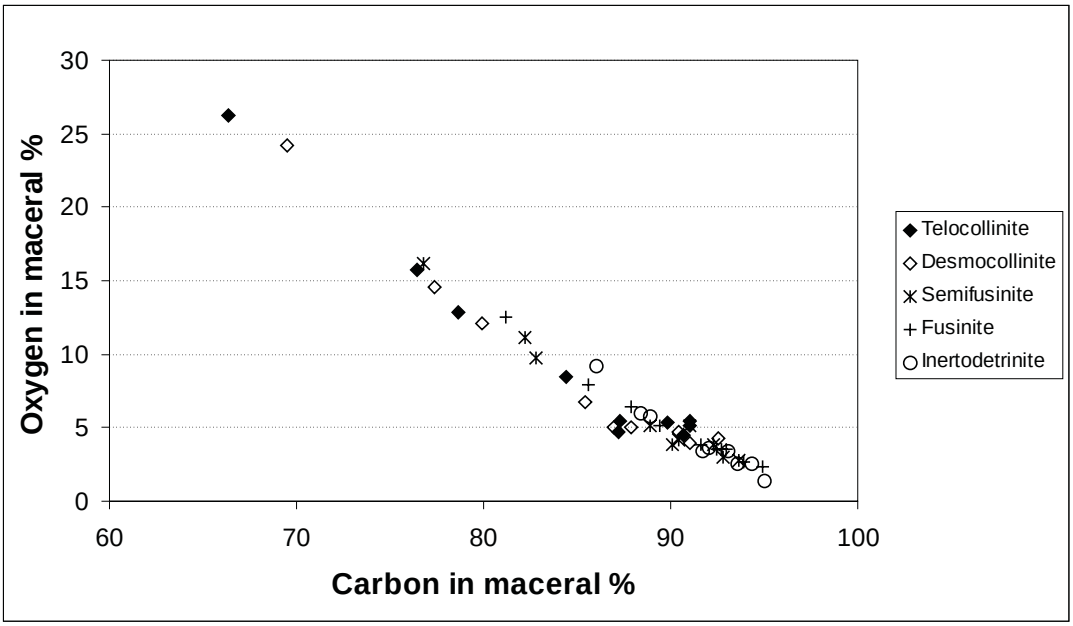

Figure 2: Plot showing relation between organic carbon and oxygen contents of each maceral for each sample from the German Creek Coal Measures.

Figure 2 shows the relation between the carbon and oxygen contents of each individual maceral group, for each of the coal samples studied. Despite the contrasts between the vitrinite and inertinite macerals in the same coal samples, especially at lower rank levels, and despite the variation in elemental composition of the different macerals with rank, the carbon and oxygen contents of each maceral group appear from this plot to remain related to each other throughout the rank range. All of the data points in Figure 2 plot on or close to the same linear trend, regardless of the maceral group or rank level involved.

This line follows closely that produced on a similar plot by whole-coal ultimate analysis data (Gurba & Ward, 2000). The vitrinite macerals, however, especially for the lower rank coals, are spread towards the upper left part of this trend, whereas the inertinite macerals are grouped nearer the lower right-hand side. Recognition of the individual macerals in such a plot identifies more clearly the contribution of the different organic components to the total coal composition, and emphasises the point, long-recognised but often overlooked, that it is the relative proportions of the different macerals (the coal type), as well as the coal rank, that determines the overall chemical composition of a coal sample. The carbon content of whole coal samples, corrected to a dry ash-free or dry mineral matter free basis, which is often used as a rank index, is actually related to more than just the coal's rank level, especially at the lower end of the rank range.

Microprobe data on the organic components can be used to provide a better understanding of the link between coal petrology and coal chemistry. This is discussed more fully by Ward & Li (2005), in a study based on combination of microprobe data on maceral chemistry with petrographic data on maceral abundance as compared to the results of conventional whole-coal ultimate analysis. In addition to providing a basis for reconciliation of chemical and petrographic information, microprobe data can be used to explain more fully particular aspects of coal behaviour, such as the proportional release of CO_2 per unit energy from different coals, or possibly variations among otherwise similar coals in coking or gasification characteristics. Identification on the inorganic constituents in particular macerals (Ward & others, 2003b) may also be of value in addressing ash problems, such as slagging, in combustion applications.

ACKNOWLEDGEMENTS

Financial support for the study was provided under the Large Grants Scheme of the Australian Research Council. Thanks are expressed to Rad Flossman for polished section preparation and Barry Searle for assistance with the electron microprobe analyses. Thanks are also expressed to Jim Beeston and Ray Smith, of the Queensland Department of Natural Resources and Mines, and to various mining and exploration companies, for provision of the coal samples. Maria Mastalerz, of the Indiana Geological Survey, provided the reference anthracite standard used in the microprobe analysis program.

REFERENCES

BEESTON, J.W., 1978: Coal reflectivity, rank and carbonisation in Departmental borehole Wodehouse NS 1, *Queensland Government Mining Journal,* **79**, 159-164.

BEESTON, J.W., 1981: Coal rank variation in the Bowen Basin, Geological Survey of Queensland Record, 1981/48.

BEESTON, J.W., 1995: Coal rank and vitrinite reflectivity. *In,* Ward, C.R., Harrington, H.J., Mallett, C.W. & Beeston, J.W. (Editors): Geology of Australian Coal Basins, *Geological*

Society of Australia Coal Geology Group Special Publication, No.1, 83-92.

BUSTIN, R.M., MASTALERZ, M., & WILKS, K.R., 1993: Direct determination of carbon, oxygen and nitrogen content in coal using the electron microprobe, *Fuel*, **72**, 181-185.

BUSTIN, R.M., MASTALERZ, M., & RAUDSEPP, M., 1996: Electron-probe microanalysis of light elements in coal and other kerogen, *International Journal of Coal Geology,* **32**, 5-30.

COXHEAD, B.A., 1997: *Queensland Coals: Physical and Chemical Properties, Colliery and Company Information*, 11th Edition, Queensland Coal Board, Brisbane.

GHOSH, T.K., 1971: Change in coal macerals. *Fuel*, **50**, 218-221.

GURBA, L.W., 2001: Distribution of organic nitrogen in Australian coals, *Proceedings of 18th Annual Pittsburgh International Coal Conference*, Newcastle, NSW, (CD-ROM).

GURBA, L.W. & WARD, C.R., 2000: Elemental composition of coal macerals in relation to vitrinite reflectance, Gunnedah Basin, Australia, as determined by electron microprobe analysis, *International Journal of Coal Geology,* **44**, 127-147.

HARRISON, C.H., 1991: Electron microprobe analysis of coal macerals. *Organic Geochemistry* **17**(4), 439-449.

JOINT COAL BOARD AND QUEENSLAND COAL BOARD 1987: *Australian Black Coals*, Joint Coal Board, Sydney.

LI, Z., FREDERICKS, P.M., RINTOUL, L. & WARD, C.R., 2004: Application of attenuated total reflectance micro-Fourier transform infra-red (ATR-FTIR) analysis to the study of coal macerals and coal maturation processes, *Abstracts and Program, 21st Annual Meeting, Society for Organic Petrology*, Sydney, Australia, September 27-October 1, 2004, 97-100.

MAHER, T.P., BOSIO, M., LINDNER, E.R., BROCKWAY, D.J., GALLIGAN, A.G., MORAN, V.J., PECK, C., WALKER, M.P., BENNETT, P.A. & COXHEAD, B.A., 1995: Coal resources, quality and utilisation. *In*, Ward, C.R., Harrington, H.J., Mallett, C.W. & Beeston, J.W. (Editors): Geology of Australian Coal Basins, *Geological Society of Australia Coal Geology Group Special Publication,* No 1, 133-159.

MASTALERZ, M. & GURBA, L.W., 2001: Determination of nitrogen in coal macerals using electron microprobe technique – experimental procedure, *International Journal of Coal Geology,* **47**, 23-30.

TAYLOR, G.H., TEICHMÜLLER, M., DAVIS, A., DIESSEL, C.F.K., LITTKE, R. & ROBERT, P. 1998: *Organic Petrology*, Gebrüder Borntrager, Berlin.

WARD, C.R. & CHRISTIE, P.J., 1994: Clays and other minerals in coal seams of the Moura-Baralaba area, Bowen Basin, Australia, *International Journal of Coal Geology,* **25**, 287-309.

WARD, C.R. & GURBA, L.W., 1998: Occurrence and distribution of organic sulphur in macerals of Australian coals using electron microprobe techniques, *Organic Geochemistry,* **28**, 635-647.

WARD, C.R. & GURBA, L.W., 1999: Chemical composition of macerals in bituminous coals of the Gunnedah Basin, Australia, using electron microprobe techniques, *International Journal of Coal Geology,* **39**, 279-300.

WARD, C.R., GURBA, L.W., LI, Z. & SUSILAWATI, R., 2003b: Distribution of inorganic elements in lower-rank coal macerals as indicated by electron microprobe techniques, *Proceedings of 12th International Conference on Coal Science*, Cairns, Queensland, 2-6 November, (CD publication).

WARD, C.R. & LI, Z.S., 2004: Comparison of elemental composition of macerals in some Australian coals determined by electron microprobe to equivalent whole-coal ultimate analysis data. *Abstracts and Program, 21st Annual Meeting, Society for Organic Petrology*, Sydney, NSW, September 27-October 1, 199-201.

WARD, C.R., LI, Z. & GURBA, L.W., 2003a: Elemental composition of macerals in coals from the Sydney and Cranky Corner Basins, *Proceedings of Sydney Basin Symposium*, University of Wollongong, NSW, 181-187.

WARD, C.R., LI, Z. & GURBA, L.W. 2005: Variations in coal maceral chemistry with rank advance in the German Creek and Moranbah Coal Measures of the Bowen Basin, Australia, using electron microprobe techniques, *International Journal of Coal Geology* (in press).

C.R. Ward*, Zhongsheng Li and Lila W. Gurba[1], School of Biological, Earth and Environmental Sciences, University of New South Wales, Sydney, NSW 2052,

* E-mail: C.Ward@unsw.edu.au

[1] Present address: CRC for Coal in Sustainable Development, Kenmore, Qld 4069

Mark Biggs

Investigations into the prediction and modelling of total sulphur in coal seams, using examples from the Bowen Basin, Central Queensland

Many steps are required to produce accurate coal quality models. The process followed at several Anglo Coal Australia Central Queensland mines to model once such parameter, total sulphur, is outlined in this paper. Success depends, in part, on creating and maintaining a database where coal quality sample intervals are matched to appropriate seam or working section intervals and that 'like' sampling interval, reporting basis, and washability process are grouped and stored together. Selecting the correct modelling algorithm to generate quality grids is only half the answer. Successfully modelling total sulphur in coal requires an understanding of its size distribution, mineralized form, and the relationship between raw and product components in washed coal, and most importantly the domain or habit of the mineralisation.

Despite total sulphur rarely being used a valid observation point for JORC calculation, spatial continuity in terms of borehole density and sample variability must also be accounted for, and often examination of this data allows confidence intervals to be calculated. This has taken on greater significance with the documentation required to substantiate JORC-compliant resources, especially where other coal quality variables are concerned. Parameters such as ash, volatile matter or crucible swelling number are often used, where the quality variability is predictable at the current borehole spacing. In contrast, sulphur and phosphorus show short-range variations (i.e. <50m) in some areas. Such parameters can vary considerably in both a vertical and lateral sense within and between seams, particularly near dykes and seam washout areas. This requires mapping by strip sampling in open cut strips or in underground gateroads to give advance warning of high spots to enable blending schedules to meet product specifications.

Sulphur is best modelled with the aid of data from complementary characterisation studies (XRD, SEM, geophysical logging). This should in turn enhance the rigorous statistical analyses of available values (by seam) carried out, and examples are given in this paper. The combination of knowing the distribution and nature of the sulphur mineralisation and having a detailed appraisal of the spatial continuity of the sulphur sample points are essential building blocks to allow areas of high sulphur to be predicted in advance of mining. Sulphur models should not be made available to end-users without complementary error bounds or 'halos of uncertainty' provided. These are defined as the potential error in terms of location and size of the relevant hazard that results from the existing data point spacing used to identify the hazard, in this case sulphur variability.

Eventually, a methodology for predicting sulphur mineral concentrations in advance of mining and reconciling 'as-sold' coal quality to that predicted will be developed. These prediction theories can then be refined at the coalface as mining progresses through high-sulphur zones.

BACKGROUND

Data from three Central Queensland coal deposits within the Anglo Coal Australia Group have been used to demonstrate the different distributions and methodologies used in modelling total sulphur in coal seams. The deposits and seams are listed in Table 1 below and are the focus of current open cut mining operations (see Figure 1):

STATEMENT OF THE PROBLEM

There is a systematic variation in rank across the Dawson and German Creek mining leases, which is exemplified by a regular increase in vitrinite reflectance in the coal from southwest to northeast. Because many of the coal's coking properties are governed by rank, there is a long-range reduction of coking parameters, such as fluidity and dilatation, towards the northeast at German Creek and north at Dawson. By comparison, the sulphur content of some coal seams can, on occasions, widely vary in both a vertical and lateral sense within and between seams, particularly near

Table 1: Location of study mines and seams

Deposit/ mine	Seam(s)	Formation	Age
Callide	Callide	Callide Coal Measures	Triassic
Dawson (previously Moura)	B, BL, C	Baralaba Coal Measures	Late Permian
German Creek	Aquila, German Creek	German Creek Formation	Early Permian

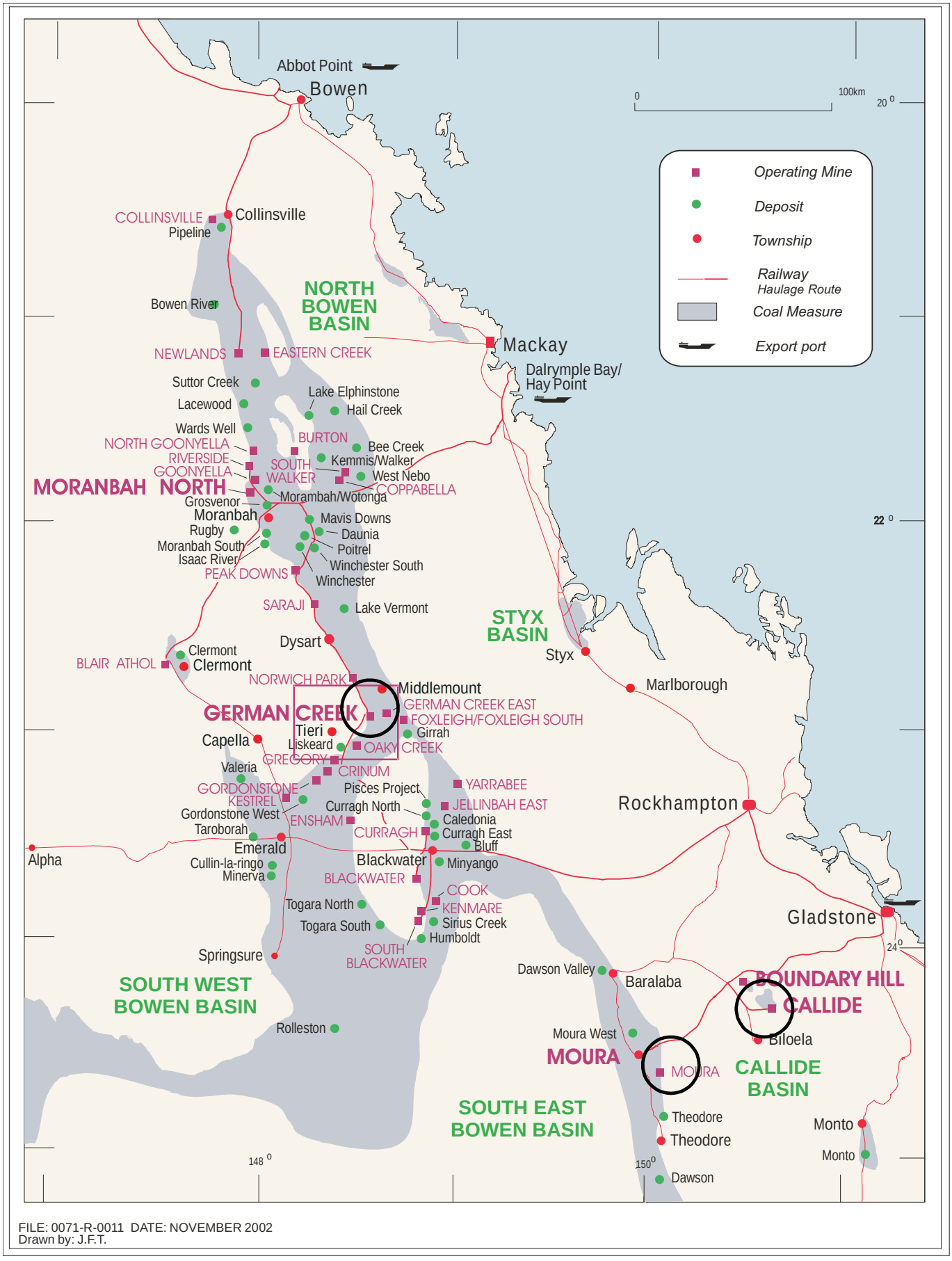

Figure 1: Location of sulphur study areas

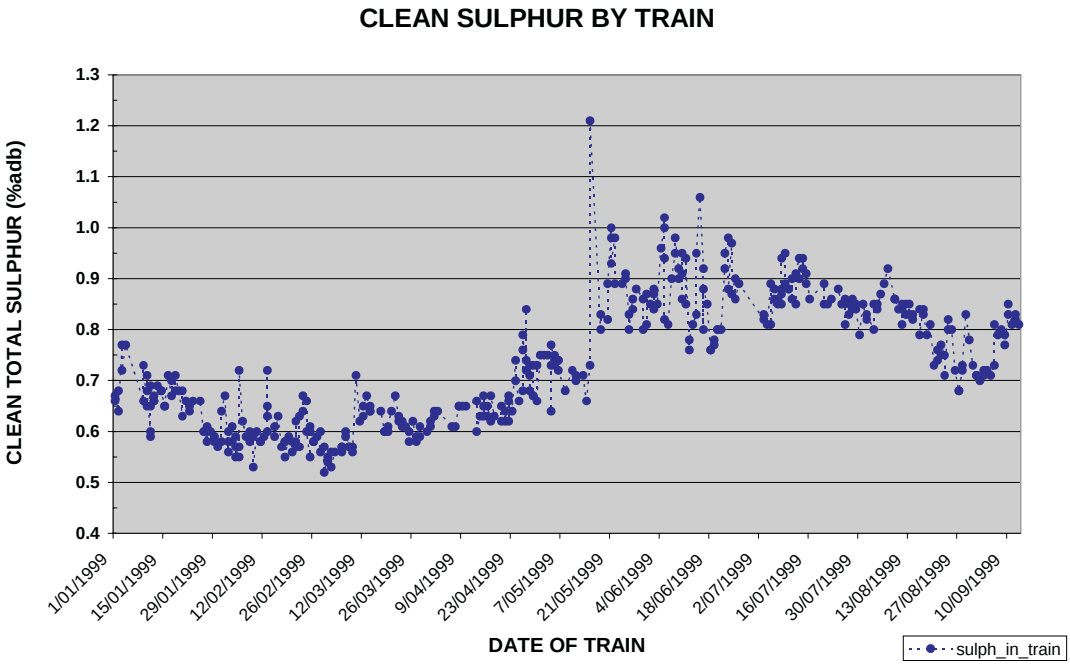

Figure 2: Train analyses, German Creek Seam

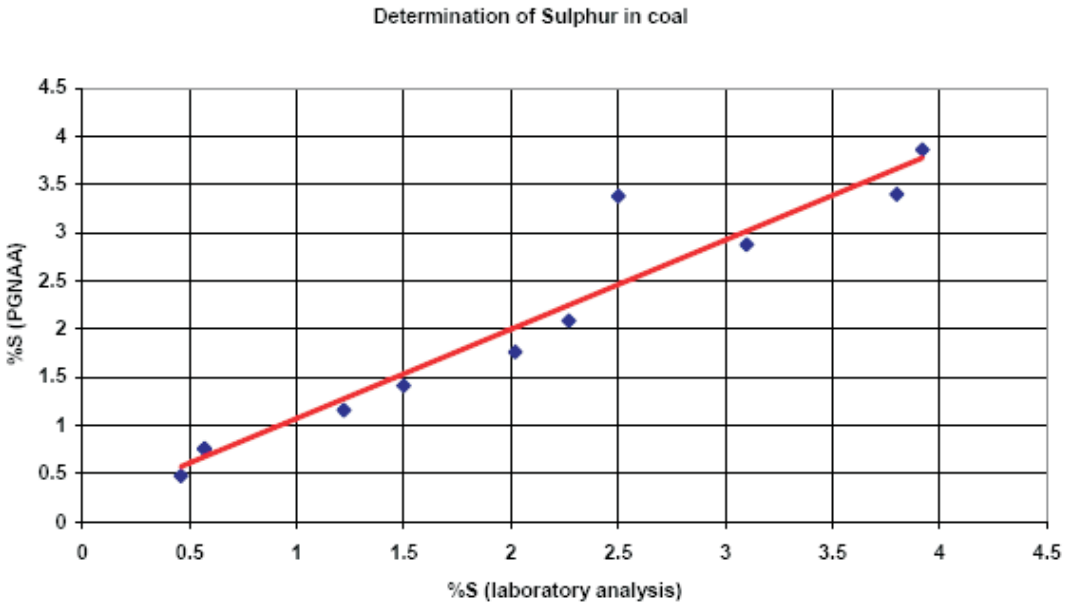

Figure 3: Correlation of laboratory sulphur with probe sulphur (modified after Borsaru & others, 2004)

dykes and seam washout areas. This short-range variability creates problems in predicting the sulphur content of washed product coal, with the possibility of coal shipments to customers being rejected if sulphur levels exceed pre-defined limits.

Therefore, if patterns in this variability could be determined and related to some geological property or process of formation of the coal seams, then areas of high sulphur might be predicted in advance of mining.

Often, in producing coal mines, such studies are initiated when production qualities change rapidly and unexpectedly (Figure 2).

The graph clearly demonstrates a step change in product coal total sulphur values, with a higher and more variable coal being produced, with site technical personnel being asked to explain and understand the divergence.

STUDY METHODOLOGY

In order to study the problem the author instigated a wide-ranging study that has as its main elements:

- background coal characterisation study,
- rigorous statistical analyses,
- spatial continuity testing;,
- computer-based grid modelling and prediction, and
- downhole geophysical logging (CSIRO's Sulphalog sonde).

Downhole geophysical logging to estimate sulphur contents is a new technique (Borsaru & others, 2003) and Figure 3 highlights the accuracy that can be obtained once site-specific correlations are established.

In a recent summary, Biggs (2000b) has argued that effective coal quality sampling and modelling is a function of:

- knowledge and understanding of the particular market specification required,
- sample density,
- seam continuity,
- modelling algorithm employed, and
- most particularly, individual parameter variability.

This paper concentrates on providing a snapshot of various aspects of the work conducted, such as statistical analysis, sample density and spatial continuity testing, as well as introducing the concept that geological domains need to be established to provide confidence bands to the estimates. Various modelling methodologies were employed, ranging from geostatistics (ordinary kriging) to polygons of influence so as to best represent the short-range variations present in the seam data sets. Although not containing sulphur levels in either coal or parting that would cause concern, Callide was included in the study as a low sulphur reference dataset to allow comparison.

COAL CHARACTERISATION STUDY

Part of successfully modelling sulphur at all three areas is recognition of what sulphur-bearing minerals are present and how they occur in relation to the coal macerals and clastic rocks encasing the coal seams. Increasingly, additional investigations, such as background coal characterisation studies are being completed. These are now seen as integral to determining lithological and structural controls to troublesome coal quality distributions. Advanced methods such as NMR, coal and parting mineral matter identification by XRD using SIROQUANT (Ward & Taylor, 1996) and/or SEM; or trace element determinations by ICP, AAS or XRF techniques are being employed.

Table 2 outlines the differing habitat and environment that the sulphur mineralisation may take.

In the example shown below (Figure 4), SEM images of two coal polished blocks show the distribution of pyrite nodules, their size, and their relationship with clays (mostly kaolinite) and the coal macerals. The larger nodules in the upper image may respond well to removal during beneficiation processes, but the scattered distribution of pyrite grains is an indicator of the ability or otherwise of potential gridding algorithms whilst modelling widely-spaced exploration borehole or channel sample. The pyrite nodules in the lower image are

Table 2: Comparison of deposit characteristics, sulphur study

Locality	Influence	Environment of Deposition	Seam structure	Nature of Sulphur Minerals	Sulphur Mineral distribution expected
Callide	Terrestrial, restricted Triassic basin, shallow dips about a central syncline	Accumulation in alluvial channel and floodbasin environments (including levees, splays and splay complexes, and mires)	Pods of thick coal, seam splitting on edges	Low organic sulphur, pyritic to dominate. Total sulphur not that variable	Uniform within seams, higher in partings, Raw Total sulphur <0.5%
Dawson	Terrestrial, extensive areally, elongate north-south	Waterlogged environment that allowed extensive coal formation was progressively replaced by a well-drained alluvial plain	Extensive thin seam development with seam zigzag splitting and coalescing	Moderate sulphur levels, may be significant sulphate sulphur as gypsum present. Pyritic still dominant	Sulphur variable throughout seam and in adjacent partings. Raw Total sulphur <5%
German Creek	Terrestrial and shallow marine (coast). Elongate north-south	Wave tide, fluvially-influenced delta	Extensive thin seam development with seam zig-zag splitting and coalescing	High organic sulphur expected. H_2S may also be present	Sulphur highly variable throughout seams and in adjacent partings. Higher near seam roofs and floors. Raw Total sulphur <15%

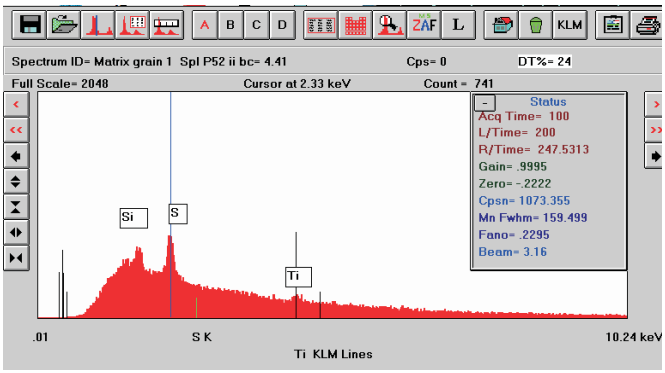

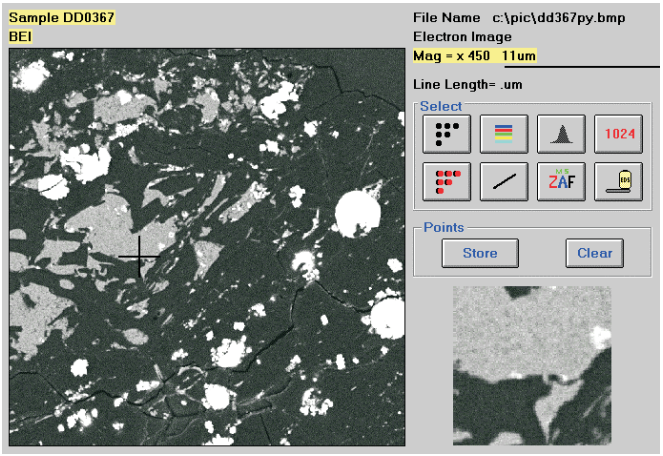

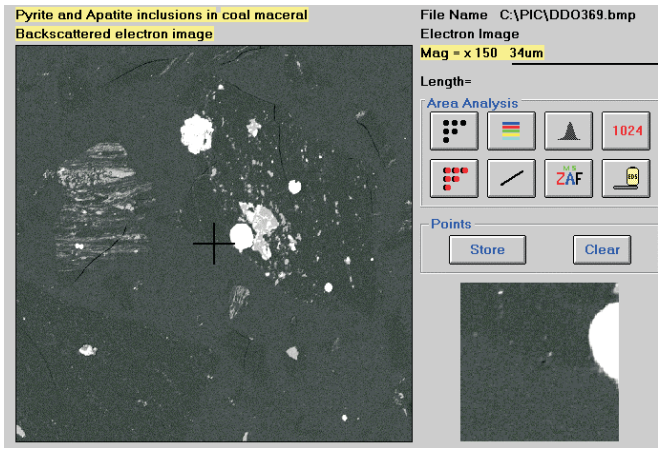

Figure 4a and b: Various backscattered images of polished coal blocks of the German Creek seam showing clays, pyrite and apatite distributed amongst coal macerals.

smaller and more widely spaced, and may not be amenable to removal by normal coal washing processes.

Also of relevance is the technique of Electron microscope energy dispersive spectra which targets particular sites on a coal polished block, to allow an estimation of sulphur organically bound to the coal structure, as shown in Table 3, below, which is from the same coal as illustrated by Figure 4, above. The value compares favourably to the published laboratory value of 0.49% (adb) for raw organic sulphur content.

Table 3: Average of 13-point counts of certain elements bound to the German Creek Seam

ELEMENT	%VOL
Na	0.004
Mg	0.028
Al	0.033
Si	0.064
P	0.005
S	0.432
Ca	0.007
Ti	0.104
Fe	0.042
C+H+N+O	99.320
TOTAL	**100.036**

Quantitative analysis of digitally recorded XRD scans provide further indications of mineral matter abundance in coal, which then provides background information during modelling. Table 4 shows the results of such an analysis for the German Creek seam for the raw coal and its washed product from an exploration borehole cored section. The seam was very slightly affected by a nearby microdiorite dyke hence the presence of some alteration products. Note the reduction in the number of minerals present, and the reduction in mineral contents, especially sulphides, carbonates, sulphides, and quartz in the washed coal. Table 5 lists the common sulphur-bearing minerals found in Australian coal seams.

DOMAINS

In reality, the variability of the resource should assessed within ‘domains’ of similar geology and within which data point spacings may need to be very different to achieve similar levels of confidence in the estimation of resources. For coal deposits ‘domains’ are likely to reflect either syn- or post-depositional conditions impacting on the coal seam. They may well impact on different critical parameters for resource estimation and require both different exploration methods and / or data point densities to achieve similar levels of confidence in the estimation of the resource (tonnage or grade). This is illustrated by Figure 5.

The examples in Table 6 illustrate some of the potential ‘domains’ that might exist within a coal lease, their impact on the geology and the type of exploration techniques that might be required to achieve comparable levels of confidence in the estimation.

STATISTICAL ANALYSES

Standard statistical analysis tools are always essential as a first pass to characterise sulphur values, spot outliers and typographical mistakes that may have been introduced during encoding. Normally 1-5 ply samples of the raw coal from the

Table 4: Borehole DD0367, German Creek, SIROQuant XRD Analyses of Raw and Clean Composite Coal

Description	Raw Coal	Clean Coal Composite	Comments
Non-Crystalline			
Coal + Amorphorous	76.0	91.7	Includes accumulated errors
Total Minerals	24.0	8.3	
Carbonates			
Ankerite	0.18	-	
Magnesite	-	0.15	
Siderite	1.61	0.11	
Clays			
Illite	2.00	0.60	
Kaolinite	3.88	3.72	Not reduced by washing
Mixed Layer	2.20	0.70	
Montmorillonite	0.52	0.35	
Hydroxides			
Boehmite	-	0.08	doubtful
Gibbsite	0.14	-	doubtful
Oxides			
Rutile	0.31	0.04	
Phosphates			
Apatite	0.70	0.10	
Silicates			
Hornblende	1.09	0.27	
Quartz	2.35	0.27	
Sulphates			
Gypsum	0.43	0.44	Not reduced by washing
Jarosite(K)	0.25	-	
Sulphides			
Marcasite	0.31	-	
Pyrite	7.20	1.10	
Salts			
Halite	0.11	-	
Minerals found	**16**	**13**	

target seam are taken and analysed (to the relevant Australian Standards) for relative density, proximate, crucible swell number, Hardgrove Grindability index, total phosphorous, and forms of sulphur. A clean coal composite of the seam is produced after processing of the laboratory float/sink washability testing.

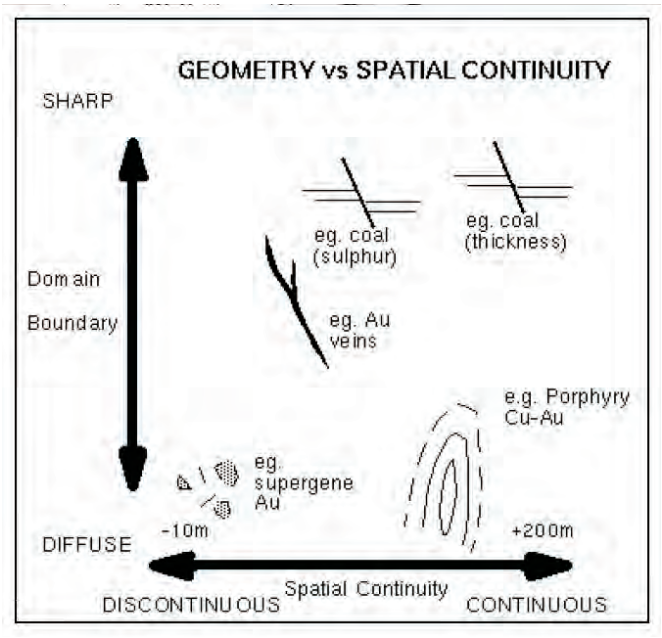

Figure 5: Concept of Domain Geometry vs Spatial Continuity, after Hanna & Cameron (1997)

Total and forms of sulphur are one of the analyses performed on this composite (see Ward, 1984 and Lowe, 1996 for a discussion on testing for sulphur). Modelling techniques such as ordinary kriging can be used from various mine planning packages to produce grid models by seam or working section for the various forms of sulphur. Though this proved moderately satisfactory for raw *in situ* data, the influence of core diameter and float/sink washing in organic liquids was also examined, as it was found that borecore size can influence the clean total sulphur result.

Figure 6 illustrates standard statistical characterisation of coal seam sulphur. It illustrates raw coal ash versus raw total sulphur for one study area and frequency histograms for other study seams.

Another standard analysis tool is shown in Figure 7, which graphs the total sulphur distribution in one of the study coals, broken down by size and float/sink density fractions. Interestingly, as the density increases, sulphur content becomes higher but more variable; however there is little correlation between the size fractions.

As some of the coals within the study area must be washed to produce a saleable product, the relationship with between the two sulphur contents is important. Figure 8 demonstrates the graphical relationship between raw and clean sulphur for the Aquila seam.

Discrepancies between raw and clean sulphur values from the models so constructed still need to be reconciled, as shown by Figure 9. This figure also demonstrates that the overall variation in clean sulphur values, as compared to its raw component also reduces. Washing the coal reduces both the sulphate and pyritic sulphur contents.

Table 5: Principal sulphur-bearing minerals identified in the study coals

	MINERAL	FORMULA	ABUNDANCE RANGE (% vol of mineral matter)
Sulphides	Pyrite	FeS_2	0–35
	Marcasite	FeS_2	0–1
	Chalcopyrite	$CuFeS_2$	trace
	Pyrrhotite	$Fe_{1-x}S$	trace
	Sphalerite	ZnS	trace
	Millerite	NiS	trace
Sulphates	Gypsum	$CaSO_4.2H_2O$	0–4
	Coquimbite	$Fe_2(SO_4)_3.9H_2O$	trace
	Halotrichite	$FeAl_2(SO_4).22H_2O$	trace
	Natrojarosite	$NaFe_3(SO_4)_2(OH)_6$	trace
	Jarosite	$KFe_3(SO_4)_2(OH)_6$	trace
	Copiapite	$Fe_{14}O_3(SO_4)_{18}.63H_2O$	trace
	after Ward (1990); Faraj (1993) ; Patterson & Marvig (1993); Patterson & others (1995); Biggs (1996)		

Table 6: Geological Domains as applied to possible Sulphur Distribution in coal seams

Environment of Deposition	Exploration Methodology	Raw Sulphur Content (%adb)	Expected Range (m)	Possible Modelling Algorithm	Anticipated Error (RMS %)
Areas of high inherent sulphur content, syn-depositional, reflects changes in groundwater chemistry in original peat swamp	Regular spacing of cored holes	0.5–12.0	100–350	Inverse distance, Mincom FEM or SMG Growth	3–5
Areas of seam splitting, syn-depositional, thickness and quality often change across split lines	Likely to require drilling to adequately define, 3D seismic may provide control of boundary of seam splitting	0.5–25	50–100	Triangulation, least squares	7–12
Areas where channels crossed peat swamp, syn-depositional, likely to impact on raw ash content of the seam and potentially on ability to beneficiate	Will require analytical data, potentially with washability by size, to evaluate. May need specialist large diameter core analyses	0.5–5	200–400	Least squares, FEM, Growth technique	3–5
Areas of sandstone roof and erosion of the underlying seam, post-depositional, irregular thinning of the seam	Close-spaced non-cored holes with down-hole geophysics for thickness determination	0–2.5	250–500	Ordinary Kriging, FEM	1–2
Areas of structural complexity (faulting), or igneous body intrusions into seam post-depositional	Detailed evaluation required confirming mineability. High-resolution 3D seismic provides best information	0.5–35	20–50 near intrusions	Triangulation, hand-contouring	10–15

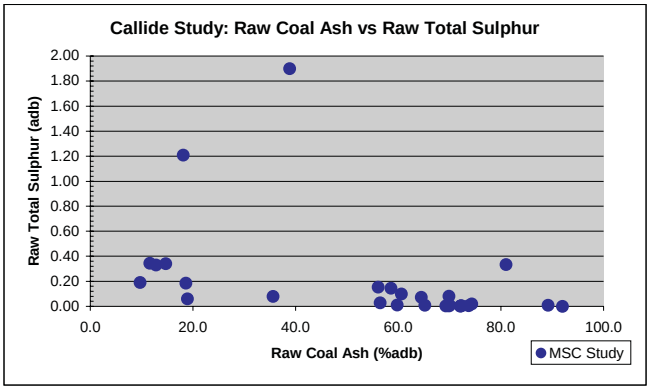

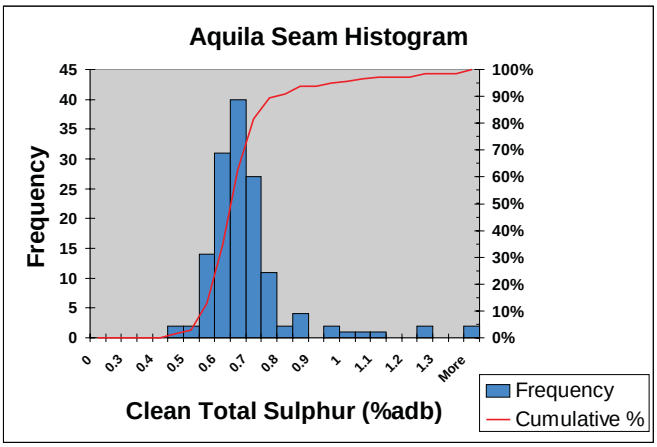

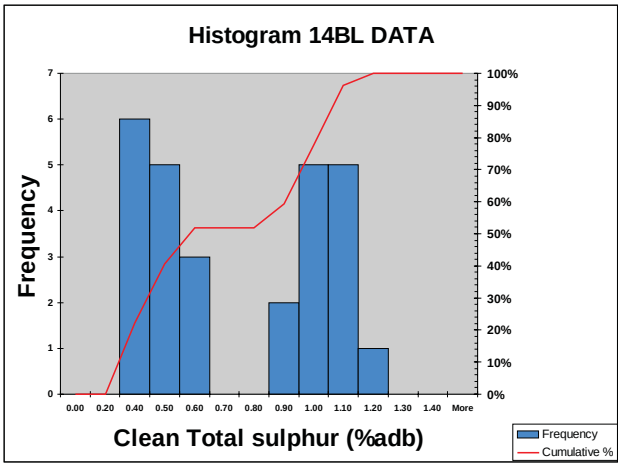

Figure 6: Standard Statistical Analyses of Coal Seam sulphur. Note the different distributions between the Aquila and BL seam

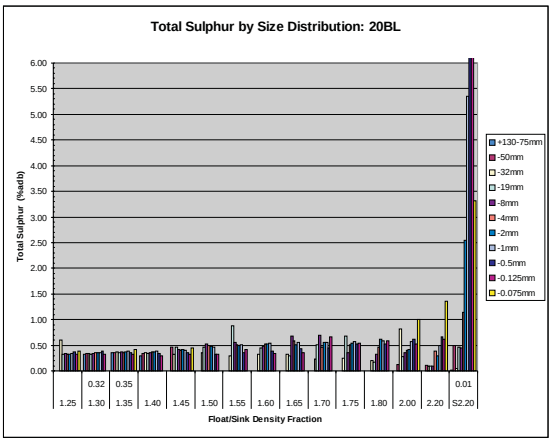

Figure 7: Total Sulphur distribution in coal Float/Sink Density fractions

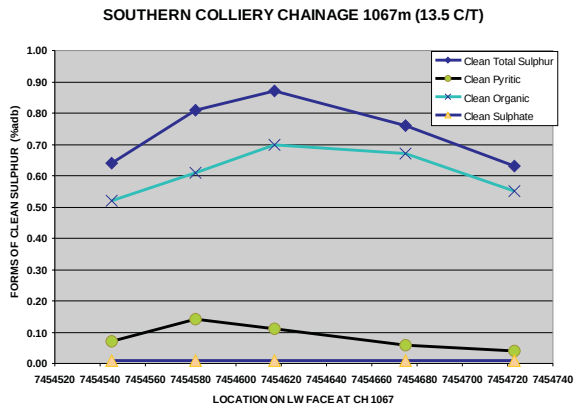

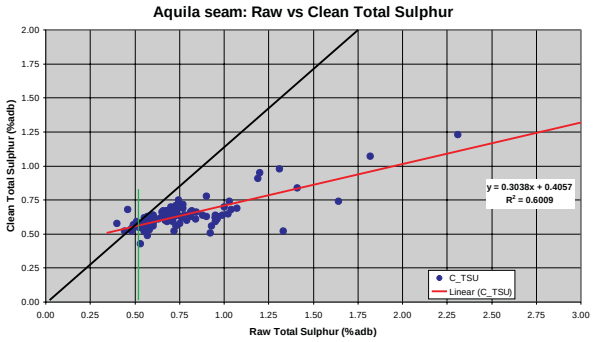

Figure 8: Correlation between Raw and Clean total sulphur for the Aquila seam. The organic sulphur breakpoint shown represents the lowest raw value at which washing will not reduce the clean sulphur value.

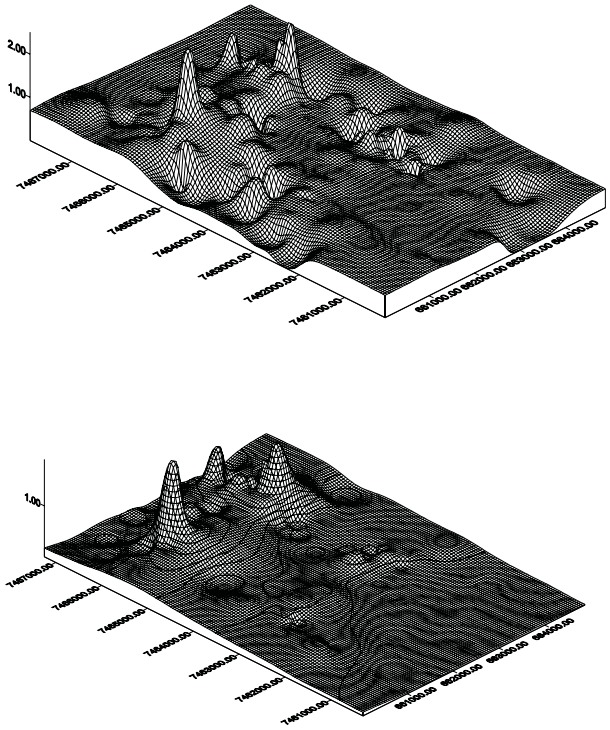

Figure 9: Comparison of ordinary kriging of raw (top) and clean (bottom) total sulphur (% adb) using the same area using the same borehole sample points. Note the reduction and variability in the clean grid.

SPATIAL CONTINUITY TESTING

Not only is it important to characterise the distribution of analysed sulphur values, but of equal importance is the spacing and spatial continuity of the sample points. It is often possible to make crude classification of deposits based on domain geometry and grade continuity, using the experience from modelling a great variety of deposits. The advantage of this approach is to establish some guidelines for what is required to build valid models for each type of deposit. This has implications both for the density of data required and the modelling methods likely to be employed. Coal from a domain sense can be regarded as highly continuous with sharp domain boundaries (Duke & Hanna, 1997).

Integral to effective coal quality modelling in this environment are techniques that have been developed to assess the adequacy of exploration borehole coverage over the lease (refer to Table 6). Borehole spacing in the north of the German Creek study area is 250m for structure and 450m for coal quality such as sulphur. At Dawson it is generally 150m for structure and 350m for quality.

Considerable thought has been given to methods to characterise the borehole coverage for structure, thickness and coal quality variables with descriptions more constructive than just holes per km^2. Two approaches were adopted. The first approach was to generate voroni tessellations (simple polygons of influence) for each borehole that intersected the Aquila seam for raw and clean coal composite total sulphur.

Figure 10 displays a plan view of the polygons generated and histogram distribution of the longest diagonal and area of each polygon.

The frequency histogram of the average radius of these polygons will give the interpreter a feeling for the underlying data point spacing, as evidenced by Figure 11, below.

The second approach was to use a set of descriptive tests devised by Swan & Sandilands (1996) to characterise data density, augmented by some tests devised by Thomas & Taylor (2000). These are generally one-sided hypothesis tests, examining the acceptance, or not, of critical chi-squared, Poisson or student-t distributions. These are separately testing for the following characteristics:

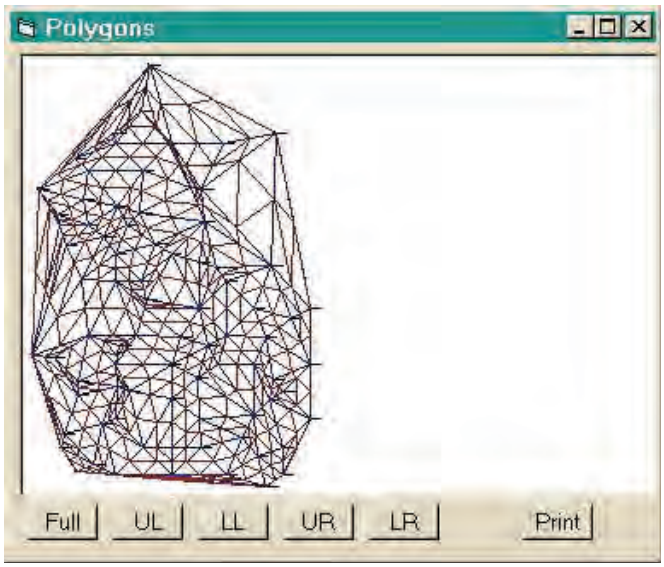

Figure 10: Aquila seam raw total sulphur, histogram of polygons of influence radii

- uniformity,
- randomness,
- clustering and regularity.

These tests for data density characterisation were described in detail by Biggs (2000a).

Hole Density and Monte Carlo Test

Software was developed for this study, which has additional output to calculate density (holes/km^2), histograms of distance to the nearest neighbour, and cell hole density.

The last test to examine hole density produces some interesting results. The essence of the test is that some optimum grid placement can be found to maximise the number of cells that have no holes, with the resultant giving a figure of merit as to how well the area is covered. The two main difficulties are deciding what cell size should be used and what is the optimal cell placement.

Initial calculations involve generating simple graphical displays such as running a user-defined rectangular-shaped window over the data in an overlapping fashion to generate

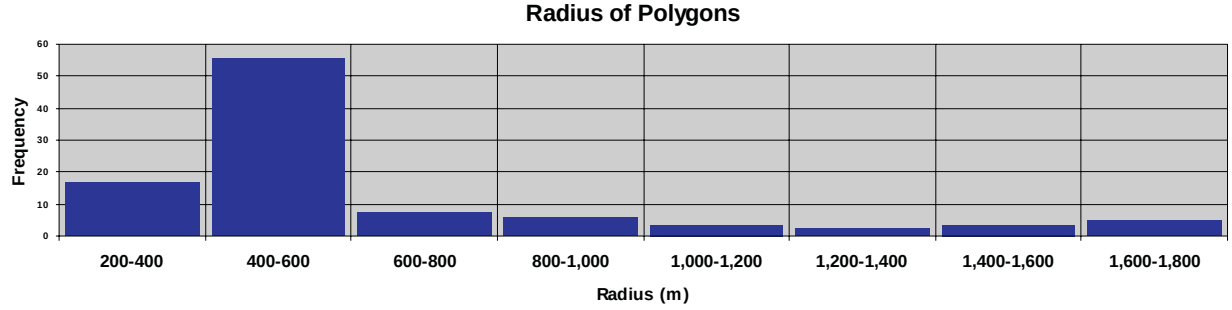

Figure 11: Aquila seam raw total sulphur, histogram of polygons of influence radii

simple moving average calculations of the parameter of interest.

In order to gauge the magnitude of anisotropy in the data variation on the Monte-Carlo test and uses a fixed cell size but varies the grid inclination in steps of 15° from 0–75°.

The program uses a cell size of 707m. This is a compromise between a small cell size which gives better results but very high granularity when holes per cell are converted to holes per km^2 and shown as a histogram; and a larger cell size which gives relatively worse resolution but reasonable density results when displayed on histograms (shown in Figure 12 below).

More advanced analysis techniques adopted are a variation on a Monte Carlo simulation. A cell of required size is added to the map area at the minimum Easting and Northing corner and then within this cell, a point at random is chosen. This point becomes the origin. By repeating the operation many times (500), the optimum grid arrangement can be established. One of the outputs of this test is the ratio of cells with no holes/cells with >1 hole per cell size (see Figure 13). This ratio is a measure of how much the reviewer may need to interpolate into empty areas and the smaller this value, the better the coverage of the project area. This value, along with the average minimum borehole spacing, is a good indicator of the density of drilling. An example of the descriptive output of these series of tests is given as Figure 13. From analysis of the program's output, Thomas & Taylor (2000) have commented upon the characteristics of the data in general:

- On the assumption that drillhole data is non-uniform, an unqualified holes/km^2 value is meaningless.
- The density distribution can be obtained by gridding the area of interest and calculating the density in each cell. The results are dependent on the cell size chosen.
- The cell size needs to be at least 5 times the average minimum hole spacing for a reasonable set of data. Smaller than this results in too many cells with zero data.
- A cell size beyond 10 x average minimum hole spacing is too coarse and the results are little more informative than just quoting an overall density.
- The number of cells with no holes is important.
- A percentage area greater than a nominated density can be obtained from the histogram outputs of the program.

DISCUSSION

Successfully modelling sulphur requires not only an appropriate gridding algorithm, but also a need to have one or more indicators such that a set of spatial data can be ranked or classed both reproducibly and without bias. Thorough analysis should summarise information extracted from the spatial data and applies additional statistical tests to quantify the nature of the data. This provides a picture of how the data varies and the level of confidence about the nature of the data. Geological domains should be established so as to allow confidence limits and 'halos of uncertainty' to be defined and applied to the relevant quality parameter. Often this is a requirement in any case if the parameter is being used to calculate JORC-standard resources and reserves.

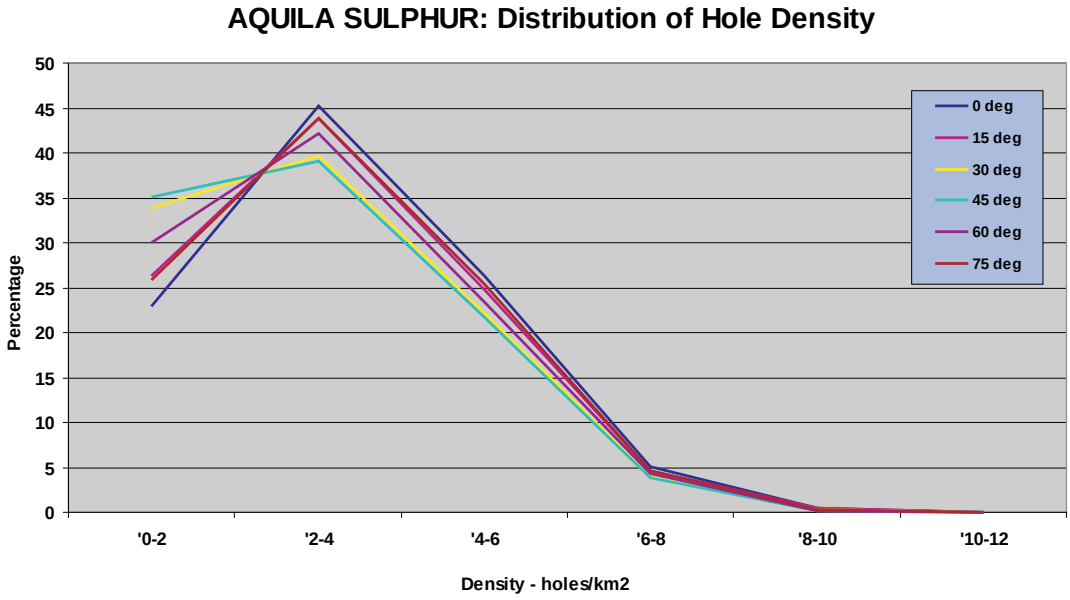

Figure 12: Variations in sample density calculations using the parameter holes per km^2 for rotated orthogonal grids 0–75°. Note the variation between densities for one quality parameter (Aquila seam raw total sulphur) above, compared to variations after various rotations for Corvus 1 seam raw ash. There are fewer data points for Corvus 1 raw ash (about ½) and the data that has been used in the model is orientated in the south-west to north-east direction.

Hole density is always a primary indicator and has been supplemented in this study with hypothesis tests for uniformity, randomness, clustering and regularity. Additional information of the sparse or otherwise nature of data is presented as the distribution of the areas of the polygons of influence. Triangulating or using least squares methods on the spatial data derives these.

The suite of tests described above does not replace geostatistics, nor in any way will it provide the depth of information that can be obtained from this technique. However it is a useful first pass classification tool because the techniques used in the tool are fixed and require no input from the user. Reproducibility and freedom from bias are automatically imposed.

Figure 14 represents the end product where raw total sulphur has been modelled for one of the study areas and is supplied with an error or confidence grid so that the end user has a feel for the uncertainty of the prediction.

CONCLUSION

Many steps are required to produce accurate coal quality models. The process followed at several Anglo Coal Australia mines has been outlined in this paper. Success depends, in part, on creating and maintaining a database where coal quality sample intervals are matched to appropriate seam or working section intervals and that 'like' sampling interval, reporting basis, and washability process are grouped and stored together. Selecting the correct modelling algorithm to generate quality grids is only half the answer. Spatial continuity in terms of borehole density and sample variability must also be accounted for, and often examination of this data allows confidence intervals to be calculated. This has taken on greater significance with the documentation required to substantiate JORC-standard resources, especially where coal quality variables are concerned.

Within the areas studied, the quality variability is predictable at the current borehole spacing except sulphur and phosphorus, which show short-range variations (i.e. <50m) in some areas. Such parameters can vary considerably in both a vertical and lateral sense within and between seams, particularly near dykes and seam washout areas. Some parameters require mapping by strip sampling in open-cuts or in gateroads to give advance warning of high spots to enable blending schedules to meet product specifications.

When it is completed, the complementary characterisation study (XRD, SEM, geophysical logging) of exploration and channel samples will enable significant updating of the existing quality database to occur. This should in turn enhance the rigorous statistical analyses of available values (by seam) carried out to date and described in brief in this paper. The combination of knowing the distribution and nature of the sulphur mineralisation and having a detailed appraisal of the spatial continuity of the sulphur sample points are essential building blocks to allow areas of high

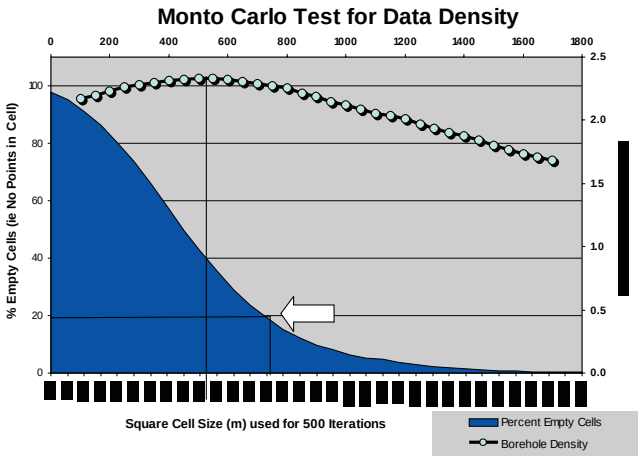

Figure 13: Monto Carlo Output to test natural data point spacing of Aquila seam raw total sulphur

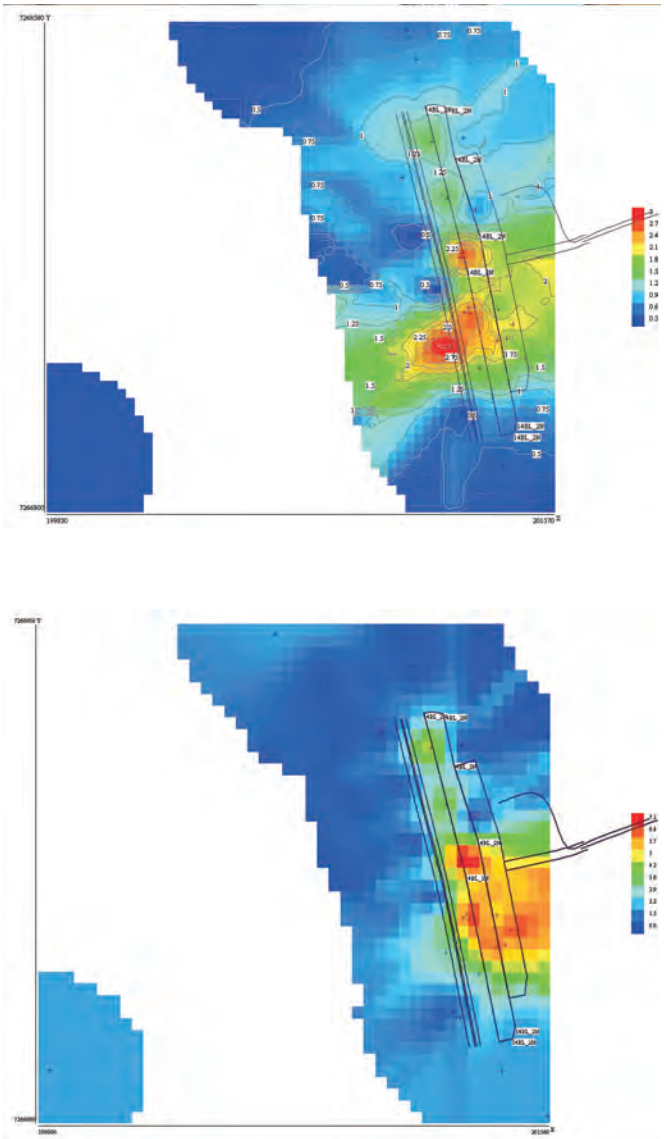

Figure 14: Raw Total Sulphur (%adb) and Anticpated RMS Error (%) gridded for seam composite of the BL seam, Dawson Mines

sulphur to be predicted in advance of mining. Eventually, a methodology for predicting sulphur mineral concentrations in advance of mining and reconciling 'as-sold' coal quality to that predicted will be developed. These prediction theories will be assessed at the coalface as mining progresses through high-sulphur zones.

REFERENCES

BIGGS, M.S., 1996: The distribution and significance of iron minerals in the Callide Coal Measures, East Central Queensland. Master of Applied Science thesis, Queensland University of Technology.

BIGGS, M.S., 2000a: Investigations into the prediction and modelling of total sulphur in coal seams, German Creek Mines, Central in Queensland. *In* Boyd, R., Diessel C.F.K. & Francis, S.: *Proceedings of the 34th Newcastle Symposium, Advances in the study of the Sydney Basin*, University of Newcastle, July 2000, 97–106.

BIGGS, M.S., 2000b: Practical data compilation and modelling of coal quality parameters for mine design at German Creek Mines, Central Queensland. *In* Beeston, J.W. (Editor): *Bowen Basin Symposium 2000 — The New Millennium — Geology*. Geological Society of Australia Inc. Coal Geology Group and the Bowen Basin Geologists Group, Rockhampton, October 2000, 163–179.

BORSARU, M., BERRY, M., BIGGS, M.S. & ROJC, A., 2003: *In situ* determination of sulphur in coal seams and overburden rock by PGNAA. *Applications of Radioactive Isotopes*, 54.

DUKE, J.H. & HANNA, P.J, 1997: Geological interpretation for resource estimation. *In: Proceedings,The Resource Database Towards 2000.* The AUSIMM Illawarra Branch, Wollongong, May 1997, 99–109.

FARAJ, B.S.M., 1993: Investigations into iron mineralisation in the Boundary Hill Coal. University of Queensland report for Callide Coalfields Pty Limited, May 1993, 1–3.

HANNA, P.J. & CAMERON, J.L., 1997: Computer database and geological modelling of Hunter Valley geology. *In, Proceedings of the 31st Newcastle Symposium on Advances in the Study of the Sydney Basin*, University of Newcastle, NSW, April 1997, 53–55.

LOWE, A., 1996: Coal Sulphur and oxides of sulphur. *In* Hart, J.H., (Compiler): *Proceedings of Workshop on Coal Characterisation: for existing and emerging utilisation technologies*. CRC for Black Coal Utilisation, University of Newcastle, February 1996, **C**, 7–12.

PATTERSON, J.H., CORCORAN, J.F. & KINEALY, K.M., 1995: Regional Studies of Carbonate Minerals in the Baralaba and Rangal Coal Measures. *Australian Coal Geology*, **10**, 4–13.

PATTERSON, J.H. & MARVIG, P., 1993: Characterisation of iron containing minerals in Callide Basin Coals. CSIRO Minerals Research Laboratories, Investigation Report CET/IR184R, 1–10.

SWAN, A.R.H. & SANDILANDS, M., 1996: *Introduction to Geological Data Analysis*. Blackwell Science, London.

THOMAS, R. & TAYLOR, M., 2000: VbSDAV1.01 — User Guide (A system to analyse spatial data using quantitative statistics), Emergent Technologies Pty Ltd user manual, January 2000, 1–15.

WARD, C.R., (Editor) 1984: *Coal Geology and Coal Technology*. Blackwell Scientific Publications, Melbourne.

WARD, C.R., 1990: Mineral Matter Analysis of Coal Samples from Callide, Queensland. Report by Unisearch for Callide Coalfields Pty Limited, University of NSW. Report no. R685, 1–21.

WARD, C.R. & TAYLOR, J.C., 1996: Quantitative mineralogical analysis of coals from the Callide Basin, Queensland, Australia, using X-Ray Diffactometry and Normative Interpretation. *International Journal of Coal Geology*, **30**, 211–229.

Mark Biggs, Chief Geologist, Anglo Coal (Dawson Management) Pty Limited, PO Box 225, Moura. QLD. 4718.
mark.biggs@anglocoal.com.au

Graham O'Brien, Kirsty Ferguson, John Kelly and Barry Jenkins

Bore core washability by coal grain analysis

Organic liquids such as perchlorethylene, bromoform and white spirits are extensively used by coal laboratories to determine the washability characteristics of coals by float/sink analysis. A significant proportion of this testing is conducted on borecore samples which are generally crushed to a topsize of approximately 12mm prior to undertaking float/sink testing. The use of these organic liquids carries a significant Occupational Health, Safety and Environmental (OHS&E) risk and can also alter some chemical assay values (i.e. coking performance, Gieseler fluidity, calorific values, chlorine content). Consequently the coal industry is searching for alternative methods for determining the washability characteristics of coal that does not use organic liquids.

Coal grain analysis uses microscopic imaging techniques to obtain routine petrographic information (maceral group composition and mean vitrinite reflectance) from polished grain mounts. This differs from other imaging methods as it also determines the area and the abundances of vitrinite, inertinite, dark minerals and bright minerals in each grain. For high rank coals (mean vitrinite reflectance >1.2%) that do not contain discernable liptinite macerals the density and ash percent of each grain can be estimated from the abundances of its maceral and mineral constituents in the grains. This information may be used to determine the washability characteristics without the use of organic liquids.

Comparative tests were conducted on two borecore samples. Washability information obtained from the coal grain analyses performed on samples prepared for petrographic analysis (-1mm) compared favourably to the washability results obtained by traditional sink float analyses for the 12.7 x 0.5mm w/w (wedge wire) and the 0.5 w/w x 0.0mm fractions of these borecores. Crushing the two borecores to a topsize of 1mm resulted in different amounts of additional liberation when compared with the yield Vs ash percent curves of the 12.7 x 0.5mm w/w fractions.

INTRODUCTION

Borecores are an integral component of coal exploration programs. They are collected to provide material for testing to establish what treatment if any is required to achieve market specification. If beneficiation is required, washability testing is done to determine the expected yield that can be expected from a particular area. Borecores are generally crushed to a top size of approximately 12mm and the 12 x 0.5mm w/w (wedge wire) fraction is generally subjected to float/sink analysis, and the 0.5 w/w x 0.0mm material tested by froth flotation.

Organic liquids such as perchlorethylene, bromoform and white spirits are currently used by coal laboratories to determine the washability characteristics of coals by float/sink analysis. The use of these organic liquids is associated with OHS&E (occupational health, safety and environmental) concerns and can also alter some chemical assay values (i.e. coking performance, Gieseler fluidity, calorific values, chlorine content). Consequently the coal industry is searching for alternate methods for determining the washability characteristics of coal that does not use organic liquids.

Petrography is traditionally used to evaluate borecores for coal rank and utilisation application (coking or thermal). Mostly this is a manual characterisation test although imaging techniques have been developed that provide maceral composition and vitrinite reflectance information. These techniques generally rely on using thresholding to discriminate between the background resin and the coal particles so that reflectance measurements are only recorded on the coal material. This means that most of the dark minerals contained within coal particles, or present as liberated minerals, and liptinites are generally removed along with the resin. The summary information obtained from a number of images is used to produce the samples reflectance distribution from which the maceral composition and vitrinite reflectance information is extracted.

An alternative imaging method called coal grain analysis has been developed for performing routine coal petrography assessment. This differs from other coal petrography imaging methods in that a mask is used to remove the pixels of mounting resin and consequently compositional information is obtained on each individual grain within each image. This technique is explained in detail by O'Brien & others (2003). For high rank coals that do not contain discernable liptinites this means that an accurate measurement of the amount of vitrinite and inertinite macerals and bright and dark minerals is made. Provided the densities of the maceral and mineral can be established then it is possible to estimate the density and hence the mass of each grain. Thus this method has the capability of determining the density distribution or washability of fine coals.

METHODS

Two borecore samples from BMA's Bowen Basin exploration program were selected by BMA Barney Point laboratory. The samples were of sufficiently high rank that they did not contain discernible liptinites. As part of their current borecore treatment method the borecores were crushed to -12.7mm and float/sink analysis was performed on the 12.7 x 0.5 w/w mm and on the 0.5 w/w x 0.0mm

fractions. Froth flotation testing was also performed on the 0.5 w/w x 0.0mm fraction. Subsamples of the entire borecores (12.7 x 0.0mm) material, which had been crushed to a topsize size of -1mm, were sent to CSIRO for assessment by coal grain analysis.

Microscopic analyses were conducted on polished grain-mounts of standard petrographic samples of the borecore using an oil immersion lens fitted to a reflected-light microscope. Microscope images were captured using the MACE™300 system for coal petrography. The images were first processed with the reflectogram program to determine the coal rank (mean vitrinite reflectance) and composition (maceral abundances) for the bulk sample. The reflectance-calibrated images were manually edited to ensure that the liberated dark minerals present in these raw coals were captured (liberated dark minerals are difficult for the image system to discriminate from the background resin) and that bridging between particles did not result in individual grains being classified as larger composite particles.

The edited images were then further processed to provide compositional and size information of each grain in each of the images. The area of each grain, its maximum and minimum dimensions and the abundances of vitrinite, inertinite, dark minerals and bright minerals in each grain were determined. The abundance of each constituent in the grain was used to sort the grains into 6 grain classes. Grains were classified as single component grains if they contained more than 95% of a component and as composite grains if they contained less than 95% of a single component.

The dominant phase in the composite grains was used to further classify the composite grains. An estimate of the volume of each grain was made from its area measurement. Detailed float/sink testing was conducted to determine maceral density and a relationship between mineral content and ash percent. The density of each grain was estimated from the abundances of its maceral and mineral constituents in the grains, and the ash percent of each grain was calculated. A full explanation of the process is contained in O'Brien & others, 2003.

RESULTS

Summary petrographic information was first obtained by initially processing the unedited image sets. The sample labelled 'CSIRO sample 1982' was of slightly lower rank (mean random vitrinite reflectance 1.31%) than the sample labelled 'CSIRO sample 1983' (mean random vitrinite reflectance 1.37%). The maceral group proportions and the reflectance distribution of all constituents in the samples are obtained during this process and if required detailed breakdown of the inertinite reflectance distribution, possibly to establish the proportion of the inertinites that are low reflecting and hence reactive during coke making can be determined.

The information for some of the grains in sample 1982 is shown in Table 1. Clearly if the grain volume and the grain density are known then it is possible to report the information on a mass percent basis and hence present the data as washability distributions. The washability distributions of the two borecore samples, determined by coal grain analysis (shown in Figure 1) demonstrate that the two coals had significantly different washability distributions. This test quantified the proportion of low density (<1.25g/cc) and high density (>2.2g/cc) material in each of the two coals. This information was not determined for the washability tests conducted by BMA Barney Point laboratory.

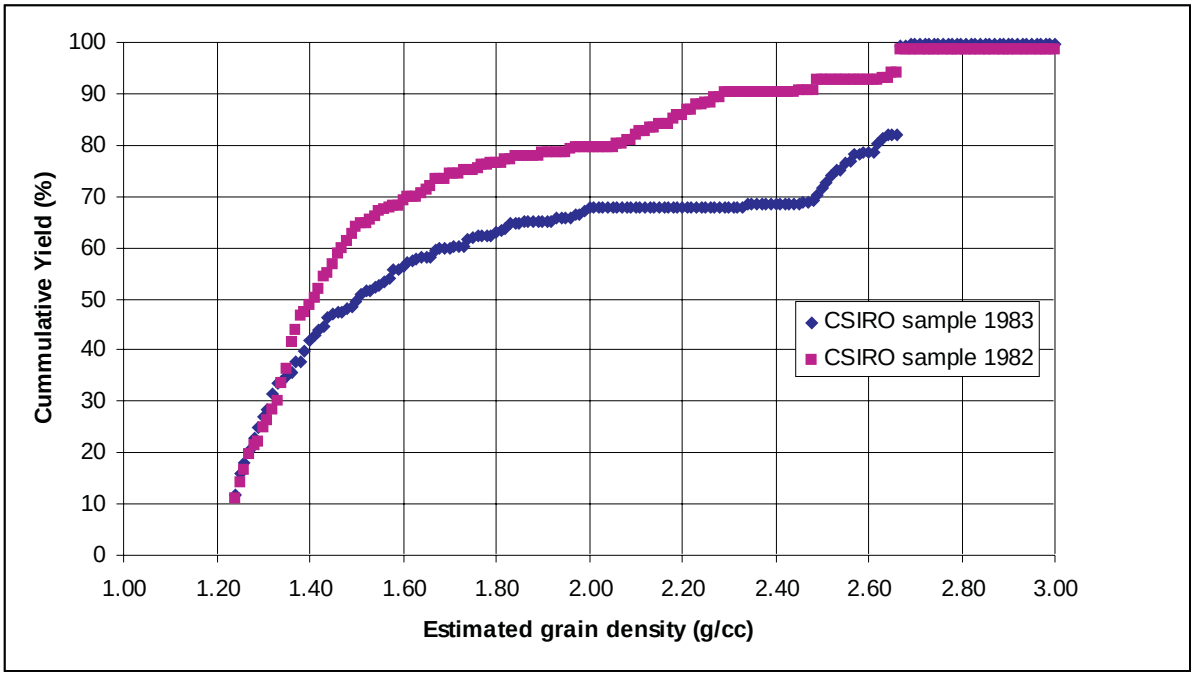

Figure 1: Washability distributions for borecore samples estimated by coal grain analysis.

Table 1: Grain information for some of the grains in CSIRO sample 1982

Raw data (pixels)					Grain composition (area %)				Calculated grain data	
Area	Vitrinite	Inertinite	Dark mineral	Bright mineral					grain	grain
pixels	pixels	pixels	pixels	pixels	% vit	% inerts	%dark mins	bright mins	density (g/cc)	ash (%)
249345	63972	169375	15998	0	25.7	67.9	6.4	0.0	1.368	10.82
3586	3586	0	0	0	100.0	0.0	0.0	0.0	1.232	0.29
73132	46122	24530	2480	0	63.1	33.5	3.4	0.0	1.302	5.96
1682	4	155	1523	0	0.2	9.2	90.5	0.0	2.533	71.95
61341	48654	7260	5427	0	79.3	11.8	8.8	0.0	1.366	14.59
243856	240739	2120	997	0	98.7	0.9	0.4	0.0	1.238	0.98
230786	158029	64942	7815	0	68.5	28.1	3.4	0.0	1.299	5.95
71699	65818	2766	3115	0	91.8	3.9	4.3	0.0	1.297	7.51
240385	28791	145220	66374	0	12.0	60.4	27.6	0.0	1.666	39.69
115392	114864	475	53	0	99.5	0.4	0.0	0.0	1.233	0.37
10373	10054	46	273	0	96.9	0.4	2.6	0.0	1.270	4.71
184	25	159	0	0	13.6	86.4	0.0	0.0	1.288	0.29
28899	28859	40	0	0	99.9	0.1	0.0	0.0	1.232	0.29
107280	624	79648	27008	0	0.6	74.2	25.2	0.0	1.640	36.83
217	206	11	0	0	94.9	5.1	0.0	0.0	1.235	0.29
150895	28934	116385	5576	0	19.2	77.1	3.7	0.0	1.335	6.45
463	452	11	0	0	97.6	2.4	0.0	0.0	1.234	0.29
1740	1740	0	0	0	100.0	0.0	0.0	0.0	1.232	0.29
3822	2573	141	1108	0	67.3	3.7	29.0	0.0	1.649	41.25
1105	0	1035	70	0	0.0	93.7	6.3	0.0	1.383	10.69
150699	147358	2931	410	0	97.8	1.9	0.3	0.0	1.237	0.75
342	342	0	0	0	100.0	0.0	0.0	0.0	1.232	0.29
297	292	5	0	0	98.3	1.7	0.0	0.0	1.233	0.29
9180	5	8882	293	0	0.1	96.8	3.2	0.0	1.341	5.63
3758	2209	1270	279	0	58.8	33.8	7.4	0.0	1.360	12.40
136375	135327	107	941	0	99.2	0.1	0.7	0.0	1.242	1.46
249	249	0	0	0	100.0	0.0	0.0	0.0	1.232	0.29
35	31	4	0	0	88.6	11.4	0.0	0.0	1.239	0.29
4	0	4	0	0	0.0	100.0	0.0	0.0	1.297	0.29
866	0	849	17	0	0.0	98.0	2.0	0.0	1.324	3.60
87811	86699	884	228	0	98.7	1.0	0.3	0.0	1.236	0.73
239791	238339	1247	205	0	99.4	0.5	0.1	0.0	1.234	0.43
115	115	0	0	0	100.0	0.0	0.0	0.0	1.232	0.29
26357	15681	9088	1588	0	59.5	34.5	6.0	0.0	1.341	10.20
113291	79972	28001	5318	0	70.6	24.7	4.7	0.0	1.315	8.07
229584	171031	50946	7607	0	74.5	22.2	3.3	0.0	1.294	5.83
242180	199594	38131	4455	0	82.4	15.7	1.8	0.0	1.269	3.39
46	46	0	0	0	100.0	0.0	0.0	0.0	1.232	0.29
53507	41350	5063	7094	0	77.3	9.5	13.3	0.0	1.428	21.13
2288	2234	27	27	0	97.6	1.2	1.2	0.0	1.250	2.29
244604	221525	18955	4124	0	90.6	7.7	1.7	0.0	1.261	3.14
19558	0	0	19558	0	0.0	0.0	100.0	0.0	2.662	69.88
94148	0	0	94148	0	0.0	0.0	100.0	0.0	2.662	69.88
245597	137115	36001	72443	38	55.8	14.7	29.5	0.0	1.664	41.84
251677	23415	205710	22538	14	9.3	81.7	9.0	0.0	1.413	14.76
226219	98886	100717	26616	0	43.7	44.5	11.8	0.0	1.429	18.96
1383	0	858	525	0	0.0	62.0	38.0	0.0	1.815	50.49
5909	2852	688	2362	7	48.3	11.6	40.0	0.1	1.816	52.45
160185	78707	59865	21613	0	49.1	37.4	13.5	0.0	1.449	21.47
251544	2328	238036	11164	16	0.9	94.6	4.4	0.0	1.357	7.67
68988	68071	354	563	0	98.7	0.5	0.8	0.0	1.244	1.67
97794	69158	19126	9510	0	70.7	19.6	9.7	0.0	1.384	15.92
2847	2847	0	0	0	100.0	0.0	0.0	0.0	1.232	0.29
251544	2328	238036	11164	16	0.9	94.6	4.4	0.0	1.357	7.67
68516	48401	6071	14035	9	70.6	8.9	20.5	0.0	1.531	31.01
3574	3534	25	15	0	98.9	0.7	0.4	0.0	1.238	1.00

The results for the washability tests conducted by BMA Barney Point laboratory are contained in Table 2. The tests conducted on the 12.7 x 0.5 w/w mm fractions were conducted as part of their routine borecore testing program and additional washability tests were conducted on the 0.5 w/w x 0.0mm fraction for this project. BMA Barney Point laboratory routinely report their washability results as recovery (yield vs ash percent) curves and the comparison of these results with the coal grain analysis are shown for CSIRO samples 1982 (Figure 2) and 1983 (Figure 3). Also shown on these graphs are the results obtained for the standard flotation tests conducted on the 0.5 w/w x 0.0 m fractions of the two borecores.

DISCUSSION

For the borecores tested the coal grain analysis method was able to determine their washability from normal petrographic samples without using organic solvents. To do this it is necessary to have reliable measurements on maceral and mineral densities and of the relationship between mineral

Table 2: Washability information determined by BMA Barney Point Laboratory

Relative Density Fraction	CSIRO sample 1982				CSIRO sample 1983			
	12.7 x 0.5mm w/w		0.5 w/w x 0.0mm		12.7 x 0.5mm w/w		0.5 w/w x 0.0mm	
	Mass%	Ash%	Mass%	Ash%	Mass%	Ash%	Mass%	Ash%
F1.35	28.6	6.0	40.7	5.8	30.2	7.0	38.1	4.8
F1.40	16.0	14.1	7.9	11.5	19.4	14.5	10.2	12.0
F1.45	8.3	19.6	5.8	16.2	11.2	20.0	6.9	15.8
F1.50	4.8	24.8	4.0	20.1	6.3	25.3	5.0	19.4
F1.55	3.5	29.8	4.5	23.8	3.6	29.8	5.3	23.0
F1.60	2.9	33.9	2.0	29.3	3.0	34.0	2.0	29.0
S1.60	35.9	73.5	35.1	66.8	26.3	67.0	32.5	63.2

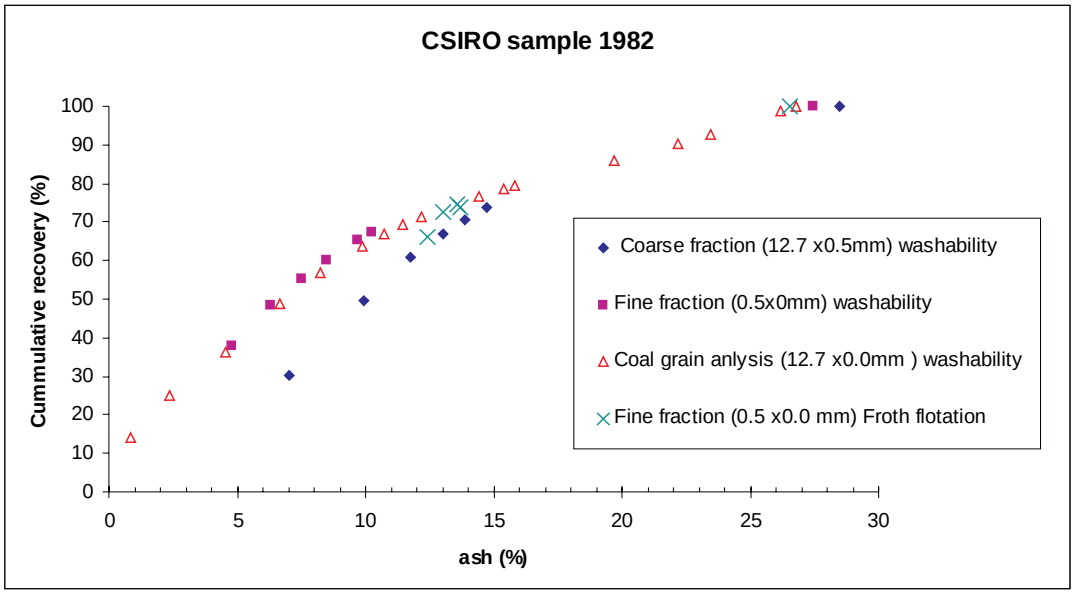

Figure 2: Comparative yield/ash percent curves for CSIRO sample 1982

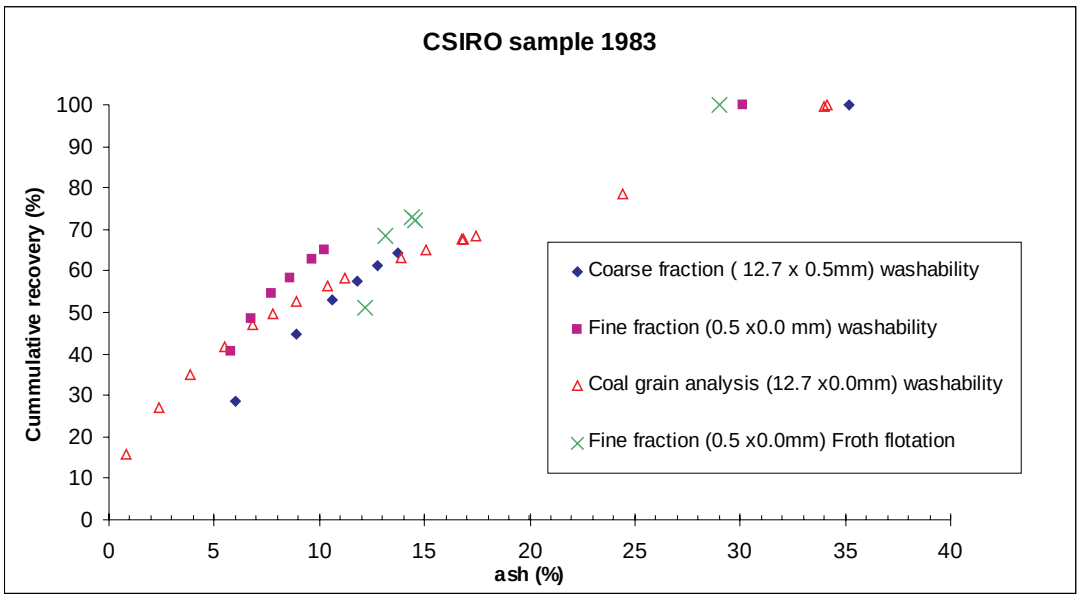

Figure 3: Comparative yield/ash percent curves for CSIRO sample 1983

abundances and ash percent. Further testing is required to extend this capability to higher and lower rank coals but the results to date are extremely promising, and differences in the yield/ash percent curves would appear to be caused by liberation issues and not by analysis methods.

For both borecores the recovery curves produced by traditional float/sink analysis for the 0.5 w/w x 0.0mm showed superior recovery to the 12.7 x 0.5 w/w mm material. These results are not unexpected as the fine fractions should have experienced additional liberation and hence show superior recoveries. The recovery curves obtained by using coal grain analysis produced on the entire 12.7 x 0.0mm fraction which was crushed to a topsize of 1mm also showed superior recovery to the 12.7 x0.5 w/w mm material.

At low ash percent values, coal grain analysis washability results (performed on the 12.7 x 0.0mm material crushed to 1mm) showed higher yield than float/sink tests performed on the 12.7 x 0.5 w/w mm fractions. For CSIRO sample 1982, the coal grain analysis result gave a similar yield/ash percent curve to the 0.5 w/w x 0.0mm fraction. This suggests that the crushing of the coal to a top size of 1mm had resulted in additional liberation, and hence higher recovery. This trend was not evident for the CSIRO 1983 sample.

For both borecores the yield/ash curves obtained from standard froth flotation tests showed significantly lower recovery to the washability results. For these two borecores the froth flotation tests did not produce a sample with an ash percent less than about 12%. This was considered to be due to the entrainment of fine minerals with the flotation product. The recovery curves obtained by using coal grain analysis, produced on the entire 12.7 x 0.0mm fraction which was crushed to a topsize of 1mm also showed superior recovery to the 12.7 x 0.5 w/w mm material.

It is not expected that crushing the borecore to -1mm prior to conducting washability tests, will replace the traditional treatment of the coarse borecore material as this part of the borecore program attempts to estimate expected liberation and yield in the coarse circuit. It does however benchmark whether further yield gains are possible. For example, further crushing of CSIRO sample 1982 resulted in a significant yield improvement whereas for CSIRO sample 1983 it did not. (For the coals that do show a yield increase the additional processing costs associated with a finer plant feed may be warranted.)

This test program highlighted that standard froth flotation testing can be of limited benefit for estimating the yield that will be obtained using column flotation technology. These devices employ froth washing and can produce low (less than 8%) ash percent products. The yield/ash percent curves produced by float sink testing provided a better evaluation of the material. Fine coal washability is seldom done as it is a relatively expensive test and may provide results of doubtful worth.

Flotation is influenced by grains surface chemistry as well as the particle size and density and hence there is some reluctance to use density information to describe a surface chemistry influenced process. Coal grain analysis provides grain chemistry as well as density information (Ofori & others, 2004) and could therefore be used to better quantify expected flotation performance than the currently used methods.

REFERENCES

JENKINS, B., O'BRIEN, G., BEATH, H. & ESTERLE, J., 2001: Automated Image Analysis System for Coal Petrographic Characterisation. ACARP Project C8056. *CSIRO Exploration and Mining Report* **809**.

O'BRIEN, G., JENKINS, B. & BEATH H, 2003: Coal Grain Analysis 2003, ACARP Project C10053.

OFORI, P., O'BRIEN, G., FIRTH, B. & JENKINS, B., 2004: Flotation Process Diagnostics and Modelling by Coal Grain Analysis, *In* Membrey, W.B.(Editor): *Proceedings of the 10th Australian Coal Preparation Conference*, Paper **C9.**

G. O'Brien, K. Ferguson,CSIRO Exploration and Mining
J. Kelly BMA, Barney Point Laboratory
B. Jenkins, Jenkins-Kwan Technology

Graham O'Brien, Sid Paterson, Mike O'Brien and John Graham

Improved coal wagon unloading by reducing loading force

Queensland Rail (QR) transports coal from Queensland coal mines to the coal ports in bottom dump rail wagons. Some coals have a propensity to be 'sticky' which hinders their unloading. Often jackhammers are needed to vibrate the wagons to facilitate unloading. The consolidating force applied to the coal during loading is a significant contributor to determining the strength of the consolidation and the position in the wagon where consolidation occurred.

A case study was undertaken at the Boonal loadout, which is located in the Blackwater system and loads coal from two mines for transport to the RG Tanna coal port at Gladstone 280km away. The unloading performance of trains carrying six coal products from the two mines loaded at Boonal between May 2003 and October 2003 (carrying approximately 1.9Mt of coal) was recorded. Each coal product carried in each of the train consist types (Stainless steel (VSA) or VSA and aluminium wagons) was evaluated separately, thereby allowing the impact of other parameters, such as loading to be assessed. The trains comprised of VSA wagons exhibited better unloading performance than the trains that also contained aluminium wagons. This was consistent with anecdotal evidence that the newer VSA wagons had better unloading characteristics (as well as carrying capacity) to the aluminium wagons.

Pilot scale laboratory testing and full scale loading trials were used to quantify loading forces and their impact on wagon unloading. Pilot scale work established that 1) loading forces increased with the drop height from the loadout slide gate to 'rail' and 2) that missing the front slopesheet so that the position of first impact was onto the wagon door significantly increased the force registered in this position.

Three audits were conducted which examined different loading methods employed at the Boonal loadout. The resultant jackhammering time required during unloading increased when the coal missed the front slopesheet and hit over the front doorset. A second consolidation force was introduced by having a varying train speed. This was thought to be due to consolidation as the result of compaction at stopped or slow speed. The effect was most noticeable when the train halted partway through the loading of a wagon.

In late 2003 the coal loading procedure at Boonal changed. This change resulted from QR requirements that wagons and their individual bogies (wheel sets) not be overloaded to the point that coal needed to be removed from the wagon before it could proceed to port. The new loading method reduced the amount of coal that was placed into each wagon by delaying wagon loading so that the position of first impact of the coal during loading was onto the front doorset of the wagon. This new loading method impacted adversely on wagon unloading.

This investigation established that the different coal products loaded at Boonal showed different unloading performances and that the VSA wagons had better unloading characteristics than the aluminium wagons. Hence improved coordination between the mines and QR to maximise the proportion of the sticky coals that are carried in the trains comprised of only VSA wagons offers the most potential benefit to reducing sticky coal impact in the short term.

Future loadouts should be designed not just to have a fast loading rate but also to minimise loading forces. This could be achieved by:

- **minimising the height of loadout slide gate above rail, and**
- **ensuring that a constant train speed is maintained during wagon loading and that the position of first impact of coal during loading is onto the front slopesheet of the wagon.**

INTRODUCTION

Queensland Rail (QR) hauls >140Mt of coal each year from >30 Queensland mines. Currently most trains consist of either 86 stainless steel (VSA) wagons or 44 VSA wagons and 56 aluminium wagons (of varying vintages and capacities). They generally take between 2–5 hours to load. Loadouts have been designed to load trains in as short a time as possible and mines have found it beneficial to install these high capacity loadouts as they reduce loading times and man hour costs.

Coal mined in the Bowen Basin for export travels through coal ports near Mackay and Gladstone in central Queensland. Coal from some mines gives varying degrees of problems with hangup during unloading and jackhammers are currently used at the ports to vibrate the wagons to generate coal discharge. This practice is labour intensive, noisy, can damage wagons and impacts on the unloading schedule of subsequent trains. Whilst trains carrying free flowing coals are generally unloaded in 2 hours, some trains can, in extreme cases, take in excess of 10 hours to unload. Coals that exhibit this characteristic are known colloquially as 'sticky coals'.

Hence, sticky coals have a significant impact on port and rail operations and on train scheduling and freight charges for the

Table 1: Unloading profiles different products loaded through Boonal between May 2003 and October 2003 (based on 1.9Mt of railed coal).

Train consist		Mine 1		Mine 2			
		Product A	**Product B**	**Product A**	**Product B**	**Product C**	**Product D**
All steel wagons	Tonnes audited	182 483	111 439	304 708	52 477	248 140	206 621
	% requiring jackhammering	75.0	30.7	56.2	14.7	24.8	32.4
	% not requiring jackhammering	25.0	69.3	43.8	85.3	75.2	67.6
	% requiring ≥15 mins jackhammering	19.0	0.0	30.8	0.0	0.0	0.0
	% requiring <15 mins jackhammering	81.0	100.0	69.2	100.0	100.0	100.0
	Longest jackhammering time (mins)	17.1	2.0	63.4	0.8	13.7	7.2
44 steel 56 aluminium wagons	Tonnes audited	172 954	146 886	323 890	48 627	270 678	345 380
	% requiring jackhammering	78.4	50.5	72.3	100.0	86.9	73.5
	% not requiring jackhammering	21.6	49.5	27.7	0.0	13.1	26.5
	% requiring ≥15 mins jackhammering	68.4	43.8	62.9	29.3	59.6	61.1
	% requiring <15 mins jackhammering	31.6	56.2	37.1	70.7	40.4	38.9
	Longest jackhammering time (mins)	198.1	49.8	287.1	29.8	103.2	54.8
10 or fewer steel wagons	Tonnes audited	12 908		25 974			6 534
	% requiring jackhammering	100.0		100.0			100.0
	% not requiring jackhammering	0.0		0.0			0.0
	% requiring ≥15 mins jackhammering	100.0		50.0			0.0
	% requiring <15 mins jackhammering	0.0		50.0			100.0
	Longest jackhammering time (mins)	105.2		40.8			12.1

mines. During 2003 and 2004, twenty five percent of the trains unloaded at the RG Tanna Coal Terminal in Gladstone required jackhammering. Gladstone Port Authority (GPA) which runs this coal terminal estimated that sticky coal costs them ~2% of annual port throughput which on an annual capacity of 40Mt equates to 800 000t a year of under-utilised port capacity.

ACARP funded research (O'Brien & others, 2002) determined that the problems associated with sticky coal were quite complex and that coal properties (size distribution, moisture content, fine clay content) and wagon properties (wagon design and material type) contributed to a particular coal's propensity to give problems during unloading. This research also found that the consolidating force applied to the coal during loading was a significant contributor to determining the strength of the consolidation and the position in the wagon where it occurred.

Although further consolidation occurred during travel, the loading force was the dominant factor in determining the strength of the consolidation that hindered unloading. Consequently it was proposed that the loading method may be modified to reduce loading force without reducing loading rate. This paper discusses ACARP funded research that tested this hypothesis.

EXPERIMENTAL

Benchmarking current loading practice

Fieldwork was conducted at the Boonal loadout. This loadout is located in the Blackwater system and loads coal from two mines producing in total six different coal products for transport to the RG Tanna coal port at Gladstone 280km away. The unloading performance of trains carrying six coal products from the two mines loaded at Boonal between May 2003 and October 2003 (carrying ~1.9Mt of coal) was recorded. The wagon makeup of each train and the coal product it was carrying was recorded.

The amount of jackhammering required during the unloading of a train was used to quantify coal unloading performance. GPA had previously established that trains that required in total more than 15 minutes of jackhammering (as measured by their data logging system) impacted adversely on port operations. Two simple indices were used to quantify unloading performance for each of the different products carried in the different train consists. The first used the percentage of coal carried that required jackhammering and the second was the percentage of coal that was contained in trains that required more than 15 minutes of jackhammering (for the whole train) during unloading (Table 1).

The data obtained enabled each coal product carried in each of the train consist types to be evaluated separately, thereby allowing the impact of other parameters, such as loading to be assessed. Clearly the trains comprised of only the steel VSA wagon classes exhibited better unloading performance than the trains that also contained aluminium wagons. This was consistent with anecdotal evidence that the newer VSA wagons had better unloading characteristics (as well as carrying capacity) to the aluminium wagons.

Figure 1: Pilot/ laboratory scaled loadout with the hopper slide gate located 7m above rail

LABORATORY RESEARCH

A pilot scale 'train loadout and slope sheet and door model wagon' was constructed by QR Redbank workshop for this project. During the loading tests 150km of coal was dropped from different heights between 4–7m 'above rail'. A plastic skirt was used to control dust loss during the loading experiments (Figure 1). Three accelerometers mounted on the front slope sheet of the model wagon and a fourth accelerometer mounted on the wagon door were used to profile loading force. The position of the wagon with respect to the hopper outlet was able to be orientated so that the slide gate opened parallel to the wagons direction of travel (as shown in Figure 1) or perpendicular to the wagons direction of travel. The slide gate of the loadout chute was

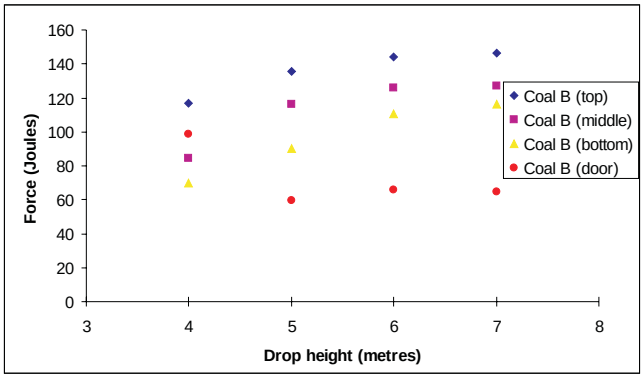

Figure 2: Force vs drop height for coal B

hydraulically controlled which enabled the speed of the slide gate opening to be varied.

Tests were conducted using the mine 1 product B coal. The relationship between drop height and loading force showed an increasing force with drop height for the three different positions on the front slopesheet, but not for the accelerometer placed on the wagon door (Figure 2).

Tests were also conducted whereby the position of first impact of the coal into the wagon was varied (top of, the middle of, and missing the slope sheet) whilst drop height was kept constant at 5m. Further experiments were carried out by dropping the coal onto the middle of the slope sheet with a slower opening time. These tests were all conducted with the slidegate opening parallel to the direction of travel of the rail wagon. Tests were also conducted with the slidegate orientated at right angles to the direction of travel of the rail wagon. The results from these experiments (Figure 3) indicated that:

- Hitting the top of the slopesheet instead of the middle of the slopesheet resulted in a lesser force being registered on the wagon door than when the middle of the slopesheet was hit.
- Missing the front slopesheet so that the position of first impact was onto the wagon door significantly increased the force registered in this position.
- The speed of opening of the slidegate showed no statistically discernible difference in force profile.
- The orientation of the slidegate (parallel or perpendicular to the direction of wagon travel) gave similar force profiles.

These tests were undertaken to replicate the initial impact obtained during wagon loading. Clearly delaying the loading sequence so that the front slopesheet is missed entirely has a major impact on the force registered on the door. Hitting the top of the slope sheet gives a small force on the wagon door. When the initial impact is at the top of the slope sheet it also allows some of the coal to strike other positions on the slope sheet before coal is dropped onto the wagon door. Consequently a bed of coal is built up over the doorset area before the wagon progress allows coal to drop directly above the door. This could reduce the amount of consolidation in the door area.

Although the orientation of slidegate door and the speed of its opening has no impact on the force profile generated by the first coal drop, these factors can influence the opportunity of placing the coal onto the top of the slopesheet. Opening the slidegate parallel to the direction of travel of the wagon, and away from the engine, makes it easier to place coal onto the top of the slope sheet, than a slidegate that opens at right angles to the line. Similarly an initially slowly opening slidegate would give the loadout operator confidence to hit the top of the slope sheet without necessarily overloading the wagon.

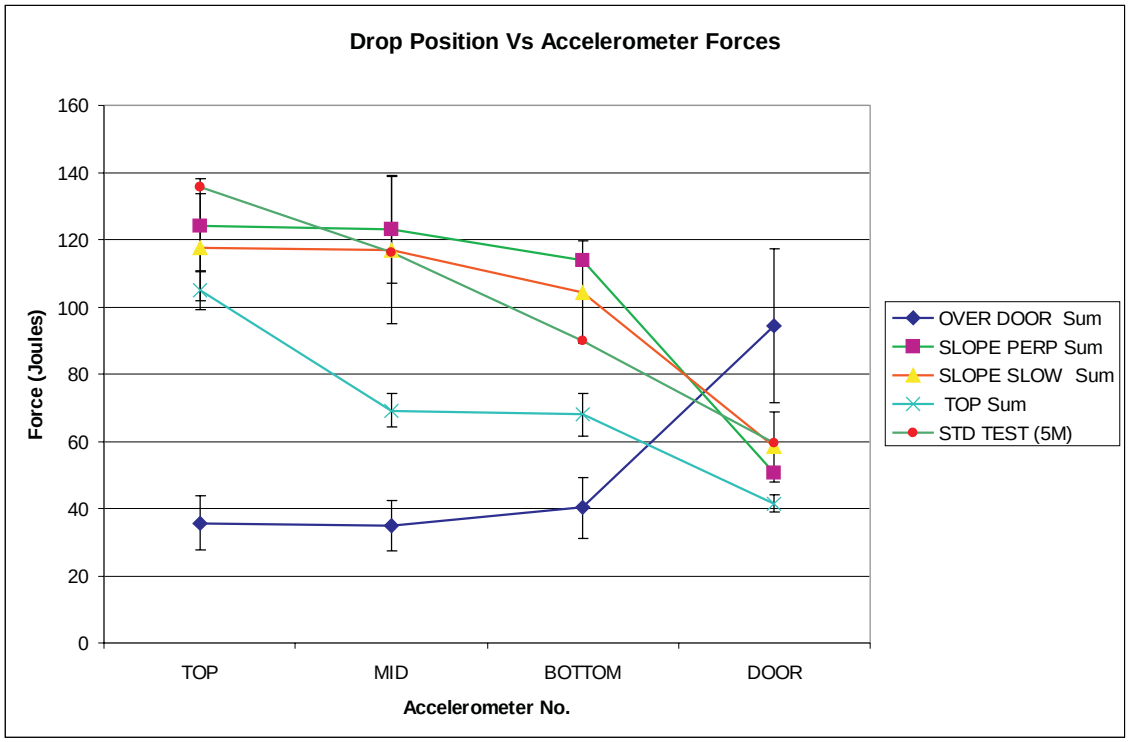

Figure 3: Force recorded at the different positions on the front slope sheet and on the wagon door when different loading methods were used with a 5m drop height.

LOADING TRIALS

The loading of three trains comprised of 44 VSA (stainless steel) wagons, and 56 aluminium wagons were audited at the Boonal loadout. These audits tested different loading methods where the position of first impact of the coal was onto the middle of the front slope sheet, the top of the front slope sheet and over the first doorset of the wagon.

The different coal product used for audits two and three required less jackhammering during unloading than the coal of audit one but showed similar trends for the different loading methods. The amount of time that jackhammers were used was manually recorded for each wagon during each of the three audits. Jackhammering was not required during the unloading of any of the VSA wagons, whereas some of the aluminium wagons required jackhammering. The results showed that when the coal missed the front slope sheet and hit over the front doorset the jackhammering time increased for the individual wagons. This audit also showed that the wagons at the end of the train required more jackhammering than the first 15 aluminium wagons (46 to 60) that were similarly loaded.

The average jackhammering time for the wagons loaded by the different methods (Figure 4) demonstrate that the first 15 aluminium wagons (46 to 60) needed less jackhammering than all subsequent wagons in the trains. For audits one and two the wagons that were loaded so that the coal's initial impact was over the front doorset required most jackhammering. For audit three the additional consolidation caused by halting the train during the loading meant that there was not a reduction in jackhammering for the last 10 wagons (when the coal hit the middle of the front slope sheet).

The two loadout operators that were on duty at Boonal when these audits were conducted had both observed that the speed of the train during loading could become variable when the engines commenced descending the grade in the track. Surges in speed meant that sometimes the loadout struggled to fully load a wagon whereas at other times a wagon could become stationary under the loadout for short periods of time. Whilst the train was stationary coal cannot flow into the wagon and the coal in the hopper can apply a second consolidation force to the coal in the wagon. The position within the wagon (i.e. the front, middle or rear of the wagon) where this additional consolidation force was applied was dependent on where the wagon stopped in relation to the loadout chute.

Assessing train unloading performance whilst a different train loading method was used

It was our intention to trial a loading method that would result in the coal first loaded into the wagon consistently hitting high up on the slope sheet of the wagon. Laboratory tests had demonstrated that this would reduce the force applied over the front door, and hence reduce consolidation that impedes unloading.

In late 2003 the coal loading used at Boonal changed. This change was brought about because of QR requirements that wagons and their individual bogies (wheel sets) were not to be overloaded. If overloading occurred the loadout was required to remove coal from that wagon before it could

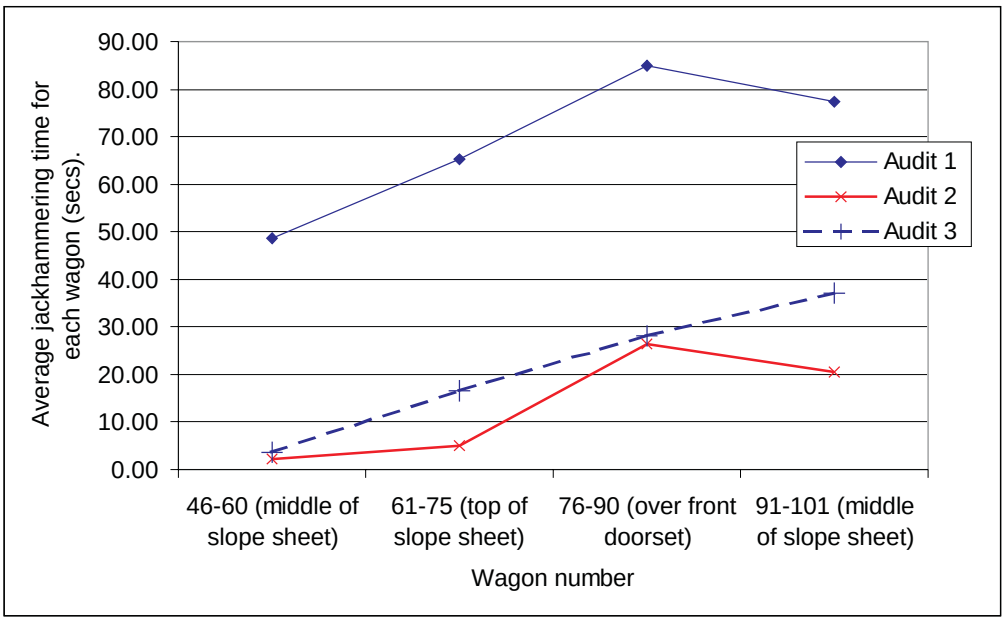

Figure 4: The average jackhammering time for each wagon loaded by different methods for the three audits.

proceed to port. The loading method that was introduced reduced the amount of coal that was placed into each wagon and achieved this by delaying wagon loading so that the position of first impact of the coal during loading was onto the front doorset of the wagon.

Between January and June 2004, 1.7Mt of coal was loaded at Boonal with this new method. CQPA recorded jackhammering requirements for the unloading of Boonal trains and the information was used to determine the unloading performance of each of the products from the two mines that was carried in the trains with different wagon consists (Table 2).

This information confirmed that the VSA wagons were less likely to cause hang up during unloading then the aluminium wagons and established that the new loading method had impacted adversely on wagon unloading. The percentage of coal that was unloaded from wagons that required more than 15 minutes of jackhammering per train highlighted that the new loading method had impacted adversely on unloading (Figure 5).

Table 2:. Unloading profiles of different products loaded through Boonal between January 2004 and June 2004 (based on 1.7Mt of railed coal)

Train consist		Mine 1		Mine 2			
		Product A	Product B	Product A	Product B	Product C	Product D
All steel wagons	Tonnes audited	59 182	81 936	47 699	34 386	61 052	259 703
	% requiring jackhammering	66.1	24.9	57.2	19.8	55.4	25.6
	% not requiring jackhammering	33.9	75.1	42.8	80.2	44.6	74.4
	% requiring ≥15 mins jackhammering	0.0	20.0	0.0	0.0	20.1	0.0
	% requiring <15 mins jackhammering	100.0	80.0	100.0	100.0	79.9	100.
	Longest jackhammering time (mins)	9.3	2.1	14.1	2.2	18.0	8.7
44 steel 56 aluminium wagons	Tonnes audited	262 675	89 024	61 431	33 760	341 070	376 048
	% requiring jackhammering	94.8	61.1	65.8	39.1	74.9	94.8
	% not requiring jackhammering	5.2	38.9	34.2	60.9	25.1	5.2
	% requiring ≥15 mins jackhammering	100.0	89.6	69.2	0.0	65.2	52.7
	% requiring <15 mins jackhammering	0.0	10.4	30.8	100.0	34.8	47.3
	Longest jackhammering time (mins)	259.4	45.2	97.8	8.9	120.2	30.5
10 or fewer steel wagons	Tonnes audited	7 000	0	0	0	25 821	19 596
	% requiring jackhammering	100.0				25.0	100.0
	% not requiring jackhammering	0.0				75.0	0.0
	% requiring ≥15 mins jackhammering	100.0				25.0	33.3
	% requiring <15 mins jackhammering	0.0				75.0	66.7
	Longest jackhammering time (mins)	107.4				28.8	15.3

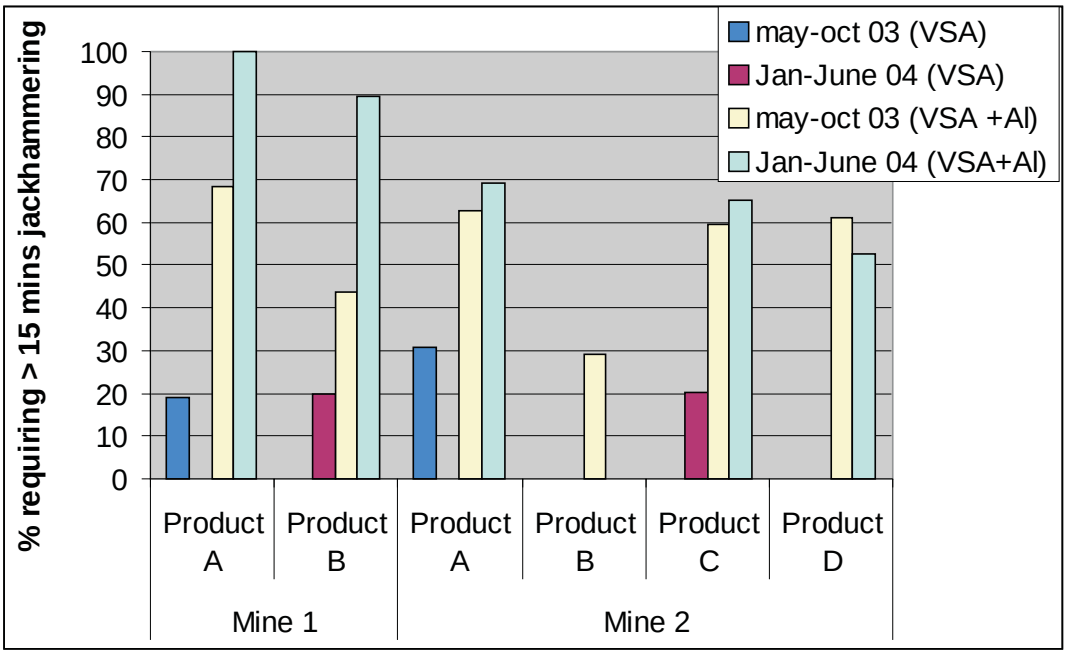

Figure 5: Percentages of coal that was unloaded from wagons that required more than 15 minutes of jackhammering.

DISCUSSION

The laboratory experiments established that there are two simple ways for reducing loading forces. These are to:

- Reduce drop height
- Ensure that coal strikes the front slope sheet of the wagon.

These tests quantified the force of the first impact of coal on the wagon and it is recognised that wagon loading is more complicated than a single loading impact force.

The reduction of drop height may not be easily achieved at existing loadouts but should be considered a priority for the building of new or replacement loadouts.

Overloaded wagons cause operational and safety issues for QR and loadouts are now required to ensure that individual bogies are not overloaded. Boonal has limited facilities to remove coal from overloaded wagons and the loading method was modified to reduce the possibility of bogies and wagons being overloaded. This method resulted in wagons being, on average, two tonnes under their desired weight and increased the problems associated with poor unloading performance. This highlights that a change in one part of the coal supply chain can impact on other parts of the chain. The underloaded wagons means that the trains loaded with this conservative method may be up to 200 tonnes underweight.

The optimum loading method (that was identified by laboratory testing) for Boonal required the initial impact during loading to be high up on the slope sheet. This does not increase significantly the frequency that the VSA wagons were overloaded, but due to their smaller size and hence tolerances it significantly increased the frequency with which the aluminium wagons are overloaded. For the loadout operators to revert to the previously used loading method (where the middle of the slope sheet was hit) or to the recommended method of hitting the top of the slope sheet will require QR to review their restrictions with respect to bogie weight limits.

The last 10 aluminium wagons (91 to 101) required more jackhammering than the first 15 aluminium wagons (46 to 60) even though they had been loaded in a similar way. This may be due to varying train speed during loading.

It is apparent that the different coal products from Boonal had different unloading performances. During the two audit periods in 2003 and 2004, on average about half of the trains were comprised of 86 VSA wagons and the other half had 44 VSA and 56 aluminium wagons. Clearly it would be desirable to have the bulk of ‘sticky’ coal loaded at Boonal carried in the trains comprised of VSA wagons, leaving the bulk of the “less sticky” coals to be carried in the trains comprised of VSA plus aluminium wagon trains. This does not mean that more trains comprised entirely of VSA wagons would be needed to service the Boonal loadout (although this would obviously help) but rather to make better use of the VSA wagon trains that do go there. This would require an additional level of logistical planning so that trains were consigned and matched to each coal product loaded at Boonal.

At Boonal six different coal products are loaded. To reduce the possibility that individual wagons and its bogies are not overloaded the current loading method is to drop the coal onto the front doorset of the wagon. Varying from this method would result in more coal being placed into the front half of the wagon, and if overloading occurred would require the removal of coal. This could be overcome if QR relaxed its overload limit for the first bogie of the smaller aluminium

wagons thus giving the loadout operators some scope to modify loading method.

CONCLUSIONS

Changing loading methods can alter the unloading characteristics of coals. In this instance for the Boonal loadout the change that had been implemented resulted in an increased need for jackhammering during unloading. The different coal products at Boonal (and probably other loadouts) show different unloading performances. Improved coordination between the mines and QR could maximise the proportion of the sticky coals that are carried in the trains comprised of only VSA wagons. This offers the most potential benefit to reducing sticky coal impact. Better train scheduling would offer significant improvements because the improved matching of wagon type to coal products (and not just to a mine) would reduce the percentage of the stickiest coals carried in the aluminium wagons.

Future loadouts should be designed not just to have a fast loading rate but also to minimise loading forces. This could be achieved by minimising the height of loadout slide gate above rail and ensuring that a constant train speed is maintained during wagon loading and that the position of first impact of coal during loading is onto the front slopesheet of the wagon.

ACKNOWLEDGMENTS

We would like to especially thank Siva Gnanananthan (QR Coal and Mainline Freight) for the assistance that he has provided. The contributions of Peter Crawford (Boonal Loadout), Caroline Camilleri (QR Coal and Mainline Freight) and Douglas Nemeth and Clint McNally (CSIRO Energy Technology) are also acknowledged.

REFERENCES

O'BRIEN, G., O'BRIEN, M., FIRTH, B., NEMETH, D., GRAHAM, J. & GNANANANTHAN, S., 2002: ACARP project C10061: Problems of Discharging Qld Coals from Bottom Dump Rail Wagons.

O'BRIEN, G., PATTERSON, S., O'BRIEN, M. & GRAHAM, J., 2004: ACARP Project C1206: Improved Coal Wagon Unloading by Reducing Loading Force.

G. O'Brien, CSIRO Exploration & Mining
S. Paterson, Central Qld Port Authority
M. O'Brien, CSIRO Energy Technology
J. Graham, Queensland Rail Rollingstock Engineering Division

Andrew Bowden

From exploration to audit: Build confidence in your coal resource using Evidence Support Logic (ESL)

Evidence Support logic (ESL) is a decision support method that has application to decision issues where uncertainty is a major factor. This means just about everywhere in the geosciences where geological models provide either the basic framework for the development and parameterisation of higher level process and risk assessment models (engineering and environmental projects) or are the primary justification for a major development project (in exploration and mining). In mineral exploration, there are several decision points, associated with different levels of uncertainty and risk, between the identification of a potentially mineable resource and the submission of a Final Reserve in accordance with JORC code. Evidence Support Logic (ESL) provides a methodology for examining the support base and exposing the key uncertainties at each stage in the estimation process. Confidence in the reserve estimate is built through the strategic targeting of future work on those key risk areas. In this paper I review the basis of the ESL method in the context of mineral exploration and present a number of examples to demonstrate the application of the method at different stages in the development of an exploration programme.

UNCERTAINTY AND RISK: EVIDENCE AND PROBABILITY

All geological models are inherently uncertain constructed inevitably from sparse, incomplete and sometimes inconsistent, data. The cartoon in Figure 1 illustrates the two sides of the opportunity-risk choice presented by lack of complete information.

In the initial stages of exploration the focus is on the opportunity for discovery of a deposit presented by uncertain knowledge. Interestingly in the exploration context uncertainty is not just a good thing, it is essential. By separating the upside uncertainty-opportunity from the downside risk we create a real option that has value.

Furthermore, the capability to obtain extra information adds significant additional value due to the possibility for reducing downside risk and capturing upside potential. As exploration progresses and we become a) technically committed to a particular geological model-reserve scenario, and b) financially committed to a go-no go mining decision we become locked into downside risk. That is, the risk of either under or over investment. However, we cannot deal with 'risk' unless we have a good understanding of uncertainty in all its forms.

In exploration terms we can formulate the uncertainty as illustrated in Figure 1 "Is it the tail of an elephant or the tail of a mouse?" All we see in terms of data to inform our assessment is the tail. The available data provides evidence that may be positive or negative or, more likely, partially positive-partially negative, and with differing degrees of quality and relevance. The explorationist's job is to examine the evidence provided by the 'tail' and make a justified recommendation on whether or not the tail is worth tugging. This should not be a probabilistic assessment – the probabilistic assessment requires us to close down the uncertainties by making a judgement about whether the 'unknowns' fall on the positive or negative side with respect to the decision issue. Of course, this is what management want us to do — to close down uncertainty — but more often than not this yearning for certainty pushes us to come up with a single answer that depends more on our risk attitude than on relevant evidence and obscures the line between what is known and what is not known (Figure 2).

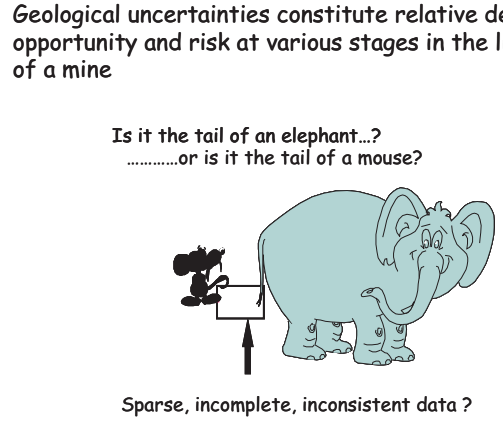

Figure 1: Uncertainty - or risk

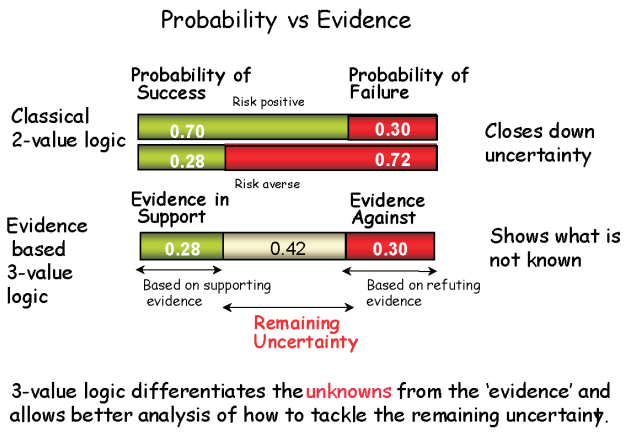

Figure 2: Probability vs Evidence based reasoning

If we take a step back from the two-value logic of probability and allow ourselves: a) to ascertain the balance of evidence, and b) to identify uncertainties explicitly, we can give ourselves a much better opportunity of understanding the level of support for our models and of using the type and nature of the uncertainties to improve the quality of our decisions.

Uncertainty can arise in a number of ways (Bowden, 2004b):

- Incomplete information about the system — our sampling of the system is inadequate,
- incomplete understanding—- we may have data and information but we don't know what it means,
- uncertain quality of data — we have information but we don't know whether it can be trusted,
- uncertain relevance — we have information but it doesn't address the issues,
- conflict — we have information from different sources that points us in different directions, or
- variability — we have information but it does not give a clear answer.

If we have a method for identify and discriminate between, the different sources of uncertainty and if we can quantify their impact through sensitivity analysis and what-if? scenarios then we may well choose very different means of progressing future work. For example, in an exploration context, we may focus future work much more specifically to target reduction of a specific type of uncertainty that has been shown through the ESL study to have the most impact on the success or failure of the prospect.

Evidence Support Logic – Constructing the ESL model

Evidence Support Logic (Bowden 2004b) provides us with a structured method for evaluating evidence and uncertainty that enables us to measure the value of information in a meaningful way. There are several steps required to develop an [1]ESL decision model; these are developed below with reference to a fairly simplistic example (Figure 3). The example in Figure 3 examines some of the technical and commercial aspects of evaluating an area considered prospective for coking coal. The framework shown in Figure 3 is neither unique nor definitive; it is used merely as an example of the top-down logic used to examine support for the top-level hypothesis.

Step 1. Identify and describe the hypothesis/model that is to be evaluated. For the model in Figure 3 we wish to test support for the hypothesis that a particular prospect is suitable for mining coking coal in an open-pit.

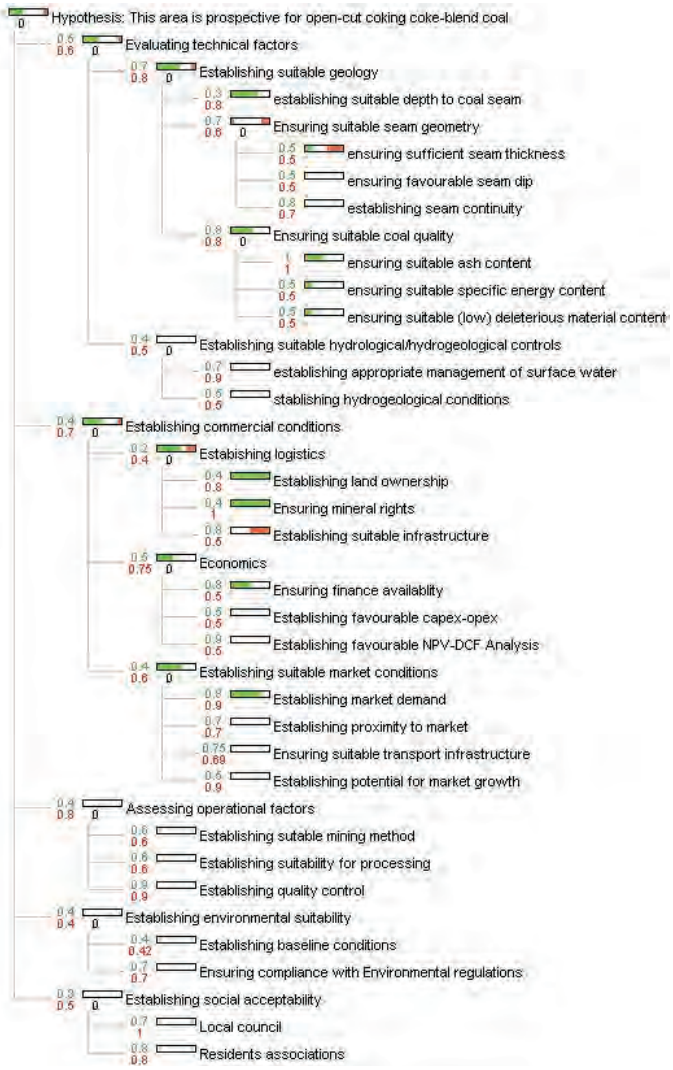

Figure 3: Decision Plot for the evaluation of open-cut coking coal prospectivity

Step 2. Construct a framework that includes all the 'processes' that contribute to testing the hypothesis. Framing the decision issue is extremely important – there is no 'correct' solution but is essential to be as inclusive as possible in order to satisfy all who will be affected by the decision that all relevant events and processes have been taken into account.

Step 3. Develop the framework to a level at which individuals (experts and lay persons) would be willing to provide judgments of evidence on the likelihood of success and failure of a contributing process.

Step 4. Develop the inference logic that describes the relationships between contributing processes. Three inference parameters are required to control the propagation for each process:

- 'sufficiency' — a parameter with range between 0 and 1, the value of which effectively weights the contribution of a process to the success or failure of

1 The ESL method is supported by TESLA software developed by Quintessa Limited in the UK and available as a download from the TESLA website http://www.quintessa-online/TESLA/

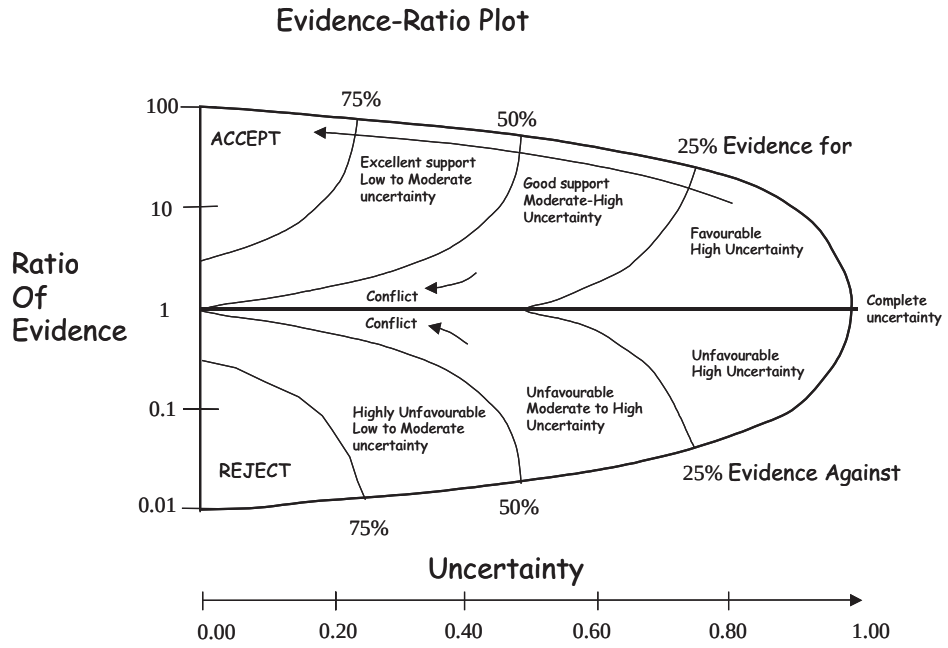

Figure 4: The basics of the Evidence-Ratio Plot

the parent process. Sufficiency values may be assigned separately for success and failure (Figure 3). The sufficiency values for several child processes contributing to the same parent process are not normalised i.e. they do not have to sum to unity as it is possible to have more than enough evidence to support a belief in the success or failure of a particular process.

- 'dependency' — a parameter with range between 0 and 1, the value of which is subtractive in effect and allows for double counting of evidence. A value of 0 signifies independence, a value of 1 indicates total dependence.
- 'necessity' — a 'red flag' parameter which overrides the normal propagation algorithm for processes considered as essential to the success of the higher level process and which is activated when supporting evidence for the process falls below 50%.

Step 5. Elicit judgements of evidence and uncertainty

Thus far we have constructed the generic model that will be used to test the hypothesis. Application of the model to a particular site requires judgements of evidence in respect of the lowest level processes contributing to the model. Judgements of evidence can be elicited in several ways: the approach recommended here involves separate elicitation of 'evidence in support' and 'evidence against' using qualitative linguistic judgements that are subsequently converted to numbers via a utility function.

In practice, linguistic scales help geoscientists and engineers to express their individual subjective belief in the various processes. It is recommended that, in the first instance, judgement is made on the face value of the information available assuming that the information is of high quality with subsequent modification of that judgement based on checks for quantity and quality of the information. (see Bowden, 2004b for details).

Step 6. Run the model. Evidence provided at the lowest level of the process tree is propagated through the model to provide a measure of support for the top-level hypothesis. The propagation algorithm derives from Interval Probability Theory (IPT), an approach to evidential reasoning developed at Bristol University. Readers interested in the full mathematical formalism of IPT are referred to the original research (Cui & Blockley, 1990). At a basic level the IPT propagation is the algebraic summation of evidence such that the result is always equal to or greater than the largest contributing value. The effect is additive such that two or more lines of evidence that support (or refute) a hypothesis reinforce each other sp that their combined evidence is more supportive than either piece of evidence taken individually (Bonham-Carter, 1994).

Step 7. Evaluate the outcome. Examine the Ratio plot. Carry out sensitivity analysis. Examine Tornado Plot to identify high impact processes.

(For a more detailed description of the ESL method the reader is referred to Bowden, 2004(a) and (b)).

Evidence Support Logic — Analysing the Outcome

The Evidence-Ratio Plot

As with most tree-models the logic tree for a 'real-life' ESL model can be very large and difficult to visualise in 'tree' form requiring scrolling on computer screen or large paper output in hardcopy. The evidence-ratio plot (Figure 4 (see

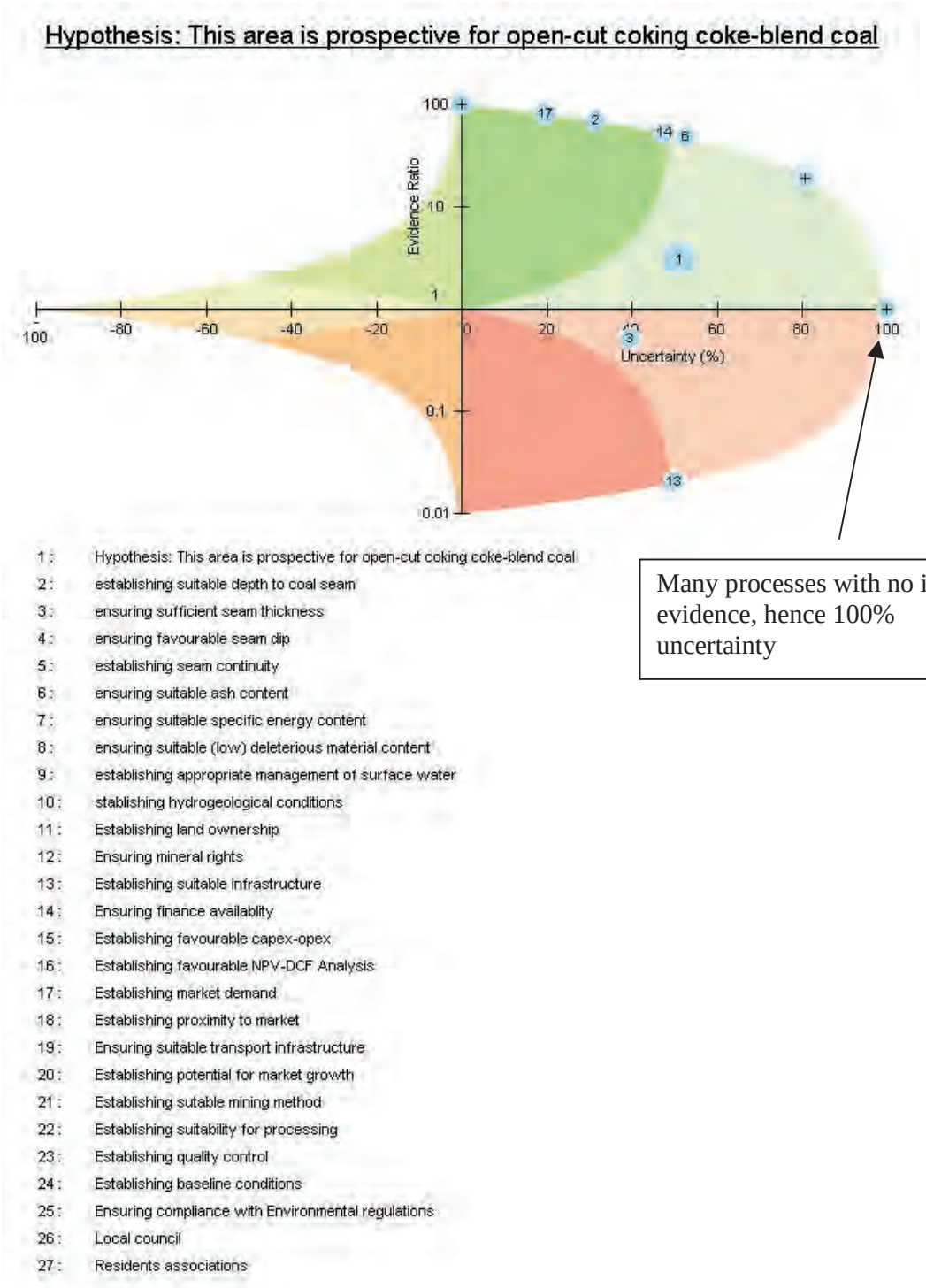

Figure 5. Evidence-ratio plot of the evaluation of open cut coking coal prospectivity of Prospect X

also Figure 5)) was designed to overcome this difficulty by presenting the same information in a single screen or A4 plot. In the evidence-ratio plot both the three-value outcome and the evidence inputs may be presented graphically in terms of the balance of evidence (i.e. the ratio of evidence in support of the hypothesis to evidence against) versus the remaining uncertainty.

The ratio of supporting to refuting evidence is plotted on the vertical axis; remaining uncertainty is plotted on the horizontal axis. Values plotting above the abscissa represent a balance of evidence in support, those below a balance of evidence against. To avoid division by zero or division of zero in this calculation, any evidence values of zero are converted to a minimum value of 0.01. This results in a possible ratio of between 0.01 and 100.

The values are then plotted using a logarithmic scale on the vertical ratio axis. Different zones in the plot may be identified for example by plotting lines of equal evidence for and against. In Figure 4 eight zones are differentiated based on evidence values of 25%, 50% and 75%. A prospect

plotting in Zone 1 for example, would indicate a balance of evidence in support of the hypothesis but with high remaining uncertainty. For large or complex ESL models it is possible to obtain a top-level outcome with accumulated evidence greater than unity which plots to the left of the vertical axis. The horizontal axis in this event represents remaining uncertainty due to inconsistency and conflict.

Sensitivity analysis – the Tornado plot

Sensitivity analysis examines the impact on the top-level result of changes in the evidence for each of the lower level processes. The results are presented in the form of a Tornado plot (Figure 6). Because of the differences in the inference logic propagation as a result of the different sufficiency weightings applied to evidence for and against the Tornado plot may not be symmetrical implying that positive changes in evidence for a particular process may have a different impact on the top-level outcome than negative changes for the same process. What-if scenarios can be used to identify those processes having the greatest impact on the top-level outcome in order to target future confidence building activities.

Application of ESL to Exploration

Prospect evaluation

ESL models can be developed for single prospect evaluation and/or for the exploration portfolio. Figures 5 and 6 illustrate a typical outcome for a single prospect evaluation developed from the framework model shown in Figure 3. The example shown here is entirely fictitious but it demonstrates the application of the method. Initially, the success of the prospect is deemed to be dependent upon two contributing factors namely, technical and commercial. In a more thorough evaluation of the prospect or at a more advanced stage in the assessment we could, for example, include evidence concerning the operational, environmental and social/community factors. Subdivision of the second-level process is continued to a level to which the individuals required to provide evidence are comfortable that they can do so with some confidence that their judgments can be supported. Support may come from data, modelling and/or from analogues.

In this example, some evidence has been input for technical and commercial factors which has resulted in an outcome of [36, 51, 12] i.e. the prospect has three times more evidence in support than against but the remaining uncertainty is still very high at 51%. This is not surprising given that no evidence has been submitted for the operational, environmental and social processes. The evidence-ratio plot for this outcome is shown in Figure 5.

It is clear from Figure 5 that whilst may processes support the proposition with little evidence against, there are two processes for which evidence against success outweighs evidence in support and, as noted above, a large number of processes with high uncertainty. The Tornado plot (Figure 7) shows that as a rule the failure to establish success has a much greater impact on the overall outcome than establishing success for any particular contributing factor

The top five factors having the greatest impact on the success of the prospect are firstly the technical factors i.e. failure to demonstrate suitable coal quality followed by failure to establish suitability for open-cut mining and suitability for processing and secondly social acceptability factors.

Prospect 'risking' applied to Financial Measures and Economic Indicators

Commonly the value of success for exploration prospects is based on a financial measure derived from a discounted cash flow analysis, usually net present value (NPV) or expected value (EV). At the exploration stage these are generally very rough and ready measures likely to undervalue a project because they do not take into account: a) technical and economic uncertainties and, b) the flexibility allowed to the company to take on real options in terms of the timing of development. More sophisticated analysis using sensitivity analysis, scenarios, Monte Carlo Simulation, real options theory, Black-Scholes equation etc may be used improve the prognosis but these are only useful when exploration has proved successful i.e. at an advanced stage in the exploration programme.

For grass roots exploration, managers still call for 'economic' indicators of success for a particular target deposit however 'unreal' these may be in practice. An ESL evaluation provides a useful means of 'risking' the indicator for a particular prospect and for 'levelling the playing field' when comparing prospects at different levels of advancement in their respective exploration programmes. Figure 7 shows an expectation curve for the NPV of an exploration prospect derived from a discounted cash flow analysis with Monte Carlo simulation. An ESL model carried out to test support for the likelihood of success at the prospect resulted in an outcome of [55,25,20]. We can 'risk' the expectation curve directly using the ESL result to give an upper bound and lower bound risk (Figure 7). Of course the risk-weighted NPVs are unreal numbers, they combine the NPV at a stated level of probability assuming a successful prospect with the upper and lower bound estimates of the prospect being a success. This approach is useful in that it provides a means of directly comparing prospects with differing potential in value terms and with different levels of support and remaining uncertainty, for example, within an exploration portfolio (Figure 8).

Evaluating the Exploration Portfolio

In this example (Figure 9) the success of the exploration portfolio is viewed in terms of the evidence of success for the contributing prospects. Figure 9 shows only the top- level outcomes, each prospect within the portfolio being underpinned by an ESL model similar to that described in the

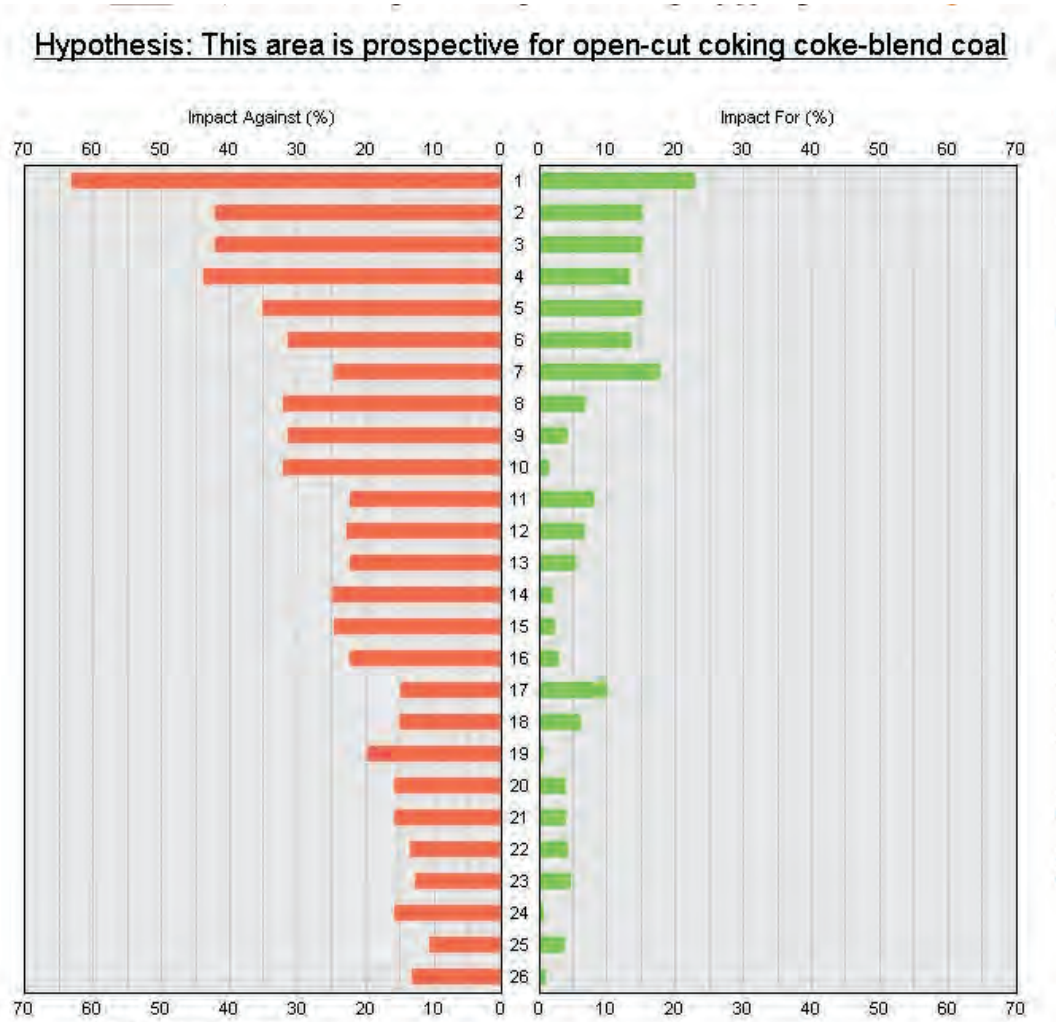

Figure 6: Tornado plot of the evaluation of open cut coking coal prospectivity for Prospect X

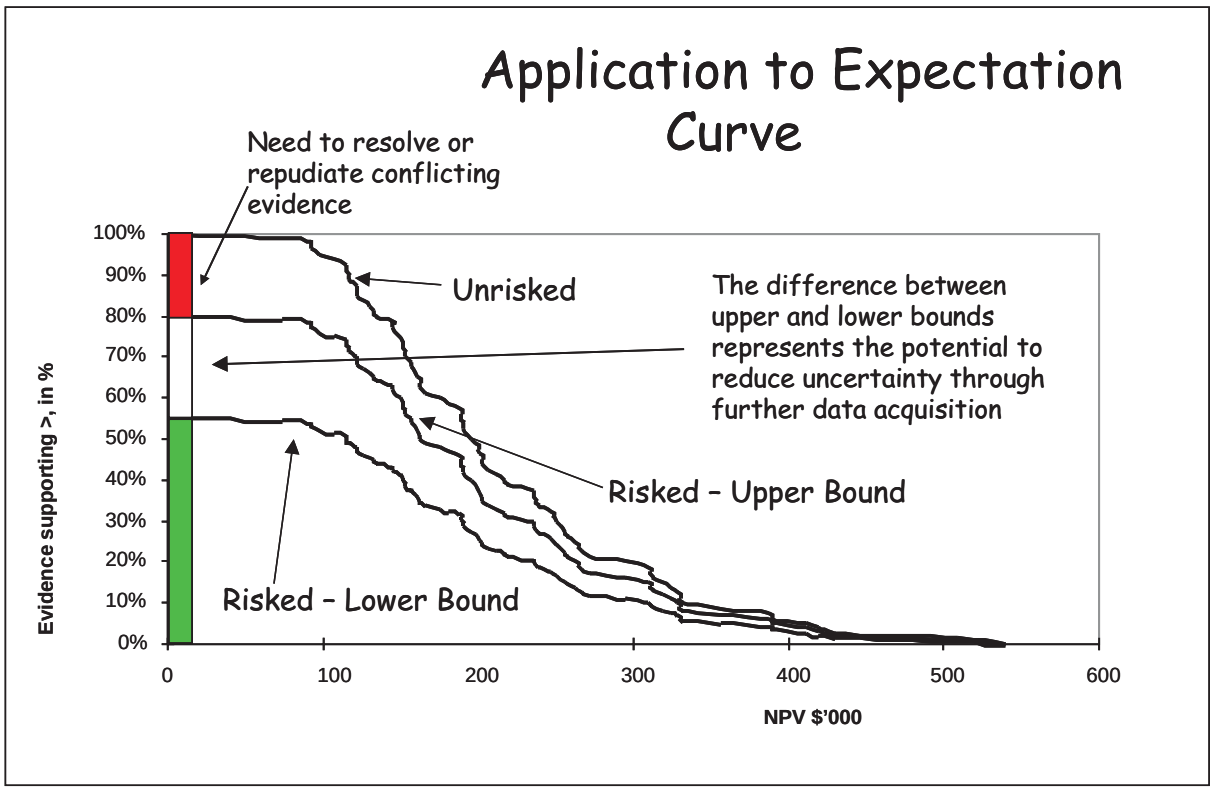

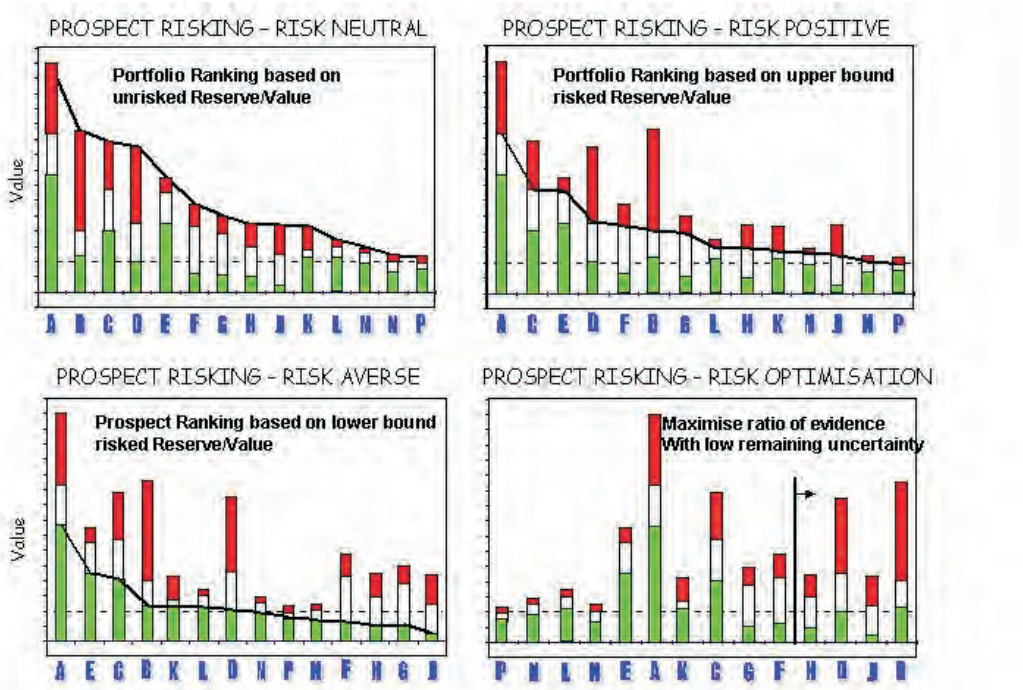

Figure 8: Prospects in a portfolio ranked according to; a) Unrisked NPV; b) Upperbound risked NPV; c) Lower bound risked NPV and d) Maximum evidence ratio plus lowest remaining uncertainty

previous example. The portfolio will be considered successful if any individual prospect is successful hence each prospect carries a nominal sufficiency weighting for supporting evidence of 1.

In this portfolio the sufficiency weighting of each individual prospect is further weighted by the relative NPV for the prospect hence the support sufficiency is given by $1*(NPV_p/NPV_{max})$ where NPV_p is the NPV of the specific prospect and NPV_{max} is the highest NPV of all the prospects. Failure of a single prospect will not imply failure of the portfolio whereas failure of all the prospects will. Therefore the sufficiency for failure of an individual prospect is given by 1/n where n is the number of prospects in the portfolio. Failure sufficiencies are not weighted by NPV as the NPV measure becomes irrelevant in the event of failure.

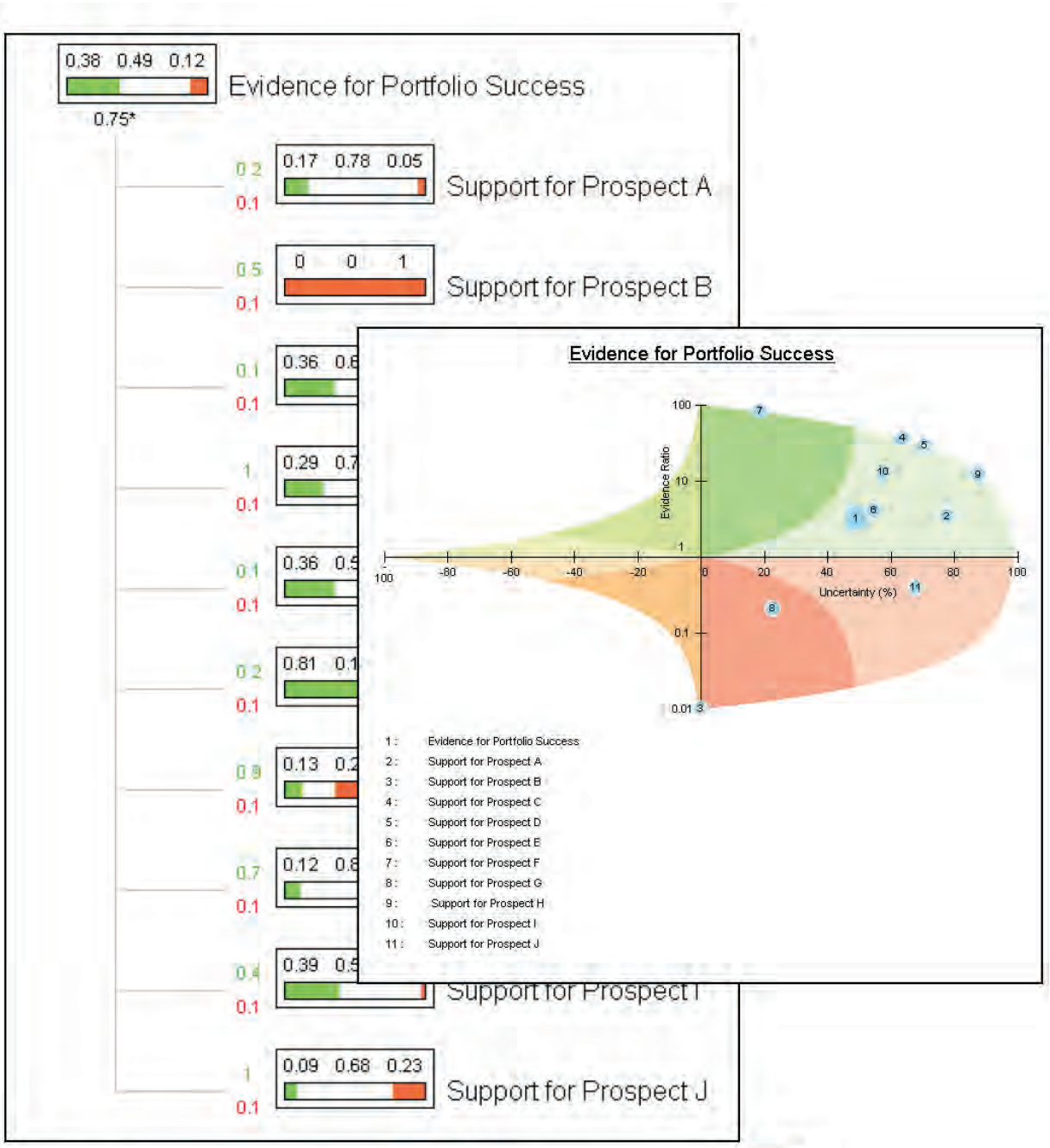

Figure 9. Assessing the evidence for portfolio success

Reserve Estimation

In the context of reserve estimation the question is one of how to build confidence in the management and execution of the process of reserve estimation including those subjective elements of the interpretation process. Simple adherence to or compliance with JORC requirements does not guarantee a high quality reserve estimate. As noted by Dominy & others (2002a) reporting codes such as JORC are effectively only a minimum standard for reporting, the actual business of estimating the resource/reserve is up to the Competent Persons.

It is clear that for the example in Figure 9 the three prospects are not contributing to the overall likelihood of success in the portfolio. Prospect B is a proven failure and should be relinquished, Prospect G appears unlikely to succeed and, depending on the results of sensitivity analysis and cost effectiveness of definitive investigations should also be relinquished. Prospect J whilst having more evidence against than for success has a very high uncertainty (68%) and therefore would merit further investigation before a decision is taken to relinquish the prospect.

Building confidence in the Reserves Estimate

Building confidence in the reserves estimate should be aimed at demonstrating their dependability with emphasis on the quality of the data and of the processes involved in crafting the available data into an estimate of reserves. At the same

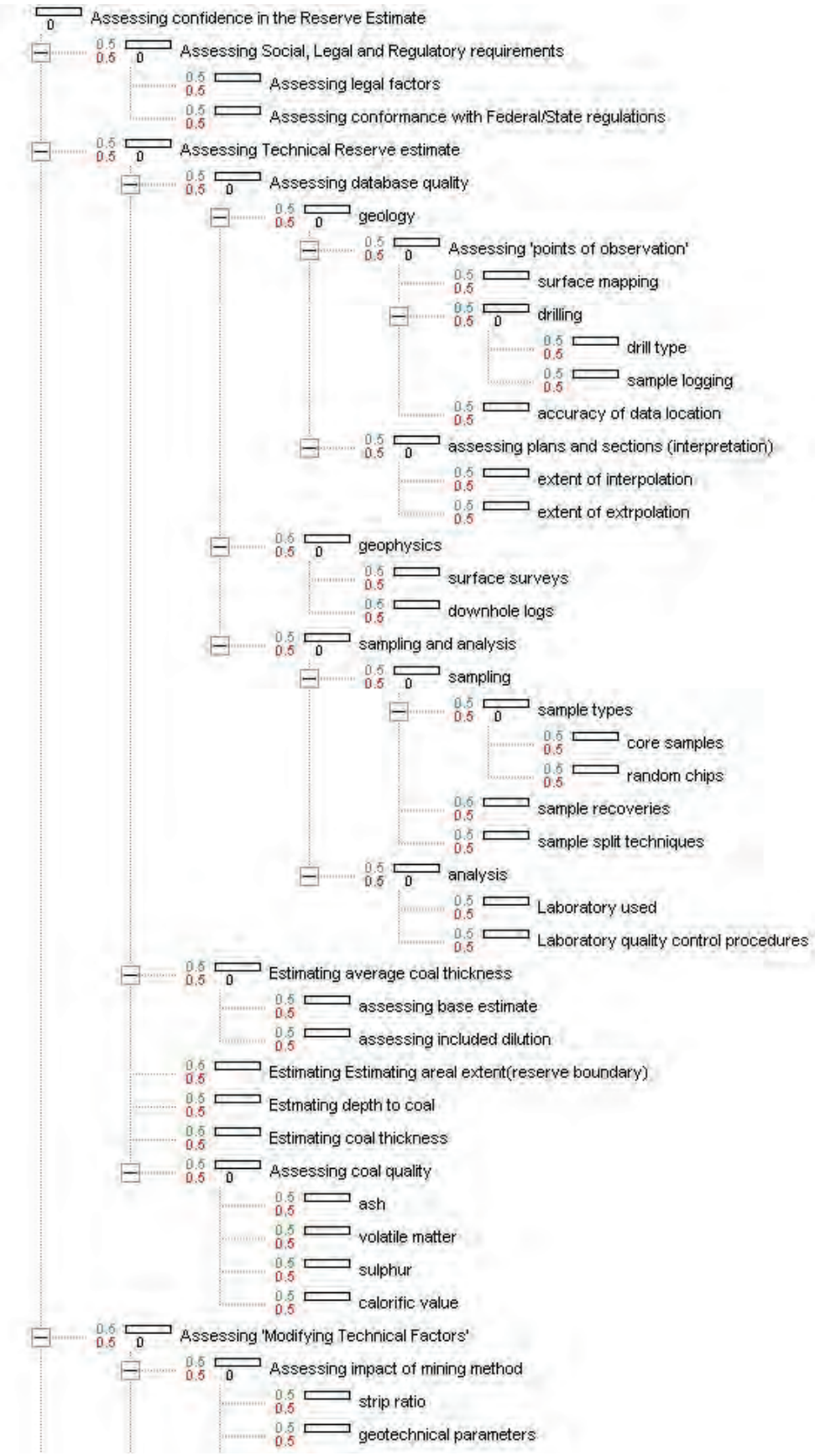

Figure 10: Part of an ESL framework model for auditing a coal reserve estimate (illustrative only)

time any remaining uncertainties should be acknowledged together with an estimate of the impact of those uncertainties on the dependability of the estimate. In order to provide a justified/justifiable estimate which can be audit-tracked from start to finish we need to examine, and make judgement on the quantity and quality of the data, and on the quality of the geological interpretation, modelling and reserve estimation processes.

A complete expression of the estimate would ideally include the observed/measured data, definitions of the currently preferred and possible alternative geological possibilities (and their impact on the reserves estimate), presentations of the supporting and the conflicting or refuting evidence and some form of representation of the remaining uncertainties.

In the context of reserve estimation the question is one of how to build confidence in the management and execution of the process of reserve estimation including those subjective elements of the interpretation process. Whilst there are clear guidelines and requirements for controlling the estimation process (e.g. Australian Guidelines for the Estimating and Reporting of Inventory Coal, Coal Resources and Coal Reserves; The JORC Code 2004) simple adherence to or compliance with these does not guarantee a high quality reserve estimate.

As noted by Dominy & others (2002a) reporting codes such as JORC are effectively only a minimum standard for reporting, the actual business of estimating the resource/reserve is up to the Competent Persons.

In order to provide documented support for the estimation process ESL can be used as an audit tool. Figure 10 illustrates part of a possible ESL framework for such a process. The framework shown in Figure 10 is illustrative only, it is not intended to be definitive; nor is it unique (although it should be possible to construct a definitive model that is acceptable to a given situation).

In effect the framework provides a checklist -similar to that in the JORC code Table 1 – but unlike the yes/no straitjacket of the checklist this approach allows the user to scale the yes/no responses according to how well the particular process has been carried out and to include a specific measure of uncertainty.

I have not, in this example, attempted to provide values for the inference parameters for the ESL framework for Figure 10 but it would be an interesting and valuable exercise to attempt to do so. Ideally, the framework model and its parameterisation should be carried out by formal elicitation of a team of qualified experts from within the industry. The technique has high value in identifying areas of a reserve estimation process that are weak on evidence or for which remaining uncertainty is unacceptably high, thus enabling improved targeting of future effort.

CONCLUSIONS

Evidence Support Logic is a tool for identifying and analysing uncertainty. The method allows the user to construct a logical structured framework that captures all

the factors that contribute to the success or failure of a particular project, and their inter-relationships. In ESL a three-value logic is applied to the elicitation of judgements of evidence using a sliding scale that allows much greater discrimination of the quantity and quality of information and of the remaining uncertainties for any given contributing process. A number of examples are presented that demonstrate application of the ESL approach to mineral exploration. ESL is a tool that merits a place alongside other decision support tools such as Monte Carlo simulation, Decision Trees and Bayesian updating.

REFERENCES

BLOCKLEY, D. & GODFREY, P., 2000: *Doing it Differently – systems for rethinking construction*. Thomas Telford.

BONHAM-CARTER, G.F., 1994: *Geographic Information Systems for geoscientists, Modelling with GIS*, Pergamon. Ontario, 295-302.

BOWDEN, R.A., 2004a: *The Application of Evidence Support Logic (ESL) in Mining Geology with particular reference to Mineral Resource and Reserve Estimation*, Mining Geology 2004, Brisbane.

BOWDEN, R.A., 2004b: Building Confidence in Geological Models. From Geological Prior Information Informing Science and Engineering. *Geological Society Special Publications*, **239**, 157-173.

COALFIELDS GEOLOGY COUNCIL OF NEW SOUTH WALES AND THE QUEENSLAND MINING COUNCIL, 2003: *Australian guidelines for estimating and reporting of inventory coal, coal resources and coal reserves*, 2003 Edition.

CUI, W. & BLOCKLEY, D.I., 1990: Interval Probability theory for evidential support, *International Journal of Intelligent Systems*, **5**.

DOMINY, S.C., NOPPÉ, M.A. & ANNELS, A.E., 2002a: Error and Uncertainty in Mineral Resource and Ore Reserve Estimation: The Importance of Getting it Right, *Exploration and Mining Geology* **11** (1-4), 77-98.

JORC, 2004: *Australasian Code for the reporting of Exploration Results, Mineral Resources and Ore Reserves*. The JORC code, 2004 Edition prepared by the Joint ore Reserves Committee of the Australasian Institute of Mining and Metallurgy, Australian Institute of Geoscientists and Minerals Council of Australia.

A. Bowden, GeoDec Consulting, 2928 Moggill Road, Pinjarra Hills, Brisbane, geodec@ozemail.com.au

John Draper, Atsushi Aoki, Nirou Okamoto, Hiroshi Karashima, Hideo Aoyama, Masayoshi Tanoue, Takao Aizawa, Ken-ichi Yamazaki, and Mark Covington

A collaborative approach between Japan and Australia in the Bowen Basin – a trial of an integrated geoscience data base for exploration

Joint research on geophysical exploration for coal between the New Energy and Industrial Technology Development Organisation (NEDO) in Japan and the Queensland Department of Natural Resources and Mines covers three main components: (1) verification and evaluation of a previously developed coal exploration and assessment system; (2) a Coal Potentiality Evaluation System; and (3) the regional geophysical and geological framework.

A test site at Coppabella Mine was used to create a geological model using the Kinematic Modelling System. Input into the model included drilling, geophysical logging, vertical seismic profiling, 2D and 3D seismic and gravity. The model is being assessed against the results of mining. Airborne magnetic and radiometric data were progressively collected over the Bowen Basin. Data collected and interpreted to date have enhanced our understanding of the basin, in particular, the tectonic and structural history. The Coal Potentiality Evaluation System consists of three main parts: a series of databases; a GIS; and the coal potentiality system which is an expert system.

The databases provide geological, environmental, mining and economic data. The Coal Potentiality Evaluation System was used to help define two project areas in the northern Bowen Basin for further testing of the geophysical methods and to identify potentially economic coal resources. During November – December 2003, a 10km seismic line was recorded using the updated equipment. The seismic data were supplemented by three fully cored boreholes, the deepest borehole being 301m. The upgraded wireline log sonde was run in all three holes. This was followed up in late 2004 and early 2005 with two fully cored boreholes and 14.2km of seismic surveys. A potentially economic coal resource was identified. Collaboration at an international and a local scale has been highly effective. It has provided ongoing development of geophysical exploration techniques, has provided an impetus for the re-evaluation of the geology of the Bowen Basin and has provided an avenue for the exchange of geophysical technology and ideas.

Key words: Seismic, wireline logging, airborne geophysics, geographic information system, expert system

INTRODUCTION

A joint Australian/Japanese initiative to develop new exploration techniques based on the latest geoscientific data is underway in the Bowen Basin. The New Energy and Industrial Technology Development Organisation (NEDO) is attached to the Ministry of International Trade and Industry (MITI) in Japan. The responsibilities of NEDO include co-ordination of research and development projects, creation of large-scale research facility development projects, developing a co-operative international research program and a global environment protection project.

Since 1992 NEDO has been involved in a long-term project entitled 'Basic Survey For Coal Resources Development / Research And Development Of New Exploration Technology For Coal Resources'. From 1992 to 1996 NEDO and the then Queensland Department of Minerals and Energy carried out studies in Queensland under the umbrella of the project (Department of Mines & Energy, 1997). From 1997 to March 2000, the project was focussed in NSW at Caroona (Condell, 2000).

A new joint project between NEDO and Queensland Department of Natural Resources and Mines (NR&M) has been completed. The joint project had three components. The first was to test the techniques NEDO had previously developed and to test further enhancements. The second was to develop a Coal Potentiality Evaluation System using GIS and artificial intelligence. The final component was an improved understanding of the geological framework of the basin. Airborne geophysics was used to underpin this understanding. A formal agreement was signed between the Minister for Mines and Energy and NEDO in November 2000 and January 2001. The agreement ended in 2005.

The testing of techniques and evaluation of the techniques was undertaken in three separate areas of the Bowen Basin with the collaboration of the coal miners and explorers. The first field area was at Australian Premium Coals' Coppabella Mine and the second and third were in an exploration permit held by Xstrata Limited in the northern Bowen Basin (Figure 1).

The individual components are described briefly and the value of such collaborative projects assessed. The Role of the Coal Potentiality Evaluation System will be highlighted. Reults to 2004 were described by Draper & others (2004).

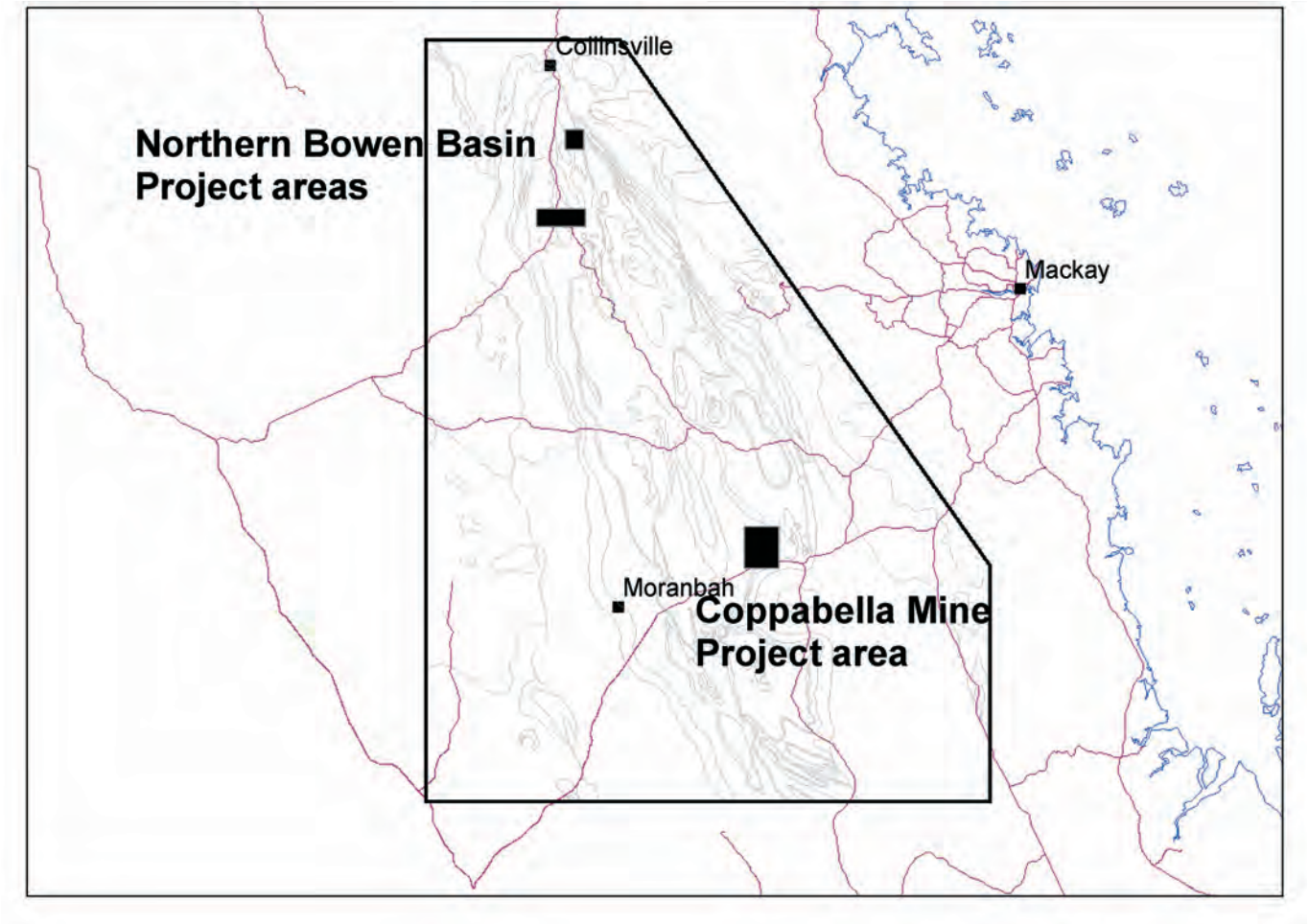

Figure 1: Location of northern Bowen Basin study areas

METHOD AND RESULTS

Coppabella

The objective of the Coppabella project was to verify and improve a high-resolution and high-efficiency seismic reflection survey and evaluation technology for an Integrated Coal Resource Evaluation System (ICRES). Coppabella is an open cut mine in the Rangal Coal Measures producing mainly PCI coals for export from the Rangal Coal Measures. The test area is in the Johnson Pit (Figure 2). In 2001 a 3D seismic survey was carried out over an area of 1.35km x 0.96km as was 3km of 2D seismic split into four lines. Four fully cored boreholes were drilled and subjected to geophysical logging and vertical seismic profiling. The geophysical logging also investigated the direct measurement of sulphur and ash content using a neutron-gamma tool. A 2km^2 area gravity survey was also carried out. The data were integrated to produce a geological model based on the Kinetic Modelling System under development by NEDO since 1997. The model is being progressively compared to the results of mining.

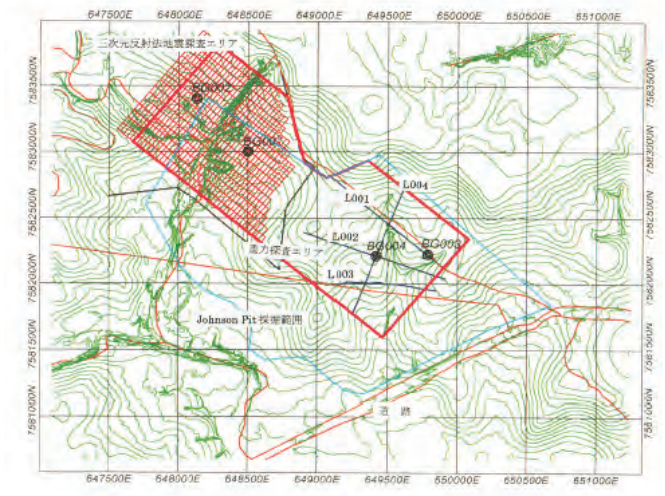

Figure 2. Coppabella project area showing the location of the four 2D seismic lines, the area of 3D seismic and the location of the boreholes (Grid – AMG55).

The seismic source used was an electromagnetic vibrator. The vibrator has a vibration force of 800kgf and a sweep range of 6.5 to 500Hz. The high sensitivity geophone has a natural frequency of 150Hz and a sensitivity of 1.8V/kine. The recording parameters for the 2D survey involved a 2.5m interval with a single geophone, a split spread with near offset of 13.75m and a shot interval of 10m. Sweep parameters were determined from point tests on each line.

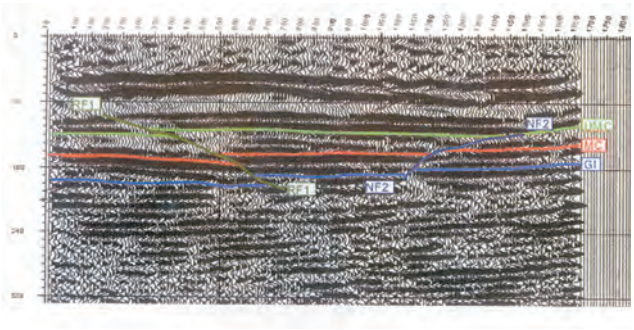

Figure 3: Example of in-line seismic line from 3D survey, Coppabella (TWT)

Recording parameters for the 3D seismic survey were 10m station interval with 60m line spacing of station lines, 20m shot interval with 30m spacing of shot lines. This resulted in 20-fold maximum common mid point coverage and bin size with 5m in-line and 10m cross-line. An example of the processed seismic is shown in Figure 3.

Geological Framework

As part of the project, the Department of Natural Resources and Mines flew airborne geophysics over much of the Bowen Basin (Figure 4). The magnetic and radiometric data were obtained to assist in the development of an improved knowledge of the geological framework of the basin. The surveys were flown over three years (2002-2004) and at a line spacing of 400m and a flying height of 80 m.

A new Northern Bowen Basin Solid Geology Map (Sliwa & Draper, 2003) was prepared jointly by CSIRO (Renate Sliwa) and NR&M (John Draper), but the remaining airborne data are still being interpreted. The northern Bowen Basin map can be downloaded from this website: http://www.glassearth.com/terranepages/NBB/Level2-rbbstory.htm.

Highlights from the data interpretations to date are: the verification and better definition of structural compartmentalisation, the mapping of much greater extent of basalt than that previously mapped, enhanced mapping of faults, identification of previously unknown structures, high potassic nature of tuffaceous units and identification of previously unknown intrusions. The mapping in the northern Bowen Basin will be extended throughout the Basin to produce a revised solid geology map of the Basin.

In 2003, Pitt Research P/L, under licence from Vector Research P/L, undertook overburden filtering (OB filter) of a test area across the central Bowen Basin, near Blair Athol. The aim of the commission from GSQ was to test the technique's ability to resolve geology from an area of basalt cover, deep structures, strong curvilinear features (dykes, faults and bedding) and stock-like intrusions. The results showed that:

- These new datasets allow the sub-basalt response to be better resolved,

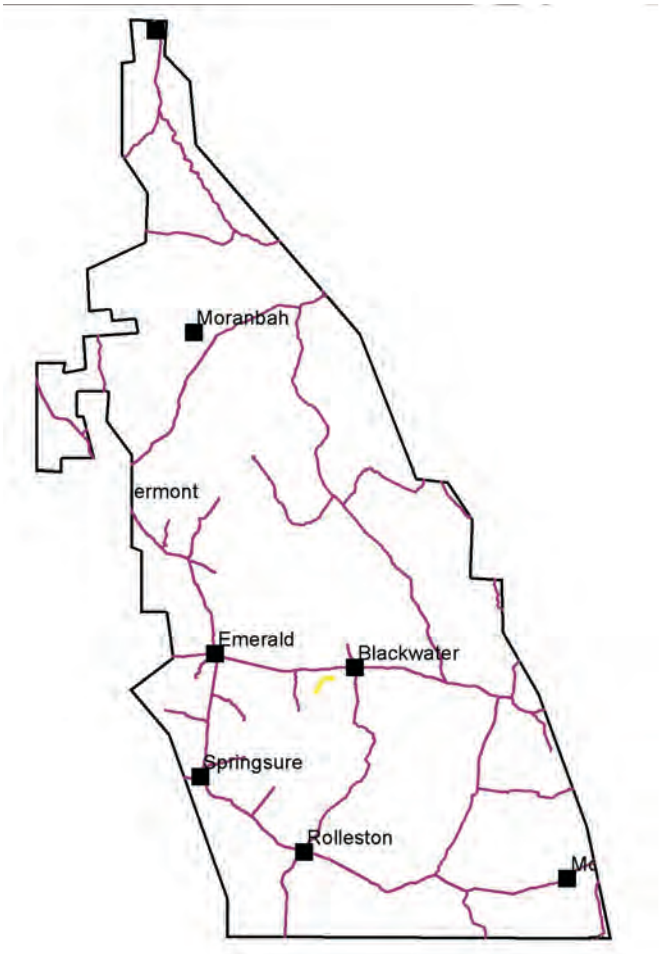

Figure 4: Area covered by airborne geophysical surveys. Red lines are major roads

- details of the near-surface geology are clearer., and
- Linear and stock-like features are resolved.

Coal Potentiality Evaluation System

The Coal Potentiality Evaluation System consists of two main components, a coal GIS and an expert system (Coal Potentiality System). The two components communicate via a mediator (Figure 5).

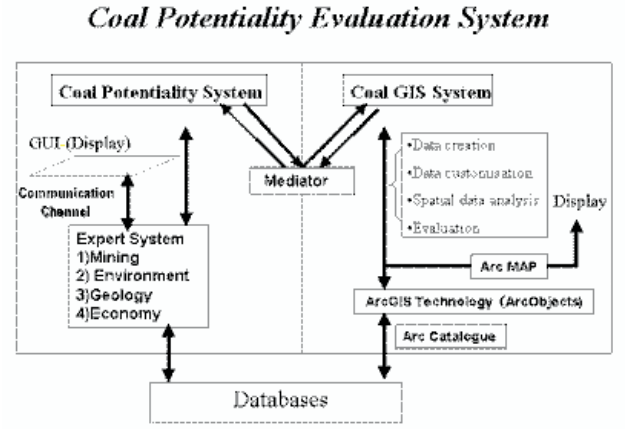

Figure 5: Summary diagram of the Coal Potentiality Evaluation System showing the basic contents of the two components.

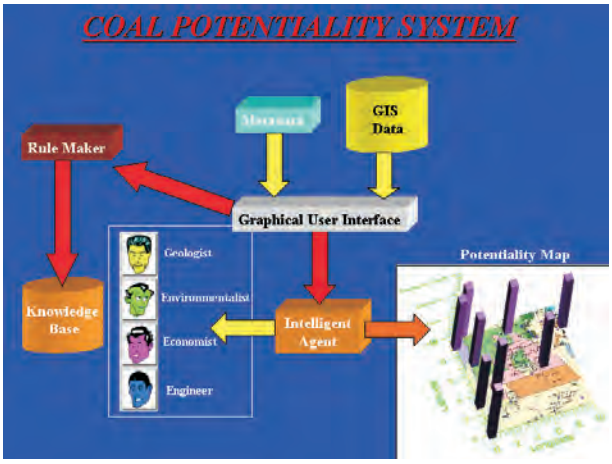

Figure 6: Flow chart for coal potentiality system

The spatial datasets are divided into two groups: Coal Data and General Data. Coal Data include data about resources, geology and geophysics, and coal tenure. General data include data relating to land use, conservation, topography, hydrography, infrastructure and digital elevation model. The data are sourced from NR&M, and Geoscience Australia (AUSLIG). Metadata were defined using the ANZLIC standard. The importance of metadata in GIS development cannot be overstated as it provides a control on the quality and completeness of the data as well as showing the currency of the data. The Coal GIS System is for decision support.

The Coal Potentiality System (Figure 6) also draws on the GIS data and the metadata which are fed via a graphical user interface to a rule maker and a knowledge base. Four knowledge bases are developed: geologist; environmentalist; economist; and engineer. The GIS data, metadata and expert knowledge is utilised by an intelligent agent to produce a potentiality map.

The Coal Potentiality Evaluation System was used to assess field study areas in the northern Bowen Basin (Figure 7). An area was required to test upgrades of the seismic system and of the downhole logging tools. A potentiality map was prepared for the area covered by the northern Bowen Basin airborne geophysical survey. Areas of high potential were identified. Field test areas proposed by titleholders in the area were assessed against the potentiality maps. The final decision of a field test areas was a combination of the potentiality mapping and practical field operational and logistical considerations.

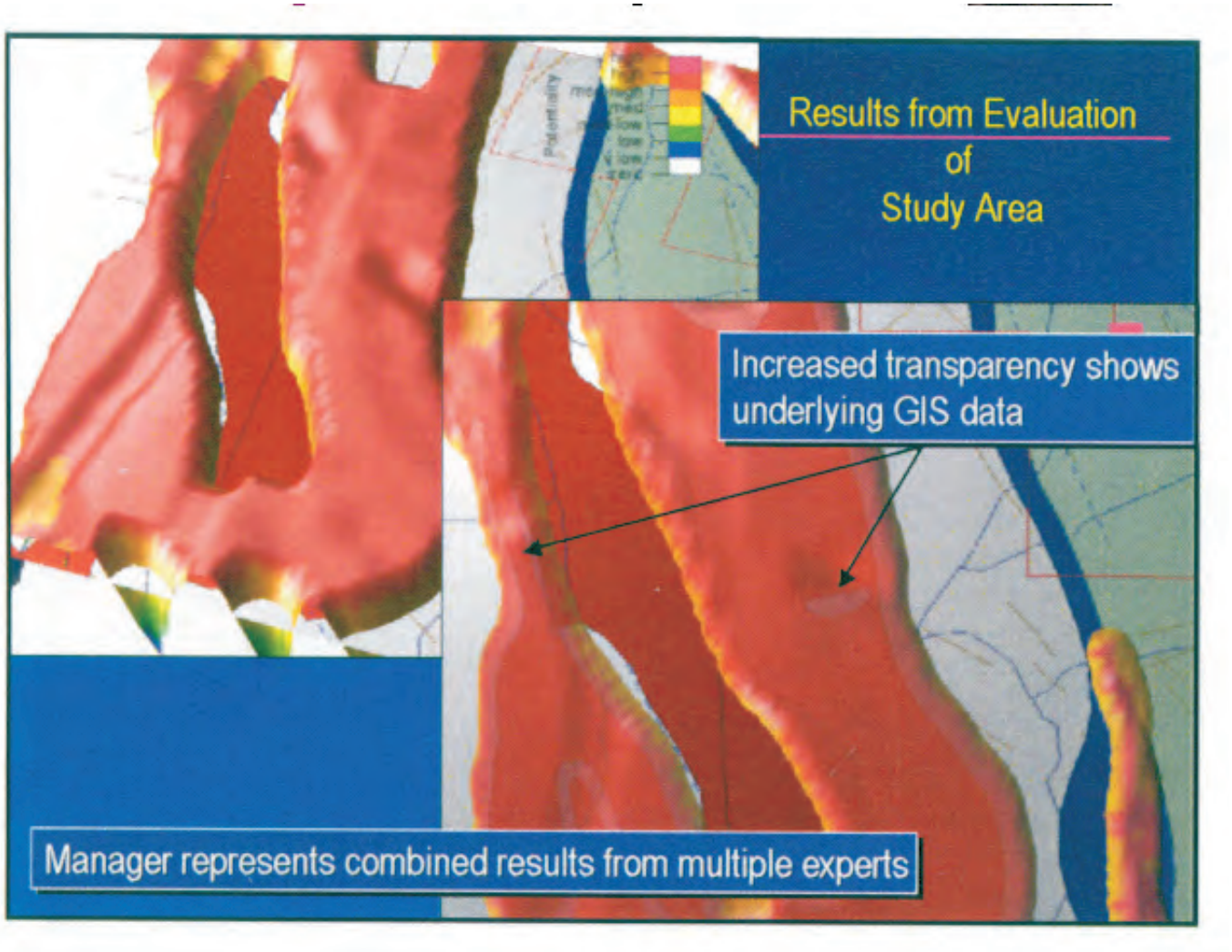

Figure 7: Results from evaluation of study area

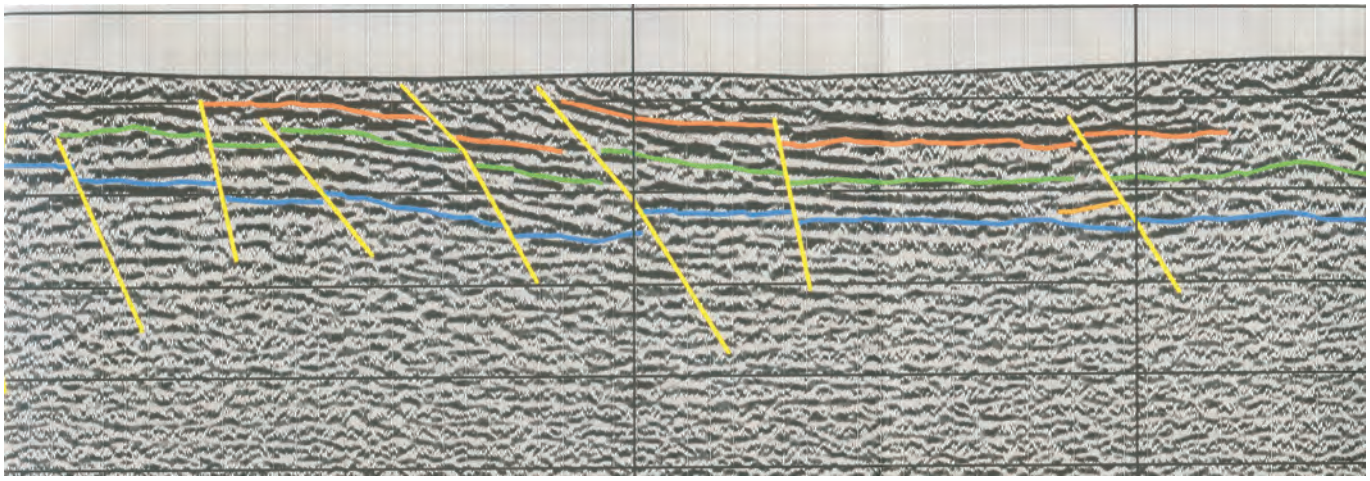

Figure 8: Sample of seismic from 2003 survey

Northern Bowen Basin Field Tests

The field test areas were required to evaluate improvements in the seismic equipment and the logging sonde as well as testing the Coal Potentiality Evaluation System. An area was selected within an Exploration Permit for coal held by Xstrata Limited. The area proposed by Xstrata and selected by NEDO is in an area of active exploration. The main target for the study was the Moranbah Coal Measures.

For the seismic system, a pseudo-random code signal has been introduced to the electromagnetic vibrator and recording system. This signal is introduced for improved measurement of high-velocity near-surface layers such as basalt.

This is to be tested in an exploration setting. Further development of the neutron-gamma sonde and software also needed testing in an exploration setting. New GPS equipment and surveying software were also included in the testing. Further enhancements have also been made to the modelling software.

During November – December 2003, a 10km seismic line was recorded (Figure 8) using the updated equipment. The seismic information was supplemented by three fully cored boreholes. The deepest borehole was 301m. The upgraded wireline log sonde was run in all three holes. The data are being processed and interpreted as this abstract is being prepared. Xstrata Limited drilled additional holes in the area and extended the seismic line another 9.5km using the same equipment.

In December 2004 and January 2005, a further area was tested. Two fully cored boreholes were drilled and 14.2km of seismic was recorded. Potentially economic coal resources were identified.

DISCUSSION

As discussed above, this paper is not about the results, but about the value of collaborative research and the use of GIS and expert systems. Within the project, collaboration existed at several levels. At the highest level was collaboration at government level between a Queeensland Government agency and a Japanese Government agency. Without the collaboration of the companies, the field testing could not have proceeded. The interpretation of the northern Bowen Basin solid geology map was the result of collaboration between CSIRO and NRM&E.

The NEDO part of the project was facilitated through JCoal and Mitsubishi Materials and involved various subcontractors: DIA Consultants; SUNCOH Consultants; Mitsui Mining Engineering; ECS International; and Velseis, plus local drilling contractors.

A critical element of a project this size was the management of the project and effective communication. This became particularly important with language and cultural differences between the parties. Both NR&M and NEDO had project manager/co-ordinators who maintain regular communication, mainly via email. Regular meetings were held of a Technical Committee and a Steering Committee. The Technical Committee met twice a year to plan the technical aspects of the research. Progress was also reviewed at these meetings. The Technical Committee reported to the Steering Committee, which was responsible for approving the annual work plan, reviewing progress and dealing with major policy issues. The committee system worked well, as indicated by the project operating to plan.

The project benefits included the six listed here:

- Extending the good relationship between Japan and Australia,
- obtaining/increasing geological information on the Bowen Basin,
- confirming the potential for new coal deposits in Queensland,
- improved evaluation of coal deposits,
- encouragement for exploration, and
- development of new integrated exploration and assessment systems.

In addition, the project will provide some direct benefits. The variation of coal type and quality in the Bowen Basin will enable the coal industry to adjust to changing market needs and to service niche markets. A better knowledge of the basin will enable the trends of rank and quality to be predicted. The exploration methods tested should open up new areas for exploration. The Bowen Basin is Queensland's highest income earner and, in an expanding world energy market, we need to be able to increase production rather than remain static. This study should enable the Bowen Basin to retain its status as a high-quality, reliable coal source.

Co-operative research brings together a wider knowledge and expertise base, and provides opportunities for project scales that are often beyond the reach of most organisations. By combining strengths and enlisting industry support, projects can proceed in real settings rather than idealised settings. In the long run, geophysical techniques have to be viable in the exploration and mining environment. Bridges are needed to take research from the laboratory to the operational environment. Co-operative projects can provide these bridges.

The opportunity to test techniques and models against the results of mining, as at Coppabella, is only possible through co-operation at several levels. Co-operation is necessary at a strategic, policy level, and at a local technical level.

FUTURE ACTIVITIES

A number of studies are planned for the Bowen and Surat basins. The airborne surveys are to continue further south to the New South Wales border as part of a new Queensland Government initiative called the Smart Exploration Program. A major structural synthesis will be carried out and geological maps updated. We will continue to build our databases. Discussions are continuing on developing the Coal Potentiality Evaluation System into a general decision making tool.

CONCLUSIONS

The joint NEDO/NRM&E Project in the Bowen Basin is an example of a successful co-operative project. It has involved not just two government bodies but has involved a number of sub-contractors and coal companies. Co-operation has operated at strategic and policy levels and at technical levels. The project is on track to produce the planned outputs and to achieve the planned outcomes. It has been a technical and an organisational success. The Coal Potentiality Evaluation System demonstrated its ability to identify areas with potentially economic coal resources.

ACKNOWLEDGMENTS

Without the support of Australian Premium Coals, the operators of Coppabella Coal Mine, and of Xstrata Limited, the title holders of the EPC in which the test project is proceeding, the project would not have been successful. We thank them for their assistance and unstinting support. In particular we would like to acknowledge John Williams of Australian Premium Coals and Todd Harrington of Xstrata Limited and other staff of those companies that were involved.

REFERENCES

CONDELL, J., 2000: Integrated coal exploration technologies, Caroona resource area, Gunnedah coalfield, NEDO-DMR Seminar 2000, Monday 13 March 2000, Pokolbin, Hunter Valley, NSW. New Energy and Industrial Technology Development Organization, New South Wales Department of Mineral Resources.

DEPARTMENT OF MINES AND ENERGY, 1997: Coal search technology. DME, Symposium proceedings, Brisbane, Queensland.

DRAPER, J.J., AOKI, A., OKAMOTO, N., KARASHIMA, H., AOYAMA, H., TANOUE, M., AIZAWA, T., YAMAZAKI, K. & COVINGTON, M., 2004: Geophysical studies in the Bowen Basin: a collaborative approach. *ASEG 17th Geophysical Conference and Exhibition*, Sydney 2004 (extended abstracts).

SLIWA, R. & DRAPER, J., 2003: Solid geology Northern Bowen Basin: an interpretation based on airborne geophysics. Map published by CSIRO and Queensland Department of Natural Resources, Mines and Energy.

John Draper, NR&M, Australia, john.draper@nrm.qld.gov.au\
Atsushi Aoki, NEDO, Japan, aokiats@nedo.go.jp
Nirou Okamoto, NEDO, Japan, okamotonro@nedo.go.jp
Hiroshi Karashima, JCOAL, Japan, karajan@jcoal.or.jp
Hideo Aoyama, Mitsubishi Materials, Japan, aoyama@mmc.co.jp
Masayoshi Tanoue, DIA Consultants, Japan, M.Tanoue@diaconsult.co.jp
Takao Aizawa, SUNCOH Consultants, Japan, aizawa@suncoh.co.jp
Ken-ichi Yamazaki, Mitsui Mining Engineering, Japan, ken_yamazaki@m.mec.co.jp
Mark Covington ECS International, Australia, mark.covington@ecsi.com.au

John Draper

A regional airborne geophysical survey of the Bowen Basin – Insights into geology and structure

Between 2002 and 2004, the Department of Natural Resources and Mines (NR&M) obtained aerial magnetic and radiometric data over the Bowen Basin from Collinsville in the north to just south of Moura in the south. This formed part of a joint project between the New Energy and Industrial Technology Development Organisation (NEDO) of Japan and NR&M in the Bowen Basin. The data will be used to revise the Bowen Basin Solid Geology Map and be utilised in a structural interpretation of the basin. The data have also been used for natural resource management studies. An overburden filter was applied to the magnetic data in the area east of Blair Athol to 'see through' the basalt. The regional magnetic data revealed much larger areas of basalt than previously mapped. Some of the basalts are sheet basalts beneath covers whereas others are preserved as palaeovalley fills. Many of these basalts represent potential groundwater resources. There have been some distinct changes in drainage patterns since the basalts were deposited. The combination of the magnetic data and the radiometric data will enable a better understanding of the Cainozoic geology. Mapping of dykes, fractures and faults has indicated complex domaining of structural elements in the Bowen Basin. The major faults show a strong north-south component as well as a strong north-northwest component. The major faults in the southern area are dominantly normal faults with later reversal whereas thrust faulting dominates in the central and northern areas. The data provide insights into areas of potentially enhanced permeability suitable for coal seam methane plays by examining regional and local structure. The widespread fracture networks have acted as a focus for mineralisation and Tertiary plugs. The main outcome of the airborne data collection will be an improved understanding of the geology of the Bowen Basin.

INTRODUCTION

A joint Australian/Japanese initiative to develop new exploration techniques based on the latest geoscientific data was undertaken in the Bowen Basin. The project is discussed by Draper & others (2004, this volume).

As part of the project, the Department of Natural Resources and Mines flew airborne geophysical surveys over much of the Bowen Basin (Figure 1). The magnetic (Figure 2) and radiometric (Figure 3) data were obtained to assist in the development of an improved knowledge of the geological

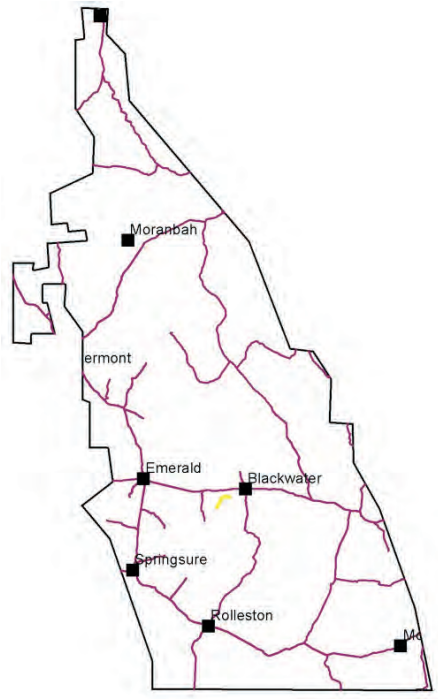

Figure 1: Area covered by Department of Natural Resources and Mines 2002-2004 airborne geophysical surveys. Red lines are major roads.

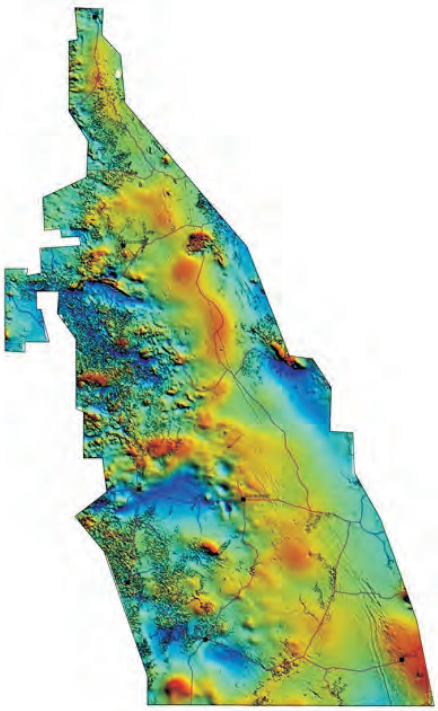

Figure 2: Total magnetic intensity image for the 2002-2004 survey areas

Figure 3: Ternary radiometric image for the 2002–2004 survey areas (K-red, Th-green, U-blue)

framework of the basin. The surveys were flown over three years (2002-2004) and at a line spacing of 400m and a flying height of 80m. The surveys will be extended south to the New South Wales border in 2005/06 to cover the subsurface Bowen Basin as well as the eastern Surat Basin.

The data were also used for natural resource management studies such as the joint NR&M, Geoscience Australia and CRCLEME project carried out in the parts of the Burdekin and Fitzroy catchment areas (Figure 4). This project will be published online on the Geoscience Australia website. Layers integrated in this study included:

- physiographic regions and soil parameters,
- hydrology and hydrogeology,
- climate, meteorology,
- land use,
- environmental data: vegetation, biodiversity,
- infrastructure,
- digital elevation models,
- bedrock geology, including structural geology,
- remotely sensed data (LANDSAT/ASTER/satellite photos, orthophotos),
- regolith features: landforms, materials, thickness,
- regional geophysics: magnetics and radiometrics; electromagnetics where possible,
- baseline geochemical features, including hydrogeochemistry, and
- mines, other known and potential mineralisation.

A new Northern Bowen Basin Solid Geology Map (Figure 5) was prepared jointly by CSIRO and NR&M (Sliwa & Draper, 2003), but the remaining aerial data are still being interpreted. Highlights from the data interpretations to date are: the verification and better definition of structural compartmentalisation, the mapping of much greater extent of basalt than that previously mapped, enhanced mapping of faults, identification of previously unknown structures, high potassic nature of tuffaceous units and identification of previously unknown intrusions. The mapping in the northern Bowen Basin will be extended throughout the basin to produce a revised solid geology map of the basin.

In 2003, Pitt Research P/L, under licence from Vector Research P/L, undertook overburden filtering (OB filter) of a test area across the central Bowen Basin, near Blair Athol. The aim of the commission from GSQ was to test the technique's ability to resolve geology from an area of basalt cover, deep structures, strong curvilinear features (dykes, faults and bedding) and stock-like intrusions.

This paper presents some preliminary results and ideas from the data. The data will be used in an ongoing mapping project and a structural synthesis in the Bowen Basin.

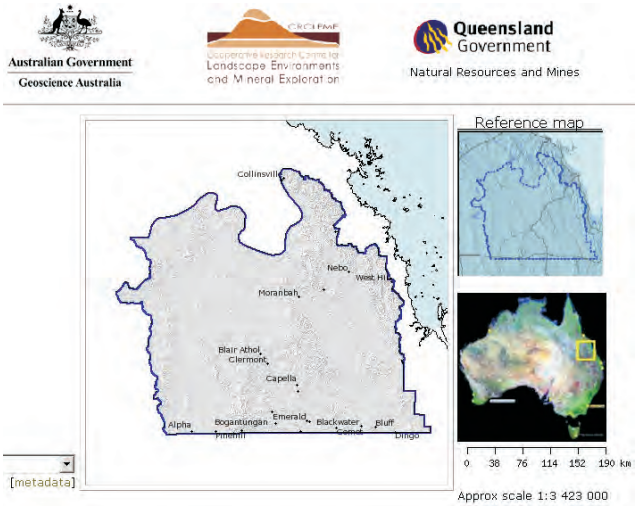

Figure 4: Portion of the Burdekin-Fitzroy project website showing project area

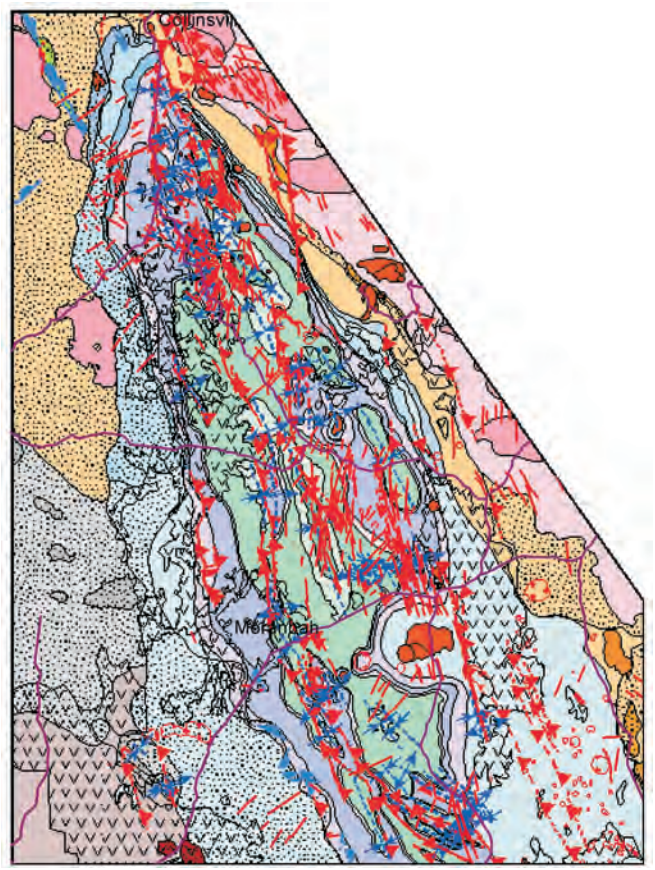

Figure 5: Solid geology map, northern Bowen Basin (Sliwa & Draper, 2003)

BASALTS

Significant areas of the Bowen Basin are covered by basalts of Tertiary age. The geology of the basalts is described in Johnson (1989). Small patches of basalt were thought to be mainly remnants of more widespread sheets of basalt. The new data shows that in some cases the small patches are surface expressions of basalts covered by sediments. Figure 6 shows the area of basalt mapped from the magnetic data compared to the basalt mapped during regional mapping. The identification of the basalts are important from

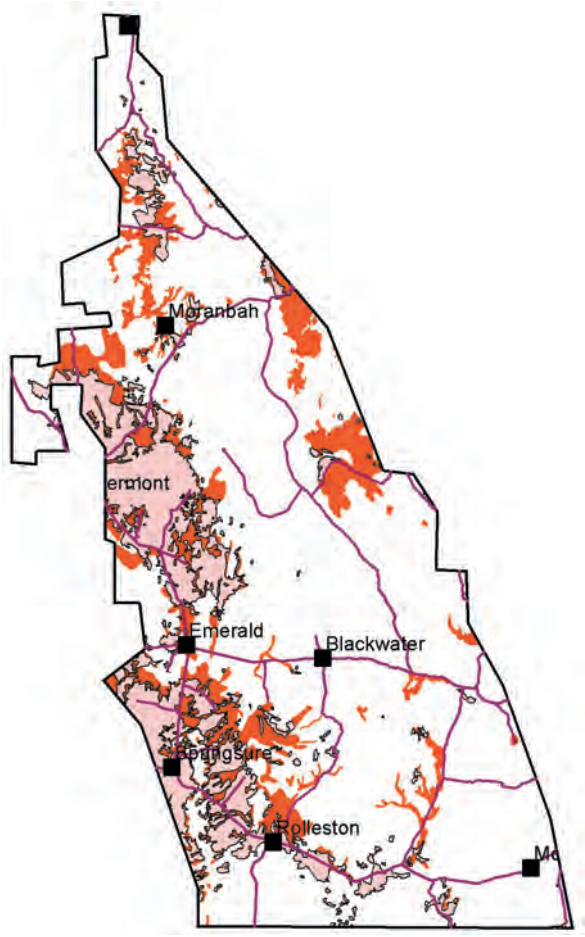

Figure 6: Comparison of area of basalt shown on geological maps with area of basalt mapped using magnetic data. Pink areas represent basalts included on geological maps and orange basalts mapped using airborne magnetic data.

a groundwater perspective as basalts are an important source of groundwater.

The original basalt flows covered large areas. The erosional remnants seen today are often the infills of palaeo-drainage channels. These are best developed in the northern part of the study area and in the southern part. The basalts are generally Eocene to Oligocene in age (Johnson, 1989). Figure 7 shows a palaeo-valley basalt overlying the Mimosa Syncline. The age of the basalts in this area is about 25Ma. As can be seen on Figure 8, the current drainage is to the east rather than to the south. Since the basalt was extruded, the flow has been eroded and more than 50m of sediment cover the basalt in places. Note also structural control of modern drainage in the Springsure-Rolleston area.

The change in drainage patterns is probably related to uplift of the eastern highlands to form the recharge areas of the Great Artesian Basin at about 10Ma (Bowering, 1982; Eadington & others, 1996; Draper, 2002). The change is associated with major landscape change (Jones, in preparation). The driving force behind the uplift may be related to collisional orogenesis of the same age associated with the formation of New Guinea (Quarles van Ufford & Cloos, 2005).

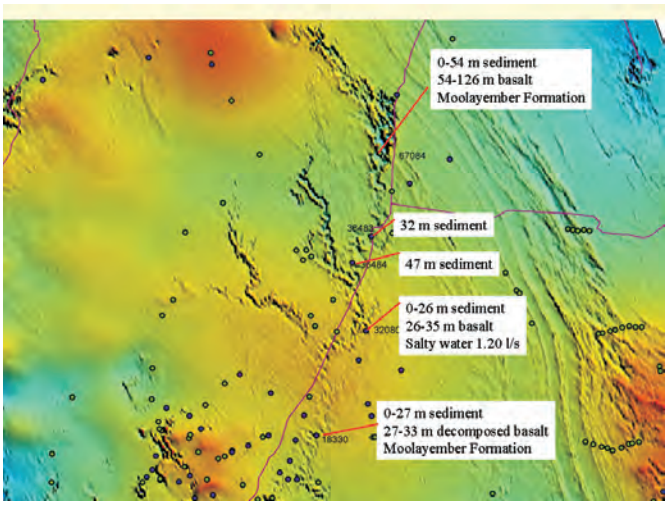

Figure 7: Paleodrainage shown by basalt overlying Mimosa Syncline. Woorabinda is located at the major road intersection. Small circles represent water bores.

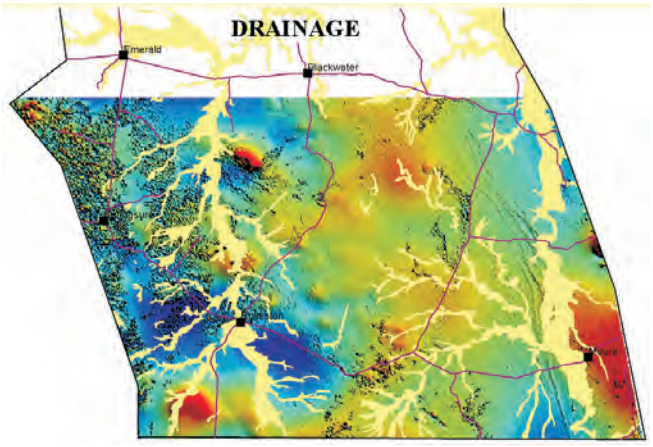

Figure 8: Modern drainage compared to palaeodrainage in the southern Bowen Basin.

OVERBURDEN FILTER

Basalts provide a major challenge to the use of magnetic data. Various techniques are applied with variable success to penetrate beneath basalt sheets. For the Bowen Basin data it was decided to experiment with one offered method. Vector Research P/L have developed The Overburden Filter^{tm} which it is claimed can 'see through' overburden and cultural noise, and resolve near surface and deeper geology below the basalt. It can resolve linear, curvilinear and spot anomalies.

In 2003, Pitt Research P/L, under licence from Vector Research P/L, undertook overburden filtering (OB filter) of a test area across the central Bowen Basin, near Blair Athol (Figure 9). The aim of the commission from GSQ was to test the technique's ability to resolve geology in an area of basalt cover, deep structures, strong curvilinear features (dykes, faults and bedding) and stock-like intrusions. For details of the filter, including images from this study, refer to the following website http://www.vecresearch.com/overburden-filter.html.

Using the various filter and bandwidth combinations, the data has and will continue to provide information from beneath the basalt. The continuation of the Anakie Inlier rocks eastward beneath the basalt cover can be clearly demonstrated (Figure 9). Areas of Permian and of Devonian sediments can be mapped. Areas of granite can be differentiated. Linear control of gold and copper mineralisation can be demonstrated. The structural patterns evident in the open cut coal mines reflect strongly developed regional structures.

MAPPING

The first of the surveys, flown in 2002, was used to prepare a solid geology map of the northern Bowen Basin (Sliwa & Draper, 2003). The experience gained in this exercise will be used to map the remainder of the basin. This mapping exercise will also utilise all open file company mapping. The mapping in the northern area has provided insight into the geophysical properties of many of the rock units.

The Anakie Inlier contains metamorphic, intrusive and volcanic rocks. Overall the Inlier has a characteristic magnetic pattern. This pattern can be mapped to the east under cover. The Overburden Filter proved to be an excellent tool for this purpose. There is a sharp truncation in magnetic properties between the Bowen Basin and the volcanic-intrusive terrains to the east of the Basin.

Permian and Triassic rocks in the Bowen Basin generally have low magnetic susceptibilities, making them partly transparent to underlying sequences. Although the Rewan Group in the Northern Bowen Basin does not have a noticeable response, in areas towards the south, where it has a higher dip, it does have a magnetic response. Likewise, the lower Moolayember Formation shows some response.

Anderson & Koppe (1973) measured magnetic susceptibility in rocks either side of the Jellinbah Fault. The highest values were in the Rewan Group. The red beds gave the highest value (45 c.g.s. units), green mudstone and siltstones moderate values (30) and sandstones gave the lowest values (27). This compared with values in the Rangal Coal Measures of 20 in sandstones and 18 in mudstones and siltstone.

The German Creek Formation had values of 13 in both sandstone and the finer grained rocks. Mudstones of the Ingelara Formation produced values of 20. In the Freitag Formation values of 12 (sandstone) and 15 (mudstone, siltstone) were measured. The contrast in magnetic susceptibility between the Rewan Group and the Rangal Coal Measures enables the thrust faults to be mapped in detail where these units are juxtaposed at the surface (Figure 10).

Because of the paucity of outcrop in the basin, the radiometric data have limited use for mapping the rock units, but provide a major tool for mapping the Cainozoic units. Some of the Bowen Basin units have a strong radiometric response, particularly the tuffaceous units which show a strong potassic response. The radiometric data show some regional variations in units. The Clematis Group in the northern Bowen Basin has a strong potassic response reflecting the high feldspar content in the sandstones (Figure 11). In the south, the Clematis Group is more quartzose and this is reflected in the low potassic response.

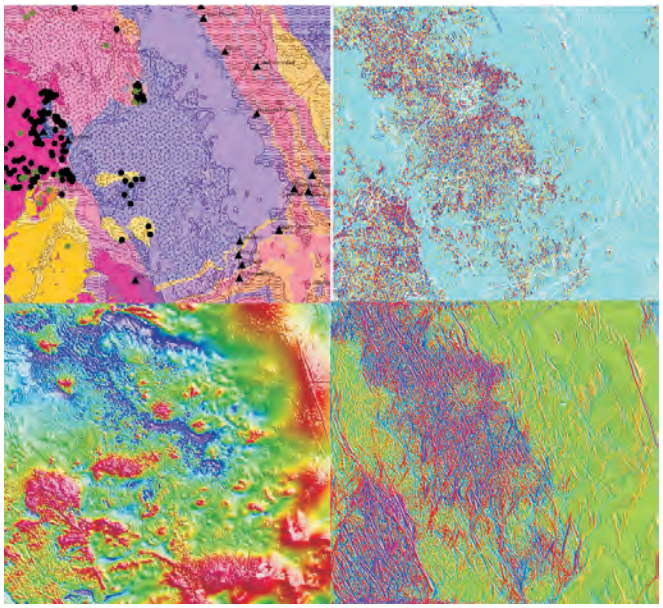

Figure 9: Examples of some overburden filters applied to magnetic data near Blair Athol. Upper left - Generalised geological map of the area, lower left - total magnetic intensity, upper and lower right - examples of applied filters.

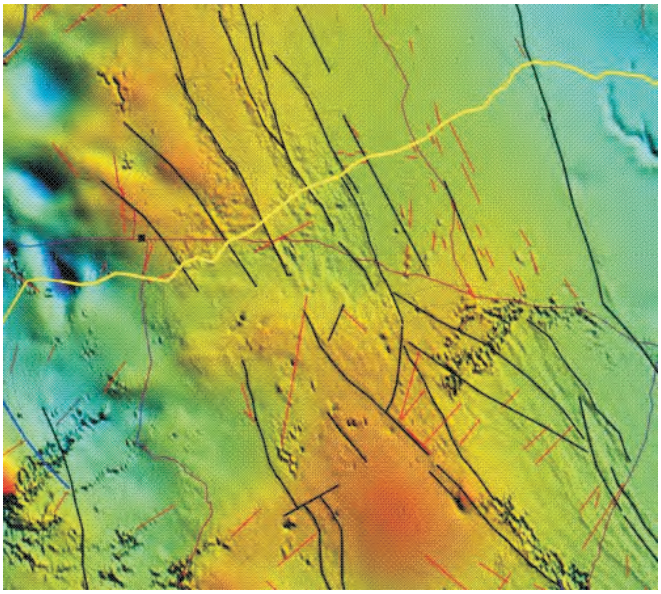

Figure 10: Variation in magnetic properties in the vicinity of the exposed Jellinbah Fault. The 'noisy' magnetic pattern adjacent to the faults marks Rewan Group sediments

The aerial data is just one of many tools to be used in a mapping exercise. Seismic, drilling data, satellite imagery, existing mapping and gravity data when integrated with the aerial data will provide the basis for remapping.

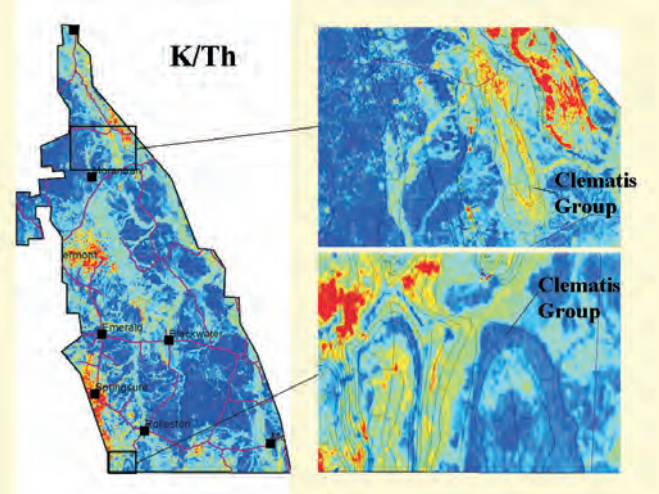

Figure 11: Variation in radiometric character of Clematis Group, northern and southern Bowen Basin. High K/Th ratios are red and low ratios are blue

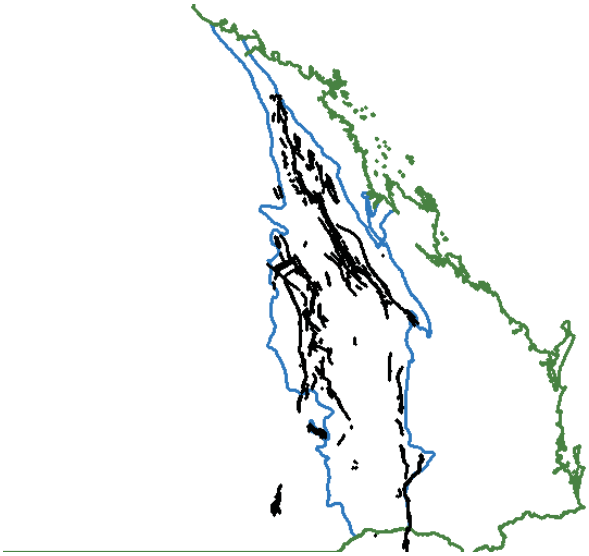

Figure 12: Major structural trends Bowen Basin

STRUCTURE

The tectonic history of the Bowen Basin was been discussed by a number of authors (Murray, 1990; Elliott, 1993; Mallett & others, 1995; Korsch & others, 1998; Fielding & others, 2000; Esterle & Sliwa, 2000). The basement to the Bowen Basin is not well defined. In the northern part of the basin, rocks of the Anakie Inlier underlie the western part of the basin with the contact with the rocks of the New England Fold Belt obscured. Further south the western part of the basin is underlain by rocks of the Timbury Hills Formation and the Roma granites (Murray, 1994). The contact with the New England Fold Belt is unmapped. It is difficult, therefore, to determine all pre-existing structural trends underlying the Bowen Basin.

The Bowen Basin began with an Early Permian extensional phase in a back arc rift setting (Fielding & others, 2000). The rifting was accompanied by volcanism in the east and continental deposition in the Denison Trough. Further south the base of the Taroom Trough is marked by extensive volcanism (Murray, 1994). A period of thermal subsidence followed in the Late Permian resulting in widespread marine deposition. This was followed by foreland loading and the development of thrusts with final basin closure in the mid Triassic. The intracratonic Surat Basin formed above the southern Bowen Basin in the Jurassic to Cretaceous. Cretaceous folding affected the Bowen Basin. The northern Bowen Basin was the site of Cretaceous igneous activity, and Tertiary basalt flows covered much of the basinal area.

This tectonic history has resulted in a complex structural framework that is difficult to unravel. The role of major linear features is also difficult to quantify. South of Moura, there is dominant north-south trend whilst north of Moura there is a dominant north-west trend, albeit with remnants of a north-south trend (Figure 12). The north-south trending faults are predominantly normal faults with younger reversals whereas the north-west trending faults are

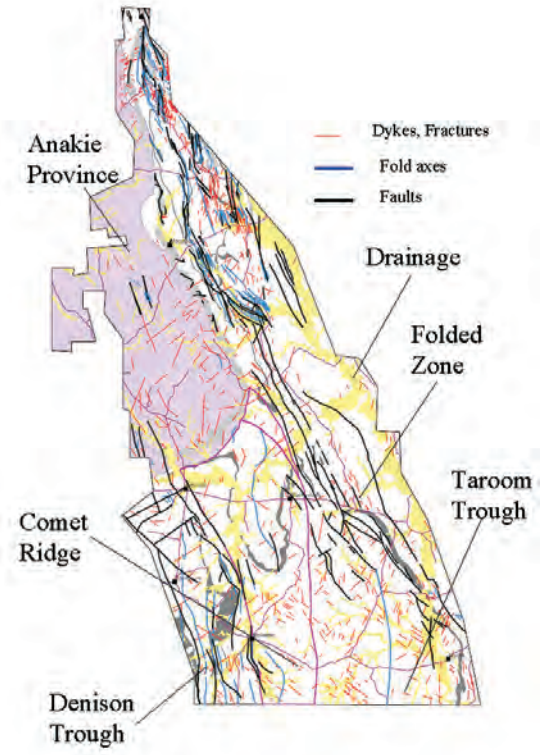

Figure 13: Montage of tectonic elements and structural features in the study area

predominantly thrust faults. The north-west trend is superimposed on the north-south trend. Structural/tectonic studies have focussed either on the southern or northern portions and need to be better integrated. The 2005/06 survey will provide additional data to provide an improved overview.

Figure 13 shows a number of different structural elements in the study. Dykes and fractures show a complex domaining (Figure 14). There are a set of radial dykes in the north and

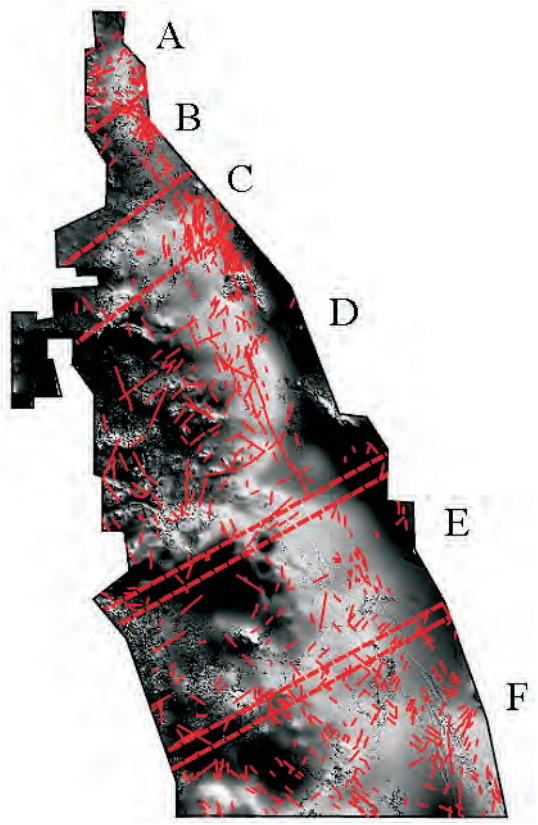

Figure 14: Possible domains delineated by dykes and fractures (greyscale magnetic background)

another near Moura. The northern most domain (A) is dominated by north-easterly trends with minor north-westerly trends and cross cutting radial trends. Domain B contains both north-easterly and north-westerly trends plus the radial trends. Curved north-south trends are dominant in Domain C. Within Domain D, north-north-westerly trends and north-easterly trends are common, but there is an east - west separation with the north-north-westerly trends dominant in the east. This latter trends appears to be associated with the thrusting and not inherent in the basement. Similarly, Domain E has north-north-westerly trends in the east and north-westerly trends to the west reflecting different basic controls. Domain F has a strong north-west trend, a north-easterly trend, a north-north-westerly to northerly trend and radial trends. The dykes patterns reflect a combination of basement trends with superimposed structural and intrusive trends.

The domain boundary between D and E is marked by a general change of major structures from north trending to north-west trending and corresponds to a change in polarity of the half grabens in the Denison Trough. The boundary between Domains C and D is marked by major dykes intrusion and dextral displacement of folds. The other domain boundaries are marked by the changes in trends. The two southernmost boundaries may represent fundamental crustal structures.

Fractures are often infilled by dykes, but mineralisation is often associated with intersection of fractures. Mineralising fluids become localised along the conduits thus developed. Mineralisation associated with the Bowen Basin is in the volcanics on the eastern side (for example, Cracow) or Permian sediments in the Clermont area (for example, Miclere) as well as the Cretaceous intrusions in the northern part of the basin.

CONCLUSIONS

Aerial geophysical data obtained over a large part of the Bowen Basin has indicated the value of such data for regional geological studies. Radiometric data have been used for geological mapping purposes and for natural resource management studies in the Burdekin Fitzroy Project. Magnetic data provide valuable input to mapping and structural studies. Highlights from the data interpretations to date are: the verification and better definition of structural compartmentalisation, the mapping of much greater extent of basalt than that previously mapped, enhanced mapping of faults, identification of previously unknown structures, high potassic nature of tuffaceous units and identification of previously unknown intrusions. The aerial data will be supplemented by continuing the surveys to the New South Wales border. A major structural synthesis study is being planned as well as a remapping project.

REFERENCES

ANDERSON, J.C. & KOPPE, W.H., 1973: Magnetic characteristics of the Rewan Formation, Bowen Basin. *Queensland Government Mining Journal*, **74**, no.860 (June 1973), 208-210.

BOWERING, O.J.W., 1982: Hydrodynamics and hydrocarbon migration – a model for the Eromanga Basin. APEA Journal, **23**, 227-236.

DRAPER, J.J. (Editor), 2002: Geology of the Cooper and Eromanga Basins, Queensland. *Queensland Minerals and Energy Review Series*, Queensland Department of Natural Resources and Mines.

DRAPER, J, AOKI, A., OKAMOTO, N., KARASHIMA, H., AOYAMA, H., TANOUE, M., AIZAWA, T., YAMAZAKI, K. & COVINGTON, M., 2004: Geophysical studies in the Bowen Basin: a collaborative approach. *ASEG 17th Geophysical Conference and Exhibition*, Sydney 2004 (extended abstracts).

EADINGTON, P., PERSON, M., TOUPIN, D. & HAMILTON, J., 1996: An outline of palaeoformation water compositions and flow patterns in the Eromanga and Cooper Basins through Mesozoic time. ***In*** Mesozoic Geology of the Eastern Australian Plate Conference, *Geological Society of Australia Incorporated, Extended Abstracts*, **43**, 167-171.

ELLIOT, L.G., 1993: Post-Carboniferous tectonic evolution of eastern Australia. *The APEA Journal*, **33**(1), 215-236.

ESTERLE, J. & SLIWA, R., 2002: Bowen Basin Supermodel 2000. ACARP Project C9021, Exploration and Mining Report 976C.

FIELDING, C.R., SLIWA, R., HOLCOMBE, R.J. & KASSAN, J., 2000: A New Palaeogeographic Synthesis Of The Bowen

Basin of central Queensland, Bowen Basin Symposium 2000. ***In*** Beeston, J.W. (Editor): *Bowen Basin Symposium 2000-the New Millenium*, Geological Society of Australia Incorporated, Coal Geology Group and Bowen Basin Geologists Group, Rockhampton, October 2000, 287-302.

JOHNSON, R.W., 1989: *Intraplate Volcanism in Eastern Australia and New Zealand*. Cambridge University Press, Cambridge.

KORSCH, R.J., BOREHAM, C.J., TOTTERDELL, J.M., SHAW, R.D. & NICOLL, M.G., 1998: Development and petroleum resource evaluation of the Bowen, Gunnedah and Surat Basins, eastern Australia. *The APPEA Journal*, **38**, 41-79.

MALLETT, C.W., PATTISON, C., MCLELENNAN, T., BALFE, P. & SULLIVAN, D., 1995. Bowen Basin. ***In*** Ward, C.R., Harrington, H.J., Mallett, C.W. & Beeston, J.W. (Editors): Geology of Australian Coal Basins. *Geological Society of Australia Incorporated, Coal Geology Group, Special Publication* **No 1**, 299-340.

MURRAY, C.G., 1990: Tectonic evolution and metallogenesis of the Bowen Basin. ***In*** Beeston, J.W. (compiler): *Bowen Basin Symposium 1990 Proceedings*. Geological Society of Australia (Queensland Division), 201-212.

MURRAY, C.G., 1994: Basement cores from the Tasman Fold Belt System beneath the Great Artesian Basin in Queensland. Geological Survey of Queensland, Record 1994/10.

QUARLES VAN UFFORD, A. & MARK CLOOS, M., 2005: Cenozoic tectonics of New Guinea. *Bulletin of the American Association of Petroleum Geologists*, **89**, 119-140.

SLIWA, R. & DRAPER, J., 2003: *Solid geology northern Bowen Basin: an Interpretation based on airborne geophysics*. Map published by CSIRO and Queensland Department of Natural Resources, Mines and Energy.

John Draper, Geological Survey of Queensland, Natural Resource Sciences

Adrian Buck, Warwick Smyth and Graham Parminter

The application of TSIM in defining intrusions, structure and LOX: A case study at Commodore Mine

The Thiel Surface Impedance Method (TSIM) has been successfully used in the Walloon Coal Measures in the Moreton Basin for fault location, subcrop location and dyke location at the Commodore Coal Mine. TSIM has been most successful in defining the subcrop or Line of Oxidation (LOX). Accurate delineation of the LOX has resulted in cost savings in exploration drilling.

Relatively large resistivity contrasts exist where coal subcrops at the LOX between coal and surrounding sediments. The TSIM measures electric and magnetic fields induced by VLF (very low frequency) radio waves to detect changes in the earth's electrical conductivity. The TSIM method is used to map near surface geological structures. Electrical conductivity changes can be interpreted simply and rapidly, providing a simple means of accurately targeting boreholes.

The TSIM method is able to be straightforwardly operated by a single person and consequently is a low cost geophysical exploration tool for LOX definition. It has been used successfully at Commodore Coal Mine to locate coal subcrop LOX, faulting and dykes in the Commodore Seam in the C-Pit and B-Pit.

INTRODUCTION

Geophysical methods have proven to be useful and cost effective in coal exploration. VLF geophysical techniques have developed slowly over several decades (Biggs, 1990), despite repeated success in the coal industry (Thiel, 1990; Nichols, 1995; Nichols, 1996; Nichols, 2000). The Thiel Surface Impedance Method (TSIM), developed by Professor David Thiel (Griffith University, Brisbane), is one such technique.

At very low frequencies, the surface impedance can be determined by quantitatively measuring the horizontal electric and magnetic field components. The Thiel Surface Impedance Meter (TSIM), originally described by Thiel (1979) for electric wave tilt measurements, measures the horizontal magnetic field using a shielded ferrite cored, multi-turn loop antenna and the horizontal electric field using a centre-fed insulated dipole antenna lying on the surface of the earth. This antenna has been shown to have an input impedance independent of the earth at VLF (Thiel, 1978). Traditionally, horizontal electric field measurements have been made using the staked dipole antenna configuration (Zonge & Hughes, 1992). There has been much discussion in the literature on how to best measure the horizontal electric field (Wu and Thiel, 1989a, 1989b, 1989c; Wait, 1989a, 1989b; Thiel & Mittra, 1997; Wait, 1999a, 1999b; Thiel & Mittra, 1999a, 1999b) with the conclusion being that both the staked dipole and the insulated dipole configurations yield reliable measurements of the horizontal electric field. The susceptibility to electromagnetic noise, the reliability of making repeatable measurements, the influence of a strong vertical electric field component and the reliance on a high-input impedance detector system are all important considerations in attempting horizontal electric field measurements at VLF (Thiel, 2000).

The TSIM 89 model was developed by Energy Control International Pty Ltd under agreement with Griffith University as part of the 1988 NERDDP grant "*Coal seam and strata condition prediction using electromagnetic surface impedance*", of which CCPL was a sponsor. The TSIM 91 model was developed in-house by the Radio Science Laboratory of Griffith University with particular application to ice depth profiling (Thiel & Neall, 1989; Thiel & others, 1996).

TSIM 91 Model is a cheap and seldom utilised instrument outside of Anglos Callide Mine for defining intrusions, structure and LOX during near surface coal exploration programs. Several key features make TSIM an efficient and attractive geophysical technique for coal exploration, resource definition and mine planning:

- The method is very safe.
- It is essentially passive, measuring the ground's response to radio wave sources thousands of kilometres away.
- Field acquisition can be handled by one person with completely portable equipment.
- It can be utilized to minimize drilling costs by better defining targets.
- It is cheap in comparison to other exploration geophysical techniques.

A general renewal of interest by GeoConsult in the technique led to its inclusion for the first time as part of the 2005 exploration program at Commodore Mine (Figure 1). The goal of the Commodore Mine TSIM survey was to reduce drilling costs by limiting the holes required to accurately define the location of the LOX and faulting. In addition to this, the difficult task of delineating several thin in-pit dykes beyond the highwall was attempted. The survey was highly successful, with the LOX, faulting and dykes locations delineated.

Figure 1: Commodore Mine location plan (Figure from Queensland Department of Natural Resources and Mines)

TSIM TECHNIQUE

TSIM is an electromagnetic geophysical method which employs surface impedance theory. Surface impedance is a localised measurement of the earth's resistance to the flow of an oscillating current. The resistivity at a point is determined as the ratio of the horizontal electric field to the perpendicular horizontal magnetic field. VLF radio wave transmitters, such as Northwest Cape communication signal, are an ideal source of electromagnetic energy for surface impedance surveys as they represent a powerful uniform signal which penetrates relatively deep into the ground.

The propagating VLF radio waves have two component parts, electric field (Ex) and magnetic field (Hy) that fluctuate at right angles to each other (Gharibi & Pedersen, 1999). The magnetic component of the source induces a secondary electromagnetic field (Ez and Hz) or eddy current in conductive earth materials (Wilson & others, 2000). The strength of these induced eddy currents in the Earth is a result of lateral resistivity variations (Wilson & others, 2000; Figure 2).

$$Z_s = \frac{E_x}{H_y} = \sqrt{\frac{i\omega\mu}{\sigma + i\varepsilon\sigma}}$$

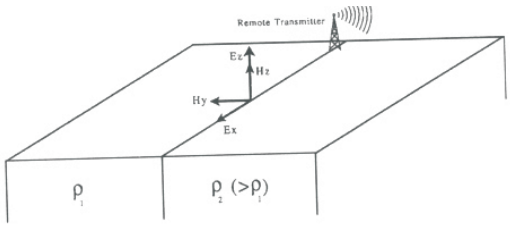

Figure 2: Surface impedance (Zs) is a relationship between the electric and magnetic fields induced by VLF radio waves. It is calculated using the above formula. Figure adapted from Gharibi & Pedersen (1999).

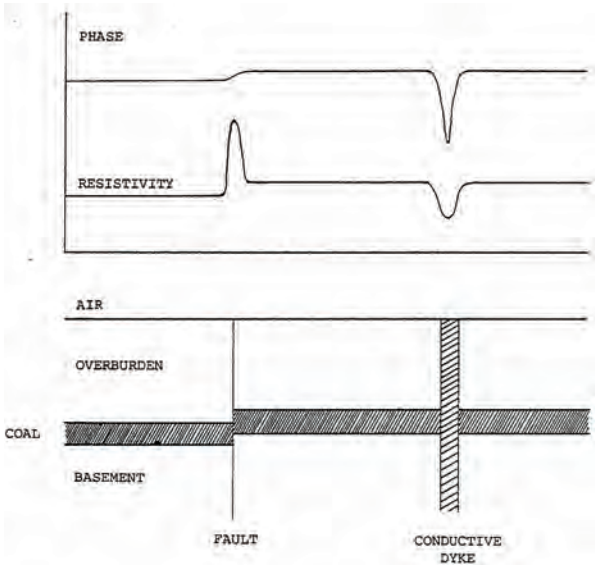

Figure 3: Abrupt changes in geology such as intrusions and faults (shown diagrammatically) produce distinct electromagnetic anomalies(phase and resistivity) that are easily identified using TSIM.

Fundamentally, the TSIM measures near surface geologic response to VLF radio waves. Abrupt changes in geology such as intrusions, faults, and LOX produce distinct electromagnetic anomalies that are easily identified using TSIM (Figure 3).

One person can easily manage the field operation of the lightweight battery-powered equipment, making it a very cost-effective and very safe method for surface exploration work. Surveys comprise lines spaced typically 50m to 100m apart orientated in a direction parallel the VLF transmitter (generally east-west). The TSIM instrument with trailing antenna is traversed taking passive apparent resistivity measurements at a set spacing typically 5m (Figure 4). The TSIM instrument simultaneously measures the electric field (Ex), the Magnetic field (Hy) and the phase difference between the primary transmitter wave and the induced

Figure 4: Typical TSIM operation. The TSIM instrument with trailing antenna is traversed taking passive apparent resistivity measurements at a set spacing.

secondary wave. From these measurements the surface impedance is calculated and variation identified.

Qualitative interpretations of geologic features and their locations are made on the curve shape of the apparent resistivity and phase angle. Detailed quantitative modelling of coal depth, thickness and fault orientation is also achievable (Wilson & others, 2000; Gharibi & Pedersen, 1999).

COMMODORE MINE

The Commodore Mine, 200km west of Brisbane in southeast Queensland is located within 10km of the town of Millmerran (Figure 1). The mine is the sole source of coal to the adjacent Millmerran Power Station. Roche Mining provides a total mine service under contract to the mine owners, Millmerran Power Partners, and are responsible for the management and operation of the mine, including exploration activities. The mine is situated at the western edge of the Moreton basin, in the Cecil Plains sub-basin. The deposit forms part of the Early Jurassic Walloon Coal measures. Tentative geologic correlation from Moreton basin across the Kumbarilla Ridge to the Surat Basin has been described by Ellis (1990) and others.

At Commodore the coal seam sequence is made up of three main intervals, in descending order (Figure 5):

1. The upper group of seams; Domeville (D), Gore (G), Koorangarra (K)
2. The Commodore Seam (M)
3. The Bottom Seam (B).

The upper group of seams (D, G and K) vary from a few thin bands of coal to a banded sequence some metres thick. The Commodore Seam is the main target mining horizon and is composed of 21 coal and stone plies which can be traced across the deposit with confidence.

The relatively low dip of the coal seams and the gently sloping topography are responsible for wide zones of coal seam oxidation. The TSIM survey layout was designed with three separate objectives:

- To define the LOX,
- to delineate a known structure, and
- to trace several thin dykes from the open pit into the current mine design.

The location of the survey is illustrated in Figure 6 below. Lines 1-7 were planned in an E-W direction north of Pit C to delineate the LOX with 1-3 lines extended slightly to the west of Pit C to delineate a known fault. Lines 8-11, 200m in length were planned in an E-W direction north of Pit B to delineate the dykes and devolatilised coal zones.

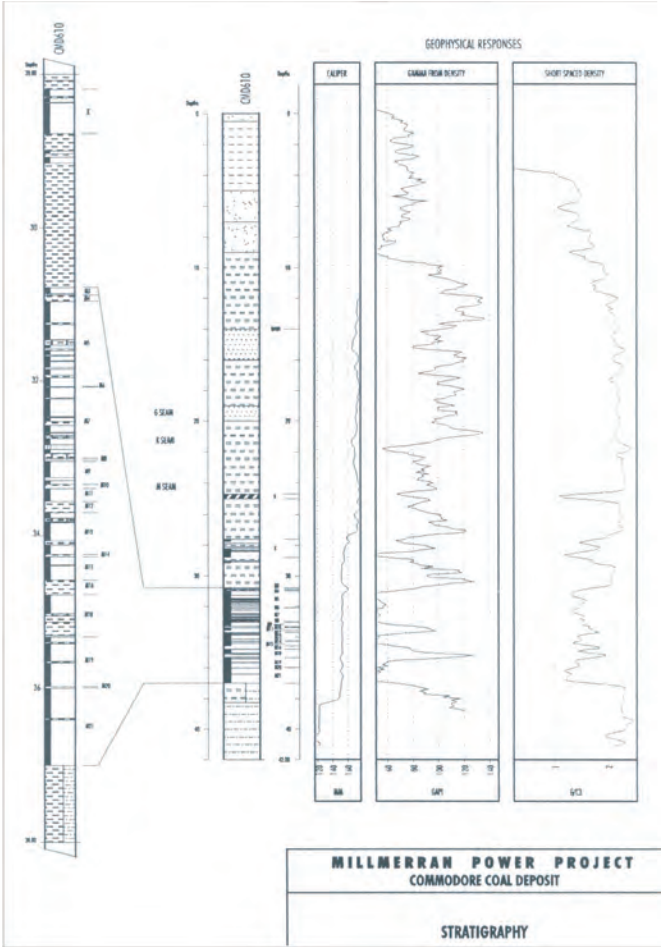

Figure 5: Typical stratigraphy of the Commodore Deposit. The target mining horizon is the Commodore Seam (M).

RESULTS – LOX SURVEY

Several TSIM lines were used at Commodore Mine's C-Pit to refine previous LOX line interpretation and design limits for open cut pit mine planning. The area had been drilled during earlier exploration programs. The drilling program established the depth to coal, the base of weathering at a depth of approximately fifteen metres, approximate LOX and structure locations.

Each TSIM line across the sparse drill hole defined LOX showed a distinct surface impedance anomaly and allowed for closer definition on the location of the LOX. Figure 7 shows geophysical traces that were used to delineate the LOX line north of C-Pit at Commodore Mine. Interpretation of the geological features was based on phase angle and apparent resistivity anomalies observed along the TSIM traverses.

RESULTS – FAULT SURVEY

Exploration drilling of the area to the west of C-Pit had previously identified a steepening in the base of coal contours. Three TSIM lines were extended to cover this area with the goal of better defining the structure. All three lines over the zone revealed pronounced fault signatures. The

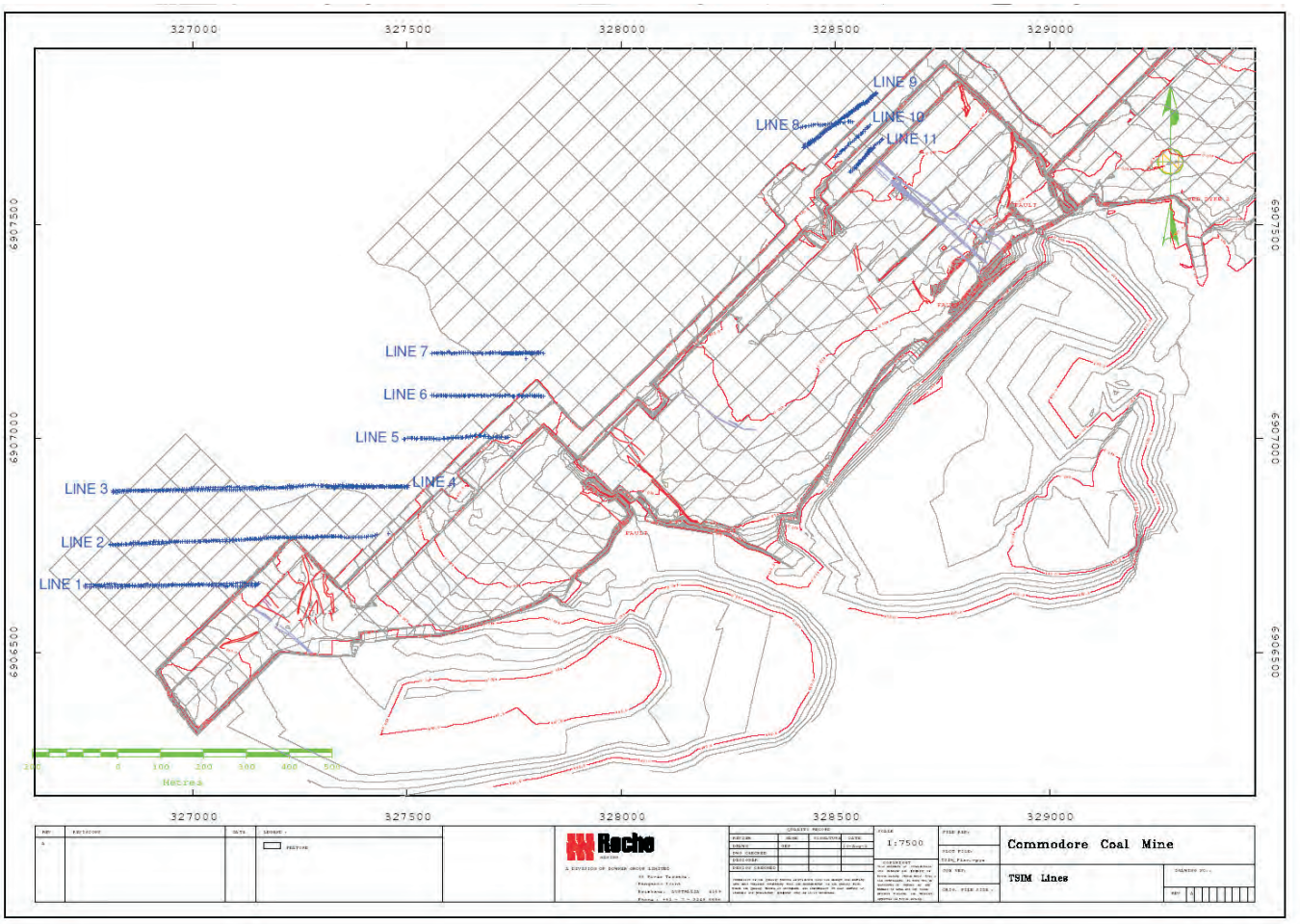

Figure 6: Layout of the Commodore Mine and TSIM survey.

location of the fault was well constrained and a minor conjugate fault recognised to the south.

RESULTS — DYKE SURVEY

The Commodore deposit is generally free from intrusion, however several less then 1m thick basalt dykes have been encountered across the site, with the greatest concentration occurring in the B-Pit. The zone of devolatilisation extends to approximately 1m on either side of the dykes. The dykes are near vertical and intrude all the coal seam. The strike of the dykes in the current strip varies slightly from 300° to 330° magnetic. The dykes had proven difficult to trace on the surface and were virtually undetected by exploration drilling. Several TSIM lines were set out to map the direction and extent of two dykes observed in the B-Pit highwall and thought to be striking near perpendicular to the highwall.

Surface impedance proved to be an ideal tool for tracing dykes at Commodore Mine. Each line revealed a characteristic and readily identifiable signature over the intrusions. Figure 8 shows the apparent resistivity and phase angle anomalies.

The TSIM interpretation of one 50cm thick dyke was confirmed by subsequent validation drilling. The hole did not intersect the dyke but, did intersect the heat affected margin around it.

LIMITATIONS

The TSIM VLF survey method is limited to shallow and near surface deposits. It is estimated that in normal and favourable conditions the technique will detect geological features up to 50m depth of cover.

Investigation of utilising a portable transmitter with variable wave magnitude is underway. This will investigate using the technique to define deeper structures and optimise the orientation of the survey to the geological feature to be defined.

CONCLUSIONS

This paper has outline a case study for a successful and positive interpretation of coal subcrop and LOX, faulting and dykes at Commodore Coal Mine in the Walloon Coal Measures using the TSIM geophysical technique. The TSIM method has again proved to be a significant cost saver in

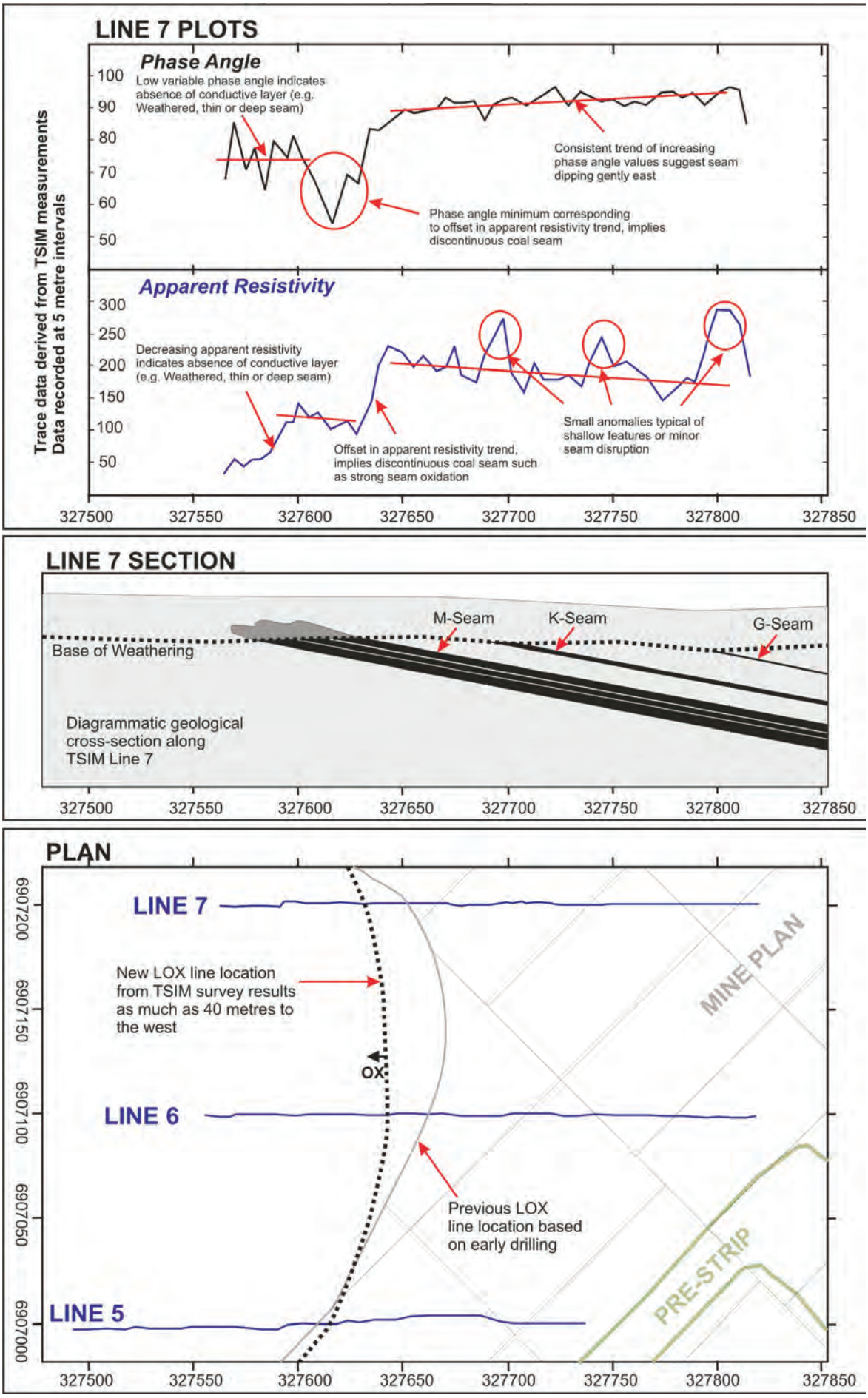

Figure 7: TSIM delineation of Commodore Mine LOX line

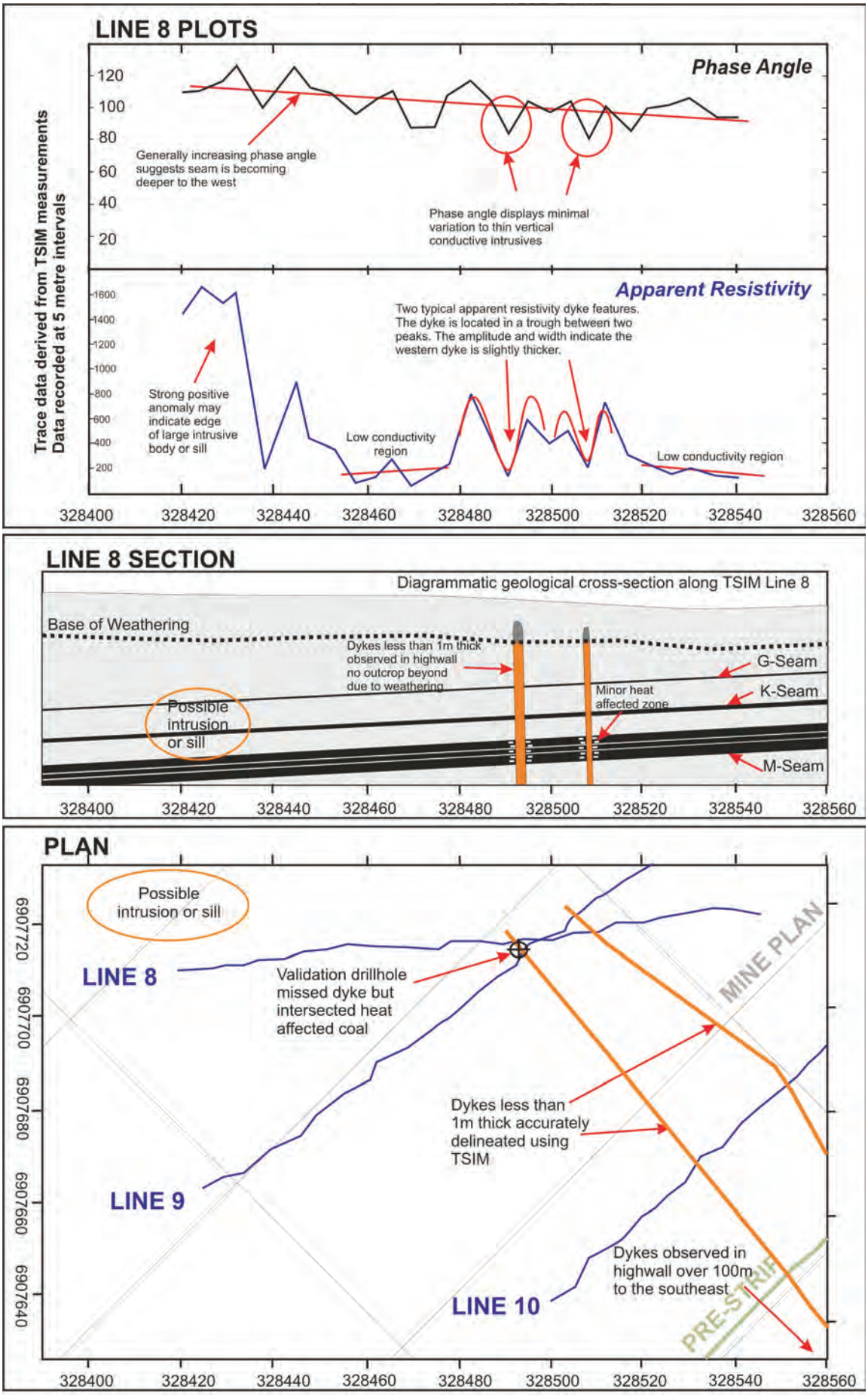

Figure 8: TSIM mapping of Commodore Mine Dyke

determining target drilling and locating and interpreting concealed intrusions and structure. In this case the interpretation of the fault and dykes has been confirmed by drilling. The TSIM technique is easy to administer and provides cheap geophysical data for the identification of near surface shallow geological anomalies.

Despite the current spectrum of advanced geophysical techniques currently available for coal exploration, a number of simple yet effective methods are still being overlooked. The TSIM surface impedance method is continually developing and improving. Natural radio signals such as lightning is being looked at as alternate VLF source and advanced electrical and magmatic sensing technology is now becoming available. These improvements along with enhanced on site data manipulation is making TSIM a reliable technique for real time identification of near surface geology.

ACKNOWLEDGMENTS

The authors would like to acknowledge Roche Mining Pty. Ltd. and Millmerran Power Partners for granting permission to publish this paper. The authors would also like to acknowledge the assistance provided by the staff of Commodore Mine during the survey data acquisition and Professor David Thiel for his expertise during the data interpretation.

REFERENCES

BIGGS, M., 1990: Results From Trials of the TSIM Surface Impedance Geophysical technique at Callide Coalfields. *In, Bowen Basin Symposium Proceedings*, Geological Society of Australia, 181-184.

GHARIBI, M. & PEDERSON, L., 1999: Transformation of VLF Data into Apparent Resistivity and Phases. *Geophysics*, **64**(5), 1393-1402.

NICHOLS, W., 1995: Location of Coal Subcrop at Callide Coalfields using the TSIM Geophysical Method. *In, Bowen Basin Symposium Proceedings*, Geological Society of Australia, 257-264.

NICHOLS, W., 1996: Geophysical trials for Fault Location at Callide Coalfields' Trap Gully Mine, Callide Basin, East Central Queensland. *In, Mesozoic Geology of Eastern Australia Plate (Extended Abstracts)*, Geological Society of Australia, 414-423.

NICHOLS, W. & WILSON, G., 2000: Applications of multiple geophysical techniques for the identification of a suspected intrusion at Callide Coalfields. *In,* Beeston, J.W. (Editor): *Bowen Basin Symposium 2000 - The New Millennium - Geology*. Geological Society of Australia Inc. Coal Geology Group and the Bowen Basin Geologists Group, Rockhampton, October 2000, 335-342.

THIEL, D., 1979: Relative Wave Tilt Measurements at VLF, *Geoexploration*, **17**, 285-292.

THIEL, D., 1990: Surface Impedance Changes in the Vicinity of an Abrupt Lateral Boundary at the Earth's Surface. *IEEE Transactions on Geoscience and Remote Sensing*, **28**(4), 500-502.

THIEL, D., JAMES, D. & JOHNSON, P., 1996: VLF Surface-Impedance Measurements for Ice-Depth Mapping – An Assessment of some Commonly Encountered Interference Effects. *Journal of Glaciology*, **42**(140), 33-36.

THIEL, D., & MITTRA, R., 1997: Surface Impedance Modelling Using the Finite-Difference Time-Domain Method. *IEEE Transaction on Geoscience and Remote Sensing*, **35**(5), 1350-1356.

THIEL, D. & NEALL, F., 1989: VLF Surface Measurements for Ice Depth Mapping in the Antarctic, *Journal of Glaciology*, **35**(120), 197-200.

WILSON, G., THIEL, D. & O'KEEFE, S., 2000: VLF Surface Impedance Modelling Techniques for Coal Exploration. *In,* Beeston, J.W. (Editor): *Bowen Basin Symposium 2000 - The New Millennium - Geology*. Geological Society of Australia Inc. Coal Geology Group and the Bowen Basin Geologists Group, Rockhampton, October 2000, 347-353.

WU, X., & THIEL, D., 1989: Electric Field Sensors in Electromagnetic Soundung, *IEEE Transactions on Geoscience and Remote Sensing*, **27**(1), 24-27.

Adrian Buck, GeoConsult Pty Ltd, PO Box 1002, Spring Hill Qld 4004
Warwick Smyth, GeoConsult Pty Ltd, PO Box 1002, Spring Hill Qld 4004,
Graham Parminter, Roche Mining Pty Ltd, 66 River Terrace, Kangaroo Point Qld 4169

Bill Withers, Ian Rose and Jared Armstrong

Geological digital asset management in coal: towards an optimum solution

The objective of all mining organisations is to maximise their financial return by accurately defining the extent and economic viability of their deposits. This is true, regardless of the commodity being mined. To meet this objective, a wide variety of data is collected using an ever increasing range of technologies and procedures. This in turn has created a data explosion that can cause serious problems for the geoscientific teams responsible for collection, analysis and modelling.

Even in year 2005, geoscientific data for one deposit may still be collected and stored in a multitude of formats; paper, spreadsheets, Access databases and propriety corporate databases. Traditionally, in the coal industry, proprietary databases attached to modelling and mine planning systems were the preferred repository for the delivery of data management solutions. However, there are many reasons why this is no longer the most optimal solution.

Some of these reasons include:

- **Evolving technologies providing a better data architecture,**
- **complex data sets are better managed,**
- **a more generic solution can be independent of any specific process,**
- **open access/integration with other applications (including GIS systems),**
- **porting of corporate data validation rules to field/laboratory entry platforms.,**
- **better integration of workflow and data capture procedures within the data management system,**
- **total cost of the data collection process is reduced,**
- **lithological intervals can be graphically corrected against geophysics, and**
- **complex queries incorporating budget expenditure, lithological, geophysical, quality and geotechnical data sets can be achieved efficiently.**

This paper investigates this topic and provides two case studies where Digital Asset Management Systems have been installed. Some of the major achievements of these installations include reduction in cost of data collection, enhanced functionality for the project geologist and considerable time reduction in the data management process. It has also provided a solution to a management objective that the base data being used for all subsequent processing has a higher degree of validation.

PART A. TOWARDS AN OPTIMUM SOLUTION

To achieve success companies must have a full understanding of their geologic deposits. This understanding is driven by a digital representation of an ore-body that is modelled based on the collection of a plethora of observations and measurements. Given that all subsequent decisions made by a mining company are based upon this collected ‘data’ it is critical to establish rigorous solutions for its collection and management. These measurements are the fundamental building block of a mining company’s value chain.

History of Geoscientific Data Management

In the last 25 years there has been a rapid transformation in the processes associated with resource estimation and mine planning. The retirement of paper based solutions and the establishment of computer based solutions has provided for all of the following:

- Analysis of far greater outcomes is possible,
- utilisation of a much wider range of measurement systems, and
- enhanced Integration of the geological, engineering and financial processes.

However, the uptake of these systems took place without many controls in place, which leads to many problems and issues that we are only addressing today. The greatest single problem being that the management of companies at the inception of these digital systems could not fully digest the implications of electronic data and digital modelling. Even today, many companies do not fully understand that the information systems used are critical to their decision making processes.

This consequently provided for an explosion in utilisation of computer-based analysis but without the rigour of the paper based solutions that existed in many companies previously. This subsequently impacted on audit ability and allowed the explosion of data utilisation without controls (Figure 1). At the same time, methods of measurement in areas such as geophysics increased, providing an information overload and serious challenges to geoscientists. The geoscientists often had the tools to do analysis and processing but did not have effective management systems to deal with these new data

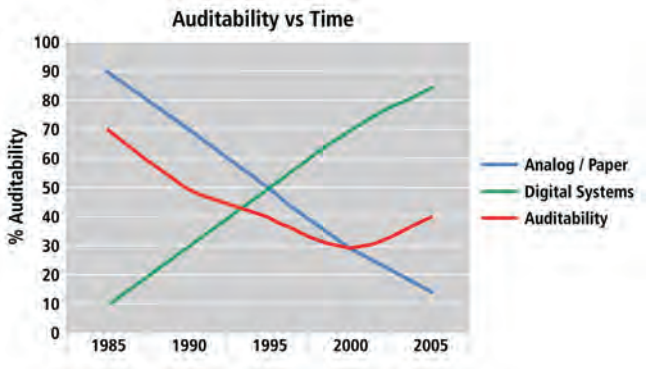

Figure 1: Graph showing volume explosion of geoscientific data over the last 20 years

types and the increased data volumes. Given this, at any exploration or mining site in the world a large percentage of data is still in any of the following formats; ASCII files, Microsoft Excel, Microsoft Word, Microsoft Access and proprietary binary formats. The implications are that the company is paying for the collection of data that may never be turned into information usable for analysis and decision-making.

Another way of thinking about geo-scientific data is by looking at the definition for 'data' and 'datum'. Data is defined as the plural of datum. Datum is defined as:

'Any position assumed or given, from which conclusions can be drawn.'

Although this is well known by most, it is still an area where many geoscientists easily get confused. When does a piece of text stored in a computer become a piece of data? This text may represent field observation or measurement. As the definition implies, when a conclusion can be drawn from the piece of text it becomes data.

There are two major areas to clarify:

1. **The fundamentals or how observations and measurements are stored:**

For Human consumption

Examples: WORD, Excel and Text files

In these structures no declaration is available for any piece of text and relationships are implied. For instance, an author can draw a conclusion from a cell in a spreadsheet by a visual inspection. The inspection might reveal the cell has a certain position in a spreadsheet, the cell may be formatted a certain way or the cell might be linked to other cells via some formula. Although it could be argued this is data to the author, it can often be simply a string of unrelated text to a different audience. The key to the success of these systems as a means of deriving information from the data, is the documentation of the files content. Even then it may not be in a convenient form for a processing system.

For machine or computer consumption

Example: Binary structures of a Geologic Modelling and Mine Planning system

Since the advent of the digital era many mining software systems evolved to deliver a raft of sophisticated solutions in the geologic modelling and mine planning areas. To facilitate these systems data storage and management, proprietary data structures optimised for processing were used. The data structures had rigorous structures where all fields were declared and known to their application. This streamlined the application-data processes however the data were not open to external systems and applications. Also in some situations specific measurements and observations had to be modified to fit internal system structures. In doing so a lot of data were never loaded and consequently not used in downstream processes. Also, these system data structures were not well designed for the purpose of storing metadata or establishing validation rules.

For machine or computer consumption and more convenient human consumption

Example: Relational Database Management Systems (RDBMS)

A number of digital storage solutions and data structure technologies have evolved to optimise the housing of data, and one of these was relational database systems. These systems and a number of peripheral technologies facilitated the following:

- A higher degree of declaration was available for defining data structures,
- provided a greater ability to build validation rules into the data structure.,
- provided the capability to relate data,
- provided a more flexible model for the storage of data so that subsequent reporting could be achieved, and
- a more open architecture was developed so that more applications could utilise the same primary data source.

The technologies supplied by RDBMS vendors such as Oracle or Microsoft (SQLServer and Access) were designed as very generic solutions to solve data issues in a wide variety of industries and for companies of every size. Significant use of these technologies has been made by a variety of exploration and mining companies with varying degrees of success. However, the opportunities provided by these technologies, has created the possibility for a new model to be considered for management and delivery of exploration and mining data.

In essence, the model consists of de-coupling the collection of geologic data from the processing and analysis of geologic data (Figure 2).

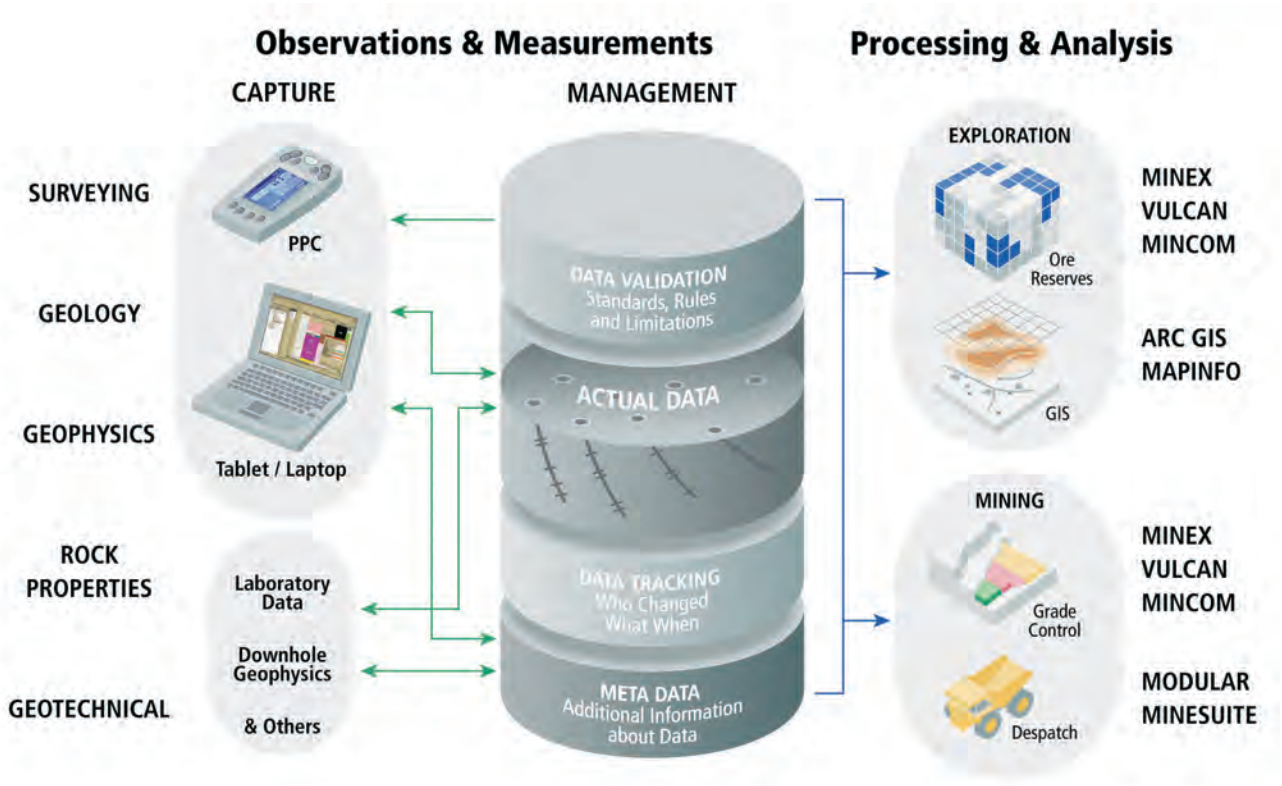

Figure 2: Schematic showing data collection and management processes "de-coupled" from data analysis processes

This is absolutely vital to achieving more value from the investment made in collecting geoscientific data.

The benefits gained by doing this are:

- There is one store for all geoscientific data (measurements and observations) regardless of what analysis systems are used.
- The potential for data silos is reduced because different groups in the one site or organization will use the same repository.
- Business rules regarding data integrity can then be distributed to a larger percentage of collected data and workflows can be optimised.
- As new technologies evolve a specific processing system may not have the infrastructure to house the data in question. An example of this may be face mapping photography like that produced by SIROVISION and Adam Technologies.
- Metadata can then be collected that will assist in down stream decision making.
- Systems become self documenting so problems are avoided like those outlined when using data storage structures for human consumption (like Excel).

2. The importance of control or measured data versus processed data

In many industries data captured in the field is subsequently used to make decisions but it is not necessarily the basis of extensive downstream computation. In the exploration and mining industry the field measurements made are critical to the geo-mathematical models constructed downstream. Given this any error in the base data can cause significant issues in the downstream models. Table 1 summarises some problems that can be found in a drilling data capture exercise.

The interpolated data are calculated from the 'control points' (observations and measurements) measured in the exploration phase.

To put it in JORC (2004) terms:

> "The location, quantity, grade, geological characteristics and continuity of a Mineral Resource are known, estimated or interpreted from specific geological evidence and knowledge."

Any error(s) at the data collection phase (geological evidences) will impact down stream decision making.

The primary benefit for a company to improve the management of geologic data is to increase the potential for better decision making and hence improve their financial bottom line. In addition, a growing need has emerged for companies to comply and be more transparent with resource reporting standards.

The competent person responsible for the resource reporting now requires a higher degree of knowledge about not only the data but also the collection methodology. Given this, the establishment of comprehensive systems for the management of observations and measurements is a fundamental step in contributing to the compliance process.

Table 1

Data Type	Description of typical errors and issues
Collar	Coordinate systems – Measured versus computed. Many current systems have no solution for storing the grid genealogy and store the calculated coordinate instead of the measured. For instance if a GPS was used the latitude and longitude should be stored and any derivative can be calculated from that measurement.
Downhole surveys	Cross data validation on hole depths is required. From these measurements de-surveying (computed hole traces) can be applied by the modelling system. This is an area where significant scrutiny is required as there is a number of de-surveying algorithms that all deliver a slightly different result.
Quality	The transfer of data from laboratories can be problematic. Check systems to validate laboratory performance need to be established. If possible washability data should be stored as part of the primary database.
Sample data	Cross data type constraints need to be in place. Some times the total depth of a hole defined in the collar area of the database may be less than the sample from and to values. Metadata about sample preparation is often not loaded.
Geology	In cases where holes have been re-logged, the previous version is eliminated. All versions of interpretation should be retained. As a result of typing errors, negative thicknesses may be stored.
Geophysics	Often this data type or its associated metadata has not been input into the database management system. Consequently only a limited amount of cross drillhole analysis can take place. Seam thicknesses may be stored and not recognised as based on geophysically uncorrected data.

Volume of data collected versus volume of the orebody

To reiterate from another perspective the value of the measurements and observations made in the exploration phase, it is worth assessing the volume of data analysed as a function of the volume of the ore body in question (P Fell, personal communication, 2005). The following table and graph (Figure 3 and Table 2) display the percentage of material used for the measurement process as a function of the drilling metreage completed. The percentage of material is equal to the volume of core divided by the volume of the orebody.

Assumptions have been made with respect to the ore-body volume and drilling costs. In this case there was no pre-collar. However, it clearly displays that in the exploration and mining industry decisions are established based on a remarkably small sample. Given this, it is critical to optimise the derived knowledge and we must therefore be confident of the original measurements and observations.

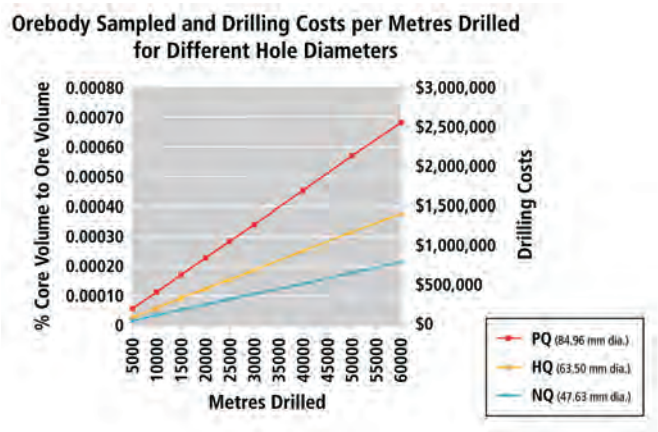

Figure 3: Sample volume verses orebody volume (see Table 2 for orebody volume computation)

Part A Conclusions

For companies wishing to establish a more optimum environment for the management of geologic observations and measurements, the following is recommended:

- De-couple the data capture technology from the geologic modeling and mine planning technology without compromising on an integrated solution. This will facilitate the utilization of the data by other evaluation technologies such as Geographic Information Systems.
- Centralise and integrate the data by removing ‘data silos’ traditionally built around like data types. Attempt to have ALL measured data in one integrated solution so the utility of the measurements taken is fully realised.
- Increase validation capabilities such that as measurements and observations are captured, they are validated. Integrate field practices with the data hub so specific validation processes are the same regardless of where data entry takes place geographically.
- Provide a digital infrastructure so that as new measurement technologies eventuate, the resultant data can be integrated into the geologic modeling process.
- Establish auditing systems so that lock down and signoff concepts that existed in the pre-digital age can again become common practice.

Table 2: Calculations relating core volume to ore body volume as a percentage.

Core Volume - Reality				
Ore Body Thickness	5 m			
Orebody Length	1000 m		OreBody Volume	2500000 m^3
Orebody Width	500 m		Depth to top of ore	95 m
Average length of hole	100 m			
Assay Cost per sample	$25.00			
Cost for RC/m	$45.00			
Cost for DD/m	$60.00			

Orebody Intersectioned Core Volume m^3 per metres drilled									
Metres Drilled	5000	10000	15000	20000	25000	30000	40000	50000	60000
No of Holes	50	100	150	200	250	300	400	500	600
Spacing	143m by 71m	100m by 50m	83m by 42m	71m by 36m	67m by 33m	59m by 29m	50m by 25m	45m by 23m	42m by 21m
No of Samples	250	500	750	1000	1250	1500	2000	2500	3000
Cost (drilling & assaying)	$235,000	$470,000	$705,000	$940,000	$1,175,000	$1,410,000	$1,880,000	$2,350,000	$2,820,000
PQ (84.96mm diameter)	1.42	2.83	4.25	5.67	7.09	8.50	11.34	14.17	17.01
HQ (63.50mm diameter)	0.79	1.58	2.38	3.17	3.96	4.75	6.33	7.92	9.50
NQ (47.63mm diameter)	0.45	0.89	1.34	1.78	2.23	2.67	3.56	4.45	5.34

% Core Volume to Ore Body Volume									
PQ (84.96mm diameter)	0.00006	0.00011	0.00017	0.00023	0.00028	0.00034	0.00045	0.00057	0.00068
HQ (63.50mm diameter)	0.00003	0.00006	0.00010	0.00013	0.00016	0.00019	0.00025	0.00032	0.00038
NQ (47.63mm diameter)	0.00002	0.00004	0.00005	0.00007	0.00009	0.00011	0.00014	0.00018	0.00021

- Recognise that people, processes and technology all play a part in the enhancement of digital asset management solutions.

PART B. DIGITAL ASSET MANAGEMENT CASE STUDIES

The arguments made in Part A of this paper relate to the generic objectives associated with the establishment of a digital asset management solution. In Part B two recent implementations of the acQuire solution (a digital asset management technology) are discussed to highlight both the benefits and issues raised. The implementations chosen are vastly different in both their geographic location and the conditions that existed on site prior to implementation.

Case Study 1 focuses on the Newlands Collinsville Abbott Point (NCA) Coal Project. NCA is owned and managed by Xstrata Coal and is 130km west of Mackay in the Northern Bowen Basin The combined output of NCA's open-cut and underground operations is around 7Mt of washed coal per year.

Case Study 2 focuses on the Sebuku Mining operations. Sebuku produces 3Mt per annum of washed coal, is located on Sebuku Island off the south eastern corner of Kalimantan in Indonesia and is operated by Straits Resources Limited. Straits Resources Limited are a diversified resource company with a copper leaching operation in Western Australia and a Coal operation in Indonesia. This is supported by a range of gold, base metals and coal exploration projects in Australia and Indonesia.

CASE STUDY 1: NCA Project, Xstrata Coal — Central Queensland

Overview

Management from the NCA Coal Project knew about acQuire's existence from other Xstrata sites. These sites were visited by Todd Harrington (Newlands), Richard Gibson (Oaky Creek) and Paul Bannerman (Oaky Creek) prior to a coal forum in 2003. Metech and a number of Queensland based coal industry geologists met at this coal forum to discuss whether acQuire would be a suitable technology for the coal industry. Following an assessment it was concluded that if acQuire was expanded to meet certain coal specific objectives, it could meet the needs of the NCA coal project.

Site status prior to the implementation

The majority of the lithology data was gathered in the field on paper logs, geophysically corrected and then entered into a text editor in the format of a Vulcan DBL (Database Listing File). Some of this correction work was completed

off site. The data was then validated via a series of Vulcan scripts before a final import into a Vulcan database.

Databases existed based on geographic mining areas, ie Suttor Rangals, Suttor Coking, Eastern Creek and Newlands Main. Several other Vulcan databases existed as geographically overlapping projects. Managing the databases was a complex and time consuming process relying on an Excel spreadsheet to track each hole status and the databases where each hole resided. The main database(s) did not contain holes from mined out areas. The database structure was based on the assumption that the holes would be used for modelling, thus many holes not considered appropriate for modelling were often deleted, wiping out any record of that hole.

It was possible for one hole to exist in several databases yet be associated with different data in each database. One hole could have several different names, made unique by the use of a non-rigid naming convention. This led to some holes being more up to date in one database than another.

Other issues included:

- A large amount of date formats were corrupted by processing through Excel spreadsheets.
- Overflow / additional lithology description codes for a single interval were handled on separate lines with the use of bed relationship characters (continuation codes). This is common in the coal industry.
- Many historical lithology codes were not present in the current dictionary.
- Truncated historic comment fields over the years had lost the associated hole depth values.
- Source quality data were stored in Excel files, separate to any associated lithology or LAS data.
- Most of the down hole geophysics was stored in a separate Vulcan database. The process was very time consuming and costly to convert LAS files to text files, then import to Vulcan.
- The majority of geological data was processed off site by external consultants giving Newlands limited ownership and control of the data. It was an inefficient and costly exercise to retrieve data back from consultants.
- Workflows were inefficient.

Business objectives

Business objectives prior to implementation included:

- The database solution must be able to contain all types of coal data relevant to Newlands. This included raw coal quality, washability data, clean coal composite data, down-hole geophysics (1cm resolution), and lithology data.

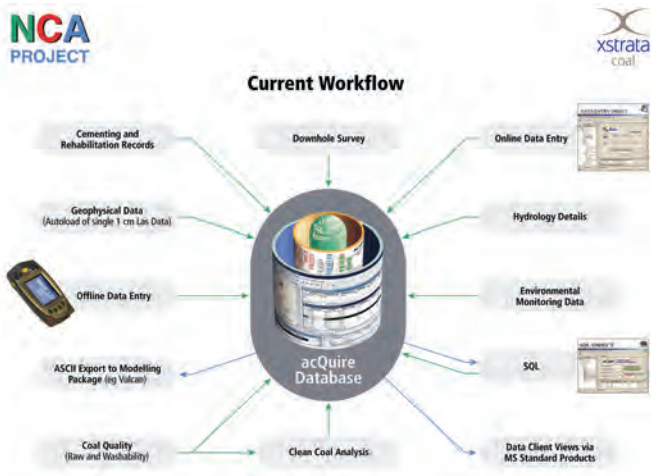

Figure 4: Current workflows for Newlands Coal

- The database should be able to store the immediate digital data but also the long term historical data without any major speed impediments.
- The solution should have abilities to port the data efficiently to both Mapinfo and Vulcan.
- To have a depth adjustment tool incorporated into the database that was both easy and efficient for lithological corrections to geophysical boundaries.
- Implementation on a dedicated SQL 2000 server.

Implementation

The NCA Coal Project implemented acQuire over two stages in April and June during 2004 in a four to six week period. Collar, geology, down hole survey, coal quality, LAS, hydrology and water chemistry were loaded.

Once the initial phase of data loading was complete, a user interface was set up to cater for NCA data management requirements. This interface was constructed within the acQuire system to meet NCA workflow requirements.

Benefits Gained from the Implementation

The following is a summary of direct benefits gained from the implementation:

- The data is now managed on site. This has resulted in immediate data management cost savings.
- Storage of the different coal data types into one central database has been achieved. This means the retrieval of any data type is more efficient.
- Multiple users can access the database at any time. A hierarchy of permissions exists for different levels of users.
- The data entry process is governed by acQuire business rules which have streamlined Newlands data collection workflows. Figure 4 shows these current workflows.

Figure 5: (i) Drill pad, the stick with flagging tape on the right marks the collar location. (ii) Preparing to Geophysically log the hole. The tool is about to be lowered down the hole over the tripod in the foreground. The personnel in the background control the computer and logging unit. (iii) Logging the hole. The cable is lifted up manually away from water and weeds.

- Data entry is via an acQuire interface and there is no need for intermediate third party software (eg Logbase, Notepad, Excel etc).
- Flexibility — the creation of virtual fields (site specific database fields) allows storage of nearly all the data types Newlands uses.
- Users can now extract acQuire data using any ODBC compliant application like Vulcan or Excel. Dynamic ODBC Links between Vulcan and acQuire can be refreshed at any time. Mapinfo Discover has the acQuire API built in and works seamlessly when accessing collar data from acQuire. The one central database providing the external links has been a very effective part of the solution.

The workflows established are outlined in Figure 4.

Where to from here

The following summarises issues that need to be resolved going forward:

- The biggest problems for NCA moving forward is loading and validating huge quantities of old historic data.
- The **Vulcan - acQuire API** is available soon. Maptek are releasing the acQuire API in version 6.0. This should improve data handling practice at Newlands.
- Being able to update the database with data returned from consultants after primary key changes resulting from modelling is an ongoing issue.
- The development and implementation of a depth adjustment tool from within acQuire is still outstanding.
- Storage of geotechnical and gas data.
- Slight improvements to the coal quality sub-system are required.
- Newlands are hoping to integrate underground, open pit, plant and coal quality operations data in the future.

CASE STUDY 2: Sebuku Mine, Straits Resources Limited — Indonesia

Overview

Sebuku island is mostly a tidal swamp with raised Cenozoic ultramafics along the eastern edge. The coal is of Tertiary Eocene age and often sub-crops less than 5m below ground level. The coal measures that contain these economic seams exist as several small basins, the largest being no longer than 3km. Once an area has been proved to resource level, embankments are built and dewatering takes place before earthmoving equipment is introduced to move the overburden. Raw ashes average values range between 7-10% with a relative density of 1.37–1.41g/cm^3.

Exploration activities still take place in 0.3–1.0m deep water covered marshlands. All the tracks are cut through marshlands for access to drill sites. Drilling and logging equipment are carried to each site. Sites are surveyed using differential GPS. Every hole is geophysically logged, however due to poor logging conditions (see Figure 5) only one in two holes are successful. Down hole geophysics has been collected since the mine started and stored digitally but not in LAS format. Lithological data is manually keypunched then corrections are made against geophysics afterwards. About one in five holes are sampled for lab analysis however only proximate analysis on raw coal is performed. Strip sampling for quality analysis is performed extensively across site.

A further 18Mt of coal had been discovered in the past two years extending the mine life by another six years (R Heeks, personal communication, 2004, 24 October). As a part of this increased focus on the coal data a number of data management inefficiencies were revealed. Straits Resources contacted Metech in 2004 for discussions about the possibility of upgrading the existing geological data storage system at Sebuku.

Site status prior to the implementation

The following issues needing resolution were raised:

- Inflexible interface to other programs. The database was part of the Mine Planning System used on site. It (the database) served the purpose of feeding data directly to the modelling section of the software. It was not designed to interface directly with external mining systems. However data exporting via CSV format existed.
- No back end validation. Data was digitally stored in an Access database. However the database was only used as a repository rather than an efficient management system. The database performed almost no validation.
- No consistent seam/ stratigraphy lists were used to control data entry. Often colours were used in the stratigraphy and lithology fields. “Green” meant basement rock and “green” meant serpentinite. “Black” was sometimes used in the lithology field for coal.
- Lack of ability to store and use coal specific data. Not all data could be stored in the existing system so it was stored in filing cabinets. The database used was eight to ten years old and not designed to handle coal specific data types.
- No process existed that allowed sub setting of the database.

Business objectives

The following points summarise Straits Resources objectives in enhancing their data management processes:

- A data management solution was required that could deliver their geological data seamlessly to the new modelling system. This was the main business objective.
- Be able to store coal specific data types. This included down hole geophysics and coal quality data.
- Load all down hole geophysics files. The objective was to move away from only paper copies of the logs stored in filing cabinets to digital storage and thereby better utilizing this information.
- The solution must have some measure of data validation. Data validated prior to system entry was preferred.
- Be able to subdivide the database. This was for the purposes of moving all the data or sections of the database to head offices in Balikpapan and Perth for backup, resource modelling, and reporting purposes.
- The geologist’s workflow had to be provided for from within the data management software interface.

Implementation

Implementation, workspace customization and training took place in February 2005 over an initial two week period. A follow up visit by a company database geologist over another two weeks in March 2005 resulted in further upgrades and completion of the workspace customisation.

Benefits gained from the implementation

The following benefits have been gained following the installation:

- Loading the LAS files (for the first time) to a digital resource management system was only a minor part of the installation. However the results of this process appeared to be a real highlight for the geological staff and demonstrated the usefulness of acQuire’s new geophysics subsystem on site at Sebuku.
- All Sebuku’s coal specific data types are now stored in one database management system.
- Manual site specific processes and local look-up lists were incorporated into acQuire. These now assist with error control during data entry.
- Interface setups to external data formats (access databases) and the API have streamlined the whole process of data presentation to external systems.
- Customised strip logs have enhanced the reporting process and geological evaluation process by combining quality, lithology and down hole geophysics on the same page.
- Database subsetting has been occurring since implementation.
- Basic workflows emulated in the user interface have enabled more efficient execution of repetitive tasks.

Where to from here

Once field logging procedures are tightened and the LAS export software improved, LAS files should become a lot cleaner. Sebuku may then move to a LAS auto-load process where a SQL Server 2000 Schedule is set up to run the importer at a pre-set daily or weekly time.

Some of the strip log reports may need refining. This will be handled in-house by Straits geologists as the need arises.

The laboratory reporting process is still via fax and quality results are hand entered. Potential exists to get this data digitally from the laboratories for direct import to acQuire.

- Dummy boreholes and dummy intervals are still stored in the database. These were required for the previous modelling system but are no longer needed. A script could be written to isolate, check and delete these dummy items from the database.
- Implementation of the acQuire programming interface (API) to the new modelling package for even more efficient data transfer.
- Enhance the user interface to more specifically emulate geological data workflow on site. This can be

done once users are more familiar with using acQuire.

DEFINITION OF TERMS

API. acQuire Programming Interface. This technology allows external software providers from within their own interface to 'pull' data directly from the acQuire data management system.

Data hub. A regional digital storage location for data gathered from different geographic centres.

Data silos. Data silos are applications that don't share their data with the rest of the enterprise system (Pastore, 2003).

Digital Asset Management System. A term used to describe the technology, people and processes that deliver a management solution for digital information that is a key asset of the company. acQuire is a Digital Asset Management Technology for geoscientific data in the exploration and mining industry.

Digital infrastructure. There are two key components to the digital infrastructure of a company — Information Technology and Information Systems. Information Technology is the hardware, network and operating systems that provide the platform for Information Systems. Information Systems are solutions that operate in specific business units to optimise that business.

JORC. Joint Ore Reserves Committee. The committee responsible for published the JORC Code. The committee consists of the Australasian Institute of Mining and Metallurgy, the Australian Institute of Geoscientists and the Minerals Council of Australia. This code sets out minimum standards, recommendations and guidelines for public reporting in Australia of exploration results, mineral resources and ore reserves (JORC, 2004).

Metadata. Information stored in the catalogue of a database that describes the database structure, constraints, application, authorizations, objects, keys and so on. More simply described it is 'data about data' (Rankin & others, 2003).

Primary key/s. Essential to relational databases. They enforce uniqueness among rows, providing a way to uniquely identify every item you want to store.

Relational database. A relational database is a database where information is stored based on its relationship to other data. The aim of a relational database is to eliminate duplication of data. This means that the data is entered once and through its relationship to other data can be retrieved in a number of formats and for a number of different purposes.

BIBLIOGRAPHY

JORC, 2004: Australasian Code for Reporting of Exploration Results, Mineral Resources and Ore Reserves, clause 19 page 7 and clause 1 page 2.

PASTORE, M., 2003: *Making Your Single-Purpose Database a Collector's Item*. Viewed 7th June 2005. http://www.intranetjournal.com/articles/200303/ij_03_13_03a.html

RANKIN, R., BETTUCCI, P. & JENSEN, P., 2003: *Microsoft SQL Server 2000 unleashed*, 2nd edition, SAMS Publishing, Indiana.

Bill Withers, Managing Director Metech P/L
Ian Rose, Exploration Geologist, NCA Coal Project
Jared Armstrong, Coal Geological Data Analyst, Metech P/L

Mihai Borsaru, John Merritt, Craig Smith and Andrew Rojc

Quantitative tool for managing acid mine drainage

The paper presents the application of the Prompt Gamma Neutron Activation Analysis (PGNAA) borehole logging technique developed by CSIRO Exploration and Mining for acid mine drainage.

INTRODUCTION

Acid Mine Drainage (AMD) is one of the biggest environmental issues facing most sectors of the mining industry including coal, precious metals, base metals and uranium. Once established, acid drainage may persist for hundred of years and is extremely costly to monitor and remediate. Acid Mine Drainage is produced by the oxidation of sulphidic mine wastes that are exposed to atmospheric conditions. In mining situations this process is accelerated when large volumes of sulphide rich minerals are exposed. Acid drainage results from oxidation of these materials and may impact on the environment. AMD occurs as run off or seepages from waste-rock stockpiles, tailings impoundments or coal rejects. It may also be discharged from underground mine workings via adits or shafts, or seep from open-pit walls where groundwater is intercepted.

Pyrite, FeS, is a common sulphide mineral present at mines and its oxidation has a major contribution to AMD. AMD in coal mining environments is characterised by low pH (leachate pH values may be as low as 2) and high sulphate (>2000mH/L) and iron. Other metal sulphides can also occur increasing the levels of soluble metals. The potential for and nature of AMD is site specific and a function of mineral deposit (Managing Sulphidic Mine Wastes and Acid Drainage — Best Practice Environmental Management in Mining, Environment Australia, May 1997 Commonwealth of Australia).

It is very important in mine planning, design, operation and closure to assess at an early stage the sulphide oxidation potential at all sites of the mine and incorporate proper strategies to minimise AMD. **The best way to deal with acid mine drainage is not to create it.** Prevention and management at source is the best strategy. Addressing the risk of acid drainage should be an integral part of mine planning and environmental management systems for the whole of the mining industry. One important parameter used in the Asia Pacific region in an environmental management system is the net acid producing potential (NAPP). It is calculated by subtracting the acid neutralizing capacity (ANC) from calculated maximum potential acidity (MPA) using the following equation (Miller & Jeffrey, 1995):

$$NAPP(kg\ H_2SO_4t^{-1}) = MPA - ANC(kg\ H_2SO_4t^{-1})$$

where MPA is (%S x 30.6).

The stoichiometric conversion factor 30.6 assumes all sulphur is present as reactive pyrite and that the reaction proceeds to completion. The ability to profile the total sulphur content in boreholes will therefore assist to estimate the Net Producing Potential of the rock (waste).

The work described in the paper deals with the *in situ* determination of the total sulphur and NAG (net acid generation) of the overburden by nuclear logging. Nuclear logging is well established and used routinely in the oil, gas, uranium and coal industries. It is essential for the oil and gas industries, in which very deep holes are drilled (thousands of metres). Owing to the deep penetration of γ-radiation and neutrons, nuclear logging can locate the presence of oil or gas behind the well casing.

Laboratory analysis of core samples retrieved from boreholes and nuclear logging are complementary. Although the core can provide all the information that can be extracted from a borehole, nuclear logging is able to provide information almost instantaneously. Informed use of nuclear logging can indicate which sections of the core deserve more detailed analysis. The volume of rock sampled by nuclear borehole logging is also much larger than the core samples and thus provides better sampling statistics, especially in heterogeneous deposits. Nuclear borehole logging techniques are either passive (natural γ) or active. In passive logging, the natural radiation in the borehole is measured by an appropriate detector, whereas in active logging an artificial radioactive source provides the radiation measured by the detector. Nuclear logging can be classified according to the radioactive source employed in the logging tool.

The technique employed for this work was Prompt Gamma Neutron Activation Analysis (PGNAA). PGNAA requires the use of a neutron source. This technique has been developed by CSIRO Exploration and Mining for *in situ* determination of the elemental composition of rock/coal. It has been shown that PGNAA can be used for the determination of density, ash, Fe, Si, Al, S, depth and thickness of coal strata in water-filled and dry boreholes (Borsaru & others, 1993; Borsaru & others, 2001; Borsaru & others, 2004).

THE FUNDAMENTALS OF PGNAA LOGGING AND ITS APPLICATION FOR *IN SITU* ANALYSIS

When fast neutrons emitted by a neutron source enter a medium they undergo collisions with the nuclei present in the matrix and lose energy. If they are not absorbed during this slowing down process, they will ultimately reach the thermal energy of 0.025eV. These thermal neutrons continue

Table 1: Neutron capture data for major components in iron ore

Element (atomic mass)	Cross-section σ(barn)*	Major γ-rays (MeV)	γ-ray intensity (I) per 100 neutron radiative captures
Aluminium (26.98)	0.23	7.72 7.69 6.10 5.13 4.91 4.69 4.66 4.13	27.4 4.2 2.3 2.6 2.6 3.9 2.1 6.4
Iron (55.85)	2.55	7.65 7.63 6.02 5.92	28.5 24.1 9 9
Silicon (28.09)	0.16	7.2 6.38 4.93 3.66 3.54 2.09 1.16	7.8 12.4 62.7 3.9 68.0 21.5 19.9
Sulphur (32.06)	0.52	0.84 2.38 2.93 3.22 5.40	75.5 44.5 22.3 27.1 59.1
Calcium (40.08)	0.43	1.94 4.42 6.42	72.5 14.9 38.9

*Thermal neutron capture

to diffuse through the medium until their life is terminated by other processes such as neutron capture or spontaneous decay.

In the capture process, the thermal neutron enters the nucleus, and produces an unstable compound nucleus, which decays by emission of one or more γ-rays. These γ-rays are characteristic of the particular nucleus and are normally named neutron capture γ-rays. The neutron capture technique is commonly used in nuclear borehole logging and on-stream analysis, and its common name is prompt gamma neutron activation analysis (PGNAA).

Table 1 shows the neutron capture data for Fe, Si, S and Al that are common elements in the earth's crust. The table also shows that the major gamma rays produced by the main constituents of the earth crust (Si, Fe, Al) have energies above 3MeV. However, the gamma rays produced by neutron activation, neutron inelastic scattering, or natural radioactivity have energies mainly below 3MeV which makes the prompt neutron-gamma method less sensitive to interferences from these neutron interactions. Also, the deeply penetrating high-energy gamma radiation detected in a borehole logging probe emanates from a large volume of the matrix and hence the technique is not as sensitive to the rugosity and condition of the borehole.

The most intense γ-rays released by sulphur (Table 1) have energies of 0.84, 2.38 and 5.4MeV. The 5.4MeV γ-ray is most suitable for the determination of sulphur. This γ-ray is well separated from the major γ-rays released by the other major elements forming the earth crust. Determination of sulphur in this work is based on recording the variation of count-rate in this energy peak.

THE SIROLOG PGNAA LOGGING TOOL

The logging tool was fabricated from aluminium and has an external diameter of 70mm and a wall thickness of 3.2mm. Aluminium was chosen instead of carbon fibre, that was used earlier to manufacture SIROLOG tools, because it can withstand higher pressures and therefore be able to log deep holes, more than 400m deep. The tool was fitted with a 100mm x 50mm diameter BGO detector. The detector was coated by the manufacturer with a layer of ^{10}B to protect it from the thermal neutrons surrounding the tool.

A section of 30cm length of the logging tool, surrounding the BGO detector assembly, was also covered externally with a

thin layer of ^{10}B (~16mg/cm^2). This layer of ^{10}B stops the thermal neutrons from interacting with the tool and the detector assembly thus producing unwanted γ-rays that contribute to the overall background. The intensity of the 478keV γ-ray peak produced by the ^{10}B can provide a measure of the thermal neutron flux around the detector and can be used as a neutron flux normalization. As ^{252}Cf releases both γ-rays and neutrons, the BGO detector and the neutron source were separated by 60mm of lead to stop the γ-radiation reaching the scintillation detector.

The lead shielding also scatters the neutrons released by the neutron source. The lead shielding has a conical shape and was placed in a high density polyethylene cylinder. A 40mm spacer made of high-density polyethylene was also placed between the neutron source and the scintillation detector. The polyethylene contributes to thermalisation of the neutrons and produces a 2.2MeV hydrogen peak in the capture spectrum. This peak is used to stabilise the gain, especially when the tool is in a dry hole and the hydrogen peak is less pronounced. This peak is positioned at channel 111 in the energy spectrum, so that the energy dispersion is 20keV per channel. Gain stabilization is essential for BGO detectors because of the sensitivity of the BGO scintillator to temperature variations.

FIELD TESTS

Field tests for acid mine drainage were carried out at Capcoal Mine.

Field tests at Capcoal Mine in waterfilled boreholes — samples collected for laboratory analysis: Twelve test holes were drilled in area Pit D of the mine to ~30m depth and sampled in two metre intervals. The samples were taken to the laboratory and the net acid generation (NAG) and total sulphur measurements were determined. Total sulphur was not determined on all tests due to the high cost involved. The holes were filled with water for logging. The diameter of the holes was not constant; it varied from 105mm to 140mm. Table 2 shows the holes logged with the PGNAA tool as well as the diameter and interval cased with PVC.

The data analysis/interpretation consisted of establishing correlations between the laboratory results and the PGNAA logs. The technique used for the data analysis was regression analysis. The PGNAA logs in PVC casing were treated separately to the logs in open holes.

Multiple regression analysis was used for data analysis and the development of calibrations to allow direct estimation of sulphur from PGNAA measurements. This entailed setting

Table 2: Borehole diameter and casing depth of the boreholes logged at Capcoal Mine

Hole	Diameter (drilling bit)	Casing depth (m)
RD4166	120 mm Blades	5 (125 mm PVC)
RD4170	120 mm Blades	6 (125 mm PVC)
RD4175	120 mm Blades	6 (125 mm PVC)
RD4179	120 mm Blades	6 (125 mm PVC)
RD4187	105 mm Hammer	6 (125 mm PVC)
RD4189	105 mm Hammer	6 (125 mm PVC)
RD4192	105 mm Hammer	6 (125 mm PVC)
DD0713	140 mm Hammer	30 (100 mm PVC)
DD0715	140 mm Hammer	27.41 (100 mm PVC)
DD0717	140 mm Hammer	30 (100 mm PVC)
RD4200	140 mm Hammer	5.5 (100 mm PVC)
RD4204	140 mm Hammer	6 (100 mm PVC)

energy windows in the gamma-ray spectrum and fitting a linear regression model of the form:

$$\%sulphur = a0 + a1X1 + a2X2 + \ldots.+ anXn$$

where a0, a1, ….an are constants and X1, X2,….. Xn are variables. The variables X are normally ratios of count rates in the selected energy windows.

Results based on regression analysis from the holes with diameter less than 120mm: Table 3 shows the RMS deviations for the neutron-capture predictions given by the regression equations obtained for NAG and sulphur (total sulphur) for the open holes (no casing) with diameter less than 120mm (RD4166, RD4170, RD4175, RD4179, RD4187, RD4189 and RD4192). Other holes were not considered in this analysis because large differences in diameter can affect the accuracy of prediction.

The regression equations derived for NAG and S are listed in Table 4. The table also shows the energy windows (channel No.; 20keV/ch) selected for each ratio used in the regression equation.

Table 3: Results from PGNAA logging at Capcoal Mine, area Pit D in uncased holes of diameter 105mm and 120mm

Parameter	RMS deviation	Number of strata used	Correlation coefficient (%)	Standard deviation of the population
NAG	0.3	27	86	0.57
S	0.41	15	85	0.71

Table 4: The regression equations for NAG and S derived from uncased holes

Parameter	Regression equation	Ratio 1	Ratio 2
NAG	NAG = 17 + 1012.4 x Ratio 1 – 537.1 x Ratio 2	(280 – 300)/(18 – 30)	(280 – 300)/(130 – 380)
S	S = -13.9 – 518.1 x Ratio 1 + 451.4 x Ratio 2	(280 – 300)/(18 – 30)	(262 – 280)/(130 – 380)

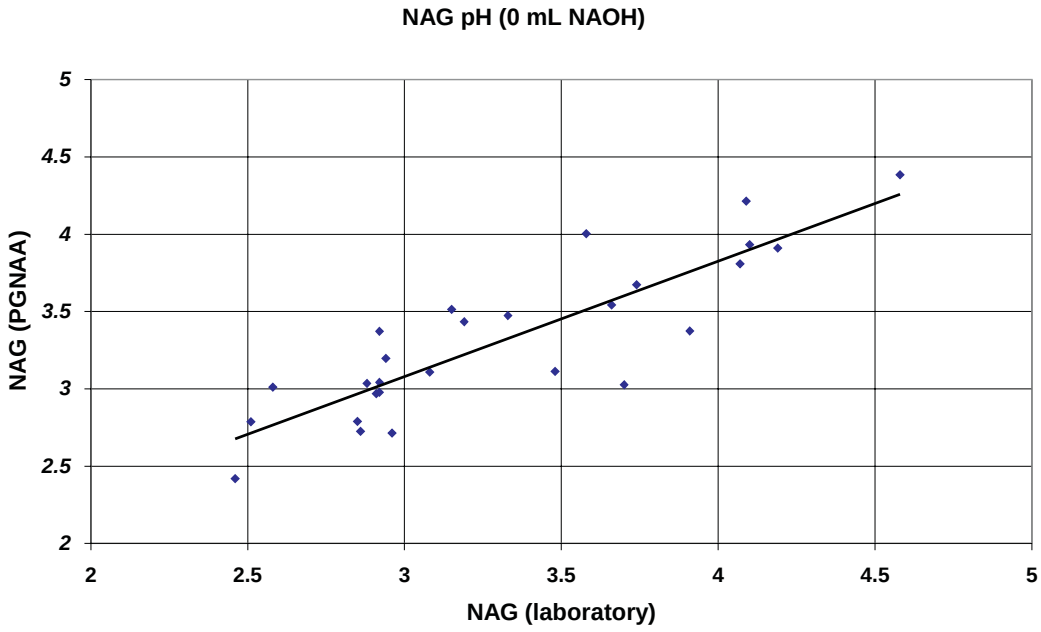

Figure 1: NAG – laboratory analysis vs. PGNAA prediction in open holes of diameter <120mm

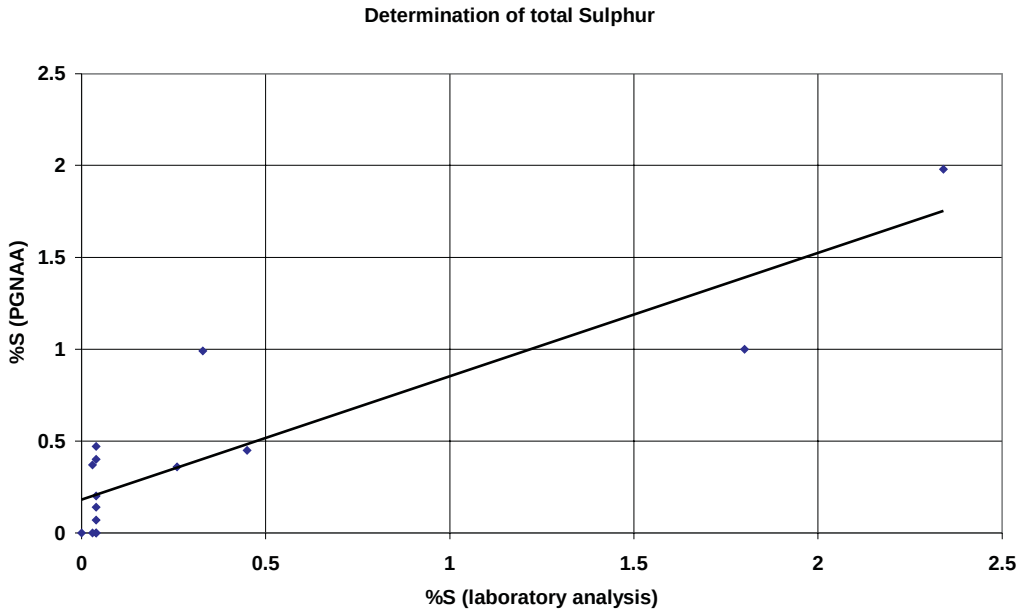

Figure 2: %S – laboratory vs. PGNAA prediction in open holes at Capcoal Mine area Pit D of diameter <120mm

Determination of NAG

The determination of NAG relies on count-rates recorded in three energy windows shown in Table 4. The (18 – 30) energy window is set around the boron peak which is prominent in the recorded γ-ray spectra. The count-rates in this peak are proportioned to the thermal neutron flux around the BGO detector. The other two windows are not related to a particular element and the regression shows that more than one element (e.g. sulphur) contribute to NAG. Figure 1 shows a cross-plot between NAG prediction by laboratory analysis and PGNAA.

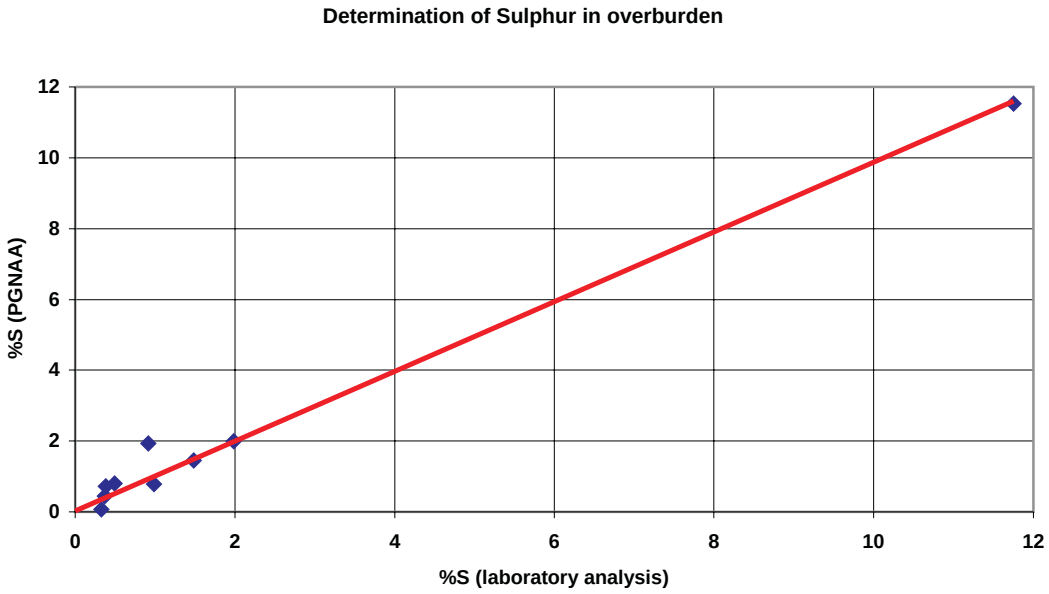

Figure 3: %S (in overburden) – laboratory analysis vs. PGNAA prediction (12 strata) at Capcoal for open hole

Determination of total sulphur

The determination of sulphur relies on the 5.4MeV γ-ray peak produced by sulphur following the neutron capture process. This peak is recorded in the window between the channels (262 – 280). The second parameter in the regression equation (280 – 300)/(18 – 30) takes care of γ-rays produced by other elements like Fe, Al, Si, Cl and Ca that can interfere with the γ-rays recorded for the sulphur peak. Figure 2 shows the comparison between total sulphur measured in the laboratory and PGNAA prediction in the regression analysis. Figure 2 shows that most of the sulphur assays were below 0.04%S with only a poor distribution between the low and high values of sulphur. However, Figure 2 shows that PGNAA is sensitive to the variation of total sulphur in overburden.

A better distribution in sulphur assays was obtained from another open hole specially drilled at Capcoal Mine to test the suitability of PGNAA logging for the determination of sulphur in the overburden. The hole was drilled to a depth of 60m and sampled for sulphur at 0.5m or 1.0m intervals. The PGNAA logging tool used to log this hole was slightly different than the tool used for logging the holes in Area Pit D and therefore the data could not be treated together. Figure 3 shows the comparison between sulphur measured in the laboratory and predicted by PGNAA for 12 strata. The RMS deviation given by the regression analysis was 0.44% S, the standard deviation of the population was 3.3% S and correlation coefficient 99%. Another regression analysis was carried out on the same data set but excluding the 11.7% S point and is shown in Figure 4. This was done due to the single outlaying point having undue influence on the statistics. The RMS deviation for 11 strata was 0.33% S, the standard deviation of the population was 0.62% S and correlation coefficient 88%.

Correlation between NAG and total sulphur

A regression analysis for laboratory assayed total sulphur and NAG determinations on samples collected in Area Pit Dwas run to establish whether a correlation exists between them or not. No correlation was observed. The standard deviation of 1.02 for NAG given by regression was almost identical with the standard deviation of the population 1.07 for NAG. The correlation coefficient of 34% is poor. This shows that total sulphur is not an indication for the net acid generation of the rock for this area. The correlation found between the PGNAA tool's response and NAG is not based on the response to sulphur but on other elements (salts) that are present in the rock.

Results when all holes (diameter from 105mm to 140mm) are considered together

Although the PGNAA technique is not as sensitive as the gamma-gamma technique to the variation of the borehole diameter, the accuracy of prediction will be worse for large variation (e.g. 25mm) in diameter. An attempt was made in the present work to add extra samples collected from the 140mm holes to the samples used in the analysis mentioned above (from holes with diameter <120mm). The samples correspond to the uncased sections of the holes. The results given by regression analysis are given in Table 5.

Table 5 shows that one can get a calibration for NAG and sulphur for holes with a diameter from 105mm to 140mm. However, the correlation coefficients and RMS deviations (relative to the standard deviation of the population) are worse than when the diameters are less variable.

Table 5: Results from PGNAA logging at Capcoal Mine, area Pit D in uncased holes of diameter 105mm, 120mm and 140mm

Parameter	RMS deviation	Number of strata used	Correlation coefficient (%)	Standard deviation of the population
NAG	0.39	33	72	0.54
S	0.44	22	74	0.62

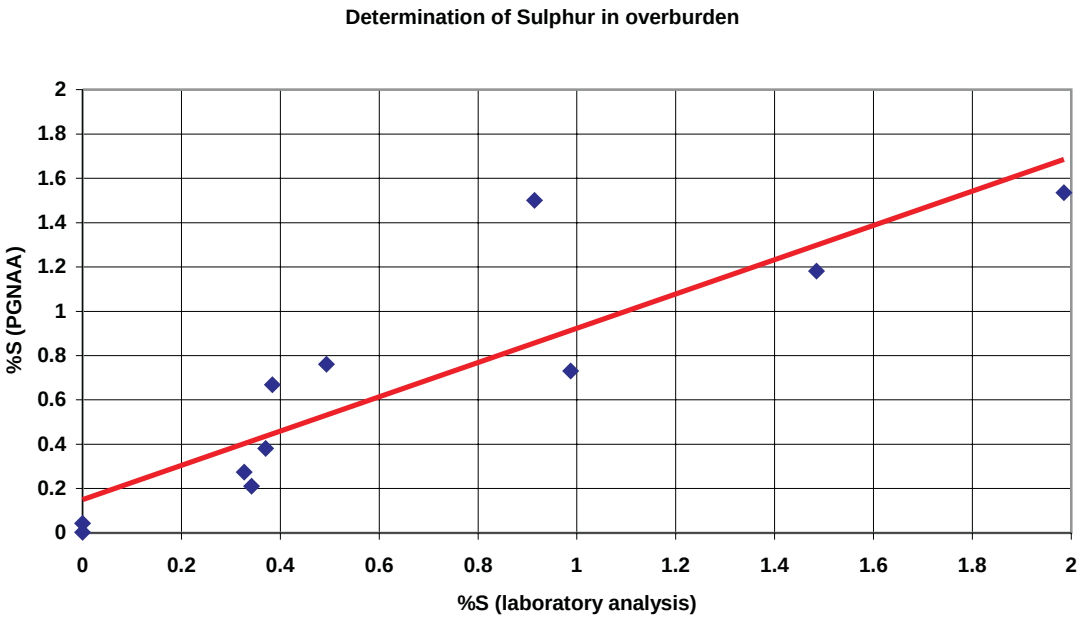

Figure 4: %S (in overburden) – laboratory analysis vs. PGNAA prediction (11 strata) at Cap coal for open hole

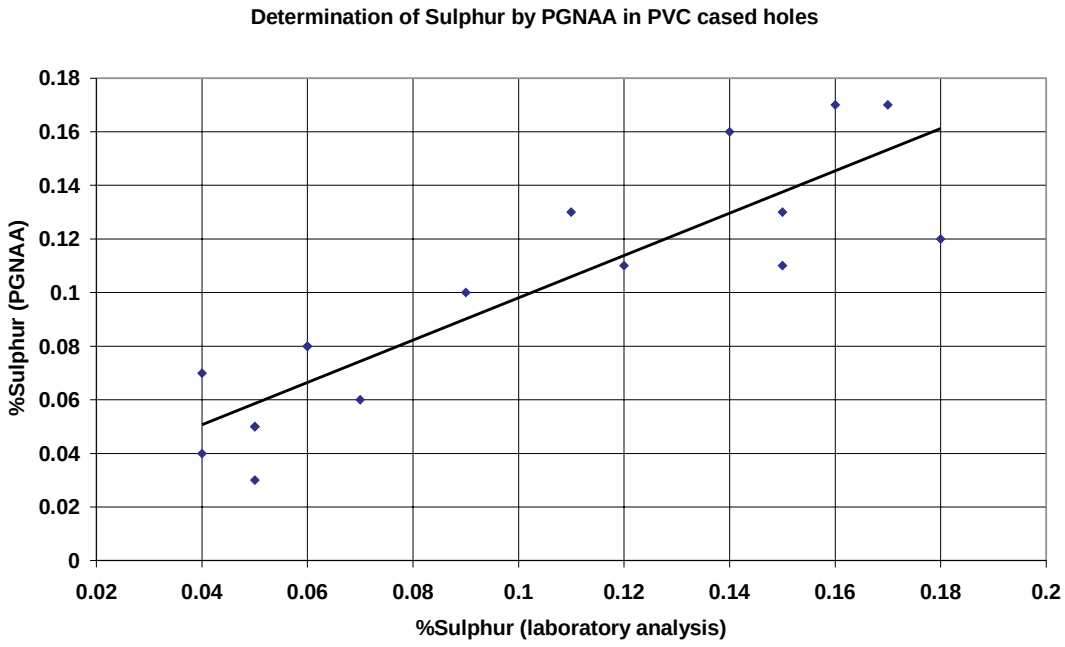

Figure 5: %S – laboratory vs. PGNAA prediction in PVC cased holes at Capcoal Mine area Pit D of diameter 140mm

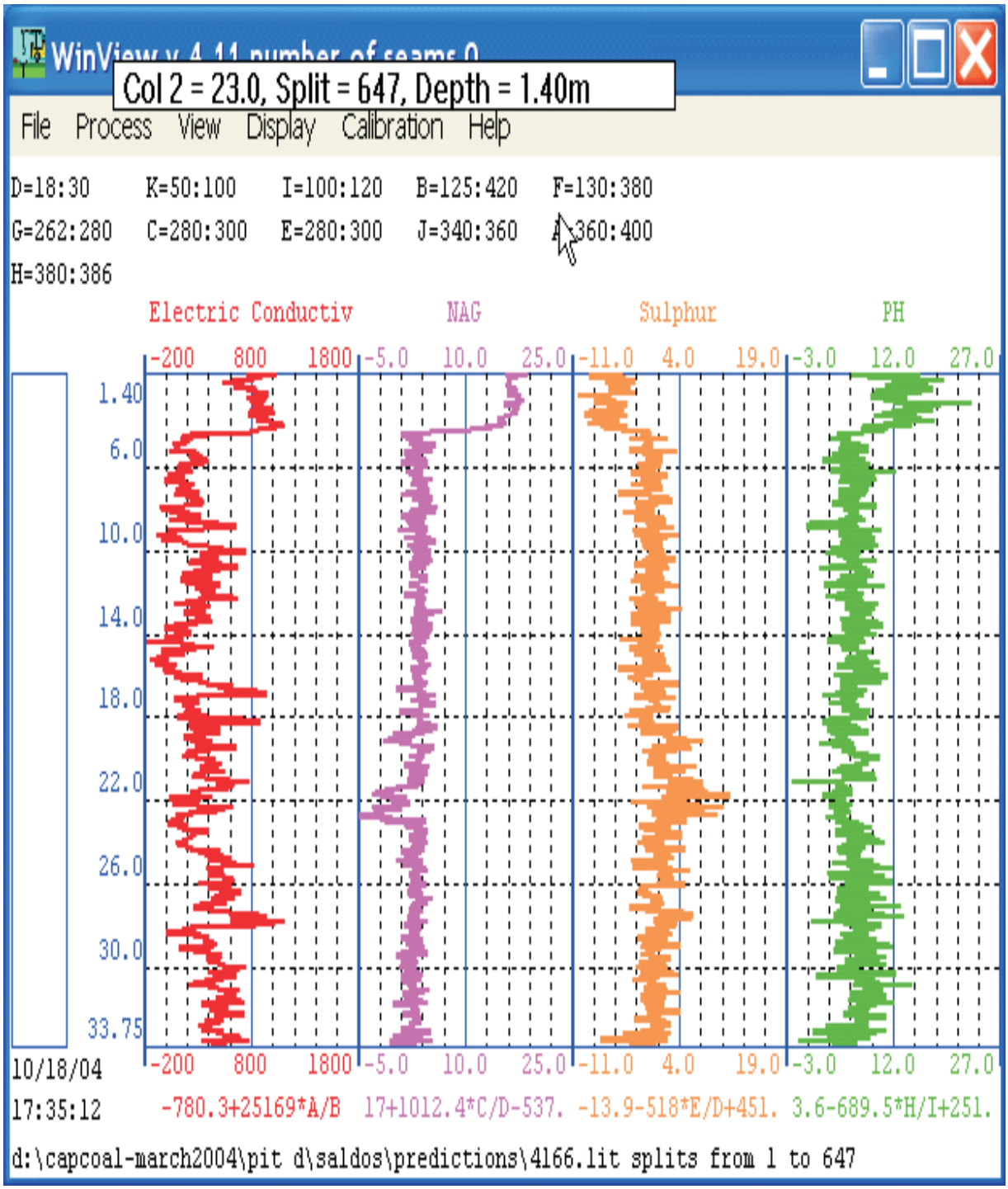

Figure 6: Variation of NAG and S predicted by PGNAA for the hole DH4166

Measurements in holes cased with PVC

A number of holes 140mm in diameter were cased with PVC at the time they were logged. Cased and uncased holes have to be treated separately. If PGNAA logging could be used in PVC cased holes, the calibrations would be different to calibrations in uncased holes. The laboratory assays did not have a good spread for NAG and no conclusion could be drawn. However, the assays for sulphur had enough range for regression analysis to be performed. The RMS deviation given by the regression analysis was 0.020% S for a standard deviation of the population of 0.05% S with a correlation coefficient of 89%. Figure 5 shows a cross-plot between laboratory assays and PGNAA prediction by the regression analysis.

Predictions of NAG and Sulphur by PGNAA

The calibrations for NAG and S have been used in the 7 uncased holes to predict their variation down the boreholes. The predictions are given by WINVIEW, a programme specially written to process data collected with SIROLOG logging tools. Figures 6 and 7 show predictions for the holes RD4166 and RD4170 as given by WINVIEW. The software can also generate average values of these variables for different sections of the holes.

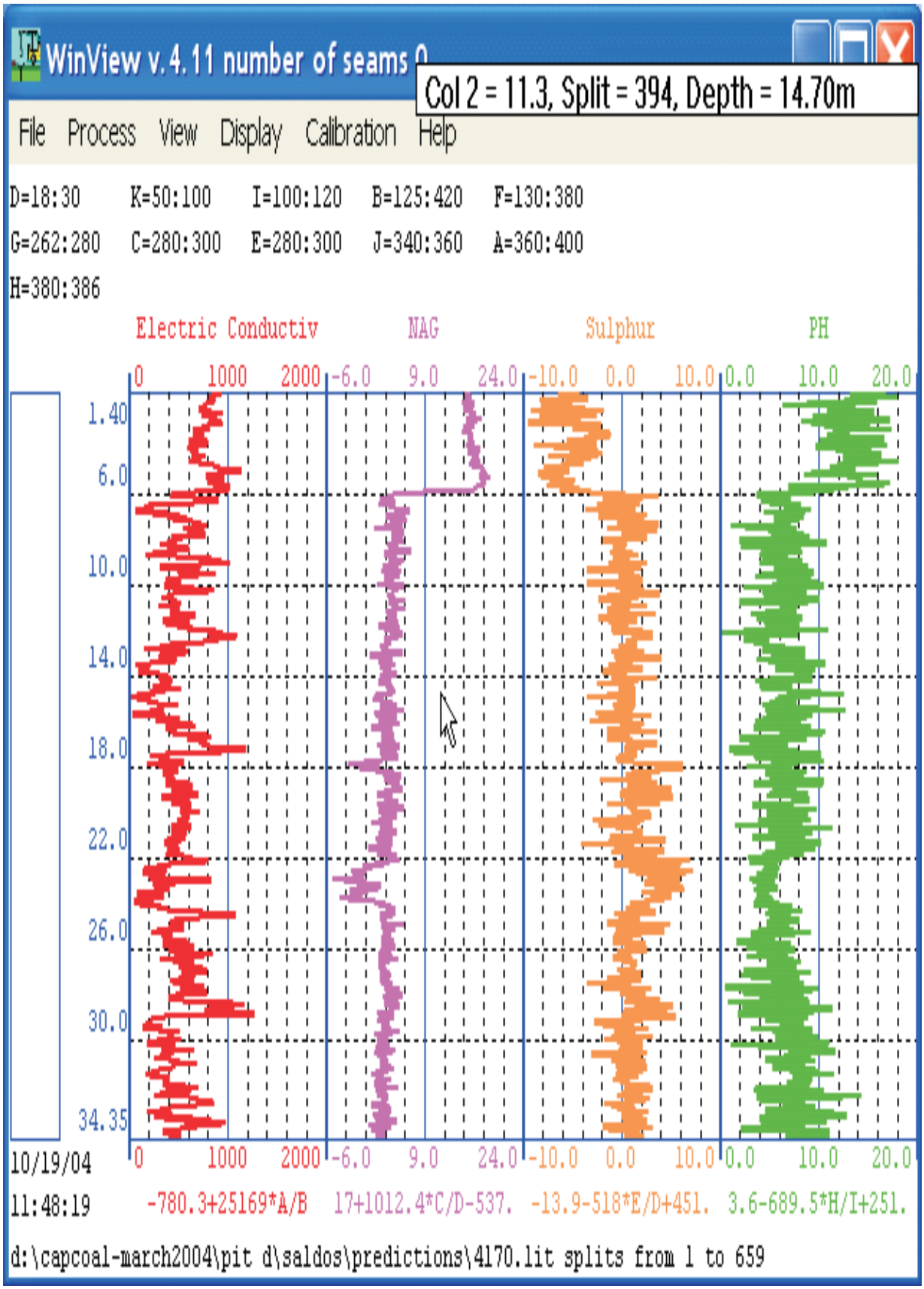

Figure 7: Variation of NAG and S predicted by PGNAA for the hole DH4170

SUMMARY AND CONCLUSIONS

The present work shows that the PGNAA technique has potential for acid mine drainage. This work established that:

1. PGNAA can measure total sulphur in overburden rock. Total sulphur is an important parameter in the estimation of the net acid producing potential (NAPP) of the rock and its estimation has a substantial contribution for developing an acid rock drainage and acid spoil control management plan.

2. A correlation between net acid drainage (NAG) and the PGNAA log was established at Capcoal area Pit D. This is important especially when NAG and total sulphur in the rock are not correlated, as was the case at Capcoal area Pit D where the tests were carried out. This conclusion is based on data available from 7 holes logged with the PGNAA technique and laboratory assays of NAG determinations. However, more tests are needed to prove that this is universal and not restricted to some areas.

3. The work indicated that sulphur can also be measured in PVC cased holes. This conclusion is based on tests carried out in three PVC cased holes. More tests are needed to prove this beyond any doubt.

The SIROLOG logging system has proved its reliability. Callide Coal Fields has been using it for routine logging since 1992. The system at the Callide Mine is used for logging control and exploration boreholes. The current work has expanded its range of applications in the environment.

Another objective of this work was to develop a practice for incorporating PGNAA logging in the environmental management of acid mine drainage. We propose that PGNAA logging should become one of the routine geophysical logs and used to log all holes. When the NAG and sulphur values predicted by the log along the borehole are above the acceptable levels, more accurate laboratory assays should be taken. PGNAA logging will identify the problem areas at a much lower cost. The PGNAA logging for Acid Mine Drainage will also determine the density, ash, sulphur, Fe, Si and Ca in coal seams.

The tool must be calibrated in cored holes rather than models. Calibration holes must be of the same diameter as the holes to be logged. Variation in the diameter of the boreholes decreases the accuracy of the tool's prediction. It is worth mentioning that recent work in CSIRO has demonstrated that PGNAA logging also has applications in identifying the lithology of the rock intersected by the boreholes and in estimating the rock strength.

The tool manufactured for this project can be ordered from CSIRO or SCINTREX/AUSLOG, a company located in Brisbane that manufactures geophysical equipment. The next generation SIROLOG logging system is currently being developed at CSIRO Queensland Centre for Advanced Technologies (QCAT).

RECOMMENDATIONS

The present work in conjunction with previous CSIRO work has demonstrated that PGNAA geophysical logging is a powerful technique and should be developed as a routine method alongside the established gamma-gamma and neutron-neutron nuclear logging techniques widely used in the coal mining industry.

Although the application of PGNAA logging for acid mine drainage was tested in the current work for the coal mining industry, it can also be applied to the metalliferous mining industry.

ACKNOWLEDGEMENTS

The authors wish to thank Anglo Coal, Capricorn Coal Management Pty. Ltd. for the strong support offered during this work.

We wish to thank Darren Pisters and Max Ayliffe (Capricorn Coal Management Pty. Ltd.) for their help and support.

This work was supported under the Australian Coal Association Research Program (ACARP).

REFERENCES

BORSARU, M., BIGGS, M.S. & NICHOLS, W.J.F., 1993: Neutron-gamma logging for iron in coal and implications for estimating the ash fusion characteristics at Callide Mine. *Nuclear Geophysics*, **7**, 539–545.

BORSARU, M., BIGGS, M., NICHOLS, W. & BOS, F., 2001: The application of prompt-gamma neutron activation analysis to borehole logging for coal. *Applied Radiation and Isotopes*, **54**, 335–343.

BORSARU, M., BERRY, M., BIGGS, M. & ROJC, A., 2004: *In situ* determination of sulphur in coal seams by PGNAA. *Nuclear Instruments and Methods in Physics Research B*, **213**, 530–534.

MILLER, S. & JEFFERY, J., 1995: Advances in Prediction of Acid Generating Waste Materials. *In* Grundon, N.J. & L.C. Bell (Editors): *Proceedings of the Second Australian Acid Mine Drainage Workshop*.

M. Borsaru, C. Smith and A. Rojc, CSIRO Exploration and Mining, P.O. Box 883, Kenmore, Qld 4069, Australia
J. Merritt, Anglo Coal (Capcoal Management) Pty. Ltd., PMB, Middlemount. Qld 4746, Australia

Jan Nemcik, Winton Gale and Ken Mills

Statistical analysis of underground stress measurements in Australian coal mines

This paper presents a summary of 235 underground stress measurements conducted in the virgin ground of NSW and Queensland mines. The main objective of this study is to analyse the statistical information from the measurements that are relevant to strata control and mine planning with a view to providing help with a practical approach to estimate the risks involved with strata failure.

Major findings include the statistical increase of maximum horizontal stress with depth in Queensland and NSW mines, a comparison of normalised lateral stress magnitudes and measurements in rock of a different stiffness, 'Tectonic Factor' concept, and maximum lateral stresses and their directions in NSW and Queensland coalfields. These findings can provide a valuable benchmark for mine planning and strata control with potential savings in mine operating costs.

INTRODUCTION

To date, SCT has conducted some 430 successful underground stress measurements in Australian and overseas mines. From these, 349 measurements were conducted in Australian mines and 235 tests measured pre-mining stress conditions. All stress measurements used the overcoring method of 3-dimensional stress determination predominantly using the ANZI stresscell (Mills, 1997). The overcoring method is currently considered to be the most accurate method of determining the *in situ* stress in underground mines.

The aim of this paper is to present the stress measurement data and methods to interpret these measurements made in typical coal measure strata. The measured stress levels are sensitive to parameters such as rock stiffness, geological discontinuities, pore water pressure and gas desorption. It can be misleading to use stress measured in different types of rock and locations without taking these parameters into consideration. Some of these parameters are addressed here to provide understanding how they influence stress flow in rock and what methods can be used for the correct data interpretation.

Influence of strata stiffness on stress

The vertical stress is driven by the gravitational load of the overburden strata. Horizontally bedded strata of different stiffness compress fully until they are able to carry the full overburden weight. The vertical stress will therefore be the same in all types of rock or coal strata. On the other hand, a large portion of the regional lateral compressive stress is usually of the tectonic origin caused by the movement of the Earth's crust. In the horizontally bedded strata, stiffer rock would attract more of a tectonic lateral stress than strata of a low stiffness. The principle of stress distribution in materials of variable stiffness is illustrated in Figure 1.

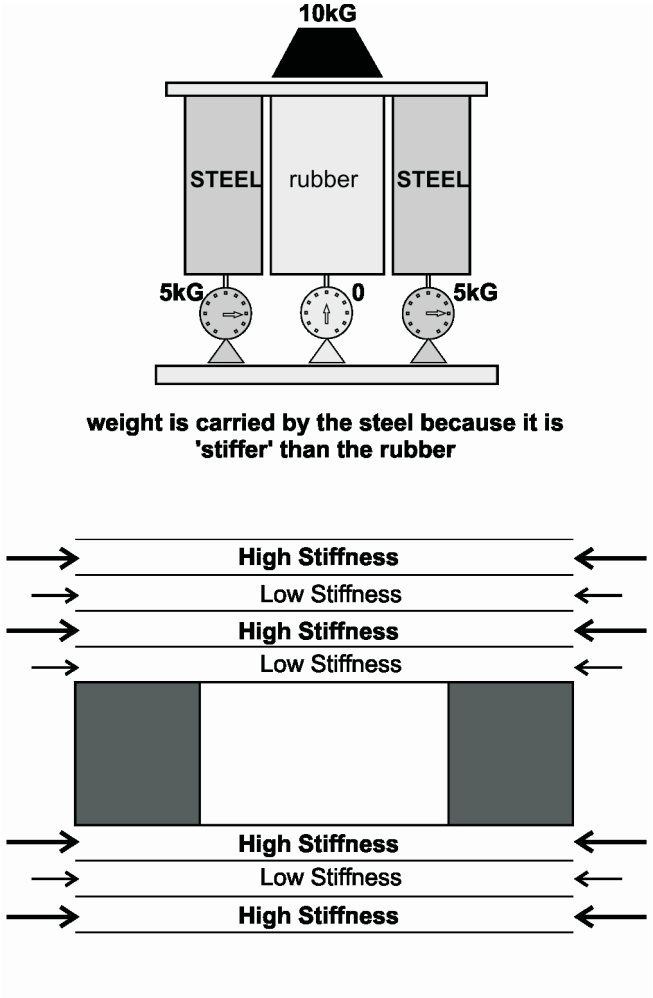

Figure 1: Variation of stress in different layers

In many cases the maximum compressive stress in rock strata is expected to be horizontal and oriented in directions typical to the region. Experience indicates that rock stiffness and therefore the measured lateral stress magnitudes vary considerably in stratified roofs. To compare stress levels between two sites, stresses in rock of the same stiffness must be known. It would be impractical to look for rocks of similar properties during the measurements and therefore a 'normalising' (scaling) technique was developed to calculate stress in rock of any stiffness.

Normalising stress tensor

Three principal stresses σ_1, σ_2, σ_3 describe the 3-dimensional stress tensor oriented in the unique direction at which all shear stresses are equal to zero (Herget, 1988). A change in magnitude of any principal stress would influence other principal stresses via the Poisson's Ratio (ν). The vertical stress in continuous bedded strata would be the same in all types of rock while the lateral stress would vary with rock stiffness. When scaling the 3-dimensional stress tensor to a rock of different stiffness, the vertical stress must remain the same while the lateral stress components would change.

The gravity driven vertical stress (σ_v) induces a lateral compressive stress in strata equal to $\sigma_v\nu/(1-\nu)$ (Goodman, 1989). Assuming that the *in situ* Poisson's Ratio (ν) is similar in most rock types ranging 0.2–0.3 in value, the gravity induced lateral stress within the adjacent rock beds will range from 0.25 to 0.42 times the vertical stress. However, the *in situ* stress measurements indicate that the lateral stress magnitudes are in most cases much larger than the gravity induced lateral stress with a typical range from 1.5 to 4 times the vertical stress depending on location and the overburden depth. In virgin ground the 'excess' lateral stress is usually of a tectonic origin (Herget, 1988) and proportional to the rock stiffness (see Figure 1).

To normalise (scale) the lateral stresses to a chosen rock stiffness, the 'tectonic' component of lateral stress is multiplied by the ratio of Young's Modulus of chosen and measured rock stiffness. To summarise the 'normalising' process:

- choose a convenient Young's Modulus to normalise the lateral stress into,
- subtract the gravity induced lateral stress component from the measured lateral stress to obtain the 'tectonic' portion of lateral stress,
- multiply the 'tectonic' lateral stress with the ratio of Young's modulae ($E_{normalised}/E_{measured}$), and
- add the newly calculated 'tectonic' lateral stress to the gravity induced lateral stress component.

The 'Normalising' process is summarised in the equation below:

$$\sigma_{NL}=E_N/E_M\{\sigma_{ML} - \sigma_v\nu/(1- \nu)\} + \sigma_v\, \nu/(1- \nu)$$

where:
- σ_{NL} = Normalised Lateral stress
- E_N/E_M = Ratio of Normalised and Measured Young's Modulae
- σ_{ML} = Measured Lateral stress
- σ_v = Measured Vertical stress
- ν = Poisson's Ratio

Consider a hypothetical case where the overcore stress measurements were conducted at two underground sites. At a depth of 290m a maximum compressive lateral stress of 19MPa was measured in siltstone with elastic modulus of 24GPa while at a depth of 400m the maximum compressive lateral stress equal to 18MPa was measured in sandstone with Young's Modulus of 15GPa. The lateral stress at 290m depth was scaled down to what it would have been if the measurement was conducted in rock with elastic modulus of 15GPa. Calculations indicate that the normalised (scaled) maximum lateral stress at a 290m depth is 13MPa, 5MPa lower than at a depth of 400m. The higher lateral stress at 400m depth is consistent with the increase in overburden depth.

Figure 2 shows measured and normalised maximum lateral stresses versus the overburden depth in Australian mines (SCT measurements only). The overall stress distribution shows no significant differences between the measured and normalised values of stress indicating a good selection of 'average rock stiffness' chosen for normalisation. When considering single measurements at a particular mine, the normalised lateral stress values describe the true nature of the lateral stress state at a mine site. Note that many existing discontinuities in underground mines may vary the stress flow and it is sometimes possible to experience unusual stress fields at the same depth in the same mine.

Note: Typically, coal has a lower stiffness than surrounding rock and therefore the maximum lateral stress in coal is usually much lower (often less than the vertical stress). Complex stress changes that occur during pore pressure loss and gas drainage within the coal can further reduce the measured stress magnitudes in coal strata. At this stage the normalisation process is not recommended for coal due to the complex issues affecting the stress in coal.

INCREASE IN STRESS MAGNITUDE WITH OVERBURDEN DEPTH

Numerous stress measurements in Australia and overseas compiled on the World Stress Map (Reinecker, 2003) indicate that the vertical and also the horizontal stresses increase with overburden depth. The normalised values of maximum lateral stress measured by SCT in NSW and Queensland coal mine roofs (Figure 3) clearly indicate increase of lateral stress with depth.

To explain the possible mechanisms of lateral stress increase with depth, several issues need to be considered. In response to a constant tectonic interaction within the ground, the rock mass on a large scale is literally broken (intercepted with many discontinuities such as faults, bedding planes, weathered dykes etc). When subject to loading, these large rock geometries would exhibit complex post failure behaviour. This behaviour can be compared to a triaxial test on broken rock sample where the maximum load (σ_1) that the rock sample is able to sustain without further failure increases with the confining stress (σ_3) applied to the sample. The triaxial test is described in Figure 4.

The exact nature of the ground behaviour may not be known, however the confining stress (σ_3) that increases with the depth of cover would provide a mechanical lock to the

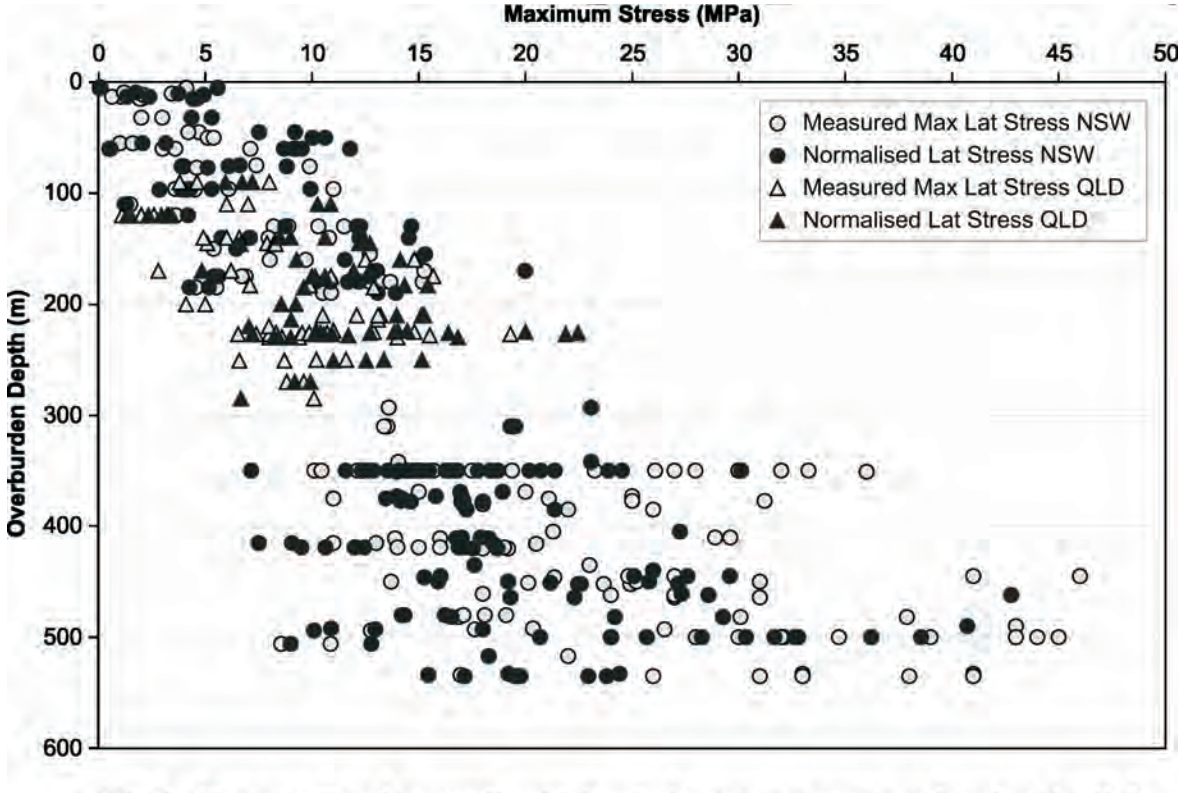

Figure 2: Measured and normalised maximum lateral stresses vs. overburden depth in Australian coal mines (SCT measurements only)

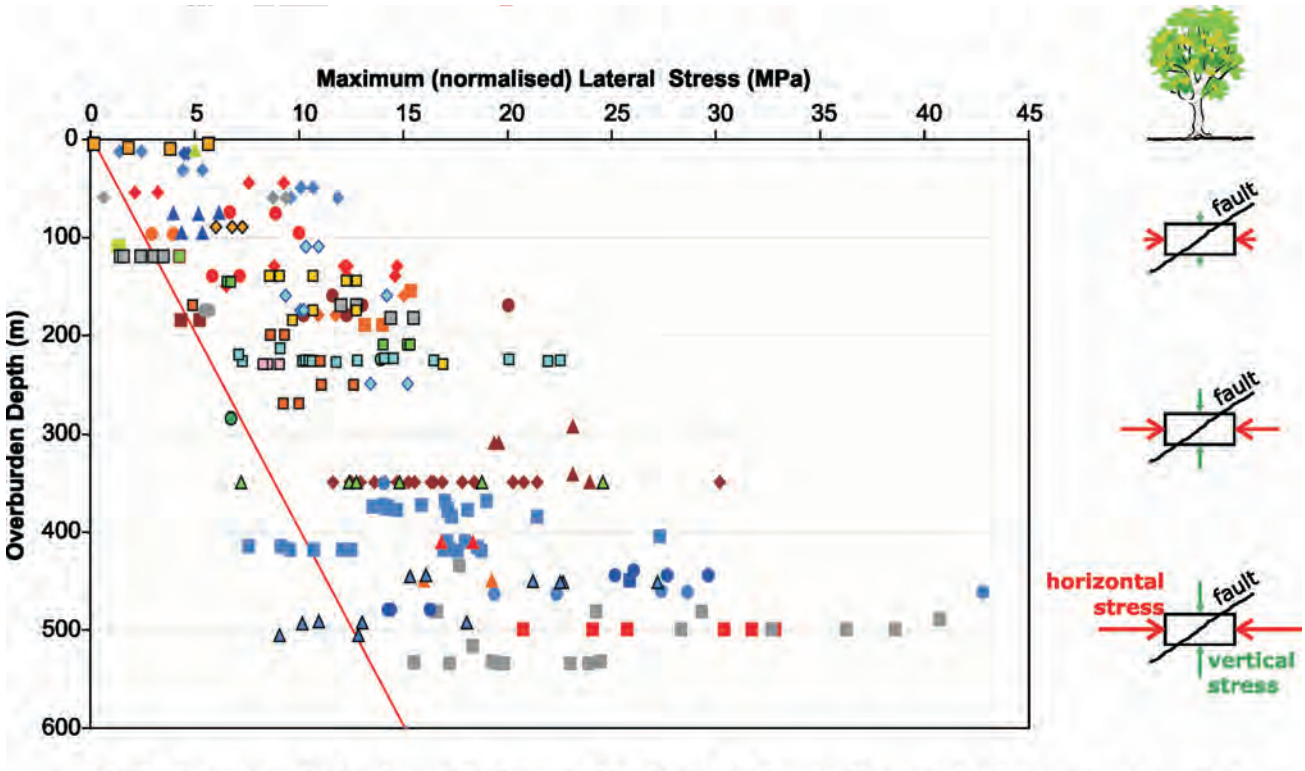

Figure 3: Increase in horizontal stress with depth in Australian coal mines as measured underground (SCT measurements only)

discontinuities within the ground rock mass. It is therefore not surprising that when loaded, deeper sections of a broken rock mass would sustain larger lateral strains while near the surface where the confinement stresses are low, displacements (slips) along the discontinuities would occur more often relieving excess lateral stress until stress equilibrium is reached. The principle of this mechanism is depicted on the right hand side of Figure 3.

The stress measurement data clearly indicate that the lateral stresses measured in NSW and Queensland sedimentary strata are considerably higher than the vertical stress. These

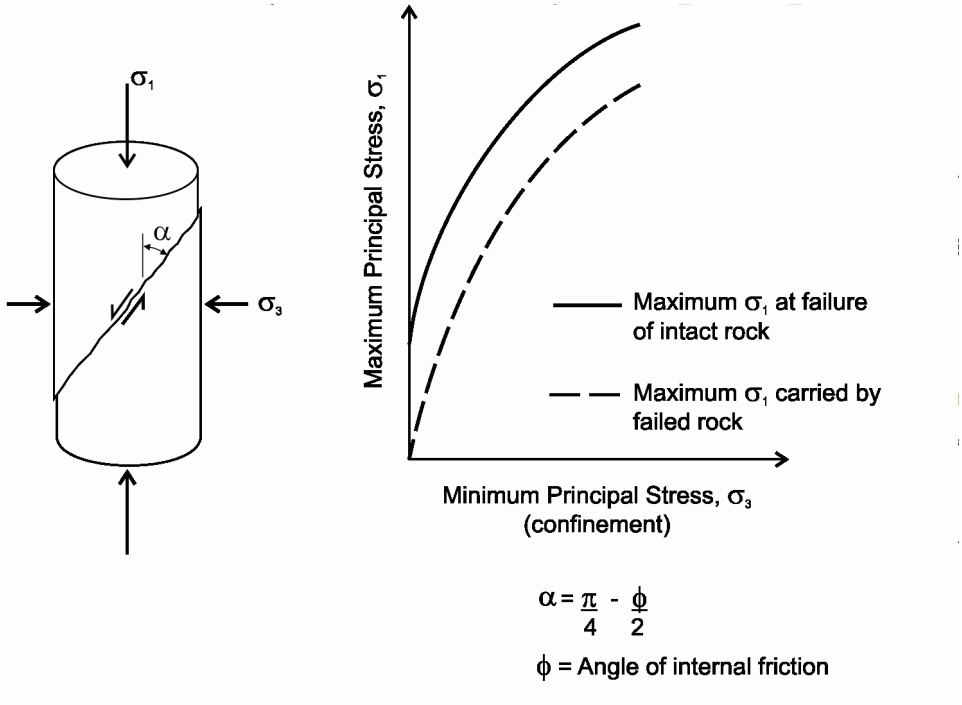

Figure 4: Increase in rock strength versus applied confinement during the triaxial rock strength test

large lateral stress magnitudes and their increase with depth appear consistent with an active tectonic plate movement that would provide stress equilibrium within the ground (as discussed above).

A wide spread of lateral stress values is typically attributed to many discontinuities and non-homogeneous rock that exist within the ground. The faulted or otherwise disturbed ground can either concentrate or reduce the stress field depending on their location and depth. The probable range of lateral stress (Figure 3) versus the overburden depth can be used effectively together with geophysical logging and borehole breakout analysis (MacGregor, 2004) to estimate the probable stress at green field sites.

While substantial amount of stress measurement data has been compiled all around the world and presented in the compilation of the World Stress Map (Reinecker, 2003), SCT measurements are unique to the Bowen and Sydney Basins. The role of horizontal stress and its affect on strata behaviour in underground coal mines has been well documented (Siddall & Gale, 1992; Hebblewhite, 1997; Mark, 2002). In most mines it can be expected that both, the vertical and the lateral stresses will increase as the mine advances to deeper ground.

Tectonic factor

The Tectonic Factor is a useful parameter that describes the amount of lateral strain induced by tectonic forces within the ground. The regional tectonic factor can be used to estimate an average 'background' lateral stress in undisturbed virgin ground where no discontinuities or other major structures exist.

The Tectonic Factor can be calculated by dividing the 'excess tectonic lateral stress' by Young's Modulus. The calculations can be described by:

$$TF = \{\sigma_1 - \sigma_v \nu/(1-\nu)\}/ E_M$$

Tectonic factors calculated for all SCT virgin stress measurements in Australian mines are plotted in Figure 5.

The results indicate that the tectonic factors increase with the overburden depth. This is consistent with the higher strain equilibrium present within the deeper ground. The lateral spread of the Tectonic Factor data is attributed to the geological discontinuities and non-homogeneous rock that exist underground.

Directions of major horizontal stress

Underground stress measurements indicate that lateral stress directions can vary substantially due to a large number of geological structures underground. In the Bowen Basin the directions of major lateral stress are in most cases confined to the North to North-East quadrant as shown in Figure 6. In NSW coalfields the maximum lateral stress directions can vary with the location and are best plotted on the regional map. Currently, other stress direction maps are being constructed in SCT to provide better understanding of the regional stress.

Variations in lateral stress direction that are sometimes measured in the mine are usually caused by at least two factors:

1. The *in situ* geological structures that can change directions of the stress flow in the mine.

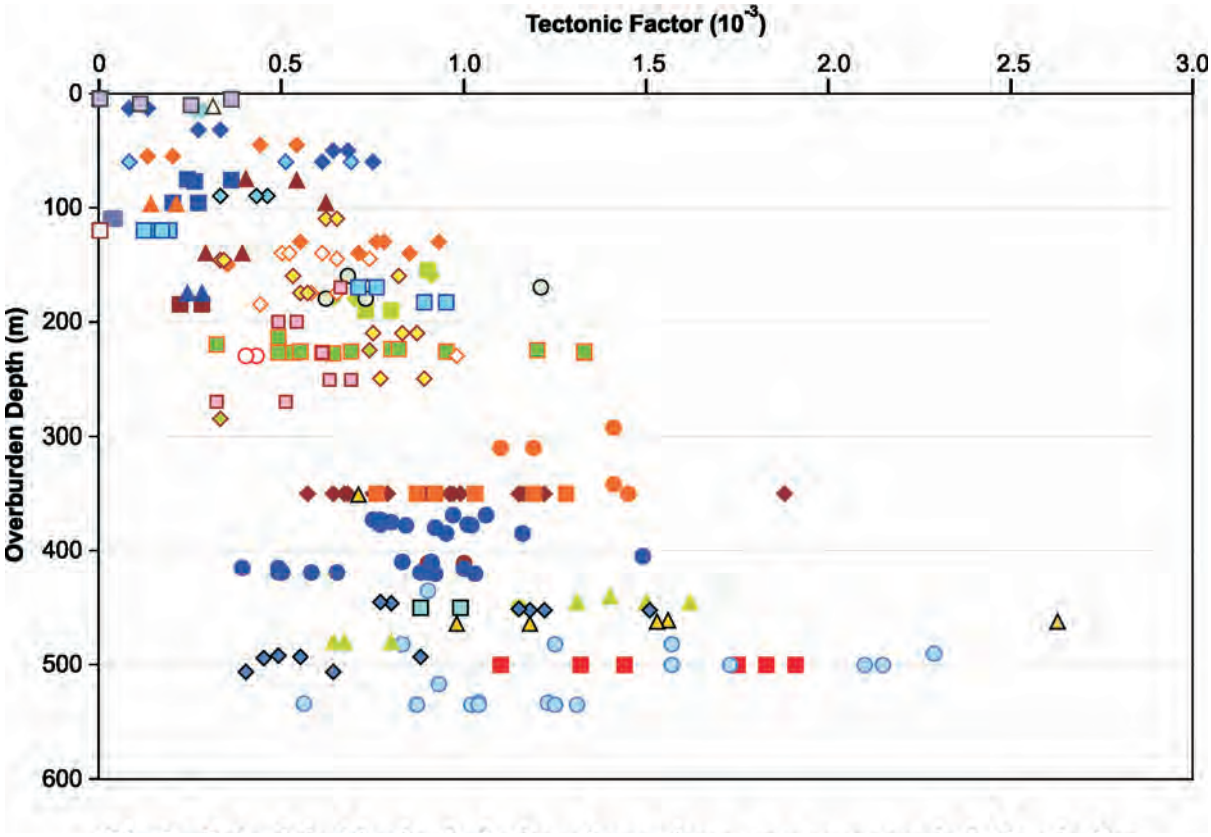

Figure 5: Calculated Tectonic Factors from stress measurements in Australian coal mines (SCT measurements only)

Figure 6: Range of maximum lateral stress directions in Bowen Basin (SCT measurements only)

2. If the lateral stresses are almost equal in all directions, the direction of maximum lateral stress can vary with even a slight change in stress.

The borehole breakout survey that is usually undertaken as part of the geophysical investigations during the exploration drilling is the best method to accurately determine the directions of maximum lateral stress flow in the explored area (MacGregor, 2004).

CONCLUSIONS

This study presents numerous *in situ* virgin stress measurements conducted by SCT. The complexity of the *in situ* ground behaviour suggests that it may be difficult to accurately predict stress levels in the mine without actual measurements, however, a preliminary stress estimation is possible using the data presented in this paper together with other nearby stress measurements and borehole surveys.

Several important points can be deduced from this study:

- the measurements clearly indicate that in most cases, the lateral stresses are considerably higher than the vertical stress,
- an increase in lateral stress with the depth of cover can be expected in the Sydney and Bowen Basins, and
- geological discontinuities and non-homogeneous sedimentary strata can significantly influence the stress directions and magnitudes in the mine.

The data presented here strengthens the understanding of stress behaviour in underground coal mines. In response to the stress range in rock of various stiffness, normalisation (stress scaling) technique was developed that allows calculations of stress in rock of any stiffness. Recognising

that a large portion of the lateral stress is probably of a tectonic origin, the tectonic factor was developed to help identify areas of highly stressed ground. Construction of stress maps showing detailed lateral stress directions in selected areas is currently in progress to help with mine layout designs.

Many geotechnical methods including numerical modelling are commonly used to predict ground behaviour. These methods require a detailed knowledge of stress distribution in the ground. A reliable source of stress information is now available to provide realistic estimates of stress in underground workings and to establish correct boundary conditions in numerical models.

Further research is in progress to enhance current understanding of stress and its influence on stability of underground workings in coal mines.

REFERENCES

GOODMAN, R.E., 1989: *Introduction to Rock Mechanics, 2nd Edition.* John Wiley & Sons, 562.

HEBBLEWHITE, B.K., GALVIN, J.M. & FOROUGHI, M.H., 1997: Geotechnical mine design issues for thick seam mining. *In Proceedings of 7th New Zealand Coal Conference.,* Wellington New Zealand, October 1997, ISBN No. 0 473 04618 0, 402–411.

HERGET, G., 1988: *Stress in Rock.* AA Balkema, Rotterdam 1988, 179.

MacGREGOR, S.A., 2003: Definition of stress regimes at borehole, mine and regional scale in the Sydney Basin through breakout analysis. *In Proceedings of 35th Symposium on "Advances in the Study of the Sydney Basin"*, School of Geosciences, University of Wollongong, 29-30 September 2003, 223–232.

MARK, C., 2002: The introduction of roof bolting to U.S. underground coal mines (1948-1960): a cautionary tale. *In Proceedings 21st International Conference on Ground Control in Mining*, 2002.

MILLS, K., 1997: *In situ* stress measurements using the ANZI stress cell. *In proceedings of International Symposium on Rock Stress*, 7-10 October 1997, Kumamoto, Japan, 149–154.

REINECKER, J., HEIDBACH, O. & MUELLER, B., 2003: *The 2003 release of the World Stress Map* (available online at www.world-stress-map.org).

SIDDALL, R.G. & GALE, W.J., 1992: Strata control — A new science for an old problem. *IMM Annual Joint Meeting,* Harrogate U.K, 1992.

J.A. Nemcik, W.J. Gale and K.W. Mills, SCT Operations, PO Box 824 Wollongong NSW 2520 Australia

Wes Nichols and Glenn Wilson

Trap Gully Mine structural interpretation: a geological and geophysical odyssey

Over the past 15 years, the interpreted geological structure at Trap Gully has been modified several times with increasing geological complexity. The modifications have arisen due to additional acquisition and improved interpretation of both geological and geophysical data. The initial structural interpretation for the Trap Gully structure was a single normal fault that was down-thrown by 20m to the east. This interpretation was derived mainly from drilling data alone. Following a host of geophysical surveying techniques (including resistivity and various seismic, electromagnetic and borehole techniques) and further drilling targeted from the geophysical surveys, the structure has now been resolved as a monoclinal fold with minor-scale reverse faulting super-imposed on it. This case study is the modern history of how this structure was investigated and defined (in advance of mining), and explores the limitations of the different techniques deployed to do so.

INTRODUCTION

The Trap Gully Mine is situated along the western margin of the Callide Basin. Mining commenced there in 1982 and, consequently, much of the subcrop area has been mined out. Several major faults have been encountered during mining and some are still evident in the existing highwalls. Mining has progressed eastwards and is poised to encounter a major monoclinal fold that will prove to be a formidable task for future mining, expected to commence sometime between 2008 and 2010. The structure's general location and effective throw was known from previous widely-spaced drilling. It was estimated to be down-thrown around 20 m to the east and was originally interpreted to be a single normal fault.

The real challenge was to define this structure accurately for mine planning. Other structures striking orthogonal to this structure were known from exposure during mining activities. In particular, a 10m fault encountered in the Trap Gully 3A pit was clearly evident in the highwall and this formed a target for some early TSIM surveys. Although this fault was not the main structural target in the Trap Gully study, it did constitute a valid preliminary test target for the early TSIM trials. The first concerted attempt at defining the suspected large normal fault using geophysics was via a Mini-SOSIE survey. This was commissioned in early 1990 but proved to be of dubious quality. Later that year, borehole-surface and refraction seismic techniques ascertained that the near surface overburden static characteristics were detrimental to the propagation of surface seismic waves.

In 1994, because mining was not planned across the structure, it was not deemed necessary to further investigate this structure. However, by 1995, although not officially planned at that stage, there were rumours that mining would, in fact, progress through the structure and further on towards the east. To pre-empt the official scheduling of this into the mine plan, further geophysical surveys were conducted (Nichols, 1996). Experiments with seismic methods and the subsequent re-processing of the data yielded inconclusive results due to the unconsolidated near-surface sediments. Results from initial RIM surveys in 1996 were the first to indicate that the style of faulting was reverse rather than normal. This was totally unexpected and led to a geotechnical drilling program and further RIM surveys were conducted across the entire area to confirm this trend in 2001. Some of the geoelectrical images produced from the RIM survey results were conclusive and confirmed the existence of reverse faults in general agreement with the geotechnical drilling but the majority of the images displayed wide 'blurred' zones in which no definite structural features were resolved. In an attempt to confirm the geoelectrical model obtained from the RIM surveys, a series of resistivity surveys were conducted in 2002 but these contributed very little in terms of new information about the geological structure.

1990 – 1994: Preliminary drilling and geophysical surveys

Drilling in advance of the Trap Gully mining areas prior to 1995 had located an area with anomalous dip to the east. It was suspected that this area contained a normal fault with a throw between 15 and 20m down to the east. Borehole spacing at that time was wide (approximately 200m in the vicinity of the presumed fault) and no drilling was done specifically to locate the fault.

VLF surveys

The TSIM for VLF electromagnetic surveying had been successfully trialled at Callide Coalfields for fault and intrusion location, blasted overburden characterisation and subcrop location (Biggs, 1990). Relatively large resistivity contrasts exist at lateral structural boundaries in otherwise homogenous, stratified sedimentary media. In the case at Trap Gully, the interpreted resistivity contrasts are due to the dry, air-filled and rubbled crush zone along predicted fault planes in the near surface. VLF techniques such as TSIM can easily detect this contrast and locate structural anomalies approaching depths of 50m, depending on the frequency of the VLF radio waves and resistivity of the local earth.

Hence, TSIM served as a simple means of accurately targeting boreholes. The surveys were conducted along the bench directly above known structural targets (faults) that were observed in the adjacent exposed highwall.

Seismic surveys

Conscientious efforts to locate this major undefined structure, suspected to be a fault, began in early 1990. The first major trial involved Mini-SOSIE surveys across the entire target area but was focussed on Line 5. This was followed by shallow refraction and downhole seismic methods. The original Mini-SOSIE data was reprocessed by Lambourne (1991). However, the ground in the fault area was not generally conducive to seismic methods and these methods proved to be too inconclusive for defining the fault. A further vertical seismic profiling (VSP) borehole-to-surface survey was conducted at Trap Gully in 1992 but, again, the results did not clearly define the fault structures. However, this survey did define two low-velocity zones, which appeared to coincide with the presumed faulting.

In 1990, Velseis performed Mini-SOSIE surveys along 7 lines at Trap Gully. The data that were collected along these lines remained inconclusive for seam and fault location. Line 5 proved to have easiest access and intersected the presumed fault location at 90°. Subsequently, Line 5 was selected for further trials. The original data from Line 5 were later reprocessed by ACIRL at Curtin University of Technology (Lambourne, 1991). Even though the result showed more continuity than previous processing (mainly due to inclusion of the variable refraction static data collected by Whitely in later 1990), interpretation remained inconclusive.

In late 1990, high resolution optimum offset surveys were conducted (Whitely, 1991) along Line 5 using the optimum offset technique. Shot holes (10m spacing) were drilled to the base of weathering (25 to 40m depth) and 'D' size detonation boosters were used as the sound source. Only one dipping reflecting surface (presumably the upper surface of the coal seam) was identified from the results of these surveys. There were no obvious reflections associated with the base of the coal seam or structures within the seam. Due to the lack of clarity from the Mini-SOSIE section, it was difficult to relate the data from the two techniques. Whitely (1991) also conducted shallow layer refraction and uphole surveys along Line 5. The results from these surveys outlined the main reason for previous difficulties with collecting seismic data in the area. Several low velocity anomalies existed in the near-surface layers. The existence of these rapid lateral velocity variations posed problems for both data collection and processing.

In 1992, a reversed vertical seismic profile (VSP) survey was conducted along Mini-SOSIE Line 5 between two shot holes (S0007 and S0020), 130m apart and each 80m deep (Hatherly & others, 1993). These holes were selected because of their close proximity to the expected fault and the intention was to determine whether the fault could be mapped by the VSP method. Initial results showed strong first breaks but these did not display the usual hyperbolic move-out expected under normal lithological conditions. Reflections were not immediately evident, but post-processing yielded the possibility of two locations for faults. An isotropic tomographic image was produced which indicated, concordant with Whitely's refraction and uphole surveys, that a complex velocity structure existed within the near-surface along Line 5. Two distinct low velocity zones were present and these were inferred to be indicative of faulted and sheared rock and, thus, were interpreted as expressions of faults.

Following the seismic surveys at Trap Gully, a cored hole was drilled adjacent to shot hole S0020 on Mini-SOSIE Line 5. Good evidence for at least minor faulting was logged in the core with several sutured micro-faults, both normal and reverse, and of up to 5cm of movement recorded (Jorgensen, 1993).

1995 – 1999: Further drilling and geophysical surveys

VLF surveys

The TSIM surveys conducted prior to 1990 were purely experimental as they were not targeted at investigation of unknown structures. From 1995 onwards, eleven TSIM surveys were conducted to locate the major structure down-dip of the mining area. The lateral location of an anomaly, interpreted as the near-surface manifestation of a fault, was easily detected by the TSIM instrument. This was the first time the 'fault' had been defined with any lateral precision. Following the apparent lateral location of the 'fault' by the TSIM method in 1995, two boreholes were drilled (50m apart, one on each side of the anomaly) along several of the TSIM lines. The set of holes (R1833 and R1834) on TSIM Line 2 was selected for investigation by the radio imaging (RIM) technique to verify the TSIM method and further investigate the structural anomaly.

RIM surveys

METS Pty Ltd performed the first RIM surveys on TSIM Line 2 in 1996 (Neil, 1996). The initial RIM survey was sited to better constrain the results of the previous TSIM surveys, which predicted the lateral location of the fault, but could not yield dip or structural information. The same two holes, R1833 and R1834, drilled for verification of the TSIM results, were utilised for surveying. Figure 1 shows the resulting tomogram generated using CSIRO's MIRP program. This tomogram gave the first indication that the fault structure was not normal as first thought, but reverse with the offset being taken up by two en echelon faults dipping at 45° to the west. Further interpretation of the results from this tomographic survey indicate the anomalous structure to be a set of two *en echelon* reverse faults which constitute a total throw of approximately 21–23m down to

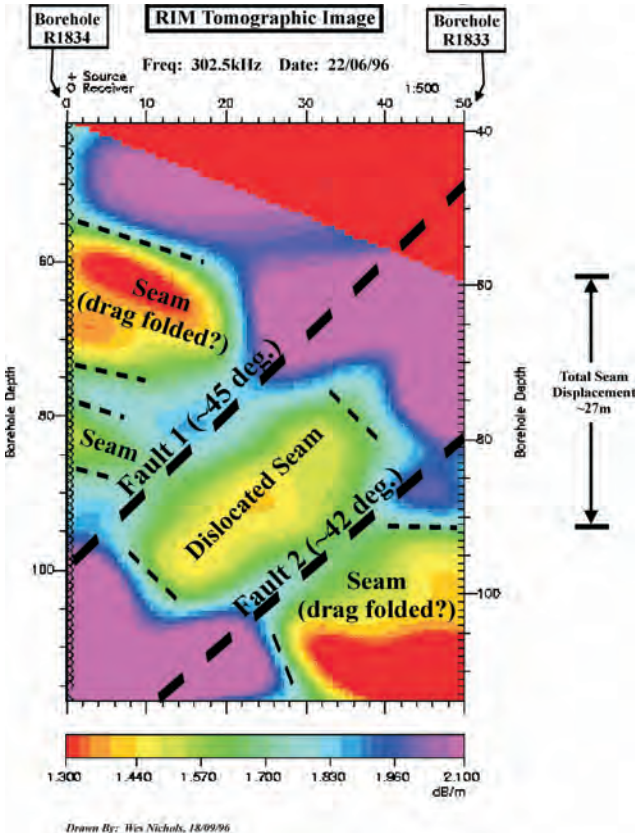

Figure 1: 302.5 kHz radio-frequency tomograph for R1833 and R1834 RIM panel using MIRP imaging package.

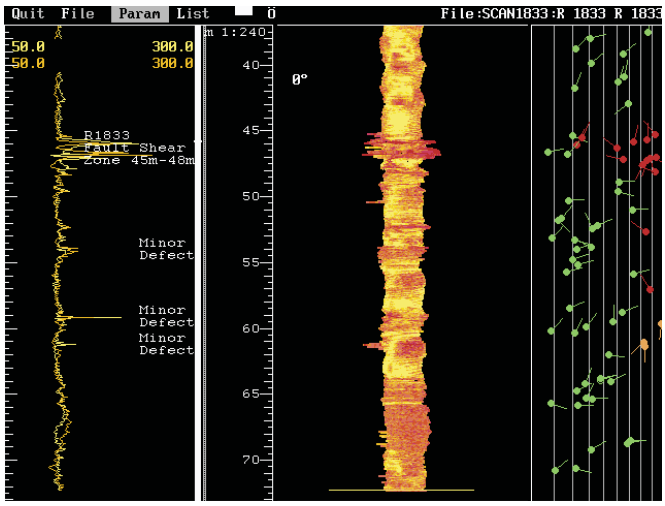

Figure 2: Full depth acoustic scanner log of borehole R1833 with a false colour acoustic impedance image

the east. This correlates with the interpreted throw between 15m and 20m from borehole results. Also, the lateral location of the two-fault anomaly between 25m and 45m along the survey line from borehole R1834 correlates with the TSIM results.

Borehole logging and geotechnical analysis of drill core

In an attempt to detect the structures identified from the RIM survey, in 1998 the Reeves borehole acoustic scanner was run in borehole R1833. Unfortunately, because of the time interval between when the hole was drilled and when it was logged with the scanner, the hole was blocked at 72.50m. Also, the borehole was cased to 31.00m and logging above 37.05m was not practical for several reasons. Figure 2 shows the full depth of the logged interval (37.05m to 72.27m). The caliper logs on the left-hand-side of the figure indicate the hole diameter from 50– 300mm and as indicated, the average hole diameter is at 125mm. The scale just off-centre indicates the depth down the borehole. The 'tadpoles' on the right-hand-side of the figure indicate the dip and azimuth of features (e.g. bedding, joints and shears) mapped from the scanner image.

The set of vertical lines on the right-hand-side of the figure indicate the dip from 0–90° (the leftmost line is 0° and rightmost line is 90°). The head of the 'tadpole' denotes the dip of the feature while the tail indicates the dip direction relative to true north (directly up the page). Red 'tadpoles' represent shear planes; green indicates bedding and beige represents joint planes. As can be observed, bedding is fairly consistent at a north-east-east azimuth with dips ranging from 10° to 70°. Joints are steep to subvertical (75° to 90°) with azimuths south-south-west. Shears are random in azimuth and dip and the major shear zone is easily recognisable between 45 and 48m depth. Whilst not shown here, expansion of the image of this shear zone demonstrates how the rock has been broken and mylonised.

Downhole focussed electric resistivity logs were also conducted by Reeves on both borehole pairs along lines T02 and T03. The log (Figure 3) shows the resistivity profiles for both deep and shallow resistivity logs for R1833 in the borehole wall. The deep focus log maps more of the rock mass and gives a better indication of the resistivity of the bulk rock mass. The shallow log maps subtle changes in resistivity at the immediate surface of the borehole wall. From the deep log, it can be seen that the resistivities in the overburden average at around 100Ωm while, in coal, resistivities increase to around 500Ωm. Smyth & Nichols (1999) geotechnically analysed the core and acoustic scanner logs from boreholes in the Trap Gully monocline area. Using dipmeter interpretation techniques described by Roestenburg (1985), Smyth & Nichols (1999) prepared detailed cross-sections of the Trap Gully monocline.

2000 – present: Recent geophysical surveys

RIM surveys

Geophysics Australia Pty Ltd performed additional RIM surveys at Trap Gully in 2000 and 2001 (Figure 4) using RIMTECH RIM-2 equipment. The data were processed using the ImageWin package developed by the CRC for Mining Technology and Engineering. Figure 5 shows the results from Panel 7 between R0207212 and R0207247, acquired in 2000. These holes were aimed at defining the monocline structure. A schematic diagram of this interpreted structure is shown in Figure 6 (Miller & Nichols, 2001). The RIM image shows good correlation with the logged geology

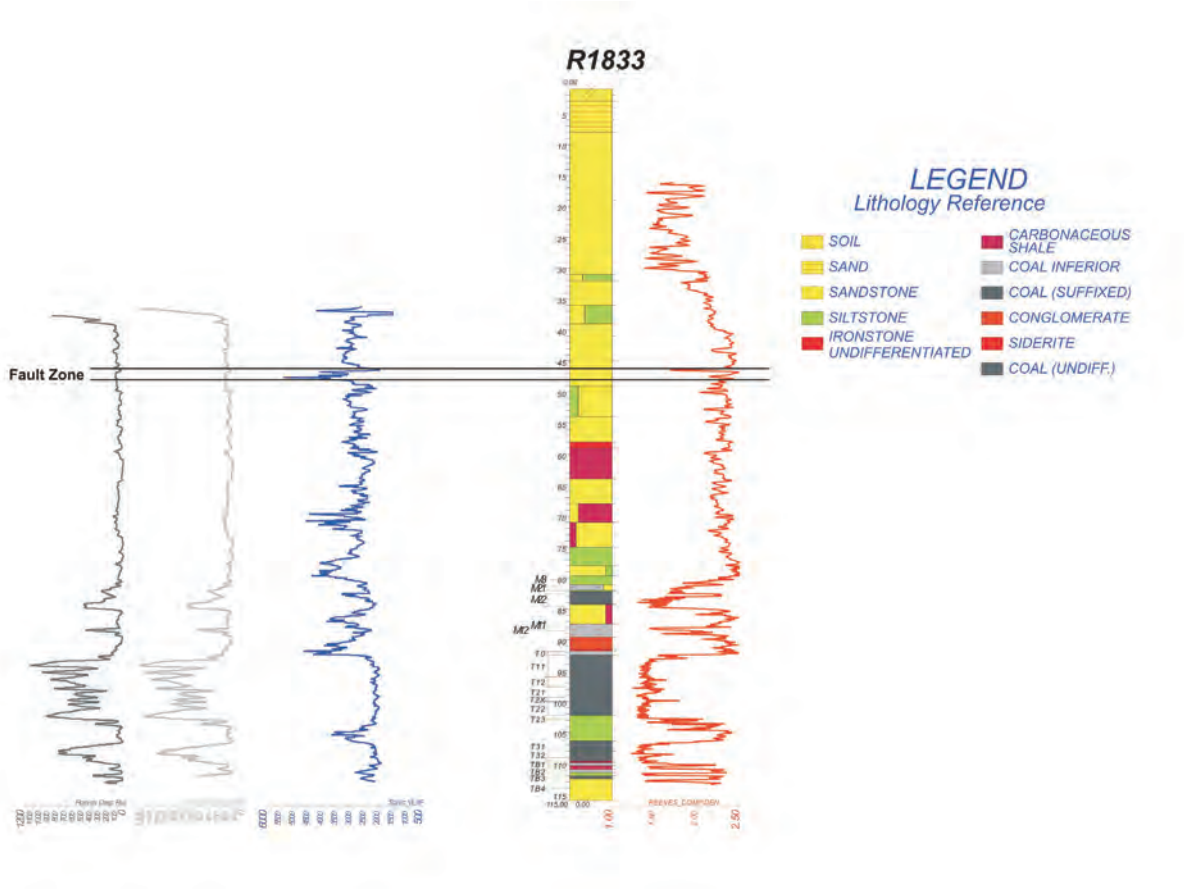

Figure 3: Plots of Reeves downhole logs for borehole R1833 (L-R: Deep Resistivity, Shallow Resistivity, Sonic, Density)

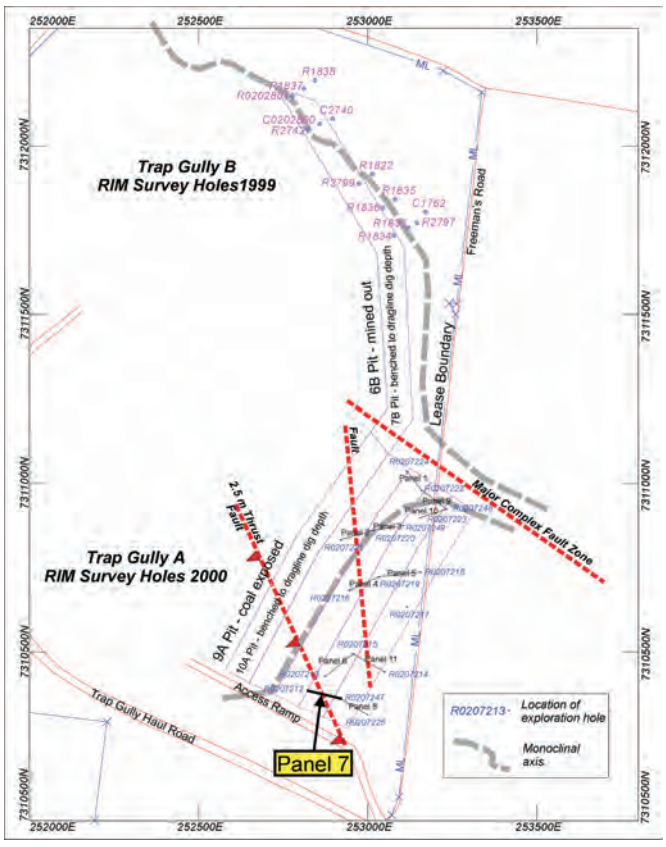

Figure 4: Schematic diagram of the eastern boundary of Trap Gully Mine with the suggested monoclinal fold axis shown. The locations of all RIM panels are shown.

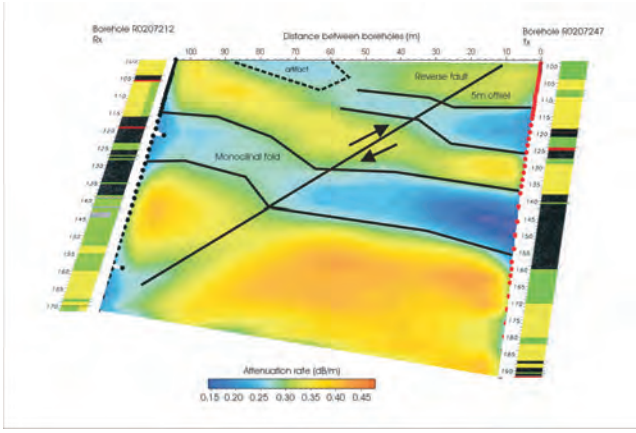

Figure 5: 52.5 kHz radio-frequency tomograph for Panel 7, between R0207212 and R0207247, using ImageWin imaging package

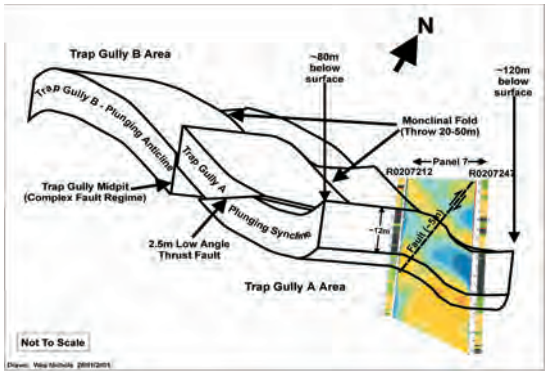

Figure 6: Schematic diagram of the monocline structure at Trap Gully

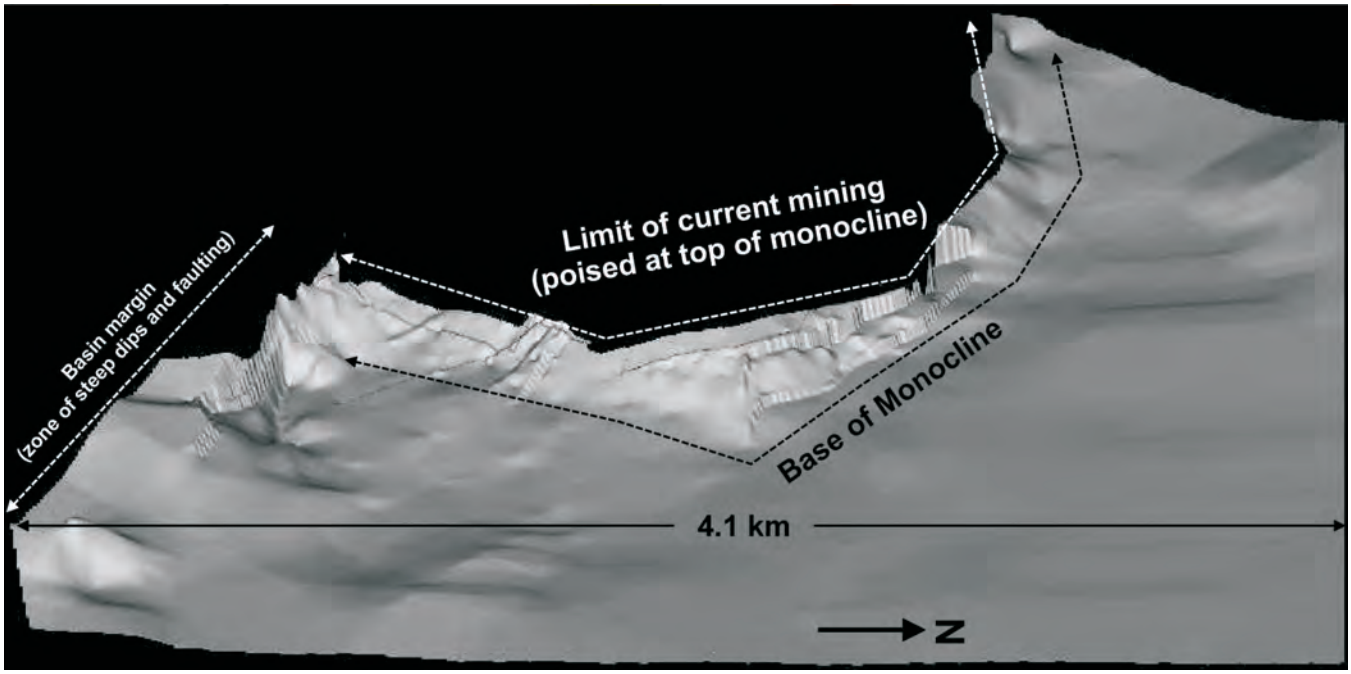

Figure 7: Current model of topography of the top of coal in the Trap Gully monocline area, showing faulting

at the borehole positions. The monoclinal fold is clearly seen with the 20m differential in seam level taken up by the fold close to hole R0207212. The two thin upper seams in hole R0207247 have not been imaged separately. The sample density in this region was 4 m x 4m and was too widely spaced to differentiate the two seams. Two reverse low angle faults (~35°) are also interpreted as being associated with the monoclinal fold. A low attenuation artefact at the top of the image is attributed to poor data coverage in this part of the image. A similar artefact is observed in the lower left corner of the image. However, this may also be associated with the eastern fault.

Resistivity surveys

However, not all RIM images were conclusive. The majority of the images displayed wide 'blurred' zones in which no definite structural features were resolved. In an attempt to confirm the geoelectrical model obtained from the RIM surveys, a series of resistivity surveys were conducted in 2002 by Subsurface Imaging Pty Ltd (Miller & Morelli, 2002) using a data acquisition system that automatically cycled through pre-set Wenner and dipole-dipole electrode arrays. Borehole controls were available for constraining subsequent inversions. Due to the depth of coal and low resolution of the resistivity method at depth, it was concluded that the surveys had not contributed any new knowledge about the geoelectrical model of the area.

STRUCTURE DEFINITION AND CONCLUSIONS

By considering all available geological and geophysical data and imposing the subjectivity that can be called intuition, the current model for the top of coal for the Trap Gully monocline is shown in Figure 7. In the course of constructing this model, the following lessons were learnt:

- The seismic methods employed were highly variable in their results and lacked success in locating the target anomaly. This was largely due to the severe lateral velocity variations in the near-surface layers. In hindsight, it would have been more prudent to perform a seismic refraction survey, prior to the much more costly reflection surveys, to detect these velocity variations.
- VLF (TSIM) was very successful in locating the lateral position of the apparent near-surface manifestation (expected to be a dry, rubbled and air-filled crush zone along the fault plane) of the anomaly and allowed drillhole targets to be located effectively. The information from the holes drilled following TSIM surveying indicated that a 'fault' with between 15 and 20m throw (down to the east) existed between them.
- RIM surveys, subsequently, revealed that the lateral location of the 'fault' from TSIM surveys and the vertical displacement from drilling correlated well, and that both could be interpreted as a two-step, *en echelon* reverse fault structure.
- Due to the depth of coal at Trap Gully and the low resolution of resistivity method at depth, the 2-D resistivity surface surveys did not yield any new information about the geoelectrical model. It could be argued that extensions to 3-D surface surveys would not be any more effective, but there is a case for potentially trialing cross-borehole resistivity surveys.

Overall, the structure was far more easily, cheaply and successfully located by TSIM and RIM than by seismic and resistivity methods. However, this is a Callide Basin result

and that may not be the case for other mines or environments. Possibly the most important lessons learnt in the whole exercise involves the commissioning of 2-D and 3-D computer model studies *prior* to any geophysical surveying to determine the best survey technique and to optimise survey configurations so that one will, at least in theory, be able to extract the maximum amount of information from acquired data. So with that said, on-going work at Trap Gully now involves 3-D nonlinear forward modelling of RIM data to test the current geological model. The ultimate ground truth (mining) scheduled to commence sometime between 2008 and 2010.

ACKNOWLEDGEMENTS

This case study represents more than fifteen years of exploration work in and around the Trap Gully Mine. The authors particularly thank Mark Biggs, Peter Hatherly, Iain Hodge, Peter Jorgensen, Craig Miller, Byron McKavanagh, Warwick Smyth and David Thiel for their assistance and contributions. The authors also acknowledge Anglo Coal (Callide Mine) Pty Ltd for permission to publish.

REFERENCES

BIGGS, M., 1990: Results from trials of the TSIM surface impedance geophysical techniques at Callide Coalfields. *In, Bowen Basin Symposium Proceedings*, Geological Society of Australia, Australia, 181–184.

HATHERLY, P.J., YU, G., ZHAO, P., McKENZIE, K.B. & WENZEL, F., 1993: The borehole vertical seismic profiling method for detailed coal seam mapping. ACIRL final report for ACARP project C8002.

JORGENSEN, P.J., 1993: Exploration drilling program – drill site geologist's report. Report to Callide Coalfields Pty Ltd.

LAMBOURNE, A.N., 1991: Re-processing of Trap Gully seismic line 5. Report to Callide Coalfields Pty Ltd.

MILLER, C. & MORELLI, G., 2002: 2D resistivity imaging at Trap Gully, Callide Mine. Report to Callide Coalfields Pty Ltd.

MILLER, C. & NICHOLS, W., 2001: Borehole to borehole electromagnetic tomography at Trap Gully, Callide Mine, East Central Queensland. *Exploration Geophysics*, **32**, 246–349.

NEIL, M., 1996: Trap Gully Mine, Radio imaging method survey. Report to Callide Coalfields Pty Ltd.

NICHOLS, W., 1996: Geophysical trials for fault location at Callide Coalfields' Trap Gully Mine, Callide Basin, East Central Queensland. *In, Mesozoic Geology of the Eastern Australian Plate Conference*, Geological Society of Australia, Australia, 414–423.

ROESTENBURG, J.W., 1985: *Dipmeter interpretation handbook with selected references*. Schlumberger Seaco, Australian Division.

SMYTH, W. & NICHOLS W., 1999: Geotechnical drilling and site investigation, Trap Gully B Pit. Report to Callide Coalfields Pty Ltd.

WHITELY, R.J., 1991: Callide Coalfields high resolution seismic trial surveys, Trap Gully area. Report to Callide Coalfields Pty Ltd.

W. Nichols, Anglo Coal (Callide Mine) Pty Ltd, PO Box 144, Biloela Qld 4715, Phone: (07) 4990 1627, wes.nichols@anglocoal.com.au.

G. Wilson, C.S.I.R.O. Division of Exploration and Mining, PO Box 136, North Ryde NSW 1670, Phone: (02) 9490 5416, glenn.wilson@csiro.au

Natasha Hendrick

Converted-wave seismic reflection for open-cut coal exploration

Two 2D converted-wave seismic trials designed to image very shallow coal seams have been conducted in the Bowen Basin, Australia. Converted-wave seismic is an alternative seismic method that takes advantage of shear-wave seismic energy arriving at the surface during a seismic survey. In contrast, conventional seismic utilises only compressional waves arriving at the surface. Due to differences in the way compressional waves and shear waves propagate through the Earth, there is potential for converted-wave seismic to yield better quality images of very shallow targets compared to conventional seismic.

Some changes to conventional recording equipment and field procedures are necessary to accommodate converted-wave seismic acquisition. A multi-component geophone replaces the vertical geophones used for conventional acquisition at each receiver station. Processing of high-resolution converted-wave data is technically challenging and requires specialised approaches to shear-wave receiver statics, converted-wave normal moveout correction and common conversion-point binning.

The converted-wave image of Field Trial A provides a cleaner image of the shallow coal seam compared to the conventional seismic stack. For Field Trial B the conventional seismic section is unable to image the coal seam at depths less than approximately 45–50m. In contrast, the converted-wave seismic image can track the shallow coal seam along the full extent of the survey line, to depths of approximately 25–30m. These experiments demonstrate the potential for converted-wave seismic to yield high-resolution images of open-cut coal reserves.

INTRODUCTION

Seismic reflection involves using artificially-generated sound waves to map structural and stratigraphic features in the subsurface, and has become a valuable geophysical tool for the accurate and cost-effective imaging of coal seams ahead of longwall mining. In contrast, the seismic method is not often utilised for open-cut coal exploration. This is related to the fact that borehole drilling is relatively cheap for open-cut seam depths, and continuous imaging of the seam is not always as critical as it is for underground mine planning and development. In addition, conventional, economic seismic surveys tend to produce inconsistent results when imaging very shallow coal seams (less than approximately 50m in depth). When continuous mapping of open-cut coal seams is important, conventional seismic survey designs can be adjusted (e.g. source and receiver spacing reduced) to successfully image shallow coal seams.

However, such field-intensive surveys are necessarily more expensive and time consuming. Converted-wave seismic technology offers an alternative geophysical tool for the continuous mapping of open-cut coal reserves that, for some situations, may provide a more cost-effective approach than conventional seismic methods. ACARP-supported research conducted by Velseis Pty Ltd over the past three years (Velseis, 2003; Hendrick, 2004) has demonstrated the ability of converted-wave seismic to successfully produce coherent, high-resolution images of very shallow coal seams. This paper introduces the basic concepts of converted-wave seismic, and presents the results from two 2D converted-wave seismic trials conducted in the Bowen Basin, Australia. Despite technical challenges associated with producing the converted-wave seismic sections, these trials have successfully achieved their objective of imaging very shallow target coal seams.

CONVERTED-WAVE SEISMIC EXPLORATION

Seismic Waves

There are several types of seismic waves, including body waves, surface waves and air waves, that are generated during a seismic survey. In terms of imaging coal seams, the most important and useful seismic waves are body waves. Both compressional (P) and shear (S) waves are seismic body waves. P waves are longitudinal waves that have particle motion in the direction of travel. In contrast, S waves are transverse waves that have particle motion perpendicular to the direction of travel. Figure 1 is a schematic illustrating the ground vibrations associated with P and S seismic waves.

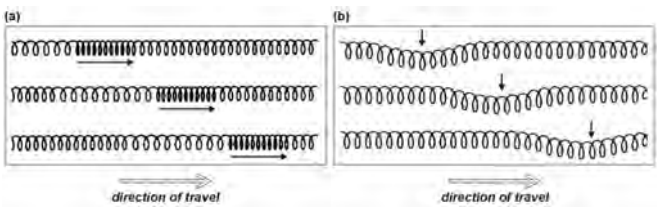

Figure 1: Ground vibrations associated with (a) P-waves and (b) S-waves. In this schematic, the seismic waves are travelling from left to right. The particle motion of the P wave is in the direction of travel. The particle motion of the S wave is perpendicular to the direction of travel.

Conventional vs Converted-Wave Seismic Surveys

Since coal-seismic sources (e.g. small dynamite explosions; mini-SOSIE) dominantly produce P-wave energy, the conventional approach to coal-seismic acquisition assumes that only P waves will arrive at the surface. Recall that the particle motion of a P wave is in the direction of travel. Hence reflected P-wave energy travelling upwards from a geological boundary will have particle motion with a strong vertical component at the surface receiver (Figure 2(a)). Conventional seismic acquisition records only the vertical component of seismic energy arriving at the receiver. This type of seismic recording can also be referred to as single-component (1C) recording.

In reality, both reflected P and S waves typically arrive at the surface during a seismic survey. Most of the S energy arriving at the surface will be mode-converted PS energy - that is, energy from a wave that travels down to a geological boundary as a P wave, gets partially converted to S energy at the boundary, and then travels back to the surface as an S wave. Coal seams are particularly efficient at generating strong PS waves (e.g. Fertig &Müller, 1978; Greenhalgh & others, 1986). Any PS-wave (converted-wave) energy arriving at the surface will have a dominantly horizontal component of particle motion (Figure 2(b)).

Multi-component seismic recording measures both the vertical and horizontal components of ground motion to enable exploitation of both the P and PS energy arriving at the surface. Note that, multi-component recording may also be referred to as three-component (3C) recording since the vertical and two orthogonal horizontal components (inline and crossline components) of ground motion are generally recorded.

P- and PS-Wave Behaviour

The different modes of propagation of P and S waves mean they travel at different speeds through the earth, and respond differently to various geological situations. Of particular relevance to the imaging of very shallow coal seams is the fact that S waves typically travel at about half the speed of P waves. Thus reflected PS waves will arrive later than P waves from the same geological boundary. For very shallow target coal seams, this will mean that PS waves should arrive after near-surface noise that typically contaminates the corresponding P-wave reflection energy.

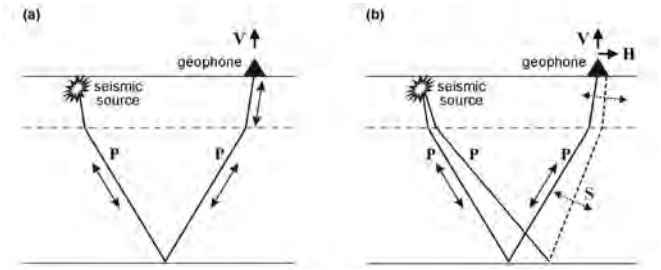

Figure 2: (a) Conventional seismic reflection assumes that only P waves arrive at the surface. Since the particle motion of an upward travelling P wave is largely vertical (indicated by the solid arrows), a vertically-oriented geophone is used for acquisition. (b) Multi-component seismic recording recognises that both P and mode-converted PS waves will arrive at the surface. The particle motion of an upward travelling S wave is largely horizontal (indicated by the dashed arrows). Thus both the vertical (V) and horizontal (H) components of ground motion must be recorded to take advantage of both wave types.

Figures 3 and 4 show synthetic multi-component seismic records that illustrate the relative behaviour of P and PS reflection energy when imaging shallow coal seams. These seismic records have been generated via the elastic finite-difference modelling technique of Virieux (1986). As discussed above, the reflected P-wave energy will be dominant on the vertical-component record, while the PS reflection event will be dominant on the inline (horizontal) component. Note that, in addition to reflected energy, surface waves (groundroll energy), refracted arrivals, and surface and interbed multiples are generated by the forward-modelling scheme. The earth models used to generate these data comprise three layers — a 15m thick weathered surface layer, country rock and a single 7m thick coal seam. To generate the seismic data in Figure 3 the coal seam has been placed at a depth of 35m. In contrast, the earth model used to produce the records shown in Figure 4 has a coal seam at a depth of 23m.

In Figure 3(a) the hyperbolic P-wave reflection event from the coal seam has a zero-offset arrival time of approximately 0.05s. The corresponding PS reflection event (Figure 3(b)) has a zero-offset arrival time of approximately 0.074s. As expected, the PS reflection event from the target coal seam arrives approximately one-and-a-half times later than the P reflection event.

As illustrated in Figure 4, this delay is advantageous when the coal seam becomes shallower. The P-wave reflection event in Figure 4(a) has a zero-offset arrival time of 0.04s. However, the P energy has been contaminated by strong groundroll energy (steeply dipping linear noise) and base-of-weathering refraction events, and the target reflection event is difficult to detect. The resultant P-wave section would exhibit poor reflector coherency. In contrast, the PS reflection event (Figure 4(b)) has a zero-offset arrival time of 0.055s, and is sufficiently removed from the near-surface noise to facilitate reliable seismic imaging of the very shallow coal seam.

Converted-Wave Acquisition and Processing

Some changes to conventional recording equipment and procedures are required to accommodate both P-wave and PS-wave recording. The primary difference is the receiver device. A purpose-built high-resolution, high-output 3C geophone replaces the vertical geophone(s) used for conventional acquisition at each receiver station. Note that, the use of three recording channels at each receiver station also necessitates the use of additional field units and acquisition cables.

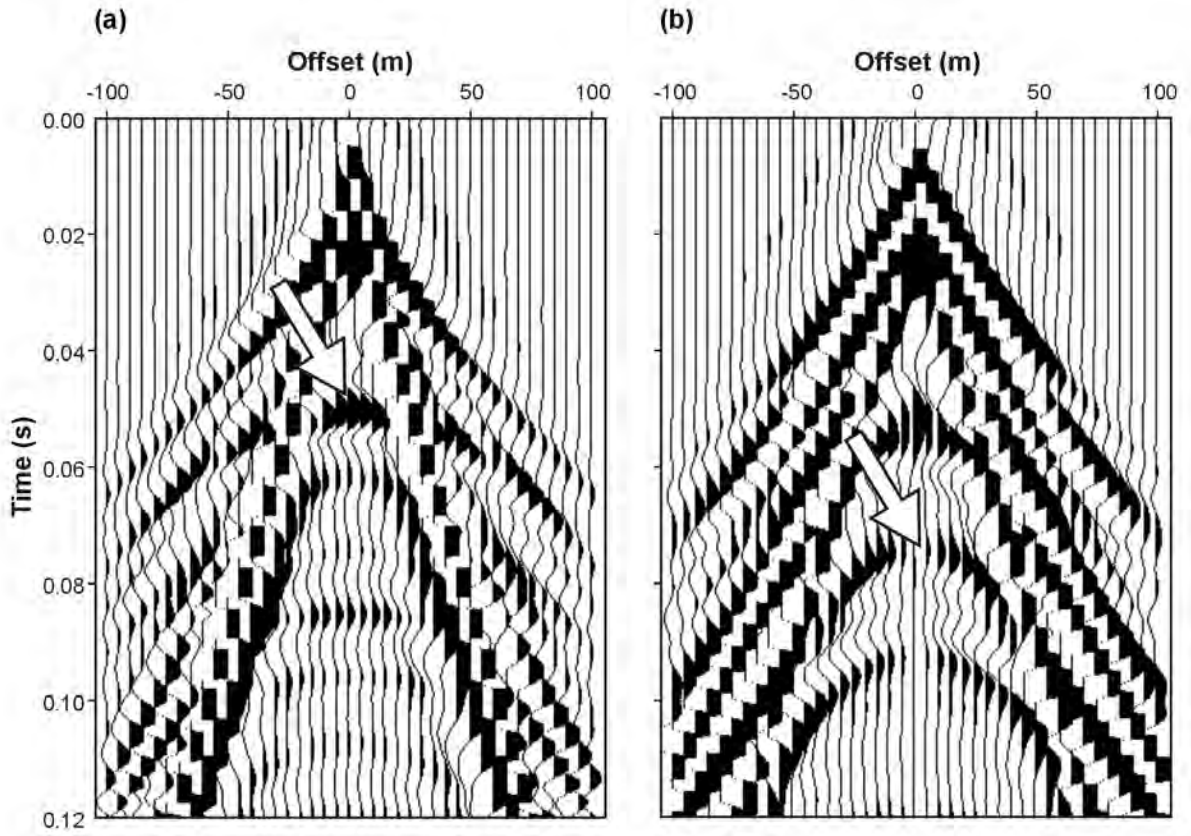

Figure 3: (a) Vertical-component and (b) inline-component of synthetic seismic record generated using an earth model with a coal seam at a depth of 35m. The P and PS coal-seam reflection events are indicated by the white arrows on the vertical and inline records, respectively. The horizontal axis represents offset, the distance between the source and each receiver. Seismic energy travelling to receivers with small offsets arrives earlier than energy that travels obliquely to receivers at far offsets. Hence reflection events will appear approximately hyperbolic in the seismic records.

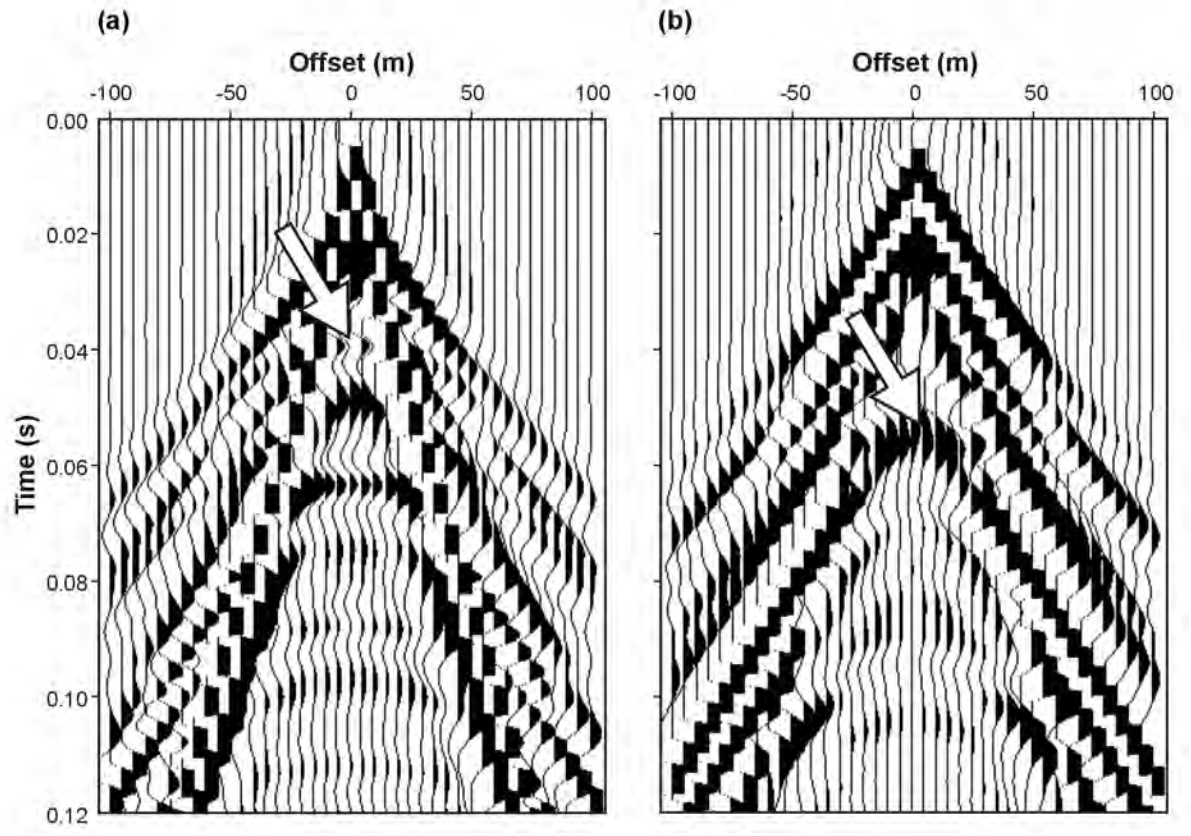

Figure 4: (a) Vertical-component and (b) inline-component of synthetic seismic record generated using an earth model with a coal seam at a depth of 23m. The arrival times of the P and PS coal-seam reflection events are indicated by the white arrows on the vertical and inline records, respectively.

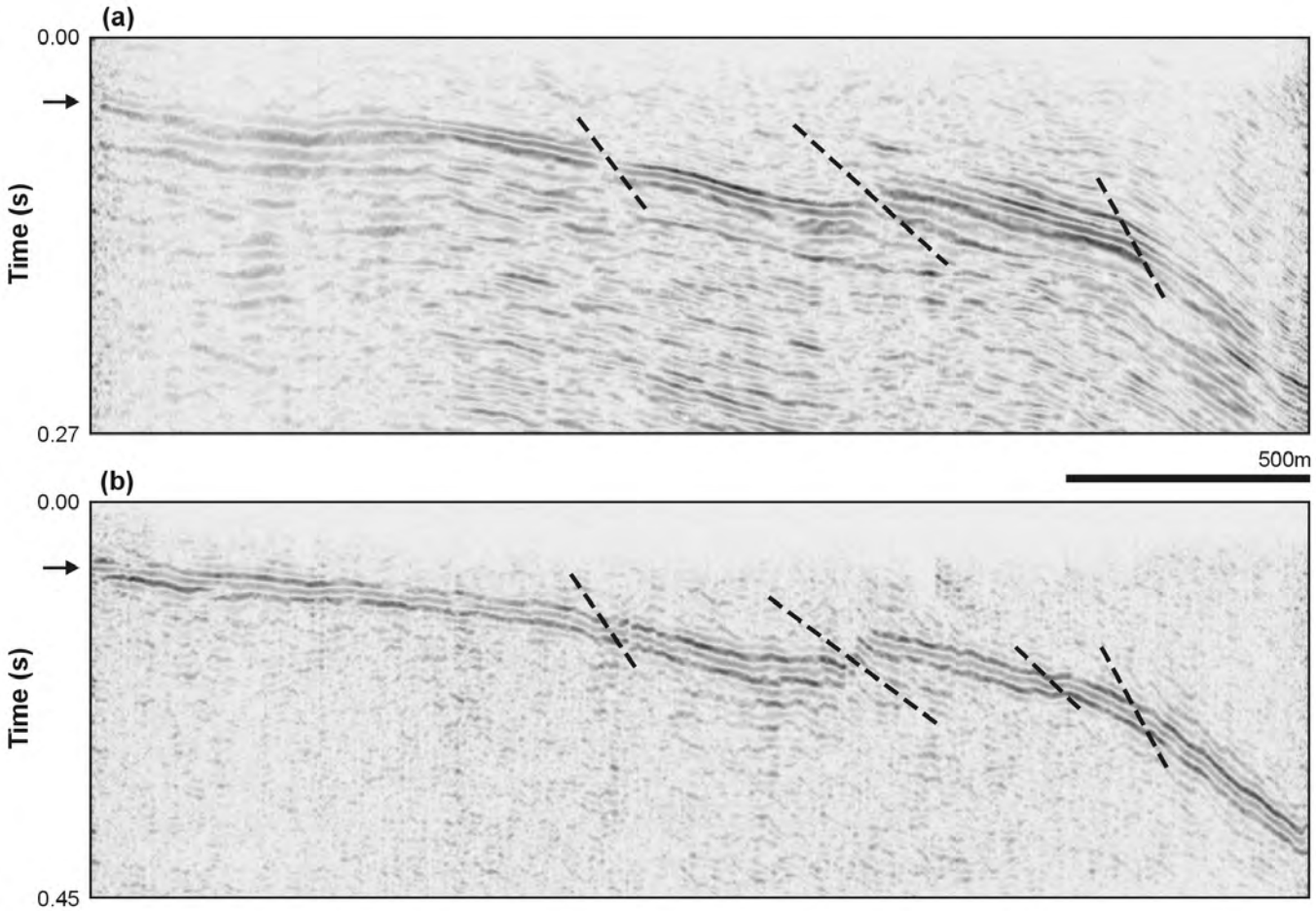

Figure 5: (a) Conventional P-wave image and (b) converted-wave (PS) image derived from Field Trial A. The target coal seam reflection events are indicated by the arrows. Interpreted faults are approximately marked by the dashed lines. The PS image exhibits greater resolution than the P-wave image where the coal seam is shallowest.

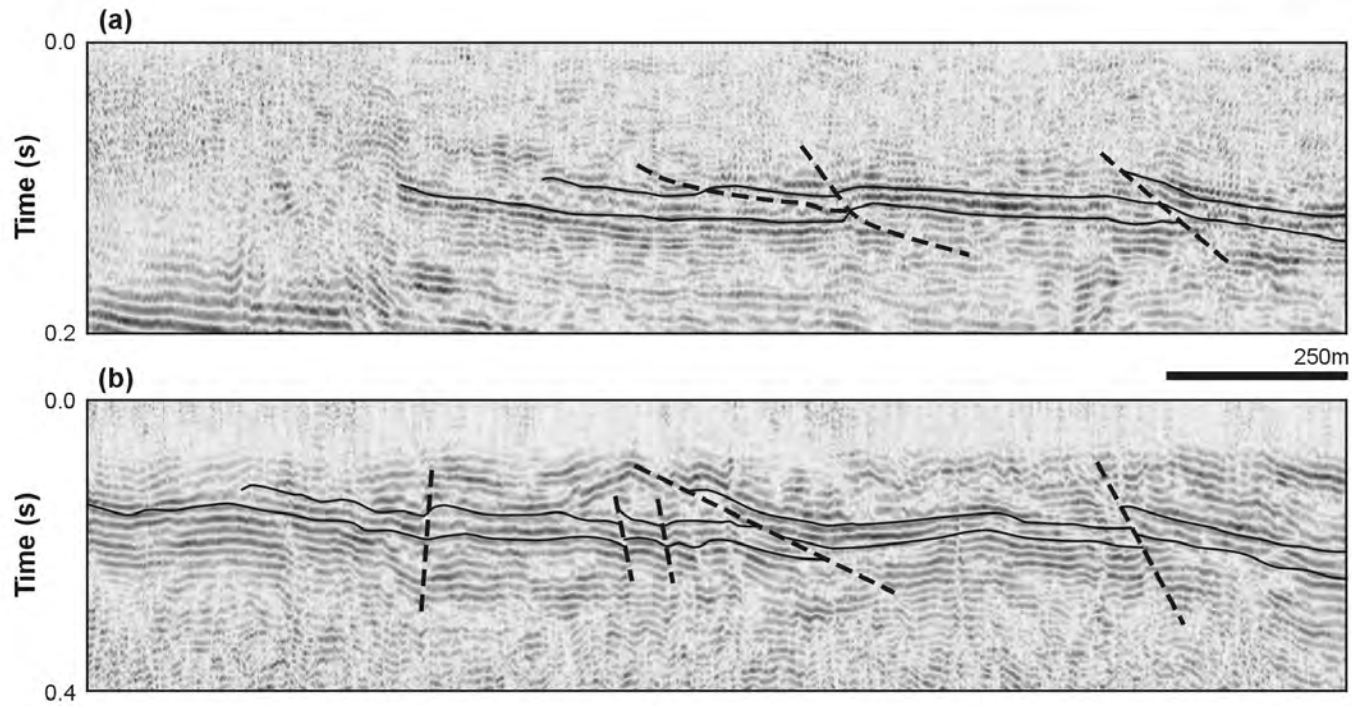

Figure 6: (a) Conventional P-wave image and (b) PS image from Field Trial B. The target coal seams are indicated by the solid lines. Interpreted faults are approximately marked by the dashed lines. The PS section is able to image the shallow coal seams to depths of approximately 25–30m.

Arrays of 3C geophones are not used since S waves are very sensitive to lateral variations in the near surface, and geophone arrays would severely distort any S energy arriving at the surface (Hoffe & others, 2002). Our field experiments indicate that the quality of the conventional P-wave data is not compromised by replacing arrays of vertical geophones with single geophones.

The vertical component of data recorded on a 3C geophone can be subjected to standard seismic-processing algorithms to produce a conventional P-wave seismic section. The converted-wave stack is generated via processing of the data acquired on the horizontal components of the geophone. This involves a number of steps that are substantially different from, and significantly more challenging than, conventional P-wave processing.

In particular, converted-wave processing involves specialised approaches to S-wave receiver statics, PS normal moveout (NMO) correction and common conversion-point (CCP) binning (Cary & Eaton, 1993; Zhang, 1996). Perhaps the most critical stage of processing high-resolution converted-wave data involves the computation of S-wave receiver statics. This information is required to compensate for delays associated with converted S-wave energy travelling through the weathered layer. S-wave receiver statics are generally not related in any way to the conventional P-wave receiver statics. This is largely due to the difference in effective thickness of the near-surface low-velocity layer that the P and S waves 'see' (e.g. S waves will only travel through solid material, and will therefore not be influenced by any near-surface water table; P waves will have their propagation speeds influenced by the presence of ground water). In addition, S-wave velocities in the near-surface can be up to ten times slower than P-wave velocities. Hence S-wave receiver statics are typically much larger than P-wave receiver statics. In practice, several iterations of S-wave receiver statics computations are necessary when trying to extract optimum static corrections.

BOWEN BASIN TRIALS

The past three years has seen a number of converted-wave trials conducted in the Bowen Basin, Australia (Velseis, 2003; Hendrick, 2004). Of these, two have been designed to specifically image very shallow coal seams (less than approximately 50m in depth). Processing of these converted-wave data has proven non-trivial. Nevertheless, viable PS images have been achieved for both of these multi-component surveys, highlighting the potential for converted-wave seismic to yield high-resolution images of open-cut coal reserves.

Field Trial A was conducted in an environment with a single target coal seam, using a buried dynamite source. Figure 5 shows the final P and PS images. As is conventional practice, the vertical scale of the PS image has been adjusted (based on an estimated P-wave to S-wave velocity ratio) to provide a comparable depth perspective to the P-wave image. The PS section yields structural information that is comparable to that derived from the conventional P-wave image. However, the most interesting aspect of this trial is the fact that the PS section (Figure 5(b)) has produced a better quality image over the left end of the line. This is due to the fact that the target coal seam is very shallow (less than 50m deep) along this portion of the line, and the later-arriving PS energy avoids contamination from refracted and surface waves. Consequently, the PS image exhibits greater vertical resolution than the P-wave image where the coal seam is shallowest.

Field Trial B was carried out in a multi-seam environment using a surface mini-SOSIE source. The final P and PS images for a portion of one of the 2D lines acquired as part of this experiment are shown in Figure 6. Significant faults interpreted on the conventional P-wave image have been independently validated by the converted-wave image. A number of additional structural features have also been identified on the PS section.

As for Field Trial A however, the most significant outcome of this experiment has been the success of the PS data to image the very shallow coal seams across the left end of the line. In contrast to the target P-wave reflection energy, the later-arriving PS energy has not been eliminated by near-surface noise. Consequently, the PS data can effectively map the target coal seams across the full extent of the survey line, to depths of 25 – 30m. The PS interpretation results along the left hand end of this line have been tested with borehole drilling, and have proven accurate.

CONCLUSIONS

Seismic reflection is not commonly utilised for open-cut coal exploration due to relatively cheap drilling costs and the inconsistency of conventional, economic seismic surveys to image very shallow coal seams. However, when continuous mapping of the coal seam is important, PS seismic technology offers a reliable alternative to more field-intensive P-wave seismic surveys for producing high-resolution images of open-cut coal reserves.

Some changes to conventional acquisition equipment and seismic surveying procedures are needed to record both P and PS energy. Single 3C geophones replace the conventional vertical geophones at each receiver station. In addition, greater numbers of field units and acquisition cables must be deployed to handle the larger number of live recording channels.

Our experience indicates that processing of PS data is significantly more challenging, and requires more geological input, than conventional P-wave processing. Nevertheless the two Bowen Basin converted-wave trials discussed here have yielded viable PS images and successfully achieved their objective of imaging very shallow coal seams.

Currently, the cost of acquiring a 2D integrated P/PS seismic survey is some 30% greater than for a standard P-wave survey if using a dynamite source, and approximately 45%

greater if using a mini-SOSIE source. In addition, processing and interpretation of the converted-wave dataset effectively doubles data processing and interpretation costs. These extra costs may be reduced in the future as acquisition and processing technology is refined, and converted-wave seismic becomes a more popular geophysical tool for open-cut coal mines. Nevertheless, our experiences to date suggest that, at least for certain situations, this impost is justified in terms of increased information content.

ACKNOWLEDGEMENTS

Parts of this work received financial support from the Australian Coal Association Research Program (ACARP Project C10020). The author would like to thank the Bowen Basin coal mines who have shown support for this new technology, and those who have made their data available for this publication. Thanks are also extended to Steve Hearn for his technical contribution to this research.

REFERENCES

CARY, P.W. & EATON, D.W.S., 1993: A simple method for resolving large converted-wave (P-SV) statics. *Geophysics*, **58**, 429–433.

FERTIG, J. & MÜLLER, G., 1978: Computation of synthetic seismograms for coal seams with the reflectivity method. *Geophysical Prospecting*, **26**, 868–883.

GREENHALGH, S.A., SUPRAJITNO, M. & KING, D.W., 1986: Shallow seismic reflection investigations of coal in the Sydney Basin. *Geophysics*, **51**, 1426–1437.

HENDRICK, N., 2004: Shallow, high-resolution converted-wave seismology for coal exploration. *In* Berry M.V. & Quigley, M.L. (Editors): Mining Geology 2004 Workshop, *AIG Bulletin* **41**, 85–91.

HOFFE, B.H., MARGRAVE, G.F., STEWART, R.R., FOLTINEK, D.S., BLAND, H.C. & MANNING, P.M., 2002: Analysing the effectiveness of receiver arrays for multicomponent seismic exploration. *Geophysics*, **67**, 1853–1868.

VELSEIS, 2003: Investigation of converted-wave seismic reflection for improved resolution of coal structures — Final Report: ACARP Project C10020.

VIRIEUX, J., 1986: P-SV wave propagation in heterogeneous media: velocity-stress finite-difference method. *Geophysics*, **51**, 889–901.

ZHANG, Y., 1996: Nonhyperbolic converted-wave velocity analysis and normal moveout: 66th Annual International Meeting, SEG, Expanded Abstracts, 1555–1558.

Natasha Hendrick, Velseis Pty Ltd, Australia, natasha@velseis.com.au

Natasha Hendrick

A preliminary evaluation of integrated P/PS seismic interpretation for improved geological characterisation of coal environments

A preliminary investigation into the potential of integrated P/PS seismic interpretation to help characterise geological properties of the sub-surface ahead of longwall mining has been conducted. This interpretation methodology requires seismic data to be acquired using multi-component (3C) geophones, such that both compressional (P) and shear (S) seismic waves are recorded at the surface. Synthetic and real seismic data have been used to conduct this initial evaluation. Interval *Vp/Vs* analysis (where *Vp* is the interval P-wave velocity and *Vs* is the interval S-wave velocity) has been performed to map lateral changes in lithology and rock properties. This involves computing the time difference between the P and PS reflection events at the top and bottom of a selected interval in the conventional and converted-wave seismic sections, respectively, to determine the P-wave to S-wave velocity ratio.

Synthetic trials highlight that conventional seismic resolution limits govern the ability of *Vp/Vs* analysis to detect lithological anomalies. It is also demonstrated that absolute *Vp/Vs* values can be recovered for thick geological intervals. However, for thin geological intervals (thickness less than seismic wavelength), only relative *Vp/Vs* values can be recovered. Nevertheless, relative *Vp/Vs* estimates are shown to reveal more information about the geological characteristics of the sub-surface than using conventional P-wave seismic data alone. Results from a Bowen Basin trial illustrate that *Vp/Vs* analysis has the potential to discriminate between shale-rich and sand-rich material, as well as potentially highlight zones of intense fracturing about small faults.

INTRODUCTION

Seismic reflection is widely recognised as a significant geophysical tool for the remote imaging of coal seams ahead of longwall mining. Conventional seismic reflection, which records compressional (P) seismic waves, is routinely used to detect faults and highlight stratigraphic anomalies to help establish the viability of mining projects and determine mine layouts. However, geological data such as roof/floor lithology and rock strength, which are also beneficial to the early mine-planning process, are not easily recovered from conventional seismic interpretation. Converted-wave seismology is an alternative geophysical tool that can potentially yield this type of geological detail. The converted-wave seismic method takes advantage of both P and shear (S) seismic waves arriving at the surface during a seismic survey. The latter generally originate from P-to-S mode conversion occurring at the coal seam, and are commonly referred to as PS or converted waves. With the support of ACARP, Velseis Pty Ltd has recently demonstrated the viability of implementing converted-wave seismic technology in the coal environment (Velseis, 2003; Hendrick, 2004).

Our current research is directed towards evaluating the quality and quantity of additional geological information that can be extracted using converted-wave seismic surveys. This paper reviews the basic concepts of conventional and converted-wave seismic, and presents results from a preliminary evaluation of integrated P/PS seismic interpretation. A number of coal-scale synthetic seismic data trials have been conducted to examine the resolution and accuracy of geological information recoverable via integrated P/PS interpretation. In addition, a preliminary attempt to map sub-surface lithology using real P and PS coal-seismic data from the Bowen Basin is given. These early results suggest that, whilst absolute rock strength and lithology is unlikely to be recovered via integrated P/PS interpretation, useful information about relative lateral changes in rock strength and lithology can be extracted.

P-WAVE AND PS-WAVE SEISMIC

Conventional P-Wave Seismic

Conventional coal-seismic assumes that only compressional (P) waves will arrive at the surface during a seismic survey. P waves are longitudinal sound waves that have particle motion in the direction of travel. Hence a P wave travelling upwards from a geological boundary will have particle motion with a strong vertical component. Conventional seismic surveys will record only the vertical component of seismic energy arriving at the receiver (Figure 1a). This type of seismic recording can also be referred to as single-component (1C) recording.

Converted-Wave (PS-Wave) Seismic

In reality, both reflected P and shear (S) waves typically arrive at the surface during a seismic survey. S waves are transverse sound waves that have particle motion perpendicular to the direction of travel. Note that most of the S energy arriving at the surface will be mode-converted PS energy — that is, energy from a wave that travels down to a

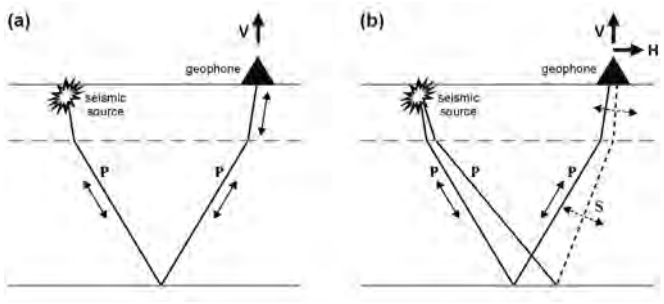

Figure 1: (a) Conventional seismic reflection assumes that only P waves arrive at the surface. Since the particle motion of an upward travelling P wave is largely vertical (indicated by the solid arrows), a vertically-oriented geophone is used for acquisition. (b) Multi-component seismic recording recognises that both P and mode-converted PS waves will arrive at the surface. The particle motion of an upward travelling S wave is largely horizontal (indicated by the dashed arrows). Thus both the vertical (V) and horizontal (H) components of ground motion must be recorded to take advantage of both wave types.

geological boundary as a P wave, gets partially converted to S energy at the boundary, and then travels back to the surface as an S wave. Any PS-wave energy travelling upwards to the surface will have a dominantly horizontal component of particle motion. To enable exploitation of both the P and PS energy arriving at the surface, converted-wave seismic surveys use multi-component receivers that measure both the vertical and horizontal components of ground motion (Figure 1b). Note that multi-component recording may also be referred to as three-component (3C) recording since the vertical and two orthogonal horizontal components (inline and crossline components) of ground motion are generally recorded.

The viability of implementing converted-wave seismic technology in the coal environment has been demonstrated by Velseis Pty Ltd over the past few years (Velseis, 2003; Hendrick, 2004). Standard seismic sources can be used (small dynamite explosions; mini-SOSIE). However, a purpose built high-resolution, high-output 3C geophone replaces the array of vertical geophones used for conventional acquisition at each receiver station. Data recorded on the vertical component of the 3C geophone is subjected to standard seismic-processing algorithms (Yilmaz, 1987) to produce a conventional P-wave seismic section. Our field experiments indicate that single-geophone acquisition does not compromise the quality of the conventional P-wave stack (Velseis, 2003).

The PS stack is generated via processing of the data acquired on the horizontal components of the 3C geophone. This is typically challenging and requires considerable geological input. Furthermore, specialised approaches to S-wave receiver statics, PS normal moveout (NMO) correction and common-conversion point (CCP) binning (Cary & Eaton, 1993; Zhang, 1996) are necessary. Nevertheless, viable PS images have been achieved for the four 2D converted-wave coal-seismic trials conducted in the Bowen Basin to date.

Physical characteristics of P and PS waves

The subsequent integrated interpretation of the P and PS sections takes advantage of the fact that P and S waves travel at different speeds through the earth, and respond differently to various geological situations. For example, S waves typically travel at about half the speed of P waves and, in contrast to P waves, S waves will only travel in solid materials. Hence, while P waves are influenced by pore space and/or fluid and gas saturation, S waves are not. In recent years these differences have been exploited in the petroleum industry, where integrated P/PS interpretation has permitted imagery through gas-filled sediments (e.g. Granli & others, 1999), improved lithology/fluid classification (Engelmark, 2001) and detected reservoir fracture systems (Potters & others, 1999). By analogy, these applications suggest interesting possibilities for the coal environment, such as gas detection, mapping of sandstone lenses or channels, and detection of fracture swarms associated with very small faults or flexures.

INTEGRATED P/PS INTERPRETATION

The fundamental approach to integrated P/PS interpretation is interval *Vp/Vs* analysis (where *Vp* is the interval P-wave velocity and *Vs* is the interval S-wave velocity). The ratio of P-wave to S-wave velocity (*Vp/Vs*) can be estimated from the P and PS seismic sections via:

$$Vp/Vs = \left(2\frac{\Delta t_{PS}}{\Delta t_P} \right) - 1 \qquad (1)$$

where Δt_P and Δt_{PS} are the time differences between the reflection events at the top and bottom of an interval of interest in the P and PS sections, respectively. Inherent in this technique is the assumption that the reflection events correlated between the P and PS sections originate from the same geological boundaries. Accurate correlation of reflection events on the P and PS seismic sections is the most critical and difficult step in the *Vp/Vs* analysis process.

The motivation behind *Vp/Vs* analysis is that the P-wave to S-wave velocity ratio is an effective indicator of lithology and/or fractures, cracks and pore space (Tatham, 1982). For example, sandstones will typically have *Vp/Vs* values in the range of 1.5 to 1.7, while shales have variable *Vp/Vs* values ranging from 2.3 to 2.9 (McCormack & others, 1984). The *Vp/Vs* in coal is typically about 2.5 (Stewart, 2003). Poorly consolidated or fractured material will also exhibit high *Vp/Vs* values. In addition, *Vp/Vs* analysis can yield estimates of Poisson's ratio (Sheriff, 1991):

$$\sigma = \frac{\left(\frac{Vp}{Vs}\right)^2 - 2}{2\left(\frac{Vp}{Vs}\right)^2 - 2} \qquad (2)$$

This elastic constant is an indicator of rock strength, and may be useful for determining additional information about roof and/or floor conditions in underground mining situations.

SYNTHETIC DATA TRIALS

A number of synthetic seismic data trials have been conducted to examine the resolution and accuracy of geological information recoverable via *Vp/Vs* analysis. Such numerical modelling provides an objective benchmark for analysing the overall accuracy and/or relevance of lithological information extracted from real multi-component data.

The synthetic data used in this research have been generated via the elastic finite-difference modelling technique of Virieux (1986). A causal, mixed-phase pulse (the derivative of a Gaussian pulse) with a dominant frequency of 90Hz has been used to approximate an explosive seismic source. Synthetic shot records are constructed at regular intervals along a specified earth model. The resultant P and PS seismic sections are produced using approximately the same processing sequences required to process real multi-component data. This helps to highlight issues relevant to real-data *Vp/Vs* analysis.

Detection of geological anomalies

Recall that *Vp/Vs* analysis involves computing the time difference between the P and PS reflection events at the top and bottom of a specific interval in the seismic sections, and calculating the P-wave to S-wave velocity ratio via Equation 1. It follows that *Vp/Vs* analysis can only be conducted on geological intervals that are thick enough for the top and bottom boundaries to produce discrete seismic reflection events (Sheriff, 1991) for further discussion on vertical seismic resolution limits).

In addition, the *Vp/Vs* attribute will only detect a lateral variation in lithology if the geological anomaly can be detected in the actual seismic sections (Sheriff, 1991) for further discussion on horizontal seismic resolution limits). That is, conventional seismic resolution limits govern the resolution of *Vp/Vs* analysis. However, while *Vp/Vs* analysis doesn't provide greater resolution than seismic imaging, it does provide the opportunity to acquire additional geological information about an observed anomaly.

Note that, it is possible for a lateral geological anomaly to not be seen in a conventional P-wave section, but be detectable in the corresponding PS section (or vice versa). This can occur because S waves respond differently to P waves in various geological situations. In this instance, the *Vp/Vs* attribute will detect a lateral change in lithology because the geological anomaly is imaged in at least one of the seismic sections.

Care must be taken to not over-interpret the *Vp/Vs* attribute. Synthetic data trials suggest that any *Vp/Vs* amplitude variations less than ~0.2 should be interpreted as 'background noise'. Such small variations in *Vp/Vs* can easily result from subtle (and common) discrepancies in the processing of P and PS data. This suggests that *Vp/Vs* analysis is suitable for detecting zones of significant lithological difference (e.g. sandstone versus shale), but is not suited for delineating subtle changes within one lithology type.

Figures 2–5 illustrate the basic concept of *Vp/Vs* analysis. Figure 2 shows a simple two-dimensional (2D) coal-scale earth model comprising shale-rich country rock and two coal seams separated by a number of sandstone channels of varying widths. The corresponding noise-free 2D P and PS seismic sections are given in Figure 3. The two-way time (TWT) picks along the upper and lower coal-seam reflection events for these sections are shown in Figure 4. The computed *Vp/Vs* values for the geological interval between the two coal seams are given in Figure 5.

The average *Vp/Vs* estimate for the country-rock material lying between the two coal seams is ~2.4 (Figure 5) — this is consistent with shale-rich material. Note that, the absolute *Vp/Vs* value for the country-rock material is slightly over-estimated due to the fact that the two reflection events used to define the TWT picks at the top and bottom of the interval are in fact interference patterns created by the energy reflected from the top and the bottom of the two thin coal seams, respectively.

The resultant error in the measured seismic travel times through the geological interval of interest causes the absolute *Vp/Vs* values to be a little too high. Nevertheless, in this example, we are still able to determine that the country rock comprises shale-rich material.

Recall that for these noise-free synthetic data, *Vp/Vs* amplitude variations less than ~0.2 are not considered significant. Thus, the 2m and 5m wide channels in the synthetic earth model of Figure 2 are not reliably detected via *Vp/Vs* analysis. However, Figure 5 shows a significant drop in the *Vp/Vs* values over the 10m, 20m and 40m wide channels. Note that, the TWT horizons from the P-wave section (Figure 4a) only detect the 40m wide channel.

However, the 10m, 20m and 40m wide channels can be detected in the TWT picks from the PS section (Figure 4b). Consequently, the three channels can be detected via *Vp/Vs* analysis. (Note: the width of channel that can be detected via *Vp/Vs* analysis will change with the dominant frequency of the seismic dataset, the signal-to-noise ratio, the vertical thickness of the channel, and the relative *Vp* and *Vs* of the channel material with respect to surrounding material).

Prediction of physical rock properties

Ideally integrated P/PS interpretation would determine absolute *Vp/Vs* values for any specified geological interval to provide the best opportunity for mapping unique lithologies. However, as illustrated by the example given in Figures 2, 3,

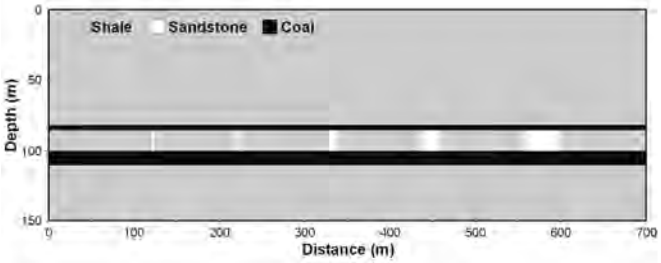

Figure 2: Synthetic earth model used to generate the P and PS seismic sections given in Figure 3. The shale-rich country rock has a *Vp/Vs* of 2.3 (*Vp*=3350m/s; *Vs*=1450m/s). The coal seams at depths of 82m and 100m (3m thick and 10m thick, respectively) have a *Vp/Vs* of 2.5 (*Vp*=2200m/s; *Vs*=880m/s). The five sandstone channels between the coal seams have a range of widths (2m, 5m, 10m, 20m and 40m, from left to right) and a *Vp/Vs* of 1.6 (*Vp*=3900m/s; *Vs* = 2450m/s).

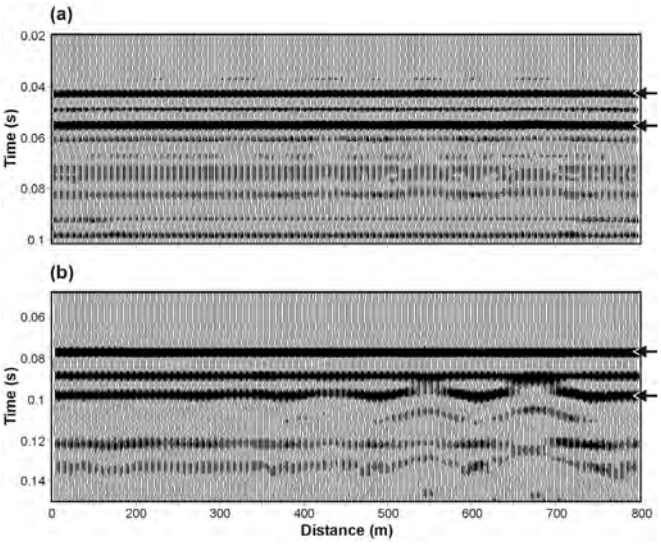

Figure 3: (a) The P and (b) PS seismic sections generated from the earth model given in Figure 2. The reflection events for the upper and lower coal seams are indicated by the arrows. Note that the time axes have been adjusted appropriately to provide a comparable depth perspective.

4 and 5, seismic resolution limits influence absolute *Vp/Vs* values. The *Vp/Vs* estimates for the 10m and 20m channels in Figure 5 are too high because the widths of the channels are smaller than the lateral resolution limit of the seismic dataset (here the Fresnel zone radius is ~40m). While the lateral resolution limit suggests that the absolute *Vp/Vs* estimate across the 40m channel should be correct, in this case it is distorted by the PS reflection event at the base of the channel being affected by an inter-bed multiple reflection event (Figure 4b). That is, noise events will also influence absolute *Vp/Vs* values. Nevertheless, integrated P/PS interpretation of these data clearly indicates the presence of the 10m, 20m and 40m wide geological anomalies, and correctly reveals that they are comprised of material that contains more sand than the surrounding country rock. Such relative variations in *Vp/Vs* contribute to our knowledge of the earth model. This type of information would not have been possible using conventional P-wave data alone.

As expected, vertical seismic resolution limits will also influence absolute *Vp/Vs* values. This has been highlighted

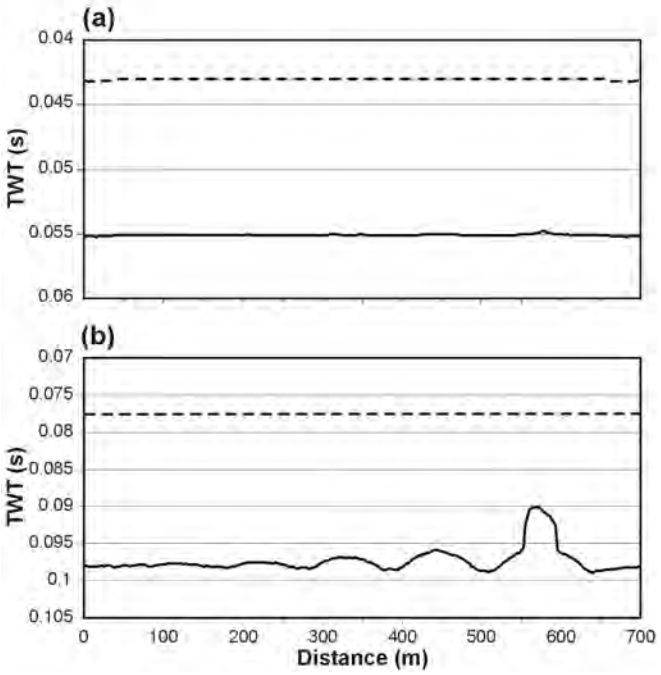

Figure 4: The two-way time (TWT) picks along the upper and lower coal-seam reflection events for (a) the P-wave section shown in Figure 3(a); and (b) the PS-wave section shown in Figure 3(b). The P data show only a subtle TWT variation over the 40m wide channel. The PS data show more significant TWT variations across the 10m, 20m and 40m wide channels due to the large contrast between the S-wave velocity of the shale-rich country rock and the sandstone channels. Note that the time axes have been adjusted appropriately to provide a comparable depth perspective.

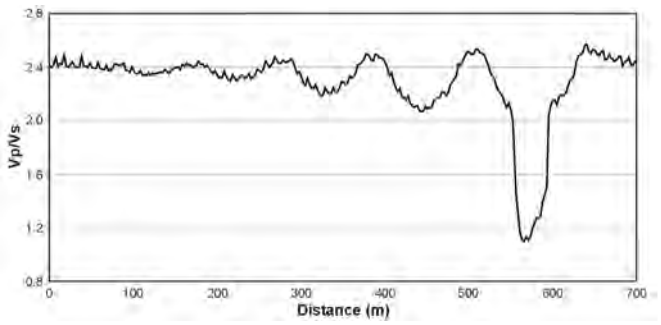

Figure 5: Vp/Vs measurements for the seismic data given in Figure 3. The background Vp/Vs is computed to be ~2.4 — consistent with the shale-rich interburden material. The 10m, 20m and 40m wide channels are correctly indicated by a relative decrease in Vp/Vs. Note however, the absolute Vp/Vs values of the detected sandstone channels are distorted due to the lateral resolution limits of the seismic dataset, and the interference of inter-bed seismic multiple energy.

previously for petroleum-scale case studies (e.g. McCormack & others, 1984; Miller, 1996), and is illustrated here using a simple coal wedge model (Figure 6). *Vp/Vs* estimates for the coal layer, computed via interpretation of the corresponding P and PS sections, are given in Figure 7. For coal thickness ranging from 40m down to 14m, *Vp/Vs* analysis correctly computes an absolute coal *Vp/Vs* value of ~2.5 (recall, any variations in *Vp/Vs*≤0.2 are insignificant).

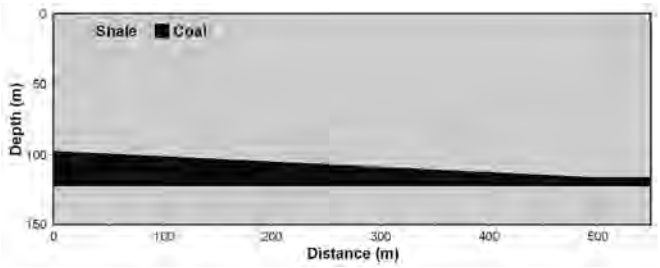

Figure 6: Synthetic earth model used to generate P and PS seismic sections for the *Vp/Vs* analysis results given in Figure 7. The coal wedge starts with a thickness of 40m and thins to 10m. The coal *Vp/Vs* is 2.5 (*Vp*=2200m/s; *Vs*=880m/s). The coal sits in shale-rich country rock with a *Vp/Vs* of 2.3 (*Vp*=3350m/s; *Vs*=1450m/s).

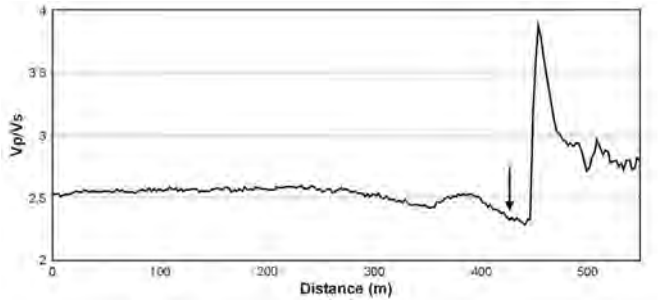

Figure 7: *Vp/Vs* measurements for the seismic data generated using the earth model in Figure 6. For coal thickness ranging from 40m down to ~14m (marked by arrow), *Vp/Vs* analysis correctly computes an absolute *Vp/Vs* of ~2.5. When the coal thickness drops below the seismic wavelength, the *Vp/Vs* estimates drop low before becoming spuriously high.

As the coal-seam thickness drops below ~14m (which is equivalent to the seismic wavelength for this dataset) *Vp/Vs* estimates drop low before becoming spuriously high. The point at which *Vp/Vs* analysis yields these significantly incorrect values is the point at which the reflection events from the top and bottom of the coal seam begin to interfere with one another.

Note: the seismic wavelength is dependent on frequency content of the seismic data, and the velocity of the material through which the seismic energy is travelling. Consequently, the distance between seismic reflectors for which *Vp/Vs* analysis ceases to yield accurate absolute *Vp/Vs* values will be site specific and dependent on local geology and data quality. (Typical coal-seismic wavelengths can vary between 12m and 40m.)

It is highly likely that many geological intervals of interest in the coal environment will have thicknesses close to or less than the seismic wavelength. This does not invalidate the *Vp/Vs* interpretation method in terms of mapping lateral changes within a single geological interval. It simply implies that the thin-interval *Vp/Vs* attribute must be interpreted in terms of relative physical rock property changes within the one interval. Further, comparison of absolute Vp/Vs values from different geological intervals should be avoided when the interval thicknesses are less than the seismic wavelength.

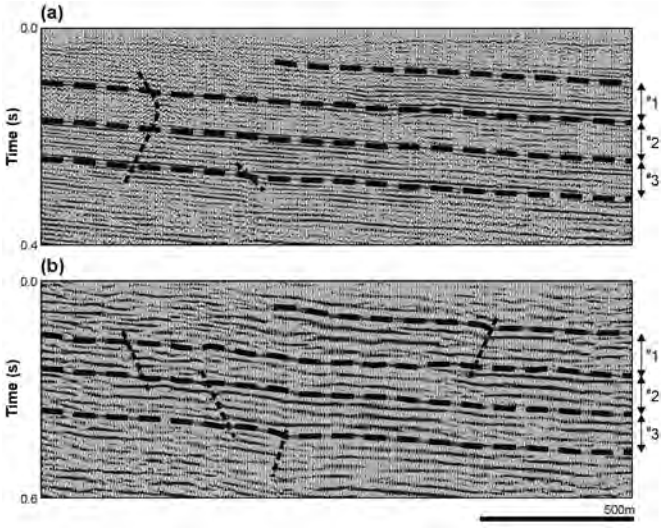

Figure 8: (a) Conventional P-wave image and (b) converted-wave (PS) image derived from the Bowen Basin trial. Interpreted faults are approximately marked. Interpreted horizons are indicated by the dashed lines. Three geological intervals have been defined. Note that the time axes have been adjusted appropriately to provide a comparable depth perspective.

BOWEN BASIN TRIAL

Of the four 2D converted-wave coal-seismic trials conducted in the Bowen Basin to date, two have been acquired in multi-seam environments suitable for trialing integrated P/PS interpretation. Here the results from one of these trials are presented. Figure 8 shows the final P and PS images from this Bowen Basin trial. Significant geological interfaces have been identified on both of the sections, and interpreted faults are indicated.

Note: in this instance, the reflection events defining the three geological intervals for *Vp/Vs* analysis do not interfere with one another (although multiple energy may still interfere with the primary reflection events). It is therefore possible that meaningful absolute *Vp/Vs* values could be recovered, in addition to *Vp/Vs* analysis indicating relative changes in lithology within each interval.

Figure 9 shows the corresponding *Vp/Vs* estimates for the three intervals. The uppermost interval (small dash) exhibits generally high *Vp/Vs* ratios, as might be expected in the shallower, less-consolidated part of the section. The second interval (dash) exhibits an abrupt lateral change in *Vp/Vs* (at distance of ~1200m). This is consistent with a change from shale-rich material on the right to sandy (or possibly gas-contaminated) material on the left. The deepest interval (solid) lies immediately above the target coal seam. This exhibits a more consistent *Vp/Vs* ratio, indicative of a shale-rich sequence. The abrupt increase in *Vp/Vs* at a distance of 500m for Interval 2 and at a distance of 750m for Interval 3 may be indicative of unconsolidated material associated with fracturing about a small fault. Note that, geological information from boreholes has yet to become available for confirmation of any aspects of this interpretation.

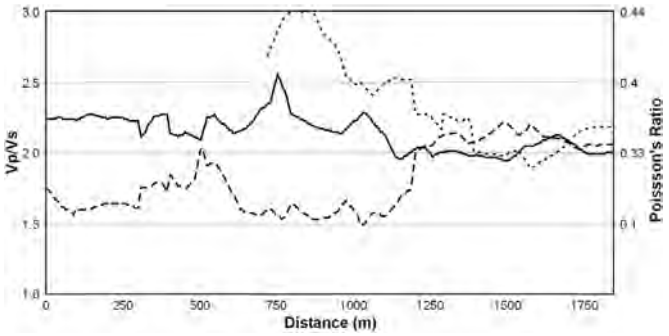

Figure 9: *Vp/Vs* for Interval 1 (small dash); Interval 2 (dash); and Interval 3 (solid) interpreted on the P and PS images show in Figure 8. A high *Vp/Vs* (greater than 2.2) corresponds to shale-rich layers or poorly consolidated material. A low *Vp/Vs* (less than 1.6) is indicative of high sand and/or gas content. As indicated on the right-hand axis, *Vp/Vs* is related to Poisson's Ratio.

CONCLUSIONS

Implementation of converted-wave seismic technologies in the coal environment provides the opportunity to take advantage of integrated P/PS interpretation methods. The potential of these methods to help characterise geological properties of the sub-surface has been evaluated here using both synthetic and real-data coal-seismic examples.

Conventional seismic resolution limits govern the resolving power of integrated P/PS interpretation. Absolute *Vp/Vs* estimates can be recovered for geological intervals thicker than the seismic wavelength, provided noise events or lateral resolution limits are not affecting the reflection events defining the interval. Thin-interval *Vp/Vs* analysis, which is likely to be more common in the coal environment, will yield relative *Vp/Vs* values. However, significant lateral variations in this thin-interval *Vp/Vs* attribute, coupled with behaviour of the individual reflection TWT curves, can be used to infer real changes in the physical properties of the geological interval.

Efficient processing of the converted-wave data and the accurate correlation of reflection events on the P and PS seismic sections are the most problematic components of integrated P/PS interpretation. Nevertheless, this preliminary evaluation of *Vp/Vs* analysis suggests there is merit in continuing to experiment with integrated P/PS interpretation methods and test their ability for improving the remote geological characterisation of coal environments.

ACKNOWLEDGEMENTS

Velseis' initial investigations to test the viability of converted-wave coal seismic received financial support from the Australian Coal Association Research Program (ACARP Project C10020). Ongoing research into integrated P/PS seismic interpretation is supported by ACARP Project C13029. The author would like to thank those Bowen Basin host mines who have helped advance research into converted-wave coal seismic. Steve Hearn is also acknowledged for his technical contribution to the real-data results presented in this paper.

REFERENCES

CARY, P.W., & EATON, D.W.S., 1993: A simple method for resolving large converted-wave (P-SV) statics, *Geophysics* **58**, 429-433.

ENGELMARK, F., 2001: Using 4C to characterise lithologies and fluids in clastic reservoirs, *The Leading Edge* **20**, 1053-1055.

GRANLI, J.R., ARNTSEN, B., SOLLID, A. & HILDE, E., 1999: Imaging through gas-filled sediments using marine shear-wave data, *Geophysics* **64**, 668-677.

HENDRICK, N., 2004: Shallow, high-resolution converted-wave seismology for coal exploration, *in* Berry M.V. & Quigley, M.L. (Editors): Mining Geology 2004 Workshop, *AIG Bulletin* **41**, 85-91.

McCORMACK, M.D., DUNBAR, J.A. & SHARP, W.W., 1984: A case study of stratigraphic interpretation using shear and compressional seismic data, *Geophysics* **49**, 509-520.

MILLER, S.L.M., 1996: Multicomponent Seismic Data Interpretation: MSc Thesis, University of Calgary.

POTTERS, J.H.H.M., GROENENDAAL, H.J.J., OATES, S.J., HAKE, J.H. & KALDEN, A.B., 1999: The 3D shear experiment over the Natih Field in Oman – reservoir geology, data acquisition and anisotropy analysis, *Geophysical Prospecting* **47**, 637-662.

SHERIFF, R.E., 1991: Encyclopedic Dictionary of *Exploration Geophysics (3rd Edition)*, Society of Exploration Geophysicists, Tulsa, Oklahoma.

STEWART, R.R., 2003: Converted-wave seismic exploration: methods and applications, *Short Course, ASEG 16th Geophysical Conference and Exhibition*, Adelaide.

TATHAM, R.H., 1982: Vp/Vs and lithology, *Geophysics* **47**, 336-344.

VELSEIS, 2003: Investigation of converted-wave seismic reflection for improved resolution of coal structures – Final Report, ACARP Project C10020.

VIRIEUX, J., 1986: P-SV wave propagation in heterogeneous media: velocity-stress finite-difference method, *Geophysics* **51**, 889-901.

YILMAZ, O., 1987: *Seismic Data Processing*, Society of Exploration Geophysicists, Oklahoma.

ZHANG, Y., 1996: Nonhyperbolic converted-wave velocity analysis and normal moveout, *66th Annual International Meeting, SEG*, Expanded Abstracts, 1555-1558.

Natasha Hendrick, Velseis Pty Ltd, Australia, natasha@velseis.com.au

Peter Fullagar, Binzhong Zhou and Roland Turner

Quality appraisal for geophysical borehole logs

Borehole geophysical logging data are routinely collected at Australian coal mines for a range of applications, especially seam picking and rock mass characterisation. Interpretation at present is usually qualitative or semi-quantitative, but in principle there is a great deal of quantitative information which can be extracted from the logs. Consistency of the wireline logs, from hole to hole and from year to year, is a pre-requisite for any form of quantitative interpretation. Absolute accuracy tends to be less important in general. Hence there is a need to efficiently assess geophysical logs, both new and historic, to ensure that an appropriate standard of repeatability is achieved.

Quality assurance of geophysical logging data can be achieved by employing both 'hard' and 'soft' control procedures. Hard control entails meticulous calibration and slavish adherence to acquisition procedures. Soft control involves thorough checking after the data have been acquired. A methodology for applying soft control was developed in a recent ACARP project. Three types of data quality criteria were identified:

- **generic criteria, applying to single logging runs in individual holes;**
- **repeat-hole criteria, for successive logging runs in 'repeat' holes; and**
- **production-hole criteria, for single logging runs in a suite of holes (usually in close proximity to one another).**

Borehole logs can be classified as acceptable, questionable, or unacceptable according to whether they satisfy the quality criteria to within tolerances specified by coal company clients. Basic log QA criteria have been codified in prototype software. The range of QA options can be expanded in the future, to satisfy specific requirements at individual coal operations.

INTRODUCTION

Geological and geotechnical information can be derived from drill core, but coring is expensive. Geophysical borehole logging and scanning is a cost-effective alternative means for extracting the information, from uncored as well as cored holes. Boreholes are drilled with limited core runs, and geophysically logged. The benefits of logging at coal mines are well recognised in Australia, and wireline data are recorded routinely.

In principle, geophysical logs can provide a basis for detailed and reliable rock mass characterisation (McNally, 1990; Hatherly & others, 2001) and coal quality estimation (Edwards & Banks, 1978), as well as litho-stratigraphic interpretation (Firth, 1999). In practice, the data are usually interpreted qualitatively or semi-qualitatively. This is in contrast to the petroleum industry, where wireline logs are a primary source of quantitative information. Therefore, the full potential of borehole logging has yet to be realised at coal mines.

Most geophysical logging data recorded at Australian coal mines is of good to very good quality. Given that borehole logs are recorded under cost and time pressure, often in difficult conditions, the overall level of quality achieved by the contractors is commendable. The quality checks proposed here are intended to assist logging contractors as well as their clients, by catching the relatively rare problem logs before they can influence decisions.

The quality of geophysical logs varies for a number of reasons, including

- different contractors at different times;
- different equipment with different specifications;
- improper or inconsistent calibration;
- variation in intensity and/or style of noise, e.g. random, coherent, spiky;
- instrumental drift;
- variation in data acquisition procedures, e.g. logging speed;
- variation in logging environment (diameter, casing, temperature, fluid);
- malfunction of equipment;
- invalid or inappropriate data reduction;
- incorrect depth registration.

Only if these variations are correctly recognised and appropriately managed will geophysical borehole logs become accepted for routine use in quantitative interpretation.

Quantitative interpretation of borehole logs takes many forms, ranging from deterministic physical modelling to purely statistical analysis. However, consistency of the wireline logs is a universal pre-requisite. In addition, for some applications, absolute accuracy is crucial.

Quality appraisal (QA) procedures are well-defined in the petroleum industry, e.g. Theys (1999), but these are not necessarily directly relevant to coal logging. Accordingly, a systematic methodology for QA of borehole logs at coal

mines was developed in a recent ACARP project (Fullagar & others, 2005). Application of the methodology should ensure an appropriate standard of repeatability is achieved.

This paper describes a series of data quality criteria for routine 'production' holes and for successive logging runs in 'repeat' holes. Data are classified as acceptable, questionable, or unacceptable according to whether they satisfy the quality criteria to within tolerances specified by the coal company clients. Prototype software has been developed to apply these criteria. On-going testing indicates that the new log QA methodology will improve the current coal industry practice and complement on-going efforts to assure data quality during acquisition.

BOREHOLE LOG QA METHODOLOGY

Current QA Procedures

At present the quality of borehole logging data at any given site is controlled by some or all of the following:

1. tool design and calibration
2. technical specifications in logging contracts
3. contractor's operational procedures and quality checks
4. repeat sections in nominated holes
5. regular repeat runs in designated 'repeat-holes'
6. graphical quality checks

Tool design and calibration are fundamentally important, but are largely beyond the control of the coal companies. Likewise, there is an implicit reliance on the contractor's operational procedures and quality checks in order to achieve the client's technical specifications.

The empirical tests (4,5,6) complement the contractor's QA checks, to ensure that unusual data is flagged at an early stage. This project was conceived with a view to vetting historic data; however, in principle the procedures could be applied 'at the truck', immediately after acquisition.

Current best-practice involves repeat logging runs in designated repeat-holes (5). Repeat -holes can provide a direct test of reproducibility between tools and contractors, and hence engender confidence in the consistency of data over long periods of time. Re-logging specified intervals (repeat-sections) in a subset of holes (4) is a valid but limited test of repeatability.

Logging repeat-holes at regular intervals can guarantee repeatability over the long term, but it does not guarantee data accuracy. In addition, appraisal of the repeat runs is usually via visual inspection, which is qualitative and subjective. There is a need for quantitative measure(s) of repeatability for the repeat-hole runs.

For production hole data recorded without repeat-hole checks, the assessment of data quality must be based on the logs themselves, supplemented by relevant geological (and drilling) information. Again, visual inspection of the logs is currently the most common approach for judging the quality of the data.

New QA Procedures

The QA methodology proposed here is quantitative and relies on application of a sequence of simple quality criteria. The QA criteria, and their associated procedures, fall into three categories, termed generic, repeat-hole, and production hole as listed in Table 1.

Table 1: Type of QA criteria

Applications	Logging mode
Generic QA checks	*single hole, single run*
Repeat-hole appraisal (2 stages) *- construct reference logs* *- check repeatability*	*single hole, multi-run*
Production-hole appraisal	*multi-hole, single run*

Generic criteria can be applied to single logging runs in individual holes; repeat-hole criteria are suitable for multiple logging runs in the same hole; and production-hole criteria are appropriate for single logging runs in a number of different holes.

Repeat-hole criteria can be sub-divided into two groups: those for generation of standard or reference logs, and those for measuring and judging deviations of repeat-hole logs from the standard.

The variety of criteria which could be applied to the logs is unlimited. We have designed a number of key criteria during the investigation of log QA procedures. Some of the criteria and procedures are described in the following sub-sections. These criteria can be refined, and others devised, as required in the future.

Software design criteria

Prototype software, LogQA, was developed during the project, in order to

- test/refine the QA methodology, and
- provide ACARP with a useful (albeit basic) QA tool.

The prototype LogQA software has been designed to be:

- Universal: not limited to single site or contractor,
- stand-alone: compatible with, but not reliant on, other software, and
- simple and practical.

In order to achieve universality, the software must operate on LAS files, i.e. the standard export format, rather than on primitive data files in contractors' proprietary formats.

Stand-alone software is inherently attractive, but only within limits. It is clearly not desirable to re-invent the wheel, e.g. for graphical display of results. Rather, new software should be designed to interface with existing software used by the coal industry. In particular, LogQA uses the existing LogTrans[1] DAT file format to specify LAS files and define depth ranges for batch processing of logs from multiple holes.

In order for QA software to be used routinely, it must be easy to understand and easy to use.

The LogQA software relies implicitly on tolerances prescribed by the user. The algorithms are configured to recognise anomalous data, not to remediate. At best, errant logs are classified as either acceptable (green), questionable (amber), or unacceptable (red).

The options implemented in the prototype software are briefly described below.

QA CRITERIA

Generic procedures

Check header information

LAS (Log ASCII Standard) format is an ASCII data transfer format, developed for the petroleum logging industry (Heslop & others, 2000). Although LAS is a standard format, it allows a great deal of latitude in terms of file headers. This flexibility can be construed as either an advantage or a disadvantage. One disadvantage is that there is no standard header layout. Therefore the nature and reliability of the information recorded in the LAS file header varies from contractor to contractor.

In the absence of a standard header, the most pragmatic approach is to scan the header for information. Accordingly, a utility has been implemented in LogQA to search the LAS header for key words selected by the user. Records containing the key words are printed. Words such as CASING, WATER, and BIT, for example, could yield information about the borehole environment.

Log verification

Measured logs should conform to 'global ranges', i.e. lie between minima and maxima prescribed for each geophysical parameters. Density, for example, should lie between 1–3g/cc in coal basins. In order to test data against global parameter ranges, there must first be agreement as to:

(a) the global maxima and minima,

(b) the parameters to which the global bounds apply, and

(c) the depth range for the test.

The application of global range criteria is complicated by the fact that different contractors use different mnemonics and, in some cases, different units for the same parameter. Sometimes the units are identical, but expressed differently, e.g. G/CC versus G/C3. Sometimes units vary for a given parameter mnemonic, e.g. sonic logs previously expressed in μs/ft are now commonly recorded in μs/m.

Prior to checking global ranges therefore, it is essential to establish which parameter mnemonics refer to equivalent measurements, and to convert equivalent parameters to a common physical unit. 'Standard' parameter names and units vary from site to site. Therefore it is necessary to generate a table for each site, to identify the aliases for each parameter, and to define the unit conversion factors.

In its simplest form, the global ranges test could be applied to all the data recorded in a particular hole. A hole could be deemed to fail if any readings for any parameter lie outside the designated limits. However, global parameter ranges will normally refer to open hole conditions, below the water level; anomalous borehole conditions, e.g. intervals above the water level or steel-cased sections, will tend to produce false negatives. Therefore, the global ranges test is more meaningful if restricted to data recorded in a normal borehole environment. The depth range(s) selected for application of global bounds can be defined manually, from driller's log or perhaps from the LAS file header, or (in principle) automatically on the basis of the log responses. In the prototype LogQA software, the user can prescribe a (single) depth interval for application of the test.

If the bounds are set to values at the extreme limits of geological plausibility or instrumental specifications, the global ranges test will flag only the grossly erroneous data, e.g. due to equipment malfunction. In this case, logs which fail the global bounds test can be rejected with clear conscience. The bounds can be tightened if more stringent quality criteria are required.

Compute histograms

One simple but effective means to check hole-to-hole consistency of geophysical logs is via comparison of parameter histograms. Usually the histogram based on logs from a small set of holes is compared with the histogram based on a larger 'reference set' of holes. Inconsistency between the histograms does not necessarily imply that the test data is erroneous, since genuine geological variation could be responsible. However, inconsistencies certainly warrant investigation.

1 A program for automatic geophysical log analysis and interpretation created by CRC Mining (formerly CMTE) in collaboration with CSIRO and Fullagar Geophysics (Fullagar & others, 1999).

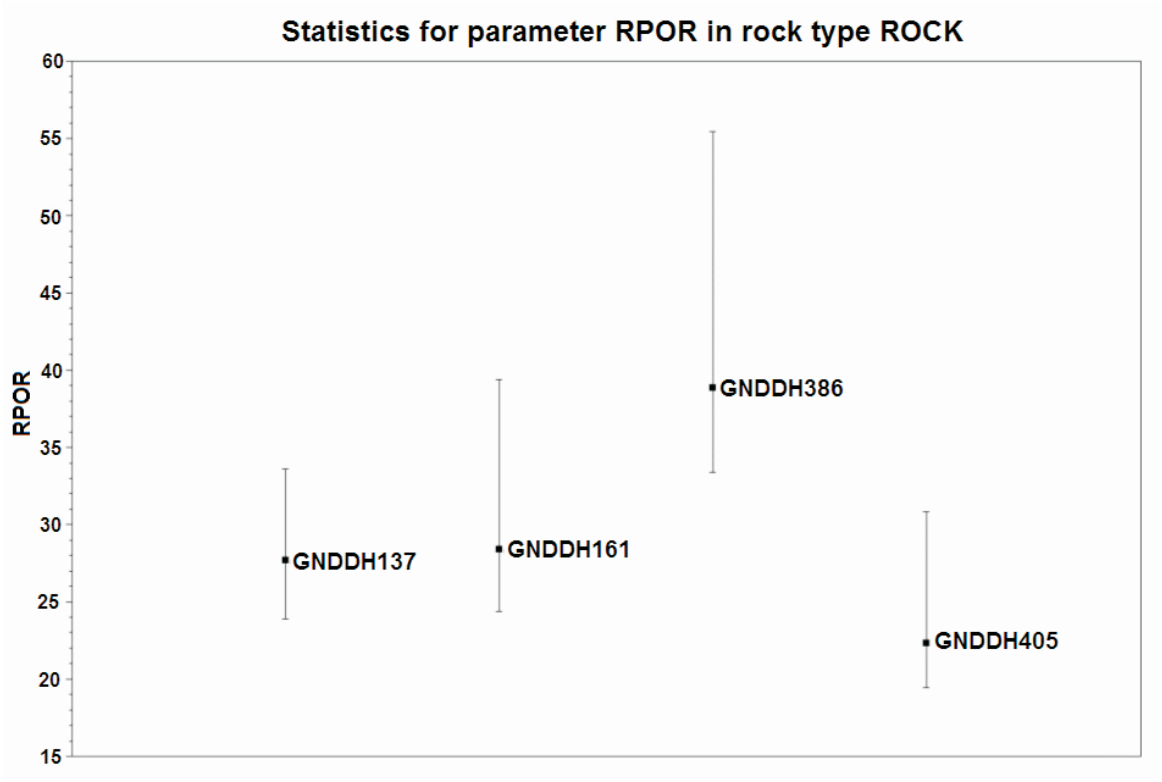

Figure 1: Comparison of neutron porosity medians (black squares) and spreads (16th and 84th percentiles) for neutron porosity in sediment for four nearby holes. Apparent porosity in one hole is spurious due to invalid data reduction. (courtesy Anglo Coal)

Comparison of histograms pre-supposes that both the test hole(s) and the reference set holes intersect the same stratigraphy. Comparison of the histograms will generally become more problematic as the distances increase between all holes involved. Thus the histogram consistency check is geo-statistical in nature. However, inter-hole distance is an imperfect measure of validity, e.g. two adjacent holes could be located on opposite sides of a major fault. Thus geological judgement must be exercised when comparing parameter histograms.

A utility for generation of histograms from LAS files has been incorporated in the prototype LogQA software.

Calculate basic statistics

Basic statistics such as mean, median, standard deviation, and percentile ranges can be computed for each parameter in each hole. Box and whisker plots (Dimitrakopoulos & Latkin, 2002) are a convenient way to present the results.

Inter-hole comparisons can be effected over the entire depth range, or over localised intervals. Analysing logs locally, according to lithotype, can be revealing, (Figure 1). Software already exists for this purpose: LogTrans, for example, offers inter-hole statistical comparison for a suite of parameters in different lithotypes as a standard option. Lithology-based analysis pre-supposes access to lithology logs. Lithology logs can be generated by a geologist, via visual inspection of core and chips, or by a computer program, via interpretation of geophysical logs.

Cross-plotting

Often a single downhole tool will record two or more very similar, or ‘redundant’, parameters, e.g. long- and short-spaced density or sonic transit times for several different transmitter-receiver spacings. When cross-plotted, redundant parameters should define a straight line with slope of unity (Figure 2).

Prior to cross-plotting, it may be desirable to smooth the shorter offset parameter in order to match the depth resolution of the other. Deviations from straight-line-with-unit-slope warrant investigation. The underlying cause could be related to instrumentation, e.g. bent probe, or to data processing, e.g. invalid calibration parameters, or to the borehole environment, e.g. severe caving of the wallrock. Quantitative tolerances could be established to supplement qualitative visual assessment of the cross-plots.

Cross-plots of different parameters can be an effective way to flag anomalies. If the parameters were recorded by different probes, the logs must be depth registered prior to cross-plotting.

A cross-plot module has been incorporated in the prototype LogQA software. Data can be plotted either for individual LAS files or for a suite of LAS files.

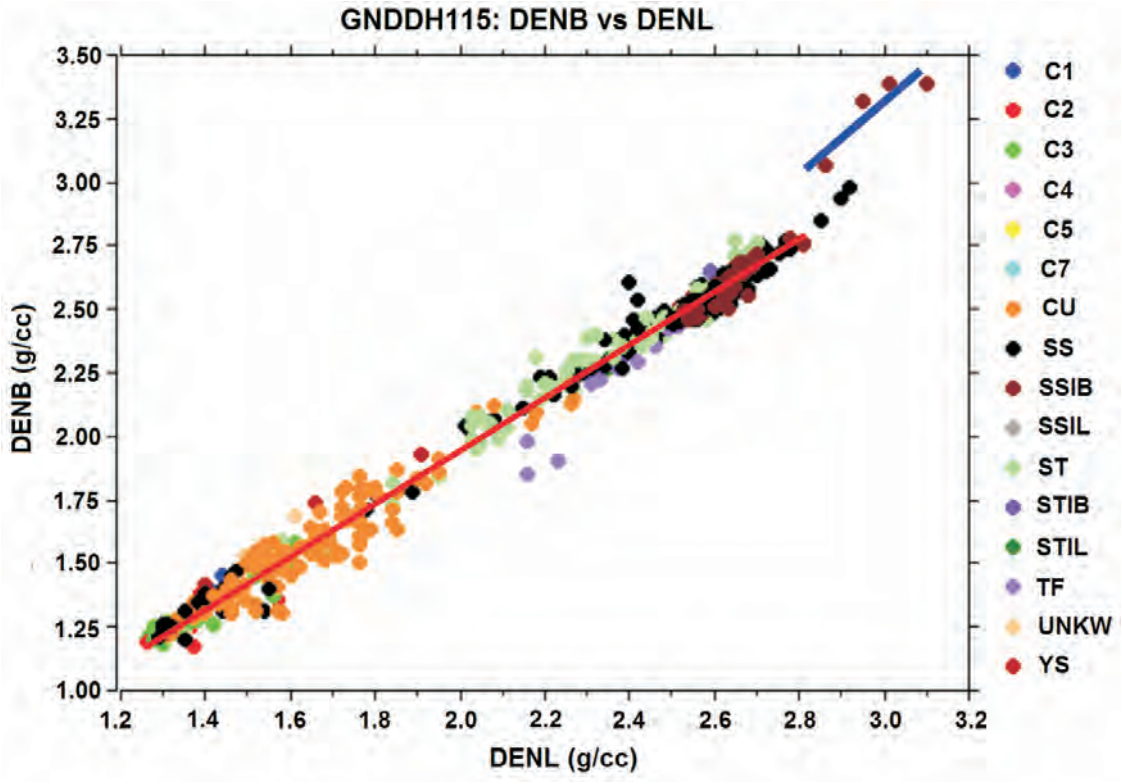

Figure 2: Cross-plot of short-spaced density (unsmoothed) against long-spaced density, with data coloured according to rock type. Two trend lines are defined: the red line is normal and the blue one with a high density trend is caused by a steel-cased section of the hole. (courtesy Anglo Coal)

Repeat-hole criteria

Auto-depth registration of logs relative to one another

For various reasons, the depth assignment for one logging run may differ from that for other logging runs in the same hole. Before assessing repeatability, we first need to ensure that all the logs are aligned in depth. Depth registration or alignment can be performed manually via visual inspection, but this may be time consuming. We have developed an automatic depth shifting procedure based on a cross-correlation algorithm, similar to that used for dipmeter analysis. Figure 3 shows an example of the auto log depth-shifting using this utility.

Construction of reference logs

Reproducibility of successive logging runs in a repeat-hole is judged with respect to a reference log. Usually the reference log is constructed via analysis of a small number of repeat runs. The first few runs in a new repeat-hole are therefore especially important, as these will define the 'target' for subsequent repeat-hole runs. Repeat-hole reference logs are somewhat subjective insofar as they are not necessarily highly accurate.

The reproducibility of repeat-hole logs is dependent on consistency of depth, borehole environment, and data reduction procedures as well as the downhole measurements *per se*. The invariance of the borehole environment is the fundamental assumption on which the repeat-hole approach is based. The depth range for reference logs and, ultimately, the repeatability checks, should be restricted to normal borehole conditions, below the water level.

Repeat-hole logs should be properly depth-registered before they are combined to define reference logs. Given a set of depth-corrected repeat logs, there are many ways to derive a reference log. The simplest method is to compute the average at each depth (Figure 4); this is the approach implemented in the prototype LogQA software. The median value at each depth is a possible alternative. Often the number of repeat logs available will be too small to warrant a more sophisticated approach.

Compute the measure(s) of deviation

The variability (statistical dispersion) of the repeat logs provides an indication of the precision which is achievable in practice. Variability can be assessed point-by-point, locally, or over the entire depth range. Point-by-point analysis is usually precluded by the small number of repeat logs available for reference log construction. However, local analysis (over limited depth range) or global analysis (over the entire depth range) are usually statistically viable.

Although different measures of variability can be defined, the root-mean-square deviation (RMSD) is arguably the simplest option. The RMSD for M repeat runs of a particular parameter is defined as

$$RMSD = \sqrt{\frac{1}{(M-1)K}\sum_{m=1}^{M}\sum_{k=1}^{K}(v_{mk}-\hat{v}_k)^2} \qquad (1)$$

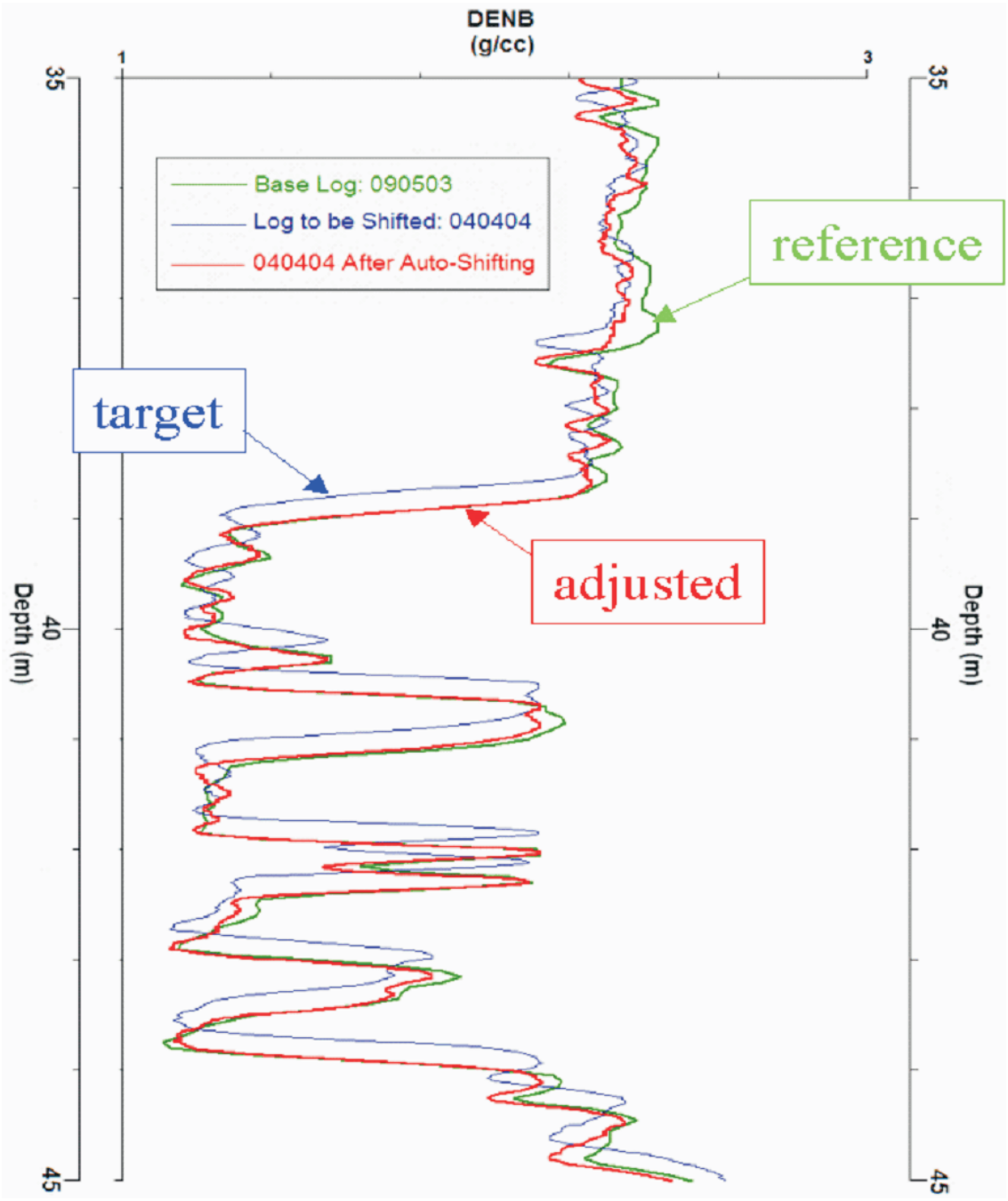

Figure 3: Example of auto depth-shifted density logs. A uniform 18cm depth increase was applied in this case (Data courtesy BMA)

where v_{mk} is the reading for the m^{th} repeat run at the k^{th} depth and where $\hat{v}_k$ is the reference log value at the k^{th} depth. If the variability at each depth can be characterised by normal random variables with mean zero and with the same standard deviation σ, then the RMSD is an estimate of σ. RMSD is expressed in the units of the log parameter in question.

Assessing repeatability of a new repeat-hole log

Once a reference log has been defined for each parameter, repeatability of subsequent logging runs in the repeat-hole can be gauged. It is possible to devise numerous measures of repeatability, both absolute and relative.

The deviation tolerance for each parameter, i.e. the degree of variability which is acceptable, is subject to the discretion of each coal mining company. The tolerance may vary according to rock type, instrumentation, or other circumstances. When setting tolerances, the company personnel should be aware of what is practically achievable as well as familiar with the minimum level of precision needed to satisfy requirements on site. Once set, however, the tolerance should be regarded as sacrosanct.

Repeatability can be assessed over a limited depth range or over the entire reference log depth range. More than one deviation may be computed for a given geophysical parameter, e.g. to assess density log repeatability separately in coal and sediment.

The deviations of the new repeat-hole logs from the appropriate reference logs are checked against the tolerances prescribed by the coal company. The results can be presented in different ways. In Figure 5 new repeat-hole logs for four

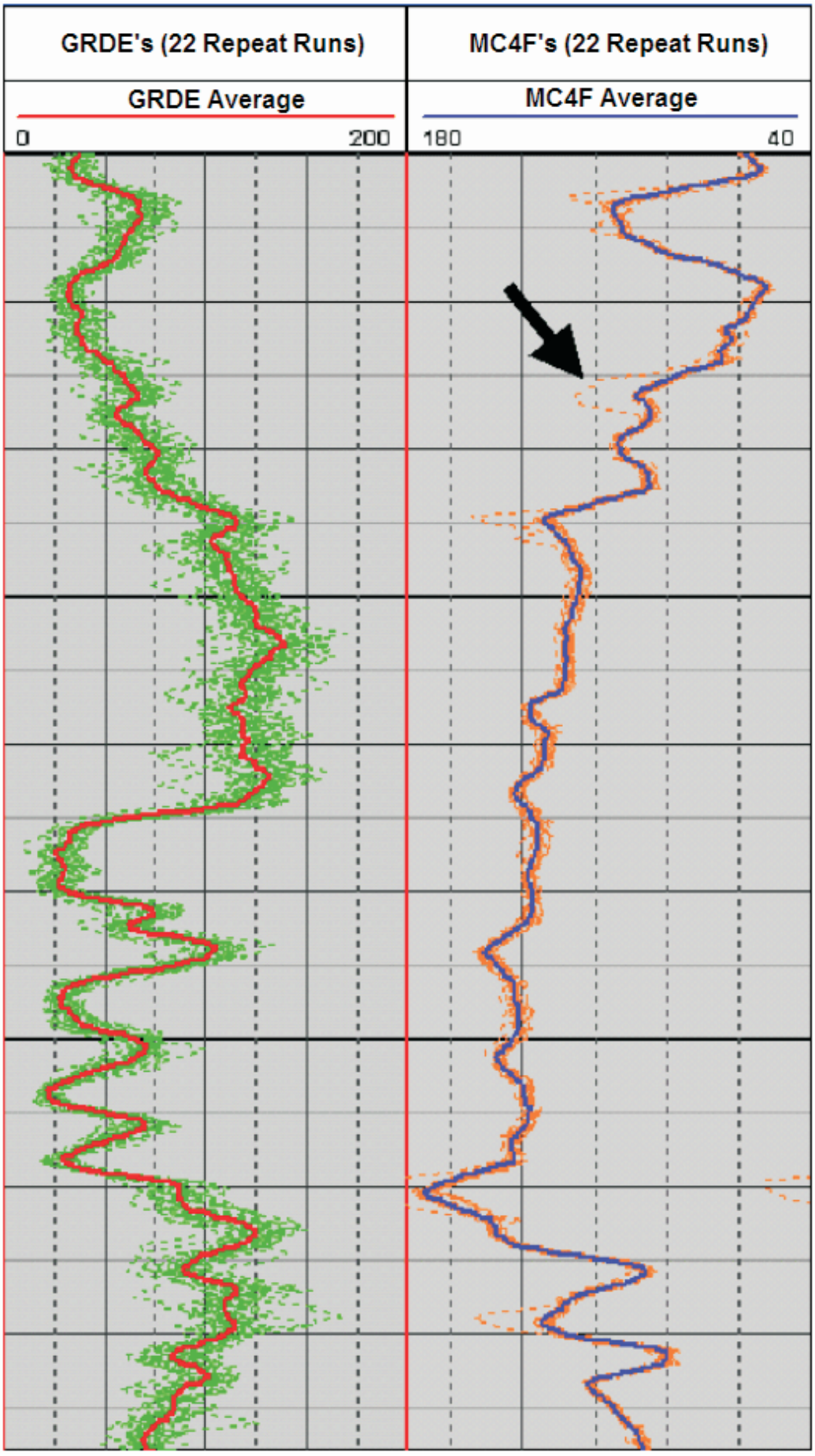

Figure 4: Natural gamma (left) and sonic velocity reference logs (bold), superimposed on the repeat logs from which they were computed. The statistical scatter of the gamma logs is normal. The repeatability of all but one (arrowed) of the sonic logs is excellent. (Data courtesy BMA)

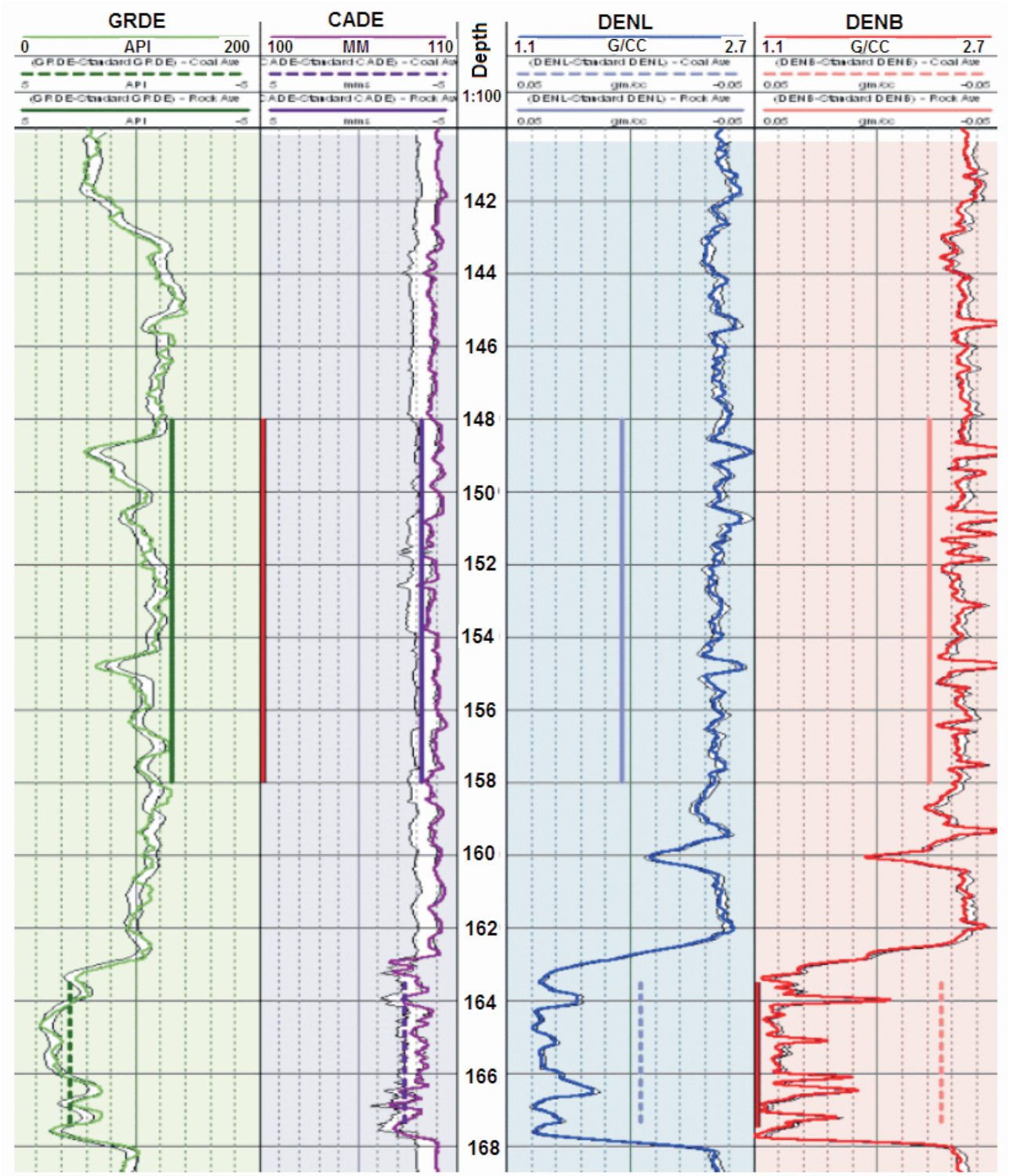

Figure 5: Repeatability check of natural gamma (GRDE), caliper (CADE), long-spaced density (DENL) and short-spaced (DENB) logs. An cceptable corridor is shown in white in each panel, bounded by the reference log ± tolerance. If a new repeat-log lies within the corridor, it is acceptable. The tolerances differ between parameters, and can differ with depth, e.g. between coal and sediment. The vertical red bar marks an interval where the caliper log is unacceptable. (Data courtesy Anglo Coal)

parameters are plotted in relation to the appropriate "acceptable corridor", with limits reference_log_value + tolerance and reference_log_value - tolerance.

QA algorithms can calculate measures of repeatability and suggest action, but ultimately a coal company representative must decide whether or not the new repeat-hole log is acceptable. The LogLQA software records a recommendation in a *Report File.* The format of the report includes provision for the company representative to document his/her decision and, if necessary, the rationale. The signed, dated report can then be filed as a permanent record of the repeatability test.

Production hole criteria

Except for repeat-sections, repeatability is of limited use as a QA criterion in production holes. Rather, QA relies on

(a) the consistency of related parameters recorded in each hole (generic criteria), and

(b) the statistical compatibility of the logs in one hole with the logs recorded in nearby holes (relative criteria).

The range of possible QA checks for production holes is very wide, and includes all the generic criteria and some of the repeat-hole criteria described above. It is likely that individual mine sites will develop specific tests to suit their geological context and achieve their operational goals. The options included in the prototype LogQA software (described above) are by no means comprehensive.

CONCLUSIONS

The motivation for the development of systematic QA procedures is the improved performance and reduction of risk which could flow from more reliable borehole logs. In particular, if a higher degree of consistency can be achieved, geophysical logs could be accepted as key inputs for quantitative rock mass characterisation and coal quality determination.

A methodology has been developed for quasi-automated quality appraisal (QA) of geophysical borehole logs recorded at coal mines. Although the quality of borehole logs is usually good, a small proportion of sub-standard or spurious data does slip through. It is highly desirable to recognise and sideline these data as soon as possible, and certainly before they can influence interpretations and decisions.

For many coal mine applications, it is the consistency of borehole logs that is paramount, rather than their absolute accuracy. Therefore the principal objective of QA is to achieve a high degree of data precision or repeatability. However, the implementation of the methodology should also be seen as a step towards improved accuracy.

Until the advent of repeat-holes, QA was left largely in the hands of geophysical logging contractors. Regular re-logging of repeat-holes, established at mine sites, now provides an objective means for testing data repeatability. However, the repeatability check itself must be conducted in an objective fashion in order for the full benefit of repeat-holes to be realised.

The QA methodology described in this paper distinguishes three types of criteria:

- generic criteria, which can be applied to single logging runs in individual holes, and hence to any logs,
- repeat-hole criteria, which apply to multiple logging runs of a single hole, and
- production-hole criteria, which apply to single logging runs in multiple holes.

The application of a repeatability check implies measurement of deviation from a reference or standard. Therefore, repeat-hole criteria can be separated into two sub-types, those used to define a reference log, and those designed to gauge the acceptability of a new log recorded in the repeat-hole.

An initial suite of QA criteria has been implemented in a prototype software, LogQA, which has been released for beta-testing prior to further development. The software is modular in structure, to facilitate incorporation of additional QA criteria in the future. The QA methodology and the prototype software can be applied to historical data as well as to new data.

ACKNOWLEDGEMENTS

This work was funded by ACARP, with in-kind support from BMA Coal Operations P/L and Anglo Coal Australia. Doug Dunn (BMA) served as industry monitor.

REFERENCES

DIMITRAKOPOULOS, R. & LARKIN, B., 2002: Maximising the benefits from downhole geophysical logs recorded in coal exploration: ACARP Project C8022a Final Report.

EDWARDS, K.W. & BANKS, K.M., 1978: A theoretical approach to the evaluation of *in situ* coal. *CIM Bulletin*, **71**, 124–131.

FIRTH, D., 1999: *Log analysis for mining applications*. Reeves Wireline.

FULLAGAR, P.K., ZHOU, B. & FALLON, G.N., 1999: Automated interpretation of geophysical borehole logs for orebody delineation and grade estimation. *Mineral Resources Engineering*, **8**, 269–284.

FULLAGAR, P.K., ZHOU, B. & TURNER, R., 2005: Quality appraisal for geophysical borehole logs. ACARP Project C13016 Final Report.

HATHERLY, P.J., MEDHURST, T., ZHOU, B. & GUo, H., 2001: Geotechnical evaluation for mining — assessing rock mass conditions using geophysical logging: ACARP Project C8022b Final Report.

HESLOP, K., KAST, J., PRENSKY, S. & SCHMITT, D., 2000: LAS 3.0 Log ASCII Standard Document #1 – File Structures: Canadian Well Logging Society and PPDM.

McNALLY, G.H., 1990: The prediction of geotechnical rock properties from sonic and neutron logs. *Exploration Geophysics*, **21**, 67–71.

THEYS, P., 1999: *Log Data Acquisition and Quality Control*. Editions Technip.

P. Fullagar, Fullagar Geophysics Pty Ltd, Level 1, 1 Swann Road, Taringa, QLD 4068, p.fullagar@mailbox.uq.edu.au
B. Zhou, CSIRO Exploration and Mining, PO Box 883, Kenmore, QLD 4069, Binzhong.Zhou@csiro.au
R. Turner, Borehole Logging Consultancy Services, turnerrt@bigpond.net.au

Binzhong Zhou, Stephen Fraser, Mihai Borsaru, Takao Aizawa, Renate Sliwa, and Tsutomu Hashimoto

New approaches for rock strength estimation from geophysical logs

ABSTRACT

There are various ways to estimate rock strength from geophysical borehole data. Most previous approaches typically require an understanding of the properties of the intact rock and of the defects within it. Geophysical logs can be used to estimate rock properties, structural defects and compositional information. This paper describes the Radial Basis Function (RBF) and Self Organizing Maps (SOM) methods to estimate rock strength from the specialist nuclear SIROLOG (spectrometric natural gamma, Prompt Gamma Neutron Activation) and conventional geophysical logs in anticipation that better performance can be achieved.

The RBF and SOM approaches do not depend on any pre-existing assumptions or models, but estimate the rock strength based on parameters and relationships derived from the internal structure and relationships within the geophysical logging data set. Our RBF and SOM methods can readily accommodate variations in rock characteristics; but their performance largely depends on the completeness of the range of lithologic variation in the available control data base.

Both specialist SIROLOG and conventional geophysical logging data from the Newlands Mine (Collinsville) has been used to demonstrate the effectiveness of the SOM and RBF algorithms to estimate the measured sonic log, and the UCS. Good results have been achieved from both the RBF and SOM algorithms, which indicates the viability of these new methods for estimating rock strength from geophysical logs.

INTRODUCTION

Geophysical borehole logging is routinely conducted at Australian coal mines for various applications such as strata correlation from borehole to borehole. One of the most attractive applications is to estimate the strength of the rocks as it is critically important to have a proper understanding and accurate estimation of the strength of the various rock types present for coal mine design and production. The importance of the rock strength estimation in coal mines is indicated by ACARP's support for a number of geotechnical projects in Australia in recent years, including geotechnical evaluation from geophysical logs (Hatherly & others, 2001); *in situ* stress estimation from acoustic scanner and wireline logs (MacGregor, 2003); and rock mass characterisation from quantitative interpretation of geophysical logs (Hatherly & others, 2004). This paper will concentrate on the estimation of the intact rock strength as measured by the uniaxial compressive strength (UCS) test.

Rock strength can be estimated in various ways but most approaches require an understanding of the properties of the intact rock and of the defects within it. Rock strength depends largely on (Schön, 1996):

- the bonding type and quality of the solid particles (solid bonds in the case of igneous rocks, cementation for consolidated sediments, cohesion for clay, friction for cohesionless unconsolidated sediments like sand and gravel);
- the internal structure of the rock skeleton (including number and type of defects).

In addition, rock strength properties can also be influenced by porosity, mineralogy, water content and other effects. The complexity of rock strength influences and dependencies suggests that estimation of rock strength is not an easy task. Various approaches were investigated by the above mentioned researches.

The regression relationship between seismic velocity and UCS has been recognised (Schön, 1996) as either a linear, polynomial or logarithmic relationship. McNally (1987, 1990) proposed an exponential relationship between the UCS and the sonic log after study of the UCS test results on thousands of core samples with geophysical logs from the Bowen Basin. This relationship is widely accepted as a conventional approach called the McNally method in Australian coal mining for estimation of the UCS from the sonic log.

The McNally method is an empirical first order estimate of rock strength. It has been found at many mines that a local relationship is required to enable UCS to be estimated with sufficient accuracy. To rectify this problem, McNally (1990) suggested a number of expressions for weak and strong strata; and the German Creek Mine derived their own local formula (Ward, 1998). As an alternative approach, Lawrence (1999) provides a UCS/sonic transit time correlation based on lithological variations. One of the primary reasons for a broad data scatter and a high uncertainty in derived relationships is due to the fundamental difference between static (UCS) and dynamic (sonic log or the seismic velocity) properties (Schön, 1996; and Hatherly, 2002).

In an effort to overcome this problem, Hatherly & others (2001) and Hatherly (2002) proposed an alternative approach

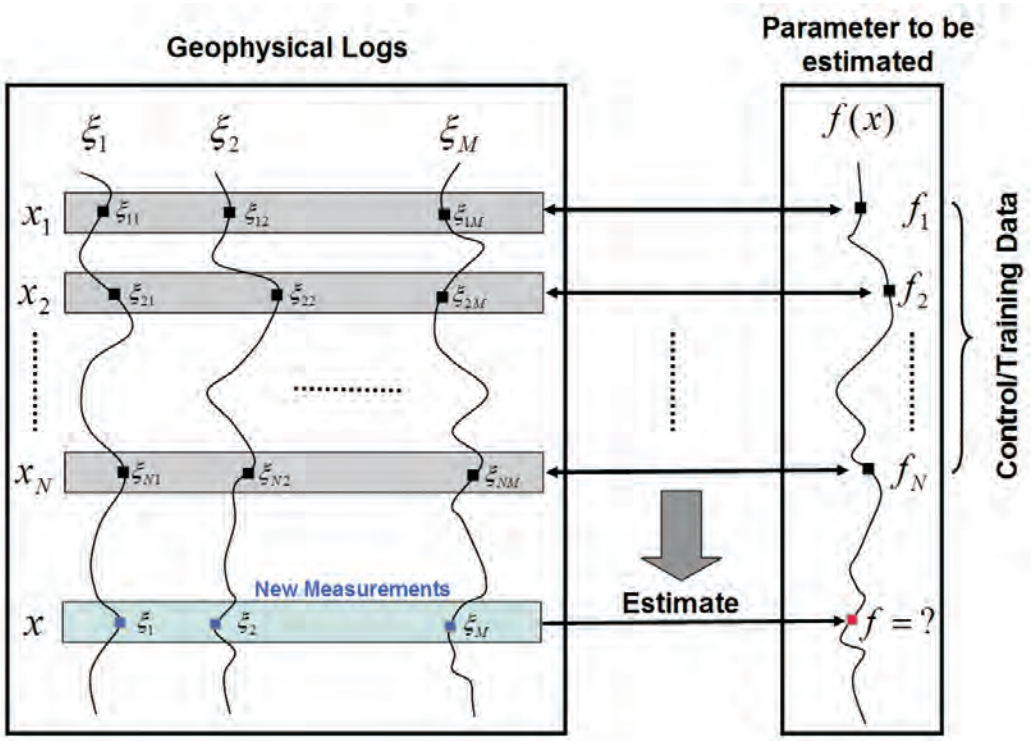

Figure 1: Illustration of parameter estimation using multiple geophysical logs. The discrete control data are used to train the parameter estimation algorithm, and the trained algorithm is then used to estimate the target parameters with new measurements.

to estimate rock strength. To estimate the UCS of clastic rocks from geophysical borehole logs, these authors first determined two compositional parameters, clay content and porosity, from a combination of standard geophysical logs and then related this to the UCS. Behind this proposition was the idea that compositional parameters would have a significant influence on rock strength and geophysical responses. While these compositional parameters also influence velocity, a method that directly utilises them to provide UCS values might be more accurate.

Reasonable estimates of UCS were made based on compositional data. However, as Hatherly & others (2004) note, the variability in the strength behaviour due to factors such as cement type and the location of the cement (around the grains or filling the pores), cannot be investigated by such an analysis. These factors also cause the development of non-uniform stresses at failure. It is well known that stress levels affect sonic velocity in rocks. This is one of the reasons why UCS estimates based on sonic velocity alone tend to be accurate only when determined for a specific site or lithology at that site. While providing an improvement over the McNally method, the compositional approach also allows UCS estimates to account for local variations.

The compositional parameters of clay content and porosity, cannot account fully for other strength controlling factors such as bonding types, grain mineralogy and defects, which is information that may still be contained implicitly within the geophysical logs. This paper proposes an alternative way to directly correlate the rock strength UCS with an extended suite of geophysical logs. In particular:

1. includes the SIROLOG spectrometric natural gamma and Prompt Gamma Neutron Activation Analysis (PGNAA — Borsaru, Rojc & Stehle, 2001) logs in data analysis/interpretation; and,

2. tests two new methods, the Radial Basis Function (RBF) and the Self-Organizing Maps (SOM), for predicting the rock strength from all available geophysical logs.

Both spectrometric natural gamma and PGNAA logs provide information on the elemental composition of the rock. PGNAA can measure the elemental composition of major elements in the rock (e.g., Si, Ca, Al, Fe and S) while spectrometric natural gamma will provide information on the amount of K, U and Th in the rock. It is hoped that the inclusion of the elemental composition of the rock, alongside the established geophysical logs, like sonic, will improve the accuracy of rock strength estimation.

ROCK STRENGTH FROM MULTI-GEOPHYSICAL LOGS

Figure 1 illustrates the basic concept of parameter estimation from geophysical logs. The parameter to be estimated can be rock-type, assay results, geotechnical properties, such as rock strength, or any other petrophysical property. The basis for this capability is that each geophysical log measures a petrophysical property, and geophysical log interpretations exploit the contrasts in petrophysical signatures between different classes of rock. We propose that increasing the number of independent geophysical logs should increase the chance of correct recognition of the rock variations.

The rock strength estimation from multiple geophysical borehole logs can be considered as a data modelling or interpolation problem from discrete known data points in multi-dimension space. There are many techniques, such as model regression and neural networks to tackle this problem, and a general review of these methods is beyond the scope of this paper, which will briefly describe two multi-parameter data analysis methods for rock strength estimation from geophysical logs: the radial basis function (RBF) algorithm and the self-organizing maps (SOM) technique. Two of the most important advantages of these methods are:

1. They provide an estimate of rock strength from parameters and relationships derived within the data set without a need for pre-existing assumptions or models;

2. They can be used to easily accommodate the rock variations by adding additional representative samples into the control data base.

Radial Basis Function Method

During the last few decades, *Radial Basis Functions* (RBFs) have found increasingly widespread use for functional approximation of scattered data. RBF applications in geophysics include geophysical data interpolation (Billings, Beatson & Newsamn, 2002; Billings, Newsamn & Beatson 2002), and prediction of log properties from seismic attributes (Ronen & others., 1994; Russell, Lines & Hampson 2003). This paper investigates the RBF method to estimate rock strength from geophysical logs by establishing a relationship between the geophysical logs and the laboratory UCS measurements.

Let $x = \{\xi_1,\xi_2,...,\xi_M\}$ denote an M-dimension variable. Given data at nodes $x_1, \ldots, x_N$ in M-dimensions, the basic form for RBF approximations can be expressed as

$$s(x) = \sum_{k=1}^{N} \lambda_k \phi(\|x - x_k\|) \qquad (1)$$

where $\|\cdot\|$ denotes the Euclidean distance between two points, and $\phi(r)$ is some function defined for $r \geq 0$. This can be understood as a synthesis of the function $s(x)$ using the basis function $\phi(r)$. In this regard, the RBF method is very similar to the discrete inverse Fourier transform. Given scalar function values $f_i = f(x_i)$, the expansion coefficients λ_k can be obtained by solving the linear system

$$\begin{bmatrix} A_{1,1} & A_{1,2} & \cdots & A_{1,N} \\ . & . & \cdots & . \\ . & . & \cdots & . \\ . & . & \cdots & . \\ A_{N,1} & A_{N,2} & \cdots & A_{N,N} \end{bmatrix} \begin{bmatrix} \lambda_1 \\ . \\ . \\ . \\ \lambda_N \end{bmatrix} = \begin{bmatrix} f_1 \\ . \\ . \\ . \\ f_N \end{bmatrix} \text{ or } A\lambda = f, \qquad (2)$$

where $A_{i,j} = \phi(\|x_i - x_j\|)$. In our case, the function value f_i is the measured UCS from the selected core sample in the laboratory while $x_i = \{\xi_{i1},\xi_{i2},...,\xi_{iM}\}$ is a suite of the geophysical logs such as gamma ray, sonic, neutron and resistivity measured at the corresponding depth of the rock sample in the borehole. The coefficients λ_k derived from equation (2) ensure equation (1) interpolates $f(x)$ exactly at $x_1, \ldots, x_N$. Therefore, the RBF method is an exact interpolator and it attempts to honour the data. The common choices of the radial basis function $\phi(r)$ are (Surfer 7 Manual, 1999)

1. Inverse Multiquadric: $\phi(r) = 1/\sqrt{r^2 + R^2}$;
2. Multi-logarithm: $\phi(r) = log(r^2 + R^2)$;
3. Multiquadratics: $\phi(r) = \sqrt{r^2 + R^2}$;
4. Natural Cubic Spline: $\phi(r) = (r^2 + R^2)^{3/2}$;
5. Thin Plate Spline: $\phi(r) = (r^2 + R^2)log(r^2 + R^2)$;
6. Gaussians: $\phi(r) = e^{-(r/\sigma)^2}$, where ó is a smoothness parameter and can be interpreted as the variance of a Gaussian distribution centred on r;

where r is a normalised relative distance from the point to the node while R is a smoothing factor in an attempt to produce a smoother surface.

The RBF method can be schematically illustrated by Figure 2. This scheme is sometimes called the radial basis function neural network (Russell , Lines & Hampson, 2003) due to its synergy to the concepts of neural networks. Russell, Lines & Hampson (2003) also discussed the relationship between the RBF method and the generalized regression neural network.

Self-Organizing Maps Technique

The Self-Organizing Maps technique (SOM; Kohonen, 2001) has previously been used to predict non-linear sequence data (Walter, Riter & Schulten 1990). The approach of these authors has been essentially followed with the use of SOM to create a 'discretisation' of the geophysical down-hole logging responses and then use of this information to estimate for each discrete 'node' a set of linear prediction coefficients. These coefficients are then used to predict the responses for 'null' or missing sample variables in the down-hole geophysical data sets.

The Self Organizing Maps procedure is a data-analysis tool, which allows visualization of relationships within and between, the various fields of complex data sets. The SOM method is described in detail elsewhere (Kohonen, 2001), and basic code is available from various web sites (http://www.cis.hut.fi/research/).

Self Organizing Maps is a powerful tool for the analysis of complex data sets. SOM has been widely used for data analysis in the fields of finance, industrial control, speech analysis (Kaski, Kangas & Kohonen, 1998; Oja, Kaski, & Kohonen, 2003), and astronomy (Garcia-Berro, Santiago

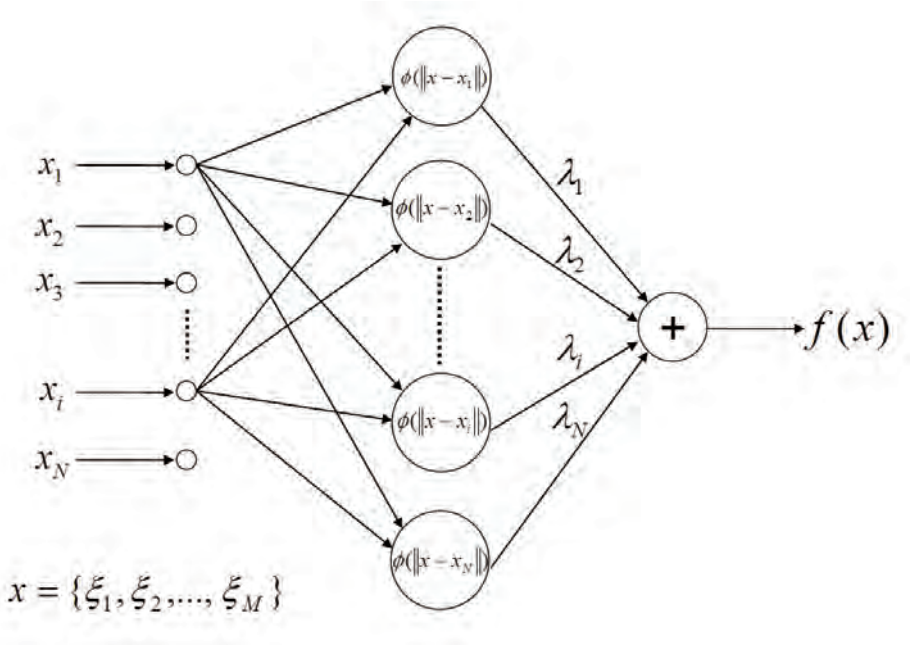

Figure 2: Schematic illustration of the RBF algorithm expressed by equations (1) and (2). It can be considered as a single layer neural network.

Torres & Isern, 2003). Over the past few years, the petroleum-industry literature indicates an increasing acceptance of the Self Organizing Map approach to assist in calibration and interpretation of drill-logs and seismic data (Essenreiter, Karrenbach & Treitel, 2001; Strecker & Uden, 2002; Briqueu & others, 2002; Coléou, Poupon & Azbel, 2003). More recently, Sliwa, Fraser & Dickson (2003) reported on the use of SOM to recognize rock types from the analysis of bore hole geophysics.

Some features of the SOM that are advantageous for data analysis include:

- Adaptivity — the ability to change if new data variables or more data become available;
- Robustness — the handling of missing and noisy data;
- Non-linearity — the ability to represent and reveal both linear and non-linear relationships amongst data variables;
- Prediction — the ability to take new data and relate these to the analysis performed on other related data, with known interpretation.

In a SOM analysis, each sample is treated as an *n*-dimensional vector. This sample vector quantization approach means that both continuous (e.g., PGNAA measurements) and categorical (assigned or named) variables can be input, making it ideal for the analysis of geological data sets. Furthermore, because the SOM is unsupervised, no prior knowledge is required as to the nature, or number, of 'groupings' within the data. These features show why the SOM technique is preferred over other more 'conventional' analysis methods such as clustering (both hard and fuzzy), factor analysis, principal components and multiple linear regressions.

The SOM method takes a set of multi-dimensional data and reduces it typically to a two-dimensional map[1] that retains the topology (relationships) of the input data points. (That is, sample vectors that are close to one-another in *n*-D space will be close to each other in the 2-D feature space). Because each sample is represented as a vector, measures of vector similarity (Euclidean distance and the vector dot product) are used to look for structure and relationships, and to produce an ordering of these data into discrete groups or clusters. The seed vector most similar to a particular input data vector is modified so that it is even more similar to it. Thus by this process of 'competitive learning', the SOM 'map' learns the position of the input data cloud. Not only does the most similar of the seed vectors move towards the data vector, the 'neighbours' of the 'most-similar seed vector are also moved. Hence via this form of 'cooperative learning', the SOM 'map' self-organizes. By these two methods, local order relationships are defined between the input data and the 'seed' vectors; with the 'seed' vectors ultimately forming code-vectors or best-matching units representing discrete groupings or clusters of input data samples as illustrated by Figure 3.

It is from these 'code-vectors' that a set of linear prediction coefficients is calculated, which can then be used to predict null or missing values in the original input data space.

The size of the SOM dictates the number of 'seed vectors' used in an analysis. A larger SOM (higher number of code vectors) allows for variation within a data set (and maintains this variability by allowing a larger range of coefficients for the predicted data). A smaller SOM clumps the input data

1 Three-dimensional, cylinder or toroid surfaces may also be used. For the analyses in this paper we have used a toroid.

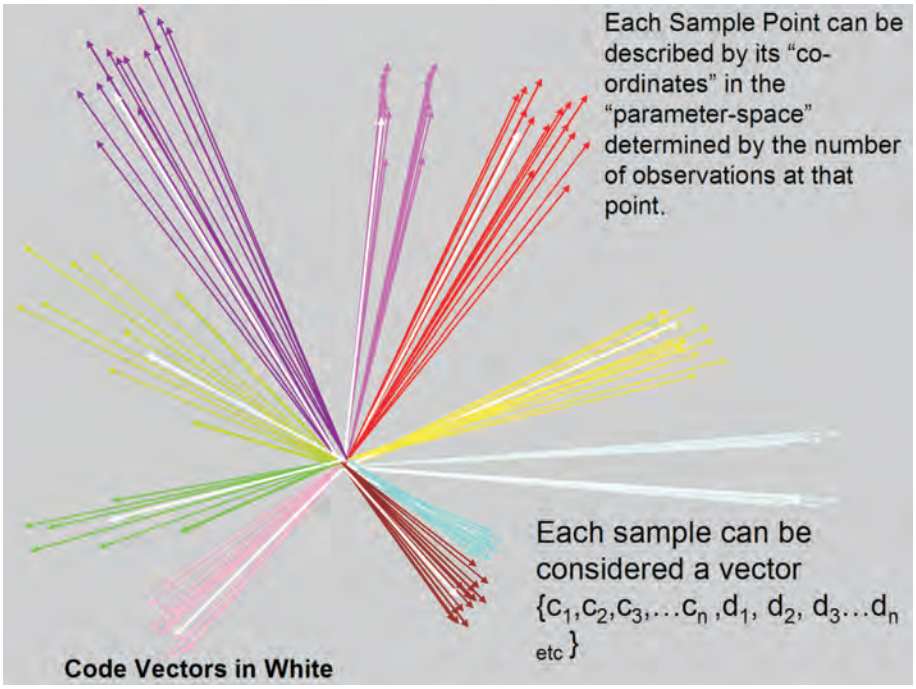

Figure 3: Schematic illustration of how SOM works

into a smaller number of 'code-vectors' (which reduces the number of discrete nodes, and hence reduces or quantizes the range of coefficients available for prediction). For this study we have chosen large-sized SOMs to provide for significant variation in the input data which consequently will accommodate significant variation, and hence more accurate predictions.

CSIRO Exploration & Mining have incorporated much of this functionality into a software package CSOM (CSIRO SOM), which has been used for this data analysis.

TEST DATA

Data Site Descriptions

The test data are from three exploration boreholes H1005, H10011 and H10035 at the Newlands Mine drilled during December of 2003. The three boreholes are aligned east to west and are positioned across a gentle anticline between two regional thrust faults (Figure 4). All three boreholes target the Moranbah Coal Measures and upper Exmoor Formation between the Middle Goonvella and Exmoor coal seams. The

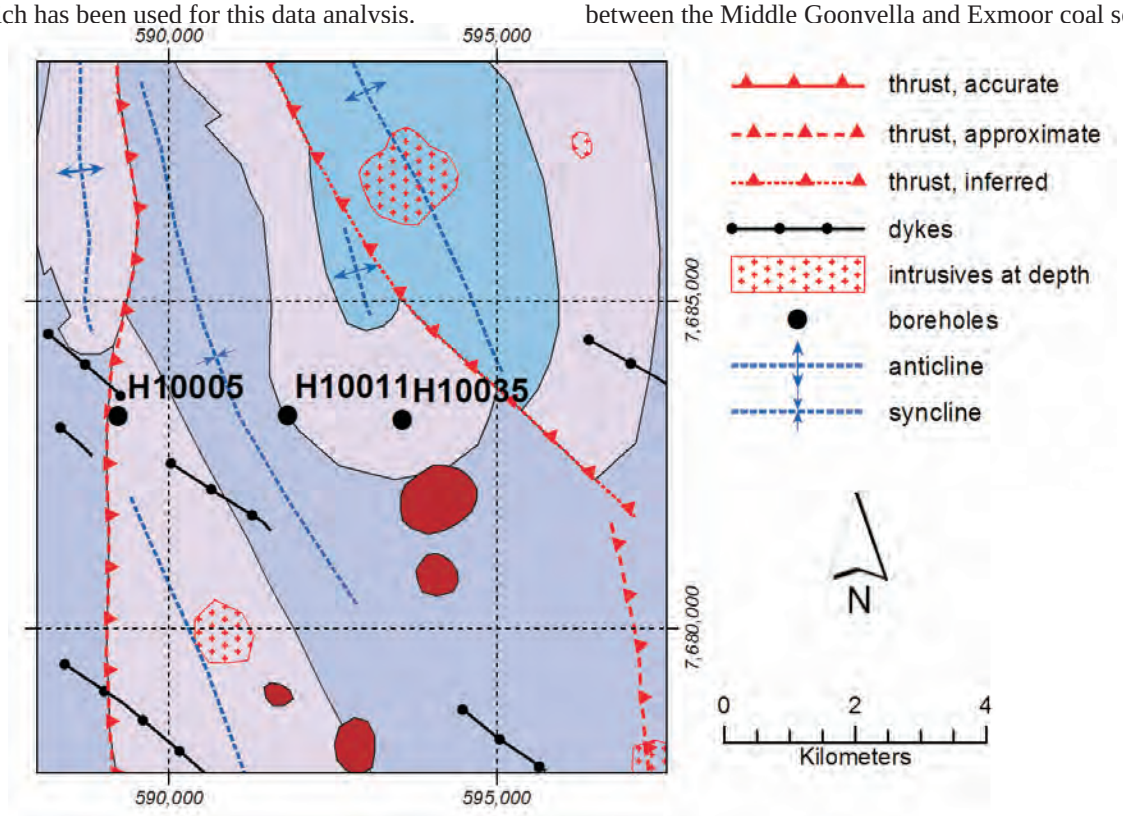

Figure 4: Borehole locations for geotechnical investigation at Collinsville area of Newlands Mine

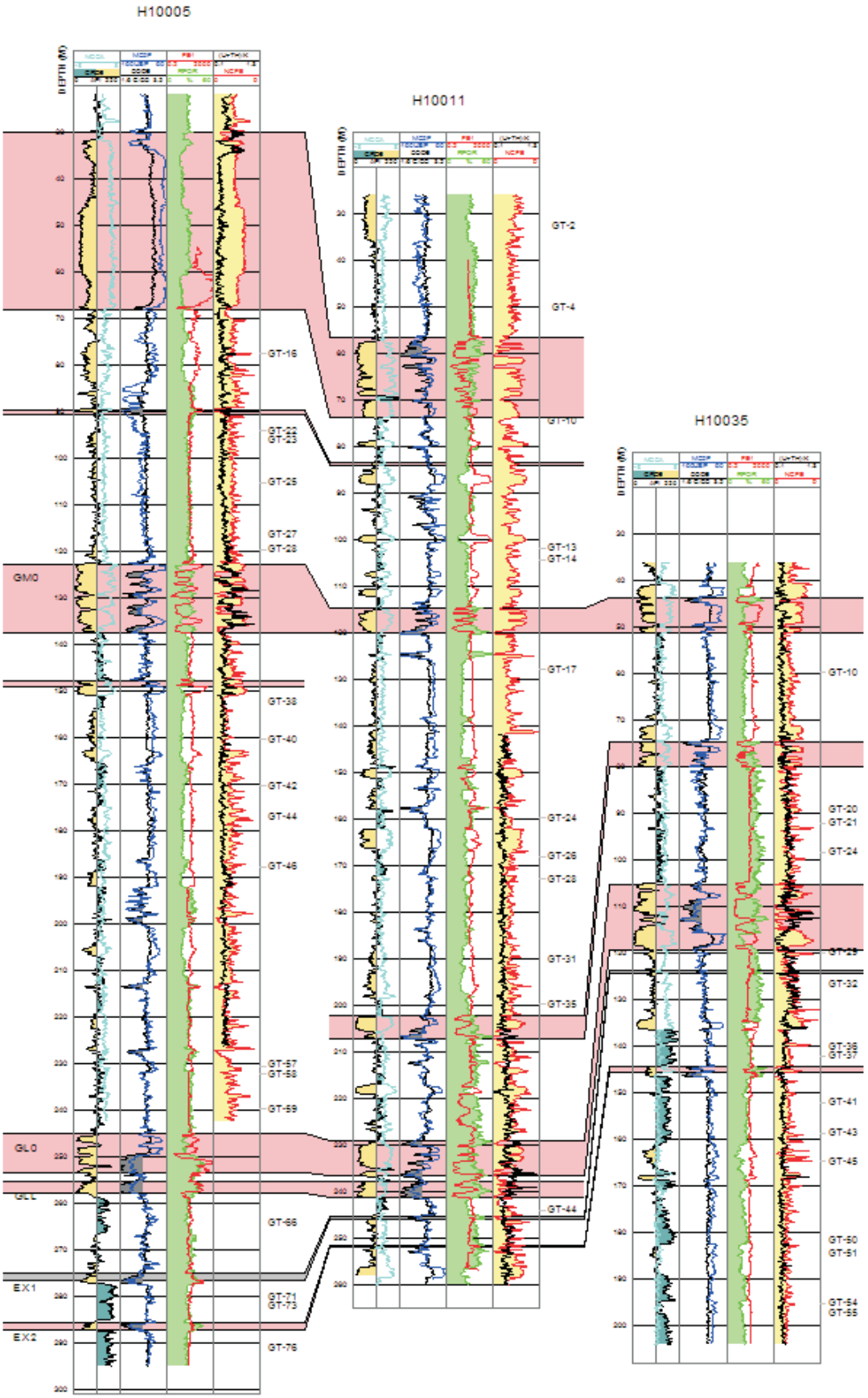

Figure 5: Selected geophysical logs (GRDE — Gamma ray; CODE — compensated density; MC2F — 20 cm sonic; FE1 — Focussed resistivity; RPOR — Neutron porosity; NGCA — Ca from NPGAA; NGFE — Fe from SIROLOG NGPAA tool; (U+TH)/K — Ratio of U, Th & K derived from SIROLOG spectrometric natural gamma.) of the three boreholes and coal seam correlation between boreholes. The logs are presented in linear scale. (GM0 — Goonyella Middle Seam, GL0 — Goonyella Lower Seam, EX — Exmoor Seam, red colour — intruded or coked).

coal measures thin considerably to the east with the Middle to Lower Goonyella seam interval decreasing from 140m in hole H10005 to 85m in hole H10035 (Figure 5). Abundant thin sills extensively intrude this succession and replace or coke most of the intersected coal seams and interburdens.

Thinly interbedded sandstones and siltstones, commonly with upward fining gamma signatures, dominate the interburden rocks of the Moranbah Coal Measures. Sandstone units rarely exceed 10m in thickness, and commonly contain significant amounts of carbonate.

The underlying Exmoor Formation is siltier, with only few thin sandstone units. Gamma signatures consistent with upward coarsening sequences are well developed in hole H10035. In general the siltstones in this unit have a much higher gamma response than siltstones in the Moranbah Coal Measures, and the sandstones contain less carbonate.

Geophysical Logs

All three holes were cored and logged. Both conventional geophysical techniques such as sonic, neutron, natural gamma, density (backscattered gamma-gamma) and focussed resistivity and the SIROLOG tools were used to log the boreholes. Limited data processing was applied to the geophysical logs. Geophysical logs were depth corrected for different tools and runs, and visually checked for anomalous responses. However, the absolute values of the geophysical logs were not calibrated, especially there are no calibration data available for the SIROLOG data. We have assumed that all the logging equipment was functioning correctly, and that appropriate data reduction procedures were followed by the logging providers. The logging data are consistent from one borehole to another. Figure 5 presents some selected geophysical logs from the three investigation boreholes. The geophysical logs used in this project include conventional logs such as calliper, density, neutron, resistivity, gamma ray and sonic logs, SIROLOG PGNAA derived logs such as for the contents of iron (Fe), silica (Si), calcium (Ca), aluminium (Al), boron (B) and hydrogen (H), and SIROLOG spectrometric natural-gamma derived logs for thorium (Th), potassium (K) and uranium (U).

Rock Testing Data

There were 187 core samples collected from the three boreholes. From these samples, 46 samples were selected and tested, with 39 samples producing usable data. The samples were chosen by the following criteria: 1) The samples should be roughly equally distributed in the three boreholes; 2) The samples should cover all major rock types from the three boreholes with even distribution among these rock types; 3) The samples should be collected from locations where the geophysical responses are relatively uniform. The following parameters: density, P-wave velocity, S-wave velocity, moisture, Poisson ratio, elastic modulus, UCS and Brazilian tensile stress were measured in the CSIRO Rock Cutting and Drilling laboratory.

RESULTS FROM SONIC LOG PREDICTIONS

To test our algorithms, we first used the combinations of conventional geophysical logs (excluding the sonic logs) and the SIROLOG data to predict the sonic logs. We compare the predicted sonic logs with the measured sonic logs from boreholes to demonstrate the appropriateness of our new approaches for rock strength estimation. We simulated a control data set by decimating the geophysical logs collected from the borehole H10035. Two basic control data sets were derived from this borehole: 1) a data set of 336 points extracted from the original geophysical logs by every 5 samples; 2) a data set of 168 points extracted from the original geophysical logs by every 10 samples. We trained our both RBF and SOM algorithms with these two basic control data set (with sonic log), and then applied our trained algorithms to new measurements (excluding sonic) to predict the sonic logs.

Results from the partially controlled borehole H10035

The trained RBF and SOM algorithms from the control data mentioned above were first applied to the borehole H10035, which was used to derive the two control data sets. The results are presented in Figure 6. The ES5 abbreviation in Figure 6 (and Figure 7) is for the sonic estimation made from the control data set decimated by every 5 samples from the original logs; ES10 designates the sonic estimation made from the control data set decimated by every 10 samples from the original logs; ‘Both’ refers to the sonic that was estimated by using both conventional logs and the SIROLOG data; ‘Conv’ implies that the estimations were made from the conventional logs only; ‘SIROLOG’ shows that the predicted sonic were derived from the SIROLOG spectral logs; The value of R indicates the correlation coefficient between the predicted sonic log and the measured sonic log from the borehole; The measured sonic log is shown in red; The RBF predicted sonic log is shown in blue while the SOM predicted sonic log is shown in green.

The quantitative comparison of the predicted sonic logs with the measured sonic log is listed in Table 1. From this table, it is evident that the sonic log prediction by both RBF and SOM methods performs well and the correlation coefficients for all the cases are above 0.9. The performance of the sonic log prediction is increased with increased control data points and increased number of geophysical logs. Comparing the SIROLOG data with the conventional data for sonic log prediction, the conventional logging data have better performance than the SIROLOG data. However, combining the conventional logging data with SIROLOG data increases the prediction accuracy and correlation with the measured sonic data.

The elemental compositional-based estimate, determined from the SIROLOG data, provides a usable estimate of the sonic log. The SIROLOG data cannot determine the specific physical property characteristics of the grain to grain bonding nor any such pattern of bonding between grains.

Table 1: The average absolute differences and correlation coefficients between the measured sonic log and the predicted sonic for the borehole H10035

	Control data decimation	Prediction Method	Conventional logging + SIROLOG data	Conventional logging data only	SIROLOG data only
Average Differences (us/ft)	5-sample	RBF	2.23	2.62	3.18
		SOM	2.64	2.46	3.65
	10-sample	RBF	2.78	3.46	4.30
		SOM	2.91	3.03	4.13
Correlation Coefficients	5-sample	RBF	0.98	0.97	0.96
		SOM	0.97	0.97	0.94
	10-sample	RBF	0.96	0.95	0.91
		SOM	0.96	0.97	0.93

Table 2: The average absolute differences and correlation coefficients between the measured sonic log and the predicted sonic logs for the borehole H10011

	Control data decimation	Prediction Method	Conventional logging + SIROLOG data	Conventional logging data only	SIROLOG data only
Average Differences (us/ft)	5-sample	RBF	5.36	10.56	6.93
		SOM	5.91	6.29	7.29
	10-sample	RBF	6.17	5.17	7.68
		SOM	5.86	6.07	6.86
Correlation Coefficients	5-sample	RBF	0.92	0.78	0.86
		SOM	0.89	0.90	0.82
	10-sample	RBF	0.91	0.89	0.84
		SOM	0.87	0.89	0.82

Additional geophysical logs also do not provide specific detail on the pattern and bonding characteristics, but their responses do contain these as dependent variables. For this example using a conventional geophysical suite and the SOM provided a prediction that out performed the RBF. If the average sonic log value is assumed to be about 90μs/ft, then the differences provide a range of 2.4 (2.2/90)% to 4.7(4.3/90)% error of prediction, with correlation coefficients ranging from 0.91–0.98.

Results from independent borehole H10011

Correct prediction of the sonic data for the partially controlled borehole using geophysical logs illustrates the feasibility of our algorithms. An assessment of the reliability of the method can be achieved by evaluating the error of prediction for estimating the sonic log from independent holes, which do not belong to the control hole set. To illustrate the application of the RBF and SOM methods to a non-control hole, we applied the trained SOM and RBF algorithms to the independent hole H10011, located some 1745m away from the control hole H10035. The results are illustrated by Figure 7. Except for the low correlation coefficient for 5-sample decimated conventional log predicted sonic, similar conclusions can be made as the ones from the control borehole H10035.

Table 2 shows the average absolute differences and correlation coefficients between the measured and the predicted sonic logs for this independent borehole. The best relative error of prediction has increased from 2.4% to 5.8% (5.2/90)%. In this example using the RBF function has provided the best statistical estimate. The calculated correlation coefficients between the predicted and measured sonic values for this independent hole are less than the coefficients calculated on the control hole. Figure 5 indicates that these two holes are in a similar section of the stratigraphy, however a component of the increase in error will be due to the natural heterogeneity of the rock sequence (facies variations, degree of alteration associated with the intrusions). It is unlikely the statistical assessment will yield results better than those achieved in the control hole; however our current results are encouraging. The predicted values produce a correlation coefficient of between 0.78–0.92.

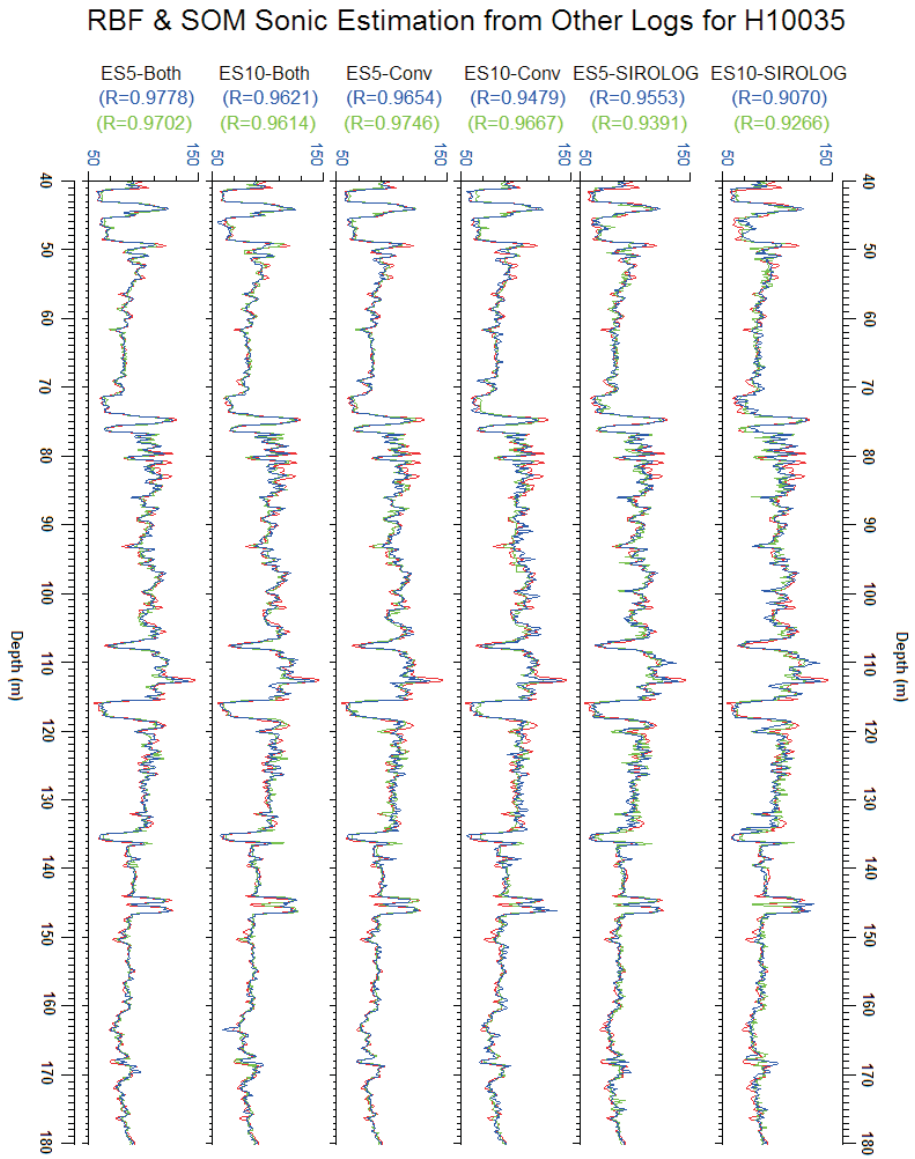

Figure 6: The sonic logs predicted using both the RBF (blue curves) and the SOM (green curves) methods for the borehole H10035. The red curves are the measured sonic log.

RESULTS FOR ROCK STRENGTH ESTIMATION

The successful estimation of sonic log from other geophysical logs demonstrates that our methods may be feasible for rock strength estimation. The geophysical logs and the rock test data from the three boreholes, H10005, H10011 and H10035, can be used to verify this hypothesis. However, there are a number of issues associated with these data:

1) there are only rock test data for 39 rock samples;

2) not all the geophysical logs are available for the rock testing samples, especially for the SIROLOG data; and,

3) the rock samples with no measurements for V_p and V_s and with relatively high moisture contents, more likely have internal defects, therefore the measured UCS values are not accurate expression for the intact rock strength.

To rectify these issues, the SIROLOG data and the rock samples with UCS <20MPa are excluded from analysis. Remaining are the conventional geophysical logs and 35 rock samples to be used in the rock strength analysis.

Statistically, 35 samples are not sufficient for a meaningful analysis of data covering a large range of rock properties. To overcome this problem, the cross-validation technique was used to verify the methods. This process involves taking out one of the known data points and measuring the difference between the estimated value at this point and the true value (the one left out). This procedure is repeated for all the data points. Table 3 lists the UCS values estimated using the SOM and RBF methods through this technique. The 13 conventional geophysical logs (e.g., caliper (CADE), density (DENB, DENL & CODE), gamma ray (GRDE), sonic (MC2F, MC4F & MC6F), resistivity (FE1 & FE2) and neutron logs (LSN & SSN) listed in Table 3 were used for the UCS estimation by the SOM and RBF methods. For comparison, the UCS values derived from the McNally

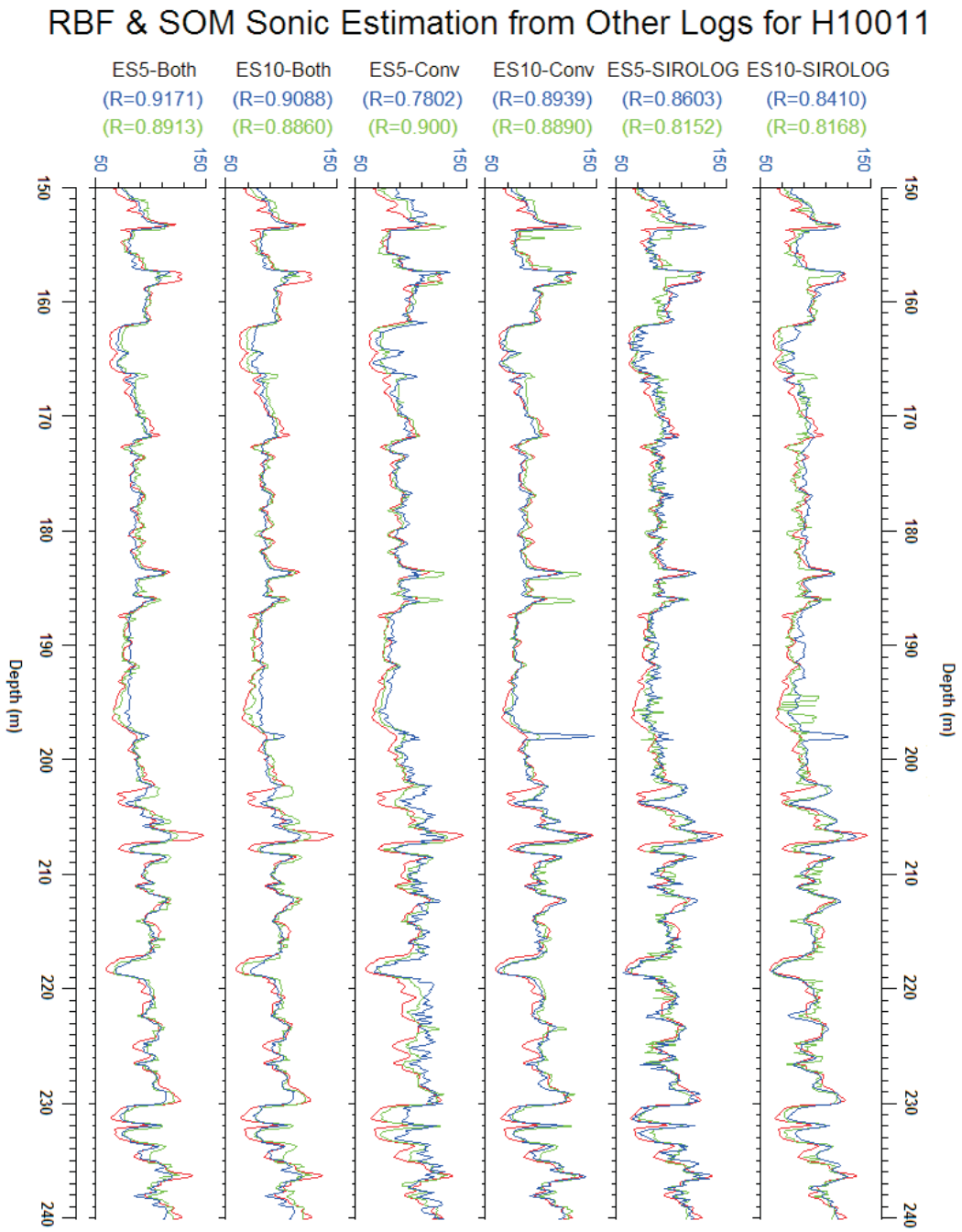

Figure 7: Sonic prediction results using both the RBF (blue curves) and the SOM (green curves) methods for the independent borehole H10011. The red curve is the measured sonic log.

method have been included with the sonic data from the log MC4F in the table. These estimated UCS values from different methods (named as McNally, SOM and RBF) are compared with the laboratory measured UCS (named as UCS in the table). The statistical results of the comparisons are shown in Table 4. All three methods produce comparable results, however the SOM and RBF methods produce slightly better results than the McNally method.

For illustration, the SOM and RBF methods using the control data in Table 3 were also applied to the borehole H10035. The results are presented in Figure 8 along with the McNally's UCS estimation from the sonic log MC4F. Again, the results from the SOM and RBF methods are similar to the results from McNally's method. Large discrepancies between different methods happen in the coal seam zones and volcanic units where control data were not available. This again illustrates the feasibility of our SOM and RBF algorithms for rock strength estimation from geophysical logs.

CONCLUDING REMARKS

Two new methods (the RBF and SOM approaches) are proposed in this paper to estimate rock strength from geophysical logs. Unlike other existing methods, such as McNally's exponential relationship between UCS and sonic log, the RBF and SOM methods do not depend on any pre-existing assumptions or models. These methods estimate the rock strength based on parameters and relationships

Table 3: The estimated UCSs from geophysical logs by McNally, SOM and RBF methods

Sample ID	Rock Type	DEPTH	CADE	CODE	DENB	DENL	GRDE	MC2A	MC2F	MC4F	MC6F	FE1	FE2	LSN	SSN	UCS	McNally	SOM	RBF
		(m)	(inch)	(g/cc)	(g/cc)	(g/cc)	(GAPI)	(ìs/ft)	(ìs/ft)	(ìs/ft)	(ìs/ft)	(OHMM)	(OHMM)	(SNU)	(SNU)	(MPa)	(MPa)	(MPa)	(MPa)
H10005 GT-16	SS	77.70	3.96	2.60	2.70	2.62	38.78	69.80	70.15	72.79	75.43	94.15	85.97	302.31	2382.11	86.00	78.26	70.02	92.89
H10005 GT-28	LM-SS-SL	119.80	4.00	2.51	2.56	2.53	88.96	82.16	82.36	84.27	84.96	28.99	27.55	252.97	2149.24	43.00	52.37	37.93	43.08
H10005 GT-38	SL	152.45	4.04	2.53	2.56	2.54	136.38	81.98	80.99	83.48	83.73	25.86	23.37	316.44	2383.47	42.00	53.84	51.03	52.68
H10005 GT-40	SS	160.50	3.96	2.49	2.52	2.50	80.58	81.75	81.29	81.68	80.19	30.61	28.15	392.36	2673.12	49.00	57.34	38.32	63.81
H10005 GT-42	S-SL	170.55	4.00	2.55	2.58	2.56	126.93	82.50	82.66	84.06	83.84	23.65	21.92	305.13	2359.52	62.00	52.75	49.66	51.72
H10005 GT-44	SS	177.15	3.97	2.66	2.71	2.66	88.79	77.34	77.15	78.12	77.60	28.11	26.18	338.58	2516.55	79.00	64.96	71.83	66.58
H10005 GT-46	LM-SL-MD	187.85	4.00	2.52	2.57	2.53	134.73	89.49	88.35	92.16	92.50	17.97	17.03	275.80	2192.01	43.00	39.74	41.81	55.74
H10005 GT-57	SL	230.75	3.95	2.60	2.60	2.61	111.65	81.01	80.15	80.57	79.03	28.72	26.30	302.24	2428.10	60.00	59.61	71.94	46.91
H10005 GT-66	LM-SL	264.35	3.94	2.52	2.53	2.54	136.51	90.14	89.91	89.88	87.33	20.80	18.27	229.22	2071.45	28.00	43.03	38.92	47.93
H10005 GT-76	LM-SL	291.25	3.89	2.57	2.61	2.58	158.73	90.09	88.00	90.19	88.48	14.86	14.38	241.66	2141.12	60.00	42.57	56.14	61.51
H10011 GT-10	LM-SL	74.55	4.38	2.52	2.50	2.51	153.32	98.86	96.76	99.00	98.59	21.07	19.33	285.57	2713.06	33.00	31.27	34.02	25.48
H10011 GT-13	SS	101.85	4.32	2.58	2.56	2.57	106.89	82.24	81.70	80.03	79.35	30.45	30.11	312.67	2997.08	31.00	60.74	50.41	37.77
H10011 GT-17	SS	127.85	4.29	2.58	2.56	2.58	87.12	80.25	79.28	79.95	79.85	32.93	31.46	403.72	3238.78	46.00	60.91	47.65	43.87
H10011 GT-24	LM-SS-SL	159.80	4.25	2.54	2.52	2.53	143.03	98.71	97.42	98.66	98.66	23.35	22.69	245.22	2538.80	24.00	31.65	33.93	26.59
H10011 GT-26	LM-SS-SL	168.15	4.26	2.60	2.58	2.59	129.65	77.90	77.92	78.46	78.33	42.02	39.18	364.92	2962.64	69.00	64.18	50.07	51.46
H10011 GT-28	IN-SS-SL	172.95	4.27	2.65	2.62	2.64	94.92	80.27	79.75	79.73	78.83	30.10	28.08	383.67	3069.17	40.00	61.38	57.07	53.65
H10011 GT-31	SS	190.30	4.24	2.63	2.59	2.62	75.32	75.22	74.86	75.59	75.80	32.78	30.83	432.43	3337.42	54.00	70.96	55.60	47.87
H10011 GT-35	LM-SL	199.80	4.19	2.57	2.59	2.57	125.81	87.70	85.70	86.88	86.46	24.10	23.35	292.34	2850.70	33.00	47.80	39.84	58.98
H10011 GT-44	LM-S-SL	244.10	4.12	2.59	2.56	2.59	131.60	84.86	83.24	83.39	83.23	26.99	26.66	277.20	2707.82	21.00	54.00	57.30	30.99
H10035 GT-10	IN-SS-SL	59.65	4.08	2.54	2.61	2.57	134.76	89.32	88.73	89.56	88.76	28.17	29.12	328.69	2772.23	68.00	43.51	45.72	38.77
H10035 GT-20	LM-SL	89.20	4.13	2.55	2.62	2.57	96.14	92.14	93.34	93.34	93.56	23.45	24.96	223.80	2234.57	31.00	38.13	36.90	45.22
H10035 GT-21	SL	92.15	4.11	2.48	2.56	2.51	114.20	96.27	97.50	97.53	97.50	19.27	20.91	210.27	2268.02	39.00	32.92	35.48	34.70
H10035 GT-32	CA-SL	126.75	4.07	2.42	2.51	2.44	92.19	100.53	100.49	102.28	102.43	13.35	14.15	160.54	2056.11	46.00	27.88	32.03	25.54
H10035 GT-36	IL-SS-SL	141.45	4.11	2.56	2.59	2.57	193.49	90.71	92.13	92.78	92.52	23.00	25.40	252.53	2343.59	51.00	38.88	48.63	54.25
H10035 GT-41	SL	152.15	4.11	2.56	2.61	2.58	144.07	84.58	85.20	86.15	85.57	17.15	18.74	288.61	2548.90	66.00	49.04	54.10	56.02
H10035 GT-43	SL	158.65	4.07	2.57	2.60	2.58	175.32	85.40	86.11	86.80	86.11	17.23	18.64	302.54	2608.91	53.00	47.93	50.81	64.89
H10035 GT-45	SS	164.80	4.05	2.58	2.61	2.59	69.36	75.60	76.91	77.31	77.17	30.64	32.25	498.38	3445.78	47.00	66.81	67.45	76.73
H10035 GT-50	IL-SS-SL	181.75	4.04	2.55	2.58	2.56	164.99	85.46	85.04	86.59	86.47	20.73	22.39	297.75	2551.68	52.00	48.28	53.31	47.83
H10035 GT-51	SS	184.55	4.00	2.59	2.60	2.59	84.62	73.33	73.92	75.53	75.42	25.20	29.08	502.91	3419.84	82.00	71.10	52.69	74.39
H10035 GT-54	SS	195.25	3.99	2.58	2.59	2.59	125.75	76.40	76.66	77.55	77.20	21.43	22.79	436.40	3092.65	68.00	66.25	53.21	54.32
H10035 GT-55	IL-SS-SL	196.75	3.99	2.68	2.70	2.68	121.19	73.83	73.98	75.07	74.98	25.05	27.63	412.03	3023.19	83.00	72.26	69.44	77.66
H10005 GT-58	LM-SS-SL	232.35	3.97	2.43	2.47	2.44	122.86	103.42	103.42	105.95	106.01	14.74	13.24	177.26	1806.79	22.00	24.52	34.30	26.13
H10005 GT-71	LM-SS-SL	280.60	3.92	2.51	2.54	2.52	170.10	82.94	82.59	83.37	83.68	16.85	16.20	255.32	2178.00	37.00	54.04	51.09	29.76
H10011 GT-04	IL-SS-SL	50.25	4.37	2.55	2.52	2.54	87.67	99.23	97.48	98.08	97.56	19.66	19.43	242.41	2713.39	27.00	32.30	33.41	15.46
H10035 GT-37	CA-SL	142.20	4.11	2.53	2.63	2.56	159.80	85.86	86.34	88.38	88.77	23.76	26.71	242.88	2371.78	60.00	45.35	52.28	76.18

Key: LM – Laminated; IN – Interbedded; IL – Interlaminated; S – Sandy; CA – Carbonaceous; SS – Sandstone; SL-Siltstone; MD -Mudstone

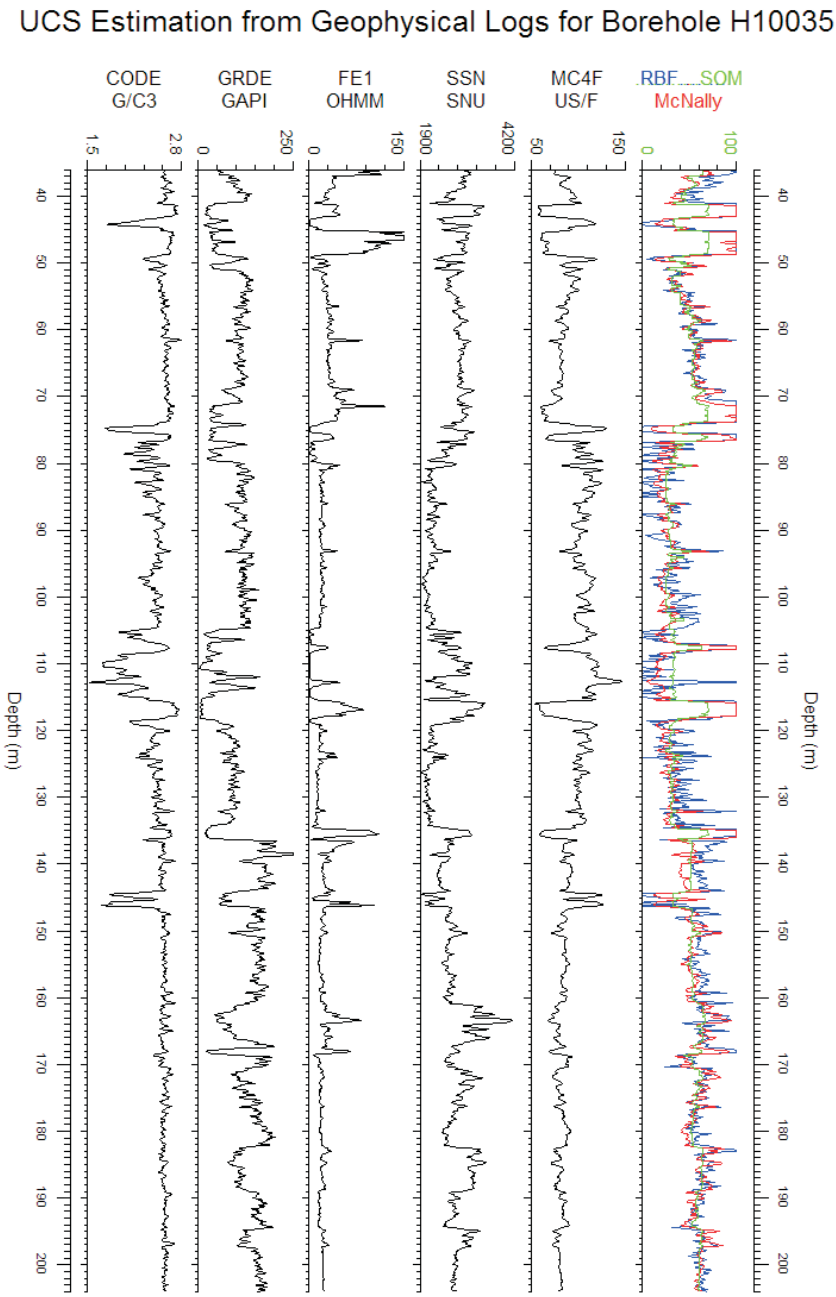

Figure 8: UCS estimation results using the McNally (red), SOM (green) and RBF (blue) method for the borehole H10035. The UCSs are in MPa.

derived from within the data set; and they are sufficiently robust to accommodate reasonable variation of the rock characteristics.

Table 4: The statistics of the estimated UCS compared with the measured UCS

Estimation method	Correlation Coefficient	Estimated UCS Relative Error[2] (%)		
		Minimum	Maximum	Average
McNally	0.62	0.65	157.140	28.90
SOM	0.65	2.51	172.85	26.19
RBF	0.72	0.08	78.73	25.19

The two new algorithms were demonstrated by both sonic log prediction and UCS estimation from geophysical logs. In the sonic prediction, we used the combination of conventional geophysical logs (not including the sonic logs) and SIROLOG spectral logs to predict the sonic logs. We compared the predicted sonic logs with the measured sonic logs from boreholes to demonstrate the appropriateness of our new methods for rock strength estimation.

The algorithms were applied to both controlled and independent boreholes; and good results were achieved in the prediction of sonic logs using both RBF and SOM algorithms from other geophysical logs. The predicted sonic logs were statistically well matched to the measured sonic

2 The relative error is calculated by (Predicted_UCS - Measured_UCS)/Measured_UCS*100.

logs. This correlation suggests that our methods for rock strength estimation from geophysical logs are viable.

Budgetary constraints limited the number of geotechnical measurements in our control data base. A cross-validation technique was used to verify both methods for rock strength estimation from geophysical logs. Both the SOM and RBF methods produced results similar to the popular McNally method. Similar UCS estimates were produced when these three methods were applied to the borehole H10035. From a correlation coefficient view-point, our new methods produce slightly better results than McNally's method.

However, this is expected as our methods were trained specifically for the 'local' test data set, while the coefficients for McNally's method were derived from the whole Bowen Basin. We do believe, however, that more representative control rock testing data will significantly improve the performance of our SOM and RBF techniques. This is demonstrated by the performances of both the sonic log prediction and UCS estimation: the performance is increased with the increased control data points and increased number of geophysical logs.

When we compare our sonic log predictions derived from the SIROLOG data with those from the conventional data, the conventional logging data produce better results than the SIROLOG logging data. For the RBF method, combining the conventional logging data with SIROLOG data increases the prediction accuracy and correlation with the measured sonic data. For the SOM method the best sonic predictions appear to result from using the conventional logging rather than the combined conventional and SIROLOG data. We note that the SIROLOG tools were not calibrated for the mineralogies present at the Newlands mine, and this may have had an adverse effect on the estimations.

However, using the SOM method on just the PGNAA data produces a reasonable estimate of the sonic log. This confirms that SIROLOG data overall can contribute to the performance of log prediction. We propose that the SIROLOG data should be more useful in complex geologic areas that exhibit wide ranging compositional variation in terms of grains and cements. It is in these areas that the ability of conventional geophysical logs should benefit from the compositional input available via the SIROLOG data. The inclusion of the quantitative SIROLOG log data into our RBF and SOM approaches, may also account for compositional variations in both grains and cements in the estimation procedure.

We believe that our RBF and SOM methodologies have particular potential above and beyond the McNally approach, or other conventional model-based approaches because they allow UCS predictions to be tailored (fine-tuned) for a particular mine site or environment. We envisage that an ideal operating scenario for a mine would be to collect and maintain a control data base of high-quality geotechnical (UCS etc) measurements and corresponding geophysical log parameters, covering most /all of the known local lithologies. This control data base could then be used in conjunction with routinely acquired geophysical logs to predict the geotechnical parameters such as UCS. Because these predicted measurements have been based on locally-acquired data, they should be more robust and matched to local conditions, than the more generic results such as those derived via the McNally method.

ACKNOWLEDGEMENTS

This project was funded by NEDO of Japan, and coordinated by Suncoh. The geophysical logs and related geological data were provided by Newlands Mine and Suncoh. The laboratory rock testing was performed by the CSIRO Rock Cutting and Drilling Technologies Group. Special thanks go to Michael Cunnington and Andrew Hughes who carried out the geotechnical measurements. Joe Clarry (Geoconsult), Ian Rose (Xstrata), Iain Miller (Geoconsult), Todd Harrington (Xstrata) and Brent Haines (consultant) are thanked for their assistance during data acquisition, logging and data provision to CSIRO.

REFERENCES

BILLINGS, S.D., BEATSON, R.K. & NEWSAMN, G.N. 2002: Interpolation of geophysical data using continuous global surfaces. *Geophysics*, **67**, 1810–1822.

BILLINGS, S.D., NEWSAMN, G.N. & BEATSON, R.K. 2002: Smooth fitting of geophysical data using continuous global surfaces. *Geophysics*, **67**, 1823–1834.

BORSARU, M., ROJC, A. & STEHLE, R., 2001: The application of the PGNAA technique to *in situ* analysis of coal. *Exploration and Mining Report 848C*.

BRIQUEU, L., GOTTLIB-ZEH, S., RAMADAN, M. & BRULHET, J., 2002: Traitement des disgraphies a l'aide d'un reseau de neurons du type «carte auto-organisatrice»: application a l'etude lithogique de la couche silteuse de Marcoule (Gard France). *C.R. Geoscience*, **334**(2002), 31–337.

COLÉOU, T., POUPON, M. & AZBEL, K., 2003: Unsupervised seismic facies classification: A review and comparison of techniques and implementation. *The Leading Edge*, **22**, 942–953.

ESSENREITER, R., KARRENBACH, M. & TREITEL, S., 2001: Identification and classification of multiple reflections with self-organizing maps. *Geophysical Prospecting*, **49**, 341–352.

GARCIA-BERRO, E., SANTIAGO TORRES, S. & ISERN, J., 2003: Using self-organizing maps to identify potential halo white dwarfs. *Neural Networks*, **16**(2003), 405–410.

HATHERLY, P.J., 2002: Rock strength assessment from geophysical logging: *8th International Symposium on Borehole Geophysics for Minerals, Geotechnical and Groundwater Applications*, Toronto, Ontario, 21–23 August.

HATHERLY, P., MEDHURST, T., ZHOU, B. & GUO, H., 2001: Geotechnical evaluation for mining — assessing rock mass

conditions using geophysical logging. *Final report ACARP Project C8022b*.

HATHERLY, P., SLIWA, R., TURNER, R. & MEDHURST, T., 2004: Quantitative geophysical log interpretation for rock mass characterisation. *Final report ACARP Project C11037*.

KASKI, S., KANGAS, J. & KOHONEN, T., 1998: Bibliography of Self-Organizing Map (SOM) Papers: 1981–1997. *Neural Computing Surveys*, **1**, 102–350. Available in electronic form at http://www.icsi.berkeley.edu/~jagota/NCS/.

KOHONEN, T., 2001: *Self-Organizing Maps: Third Extended Edition, Springer Series in Information Sciences*, **30**, Springer, Berlin, Heidelberg, New York, 1995, 1997, 2001.

LAWRENCE, W., 1999: Interpreting and understanding strata behaviour. *2nd Annual Longwall Mining Summit*, Yeppoon. AJM Conferences.

MACGREGOR, S., 2003: Maximising *in situ* stress measurement data from borehole breakout using acoustic scanner and wireline tools. *Final report ACARP Project C10009*.

McNALLY, G.H., 1987: Estimation of coal measures rock strength using sonic and neutron logs. *Geoexploration*, **24**, 381–396.

McNALLY, G.H., 1990: The prediction of geotechnical rock properties from sonic and neutron logs. *Exploration Geophysics*, **21**, 67–71.

OJA, M., KASKI, S. & KOHONEN, T., 2003: Bibliography of Self-Organizing Map (SOM) Papers: 1998-2001 Addendum. *Neural Computing Surveys*, **3**, 1–156. The papers are available in electronic form at http://www.soe.ucsc.edu/NCS/.

RONEN, S., SCHULTZ, P.S., HATTORI, M. & CORBETT, C., 1994: Seismic-guided estimation of log properties, Parts 1, 2, and 3. *The Leading Edge*, **13**, 305–310, 674–678, 770–776.

RUSSELL, B.H., LINES, L.R. & HAMPSON, D.P., 2003: Application of the radial basis function neural network to the prediction of log properties from seismic attributes. *Exploration Geophysics*, **34**, 15–23.

SCHÖN, J.H., 1996: *Physical properties of rocks: Fundamentals and principles of petrophysics*. Elsevier Science Ltd.

SLIWA, R., FRASER, S.J. & DICKSON, B.L., 2003: Application of self-organising maps to the recognition of specific lithologies from borehole geophysics. *In*, Hutton, A.C., Jones, B.G., Carr, P.F., Ackermann, B. & Switzer, A.D., (Editors) 2003: *Proceedings of the 35th Sydney Basin Symposium on "Advances in the study of the Sydney Basin"*, September 29-30, University of Wollongong, 105–113.

STRECKER, U. & UDEN, R., 2002: Data mining of poststack seismic attribute volumes using Kohonen self-organizing maps. *The Leading Edge*, **October 2002**, 1032–1037.

SURFER 7 USER'S GUIDE 1999. Golden Software, Inc.

WALTER, J., RITER, H. & SCHULTEN, K., 1990: Nonlinear prediction with self-organizing maps. *1990 IJCNN International Joint Conference on Neural Networks*, **1**, 589–594.

WARD, B., 1998: German Creek Mines Rock strength from velocity logs. Report for Capricorn Coal Management Pty Ltd.

B. Zhou, S. Fraser, M. Borsaru, R. Sliwa, CSIRO Exploration and Mining, PO Box 883, Kenmore, QLD 4069
T. Aizawa, T. Hashimoto, Suncoh Consultants Co. Limited, 1-8-9, Kameido, Koto-Ku, Tokyo, 136-8522, Japan

Troy Peters

The successful integration of 3D seismic into the mining process: Practical examples from Bowen Basin underground coal mines

This paper discusses how mine staff from a number of Bowen Basin coal mines have effectively and efficiently integrated 3D seismic information into their work practices. Comprehensive reconciliation procedures have evolved over the years to help understand how the 3D seismic data responds to particular geological conditions. High-resolution seismic imaging of fault structures has helped target borehole drilling for fault evaluation and grout pattern design. High density seam-roof elevation data extracted from seismic have been merged with borehole seam picks to assist with both in-seam gas drainage programs and the design of cutting profiles for production mining.

Stratigraphic interpretation of the 3D seismic data has contributed to the overall geological understanding of the mine area, and has contributed to predicting roof and floor conditions that impact mining operations. The full potential of the 3D seismic data has only been realised through the constant interaction of mine-planning staff and the seismic interpreters. Successful integration of 3D seismic data into the mine planning process requires the 3D seismic volume to be treated as a live commodity that is constantly evolving through the life of the mine.

INTRODUCTION

Acquisition of 3D seismic data has become a vital exploration tool for underground coal-mining operations. This is highlighted by the fact that a total of 45 3D seismic surveys designed to provide coal-mining staff with high resolution subsurface images and detailed fault delineation have been acquired in the Bowen and Sydney Basins since 1997. With this growth of 3D seismic comes the new challenge of effectively integrating large volumes of seismic data (and their derivatives) into mine planning and development. Little has been published on this subject, and to date individual coal-mine sites have endeavoured to determine their own methodologies to facilitate the successful integration of seismic data.

Drawing on the experiences of a number of mines in the Bowen Basin, this paper provides a summary of some of the more effective approaches for integrating seismic data with traditional mine planning and development information. Experience has shown that successful data integration is largely dependent on all mine staff having a strong understanding of the inherent advantages and limitations of the seismic method. Further, such information needs to be consistently included in all mine planning and development documents and discussions. When a mine makes the effort to effectively integrate seismic data into their mine planning and development, the mine is rewarded with significant technical and cost benefits.

3D SEISMIC

Seismic exploration is a geophysical method that involves imaging the sub-surface using artificially generated sound waves. Surface receiving devices, or geophones, are used to detect the seismic energy that originates from a seismic source (e.g. small dynamite explosion), travels down into the earth, and gets partially reflected back to the surface at geological boundaries. A 3D seismic survey involves using a grid of surface receivers to detect the reflected seismic energy generated by each seismic source in an exploration area, rather than using a single line of receivers (2D seismic). Figure 1 illustrates a typical source and receiver layout for a 3D seismic survey in the Bowen Basin.

The resultant volume of seismic data is a 3D representation of all geological boundaries in the survey area as a function of two-way reflection time. Seismic interpretation is the process of tracking significant geological boundaries (e.g. target coal seams) and producing two-way time (TWT) horizon surfaces. These TWT surfaces, together with the seismic volume itself, can be used to derive a number of secondary seismic attributes (TWT gradient, seismic amplitude, instantaneous frequency) to yield high-definition structural maps, locate stratigraphic anomalies and provide detailed fault information.

Such attribute maps, together with interpreted lineaments and other features can be imported into mine planning software packages. This is discussed in greater detail below. More complex seismic interpretation procedures, that involve full seismic waveform analysis and geological inversion, can also provide information on physical properties such as coal quality and rock type.

Note that, because a 3D seismic volume and the horizon picks that track any significant geological boundaries in the survey area are referenced to two-way reflection time, it is often difficult for mine geologists to integrate the actual seismic structural surfaces into mine planning packages. Provided sufficient geological control exists (e.g. borehole data), reliable time-to-depth conversion can be performed. The accuracy and dependence of seismic depth conversion

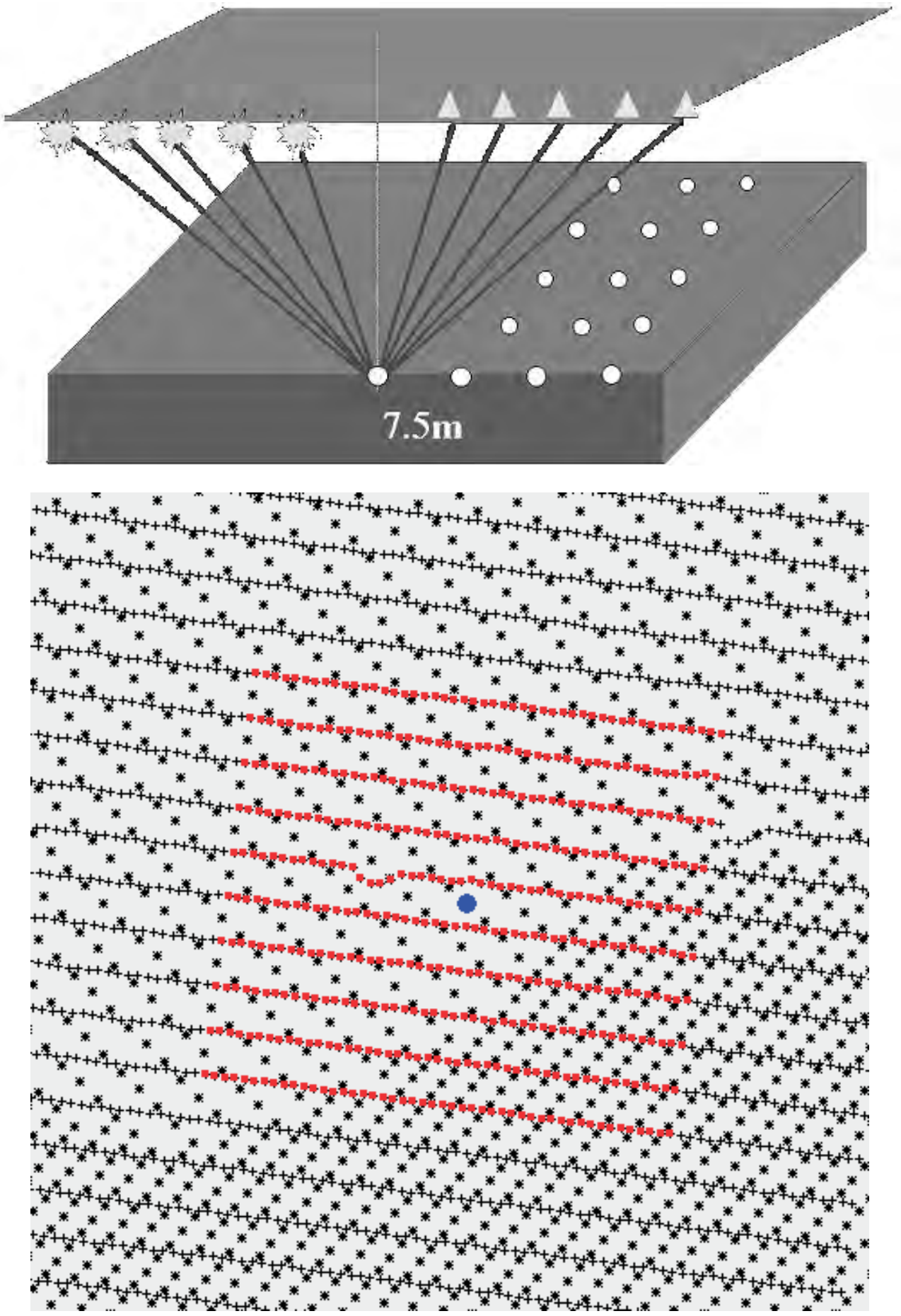

Figure 1: Typical 3D acquisition source and receiver layout. Top is the acquisition in section view and Bottom is in plan view Shots= *, Receivers= +

on geological control and mathematical gridding algorithms is examined in detail by Zhou & others (2004). Following the seismic depth conversion, there are a number of approaches resulting in the effective use of the elevation surfaces as discussed below.

Overall, interpretation of a 3D seismic volume results in vast quantities of spatial data (typically 18,000 sub-surface points of information per seismic attribute per square-kilometre). All of this information should be integrated into the mine planning and development process to maximise the benefit-to-cost ratio of undertaking a 3D seismic survey. Strategies for effectively achieving this are presented below.

Reconciliation

Reconciliation, as defined here, is the process of comparing the seismic interpretation results with hard geological data from either validation drilling or underground mine mapping. It can be thought of as a calibration process, allowing the mine to understand the advantages and limitations of the seismic method in characterising faults (predicting fault throw, location, orientation) and identifying stratigraphic anomalies. The reconciliation process helps reduce ambiguity in the seismic interpretation results.

Ambiguity exists because the physical process of sound waves travelling through the earth limits the vertical and lateral resolving power of the seismic data. This can result in the inability to distinguish a small fault from a seam roll, or impede the accurate imaging of a complex faulted zone. Reconciliation focuses on determining the accuracy of fault throws and location, by comparing structures interpreted from 3D seismic data with those intersected during mining operations. Typical fault throw and location errors are ±1.2m and ±11m, respectively.

From the surface, reconciliation of seismic fault information typically involves drilling 3 boreholes about an interpreted fault, and comparing borehole information with seismic data to assess the accuracy of the seismic image. Note that, using surface drilling to test the seismic derived structure can produce inconclusive results. If mine development is taking place, underground maps and seam elevation collected by the mine geologist are more reliable for conducting reconciliation.

Our experiences suggest that mines who most effectively integrated 3D seismic into their mine planning and development are those who are proactive about reconciliation, both through drilling and during underground mapping. In this way the mine staff and seismic interpreter are constantly learning what information the seismic volume can bring to the mine planning and development process. This continues to take place throughout the working life of the mine.

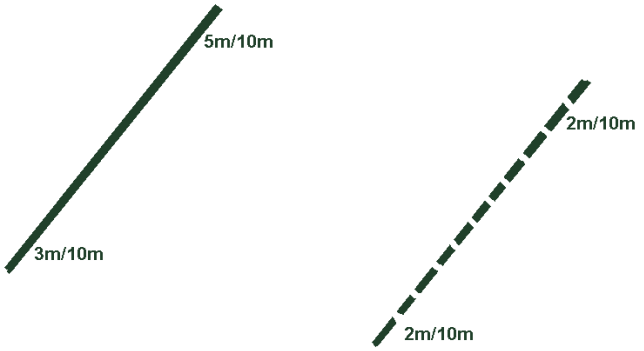

Figure 2a: Over simplified representation of fault information derived from the seismic data. Lines indicate fault position, the numbers which are annotated (e.g. 2m/10m) represent the throw and width in metres. Heavy Solid line = confident interpretation, Heavy dashed line = less confident

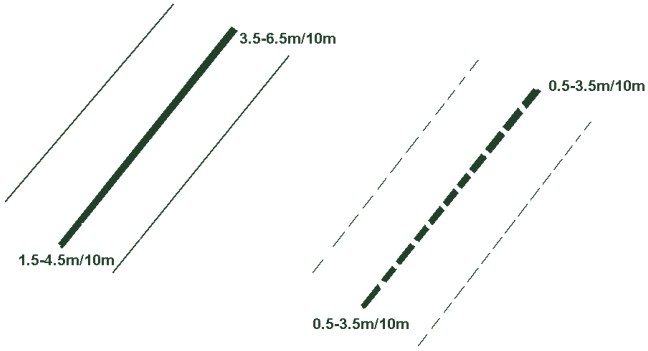

Figure 2b: A more effective way to represent fault information derived from seismic data. Secondary lines bound the fault centerline. The distance that these are offset from the fault centerline is regarded as the error in the spatial location (e.g. ±11m). In this case the fault throw is represented as a range of possible displacements rather than a single value. This range may be considered the error in the estimated displacement (e.g. 2m±1.2m).

Structural Information

Typically, accurate delineation of structure is the primary objective for a 3D seismic survey. Structural information derived from seismic data interpretation (e.g. fault throw & location) is delivered to the mine in ASCII or DXF format, which can be easily imported into most mine planning packages. Further, it is common that such interpreted structures are described with varying degrees of interpretation confidence (e.g. confident, less confident). While simply plotting these features onto mine plans conveys the basic seismic interpretation results, it is not using all available information effectively. As discussed above there is known ambiguity in seismic interpretation results. The mine planning team has to ensure that all mine-site staff understands the uncertainty in the seismic interpretation results by ensuring this information is included on all mine plans and team discussions.

Staff at one Bowen Basin mine-site have addressed this problem by incorporating secondary lines (representative of location error) and representing faults with a variable range of throws in their mine plans (Figure 2).

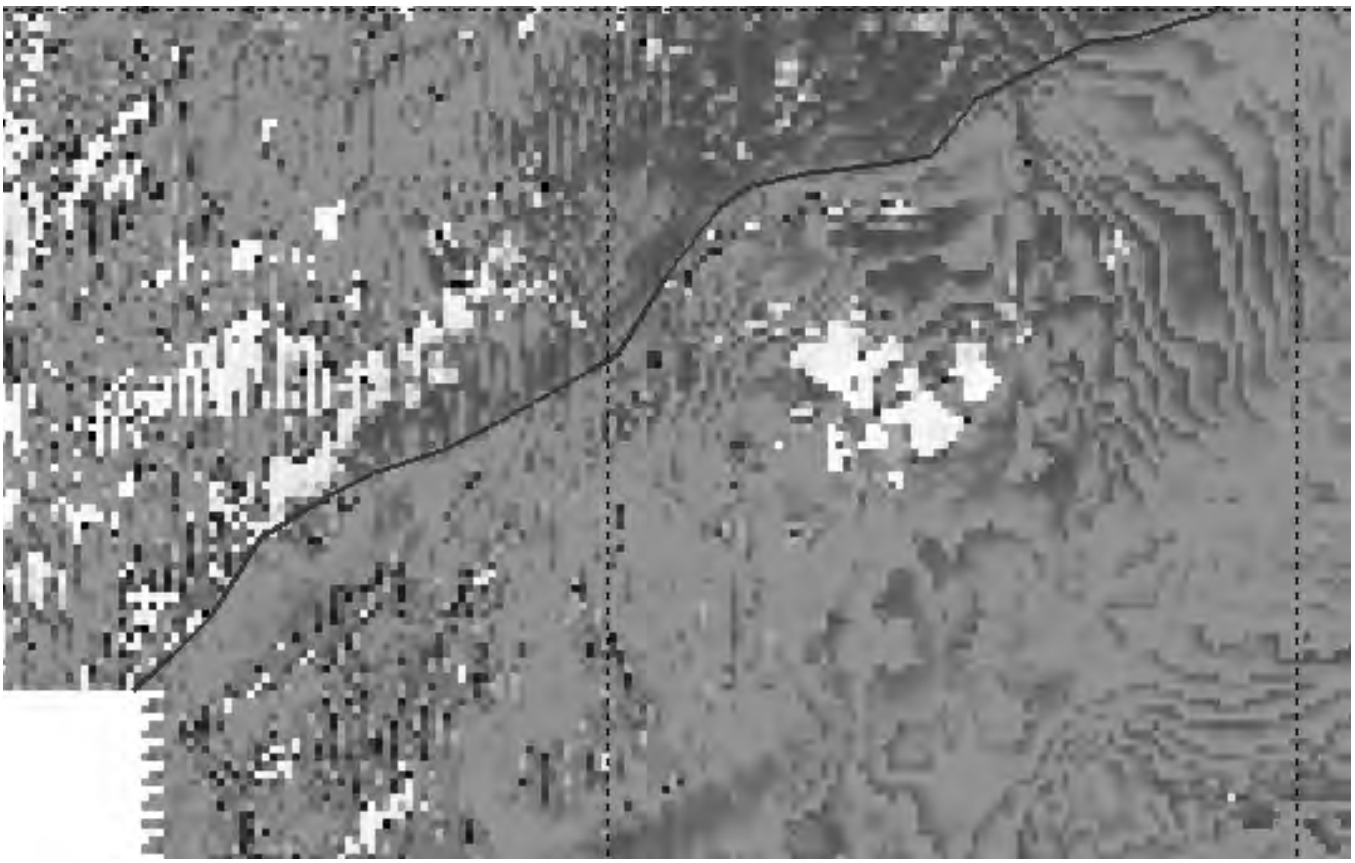

Figure 3: Instantaneous Frequency indicating seam split line. Line indicates interburden thickness or ~1.5m

As noted above these errors can be quantified through the process of reconciliation. Alternatively, draw on the experience of the seismic interpreter and adopt the suggested errors detailed in the technical report that accompanies the 3D interpretation results. Some attempt to convey errors of the interpreted results to the end-users, is better than nothing.

Stratigraphic Information

Recently there has been a growing desire to obtain more than just structural information from a 3D seismic volume. As noted above, there are complex seismic stratigraphic interpretation packages designed to recover information such as roof/floor rock properties, coal quality and gas content. However, here we will restrict our discussion to the type of stratigraphic information that is commonly presented to a mine as a result of conventional seismic interpretation methods.

Typically stratigraphic lineaments or zones will be delivered to the mine in ASCII or DXF format for incorporation into their mine planning software. As for fault information, the uncertainties in the absolute location of any stratigraphic anomaly should be marked on all maps that include the 3D seismic interpretation results. Additionally, there must be some supporting evidence of what the stratigraphic anomaly might be. Our experiences suggest that seam splitting and igneous intrusions (sills) are two of the most prevalent stratigraphic anomalies detected via conventional seismic interpretation. The following discussion is an example of how a mine might effectively incorporate a suspected seam-split seismic anomaly into their mine maps.

A stratigraphic anomaly (such as a seam split, or intrusive sill) will be detected by the seismic interpreter using a number of different seismic attribute maps (e.g. TWT gradient, seismic amplitude, instantaneous frequency). For the seam-split example being considered here, instantaneous frequency was a significantly useful seismic attribute (Figure 3). Mine geologists could correlate the seismic attribute anomaly with an expected seam split in the area.

However, reconciliation drilling was required to gain an understanding of what the anomaly represented in real physical terms. It was found that the anomaly actually marked the point at which the interburden thickness between the split and working section reached 1.5m. An effective way to present all the above information for mine-site staff is to import the ‘seismic split line’ into mine maps, but refer to it as the ‘1.5m interburden thickness line’. Further, importing the instantaneous frequency map and marking the zone over which the instantaneous frequency anomaly occurs, suggests to end-users that the ‘1.5m interburden thickness line’ has an inherent error in its lateral position.

If the rate at which the seam splits has geotechnical implications for the mine, further useful information could be extracted from the 3D seismic volume in the form of interburden thickness contours (coal ply to working seam thickness map) being overlaid onto the mine plan.

Depth Surfaces

Whilst elevation surfaces are highly valued by mine staff, it is important to keep in mind that absolute elevation derived

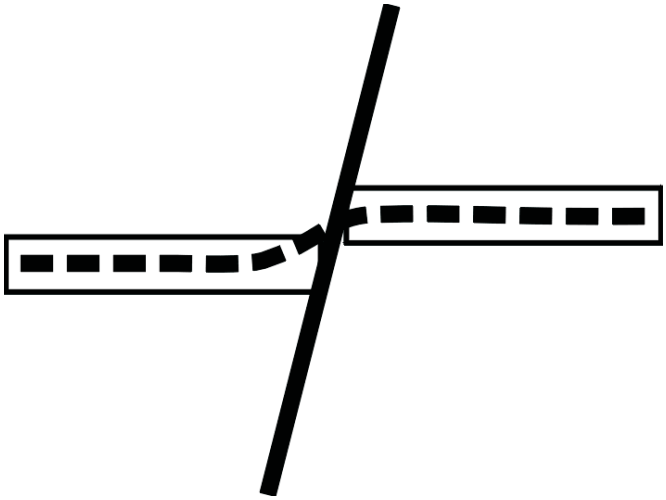

Figure 4: Example of how seismic derived depth information can be used by the mine. Flight plan indicating longwall cutting profile, Dashed line = representative long wall cutting height

from seismic can be erroneous. In contrast, experience suggests relative changes in seam elevation are quite reliable. These assumptions, however, should be tested by reconciliation prior to integrating the seismic-derived elevation into mine planning. Typically, this involves importing and comparing the seismic derived elevation data with both borehole seam picks and underground survey data.

Once the reliability of the elevation data is evaluated, the mine staff have a number of options for integrating the seismic data into their mine planning and development. Current examples include using seismic elevation data to assist with grout pattern design and flight plan design for longwall cutting profiles, and to guide inseam drilling for the purpose of gas drainage.

Figure 4 is an example of a flight plan designed to negotiate a structure with a full seam thickness throw. In this instance the seismic derived roof elevation data for the entire 3D survey area have been imported into the mine planning software. By subtracting the seam thickness (determined from boreholes) from the seismic roof elevation, a profile of the coal seam could be obtained for the entire mine area. This info was used to help plan longwall cutting profiles.

Note also, that if reconciliation determines that these elevation data are reliable, then coal seam structure maps may be used to directly derive estimates of fault throws.

CONCLUSION

A growing number of 3D seismic surveys are being acquired in conjunction with underground coal-mining operations. To maximise their benefit-cost-ratio, coal mines must ensure effective integration of this 3D seismic information into the mine planning and development process.

Mine staff should familiarise themselves with all data files that are produced from a 3D seismic interpretation project, and should have a basic understanding of the seismic method as well as working knowledge of the inherent advantages and limitations of 3D seismic. Many of these concepts are addressed in detail in the reports provided with the seismic interpretation results.

A proactive approach to reconciliation should be adopted. Information recovered from the reconciliation process, such as fault throw errors, lateral position errors or stratigraphic information, should always be included with the seismic interpretation results on any maps and/or presentations. Mines should also consider using seismic attribute maps directly in their mine-planning software to aid understanding of the strengths and weaknesses of the seismic interpretation results.

Mines must recognise that 3D seismic interpretation results are dynamic, and will need to be re-visited and updated as more geological information becomes available throughout the working life of the mine.

To date, mines will typically confine the use of 3D seismic interpretation results to two-dimensional space (i.e. plan view). However, 3D seismic data provides the opportunity to visualise 3D earth models. It is possible to combine fault, stratigraphic, seam elevation and borehole data into a 3D workspace, such that a mine planning team can immerse themselves in the 3D subsurface. We believe this will ultimately become the method of choice for successfully integrating 3D seismic into the mining process.

ACKNOWLEDGEMENTS

Experiences from a number of Bowen Basin mines have been used to compile this paper. The author would like to acknowledge all those mine staff who have supported and facilitated the use of seismic for improving their mine planning and development process.

REFERENCES

ZHOU, B., HATHERLY, P. & SLIWA, R., 2004: Integration of Seismic for Mine Planning. *ACARP Project C11038 Report.*

T. Peters, Velseis Pty Ltd, tpeters@velseis.com.au

Peter Hatherly, Binzhong Zhou and Greg Poole

Borehole controlled seismic depth conversion for coal mine planning

While there is a well established role for seismic surveying in mapping coal seam structures, seismic data may not be reliable for depth and dip determinations because velocities are needed in order to convert seismic reflection times to depth. In this paper we present a method of establishing velocities by tying the seismic data to the large number of depth control points available at boreholes, in mine workings and from in-seam drilling.

Once converted to depth, the seismic data can make further significant contributions to exploration and mine planning activities. Structure contour plans can be established with much greater accuracy, interbeds will be placed in their true spatial positions and fault attributes can be better estimated. Mining and the need for further drilling can be planned with greater efficiency.

For 3D seismic data, the method is comparatively straightforward, provided the control data are within the region of the 3D survey. For 2D seismic data, extrapolation of the seismic data to include off-line boreholes is required. The mis-ties that invariably arise at the intersections of 2D lines must also be treated.

We demonstrate the depth conversion process using 3D seismic data from Xstrata's Oaky Creek Mine and 2D seismic reflection data from the BHP Billiton Illawarra Coal exploration areas.

INTRODUCTION

Normal practice for seismic reflection surveying is to present the results in the time domain whereby coal seam levels are displayed in terms of the two-way reflection time from a datum close to the ground surface. To convert the times to depth, knowledge is required of the seismic velocities down to the reflectors of interest.

In principle, the velocities derived during seismic processing can be used to estimate the depth of seismic reflectors (e.g. Blackburn, 1980). These velocities come from the static corrections where velocities above and below the weathering are needed, from datum corrections, and from normal moveout corrections. The velocities used for normal moveout (NMO) corrections compensate for the offset between each shot point and each geophone and the slanting of the travel path followed by the seismic waves between the shot point, the reflectors and the geophone.

Depth conversion using NMO velocities, however, is not fully successful because seismic waves are refracted as they pass through the various layers and the NMO velocity determinations may not properly account for this. Anisotropy also causes a difference in velocity between horizontal and vertical directions which distorts NMO velocities.

For such reasons, alternative approaches to determining velocities for depth conversion are also employed. These include using sonic logs and data from shots deep within a borehole and the ground surface. Unfortunately there are also problems with these approaches because the frequency dependent dispersion that occurs with seismic waves leads to different (higher) velocities being measured by sonic logs and in the case of the well shooting, there can be logistical difficulties in obtaining the seismic measurements.

With seismic surveying undertaken for petroleum exploration, the issues of velocity estimation and depth conversion therefore remain problematic. For coal mining, however, it is possible to provide an alternative approach to velocity estimation based on establishing ties between the processed seismic data and the many boreholes that are typically available. This enables accurate depth conversion for the typical coal mining situation.

In this paper we describe and illustrate our approach to seismic depth conversion. The process is simpler for three dimensional (3D) seismic data sets because the seismic data are internally consistent and there will always be a seismic trace at any borehole location within the volume of 3D seismic data. The 3D process is described in Zhou & others (2004) but it has now been extended to allow depth conversion of two-dimensional (2D) seismic data. For 2D data we have needed to address the problems of mis-ties at the intersection of lines and the extrapolation of seismic data to boreholes that are off-line.

DEPTH CONVERSION

For 3D seismic data, the method involves the following steps:

- Select and identify the control horizons on the seismic section (normally the coal seams) and establish the reflection times of those horizons for the whole seismic volume;
- Match the reflection times for the control horizons with known depths at all available boreholes;
- Derive depth conversion velocities for each horizon at each borehole;

- Laterally extend the depth conversion velocities for each horizon from the boreholes to every seismic trace by using a suitable 2D interpolation method. This establishes continuously variable depth conversion velocities for each horizon;
- Between the control horizons compute a depth conversion velocity at each seismic time sample for each trace by 1D linear interpolation;
- Convert each time trace to a depth trace and resample it at an appropriate sampling rate. The end result is seismic trace data rescaled to depth.
- For 2D seismic data, the same procedure is applied but the additional steps are required to treat differences in datum, to handle mis-ties and to include boreholes that are off-line.
- Reduce all lines to the same datum and pick the reflectors;
- Determine the mis-tie times at all line intersections and apply the iterative least squares method described of Bishop & Nunns (1994) to establish a bulk constant mis-tie correction time for each line. This removes the most significant part of the error;
- Correct any residual time mis-ties at the intersections by an amount weighted by the inverse of the total number of intersection points on each line (i.e. the residual is mainly taken up by the line with the least number of intersections). Between intersection points, adjust each line by linearly interpolating the corrections at the intersection points;
- Extrapolate the reflection times of the target horizons to the borehole locations. Compute depth conversion velocities at the boreholes and then extrapolate the velocities back to the seismic lines to establish depth conversion velocities at all of the seismic traces. Convert the seismic traces to the depth domain.
- For both 2D and 3D seismic data, this method creates depth converted seismic sections for the full seismic sections. Depths to the control horizons will be exact at the boreholes. Elsewhere, the accuracy will depend upon the extent to which the true seismic velocity varies from the interpolated values.
- Example 1 - 2D data

BHP Billiton Illawarra Coal undertakes extensive seismic reflection surveys as part of their exploration activities in the Southern Coalfield of NSW (Poole & others, 2003). Since 1997 much of their exploration has focussed on the needs for West Cliff, Appin and Douglas Collieries. Using their own acquisition equipment and field crew, BHP Billiton have acquired over 120 lines of 2D seismic data in this area, with an additional seven 3D seismic surveys shot since 2004 when a new 800 channel Vibtech seismic system was purchased.

Figures 1 and 2 show results for an area of 4km^2 from within BHP Billiton's lease areas where 2D seismic lines have been shot, mainly with northerly and east-north-easterly orientations. Figure 2 shows the 2D seismic section for the line highlighted in red in Figure 1. The Bulli Seam is the working seam and is readily identified at the top of the strong reflection package with a two-way time of about 0.33 seconds. The locations of the exploration boreholes providing Bulli Seam depth control are denoted by the in-filled dots in Figure 1. Most boreholes lie on the seismic lines but some are off-line.

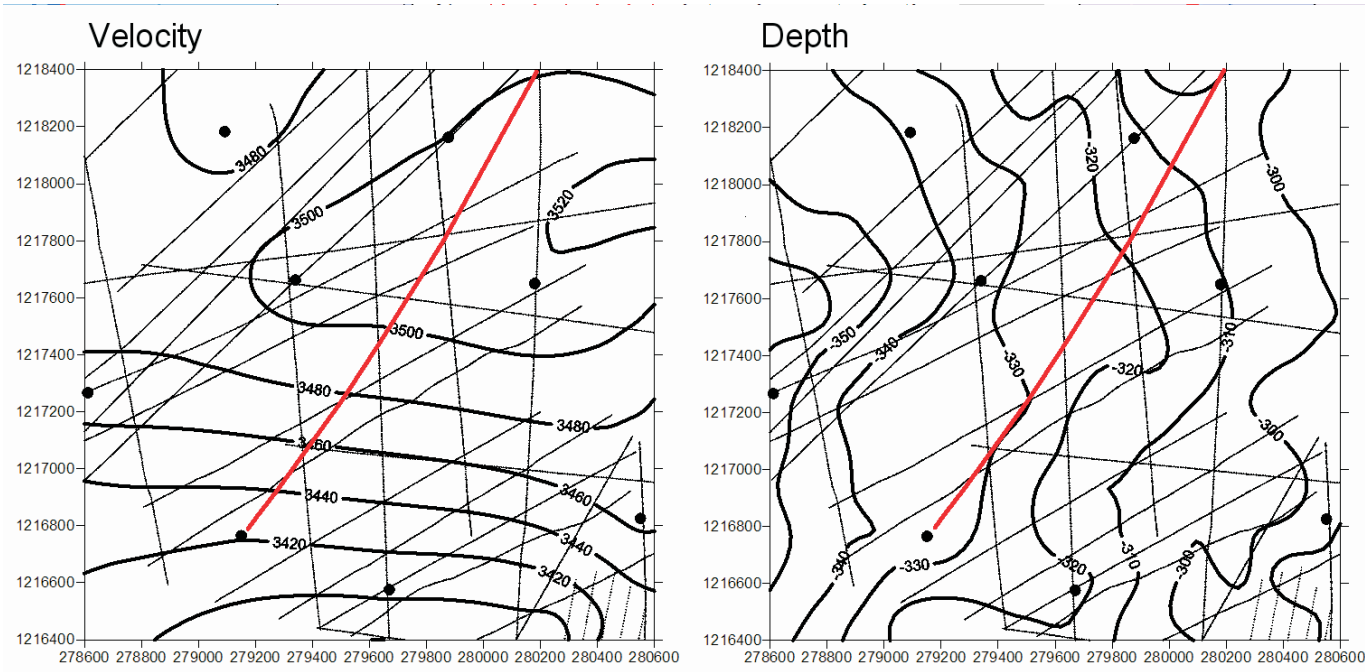

Figure 1: An example taken from the Appin/West Cliff/Douglas exploration areas. The straight lines denote the 2D seismic lines. In-filled dots denote borehole locations. The contours on the left are the depth conversion velocities required to tie the Bulli Seam reflection times to borehole depths. The contours on the right are the elevation of the Bulli Seam (below sea level).

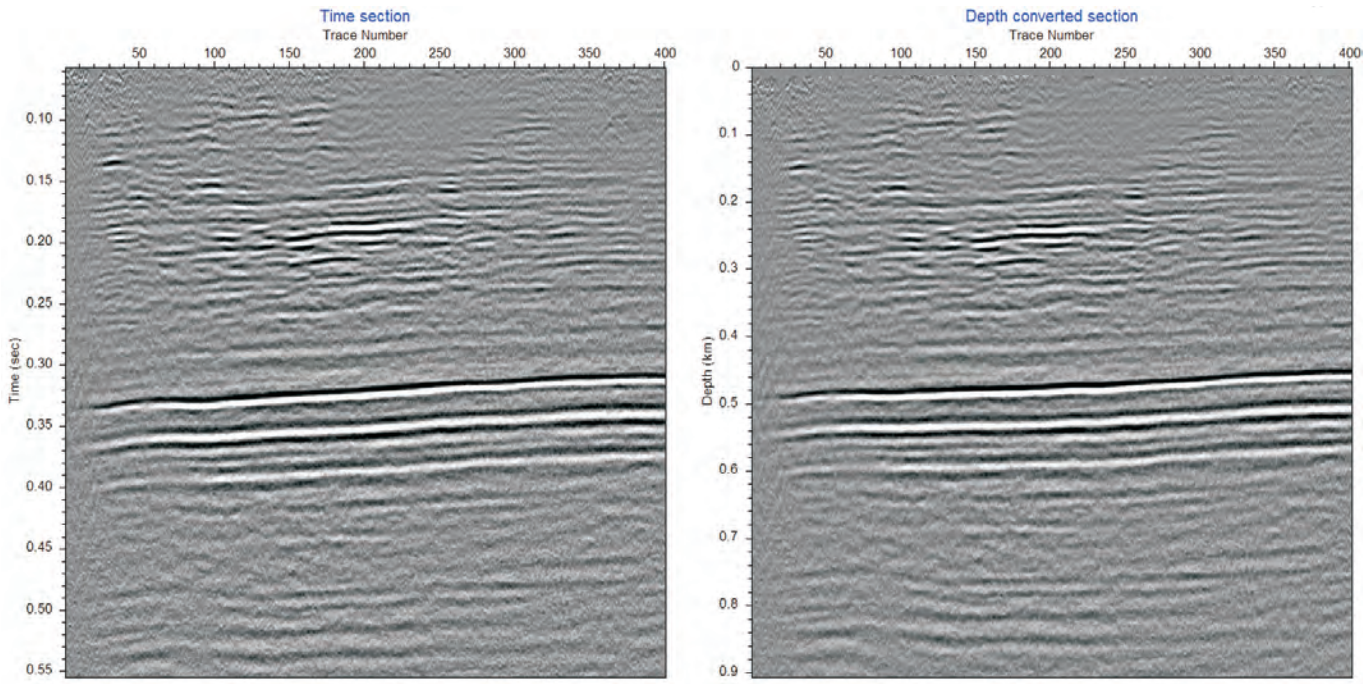

Figure 2: 2D seismic sections for the line shown in red in Figure 1. To the left is the reflection time section, to the right is the depth converted section. The Bulli Seam is the reflector at ~0.33 secs. In this case, the structure of the time section is largely unchanged by the depth conversion.

The first stage in the depth conversion process was to apply bulk shifts to the 2D lines processed to a different datum to that chosen for the depth conversion. Next, the Bulli Seam reflections were picked and used as a basis for the mis-tie corrections.

Once the mis-ties were corrected and data consistency was established, depth conversion velocities were found at each of the borehole intersections. For the boreholes on the lines, the velocities were determined from the reflection times for the traces at the boreholes. For boreholes off the line, seismic times at the boreholes were estimated using geostatistical means. In turn, these same geostatistical means were used to determine depth conversion velocities for the entire region. Depth conversion velocities determined for this area are shown in Figure 1.

For the final stage of the depth conversion, the appropriate depth conversion velocities were applied to each seismic trace. This created depth converted traces from which the depth of the Bulli Seam below datum could be established along all lines. These depths can be combined with the borehole data to provide estimates of seam depth throughout the area. Also shown in Figure 1 are the integrated depth data for this area.

EXAMPLE 2 3D DATA

Depth conversion for discrete 3D data sets is a simpler process because there is no need to the consider the mis-tie corrections present in 2D data. Provided the control boreholes are within the survey area, there is also no need to extrapolate away from the seismic lines to establish reflection times and depth conversion velocities at the boreholes. The application of the depth conversion process on 3D data is illustrated in Figures 3 to 6. This also illustrates another powerful aspect of depth conversion - the removal of potentially misleading time shifts introduced during processing.

The example is taken from Zhou, Hatherly & Sliwa (2004) and shows results for the Sandy Creek 3D seismic survey at Xstrata Oaky Creek Mine in Central Queensland. Figure 3 shows the survey area and the location of the boreholes available for depth control.

For evaluation and control purposes, Xstrata had the seismic data processed by two processing companies. Results for a 2D line cut out of the 3D volume are shown in Figure 4. The same fault structures and major reflecting horizons can be seen on both sections and the German Creek Seam, the Tieri 1 Seam and the Aquila Seam have been picked. However, there are differences between the two sections. The top section is less noisy and does not show the same broad synclinal structure centred at station 350 present in the bottom section. The amount of noise in these sections is likely to be due to differences in the frequency bandwidth and coherency filters used by the processing companies and is not an issue for this paper. However the synclinal structure is of interest because it is probably due to differences in the static corrections and choice of seismic velocities for statics and normal moveout corrections. This is the type of misleading feature that our depth conversion process should be able to resolve.

The locations of the boreholes on this seismic section are indicated in Figure 4. In Figure 5, the velocities required to

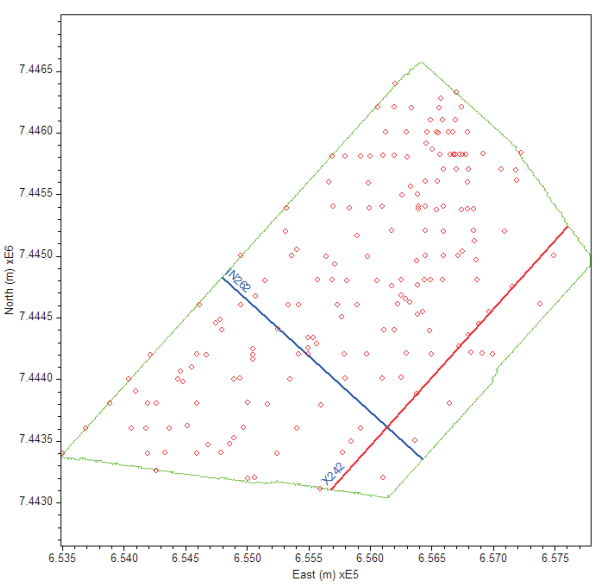

Figure 3: Plan view of a 3D seismic survey undertaken at Sandy Creek. Open circles denote borehole locations. Red and blue lines show locations of 2D seismic sections cut out of the volume. (From Zhou, Hatherly & Sliwa 2004).

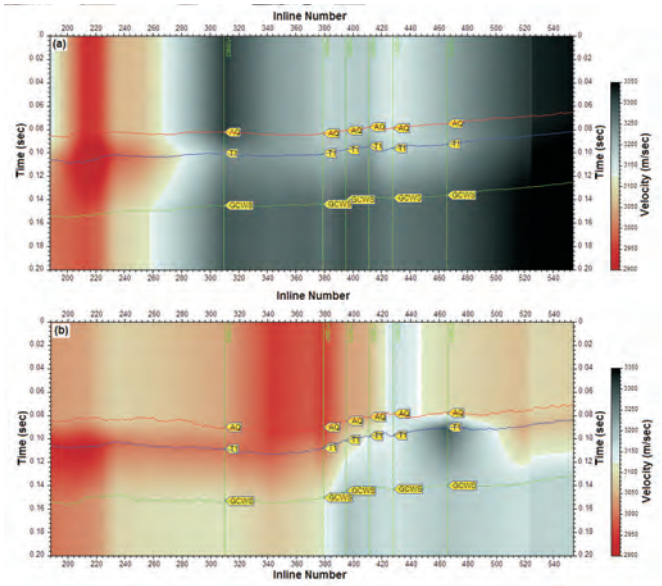

Figure 5: The velocities required to tie reflection times to the depths to the German Creek, Tieri 1 and Aquila Seams for the two seismic sections in Figure 4. (From Zhou, Hatherly & Sliwa 2004).

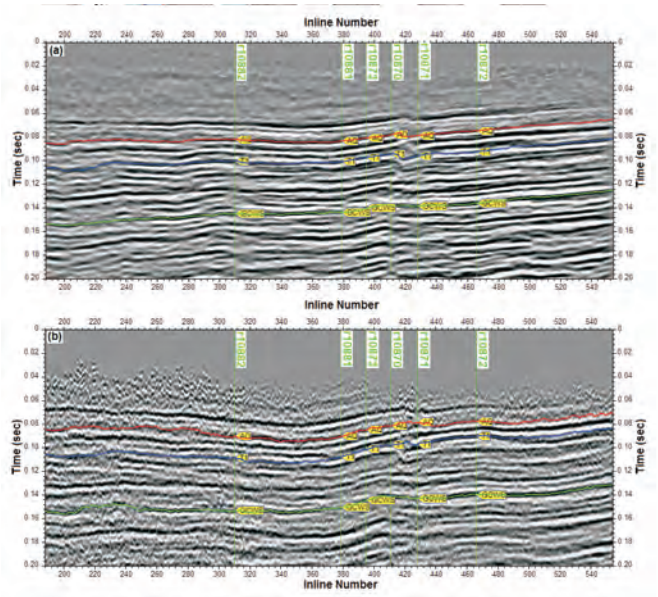

Figure 4: The 2D seismic section for cross line 242 (see Figure 3) produced by two processing companies. Three seams have been picked – the German Creek (green), the Tieri 1 (blue) and the Aquila (red). Locations of boreholes on or near this section are shown in green. (From Zhou, Hatherly & Sliwa 2004).

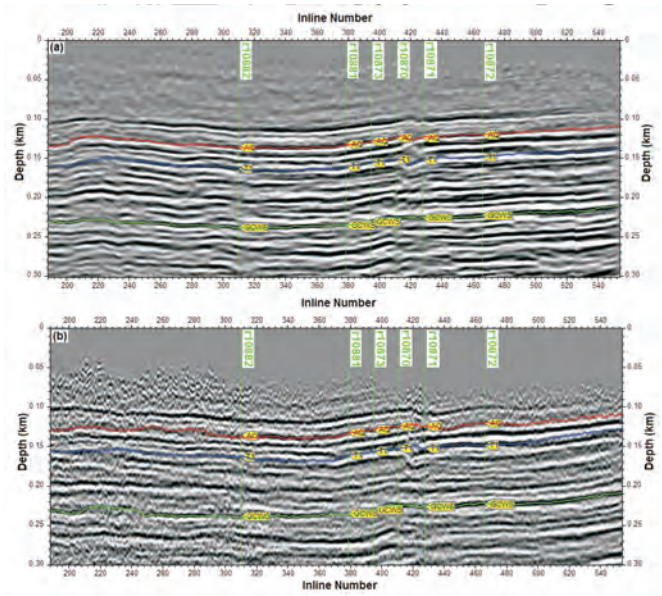

Figure 6: Depth converted seismic sections for the seismic time sections shown in Figure 4. The coal seam structures are now almost identical. (From Zhou, Hatherly & Sliwa 2004).

produce ties for the three seams at the boreholes are shown. As expected, different velocities are required for the two different sections but when these are converted to depth using the appropriate depth conversion velocities, Figure 6, the overall structure of the sections is identical.

The differences in noise remains but the synclinal structure in the lower time section of Figure 4 has been removed. Clearly it was a feature in the seismic data that was not supported by the drilling results.

DISCUSSION

We have implemented the depth conversion process through our SeisWin software for seismic interpretation (Zhou & others, 2004) and the calculations take only a few minutes on a personal computer. Given this, the depth conversion can be updated every time new boreholes and seismic lines become available.

Table 1: Statistics for the depth errors between seismic derived depths and the underground survey points for the roof of German Creek Seam.

Depth Errors	Number of Points	Percentage
≤1 m	79	71%
1–2 m	22	20%
2–3 m	7	6%
>3 m	3	3%
Minimum Depth Error	0.01m	
Maximum Depth Error	3.99m	
Absolute average depth error	0.81	

The process can also be applied to hybrid 2D and 3D seismic data sets. As indicated above, BHP Billiton has shot 3D surveys as well as a large number of 2D in their exploration area. By treating a 3D survey as a 2D survey with closely spaced lines folding back and forwards, 3D data can be introduced into a 2D data set. Because the mis-tie process can become unwieldy if there are 2D lines crossing a 3D area, we allow the choice as to which lines to utilise and whether to stage their introduction into the process.

The accuracy of the depth conversion process depends on the circumstances of each individual survey the quality and amount of seismic data, the geological complexity and the amount of depth control data from drill holes. With the Sandy Creek 3D seismic survey, it has been possible to investigate its accuracy because a NE trending longwall panel has been mined to the NW of the survey area. From those workings, depths from 111 survey points were available. The results of a comparison of the seismic and underground data are summarised in Table 1. At most points the seismic depths were within 1 m of the underground data. We also found that the larger of the depth errors tended to occur in the vicinity of faults where there was ambiguity on where to pick the reflecting horizon and where seismic resolution is generally reduced.

The large number of boreholes available at Sandy Creek also allowed analysis as to how many boreholes are required to enable satisfactory depth conversion. As drilled, the average borehole spacing over this survey area is ~200 m. By incorporating fewer boreholes in the depth conversion and using cross-validation techniques to investigate the depth errors at the unused boreholes, we found that if the borehole spacing were reduced to an average spacing of 800 m (i.e. a quarter of the amount of drilling), the depth errors for 71% of the boreholes remained better than 2.5m. Such a finding suggests that provided a seismic survey resolves the structures, and provided the seams and interburdens are adequately sampled for coal quality and geotechnical purposes, analysis of the depth errors in the seismic data can be used to indicate how much further drilling is required to provide adequate depth data for mine planning.

Depth conversion velocities can also carry geological information. For example, the greater the velocity, the greater should be the rock strength. However, consideration needs to be made of the other reasons for velocity to change. In particular, changes in velocity may also be due to changes in depth and as illustrated by the Sandy Creek example, the choice of processing parameters.

CONCLUSIONS

By converting seismic sections to depth, seismic data can make a more powerful contribution to coal exploration and mine planning. The effects of variable velocity on time sections are largely removed, be they due to changes in the geology or due to the choice of velocities in various processing steps. Overall coal seam structures will be accurately depicted by the seismic data and improved structure contours are possible.

The method we have developed uses exploration boreholes to provide tie points. This information is normally abundant for seismic surveying in coal mining areas. The method can be implemented on a personal computer and can be repeated every time new boreholes or seismic data become available. Critical evaluation of the depth converted seismic results can enable better and more cost effective drilling programs to be developed.

ACKNOWLEDGEMENTS

The Sandy Creek 3D data were originally presented in Zhou, Hatherly & Sliwa (2004). The support of ACARP and CRC Mining for this work is acknowledged as is the contribution of the processed data by Gary Fallon, formerly of Xstrata. The results shown in Figures 1 and 2 are from the geological exploration program undertaken by BHP Billiton Illawarra Coal.

REFERENCES

BISHOP, T.N. & NUNNS, A.G., 1994: Correcting amplitude, time, and phase mis-ties in seismic data: *Geophysics*, **59**, 946-953.

BLACKBURN, G., 1980: Errors in stacking velocity true velocity conversion over complex geologic situations: *Geophysics*, **45**, 1465-1488.

POOLE, G., DOYLE, J., RILEY, P. & HASELDEN, R., 2003: Exploration in the Southern Sydney Basin Coalfields: *Proceedings of the 35th Sydney Basin Symposium on Advances in the Study of the Sydney Basin*, Wollongong, 29-39 September, 215-222.

ZHOU, B., HATHERLY, P.J. & SLIWA, R., 2004: Integration of seismic data for mine planning: *Final Report ACARP Project C11038*.

P. Hatherly, CRC Mining/School of Geosciences, University of Sydney, NSW 2006, phatherly@geosci.usyd.edu.au
B. Zhou, CRC Mining/CSIRO Exploration and Mining, PO Box 883, Kenmore, QLD 4069, Binzhong.Zhou@csiro.au
G. Poole, BHP Billiton Illawarra Coal, PO Box 514, Unanderra NSW 2526, Greg.R.Poole@BHPBilliton.com

Peter Hatherly and Binzhong Zhou

Uncertainty: examples from seismic imaging and Iraq

Seismic surveying is one of key exploration methods available to the Australian coal mining industry. In some instances, unfortunately, the use of the technique has been marred by concerns over interpretations that sometimes suggest structures that do not exist and an apparent inability to map all faults that it should. In our view, this is all to do with the inability to manage uncertainty rather than a problem with the method. All exploration methods have uncertainties attached to them and it is our task as geologists, geophysicists and engineers, to understand the reasons for the uncertainties and to devise strategies to reduce the risk attached to them. In this paper, we discuss and illustrate the main causes of uncertainty in seismic surveying. The causes and management of these have many parallels to the well known search for weapons of mass destruction and justification for the war in Iraq. Just as it behoves governments to properly understand the intelligence that is provided to them, so too must mining companies. Uncertainty is a reality. Success depends on its management.

INTRODUCTION

"Without a measureless and perpetual uncertainty, the drama of human life would be destroyed", so said Winston Churchill. We are not sure that a mine manager struggling to take a longwall through a fault zone would agree with the sentiments of this quote. To him it is all about a bit less drama and as much certainty as possible. However to continue the quotations, according to poet Robert Burns, *"There is no such uncertainty as a sure thing"*, and from author Mark Twain, *"Education is the path from cocky ignorance to miserable uncertainty"*.

Figure 1 Satellite image interpreted to show activities at an Iraqi chemical facility (http://www. gwu.edu/~nsarchiv/NSA Hlt103744176EBM 1 BB/ nsaebb88/iq16.jpg accessed 9/5/2005)

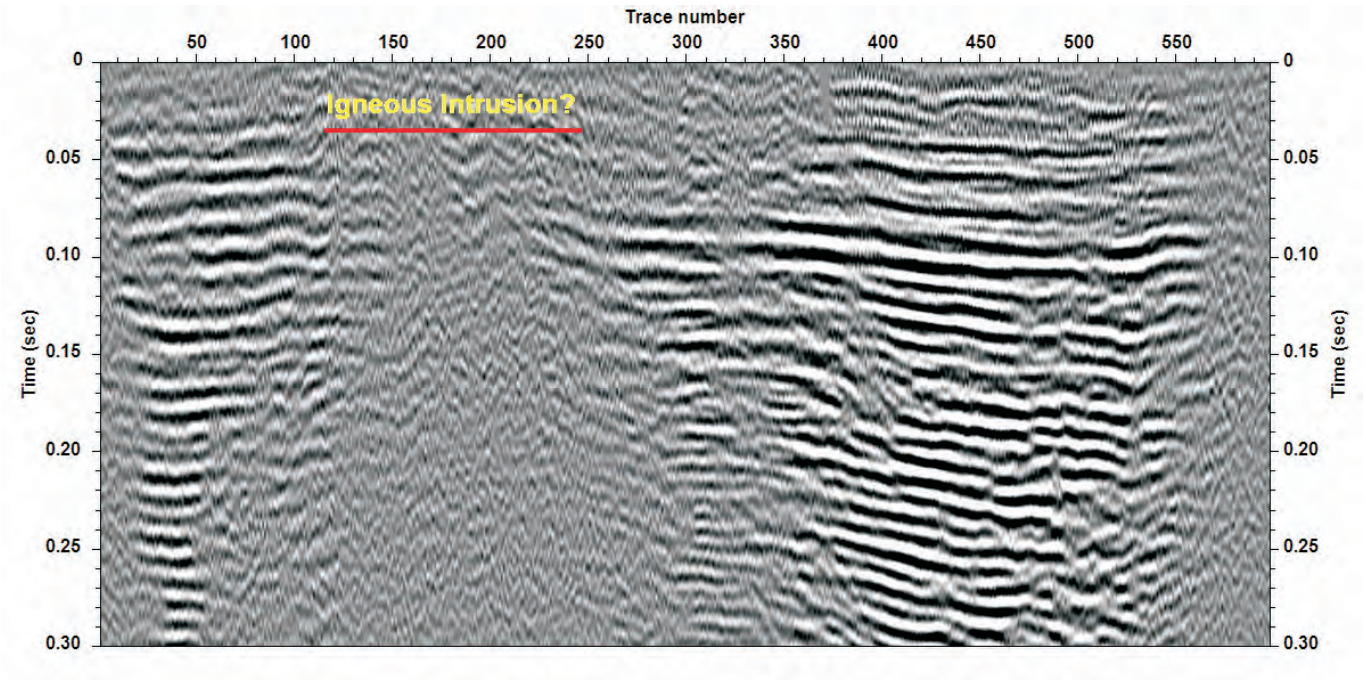

Figure 2: A 2D seismic section from the Sydney Basin showing a possible igneous intrusion

So what is uncertainty all about? On the one hand, we can accept that there is no such thing as total certainty, but on the other, we strive to manage our affairs in predictable and ordered manner, and in our quest to provide some level of certainty to our lives. This is also the case for the geological exploration in coal mining. We know that geological conditions will never be totally known in advance of mining but for productive and safe mining operations, it is our jobs to determine the geological conditions to the best of our ability.

After drilling, seismic reflection surveying is probably the next most important geological exploration tool for underground mining. In conditions well suited to seismic surveying, the technique can deliver 2D and 3D images of the subsurface superior to any other exploration techniques. However, there can be conditions, such as those associated with thick Tertiary overburden and multiple-seams, that are not always suited to seismic surveying.

Furthermore, regardless of data quality, it is a given that mine planners will want to push the seismic data to the limits of its resolution and our ability to interpret the results. In all situations, it is therefore to be expected that there will be some degree of uncertainty associated with seismic results. Quite possibly wrong interpretations will be made from seismic data and features that should have been detected will be missed.

In a sense, this situation is no different to the uncertainty associated with a drilling program but because seismic attempts to provide images and to take the data into the second and third dimensions, the issues of uncertainty are not so well accepted. It is our intention in this paper to discuss the issues of uncertainty in seismic interpretation and to propose a framework by which these should be managed.

UNCERTAINTY AND THE WEAPONS OF MASS DESTRUCTION

Without trivialising the issues surrounding the current Iraq war, the efforts of the coalition partners to mount the war partly on the basis of satellite images interpreted to show chemical weapons facilities and missile sites, provides a topical analogy to the issues of seismic uncertainty and the way it should be managed. Figure 1 shows examples of images, interpreted to show irrefutable evidence of the existence of these facilities.

Perhaps it will be one of the lessons of history that uncertainty and ways of reducing it will be factored into the future assessment and use of such images by our political leaders. In the same sense, how should the uncertainty and ways of reducing it be factored into the use of seismic data by geologists and mine planners? For example, what is the significance of the zone of poor reflections in Figure 2? Igneous intrusions are known to exist in this area. Should this zone carry a label stating ‘intrusion’?

To help answer this, consider the issues shown in Table 1. There we attempt to extend the analogy between the issues contributing to seismic uncertainty and their management and the issues contributing to uncertainty in the detection of the weapons of mass destruction and the management of them.

In the table we identify 5 key steps. The first three are mainly concerned with the decision to employ the techniques and their actual deployment.

There are some fundamental elements of uncertainty attached to the techniques that need to be considered. By the end of the third stage, input is required from other sources which

Table 1: Comparison of the issues of uncertainty and management between seismic exploration and the search for weapons of mass destruction

Steps	Seismic exploration	Imagery for weapons of mass destruction		
	Issues & procedures	**Additional aspects**	**Issues & procedures**	**Additional aspects**
1. Data capture	Geological models	- Past & additional knowledge	Intelligence reports	- Past & additional knowledge
	Seismic survey	- Survey design, - Site specific geological and land use issues, - Data processing	Capture satellite images	- Radar, IR etc., - Topography, land use and vegetation, - Image processing
2. Resolution	Seismic frequency range	-Thin beds, - Dykes, - Fault throws, - Fresnel zone	Image resolution	- Limits of current technology
	Signal to noise ratio	- Clarity of image, - Ultimate penetration	Signal to noise ratio	- Clarity of image
3. Identification	What is it?	- Experience, - Knowledge of procedures, - Intuition, - Input from other sources	What is it?	- Experience, - Knowledge of procedures, - Intuition, - Input from other sources
4. Significance	Past history		Past history	
	Potential impact on mine		Potential impact on global peace	
	Risk assessment		Risk assessment	
5. Decisions	Validation	- Follow-up investigations	Validation	- Follow-up investigations
	Vested interests		Vested interests	
	Management commitment	- Change in manager or owner?	Management commitment	- Change in government?
	Economic factors		Economic factors	
	Final decisions	- Mine?	Final decisions	- Invade?

can add to the interpretation. This then leads to the final stages where the significance of the interpretation needs to be considered and the decisions made on how to act on it.

Again, without trivialising the issues, some of the inputs to these final stages may be influences that do not rely on the facts as they best can be ascertained by the geologist or the intelligence analyst. The existence of these are a fact of life and can be changed.

However, it is the responsibility of the geologist and the intelligence analyst to ensure that there is as much certainty attached to an interpretation as possible. To achieve this, input from all data sources, thorough knowledge of the limitations of the data, risk assessment and validation programs are key activities.

SOURCES OF UNCERTAINTY IN SEISMIC DATA

The use of the seismic method requires the application of three complex and interrelated processes: data acquisition, processing and interpretation. Unfortunately different groups of people tend to get involved in these various stages and uncertainty in the outputs of any of them can have a significant impact on later stages and the final results.

The processing stage probably has the greatest scope for variation because modern processing packages allow considerable freedom in the selection of processing algorithms and parameters. For any seismic survey, it is most unlikely that different data processing staff will

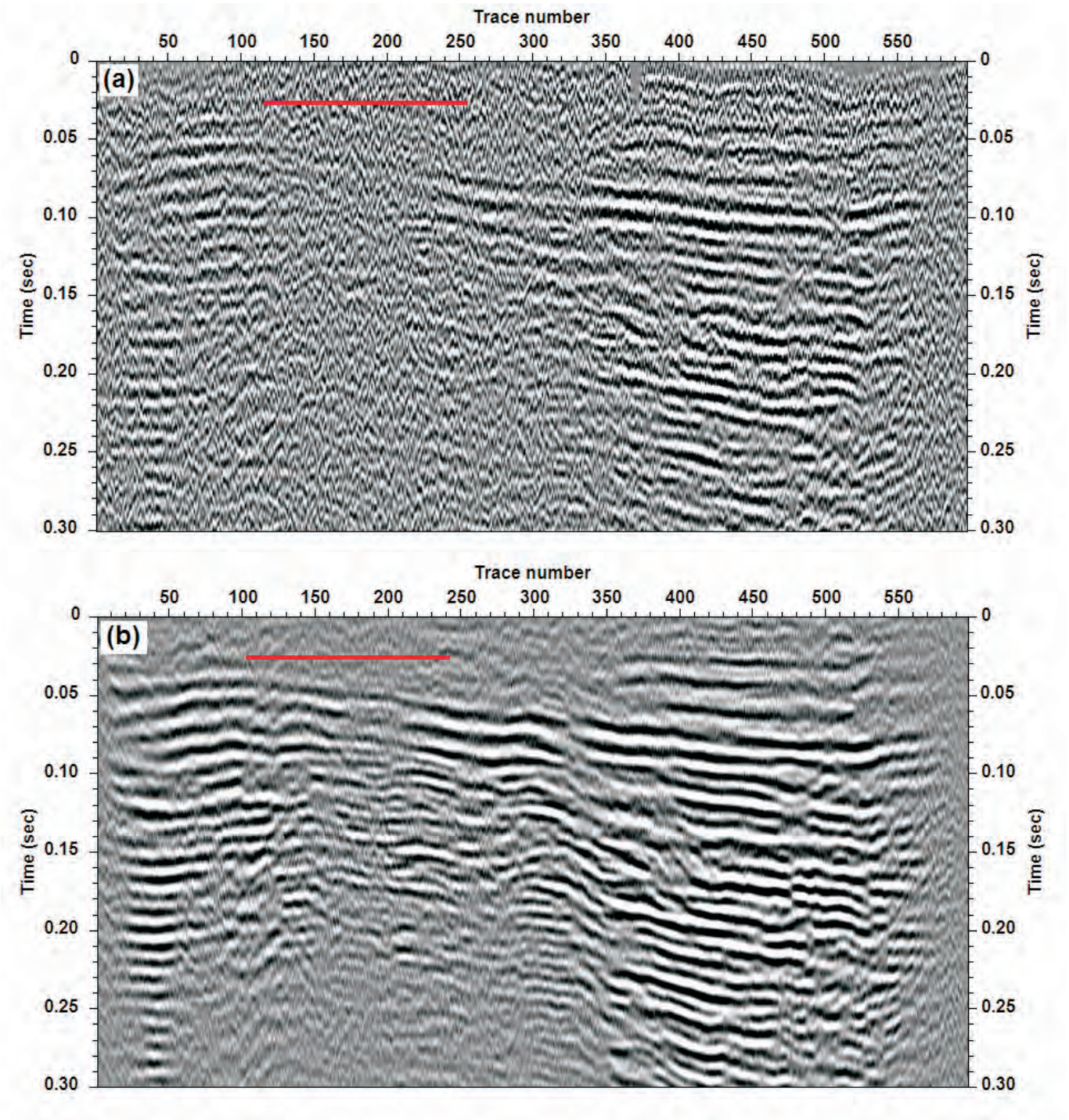

Figure 3: The same seismic sections as in Figure 2. (a) The initial brute stack section which has better continuity than the final stack section in the area of possible poor reflection zone; (b) Improved final stack section after reprocessing with special care taken with the static corrections.

independently produce the same results even if they follow the same processing path. There are simply too many decisions on input parameters required of the processor. The outputs of different processing packages will also be slightly different. Examples of processing related differences are found in Tucker & Yorston (1973), Yilmaz (2001) and in our companion paper (Hatherly & others, 2005).

To understand whether the processing is taking the seismic data to an appropriate final result requires that a watch be maintained over the processing stages. Ideally, it should be possible to see reflectors on raw field records that can be correlated with the reflectors on the final sections. The brute stack also provides an important check point. The brute stack provides the first view of what the final section should look like and subsequent processing is directed towards refining that brute stack.

The example of Figure 2 is a case in point. The brute stack for this section is shown in Figure 3a. Across the zone in question, the main reflectors are present but very weak. In the initial final stack of Figure 2, these weak reflectors were

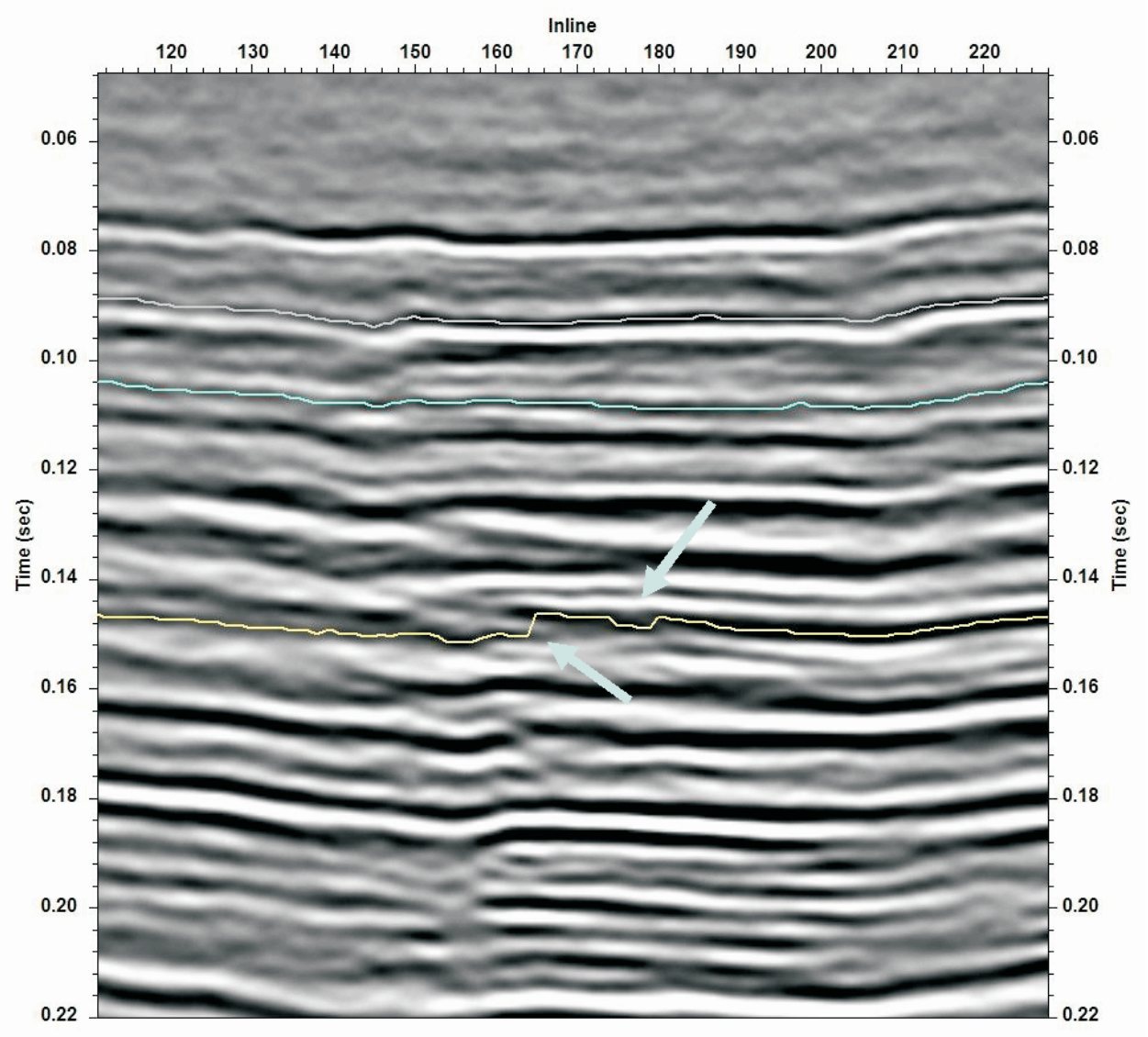

Figure 4: While the upper reflectors on this section can be picked with certainty, there is considerable uncertainty with the picking of the third reflector at about 0.15 seconds. It is a weak reflector, the pulse shape changes and its behavior around the fault is uncertain.

processed out. However, by more careful processing and attention to statics, the final section in Figure 3b was obtained. The weak reflectors in the brute stack were enhanced to reveal continuity in the coal seam, not the intrusions initially suggested.

A second example of the uncertainty that can arise as a result of processing, can be found in Figures 3 to 6 and the associated discussion of Hatherly & others (2005). Different processing centers derived different stacking velocities for these data with the result being a general synclinal structure on one result that was not present on the other. The depth conversion process we described in that paper resolved that ambiguity, but without such depth conversion the reality of that structure would not be known.

There are many causes of uncertainty in seismic interpretation. Some of these are due to the fundamental limitations of the seismic method. For instance lateral resolution is controlled by the size of the Fresnel zone defined by the depth of the reflector and the wavelength of the seismic wave. The wavelength also controls the resolution of the tops and bottoms of reflectors. When many seams are present there is a significant reduction in the reflection energy returning from the lower seams and reverberations between the seams creates additional reflection events that are difficult to identify during processing. Issues such as these are discussed in Zhou & Hatherly (1999).

Other examples of interpretational uncertainty are illustrated in Figure 4. In this case from the Bowen Basin, multiple seams are present and three have been picked. For the interpretation and use of these seismic data, consideration needs to be made of:

- Which reflectors represent the coal seams of interest. The uppermost reflectors are obvious but the deeper reflector at 0.15 seconds is not a particularly strong reflector. In this case, this reflector was picked by tying the seismic data to boreholes.

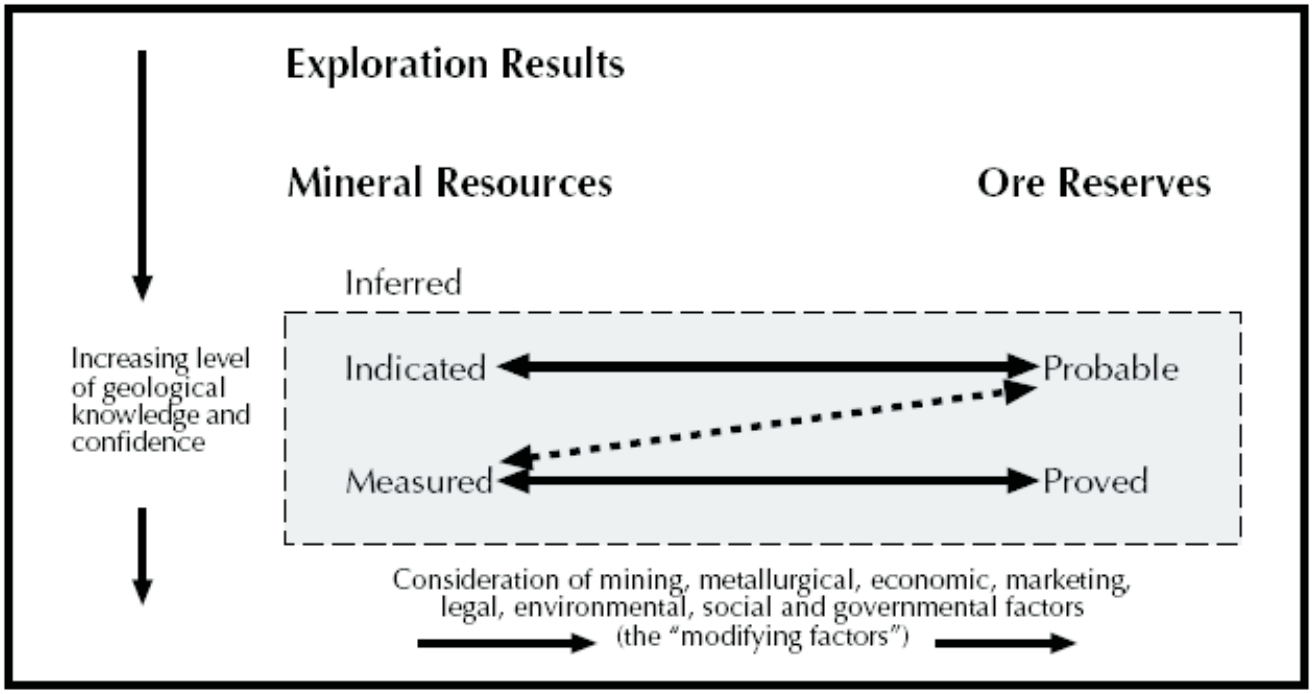

Figure 5: General relationships between exploration results mineral resources and ore reserves (from the JORC Code, http://www.jorc.org)

- Changes in the shape of the reflection signal. The upper arrow points to an area where the reflection time abruptly increases. This is unlikely to represent a change in depth. Instead, the shape of the reflection wavelet has changed slightly and the automatic event picking algorithm has moved accordingly.
- The position of the fault in the vicinity of station 150 is quite clear on the upper reflectors but on the third reflector picked, the lower arrow points to the fault region and here it is not at all clear where the fault is precisely located and how the reflector should be picked to either side.
- There is possibly another fault present to the right of the section. There is quite a distinct roll on the upper reflectors but on the third reflector, there is no evidence of it. Is a fault present on the third reflector but at a throw below the level of the seismic resolution?

Our aim in raising these uncertainties is not to alarm previously unsuspecting users of seismic data as per our quotation by Mark Twain, rather it is to point to the need for this uncertainty to be recognized and managed.

MANAGEMENT OF UNCERTAINTY

From the foregoing discussion and examples, it is evident that it is unavoidable that there will be uncertainty in seismic imaging and exploration more generally. The answer to this situation is not to remain in ignorance but instead it is to use all available data intelligently in full understanding of their strengths and weaknesses. A balanced exploration program is one where the shortcomings of the various methods are balanced by the strengths of the others. Through the process of integration, it is possible to consider the risks and consequences of the various possible scenarios. If after consideration of all available data, there is still an unacceptable level of uncertainty about the geological conditions, then the options are either to do more exploration work, or if this is not possible, act on the basis of an informed assessment of the risk.

The management of uncertainty for detailed mine planning and operations represents a continuation of the principles outlined by the JORC Code (http://www.jorc.org) for the reporting of resources and reserves to the Australian Stock Exchange. Figure 5, is taken from the Code and shows the inter-relationships between securing geological knowledge and confidence and the additional modifying factors. To establish a proved ore reserve, all need to be favourable. We suggest that to successfully mine a proven ore reserve, the strategies and processes described by the JORC Code need to be continued to provide even more detailed knowledge and increased confidence. In some regards, the inputs and uncertainties that are expressed in Table 1 are mirrored in Figure 5.

Returning to the issue of the management of uncertainty in seismic data, one way that this will be improved is through quantification of the uncertainty. Techniques for doing this are being developed for petroleum exploration (Grubb, Tura & Hanitzsch 2001; Houck 2002; Kodloff & Sudman 2002; Landr∅ 2002; Malinverno & Briggs 2004; Thore & others 2002) and may be relevant to coal mining. Regardless of the availability of these, we recommend that good practice for coal seismic exploration should ensure that:

- Field surveys are planned with full knowledge of the geological conditions and their likely impact on the seismic data.

- Processing centres have access to all geological information that can assist their activities.
- The results of each processing stage are carefully monitored and documented.
- Interpretation is made with full knowledge of the background geology, the targets and any issues with the data acquisition and processing.
- There is comprehensive integration of the seismic results, other geological data and relevant mining experience.

CONCLUSIONS

Through the quotations of Burns, Churchill and Twain there is wisdom concerning uncertainty that is very relevant to our efforts to undertake effective coal exploration programs. It is also relevant to consider the failure of an exploration program of another type – the hunt for missiles and chemical weapons in Iraq, as an example of the complex issues that come to bear and need to be managed. In the case of seismic exploration, the acquisition, processing and interpretation of seismic data have many parallels with satellite technologies.

These are both powerful techniques but their effective use requires skilful deployment and decision making that is cognisant of the uncertainties and associated risks. The JORC Code provides guidelines for establishing proved ore reserves to an acceptable level of certainty. The same approach should be followed right through to mining.

ACKNOWLEDGEMENTS

Our research into seismic methods has been supported by CSIRO Exploration and Mining, CRC Mining and the Australian Coal Association Research Program (ACARP). Data have been supplied to us by numerous mining companies. Their contribution is also acknowledged.

REFERENCES

GRUBB, H., TURA, A. & HANITZSCH 2001: Estimating and interpreting velocity uncertainty in migrated images and AVO attributes, *Geophysics* **66**, 1208-1216.

HATHERLY, P., ZHOU, B. & POOLE, G., 2005: Borehole controlled seismic depth conversion for coal mine planning: This volume.

HOUCK, R.T., 2002: Quantifying the uncertainty in an AVO interpretation, *Geophysics* **67**, 117-125.

KODLOFF, D.D. & SUDMAN, Y., 2002: Uncertainty in determining interval velocities from surface reflection seismic data, *Geophysics* **67**, 952-963.

LANDR∅, M., 2002: Uncertainties in quantitative time-lapse seismic analysis, *Geophysical Prospecting* **50**, 527-538.

MALINVERNO, A. & BRIGGS, V.A., 2004: Expanded uncertainty quantification in inverse problems: Hierarchical Bayes and empirical Bayes, *Geophysics* **69**, 1005-1016.

THORE, P., SHTUKA, A., LECOUR, M., AIT-ETTAJER, T. & COGNOT, R., 2002: Structural uncertainties: Determination, management, and applications, *Geophysics* **67**, 840-852.

TUCKER, P.M. & YORSTON, H.J., 1973: *Pitfalls in seismic interpretation,* Society of Exploration Geophysicists.

YILMAZ, O.Z., 2001: *Seismic data analysis: processing, inversion, and interpretation of seismic data*: Society of Exploration Geophysicists.

ZHOU, B. & HATHERLY, P.,1999: Interpretation of small scale geological features on seismic reflection data, *Final Report – ACARP Project C7026*.

ZHOU, B. & HATHERLY, P., 2003: Seismic imaging: Science and Art, *Preview*, **105,** 25-28.

ZHOU, B., HATHERLY, P.J., & SLIWA, R., 2004: Integration of seismic data for mine planning, *Final Report – ACARP Project C11038*.

P. Hatherly, CRC Mining/School of Geosciences, University of Sydney, NSW 2006, phatherly@geosci.usyd.edu.au
B. Zhou, CRC Mining/CSIRO Exploration and Mining, PO Box 883, Kenmore, QLD 4069, Binzhong.Zhou@csiro.au

Mark Biggs

The continuing development of downhole geophysical techniques to explore for coal deposits in the Bowen Basin, Queensland

Coal exploration continues unabated within the Bowen Basin of Central Queensland. Whilst some would argue that most of the shallow high value coal has been discovered, the prospect of finding further significant greenfields and brownfields deposits appeals. Despite the fact that exploration drilling results from more than 250 000 boreholes drilled since the last Bowen Basin symposium provide a substantial database for the evaluation of many leases, potential mining hazards such as weak roof and floor, high concentrations of insitu gas, dykes, sills, and faults exist, some awaiting discovery.

Recent advances in the use of downhole geophysics have extended their use beyond merely picking seam surfaces, thicknesses and estimating coal ash contents. They now have the potential to yield valuable data on the definition of rock mass characteristics, formation dip, *in situ* stress, near influence of intrusives and fault orientations. The application of new interpretative tools that complement structural modelling uses data from improved dipmeter logs and applies sonic, natural gamma, and core geotechnical defect logging to the characterisation of roof and floor strata have also aided the detection and prediction of mining hazards.

This in turn has provided sounder interpretations of coal seam structural models in areas of complex faulting. Improvements to downhole magnetometer sondes have allowed delineation of the margins of silling in some principal seams and the ability to trace dyke extensions from their occurrence in highwalls. Gas zone detection and subtle fault intersections in boreholes has been possible through geophysically logging using a combination of standard density and radiation-based logs as well as the latest technology Full Wave Sonic and acoustic scanner technology.

Of particular value has been the proliferation of software programs that have used some form of artificial intelligence to graft combinations of log responses to remotely classify geotechnical units (mainly seam roofs and floors) and some of their parameters, such as strength. In the case of Logtrans, borehole-derived RQD and fracture frequency indices have been included in the classification algorithms to improve the correlations and lithological predictions. Rolling improvements, in the near future, to information from CSIRO-developed automatic core logging technologies, based on visible and infrared spectroscopy, may also hold promise for providing rapid semi-quantitative analysis of the mineralogical characteristics of cores for geotechnical assessment of formations hosting coal resources. Coupled with geophysical measurements the technology may offer, in due course, a near real-time tool for improved understanding of geotechnical properties.

Based on the recent experience, the use of clearly targetted downhole geophysical surveys has provided substantial additional information to aid exploration and mine planning. Unfortunately databases and mine planning software capable of holding this quantum leap of data efficiently are yet to be in widespread use, and interpretive software is at a formative development stage for coal applications, and not widely available at mine sites.

Sonic logging methods would still appear to show the most promise for unravelling rock mass character throughout the Bowen Basin. Brief examples of each technique's application are given from some Anglo Coal Australia (ACA) operations in the basin. The keys to expanded utilisation of geophysical logs for geotechnical purposes are:

- **An improved understanding of the connection between petrophysics and geotechnical engineering, and**
- **efficient means for extracting geotechnical parameters from large volumes of wireline logging data.**

Key words: Downhole geophysical logging, dipmeter, Ferret tool, full waveform sonic logging, acoustic scanner, LOGTrans, geophysical interpretation.

INTRODUCTION

A large percentage of the shallow coal in the Anglo Coal Australia's (ACA) Bowen Basin operating mines has been mined except at Callide and Dawson where shallow, thick seams remain. Despite the fact that exploration drilling results from more than 39,000 boreholes provide a substantial database for the evaluation of coal within each of the leases, many mining hazards such as dykes, sills, and faults exist, awaiting discovery.

Recent dipmeter, magnetometer, full waveform sonic logging, and acoustic scanner surveys have shed new light on the use of these techniques to assist in delineation of such

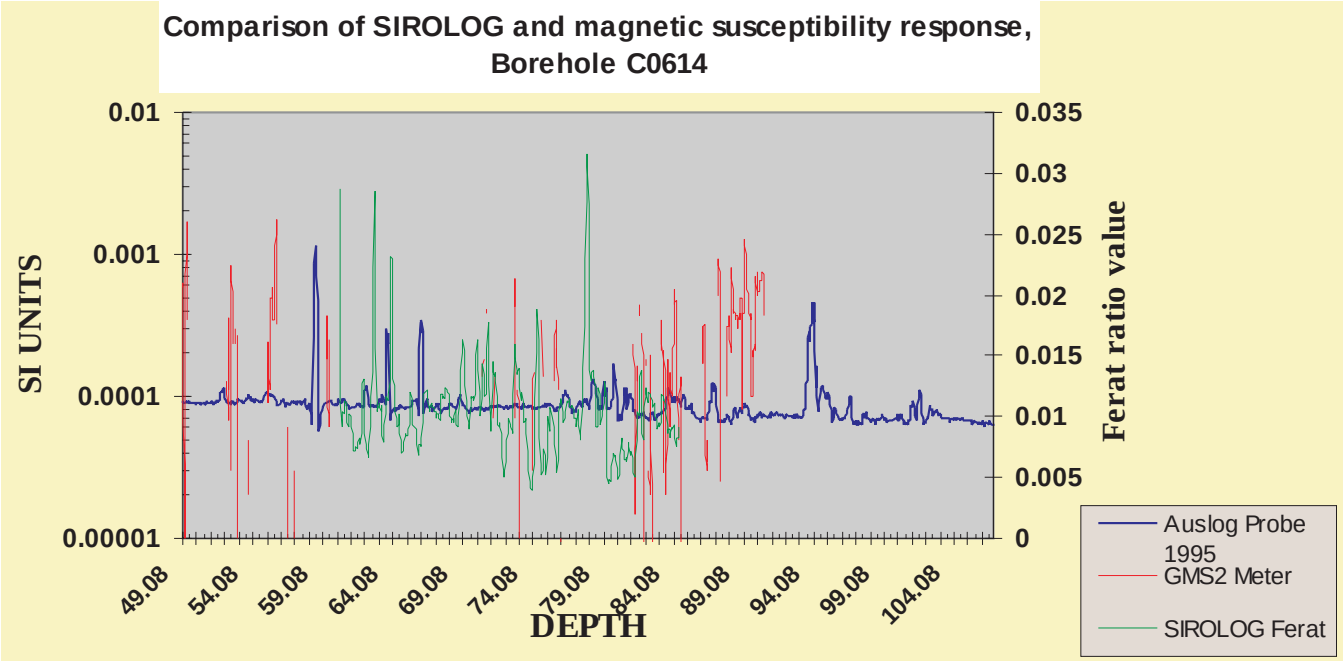

Figure 1: Comparison of SIROLOG and downhole susceptibility response, Borehole C0614, Callide Mine

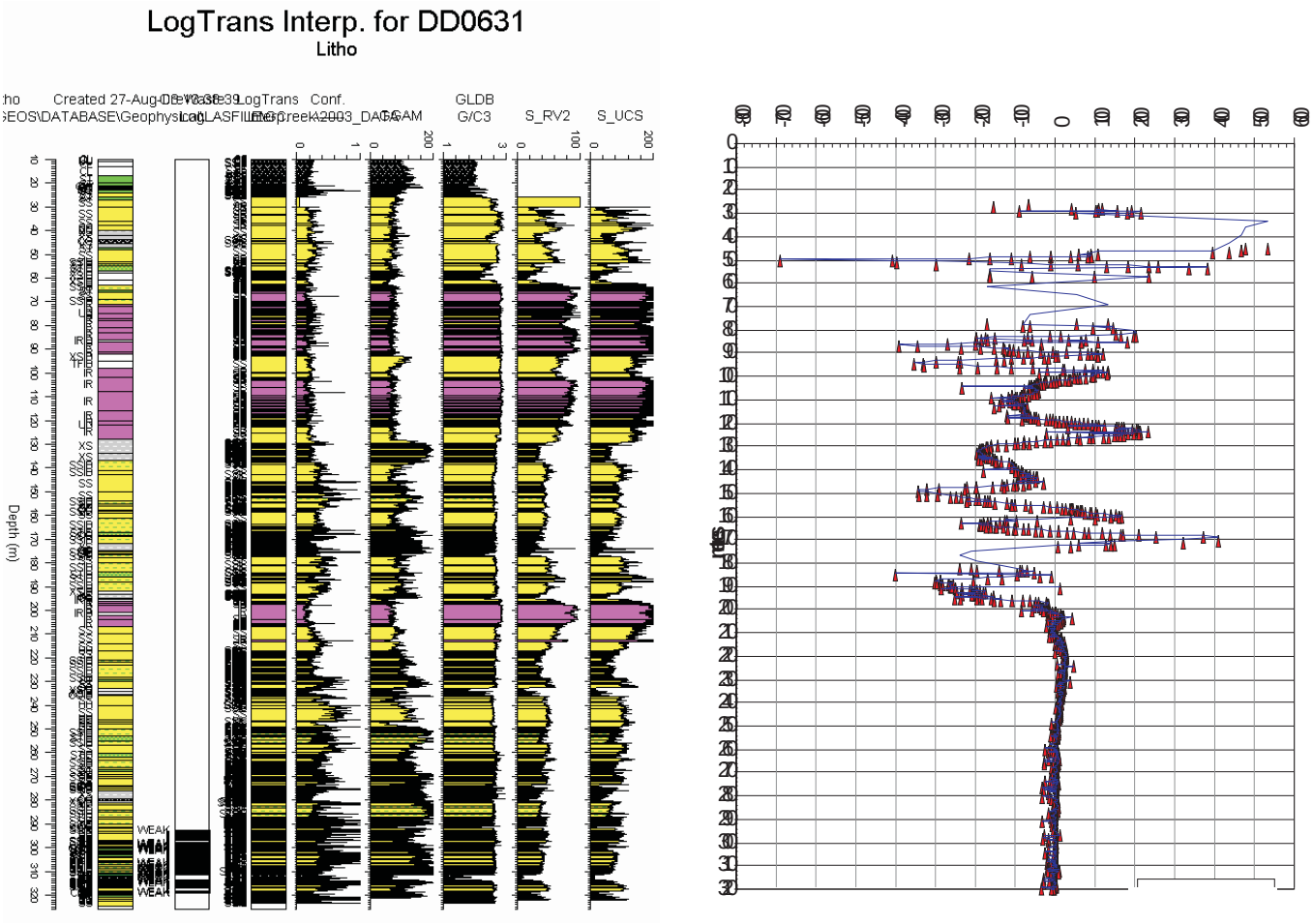

Figure 2: Example of Downhole magnetometer results, DDH631, 400's Panels, German Creek Mine

mining hazards. Brief examples of each technique's application to hazard prediction at a selection of mines are given in this paper. These techniques had been used in past exploration programs with indifferent results. Considerable pre-survey planning took place to research the best application methodology for the target. For example, rock velocities determined from full waveform sonic and acoustic scanner logging assisted planning the 2D-seismic survey. Rock petrophysical properties on dyke and country rock material assisted downhole magnetic and LOGTrans surveys.

Of course, there is and will continue to be, use of standard tools (long and short–spaced density, natural gamma, resistivity, calliper, and sonic) to aid in the exploration and evaluation of coal deposits. The uptake of other more specialised tools has been variable. Biggs & Hatherly (2000) reported on the full-waveform sonic tool but its development appears stalled (Hatherly & others, 2004). Dipmeter tools have improved and acoustic scanner use has increased but is still hampered by cost, probe availability, and lack of rapid interpretation tools (McGregor & Gale, 2000; Green & Ward, 2001; McGregor 2003; and Morrison & Smyth, 2003).

UltraMag's downhole magnetometer (Ferret tool) and others (Auslog hardness; Smith, 2003) have yet to gain wide acceptance. Of concern is that excellent research outcomes (e.g. ACARP project C11037, Hatherly & others, 2004) are yet to be assimilated into exploration or mine planning critical path evaluations. Interpretation software (Wellcad or SEISWin) is still comparably expensive and their implementation is not standardised.

Table 1 summarises the use of the specialist probes mentioned above. Detailed discussion follows of selected probes described above, and some discussion of newly developed interpretation software such as Logtrans is also included.

DOWNHOLE MAGNETOMETER

To progress standard interpretation of ground or airborne magnetic data, survey profiles must be augmented with some or all of the following:

- Shallow drilling and magnetic susceptibility logging,
- magnetic remanence determinations on oriented dyke samples,
- assumptions of 'structural continuity', and
- downhole magnetometer surveys.

Shallow drilling into the dyke and susceptibility logging would define the 'depth to magnetic top', and provide information on magnitude and lateral consistency of susceptibility. Variations in oxidation and/or depth of burial strongly affect ground profile anomalies. Several coal logging providers such as Auslog or UltraMag (McClelland, 2001) provide downhole magnetometer probes, although their limited appeal does not provide sufficient work or competition to make logging costs low enough to utilize them routinely.

A comparison of a downhole magnetometer log versus SIROLOG iron ratio (Borsaru & others, 2001) and hand-held susceptibility measurements on core from the same hole is shown in Figure 1. This borehole is from ACA's Callide Mine and the initial purpose of the logging was to detect and characterise thin dykes. Despite there not appearing to be good correlation between techniques, the methodology proved successful in delineating iron-rich mineral zones, and in particular differentiation between siderite and geothite.

Conversely, Figure 2 shows the results of the Ferret probe (UltraMag Geophysics Pty Ltd), which clearly delineates olivine dolerite intrusions intersected in the hole (coloured pink in the stratigraphy column to the left) and the use of standard anomaly profiling software suggests the dykes are present some distance from the borehole.

FULL WAVEFORM SONIC

The conventional sonic log is based on the first arrival of a refracted wave travelling up the borehole wall. If instead the analysis was on the full waveform sonic (FWS) log, far more information on geological conditions within a borehole should be available to geologists and engineers (Hatherly, 1998). In Australia, most geophysical logging contractors working in the coal mining industry (Auslog, Geoscience, Precision, Robertson Geologging, and Total Geophysics) have full waveform logging capabilities. The observed pulse is in the frequency range 10 to 25kHz and the waveforms are sampled at 4 microsecond intervals. The tools unfortunately often have their three detectors at spacings like 0.4, 0.6m, 1.0m or 1.4m from the source.

Even today within Australia's coal mining industry, work involving the use of sonic logs to estimate uniaxial compressive strength (UCS) is mainly referenced to the work of McNally (1987, 1990) and Davies & McManus (1990). They have been used extensively in geotechnical investigations throughout the industry. The estimates are based on empirical relationships between sonic transit time at a 0.2m source-to-detector spacing and UCS as measured in rock mechanics laboratories. Full conversion to FWS logging will require recalibration at most sites. However the relationship with UCS is not quantitative. Furthermore, geotechnical evaluation requires information on fracture properties as well as those of the intact rock mass. Techniques for using conventional sonic logs to characterise fractures have not been fully established, but are the subject of ongoing industry and ACARP research (Hatherly & others, 2001; Zhou & others 2002).

For rock strength assessment, the advantage of the FWS log is that it allows visualisation and analysis of the full seismic waveform – the P-wave from which transit times are determined, the slower S-wave and the Stoneley wave which travels mainly through the borehole fluid. In principle, the properties of these three wave types (velocity and amplitude)

Table 1: Comparison of Specialist Downhole Geophysical Logs within Anglo Coal Australia

Tool/ Technique	Additional Cost (per 200m borehole)	Output Products	Usefulness	Application	User Requirements	ACA Usage
Full Waveform Sonic	$60	Hardcopy printout, Raw logging format file	Interpretations of compressional, shear, and stoneley wave velocity and amplitudes. Calculation of dynamic indices such as poisson's ratio	Open-cut slope stability, Highwall Mining hazard assessment, Longwall roof and floor assessment	Needs specialist software such as WellCad or SeisWin, Interpretation methodology not well publicised. Experienced interpreter skills required. Lack of LAS provision hampers using non-expert systems	None Current
Acoustic Scanner	$975	Converted Raw logging format file to Wellcad, Image Pro, or Seiswin format	Depth, orientation, and dip of joints, bedding planes, shear zones and other structural features. Stress magnitude (estimated) and direction	Almost critical path for longwall and other underground applications as provides joint orientation, bedding, stress, and strength data	Needs specialist software such as WellCad or SeisWin, Needs specialist software such as WellCad or SeisWin, Interpretation methodology not well publicised. Experienced interpreter skills required. Interpretation can vary between practioners	Moderate at underground operations. Lack of suitable software and skilled interpreters means interpretation often not performed in-house (at extra cost for external consultancy).
Dipmeter	$310	LAS, hardcopy, Raw logging format file	Improved vendor data acquisition software, strike and dip of strata, regional trends	Mainly to check and augment structural and dip interpretations in faulted ground	Can use specialist software such as WellCad, but most coal mine planning packages will load data. Provision of LAS means spreadsheet analysis possible. Intermediate skill level required	Increasing use at some sites, useful in compressional fault regimes
Magnetometer (Ferret or Auslog)	$2,000	ASCII file, hardcopy, Raw logging format file	Too expensive to use routinely, dyke or sill interpretation	Detection of near borehole intrusions in longwall panels, provides petrophysical parameters for magnetic profile interpretation	Easily understood by novice, spreadsheet only and magnetic anomaly interpretation software, ie Intrepid etc	Trial use only
Hardness (Auslog)	unknown	Raw logging format file	Provides formation strength where sonic relationships poor or holes unable to hold water	Applications where sonic log not appropriate, i.e. dry borehole	Interpretation software not known	Trial use only

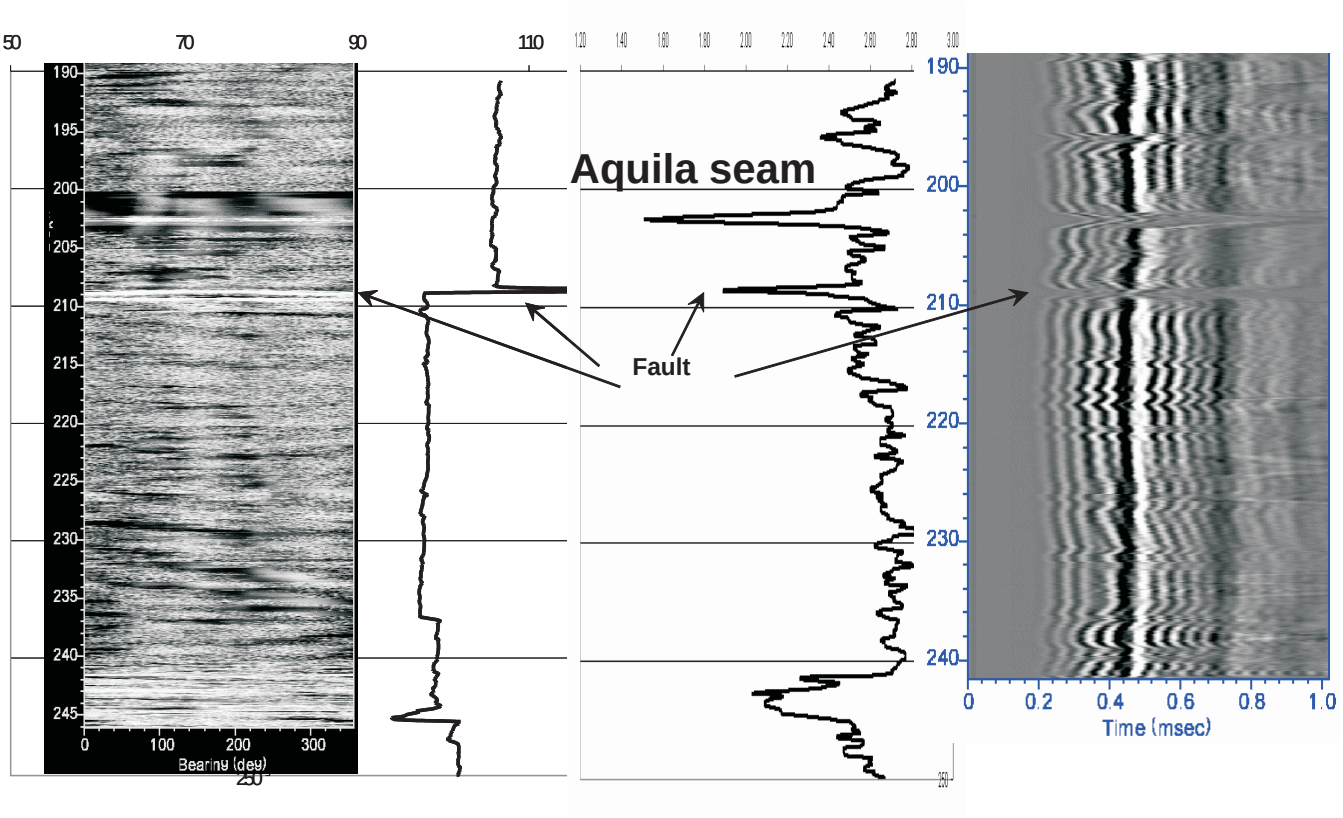

Figure 3: Comparison of logging methods in borehole DDH430. The logs from left are acoustic scanner, caliper, density, and full-wave form sonic. Note that a fault was recorded on the geologist's log occurring 7m below the Aquila seam

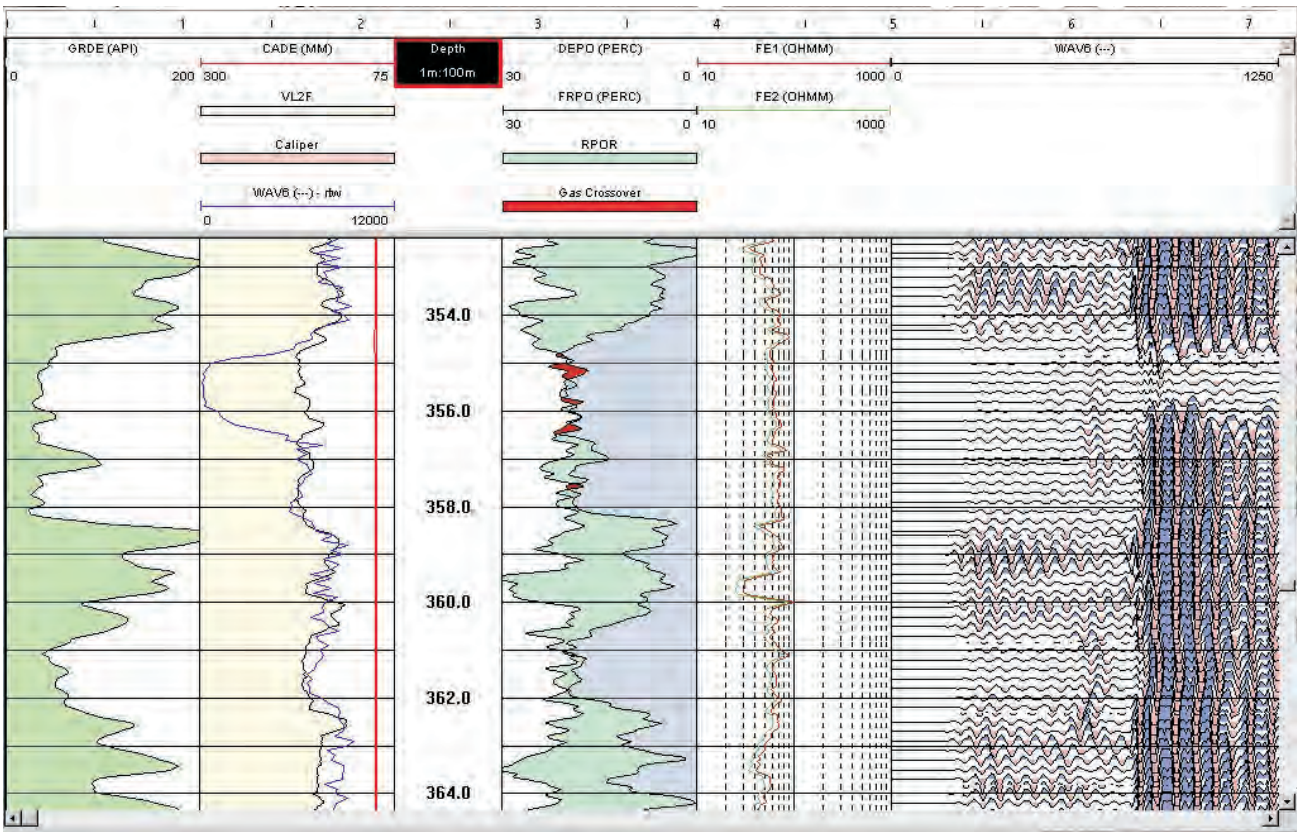

Figure 4: Example of Porosity crossover zones, indicating enhanced gas content and poor Full waveform sonic response (modified after Hatherly & others, 2004).

allow the determination of dynamic moduli and an estimation of properties of the strata and the extent and openness of *in situ* fractures. Means of doing this are currently being developed, partly through ACARP projects but for now, qualitative interpretations of the waveform images provides the most useful application to support the conventional P-wave transit time data.

Borehole DDH430, from ACA's German Creek mine (Figure 3) appeared to intersect a fault zone 7m below the Aquila seam, based on the geologist's log. Figure 3 shows an acoustic scanner image, calliper, gamma-gamma density, and full-waveform sonic trace over the interval 190 to 250m. The Aquila seam is clearly defined, and the fault intersection most clearly by the calliper. Note the different response of the FWS over the seam interval to that of the fault. Also note the additional information on sheared/jointed zones above and below the Aquila seam provided by the FWS, particularly at 221, 226, and 231m. The acoustic scanner image, whilst not showing high contrast does correspond to most of these FWS zones.

Figure 4, from Hatherly & others (2004) shows the other strength of the FWS response in delineating and/or confirming methane gas-saturated zones in boreholes (the red-shaded cross-over zone between density and neutron porosity logs on Figure 4). Particularly the Stoneley wave is attenuated at the crossover points.

ACOUSTIC SCANNER

The acoustic scanner probe is being increasingly run in ACA exploration and mine planning boreholes. These downhole geophysical sondes utilise a rapidly rotating ultrasonic beam to scan the borehole wall. A transducer, which emits repeated short burst of sound energy 1MHz energy, pulse every 1 microsecond, pairs of amplitude and travel time values are digitised and stored for each pulse cycle, and data recorded at 5cm or 10cm increments.

The amplitude of the reflected signal is used to generate an image of the borehole wall. The travel time of the reflected pulse allows the shape of the hole to be mapped. A survey package consisting of axial magnetometers and accelerometers allows the orientation of the tool to be established and thus the orientation of features on the image and any borehole breakout. The survey package also allows determination of borehole deviation. The sonde is 57mm in diameter and 3.9m long, with a logging speed 2.4m/min. The borehole must be water-filled. Poor results have been obtained from logging boreholes drilled using blades and hammers, moderate results from holes using the PCD bit, and best results from boreholes that have been fully or partially HQ-wireline cored (due to the extra conditioning work performed on sidewalls before and after coring).

Most current logging companies have an Acoustic Scanner tool (e.g. Precision and Geoscience have the ALT tool). The charge is additional to conventional downhole logging suite, and normally comprises a daily rental fee ($250-300) and a metreage survey charge ($1.00 - $3.75 per metre). At ACA's Dawson site, logging the deepest 200m of a 450m single exploration borehole typically will add $1000 to logging cost. Additionally, data conversion and storage of data to CD-ROM by the logging company can cost $150-300 per hole. Interpretation costs can vary depending whether the specialist software required is available (refer to Table 1).

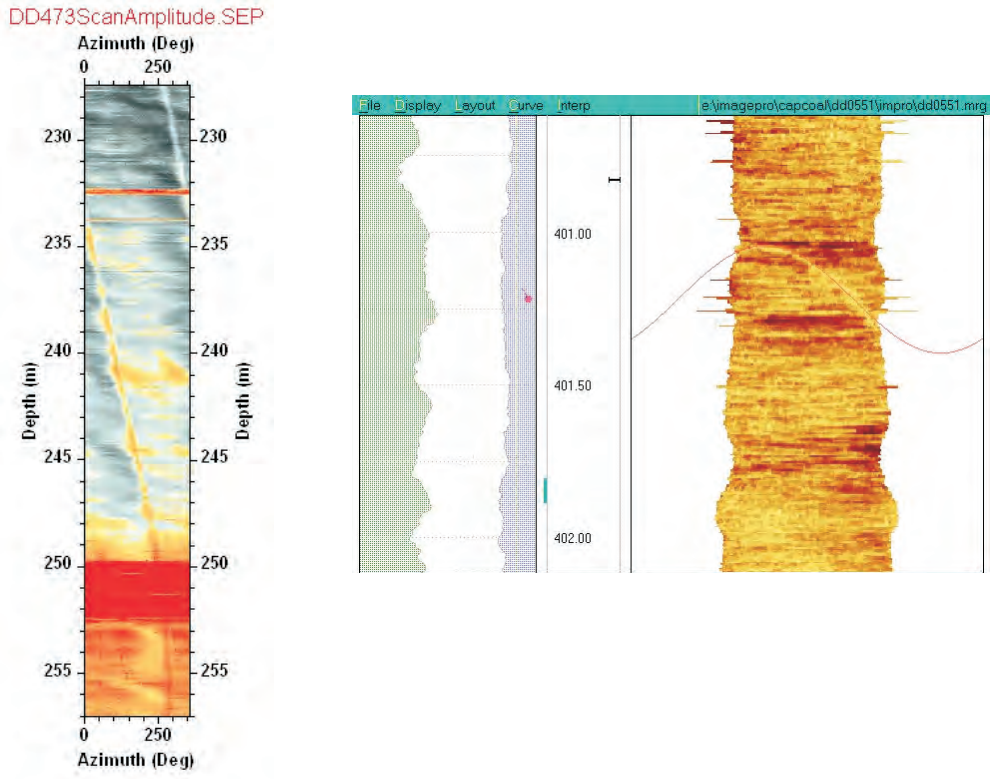

Figure 5: Typical German Creek Acoustic scanner borehole quality

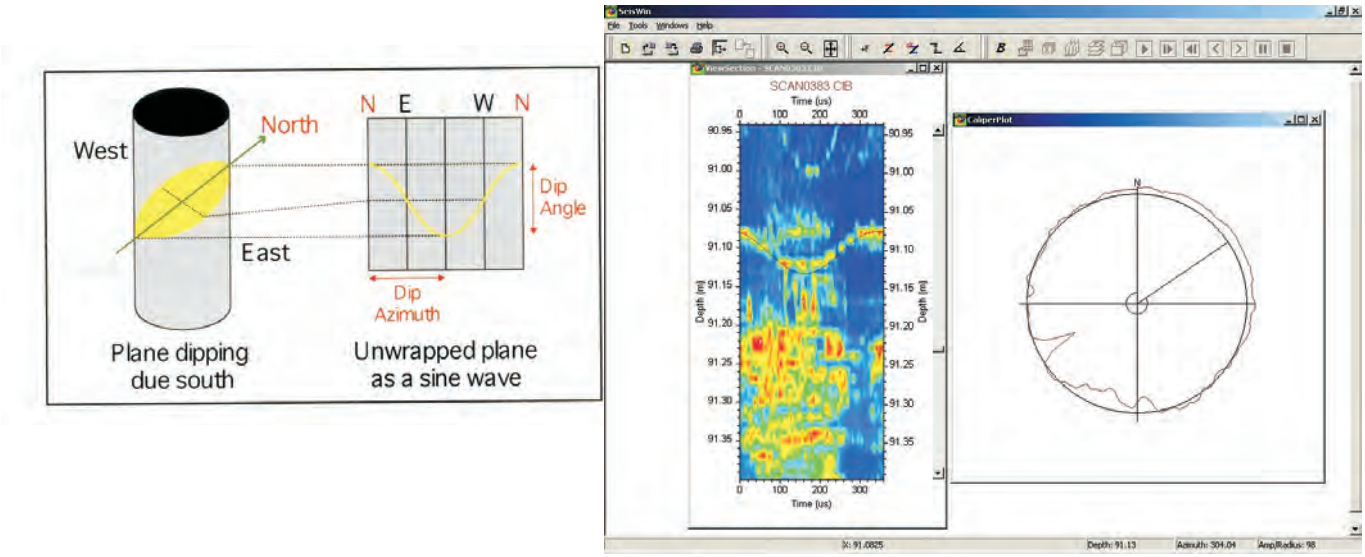

Figure 6: Acoustic Scanner Joint Detection Principles

Most available software programs are relatively usable, e.g. QLOG, PC-ImagePro, SeisWin, WellCad, but varies significantly in cost (A$500-$8000) per licence. Costs for interpretation are time (3-4 hours per hole) but are negligible if you are using your own staff that have the time and are trained. If the work is sourced externally using consultants or contractors, rates can be by hour ($65-$120) or by the metre ($10-$20 per metre). If report costs included then budget on $1500-$2500 per 200m of interpretation.

The potential uses of the acoustic scanner, despite the data acquisition and interpretation costs, are varied and useful to the mine planner:

- Additional source of verticality,
- provide detail on borehole sidewall condition,
- orientation of core once features matched,
- interpretation of bedding planes, shear zones and joints,
- borehole breakout,
- borehole ellipticity- principal horizontal stress direction,
- horizontal stress magnitude (future?), and
- rock strength /fracture frequency/ overburden characterisation (future).

Typical acoustic scanner borehole quality at ACA's German Creek Mine is shown in Figure 5. Figure 6 shows the principles behind joint detection and how software such as Seiswin is used to detect defects and ellipticity. Acoustic scan logging is currently too expensive to conduct on every hole. Its best application is in cored holes, which tends to defeat the purpose somewhat.

The probe proved most useful at German Creek for generating joint roses for the intervals immediately adjacent to the target seams in areas where there was no highwall or underground exposures present. Future application for rock mass characterisation are still at formative stages or yet to be realised (Dimitrikapous & others, 2001; Wooton 2003; Morrison & Symth, 2003; Hatherly & others, 2004).

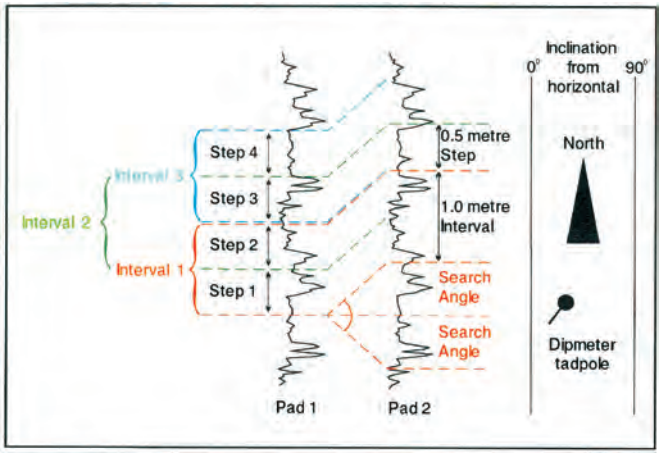

Figure 7: Dipmeter processing terminology (modified after Firth, 1999)

DIPMETER

Dipmeter tools make high-resolution micro-sensitivity measurements around the borehole circumference, which are correlated to produce apparent dip information (Firth, 1999). This is merged with tool orientation (navigation) data to provide formation dips in the earth's frame of reference. Dipmeters have a calliper, micro-resistivity electrodes, magnetometers and level cells or accelerometers needed to define the orientation of the tool in three dimensions. A minimum of three circumferential measurements is needed to define a plane. Traditional slim dipmeters therefore have 3-arms 120° apart (Figure 7). Resistivities are measured with small sense electrodes, separated by a thin insulator from the rest of the pad, which acts as a guard, current returning to the body of the dipmeter some distance above the calliper arms. Pad traces are generally correlated automatically using the interval correlation technique. This can be augmented by machine-aided manual correlation (Figure 8).

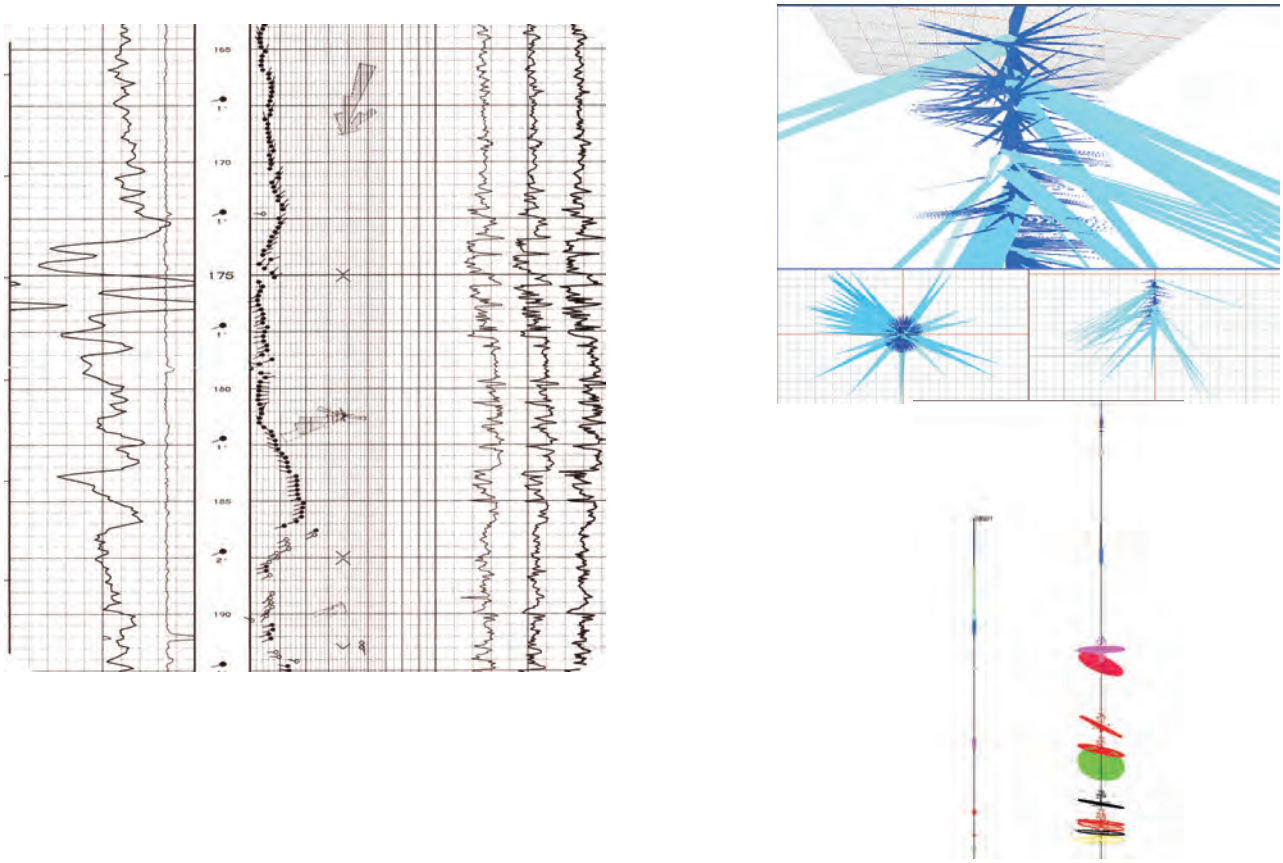

Figure 8: Different modes of displaying Dipmeter data. Image on top right courtesy G. LeBlancSmith, CSIRO

Dipmeter applications within ACA for coal are:

- Alternative method to obtain verticality data,
- aid in validation of computer structure models,
- delineation of local structures such as folding, unconformities, and faulting,
- correction for apparent coal thicknesses in high-dip areas,
- seam correlation in high-dip areas,
- adjunct to interpreting FWS and AS data, and
- can be calibrated against cored sections.

Figure 8 displays dip tadpoles showing strike (corrected to true north) and dip (scale range 0–90 degrees) from an exploration borehole at ACA's Dawson North. Improvements to the logging tool and interpretation software in recent years have vastly improved the display and value of the dipmeter tool. It has found use at Dawson North in that whole blocks of strata between major faults have been tilted, and that dips above major reverse faults are generally steeper than for strata below the fault plane (25°vs 8°). This additional data, when included in the database, vastly improves the modelling outcome. Additionally, interpretation of dip and strike trends, originally from the oil patch, can give clues to regional and local structure (Figure 9). Dipmeter data contains a certain redundancy, which must be filtered out, and interrogators need to be cognisant that dip and strike data is non-unique i.e. is it strata dip or a shear zone or major jointing or noise that you are seeing on the plots?

Validated strike and dip data has been used within ACA to correct structural grid models in areas of steep dips of highly fractured and intensely faulted ground. Figure 10 displays colour contours of average borehole seam dip for an area at the Dawson North mine. Dipmeter interpretation methodologies are still being developed for coal use.

INTEGRATION OF TECHNIQUES

Rock Classification Defect Schemes

Despite the individual usefulness of each technique described above, it is the data from each that is combined that provides real value to coal mining operations and exploration areas. Rock mass characterisation has, to date, relied upon geotechnical information derived primarily from drill core. However, coring followed by geotechnical logging is expensive and slow, providing a strong incentive to characterise the rock mass via alternative means. Hatherly & others (2001 and 2004) have commented that geophysical logging is a fertile source of geotechnical data from uncored as well as cored holes. Conventional petrophysical parameters such as sonic velocity, density, and resistivity are often correlated with *in situ* rock strength, porosity, degree of fracturing, and type of material occupying pore space. More detailed and comprehensive geotechnical characterisation can be performed if full waveform sonic and/or acoustic scanner logs are available (Figure 11).

It has long been recognised that seismic velocity has a relationship with rock strength (Davies & McManus 1990;

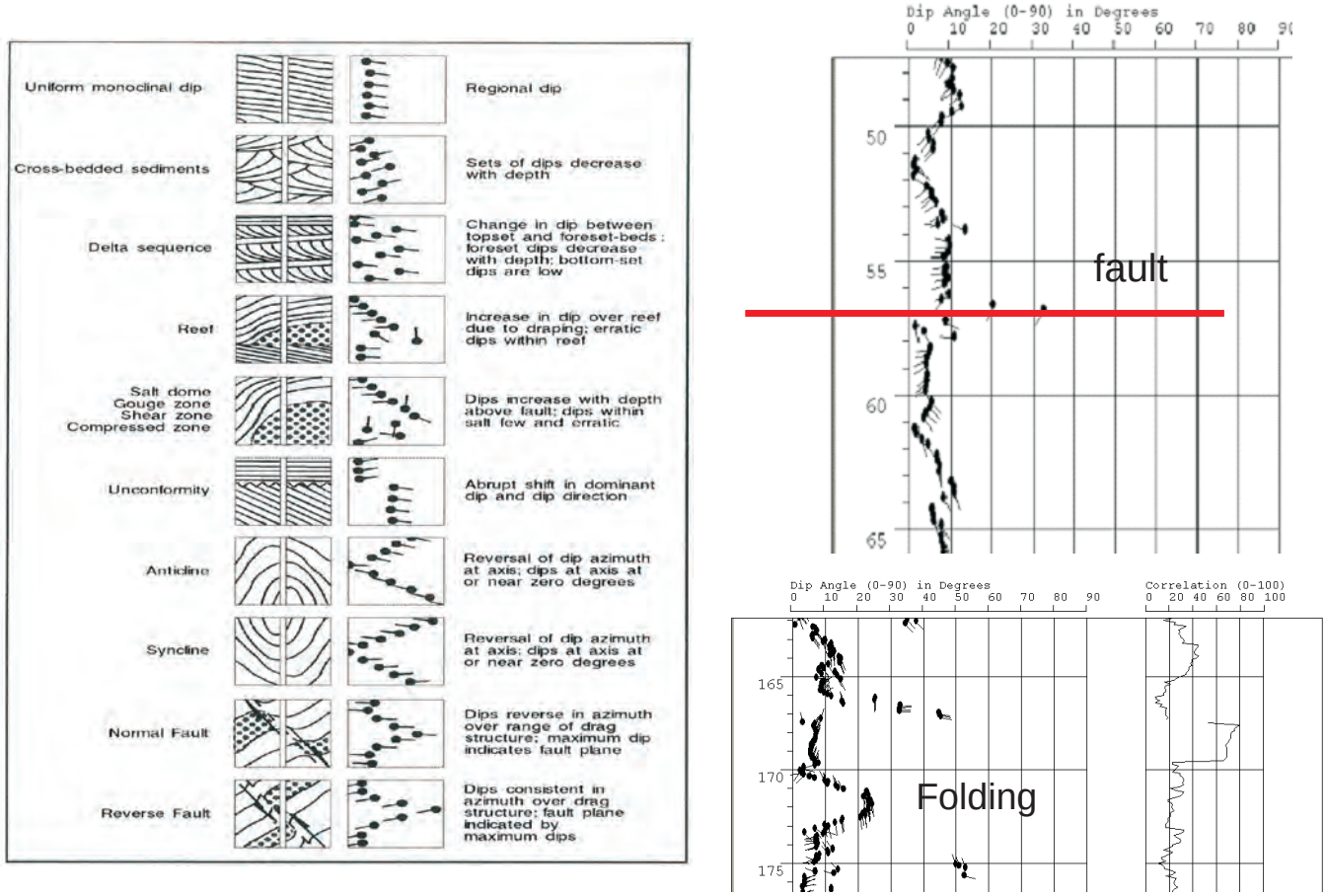

Figure 9: Idealised Dipmeter tadpole patterns with some actual examples from Dawson North Mine (modified after Firth 1999)

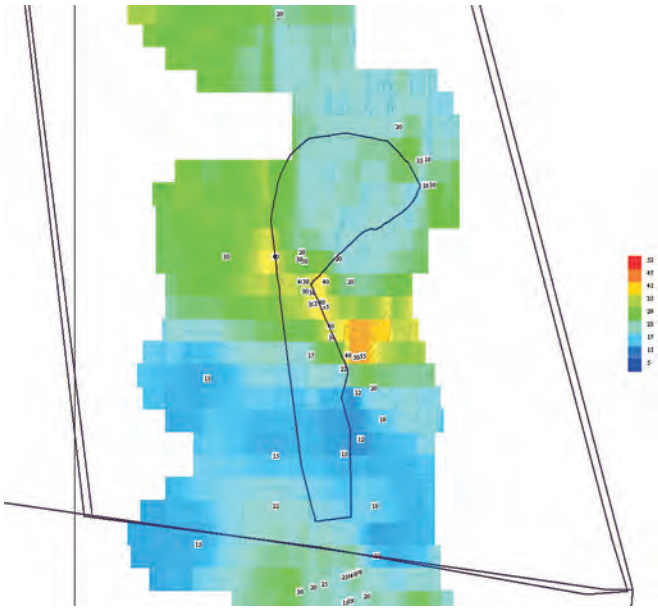

Figure 10: Example of contoured strata dip composed entirely of dipmeter data alone. Note zone of high dips associated with a major fault zone.

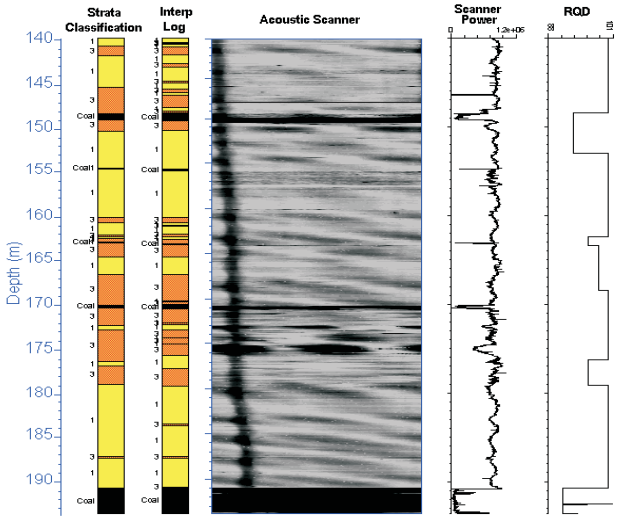

Figure 11: Preliminary Rock Classification/Defect Logs (modified after Guo & others, 2000)

Mc Nally 1987; 1990). In the case of sonic logging, empirical relationships between sonic transit time and UCS have widespread acceptance in Australian coal mining. While these provide a first order estimate of rock strength, it has been found at many mines that a local relationship is required to enable UCS to be estimated with sufficient accuracy. Sometimes a relationship cannot be found at all. The reasons for these problems mainly arise because the UCS is a measure of inelastic rock properties while seismic velocity is a measure of elastic properties. These need not be related and while an empirical relationship might exist within a given rock type, there is no reason for this to be the case when different rock types are involved.

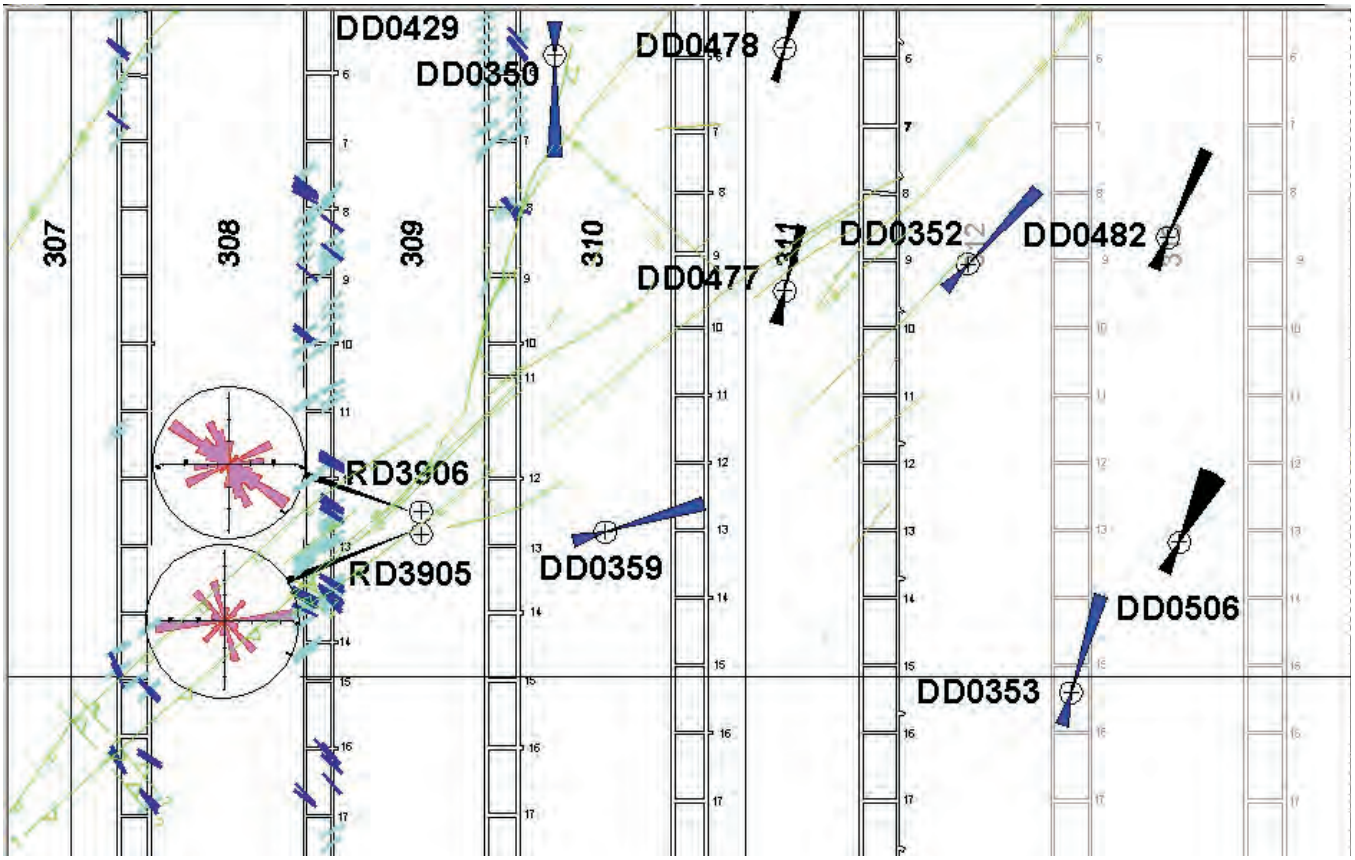

Figure 12: Integration of many techniques. Example from An ACA Longwall mine that displays combination of underground joint mapping, Acoustic Scanner joint azimuth rose diagram, and stress magnitude and direction, black from overcoring (scaled to magnitude), blue from acoustic scanner and /or CSIRO remnant core magnetism techniques. The plot outlines major stress directions and magnitudes likely to be encountered at the longwall face

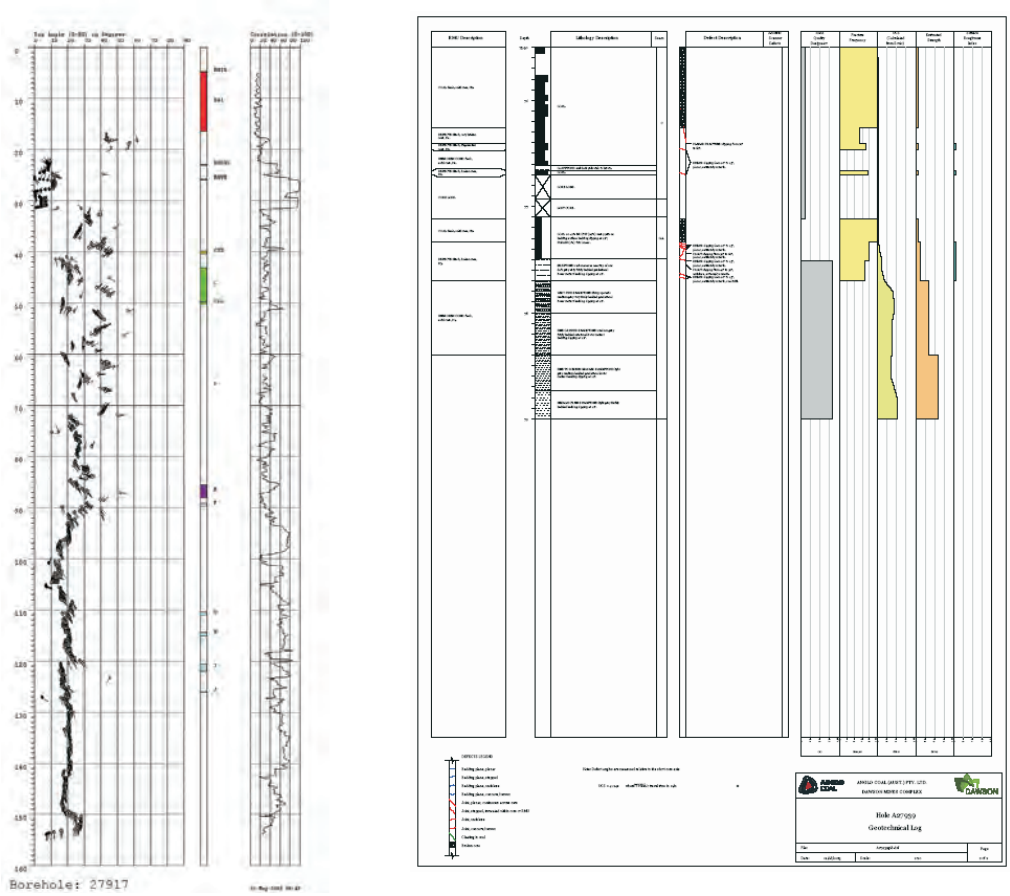

Figure 13: Further examples of integrating geological, seam pick, defect logging, dipmeter, sonic and acoustic Scanner data on downhole borehole plots, examples from ACA Dawson Mine

In Hatherly & others (2001), Stoneley wave assessment from the full waveform sonic log has demonstrated that formation and fracture permeability may be estimated. This process needs to be made into a routine procedure. In coals, it may be possible to estimate permeability using Sirolog data to determine the clay minerals present. There is an emerging link between the permeability and the amount of clay present within the cleats.

New approaches are being reported whereby more robust rock strength and fracture frequency estimation, which is based upon extracting the rich petrophysical data that can be obtained from geophysical logs (Dimitrakopoulos & Larkin, 2002; McGregor, 2003; Turner & Hatherly, 2003; Medhurst & Hatherly, 2005). In particular standard oil patch formation evaluation from geophysical logs in clastic rocks often entails estimating the quartz, porosity and clay content from density and gamma ray logs respectively.

The general assumptions that porosity in sandstone formations can be estimated using a rock matrix density of 2.65g/cc and that the natural gamma radiation from clays can be scaled to indicate clay content are not adequate and that more detailed assessments need to be made using additional geophysical data (Medhurst & Hatherly, 2005). This can come from neutron, resistivity and sonic logs. None of these logs should be interpreted in isolation because there needs to be consistency with all logs. This is an advantageous situation because a process of cross-validation can be introduced to allow the interpretation to be fine-tuned until the best match between all available data is obtained.

These estimates are made to assist lithological interpretation and to provide further insight into geotechnical properties, particularly in combination with sonic logs (Turner & Hatherly, 2003). Figures 12 and 13 demonstrate both current interpretation capabilities of the current interpretation software and how data can be combined to provide powerful background profiles to hazard planning.

LOGTRANS

ACA is investigating the potential of computer-aided interpretation of wireline logs and other borehole data for both geotechnical and geological purposes. To this end, LogTrans software is being incorporated into the processing sequence controlled by ACA's LASman (LAS processing software). The aim was to efficiently generate a 3D geotechnical model using all available wireline logs. LogTrans (Fullagar & others 1999, 2002, 2004; Alyffe 2002) interprets depth intervals according to the degree of similarity between their log signatures and the signatures recorded in a suite of representative control holes. Prior to application of LogTrans, therefore, it is necessary to statistically characterise the wireline log responses in the control holes. Preparatory control hole analysis has been completed at ACA's German Creek mine (Alyffe, 2002).

Previously geotechnical units were manually interpreted, but up to 12 different people were involved over a seven-year period that led to a loss of quality control. Preliminary auto-interpretation, based largely on UCS (uniaxial compressive strength) computed from sonic logs, successfully mapped variations in strength (Guo & others, 2000).

In the mine study (Alyffe, 2002) the immediate roof and floor strata for the German Creek seam are interpreted in terms of 'geotechnical units' which are differentiated by lithology, strength, and stratigraphic position. The geotechnical units are not uniquely defined in terms of their physical properties, e.g. strong fine-grained sandstones occur in both the roof and floor strata. Consequently, a new capability was added to LogTrans in order to ensure that the auto-interpretation is stratigraphically consistent as well as mechanically valid.

Geotechnical interpretation in the immediate roof and floor of the German Creek seam is controlled by an informal stratigraphy of geotechnical units. Initial LogTrans interpretations based primarily on sonic, density, and natural gamma logs incorporated far more detail than the original geotechnical interpretations. These initial LogTrans interpretations provided a valid indication of the variations in the rock strength, but did not honour the stratigraphic sequence of the geotechnical units. The initial computer interpretations were simplified and stratigraphically corrected using a second program, STRAT, with pattern recognition capability. The combination of LogTrans and STRAT successfully recovered the geotechnical interpretation almost everywhere within the control holes. Several independent (non-control) holes were also auto-interpreted correctly.

Given the agreement achieved between computer-aided interpretation and conventional geotechnical interpretation, a trial implementation is in progress. This trial will entail refinement of control information and processing procedures. It is recognised that the existing style of interpretation in terms of simplified geotechnical units is not optimal for mining hazard assessment, as there is a need to highlight possible delamination surfaces. The preferred final form of interpretation is likely to combine geotechnical units with a pictorial summary of thin weak zones detected by LogTrans. Outcomes of the work to date are as follows:

- LogTrans performance relies on the integrity of the control information eg the accuracy of the geological, geochemical, and geotechnical data from control holes and accuracy of geophysical logs.
- Moving from using wireline logs qualitatively to interpreting them quantitatively there are some issues between different logging companies.
- Borehole depths between the various geological and geophysical logs must be carefully reconciled to ensure proper characterisation.
- Interpretation performance is best where there is high petrophysical contrast between classes.

- The LogTrans results are encouraging for both geotechnical and lithological interpretation with prediction accuracy in excess of 90% has been achieved.

The LogTrans results are encouraging for both geotechnical and lithological interpretation (Figure 14).

CONCLUSIONS

There is a long history of surface and underground mining and mine geological experience within the ACA group. Geological and geotechnical information is collected to formulate reliable geological interpretations and forecasts to support mining operations and planning. None of the techniques outlined above could be used in isolation without the benefit of more than 39 000 boreholes compiled from various exploratory drilling programs over a period of 25 years. Recent advances in the resolution and computer-aided imaging and interpretation of the highlighted geophysical techniques have genuinely added to this substantial database for the evaluation of mine operating and statutory hazard plans.Individually, the downhole geophysical tools described above all have their weaknesses. Although downhole magnetometer results appear to be responding to the presence of dykes and sills, their resolution may not be sufficient for mine planning purposes. At present,

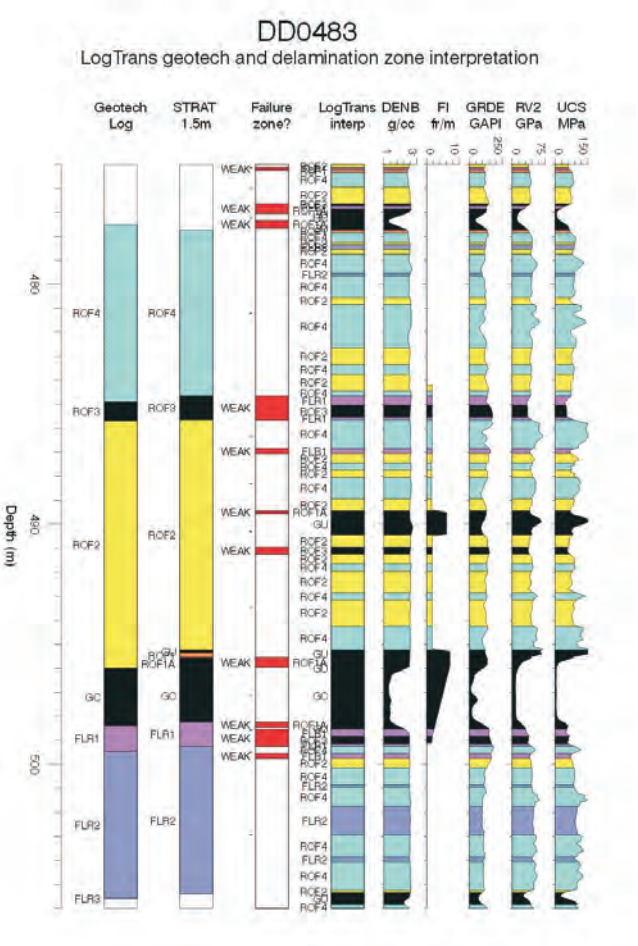

Figure 14: An Example of Logtrans Geotechnical Strata and delamination zone estimation for borehole DDH483, Grasstree Mine (modified after Ayliffe, 2002)

the potential of full waveform sonic logging has yet to be fully realised but it can help resolve faulting intersected by boreholes and provide more comprehensive rock strength estimations. Acoustic scanner data acquisition is still hampered by high logging costs and interpretation by the need to have specialist software and the necessity to develop reasonable interpretation skills. Dipmeter data contains some redundancy and requires other data to differentiate between bedding dip, joint or shear zone dip, and noise.

Despite these limitations, the use of these clearly targetted downhole geophysical surveys have provided substantial additional information to aid exploration and mine planning within Anglo Coal Australia. Unfortunately databases and mine planning software capable of holding this quantum leap of data efficiently are yet to be in widespread use, interpretive software is at a formative development stage for coal applications, and not widely available at mine sites.

Advances in full waveform sonic, dipmeter, and acoustic scanner techniques aside, sonic logging methods would still appear to show the most promise for unravelling rock mass character throughout the Bowen Basin. Therefore, the keys to expanded utilisation of geophysical logs for geotechnical purposes are:

- An improved understanding of the connection between petrophysics and geotechnical engineering, and
- efficient means for extracting geotechnical parameters from large volumes of wireline logging data.

REFERENCES

ALYFFE, M., 2002: Introduction to Logtrans: Computer-aided Geotechnical and Lithological Interpretation Wireline Logs, Anglo Coal (Capricorn Management Pty Limited), *in* Nichols, W. (Editor): Proceedings Anglo Coal Geomeet, May 2002, Gladstone, section E2, unpublished.

BIGGS, M.S. & HATHERLEY, P., 2000: An update on use of geophysical techniques to detect hazards at German Creek Mines, Central Queensland, *in* Beeston, J.W. (Editor): *Bowen Basin Symposium 2000 The New Millenium - Geology*, Geological Society of Australia Inc, Rockhampton, October 2000, 221-230.

BORSARU, M., BIGGS, M.S., NICHOLS, W.F. & BOS, F., 2001: The Application of prompt-gamma neutron activation analysis to borehole logging for coal, *Applied Radiation and Isotopes* **54**, 335-343.

DAVIES, A.L. & McMANUS, D.A., 1990: Geotechnical applications of downhole sonic and neutron logging for surface mining, *Exploration Geophysics*, **21**, 73-81.

DIMITRAKOPOULOS, R. & LARKIN, B., 2002: Maximising Benefits from Downhole Geophysics Logs recorded in Coal Exploration programs, End-of-Grant Report, Australian Coal Association Research Program, Project C8022A (unpublished report).

FIRTH, D., 1999: *Log Analysis for Mining Applications*, Reeves Wireline Pty Ltd, London.

FULLAGAR, P.K., ZHOU, B. & FALLON, G.N., 1999: Automated interpretation of geophysical borehole logs for orebody delineation and grade estimation, *Mineral Resources Engineering*, **8** (3), 269-284.

FULLAGAR, P.K., ZHOU B. & BIGGS, M.S., 2002: Automated geotechnical interpretation of geophysical logs, *in*, *Abstracts 8th International Symposium on Borehole Geophysics for Minerals, Geotechnical and Groundwater Applications, part 10*, Canadian Exploration Geophysical Society.

FULLAGAR, P.K., ZHOU B. & BIGGS, M.S., 2004: Stratigraphically consistent auto interpretation of borehole data, *Journal of Applied Geophysics*, **1441**, 360-373.

GREEN. D. & WARD, B., 2001: Determination of Goaf Delamination Horizons and other Roof Geomechanical Features using Downhole Acoustic Logs,: End-of-Grant Report, Australian Coal Association Research Program, Project C9003 (unpublished report).

GUO, H., ZHOU, B., POULSEN, B. & BIGGS, M.S., 2000: 3D overburden geotechnical characterisation for longwall mining at Southern Colliery, *in* Beeston, J.W. (Editor): *Bowen Basin Symposium 2000 - The New Millennium - Geology*, Geological Society of Australia Inc Coal Geology Group and the Bowen Basin Geologists Group, Rockhampton, October 2000, 67-72.

HATHERLY, P., 1998: Note on Full Waveform Sonic Logging, Centre Mining Technology Equipment, unpublished report, Sydney, November 1998, 1-14.

HATHERLY, P., MEDHURST, T., ZHOU, B. & GUO, H., 2001: Geotechnical evaluation for mining – assessing rock mass conditions using geophysical logging, End-of-Grant Report, Australian Coal Association Research Program, Project C8022b (unpublished report).

HATHERLY, P., SLIWA, R., TURNER, R. & MEDHURST, T., 2004: Quantitative geophysical log interpretation for rock mass characterisation, End-of-Grant Report, Australian Coal Association Research Program, Project C11037 (unpublished report).

McCLELLAND, P., 2001: High Resolution Downhole Ferret (Magnetometer) Survey, Logistics Report, 400s Panels, UltraMag Geophysics Pty Ltd, unpublished report for Capricorn Coal Management Pty Ltd, October, 1-8.

MacGREGOR, S., 2003: Maximising *in situ* stress measurement data from borehole breakout using acoustic Scanner and wireline tools: End-of-Grant Report, Australian Coal Association Research Program, Project C10009 (unpublished report).

MacGREGOR, S. & GALE, W., 2000: *In situ* stress measurement using acoustic scanner analysis of borehole breakout, *in*, Beeston, J.W. (Editor): *Bowen Basin Symposium 2000 - The New Millennium - Geology*, Geological Society of Australia Inc Coal Geology Group and the Bowen Basin Geologists Group, Rockhampton, October 2000, 97-106.

McNALLY, G.H., 1987: Geotechnical applications and interpretation of downhole geophysical logs, ACIRL Report No. 08/0621, unpublished report, July 1987.

McNALLY, G.H., 1990: The prediction of geotechnical rock properties from sonic and neutron logs, *Exploration Geophysics* **21**, 65-71.

MEDHURST, T. & HATHERLY, P., 2005: Geotechnical strata characterisation using geophysical borehole logs, *in* Peng, S.S., Mau, C., Finfinger, G., Tadolin, S., Wahib Khan, A. & Heasley, K., (Editors): *Proceedings of the 24th International Conference on Ground Control in Mining*, University of West Virginia, USA, 179-186.

MORRISON, C. & SMYTH, W., 2003: Hazard Mapping in an Australian Coal Mine, 3D modelling combining mapping with Acoustic scanner interpretation, Symposium of Sydney Basin Geologists Group and Standing Committee of Coalfield Geology, unpublished paper, Newcastle, November 2003.

SMITH, W., 2003: New Borehole Tool Developments by Auslog, Bowen Basin Geologists Group Meeting paper, unpublished, March 2003, Gladstone.

TURNER, R. & HATHERLY, P., 2003: Estimation of porosity, clay content and gas from multiparameter geophysical logs, Symposium of Sydney Basin Geologists Group and Standing Committee of Coalfield Geology, unpublished paper, Newcastle, November 2003.

WOOTTON, P., 2003: Improved Coal Seam Definition from Geophysical Log Data, Symposium of Sydney Basin Geologists Group and Standing Committee of Coalfield Geology, unpublished paper, Newcastle, November 2003.

ZHOU, B., HATHERLY, P., LE BLANC SMITH, G. & MAISON, I., 2002: Visualisation of 3D seismic and Full Waveform Sonic Data, End-of-Grant Report, Australian Coal Association Research Program, Project C9014 (unpublished report).

Mark Biggs, Chief Geologist, Anglo Coal (Dawson Management) Pty. Limited, PO Box 225, Moura. QLD. 4718.

Ross Seedsman

Evolution of geotechnical models for roadway development and longwalling in thick coal seams

In 1990, thick coal seams were defined as those greater than 4m thick and there had been continuing research on how these seams could be adequately extracted by underground methods. A National Energy Research, Development & Demonstration Council (NERDDC) funded project documented the possibility of 6m high longwalls. In 1990, the concerns with the longwall face were focussed on the difference between 2 and 4 leg supports, the possible need to increase support load density to compensate for increasing height, and on the role of joints and cleats defining unmanageable face spall. Predicted roadway conditions were based on extrapolation from other mines.

The question of 2 versus 4 legs was unresolved, the support load density was not increased, to maintain the same amount of leg closure the set to yield ratio was increased, and flippers were recommended to steer face spall to the AFC. By the end of 2005, there have been 8 faces operating in Australia between 4m and 5m, none at 6m. They are all 2 leg supports with capacities of up to 1053t, and support load densities of 112t/m^2. Face stability and spall has been of concern to some of the operations. Typically, development roof conditions have been good and some operations have experienced poor ribs. Tailgate stability has been more problematical than maingate stability. A revision of our understanding of horizontal stresses in coal has been necessary.

INTRODUCTION

The recovery of thick coal seams has been the subject of research for many years, with the objective of maximising high reserve recovery. The thicker the seam, the lower is the reserve recovery achievable from first workings; the constraints of high faces also apply in pillar extraction panels and longwalls. By 1990, high-production longwalling had been demonstrated to be achievable in Australia for seams up to about 3.5m. Reserve recovery in thicker seams was of concern, particularly to the Queensland Coal Association. In industry funded research, multi-slice longwall had been investigated for Ulan and multi-slice pillar extraction for Collinsville.

'Thick' seams were defined to be those beyond the reach of current longwalls in Australia at the time — in 1990 this meant anything greater than 4.0m. There were faces operating at between 4.0m and 4.7m height in the USA, Germany and Bulgaria at the time. In 1990 there were only 3 longwalls in the Bowen Basin — Central, Southern, and Cook. Since that time there have been a number of high reach faces installed — Dartbrook (4.8m), Moranbah North (4.8m), Newlands (5.0m), North Goonyella (5.3m), West Wallsend (5.3m), and Mandalong (5.0m). Broadmeadow (4.5m) is scheduled to start extraction in July–August 2005.

The Upper Newlands Seam was the subject of a National Energy Research, Development & Demonstration Council (NERDDC) project on the feasibility of operating a 6.0m high face (Roberts & Seedsman, 1991). The structure of the research was to use Newlands Mine as a case study to work through all the steps in specifying a longwall mine. There was excellent cooperation from the suppliers who were asked to submit equivalents to tender documents. There was no obligation for Newlands Coal Pty Ltd to accept any of the recommendations or tenders. Australian Coal Industry Research Laboratories (ACIRL) were the prime contractor for the research, and the author was their project manager. This paper compares the status of geotechnical knowledge in 1990 with a range of experiences and new insights developed over the last 15 years.

DEVELOPMENT ROADWAYS

1990

In 1990 the latest machines were the Joy 12CM20 and the Jeffrey 2048CM; the Alpine Bolter-Miners (ABM 20) had not yet appeared.

In the NERDDC project, it was recognised that development height should be less than the 6m extraction height, and for the coal quality reasons a coal roof was to be left. The roof and rib support designs were based on the extrapolation of conditions from other mines. By reference to experiences under coal tops at Ulan, Collinsville, Harrow Creek (trial colliery at Peak Downs) and Box Flat No 9 (Ipswich) it was anticipated that roof conditions would be benign under a coal roof. In particular, there was a reference to good coal roof at 550m depth at Box Flat.

In the case of ribs, the possible role of adverse orientation to cleat was recognised for the proposed 4m high roadways, and the recommendation was made not to align the roadways parallel to either cleat set and particularly a moderately-dipping angle shear. It was known that at Harrow Creek the ribs deteriorated noticeably beyond 250m depth and that large sheet-type failure developed during pillar splitting. Rib research in the 1980s referred to MIF — mining induced failure (O'Beirne & others, 1986).

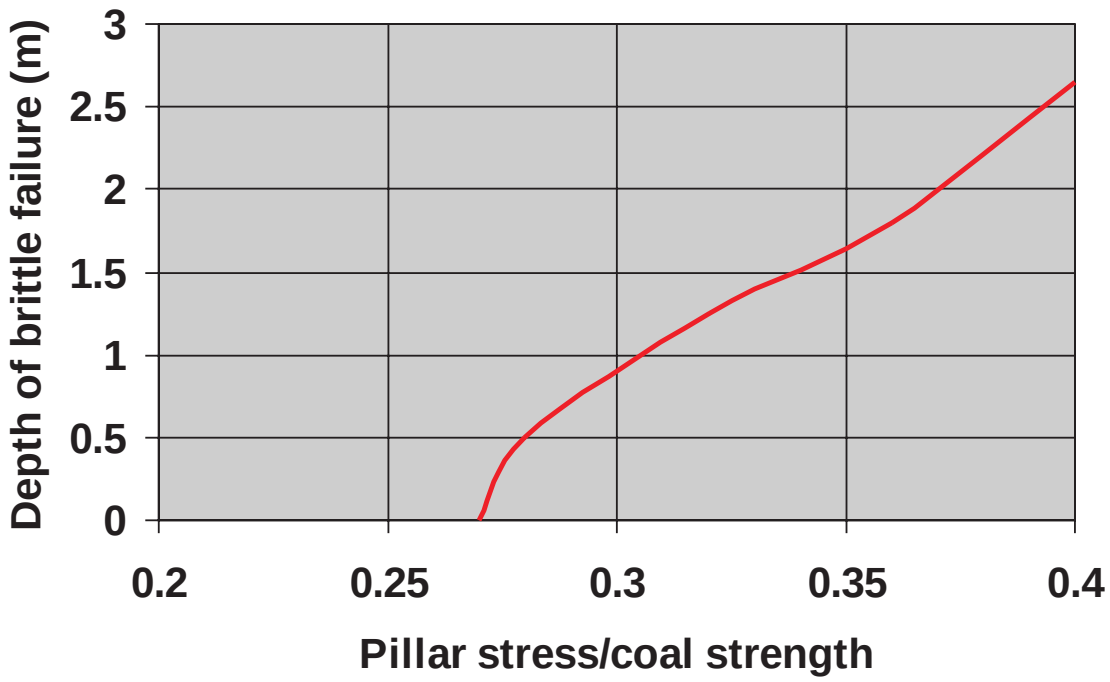

Figure 1: Onset and depth of brittle failure in coal ribs

The NERDCC report made reference to the then emerging knowledge of the role of alignment to principal horizontal stress directions. There was no incorporation of this into the specification of the roof support.

2005

Observations of roof instability in the Goonyella Exploration Adit Project (GEAP) in 1999–2000 suggested that coal roofs can be exposed to the onset of tensile stresses and that there are very high compressive stresses in the ribs (Seedsman & others, 2002). This had been partly anticipated from the work of Enever & others (2000) that had identified "anomalously" low minimum horizontal stresses in coal seams during hydrofracturing research in coal seam methane. However, the scale of the de-stressing was greater than anticipated. Subsequent measurement of the stresses in coal from underground openings at GEAP using the overcore technique indicated a stress field where the vertical stress is the major principal stress. Similar results have been reported from Moranbah North and North Goonyella and it is understood from Ulan and Newlands.

It is now believed that the stress field in coal depends on the state of drainage of water and possibly gas (Seedsman, 2004). As the seam is depressurised by the drainage of water ahead of mining, the coal compresses in response to the increase in effective stress. As it compresses it decouples from the overlying stone and any 'tectonic stress' is redirected into the stone. As the area of coal compression extends outwards, the overlying stone sags and reloads the coal. Horizontal stresses are induced in the coal under this lithostatic loading condition, with their magnitude related to the Poisson's Ratio of the coal. The induced horizontal stresses in coal immediately ahead of the face are as low as 20% of the vertical stress. The vertical stresses may increase with time depending on the rate of drainage and mining advance — there is evidence that at the face it may be about 50% of that related to simple overburden loading.

With this new model for coal stresses, the roof conditions are more readily explicable. For a stress state where the vertical stress is substantially greater than the horizontal stress, simple elastic theory states that the roof stresses will be less than the far-field horizontal stress and the ribs will be heavily loaded. These changes are greater if the width of the roadway is increased compared to its height.

Coal roofs, so long as they are thickly bedded, may be intrinsically stable and require low support densities. Thinly bedded coal seams can delaminate under self weight and be difficult to reinforce due to the loss of resin/grout in the highly dilated blocky mass. Alignment of roadway parallel to joints and normal faults can result in poor roof conditions due to the collapse of joint blocks in an environment of very low confining stresses or the onset of tension.

The new stress model for coal, when combined with evolving understanding on the behaviour of brittle rock, provides a better understanding of MIF. It is considered that coal can be considered to be a brittle material and hence the recent work in Canada on brittle rock (Martin & others, 1999) can be applied — the key one being that cohesion and friction are not mobilised simultaneously at low confining stresses. As a result, the failure criterion for coal near to an excavation should be based on the Hoek-Brown criterion with m = 0 and s = 0.11.

The combination of the stress and brittle coal models leads to the prediction that the onset of poor ribs occurs when the pillar stress/UCS ratio exceeds 0.27 (Figure 1), and that rib

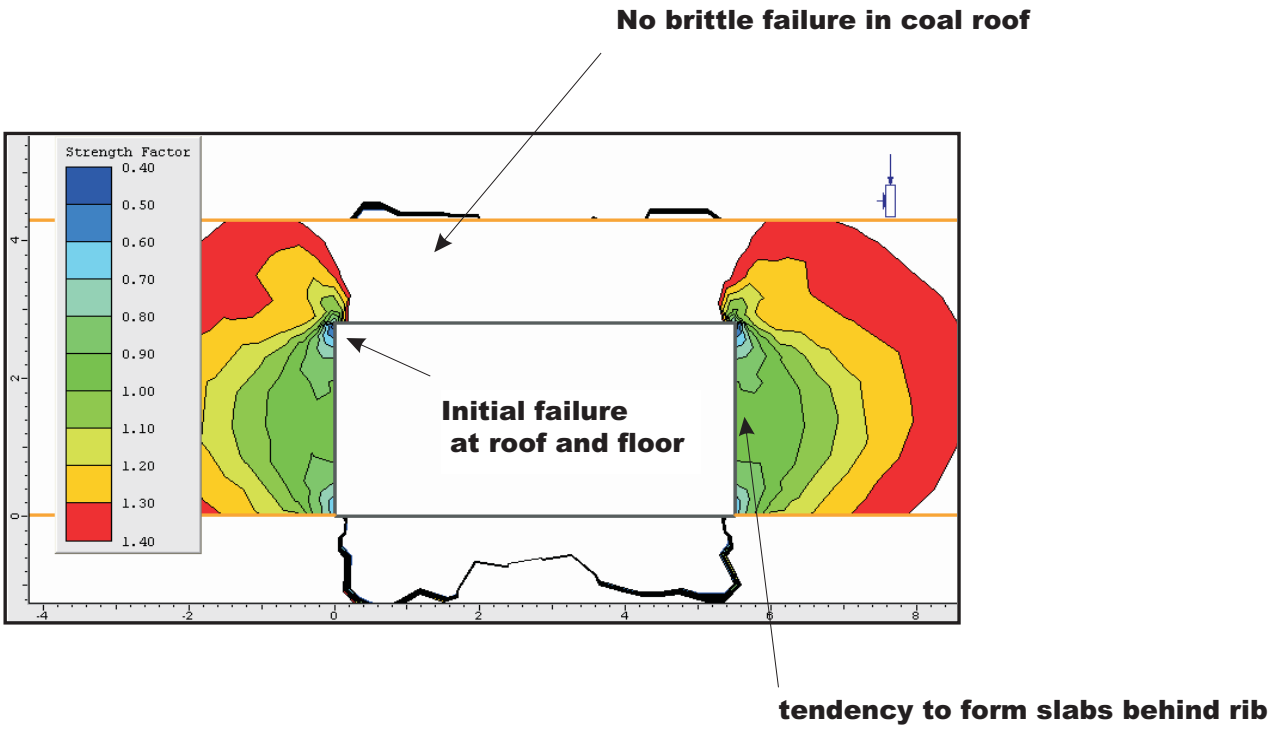

Figure 2: Patterns in the formation of mining induced fractures in coal

failure is localised initially at the roof and floor corners, with the tendency to define vertical slabs (Figure 2). This behaviour can develop not only in gateroads but also on the longwall face.

It is important to note that MIF can only form by this mechanism if there are no pre-existing discontinuities that allow a failure mode to develop at lower stresses (e.g. planar or wedge slide).

LONGWALL FACE

1990

In 1990, 19 of the 25 Australian faces used 4 leg supports whereas, for the longwalls in excess of 4m operating overseas, only 1 of 8 used 4 leg supports (Daw Mill in the UK). The NERDDC research did not make a recommendation on the leg configuration of 6m supports.

The maximum support capacity in 1990 was 800t with a support load density of approximately 100t/m^2, for a face operating in the Wollongong district. At the time, the detached block model for support capacity (Wilson, 1986) was in vogue, and this proposed that the block height was a function of the extracted thickness. It was argued that the detached block model may have some validity but that the relationship of height to extraction thickness was not justified. A support load density of 100t/m^2 was recommended for what was considered to be readily caving strata.

The issue of convergence of the face was recognised and arguments presented in terms of ground reaction curves. Maintaining the current convergence between set and yield of about 6mm was recommended, and the implication of this was a need to increase set to yield ratios from the typical 80% to about 90%.

The possibility of face spall from high on the face was recognised, and the ability to 'steer' face coal onto the AFC using a flipper was recommended. Routine deployment of face sprags was not recommended as the view was that spall blocks would only form at the top of the seam related to roof deflection and hence could be controlled with flippers. Face sprags were recommended for protection during maintenance. As part of this general concern, the use of a walkway behind the legs was recommended.

Alignment to cleat and other coal seam discontinuities was given particular attention, with the concern that the higher ribs would result in large blocks falling on the face (Figure 3). There was reference to UK work that had shown poorer face conditions develop if the face is within 20–30° of the strike of the cleat (Farmer, 1985). At Newlands, there was also a concern for a 45° dipping shear in the seam and angled bedding in the roof.

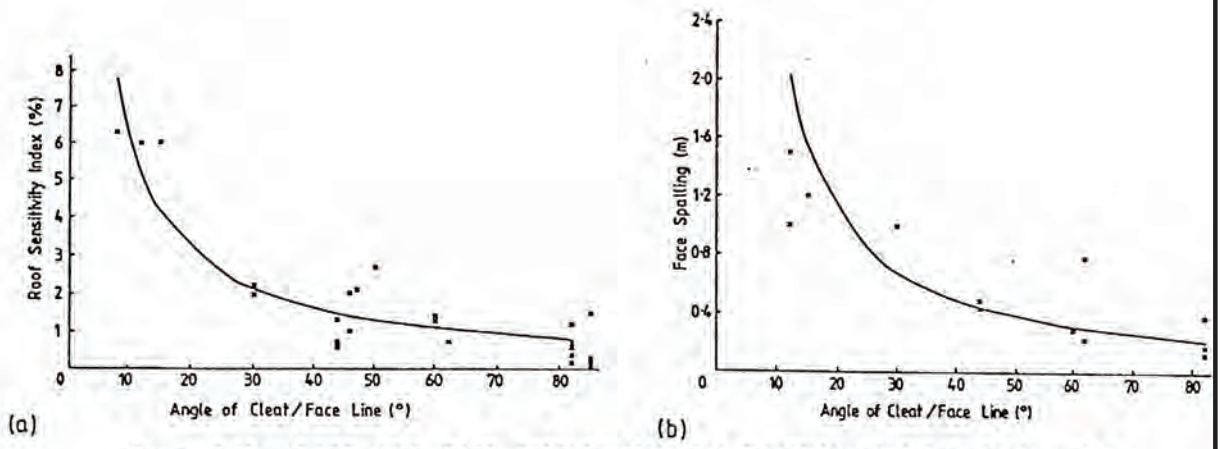

Figure 2.10 ROOF AND FACE INSTABILITY AS A FUNCTION OF CLEAT/FACE ANGLE

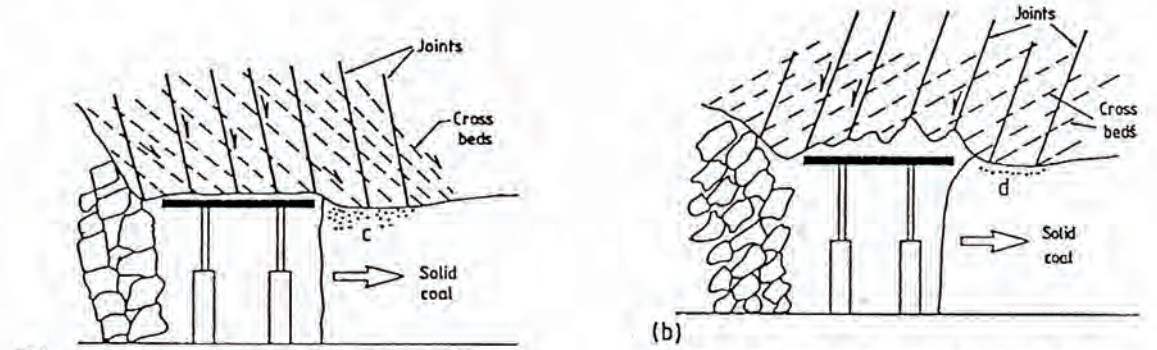

Sketch cross sections of geological structures and longwall faces (after Kidybinski 1962 and Wilson 1970). Large arrows indicate direction of face advance; small arrows indicate movement of roof blocks above support. Dotted area ahead of face indicates area of highest seam loads where c is greater than d.

Figure 2.11 ROLE OF ROOF STRUCTURE ON LONGWALL FACE BEHAVIOUR

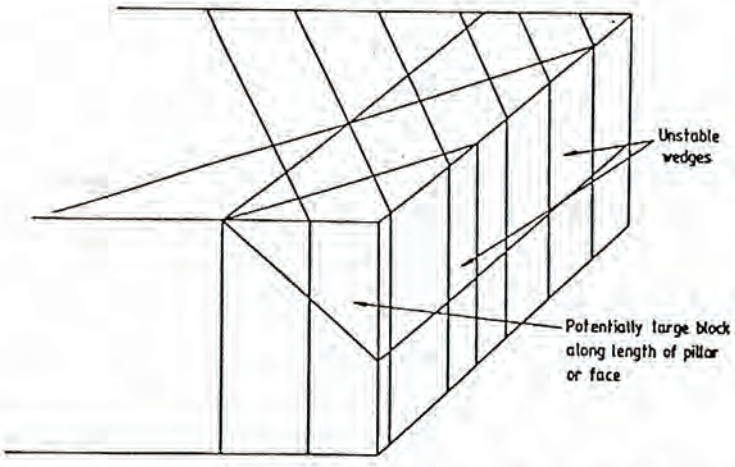

Figure 2.12 SCHEMATIC DIAGRAM OF CLEATS AND ANGLE SHEARS ON

Figure 3: Impact of seam discontinuities on face control

2005

Since 1990 all new longwall faces in Australia have been 2 leg faces, and there are now only 10 out of 25 faces that use 4 leg supports. The most recent supports for thick seams are 980t with a support load density of 106t/m^2 and a set to yield ratio of 90% (Moranbah North, Newson, 1999) and the 1053t supports at Mandalong (112t/m^2, 87% set to yield).

There has been no significant advance in specifying support capacity or support load density as a function of the geotechnical environment — it is considered that the industry is managing this risk by purchasing the highest available. There is a question as to whether this is driving the trend to heavier supports or if the demand for extended cycle life is providing the opportunity to increase capacities. Longwall geotechnical research has recognised that support performance is a function not only of hydraulic capacity but also of displacement and time, and focus is moving to maximising control of the tip to face area and avoiding adverse geologies. Ground reaction concepts have been reintroduced and good progress is being made (Medhurst, 2005).

The operational importance of alignment away from cleat is being recognised. Firstly, controlled and regular loading of the AFC is achieved if cutting of the coal by the shearer is maximised — face slumping overloads the AFC, sometimes with large blocks that cannot pass under the shearer or through the BSL. Geometric considerations reveal that this problem increases to the square of the face height. Secondly, the tip to face is better controlled if there is no face slumping, recognising that any loss of tip to face increases in direct proportion to the increased face height.

It has been observed in many of the thick coal seams that there is a dominant sub-vertical discontinuity in coal, which extends through the full thickness of the coal seam and with a very high lateral persistence. In a pure sense, this could be better termed a joint. If present, the complementary joint set is poorly developed. It would appear that the unstable wedges identified in 1990 can develop when only one joint set is present as a result of interaction between the joint and MIF. If face spall control is considered to be a major factor in determining longwall panel orientation, a longwall face at right angles to the strike of the coal joint is preferred. It is noted that such a decision introduces slab hazards in the ribs of the gateroads at shallower depths than those at which a similar hazard develops because of MIF.

PILLAR DESIGN

1990

Due to the lack of Australian guidelines at the time, chain pillar design was very conservative and used a pillar strength equation derived from laboratory testing of the Upper Newlands Seam (strength = 5.5 * (0.75 + 0.25 pillar width/pillar height), a pillar height equal to the extraction height, and an equivalent factor of safety of 1.56.

2005

In 2005, there are now 2 pillar design approaches available for Australian coal operations — Galvin & others (1999) for bord and pillar operations and Colwell (1998) for tailgate pillars. They use different pillar strength equations and it is important that these are not interchanged. An unresolved issue is the decision on the pillar height to use in these empirical equations. While it can be argued that a fall of top coal may increase the effective height of pillars, it is highly unlikely that the same concern applies if the gates are located in the top of the seam and there is a step in the floor as the shearer enters the tailgate.

Tailgates have been problematical in some of the thick seam operations, with poor ribs (Tarrant & others, 2002) and roof instability limiting egress and ventilation. A possible origin of the poor ribs has been outlined above. Seedsman (2001) has argued that tailgate roof instability is related to the reduction of roof stresses due to the rotation/extension of the roof line if the chain pillar yields at the tailgate corner. This mechanism will be particularly significant if a coal roof is already under very low confinement.

CONCLUSIONS

From a geotechnical basis, the introduction of thick seam longwalls into Australian operations in the Bowen Basin and New South Wales has been characterised by well-performing face supports, without the need to increase capacity as a function of extraction height. The impact of coal joints on face productivity is perhaps greater than expected.

By comparison, development and tailgate issues have been more significant. Coal tops are performing better than expected, although there was a precedent from the old mines at Collinsville and Ipswich. The high ribs are presenting greater problems than the roof, and there needs to be more work on how to optimise support installation and performance. There remain some unresolved issues on tailgate pillar design.

The recognition of the different stress field in coal compared to overlying stone, combined with the concepts of brittle rock failure should underpin future improvements in thick seam longwall operations.

REFERENCES

COLWELL, M., 1998: ACARP Project C6036, Chain Pillar Design – Calibration of ALPS, Report to ACARP.

ENEVER, J.R., JEFFREYS, R.G. & CASEY, D.A., 2000: The relationship between stress in coal and rock, *In* Girard, J. & others (Editors): *Pacific Rocks, Rock around the Rim:*

Proceedings of the Fourth North American Rock Mechanics Symposium, Seattle. Balkema.

FARMER, I., 1985: *Coal Mine Structures*, Chapman and Hall, London.

GALVIN, J., HEBBLEWHITE, B.K. & SALAMON, M.D.G., 1999: University of NSW coal pillar strength for Australian and South African mining conditions, *In Proceedings Second International Workshop on Coal Pillar Mechanics and Design*. NIOSH IC 9448.

MARTIN, C.D., KAISER, P.K. & McCREATH, D.R., 1999: Hoek-Brown parameters for predicting the depth of brittle failure around tunnels. *Canadian Geotechnical Journal*, **36**, 136–151.

MEDHURST, T., 2005: Practical considerations in longwall support behaviour and ground response, *In* Coal 2005, Moving Technology – Maintaining Competence. *6th Australasian Coal Operators' Conference*, Australasian Institute of Mining and Metallurgy.

NEWSON, S., 1999: A New Millenium Longwall. The Second Longwall Mining Summit, Yeppoon, Australian Journal of Mining.

O'BEIRNE, T., SHEPHERD, J., RIXON, K. & NAPPER, A., 1986: Coal rib stabilisation — a new perspective. *The Coal Journal*, **14**, 7–11.

ROBERTS, B. & SEEDSMAN, R.W., 1991: Geotechnical, mining, and equipment issues for 6m high single pass longwalls. *The Australian Coal Journal*, **33,** 15–31.

SEEDSMAN, R.W., 2001: The stress and failure paths followed by coal mine roofs during longwall extraction and implications to tailgate support, *In* Peng & others (Editors): *20th International Conference on Ground Control in Mining*, Morgantown, West Virginia University.

SEEDSMAN, R.W., MITCHELL, G. & BRISBANE, P., 2002: Strata management at the Goonyella Exploration Adit Project, *In* Aziz & Kinnimonth (Editors): *Coal 2002 3rd Australian Coal Operators' Conference*, Wollongong, Illawarra Branch, Australasian Institute of Mining and Metallurgy.

SEEDSMAN, R.W., 2004: Failure modes and support of coal roofs, *In,* Villaescusa & Potvin (Editors): *Ground Support in Mining and Underground Construction*, Balkema, 367–373.

TARRANT, G., DOYLE, R. & MILLS, K., 2002: Investigations aimed to improve tailgate serviceability at Dartbrook Mine, *In* Aziz & Kinnimonth (Editors): *Coal 2002 3rd Australian Coal Operators' Conference,* Wollongong, Illawarra Branch, Australasian Institute of Mining and Metallurgy.

WILSON, A.H., 1986: The problems of strong roof beds and water-bearing strata in the control of longwall faces. The AusIMM Illawarra Branch, Ground Movement and Control related to Coal Mining Symposium, August 1986.

Ross Seedsman, Seedsman Geotechnics Pty Ltd, Mount Kembla

Chris Hanson, David Thomas and Bob Gallagher

The value of early geotechnical assessment in mine planning

Valuable data for geotechnical interpretation and integration into effective Australian underground mine planning may often be available, yet is not always fully appreciated or utilised, particularly in the early stages of mine planning or in due diligence studies. There may be considerable benefits associated with early prioritisation of geotechnical evaluation and impact on mine planning.

Unidentified, misinterpreted, or ill-defined adverse geological and related geotechnical resource characteristics can pose significant business risk to underground coal projects and operations. Preliminary resource definition in the early conceptual mine planning stages attributes significant focus (entirely warranted) on resource quality and structural geology constraints. Yet detailed geotechnical data analysis and interpretation, which may have a substantial down stream impact and sensitivity with respect to future mine planning strategies, at times is given lower priority, or scoped and resourced in the later stages of a bankable feasibility study. Through extensive mine planning experience and observation of downstream process impacts, it has been found there is often data available for geotechnical analysis that does not readily stand out or is not adequately understood or utilised, available at the early (conceptual) stages of mine planning. Part of the issue may be that exploration geologists are not necessarily experienced geotechnical engineers and do not necessarily recognise or understand all important parameters. Subject to appropriate application of experienced professionals data can be manipulated to provide key geotechnical hazard assessment at minimal cost, and provide a framework for understanding and optimising the mine planning process.

Although there is no single prescribed strategy for resource evaluation from a geotechnical perspective, potential business risks and mitigation approaches can and should be adopted at the conceptual mine planning stage. There has been a recent focus in the metals industry to provide a reporting framework for geotechnical classification of mining projects. This paper outlines the strategies and gives examples of key analyses adopted in mine planning and discusses the relative merits of adopting a reporting framework as a tool for geotechnical classification in mine planning.

INTRODUCTION

A well known, but not necessarily implemented, fact is that geotechnical assessment forms a key driver in project viability. Primary consideration should be given to the likely mine planning implications arising from geotechnical interpretation. Significant expenditure is often attributed to the acquisition of exploration data, yet at times there appears an imbalance between resources attributed to data acquisition, processing and presentation, compared with that dedicated to comprehensive interpretation and risk assessment of relevant geotechnical data and subsequent integration into mine planning processes. There is almost always relevant geotechnical detail that can be manipulated from any form of geological exploration, that should be appropriately assessed in the conceptual mine planning process onwards.

This paper outlines experience with respect to geotechnical assessment in the context of mine planning and balanced against other key drivers. It is non-specific with respect to case histories, but rather, examines generically the experiences gained through numerous sources including:

- practical operational mining experience,
- due diligence studies, in particular auditing resource and reserves and assessment of attributed valuation and risk assessment,
- designing, costing and project managing exploration programs,
- analysing and interpreting data from exploration, in particular with respect to geological interpretation and associated geotechnical analysis at all stages of mine planning, and
- completion of geotechnical evaluation at concept, pre-feasibility and feasibility study levels for coal projects.

A discussion outlining specific forms of geotechnical data that can be interpreted to add significant value at the early stages of mine planning is outlined. In mine planning, it is desirable to establish an appropriate level of geotechnical risk assessment balanced against other key drivers at each stage of the mine planning process. In conclusion, the relative merits of a reporting framework for geotechnical classification of coal mining projects are debated.

THE MINE PLANNING PROCESS

Stages of mine planning

The major stages of mining project development are set out below in Figure 1. At the end of each stage, a business case is generally made to justify progression to the following stage. A subsequent increase in exploration, data compilation, analysis and interpretation and mine planning input is required as the project development process unfolds,

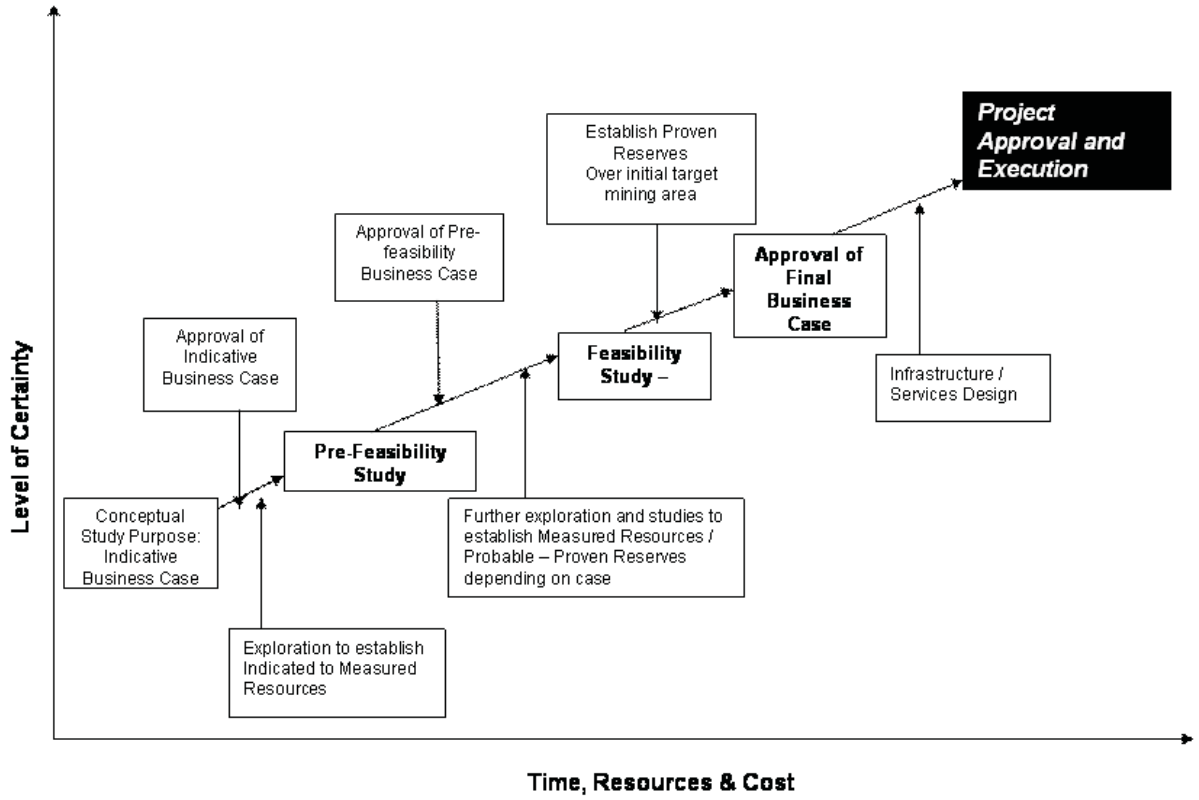

Figure 1: Typical stages in mining project development

with an associated increase in committed human and physical resources and total cost.

At each stage in the planning process, the level of certainty with respect to project value and confidence in the specific resource and reserve characteristics increases. The prime consideration is project value and ability to achieve the projected production levels, operating cost and sales price. Geotechnical aspects affect two of these three primary determinations. Key measures of project value include:

1. *Fair market* value of each project under consideration, determined by current market conditions and price.

2. The *intrinsic* value of each project under consideration, determined by current worth and potential future earning power. Intrinsic value can be assessed at a conceptual stage using appropriate Valmin Code guidelines, however, detailed intrinsic valuation is usually estimated from pre-feasibility onwards, where net present value can be attributed over a given timeframe with discounted cash flows.

3. The *strategic* value, usually reflecting a higher value attributed due to such factors as geopolitical advantages, economies of scale or reducing competition. Strategic value may also be in the context of brownfields expansions that may reduce overall unit cost of total production output and/or make exploitation of nearby deposits more attractive or more competitive to the company than its peers.

Typical project ranges with respect to the accuracy of project valuation during each of the mine planning stages are illustrated in Table 1.

Conceptual mine planning studies are typically based on a level of established exploration data, historical information and inferences from regional and benchmarked experience. From the perspective of project viability this level of analysis generically represents a broad-brush assessment of possible viability, considering as wide a range of alternative scenarios and options as necessary. None the less, a business case must be made to proceed to pre-feasibility, which upon approval often requires substantial commitment of expenditure to advance the project through pre-feasibility.

When assessing either a single project or considering a portfolio comprising a number of potential projects with a strategy to narrow the field for further development, there is considerable justification in utilising all available data sources and committing to comprehensive use of all valid data and key screening criteria at this time.

This is a fundamental requirement for:

- minimising costs and resources otherwise dedicated to projects or resource areas that may not ultimately be viable, and
- presenting a balanced and authentic assessment of project potential such that viable projects are not overlooked at the outset, particularly with respect to previous resources where preconceptions may exist.

An analysis using appropriate valuation tools on various scheduled mine plan options is justified at this stage of the

Table 1: Estimation of project valuation accuracy by stage

Type of estimate	Conceptual	Pre-feasibility	Full feasibility	Definitive
Purpose	Indicative business case for JV	Establish project scope and criteria	JV approval	Project cost control
Resource status	Inferred to indicated	Indicated to measured	First ten years measured	First ten years measured
Reserve status	Possible to probable	Probable	First ten years proven	First ten years proven
Possible range of costs around central estimate	30%	20%	15%	5%
% of design effort required to produce estimate	0.5%–5%	5%–30%	30%–45%	45%–65%
Normal estimating method	Scaled historical data	Factored budget quotes	Engineering estimates, firm quotes	Engineering estimates, full take-offs

project, and is either presented as a case for proceeding with project development or otherwise discarding. When assessing larger project portfolios, a matrix incorporating value and other strategic factors may be compiled and allow for ranking and comparison across a range of projects. Quantifying, qualifying, and benchmarking project geological and geotechnical risk should be conducted at this stage. If the business case is verified, additional resources are committed to develop a project to a pre-feasibility level of assessment.

A pre-feasibility level of study allows for detailed comparison of key mine planning and strategic alternatives and usually facilitates confirmation of one or two of the most attractive options presented at concept level. Cost estimates and economics should be sufficiently accurate to select options and justify expenditure to bring the project to bankable feasibility.

A feasibility study is used to secure a commitment to finance. It presents a summary of the risks and mitigation strategies allowing a company or bank to risk weight lending rates. Cost estimates and economics should be sufficiently reliable and robust for decision on project approval to be made. Project valuation accuracy should be targeted at 10–15% at this stage.

Often bankable feasibility study (BFS) mine plans become set in stone. Operations personnel may use limited initiative to revise or review, particularly if not privy to or informed of the key drivers leading to the derivation of the plan. If these key drivers change, then the BFS layout, schedule, and economics should be reviewed, and if warranted, revised.

The mine planning team

In a typical mine planning process, resources are assessed based on (minimum) industry guidelines. Such guidelines include:

- Australian Standard for Metallurgical Coal Projects,
- The Australasian Institute of Mining and Metallurgy Monograph 12, and
- internal company or corporate advice or structured guidelines.

Mine planning options are formulated, and productivities and costs are assigned within an economic model and scheduled to arrive at an estimated value. This may resemble more a comparative fair market value at the conceptual stage, and an NPV through discounted cash flow/rate of return over a fixed period from pre-feasibility onwards. Care should be taken as there will often be a tendency to overestimate value at this stage, unknown conditions may present a lower hurdle rate for screening. The typical involvement of relevant parties in this process is as follows:

Qualified geologists assess the resource quality, seam characteristics and structure, provide a resource status classification and, in combination with others, devise and manage exploration programs to reach required resource status classification.

Qualified mining engineers assess reserves based primarily on geological constraints provided, usually by way of a plan from geologists. Underlying geotechnical concepts are factored in, often based on a broad assessment of regional stress data and anticipated ground conditions, from the information provided by the geologists. In general, mining engineers are responsible for generating mine planning options and economic models from which reserves are generated and classified based on the assessed recoverable (economic) resource.

Business analysts and coal quality experts traditionally have a role in assessing key economic assumptions and sensitivities flowing forward, usually in the form of market placement and exchange rate or price fluctuations.

Marketers and corporate personnel who may identify a market niche and gain commitment from buyers.

As with consideration of mine planning components and parameters, a holistic approach should be used with individual parties working together as a team, rather than in isolation in defined roles on projects, as critical for delivery of an impartial and comprehensive mine planning process.

The team of professionals dedicated to resource and reserve assessment and project valuation at progressive stages of the mine planning process will clearly depend on the nature and characteristics of the project being assessed. Consistent with the mine planning approach as previously outlined, be it open cut or underground mining assessment potential, the most important point at which comprehensive analysis and risk assessment by mining professionals with appropriate relevant experience from available data is warranted is, arguably, at the conceptual stage. This is consistent with a philosophy of presenting a balanced (and in the case of multiple projects fair comparison) of project potential.

Dedicating comprehensive expertise at this stage will assist in minimising the expenditure committed to projects, which are not ultimately viable, and reduce the potential for ill-considered relinquishment of potential projects. One of the fundamental areas to minimise downstream mining risk that should be most comprehensively assessed at the concept stage, is that associated with analysis of structural geological, geotechnical and hydrological/hydrogeological parameters.

Opportunity and constraints with respect to resource coal quality, structure (faults), and resource recovery are always (rightly) key drivers in determination of project viability and mine layout. However, other geotechnical parameters may often be overlooked at the concept stage. The first mine layout option(s) is extremely important, as it forms the blue print for each successive stage of project development. Once committed to paper, it can be difficult to change, particularly if the change results in reduced resource recovery.

In keeping with the above argument, there are major benefits in utilising and integrating a team of experienced professionals in concept mine planning studies who have a broad range of exposure and skills in:

- practical geological/geotechnical open cut or underground operational mining and exploration experience,
- conceptual through to bankable feasibility level mine planning studies and due diligence studies for an extensive range of resources and clients, and
- economic evaluation and project financing.

The major benefits in applying appropriate expertise and strategy at concept level relate to:

- providing capacity (through experience base) for formulation of hazard plans, risk ranking, and risk assessment from a comprehensive review of all available data, such that critical issues and strategies are developed and integrated into the mine plan process,
- targeting future exploration and scoping feasibility studies to ensure that critical issues are addressed in appropriate depth and in a timely fashion with respect to landmark requirements in project development, and
- evaluating and comparing mine planning options and sequences incorporating assessed geotechnical risk parameters against other key drivers such as optimising resource extraction, resource quality and economic return.

Assessment of parameters

With a suitably selected team, preliminary assumptions and measured risks relating to the parameters assessed from available data can then be developed. The key in achieving a balanced assessment of parameters is to integrate the major components under the same analysis, rather than treat each in isolation.

Assessment at this stage (in addition to economics based on resource quality), should include as a minimum:

- site-specific tenement constraints or future project risks, for example subsidence under rail, road or waterways, strata title issues, property ownership etc,
- potential hydrological or hydrogeological risk associated with water ingress due to perching aquifers, surface to seam flows or associated slope stability issues in open cut mining,
- approximations of significant (mine plan constraining) geological structure from observed major RL displacements and regional knowledge,
- approximations of joint/cleat orientations from regional inferences and the associated impact on mine planning options, and
- overburden, seam and floor characteristics; more specifically rock mass and material properties and their impact on slope stability and bench orientation in open cut mining or heading stability or caving characteristics in underground mining.

Due consideration, risk analysis and sensitivity analysis of various planning options at conceptual level based on comprehensive analysis and interpretation of available data including resource quality, economic, geological and geotechnical parameters is essential to deliver:

- An assessment(s) of project risk and value that is more likely to be validated than refuted by future (down stream) exploration studies and analysis.
- Should business approval progress to pre-feasibility, an exploration program and study design can be delivered with sound logic based on the conceptual study findings and identified areas for further investigation. This can incorporate adequate and appropriate data collection and testing requirements, procedures and analysis/reporting requirements to maximise the understanding of project risks. In depth detailed team planning will almost certainly optimise exploration expenditure through prioritising exploration and analysis requirements relating to project development needs.

- Reducing the surprises in downstream project development. Getting it right here may even go a long way to delivering everyone's ultimate goal; a mine plan that evolves into a mining operation that optimises economic return and delivers few surprises.

KEY GEOTECHNICAL ASSESSMENTS AT THE CONCEPTUAL STAGE OF MINE PLANNING

There are a number of key data sources that frequently exist at a conceptual mine planning stage, from which priority geotechnical assessments can easily be made and assessed in balance with other important factors, (including hydrological, gas, etc). The following presents a descriptive general approach in such assessments and includes hypothetical examples.

Geology and geotechnical inputs at concept mine level are clearly interlinked and not mutually exclusive. The scope of a concept study would clearly reflect the type of mining being considered — open cut or underground. For example an underground longwall conceptual study may include the following sections:

- coal quality (impact on reserves and various);
- geology:
  - » description of target formation,
  - » regional geology, structural trends and coal measure sequence,
  - » specifics of exploration undertaken, exploration history and current resource status,
  - » structural trends,
  - » intrusives,
  - » description of coal measures and individual seams,
  - » topography,
  - » hydrogeology, and
  - » seam gas;
- geotechnical considerations:
  - » roof and floor conditions,
  - » seam conditions,
  - » stress magnitude and orientation,
  - » jointing and cleating,
  - » pillar dimensions,
  - » ground support requirements,
  - » consideration of longwall cavability,
  - » multiple seam mining implications, and
  - » consideration of *in situ* horizontal stress on mine layout.

Once relevant geological and geotechnical inputs have been scoped for the deposit and mining method being considered, analysis of each parameter is required. The following outlines some of the data and associated analysis regarded as essential to address key issues at this stage.

Previous research, back analysis and benchmarking previous industry experience and learning

Internet and library sources provide a ready source of publicly available information in Australia, the US, and elsewhere on everything from multi-seam mining experience and associated panel\pillar design history and methodologies, to benchmarking productivities relative to different geotechnical environments. Where appropriate and comparative, such information can be used to benchmark performance and anticipate likely ground behaviour with respect to resource and reserve assessment. This can be further used to influence downstream decisions on such factors as mining method, mine layout, and equipment selection. If possible, assess using a range of methods to achieve this, and compare and identify why different results may be derived.

In many instances when considering a conceptual mine planning study in an area not previously mined, there may be very little site-specific data relating to likely operational performance in the particular resource under consideration. In these instances however, parallels can be drawn through assessing productivity and other risks impacting operational performance, particularly when considering previous mining experience in the same seam, or in a seam with similar geological/geotechnical characteristics. This can be drawn from international experience and data. It does not necessarily have to be documented experience from a similar Australian resource as long as it can be demonstrated with confidence that the empirical comparisons are justified.

When assessing the strength of comparison with respect to geotechnical experience in comparative environments, particular parameters to comprehensively check should include, as a minimum:

- *System of mining.* Ensure that the operational data being compared derives from the same system of mining. This may sound like the obvious, however the geotechnical environment, open cut or underground, is highly sensitive to mining method. The impact of the geotechnical environment will differ subject to mining method. With any empirical comparison of mining data, this should be the first check prior to others to establish that an overall comparison is indeed valid, prior to further analysis.
- *Resource characteristics.* Check that general seam structural geological characteristics, seam thickness, seam rolling and horizon, rock mass and material strengths, and likely nature and density of seam cleat and jointing, for the resource being assessed are in

the same general range as the study data being considered.

- *Stress environment.* Check that the range of cover depths and anticipated horizontal and vertical stresses are in the same general ranges for the resource being assessed as the comparative study data being considered.

Regional geological structural trends

Regional structure can be reviewed from publicly available government sources. Aeromagnetic, satellite photos and gravity surveys may also give an insight into regional anomalies. Interpretation of geological structure over a resource area should always be checked and balanced against the wider existing regional trends and structural styles prior to more detailed structural interpretation from available exploration data.

Earlier generation seismic structural interpretation through a target area, although less advanced than more recent seismic technology, can certainly assist in structural interpretation. Often, the seismic interpretation can be enhanced through reprocessing of base information using more current technology.

Once a geological interpretation has been established, mine planning constraints, in particular based on trends, locations and displacement of faults or significant folds are normally applied.

However, in addition to fault location and displacement magnitude, assessment of the nature of interpreted geological structure with respect to orientation and dip relative to the coal seam/panel layout is important. For example, interpolated discreet near seam low-angle compressive thrust faults may have a more adverse impact (over a greater lateral extent) on strata stability, roof support requirements and potential mine planning constraints than subvertical normal faults of limited lateral extent. Structure can also have an adverse impact on roof/rib stability for both longwall and development mining.

It is largely the nature of the geological structure with respect to its orientation relative to longwall faces or development headings and associated dip with respect to the roof, rather than simply magnitude of displacement, that forms the major constraint with respect to mining. There now exists a number of Australian examples of demonstrated longwall retreat through significant faults, which have been achieved through appropriate hazard assessment and operational practice. Significant displacement faulting, although a risk, should therefore not automatically be a planning constraint. Care should be taken when assessing the risks associated with fault mine through related to seam displacement considered in the context of seam thickness and roof and/or floor strength. For example a +5m seam displacement in a 1.5m seam with strong roof and floor when fully assessed may present substantially more risk than a +5m seam displacement in a 5m seam with weak roof and floor.

For example a seam displacement of greater than 5m in a 3m thick seam with strong roof and floor when fully assessed may well present less risk than a 2m seam displacement in a 5m seam with weak roof and floor.

Where possible, attempting to assess the variations in rock mass characteristics associated with structures, to facilitate a more comprehensive assessment of geotechnical implications and associated mining risk, is also justified.

Seam splitting and rider seams

The geotechnical impact of seam split areas, particularly in the near roof of underground longwall and development headings should never be underestimated. There are numerous documented examples of major roof cavity and productivity delays associated with immediate seam splitting. Seam split zones in Australian underground coal mines are often associated with:

- Channelisation of strata and associated variation in rock mass characteristics and stress distributions where rider seams diverge.
- Differential compaction features. These are often (wrongly) interpreted as low angle shear zones, although the impact can be similar but more localised. Differential compaction is a geological depositional feature associated with basin development and sinking of overlying strata into the coal formation.
- Localised seam thinning.
- Increased density of jointing in the immediate roof.

All of the above can combine to form highly variable and low strength rock mass and cohesion in the immediate roof environment which may require tailored strata management and ground support practice. Preliminary hazard plans and risk assessment should most definitely incorporate the lateral extent of interpreted seam split zones and the associated consequences with respect to both specific ground support requirements and/or mine planning constraints. Geotechnical hazard plans can be used to generate mine planning schedules zoned for variation in mining rates using appropriate de-rating factors.

Exploration core and geophysical log signatures

It is relatively easy and appropriate to manipulate these forms of exploration data to interpret rock material composition and rock mass characterisation (using selected appropriate industry standard rating schemes), of the entire overburden section for immediate roof strata assessment and higher. Such information is particularly relevant to assessing the risks and likely requirements associated with ground control, longwall cavability characteristics, mining method, productivity, and mine sequencing.

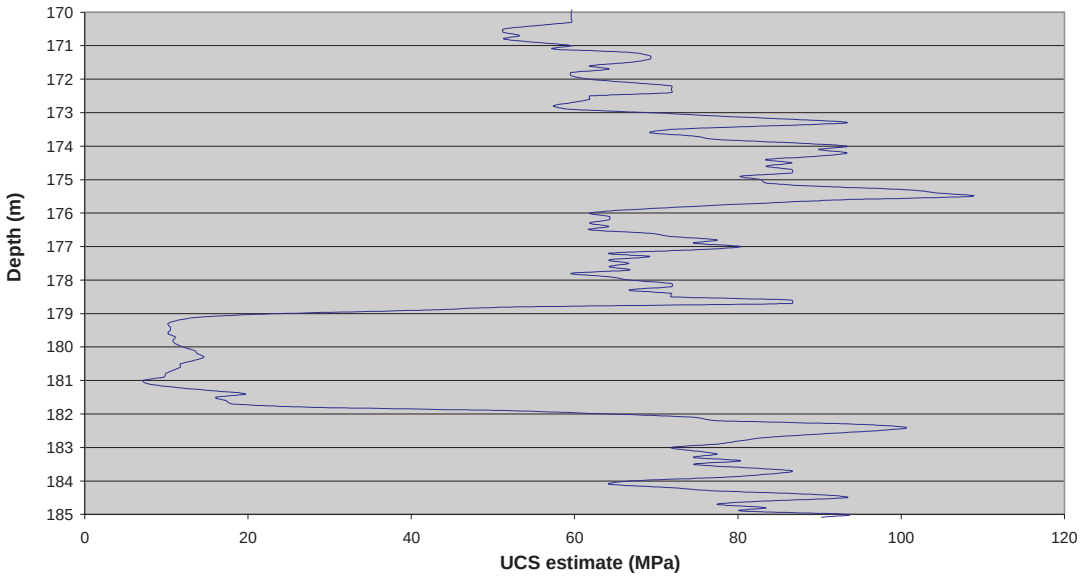

Figure 2: Example IMC plots of estimated UCS from manipulated LAS files

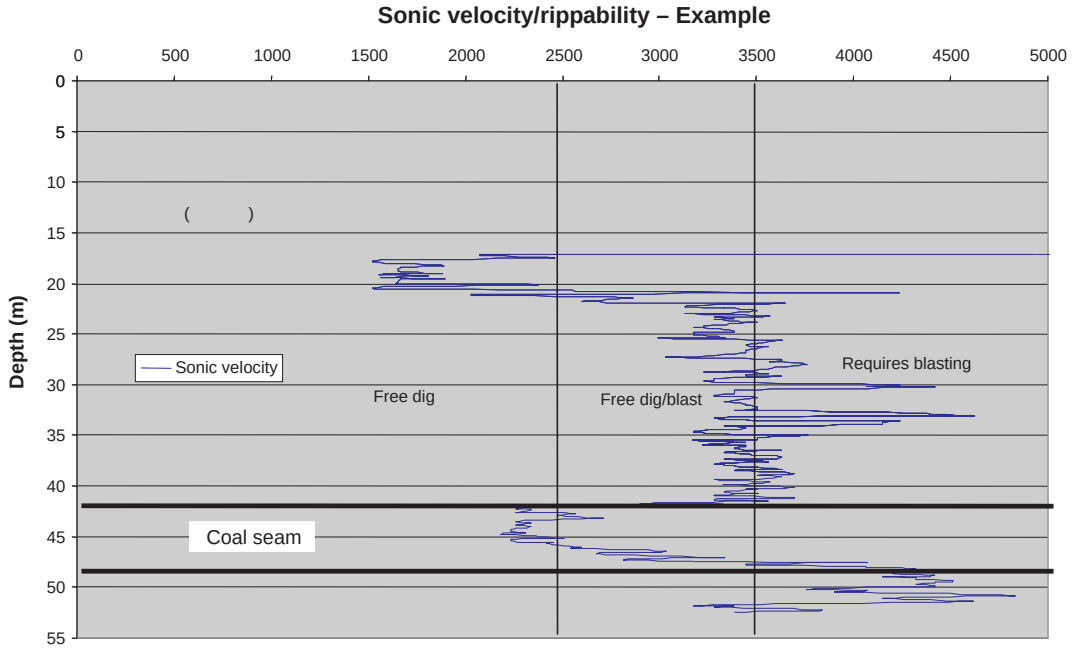

Figure 3: Example IMC plots of seam rippability from manipulated LAS files

In many instances it is possible to use existing geophysical logs or electronic LAS files, and correlate these with lithological logs. Material strength in the form of unconfined compressive strength (UCS) may be estimated if existing conversion formulae for the assessed seam in the same area to convert Sonic Velocities into UCS are available. Sonic velocity is a function of rock elasticity, and this can be correlated with rock strength. By plotting the sonic velocity for the immediate overburden to the seam, the rippability of the overburden can therefore be assessed as illustrated in Figure 3 through use of industry standard generalised rock strength correlations as illustrated in Table 2.

Such correlation facilitates estimation of the immediate roof, floor and seam material strengths. Figures 2 and 3 illustrate (relatively straight forward) LAS file manipulation to produce valid graphical output in the form of valid industry recognised geotechnical characterisations for underground and open cut scenarios.

Geophysical logs when assessed with geological (lithology logs) can be particularly useful in assessing the extent and

Table 2: Example of sonic velocity correlations with rock strength.

Sonic velocity (m/sec)	Rock strength
<1500	Very low
1500–2500	Low
2500–3500	Medium
3500–4500	High
>4500	Very high

position of any Rider seams and the extent of laminated or low strength roof units for likely support scenarios. Both of these factors warrant due consideration as they can have particular impacts on the geotechnical mining environment. Estimation of coal mass roof ratings (CMRRs) from available exploration data can easily be achieved through appropriate industry methodologies, and can facilitate early detailed geotechnical characterisation even at a very early stage of mine planning.

Assessment of floor stability from available exploration data

Weak and/or easily degradable floor may in certain instances constrain open cut or longwall mining potential, and therefore mine layout. In the case of underground development, the mining risks associated with trafficability in development headings, pillar behaviour and floor heave in such conditions warrant consideration at an early stage.

Assessment of joint and cleat orientation with respect to mine layout

In many instances detailed geotechnical interpretation of cleating/jointing from petroleum and gas exploration data, core logging, core orientation, and acoustic scanner information is possible. Such interpretation can assist in the assessment of optimum panel layouts with respect to roadway heading and longwall face stability.

Inappropriate panel layout with respect to cleat/joint orientation can have adverse rib stability impacts on development mining and under longwall abutment loading and can also result in unstable longwall faces. The risks and implications associated with cleat/joint orientation and density with respect to mine layout should be regarded as a priority geotechnical parameter warranting consideration in mine planning. Risk assessment of anticipated cleat and joint orientation with respect to panel layout is therefore necessary at the earliest possible stages of mine planning.

In the assessment of open cut geotechnical mining risk, interpreted jointing/cleating should be considered in combination with preliminary rock mass and material assessment and interpreted bedding plane orientation relative to mining direction. This can be assessed through consideration of typical failure mechanisms and in general terms, the impact and extent of potential failures will be exacerbated if the discontinuities strike parallel with the pit face. A preliminary risk assessment incorporating standard potential failure mechanisms (as outlined by Hoek & Bray, 1981), from data interpretation or inference, should be incorporated at concept level, making a preliminary assessment of the following as illustrated in Figure 4.

- The potential for toppling failure from vertical/subvertical joint sets.
- The potential for planar failure due to low angle dipping discontinuities. This can present a particular problem where low angle discontinuities intersect subvertical joint sets as illustrated in Figure 4.
- Planar failure due to low angle structures intersecting subvertical joints.
- Wedge failures due to intersection of opposing discontinuity sets.
- Mass slump mechanisms in overburden soil or heavily fractured rock.

In addition to the impact of joint and cleat orientation, both low wall and highwall stability should consider the risk associated with the following parameters relative to mining method:

- geometry, including floor dip, slope angle,
- placement sequence with respect to spoil,
- material properties including (if available or inferred) strength, shear strength, weathering, plasticity, fabric structure, saturated and unsaturated unit weight,
- floor material strength and degradability,
- identification and categorisation of discontinuities, shears or weak bands, assessment of failure potential along these surfaces and the potential for and reactivation with increased hydrostatic surcharges,
- standing water table, aquifers and general groundwater conditions, and
- blasting practice and impact on stability.

In consideration of underground mining, orientation and density of jointing and cleating can impact on the stability of the roof and rib from a geotechnical, and therefore mine planning perspective. Well developed cleating and/or jointing running near parallel to planned mining development operations will likely impact adversely on roadway rib and roof stability. Orientation of cleating relative to proposed longwall panels may also have an adverse geotechnical impact on longwall face behaviour.

Experience shows that a heading orientation of at least 20° to the cleat/joint direction is required to minimise adverse impact with respect to both roof and rib stability. However the optimum underground panel layout should be cognisant of both the predominant joint and cleat orientation, the major and minor principal horizontal stress orientations and consider the orientation of geological structural zones. Figure 5 illustrates a hypothetical longwall gateroad panel layout considering joint/cleat orientation and *in situ* principal horizontal stress.

Existing geological models

If existing geological models are available at concept level, gains can be made from comprehensive analysis of existing geological strata models from a geotechnical perspective. In many instances the seam, as well as overburden strata is modelled in the form of a three dimensional model. Mine planning is also three-dimensional. Assessing the consistency

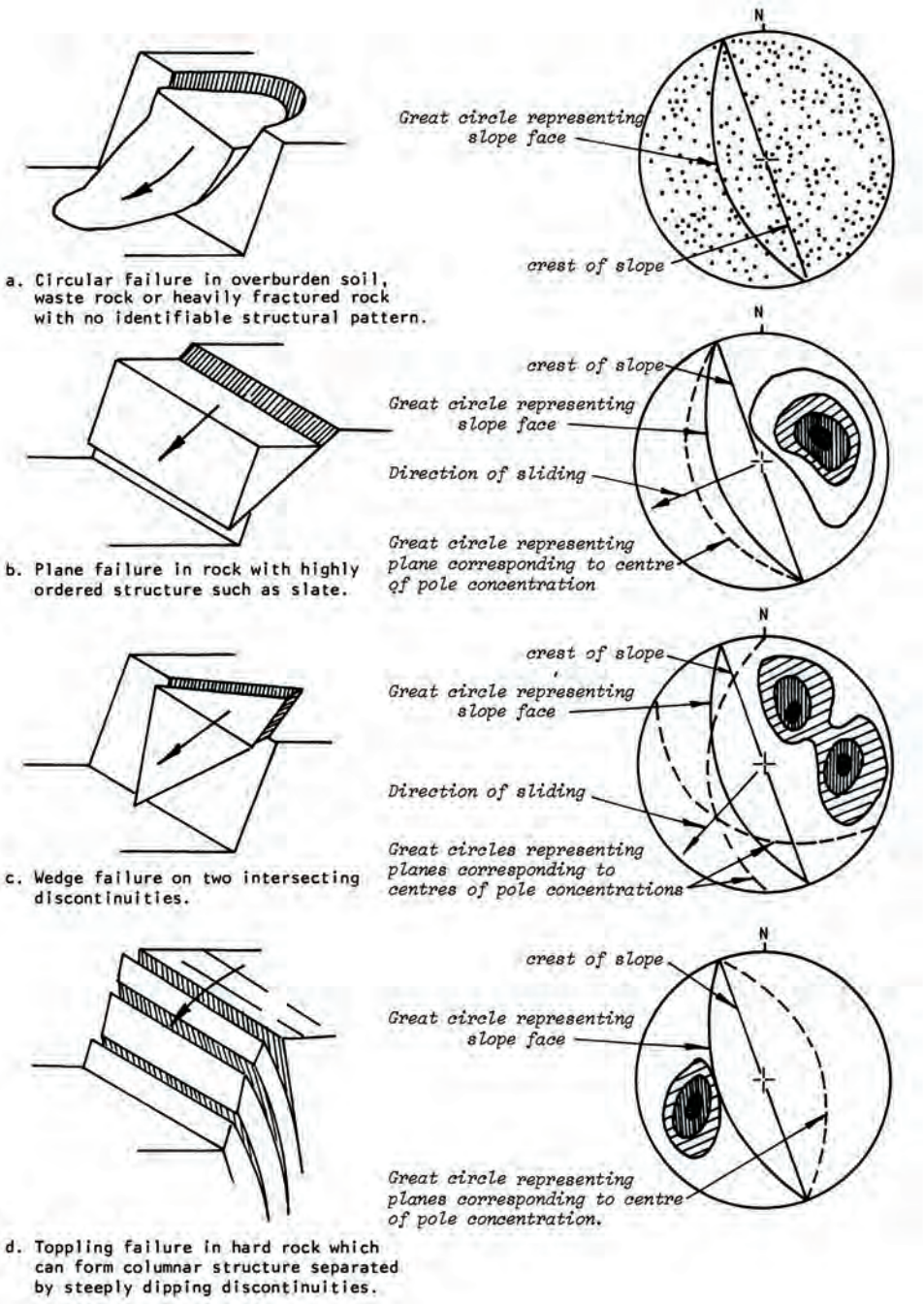

Figure 4: Preliminary open cut slope stability assessment (from Hoek & Bray, 1981)

of seam thickness and interpretation of immediate roof lithologies and overburden characteristics from the existing geological model can deliver key data which can be used for preliminary hazard and risk analysis of geotechnical parameters including:

- rock mass and material assessment of the immediate roof, seam and floor characteristics for both open cut and underground mine planning purposes,
- rock mass and material characterisation of the overburden for analysis of goaf cavability and associated impact on pillar extraction, abutment pillar loading, and longwall face performance, and
- assessing broad scale variations in dip which may pose a risk to both horizon and ground control, particularly for longwall mining.

Stress orientation and magnitude

Information on stress magnitude and orientation may be available from a number of sources, including coal seam hydrofraccing methods which are often commonplace in petroleum/gas field evaluation. In such instances, major principal horizontal stress magnitudes and orientation can be approximated by formula and assessed in the context of mine layout. Stress orientation may also be derived from caliper logs or acoustic scanner analysis using borehole breakout.

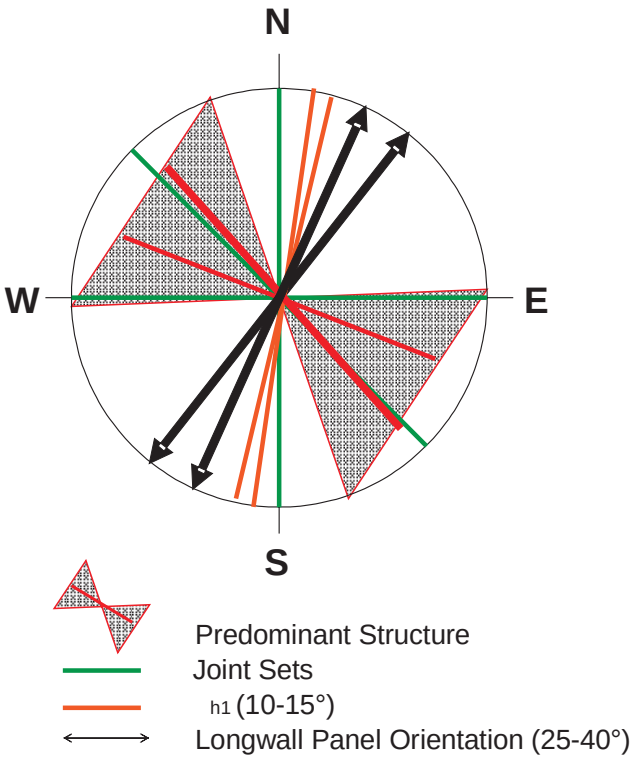

Figure 5: Hypothetical optimum mine layout with respect to interpreted joint/cleat orientation

Such information can prove useful in assessing or testing the assumption of regional horizontal stress fields. Approximated horizontal stress magnitudes should be considered with caution, as they are entirely dependant on the modulus properties (stiffness) of the rock material being considered. Stiffer materials will inherently attract higher *in situ* stresses. When approximating horizontal stress magnitude from available data and assessing likely ground behaviour/reaction, it is therefore critical to make the assessment in the context of the materials being considered. Further, a number of stress domains may exist across the resource, modified in particular by intrusives and faulting. If sufficient information is available and providing like materials are being assessed and compared, approximated horizontal stress magnitudes can reasonably be compared and variations/anomalies identified over a resource. Any differences in stress orientation or magnitude (measured or predicted) over the resource may flag the potential for adjacent associated geological structural influence which may, in itself, prompt the targeting of further exploration investigation and analysis.

Assessing the impact of *in situ* stress orientations relative to underground development driveage and strata management requirements should take into consideration:

- an estimation of *in situ* vertical stress from cover depth and consideration on rib stability and support requirements,
- assessment of the regional horizontal stress field and typical horizontal to vertical stress ratios for the seam under consideration, and

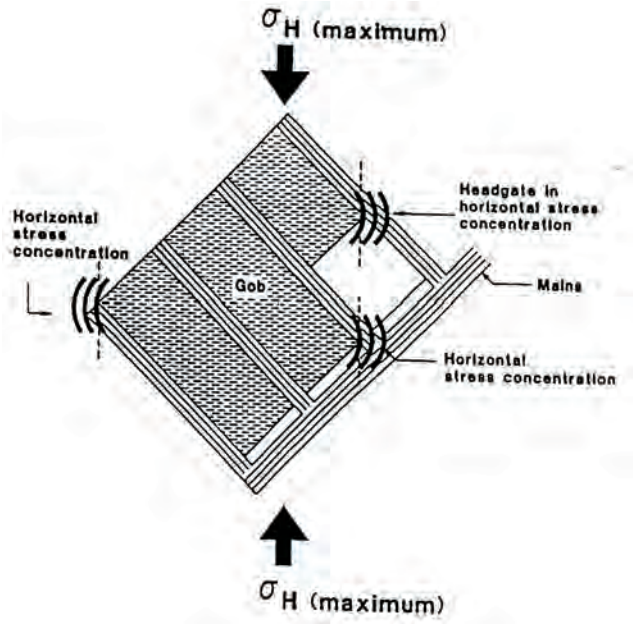

Figure 6: Horizontal stress notching in longwall mining (from Chekan & Listak, 1992)

- assessment of available *in situ* stress orientation measurements, inferences or estimations from exploration data as described above.

Assessing the impact of *in situ* horizontal stresses relative to longwall panel and face orientation is also an important consideration. It has previously been found (Hasenfus & Su, 1995) and continues to be observed in Australian longwall operations, that the maingate is stress relieved when Ø, the angle between the *in situ* principal horizontal stress direction and the maingate orientation, is between 90° and 180°, with the best conditions prevalent at Ø= 160°. Conversely, the maingate is stress concentrated when Øis between 0° and 90°, with the maximum concentration at Ø= ~70° and negligible concentration between 0° and ~25°. Figures 6 and 7 illustrate a model of this relationship between Øand the relative horizontal stress increases or decreases in the maingate.

Stress notching of *in situ* horizontal stress (eg on approaching a previous goaf leading to a 'superstressed' situation) is an important consideration for mine planning, pillar design, and tailored secondary support requirements. The degree of impact in this situation is dependant on the orientation of maingate or tailgate and/or virgin goaf areas with respect to *in situ* principal horizontal stresses. It is important to assess the risk of unfavourable panel orientation and to consider the preference for maingate or tailgate in stress notch (if panel orientation unfavourable) and preferred direction of retreat and mining sequence, balanced against other factors.

Assessment of anticipated vertical stresses on the longwall face. Variations in vertical stresses on the immediate longwall face will be anticipated as planned longwall panels advance from shallower supercritical through critical range to deeper subcritical scenarios. Preliminary assessment of subsidence profiles at various depths at assumed angles of draw could then be estimated as illustrated in Figure 8.

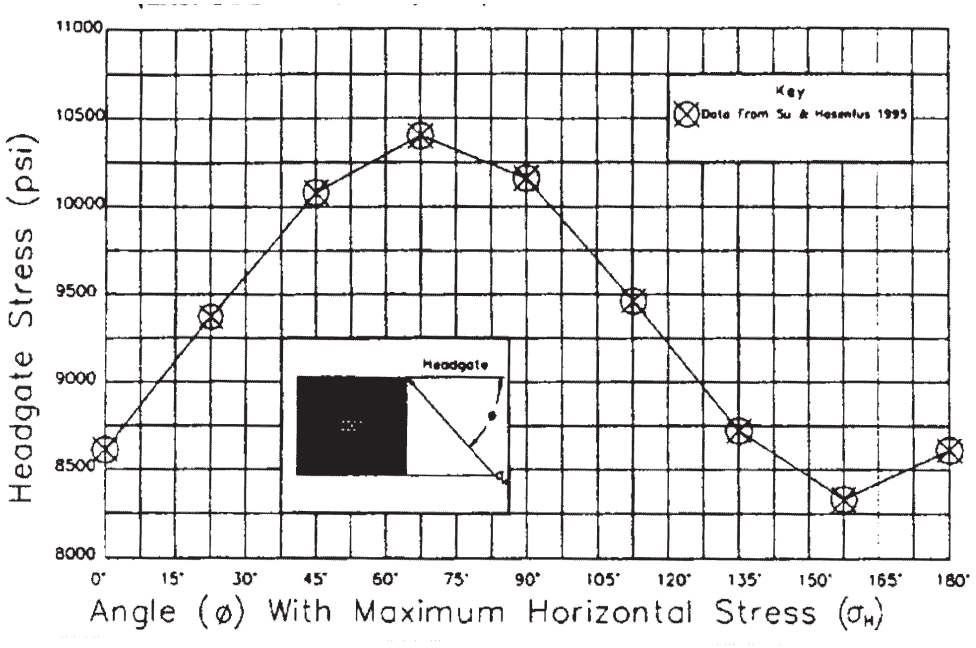

Figure 7: Effect of panel orientation on horizontal stresses (from Hasenfus & Su, 1995)

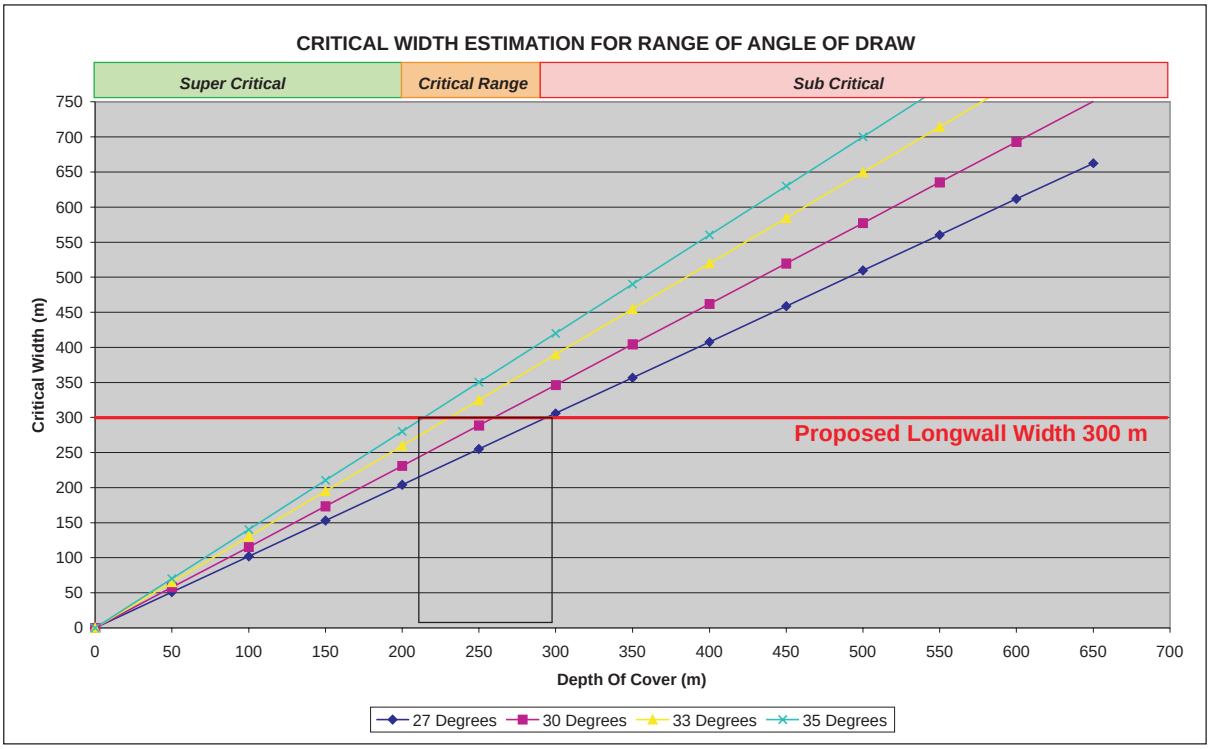

Figure 8: Hypothetical case illustrating anticipated ranges in behaviour with depth

The progression may not necessarily translate into increased anticipated loading on the longwall face. A critical factor in such an analysis is the likely goafing behaviour associated with overburden strata and the absolute vertical stress increase associated with the proposed panel face width. Sufficient overburden lithological data may well be available at a conceptual stage to assess (and in the case of multiple projects compare) likely face loading implications associated with longwall width taking into consideration overburden and caving characteristics.

Lack of horizontal stress

There are incidences of roof failures, that have been attributed to lack of confining stress, in particular where influenced by the presence of jointing. The general style of failures in these instances may be confined by parallel running joint sets and attributed to a lack of confining stress acting on the joint surfaces and therefore strata inability to maintain stability. Lack of confining stress may also be associated with proximity to geological structure (eg on the crest of seam rolls), or around faults.

The impact of potentially low magnitudes of confining *in situ* horizontal stresses and impact on the mine layout should be incorporated into hazard assessment, particularly in shallow underground environments or with limited competent material cover. In some instances, the assessed risks associated with limited competent rock cover may be of sufficient magnitude to preclude mining potential. A common rule of thumb is to maintain a minimum of 25m to 30m of competent material in the mining seam roof.

Longwall caving characteristics

Proposed longwall panel width against overburden depth ratios directly impact longwall caving characteristics, face conditions, surface subsidence profiles and chain pillar design, together with anticipated ground support requirements and productivity assumptions. A number of industry recognised empirical methodologies exist to assess estimated pillar loading, strength and design requirements which incorporate depth of mining and face width. Empirical design methodologies and bench marking mining experiences in similar geotechnical environments utilising available geological information can be used at the conceptual level of mine planning to establish base roadway development and longwall requirements and other potential impacts. Previous pillar design experience and stress modelling from the same seam in similar mining environments should be incorporated where available.

Specific interpretations/inferences to assist in assessing likely goafing and longwall face behaviour and associated geotechnical risk can be made at preliminary mine planning level. This can be assessed through the combined influences of cover depth, overburden lithology, and joint/cleat orientation relative to the longwall. Specific initial considerations may include:

- Assessing the nature of the overlying strata with respect to rock material and rock mass strength, rock composition, and bedding plane characteristics and the potential impact on longwall face and abutment loading. A broad interpretation of overburden lithology can be made though manipulating electronic LAS files to produce geophysical plots of characteristic overburden for assessment with respect to anticipated goafing behaviour.
- The longwall panel width against overburden depth ratio will impact on the caving characteristics, face conditions and surface subsidence profiles as previously discussed.
- Joint orientation with respect to proposed longwall face orientation is regarded as potentially having a significant impact on longwall face stability and goafing behaviour.
- A potential high level of risk exists in any longwall system if longwall specification based on anticipated ground behaviour is ill considered. At conceptual level, a broad assessment of the overburden behaviour based on interpretation from (in some cases limited) exploration data and benchmarking this against behaviour in comparable environments for existing longwall operations can be undertaken.

In potentially more complex or challenging geotechnical environments, more detailed numerical modelling may be justified at a later stage of mine planning when adequate high confidence geotechnical parameters can be established from exploration test work. This is likely to assist in validating empirical assumptions with respect to goafing and loading behaviour made at concept level.

Pillar design assessment

Industry recognised and current empirical pillar design methodologies (eg UNSW, various ALP based methodologies) can be undertaken at the conceptual level of study to gain an appreciation of likely mine pillar requirements based on available input data and parameters. With limited available input data this approach in general is justified at conceptual level. In the later stages of mine planning, more sophisticated measures such as numerical modelling may be used. In any geotechnical design there is value in applying and comparing separate methodologies based on available input parameters, rather than use of simply one or other methodology. This provides a check on the validity of the design tool used specific to the resource characteristics, highlights any variations and sensitivities associated with site specific input parameters and design formulae used, and provides a more considered and auditable design process. Particular care should be taken in adequately assessing the quality and sensitivity of input parameters in any geotechnical design process used.

Multiple seam mining implications

Interactive problems due to stress redistributions in multiple seam longwall operations, particularly due to transfer of stress from overlying gateroad pillars to underlying gateroad pillars where superimposed, or to the underlying longwall face where superpositioned (Figure 9), can have an adverse impact on longwall face strata control or pillar performance, unless appropriately considered and designed for in the mine planning process. Gale (2004), has recently completed an ACARP study reviewing overseas data relating to empirical experience and undertaking geotechnical modelling work in multi-seam longwall environments. From this work, Gale indicates that in general offset compared with superimposed layouts may be preferable in Australian conditions and certainly from the perspective of subsidence minimisation. The risk of adverse longwall face control under overlying chain pillars should, however, not be under-estimated.

In a case study conducted by Chekan & Listak (1992), concentrating on pillar design considerations for underlying superimposed pillars (based on ALPS pillar design methodologies calibrated with modelling), it was concluded that the two most important parameters influencing the proportion of abutment stress transferred from the upper to the lower mine pillars (referred to as the multiple seam factor

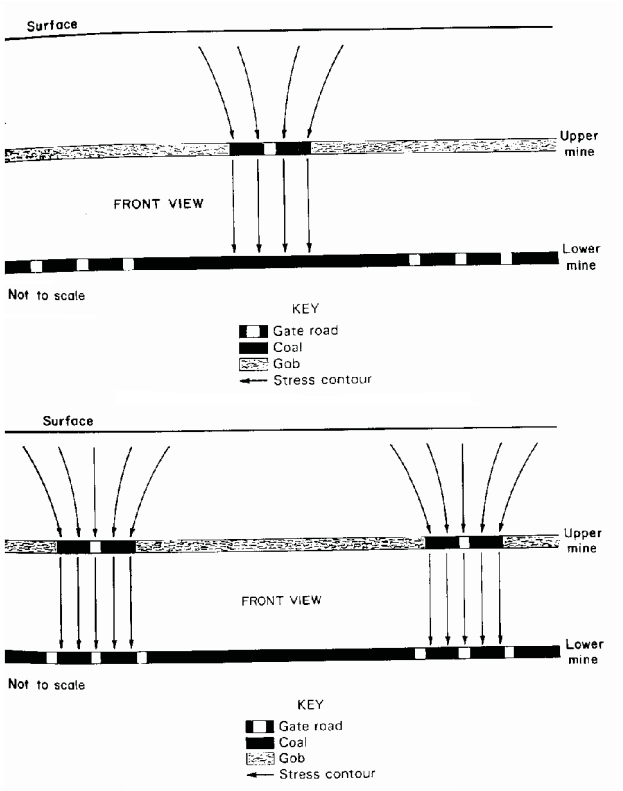

Figure 9: Schematic illustrating offset and superimposed panels and associated loading (from Chekan & Listak, 1992)

– MSF) were, in order of sensitivity, interburden thickness followed by pillar width. Pillar length was found to be a far less sensitive parameter. This study was based on three and four heading gateroad scenarios.

In a hypothetical situation, assuming an interburden thickness between superimposed pillars of 50m (165ft) and upper pillar sizes of approximately 100ft (30m), the USBM studies (Figure 10) indicate an approximate MSF of around 30%. That is, 30% of the calculated abutment load from the upper pillars can be anticipated to be transferred to the lower pillars in this situation. Although specific to American pillar design calculations (ALPS) and multi-seam longwall mining conditions for three heading gateroads, and also calculated for smaller pillar sizes, the example none the less serves to illustrate that, where the interburden between seams is <50m, there is likely to be a component of load transfer requiring that can be estimated and considered further in designing chain pillars for superimposed panels.

More recently Ellenburger, Chase & Mark (2003), NIOSH conducted an empirical study into case histories involving undermining previous longwall panels involving 12 different coal seams with seam heights ranging from 1.2–2.1m and overburden thicknesses ranging from 75–620m. A strong empirical relationship was established between the amount of damage to the lower seam caused by load transfer from the upper seam, and the overburden to interburden ratio (Figure 11).

The US database study concluded the following:

- No significant damage to the lower seam was recorded when the overburden-to-interburden (OB/IB) ratio was less than approximately seven.
- It is possible to successfully mine, even at high cover and with large OB/IB ratios, when the mining is carefully planned to take place in the stress shadow beneath fully extracted goaf areas.

In summary, there is a need to not over generalise and to recognise the complexities associated with stress redistributions in multi-seam mining operations specific to local conditions, mining timing/sequence, local geotechnical parameters, and in the context of what the mine design is trying to achieve. Nonetheless, at conceptual level with limited data and in the absence of a record of mining history,

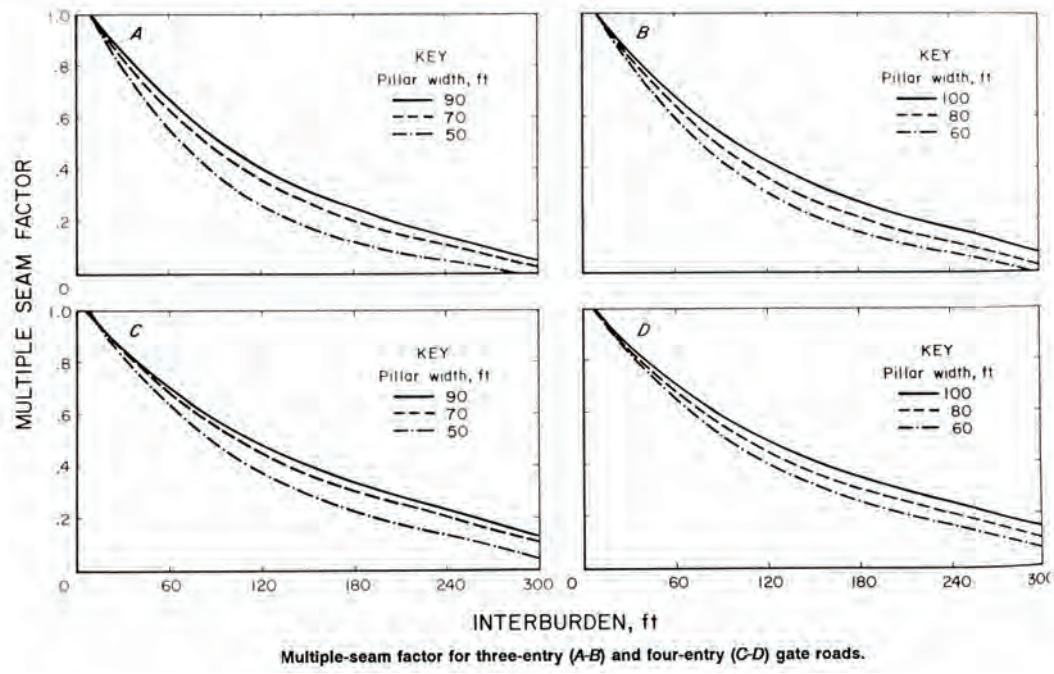

Figure 10: Abutment load transfer to lower superimposed pillars (from Chekan & Listak, 1992)

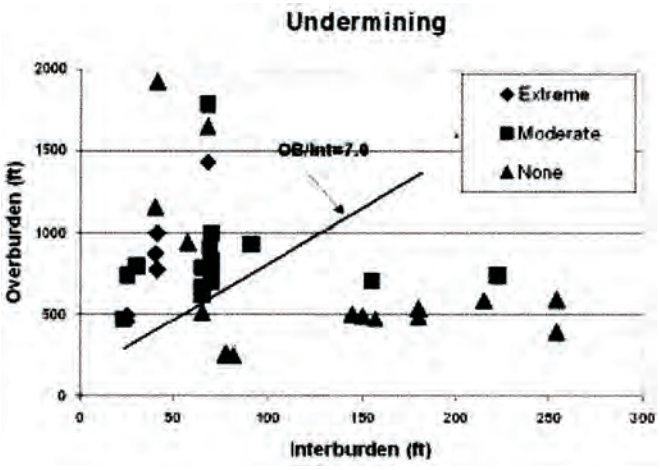

Figure 11: US case studies for undermining longwall panels (Mark & others, 1997)

assessing mining experiences in comparable geotechnical environments using published data may deliver a valid and logic based assessment of likely behaviour in a multi-seam environment. Given local specific conditions however, further assessment which may take the form of geotechnical modelling may be warranted in down stream mining studies when sufficient high confidence input data is available to validate initial assumptions and interpretations made regarding stress interactions.

Subsidence considerations

A number of alternative approaches to subsidence prediction are available, using empirical or mathematical relationships. At conceptual mine planning level, the primary purpose of this evaluation may be in regard to environmental impacts, an assessment of the further requirements of mining approvals, or to assess the potential lateral impacts on adjacent lease ownerships and associated mine layout constraints.

Analysis at conceptual level should include:

- review and back-analysis of previous regional subsidence history,
- determination of approximate subsidence magnitudes and lateral influence for the proposed mine layouts,
- potential impact with respect to perched aquifer breaching and associated inflow,
- generation of post subsidence surface contours across the proposed mining area (if sensitive and required), and
- a preliminary assessment of potential subsidence impacts and recommendations for further study should the project progress. Typical mitigation and remediation measures (including design, and pre/post mining) may be included at this stage.

A number of subsidence predictive tools, including for example empirically derived subsidence curves (eg Holla, NCB), can be used as a tool to complete analysis. However care should be taken to select the most appropriate method for the seam environment being considered. A second check analysis using a separate methodology may be warranted at this level depending on the level of mine planning sensitivity and risk in relation to projected subsidence.

A REPORTING FRAMEWORK FOR GEOTECHNICAL CLASSIFICATION OF MINE PLANNING PROJECTS

As previously outlined, there are clear input requirements for effective project valuation at various stages of the mine planning cycle. The author has argued the case for comprehensive geotechnical assessment of coal reserves at the conceptual stage, siting specific data interpretation methodologies, which can be utilised. This is particularly relevant in the case of observed trends in Australian underground coal mining which in a number of instances include assessment of resources and reserves:

- at increasing depths of cover with associated increased adverse stress acting on the roof and ribs,
- in structurally more disturbed areas,
- incorporating multi-seam extraction, and
- with complex resource characteristics including seam splitting and recovery of isolated fault bounded blocks.

There has been recent discussion, focussed primarily on the metals industry, regarding the potential advantages of reporting frameworks for geotechnical classification of mining projects. A recent AusIMM publication (Haile, 2004), argued strongly the case for such a framework and proposed a classification scheme. Table 3 illustrates the proposed data interpretation requirements at various stages of geotechnical categorisation, from implied to verified. Although focused primarily on metals orebody assessment, such a framework specific to coal could provide mining and financial Institutions with a guide to the level of geotechnical input required for a project at any particular stage of development.

From the perspective of geotechnical risk sensitivity in the process of mine planning and project development, the author raises the following questions to the industry in search of debate and feedback:

1. How well are resources currently assessed in mine planning and during project development, particularly at the early stages of assessment, from the perspective of geotechnical risk, relative t*o* other key drivers including coal quality and valuation? How sensitive is such assessment in determining the success or otherwise of a project?

Table 3: Example proposed reporting framework for geotechnical projects (from Haile, 2004)

Data type	Implied	Qualified	Justified	Verified
General requirements and geotechnical model reliability	No site-specific geotechnical data necessary	Project-specific data are broadly representative of the main geological units and inferred geotechnical domains, although local variability or continuity cannot be reliably accounted for.	Project-specific data are of sufficient spatial distribution (density) to identify geotechnical domains and to demonstrate continuity and variability of geotechnical properties within each domain	Site-specific data are derived from local *in situ* rock mass.
Geological model				
Stratigraphic boundaries	Inferred from regional geology	Reasonable knowledge of major units and geometry	Well constrained in the vicinity of the mine excavations and infrastructure	Mapped in the field
Weathering/alteration boundaries	Inferred from regional geology	Based on geology model	Well defined grading of weathering and local variability	Mapped in the field
Major structural features	Inferred from regional geology	Major 'dislocations' interpreted	Drilling sufficient to be well constrained in continuity, dip and dip direction	Mapped in the field
Rock mass data				
Discontinuity	Based on general rock type characteristics	Estimates of RQD/FF and number of defect sets from resource data (will probably contain directional bias)	RQD/FF statistics and number of defect sets representative of all geotechnical domains and directions	Multi directional FF from *in situ* mapping and visual count of defect sets
Intact material strength/ deformation characteristics	Based on general rock type characteristics	Field estimates	Field and laboratory estimates and variability	Field and laboratory estimates
Defect data				
Orientation	Inferred from regional geology	Orientation inferred from geological model	Dip and dip direction statistical data from drill holes.	*In situ* measurement of dip and dip direction from excavation mapping.
Surface characteristics	Estimated on precedent experience	Estimated on precedent experience	Statistical estimates from core logging for all defect sets. Laboratory shear strength testing of critical defects.	Statistical estimates from *in situ* measurements. Laboratory shear strength testing of critical defects.
Volumetric distribution (continuity and spacing)	Estimated on precedent experience	Estimated on precedent experience	Estimated on precedent experience	Persistence and spacing measurements
Stress regime				
Principal stress field	Estimated on precedent experience	Mean regional trend	Local magnitude and orientation based on local experience or modeling	Measured or inferred from *in situ* performance
Seismicity/earthquake	Based on general experience	Based on general experience	Based on regional trends	*In situ* experience
Geotechnical model/ domains	Based on geology model	Based on geology model	Based on geotechnical data.	Based on *in situ* data
Hydrogeological model	Based on general experience	Based on general experience	Hydrogeological study	Local observations/ measurements

2. Given the traditional role and required (defined) competencies of persons traditionally used to assess a project with respect to resource and reserve definition generally to JORC Code guidelines, is there a real justification for the involvement of experienced geotechnical practitioners and more defined input at the various process levels?

3. In view of both the above factors, are there reasonable grounds for developing a reporting framework, which can be used as a guideline for geotechnical classification of mining projects, specific to coal, which could prove beneficial to resource companies?

REFERENCES

CHEKAN, J. & LISTAK, J.M., 1992: Analysis and design considerations for superimposed longwall gateroads. Bureau of Mines Information Circular, United States Department of The Interior.

ELLENBURGER, J.L., CHASE, F.E. & MARK, C., 2003: Using site case histories of multiple seam coal mining to advance mine design. *In Proceedings 22nd International Conference on Ground Control in Mining,* Morgantown, West Virginia, 59–64.

GALE, W., 2004: Multi-seam layout guidelines and feasibility of partial chain pillar removal. *In Australian Coal Association Research Program, No C11032*.

HAILE, A., 2004: A reporting framework for geotechnical classification of mining projects. *The AusIMM Bulletin,* **5**(September/October), 30–37.

HASENFUS, G. & SU, D., 1995: Regional horizontal stress and its effect on longwall mining in the Northern Appalachian coal field. *In Proceedings International Conference on Ground Control in Mining,* Morgantown West, Virginia, 39–45.

HOEK, E. & BRAY, J.W., 1981: *Rock Slope Engineering*, *Revised Third Edition.* The Institution of Mining and Metallurgy: London.

MARK, C., MUCHO, THOMAS, P. & DOLINAR, D., 1997: Horizontal stress and longwall headgate ground control. *In* Society for Mining Metallurgy, and Exploration Inc, presentation at the SME Annual General Meeting Denver, Colorado, February 24–27.

C Hanson, MAusIMM, Principal Geologist and Geotechnical Enginee),
D Thomas, MAusIMM, Principal Mining Engineer,
B Gallagher, MAusIMM, Director (Coal Mining),
IMC Consultants Pty Ltd, Level 27, Central Plaza One, 345 Queen Street, Brisbane Qld 4000.

Nicole Baldwin and Warwick Smyth

The implementation of GPAC software on the calculation of geotechnical indices in the exploration and mining environment

The geotechnical logging software GPAC automates the calculation of geotechnical indices (Rock Quality Designation RQD, Rock Mass Rating RMR, Quality Index Q and Coal Mine Unit Rating CMUR) in a fraction of the time that manual calculation previously required, along with a higher degree of accuracy and standardisation and the removal of errors associated with data entry and calculation.

This paper will provide an overview of the computation of RQD, RMR, Q Index and CMUR. These geotechnical factors are of major importance to the coal mining industry, but are also widely used in other civil engineering and mining industries worldwide. In addition, a case study at Newlands Northern Underground will present a comparison of the new automated GPAC calculated values with the traditional manually calculated values. The computation assists with modelling and eliminates the personal rating variance in rock mass characterisation. The application of the GPAC program will provide engineers and geologists with quick, efficient and reliable data for use in the planning stage of mines. GPAC's computed indices are a step forward in geomechanics ensuring that the engineers and geologists can fully and effectively utilise the results that are investigated.

INTRODUCTION

GPAC (Geological Plotting and ASCII Collection) software is a logging system, database and automated geotechnical index calculator. Calculation of geotechnical indices is fully automated which provides a standardised methodology and an increase in accuracy. The paper provides an overview of GPAC computation for the geotechnical indices RQD, RMR, CMUR and Q index. The software is designed to calculate indices in a manner similar to manually calculated values, which provides easy to understand and follow methodology.

A comparison is presented in order to show the correlation of manually calculated indices with GPAC computed indices. RQD, RMR and CMUR are examined from 720m of core supplied by Newlands Northern Underground in the Bowen Basin. The benefits of automatic calculation can be shown through time saving, decrease in errors and a simple output which can be used in modelling of ground conditions. These values provide data that can be used in the mining development stage ensuring safer and more productive workings. An example of the use of geotechnical indices is included.

ROCK MASS CLASSIFICATION

Rock Quality Designation RQD

RQD was originally designed as an indicator of rock condition for civil engineering design purposes. Created by Deere & others, 1967 it is now one of the most common rock mass classification systems used world wide in the mining and civil industry. The calculation of RQD is simply the total length of core pieces greater than or equal to 100mm in length divided by the core run length (usually 1.5m to 3.0m) (AS 1726, 1993).

Generalised indications of rock mass conditions from RQD are as follows:

RQD 0–25%	Very Poor Rock Quality
RQD 26–50%	Poor Rock Quality
RQD 51–75%	Fair Rock Quality
RQD 76–91%	Good Rock Quality
RQD 91–100%	Very Good Rock Quality

The Rock Quality Designation number is used as a parameter in all other classification systems explained in this paper.

Rock Mass Rating RMR

Rock Mass Rating RMR was created by Bieniawski, 1988 to be used as an additional tool for tunnel design in civil engineering. Since this time the Australian mining and civil industries have adopted this tool to use as an indicator of ground conditions in underground workings. The Rock Mass Rating system is based on five parameters, each of which is given a weighted percentage based on their influence on the rock mass unit. The RMR is expressed as a percentage calculated from the sum of these parameters.

Rock Substance Strength	0–15
RQD index	0–20
Joint Spacing	0–20
Joint Condition	0–30
Groundwater	0–15

There is a rating in place for discontinuity and tunnel orientation but it is not used in GPAC. It could be applied at a later stage in the mining process.

Indications of rock mass conditions from RMR are as follows:

RMR 0–20	Very Poor Rock
RMR 21–40	Poor Rock
RMR 41–60	Fair Rock
RMR 61–80	Good Rock
RMR 81–100	Very Good Rock

Coal Mine Roof Rating CMRR and Coal Mine Unit Rating CMUR

The Coal Mine Roof Rating was created by Molinda & Mark, NIOSH (American National Institute of Safety and Health), 1994 to ensure that layered sedimentary rock was taken into account in classification systems. The stratigraphic factors that the coal industry faced with a layered mine roof meant that a rating system needed to be created to address the bedded sedimentary rocks and concentrate on the bolted horizon and its ability to form a stable mine. CMRR identifies these stratigraphic factors and weighs them against their influence on the rock mass unit.

The Coal Mine Roof Rating and CMUR can be determined from underground mapping or from core. The later method is used in GPAC. The CMUR is calculated from the parameters of RQD, fracture spacing, diametral strength and uniaxial compressive strength (UCS). In the GPAC program the Coal Mine Unit Rating is calculated for each individual rock mass unit whereas the Coal Mine Roof Rating is calculated for the borehole. The CMUR indicates the relative strength of the individual units which then determines a CMRR over a nominated bolted roof horizon rating on a scale from 0–100.

An indication of the bolted sequence conditions for CMRR are as follows:

CMRR 0–44%	Weak Roof
CMRR 45–65%	Moderate Roof
CMRR 66–100%	Strong Roof

Norwegian Tunnelling Quality Index Q

The Tunnelling Quality Index was created to assist the civil tunnelling industry and has also been adopted by the Australian mining and civil industries. Created by Barton (1988), it provides an indication of rock mass unit conditions. When used alone or in conjunction with the other rock mass classification systems it presents a very good impression of the rock conditions.

The calculation of Q index involves the determination of six parameters:

RQD	0–100%
Joint Set Number Jn	0.5–20
Joint Roughness Jr	0.5–4
Joint Alteration Ja	0.75–20
Joint Water Factor Jw	0.2–1
Stress Reduction Factor SRF	1–20

Q index is then calculated using the equation

$$Q = (RQD/Jn) \times (Jr/Ja) \times (Jw/SRF)$$

An indication of the rock mass conditions from Q index are as follows:

Q 0.001–0.01	Exceptionally Poor Rock
Q 0.01–0.1	Extremely Poor Rock
Q 0.1–4.0	Very Poor Rock
Q 4.0–10.0	Poor Rock
Q 10.0–40.0	Fair Rock
Q 40.0–100.0	Good Rock
Q 100.0–400.0	Extremely Good Rock
Q 400.0–1000.0	Exceptionally Good Rock

AUTOMATION OF GEOTECHNICAL INDEX CALCULATIONS USING GPAC

Rock Quality Designation RQD and Fracture Spacing

When determining RQD in GPAC the midpoints of discontinuities are used to calculate the length of core piece. The software is programmed to ignore drill induced and cemented defects ensuring that the number is the same as would be calculated in the field by the geologist. The user is required to record core loss and crushed zones in the defect entry panel so that all values are taken into consideration in the determination of the rock quality designation. The RQD value is calculated per core run, or per rock mass unit.

Fracture Spacing is used in RMR and CMUR. The average fracture spacing is computed for each rock mass unit (RMU). GPAC treats the ‘from’ and ‘to’ depths of the RMU as discontinuities for the calculation.

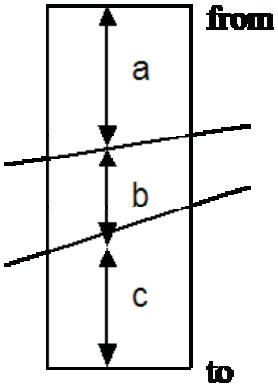

Figure 1: GPAC calculation of Fracture Spacing

In the above example the Fracture Spacing = (a+b+c)/3

Table 1: Rock Mass Ratings Calculated by GPAC

RQD	90<RQD≤100	75<RQD≤90	50<RQD≤75	25≤RQD≤50		25>RQD	
Rating	20	17	13	8		3	
UCS MPa	250<UCS	100<UCS≤250	50<UCS≤100	25<UCS≤50	5<UCS≤25	1<UCS≤5	1≥UCS
Rating	15	12	7	4	2	1	0
Fracture Spacing m	2<FS	0.6<FS≤2	0.2<FS≤0.6	0.06<FS≤0.2		0.06≥FS	
Rating	20	15	10	8		5	
Ground Water	CD-Dry	DA-Damp	W-Wet	DR-Dripping		FL-Flowing	
Rating	15	10	7	4		0	
Joint Condition							
Extent m	1>E	1≤E≤3	3<E≤10	10<E≤20		20<E	
Rating	6	4	2	1		0	
Separation	0	0<S<0.1mm	0.1≤S≤1mm	1<S≤5mm		5mm<S	
Rating	6	5	4	1		0	
Roughness	VR-Very Rough	RR-Rough	SR-Slightly Rough	SS-Smooth		SL-Slickensided	
Rating	6	5	3	1		0	
Infill Thickness	0	0<T<5mm	5mm≤T	0<T<5mm AND infill type is CL (clay)		5mm≤T AND infill type is CL (clay)	
Rating	6	4	2	2		0	
Weathering	Fresh	Slightly Weathered	Medium Weathered	Highly Weathered		Extremely Weathered	
Rating	6	5	3	1		0	

Reference source: Bieniawski, 1988

Rock Mass Rating RMR

Rock mass parameter ratings are determined from the original RMR tables. GPAC doesn't calculate RMR on a sliding scale. When GPAC has calculated the parameters needed for Rock Mass Rating the computer then compares these numbers to the appropriate rating in Table 1. Below are descriptions of methods used by GPAC to calculate the RMR parameters.

- Rock Quality Designation — GPAC calculates RQD using a weighted average over the RMU.
- UCS — Values for the uniaxial compressive strength are computed from laboratory test data, point load test data, sonic derived UCS and field strength estimates. The program seeks the required data set and if it does not exist it moves onto the next data set. GPAC determines the weighted average UCS for a RMU and from this number the UCS rating is determined.
- Fracture Spacing/Spacing of Discontinuities — The methodology for computing fracture spacing has been described above. Once this number has been calculated the fracture spacing rating is determined from Table 1.
- Ground Water — The Ground Water Condition is entered for each RMU and the rating is taken from Table 1.
- Joint Condition — In order to obtain a single value for a RMU the lowest rating that is recorded from each component of joint condition is added together.

Coal Mine Unit Rating CMUR

GPAC calculates a coal mine rating for each rock mass unit. This number provides an indication of the strength of the unit. The GPAC methodology for calculating CMUR involves the summation of Discontinuity Rating, Unit Strength Rating, Moisture Sensitivity Deduction and Slickenside Deduction.

Discontinuity Spacing Rating — GPAC uses the latest equations, in metric units, from NIOSH. The weighted RQD, fracture spacing (FS) and Diametral Strength (DS) are used in the CMUR discontinuity rating. The formulas used in GPACs CMUR are as follows:

FS 5.64 * ln(FS) + 5.8
RQD 10.5 * ln(RQD) - 11.6

RQD rule: If RQD rating is ≤20, RQD rating equals 20.

Table 2: Discontinuity Spacing Rating Formulas

Metric Specification	Formula to use
FS<63.5mm or RQD<50	RQD
63.5mm≤FS≤203.2mm and 50≤RQD≤90	Minimal rating of RQD or FS
RQD>90 or 203.2mm<FS≤1219.2mm	Minimal rating of FS or DS
1219.2mm<FS	DS

Table 3: Diametral Point Load Test Rating Formulas

Metric Specification	Metric Rating
Is(50)<0.239MPa	25
0.239MPa<Is(50)<1.296MPa	20 + 20.88 * Is(50)MPa
1.296MPa<Is(50)<2.151MPa	27.5 + 15.08 * Is(50)MPa
2.151MPa<Is(50)	60

Table 4: Unit Strength Rating Formulas

Metric Specification	Metric Rating
UCS<34.48MPa	5 + 0.218 * UCS
34.48MPa≤UCS≤147MPa	7 + 0.157 * UCS
147MPa<UCS	30

Table 5: Moisture Sensitivity Deduction

Moisture Sensitivity	Rating
N-Not Sensitive	0
S-Slightly Sensitive	-3
M-Moderately Sensitive	-7
V-Severely Sensitive	-15

Diametral Point Load Test (PLT) Rating — The Diametral Strength rating is determined from a table of formulas (Table 3). Diametral strength can only be obtained by diametral point load testing which gives a Is(50) MPa reading. The Is(50) value is taken as a weighted average of interpolated midpoint values of diametral test data for each rock mass unit.

The Discontinuity Rating is defined as the lower of the Diametral PLT rating or the Discontinuity Spacing Rating.

Unit Strength Rating — The UCS is used to determine the unit strength rating. The UCS is the weighted average for the RMU. GPAC calculates the UCS using Laboratory test data, point load test data, sonic derived UCS and lastly field strength estimates. Once the UCS is determined the rating is calculated from the equations in Table 4.

Moisture Sensitivity Deduction — The Moisture Sensitivity should be determined from the immersion test (explained in Molinda & Mark, 1994). It is recorded for each RMU and the ratings are as shown in Table 5.

Slickensided Defects — In GPAC a -5 deduction is in place if there are any slickensided defects in a RMU. This deduction was based on correspondence with Mark & Molinda (personal communication).

Norwegian Tunnelling Quality Index Q

The Q index involves intensive programming in GPAC. This section will summarise the rules that the program follows.

RQD — The simplest parameter of Q index uses the direct weighted RQD value for the RMU. If the RQD is ≤10%, then 10% is used.

Joint Set Number Jn — GPAC has to determine the joint set number. In order to accomplish this, the program separates the defect type, surface type and dip direction. Defect types are bedding, joints, faults, shears and crushed zones. Any slickensided defect is given extra weighting by being separated out as a joint set. Defects within 10 degrees of each other are considered a joint set.

Table 6: Joint Set Number Jn

Joint Set Number	Jn Rating	GPAC rule
Massive	0.5	No joints present
Few joints	1	1–3 defects (differing angles) present in entire RMU (bedding or joint defect types only)
One joint set	2	
One joint set plus random	3	
Two joint sets	4	
Two joint sets plus random	6	
Three joint sets	9	
Three joint sets plus random	12	
Four or more joint sets, heavily jointed	15	
Crushed rock, earth like	20	75–100% of unit is crushed

Table 7: Joint Roughness Number Jr

Joint Roughness Number	Jr Rating	GPAC rule
Discontinuous joints	4	If there are less than 3 joints in RMU with extent <0.5m or if no joints present
Rough and undulating or irregular	3	Rough, very rough and undulating or irregular
Smooth and undulating or irregular	2	Smooth, slightly rough and undulating or irregular
Slickenside and undulating or irregular	0.5	Slickensided and undulating or irregular
Rough and planar	1.5	Rough, very rough and planar
Smooth and planar	1.0	Smooth, slightly rough and planar
Slickenside and planar	0.5	Slickensided and planar
No rock wall contact across gouge	1.0	If separation <1mm

Table 8: Joint Water Factor Jw

Joint Water Factor	Rating Jw	GPAC rule for Ground Water Condition
Dry or minor inflow	1.0	CD-Completely dry
Medium inflow	0.66	DA-Damp
Large flow in sound rock	0.5	W-Wet
Large flow washing out joint infills	0.33	DR-Dripping
Very high flows	0.125 (midpoint)	FL-Flowing

Joint Roughness Number Jr — The joint set or random joint with the lowest joint roughness number is used in the Q index equation.

Joint Water Factor Jw — The ground water condition is recorded for each RMU and GPAC gives a rating based on Table 8.

Joint Alteration Number Ja — The joint set or random joint with the highest joint alteration number is used in the Q index equation.

Stress Reduction Factor SRF — The Stress Reduction Factor is determined from a number of factors in GPAC. The table shows the rules that GPAC follows to establish the SRF.

Once GPAC has calculated each parameter for the RMU they are then used in the quality index equation to determine the rock mass ground conditions.

THE IMPLEMENTATION OF GPAC IN THE EXPLORATION AND MINING ENVIRONMENT

As boreholes are logged straight into the GPAC program the time taken to calculate the Geotechnical Indices is negligible. This saves a good deal of time and money since the geologist or engineer is not required to re-evaluate boreholes to determine the rock condition. Coding sheets are programmed

Table 9: Joint Alteration Number

Joint Alteration Number	Ja Rating	GPAC rule (Infill type)
Rock wall in contact		Infill thickness <1mm
Tightly healed hard, non softening impermeable filling	0.75	CE, Jn=0.5
Unaltered joint walls, surface staining only	1	OP, ST
Slightly altered joint walls, non softening mineral coatings, sandy particles, clay-free disintegrated rock	2	CD, CA, FE, QU, MN, PY, CB
Silty or sandy clay coatings, small clay-fraction (non-softening)	3	CS, SA, CT
Softening or low-friction clay mineral coatings, i.e. kaolinite, mica also chlorite, talc, gypsum and graphite etc and small quantities of swelling clays (discontinuous coatings, 1–2mm or less)	4	CL, CH, LI, CO
Rock Wall Contact before 10cm shear		Infill thickness ≤mm
Sandy particles, clay free, disintegrating rock	4	SA,CA,FE,QU,MN,PY,CB,CD
Strongly over-consolidated, non-softening clay mineral fillings (continuous <5mm thick)	6	CS, CT
Medium or low over-consolidation, softening clay minerals (continuous <5mm thick)	8	CH, LI, CO
Swelling clay fillings ie montmorillonite (continuous <5mm thick)	10	CL
No rock wall contact when sheared		Infill thickness >5mm
Sandy particles, clay free, disintegrating rock	6	SA,CA,FE,QU,MN,PY,CB,CD
Thick continuous zones or bands of clay	11.5 (midpoint)	CL, CS, CT, CH, LI, CO

open	stained	coated	cemented	Calcite	iron oxide	quartz	chlorite	manganese
OP	ST	CD	CE	CA	FE	QU	CH	MN
pyrite	limonite	coal	clay stiff	clay sandy	carbonaceous	breccia	clay soft and swelling	
PY	LI	CO	CT	CS	CB	SA	CL	

into GPAC which disallows any incorrect codes providing a validation process.

GPAC has been tested on boreholes in the Bowen Basin region at several mines, including Newlands Northern Underground. There is a high correlation between GPAC computation and manually calculated indices. Twelve boreholes have been imported into GPAC with HQ core intervals ranging from 90m to 280m. The geotechnical indices were calculated for 720m of core manually and by GPAC software. The following graphs show the comparison for RQD, RMR and CMUR (Figures 2–4).

The output, in CSV format, of the geotechnical indices from GPAC allows for easy import into mining software. The information is presented in a format that can be used in modelling for the planning stage of mine development. The geotechnical indices provide an indication of ground conditions which assists engineers with anticipating poor ground where more rock support may be required.

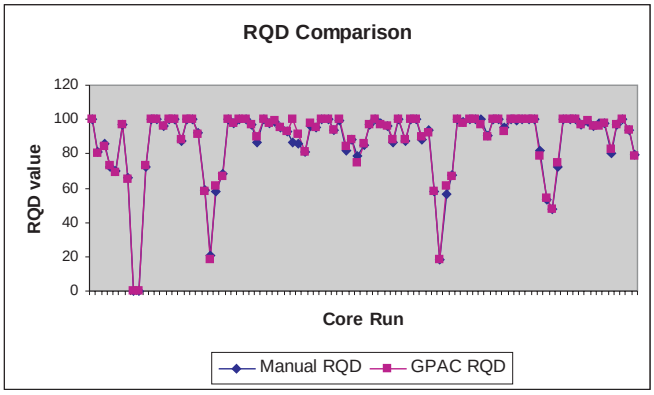

Figure 2: RQD Comparison

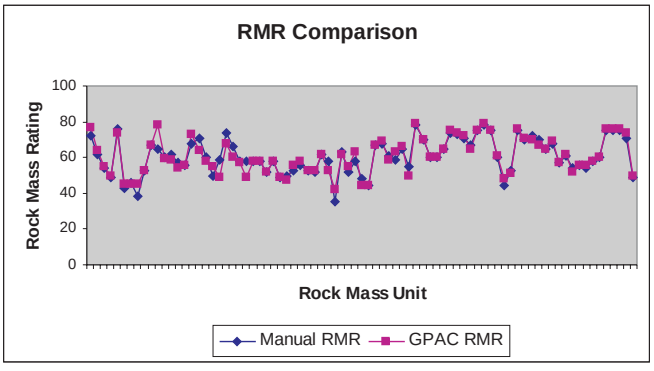

Figure 3: Rock Mass Rating Comparison

Table 10: Stress Reduction Factor

Stress Reduction Factor		SRF	GPAC rules
Weakness zones intersecting excavation, which may cause loosening of rock mass when tunnel is excavated			
Multiple occurrences of weakness zones containing clay, very loose surrounding rock (any depth)		10.0	If infill type is CS, CT, CL, CH, LI, CO *and* 9≤Jn<15
Multiple shear zones in competent rock (clay free) loose surrounding rock (any depth)		7.5	If infill type is OP,ST,CD,CE,CA,FE,QU, MN PY,CB, SA *and* 9≤Jn<15
Single weakness zones containing clay, or chemically disintegrated rock (excavation depth<50m)		5.0	If depth of RMU <50m *and* infill type is CS,CT,CL,CH,LI,CO *and* 3≤Jn<9
Single weakness zones containing clay, or chemically disintegrated rock (excavation depth >50m)		2.5	If depth of RMU >50m *and* infill type is CS,CT,CL,CH,LI,CO *and* 3≤Jn<9
Single shear zone in competent rock, clay free (depth of excavation <50m)		5.0	If depth of RMU <50m *and* infill type is OP,ST,CD,CE,CA,FE,QU,MN,PY,CB,SA *and* 3≤Jn<9
Single shear zone in competent rock, clay free (depth of excavation >50m)		2.5	If depth of RMU >50m *and* infill type is OP,ST,CD,CE,CA,FE,QU,MN,PY,CB,SA *and* 3≤Jn<9
Loose open joints, heavily jointed (any depth)		5	If Jn≥15
Competent rock, rock stress problems	UCS/major stress MPa		Only relevant if jointing is minimal Jn<3 *and* OP,ST,CD,CE,CA,FE,QU, MN,PY,CB,SA or massive
Low stress, near surface	>200	2.5	If UCS >200
Medium stress	200–10	1.0	If 11≤UCS≤200
High stress, very tight structure (usually favourable to stability, may be unfavourable to wall stability)	10-5	1.25 (mid point)	If 5≤UCS≤10
Mild rockburst (massive rock)	5–2.5	7.5	If 2.5≤UCS≤4
Heavy rockburst (massive rock)	<2.5	15	If UCS <2.5
Swelling/Squeezing rock, plastic flow of incompetent rock under influence of high pressure or water			
Mild squeezing/swelling rock pressure		7.5	If 8<Ja<10
Heavy squeezing/swelling rock pressure		15	If 10≤Ja

Reference Source: Barton, 1988

An example of the use of geotechnical indices can be seen in Figures 5 and 6. The geotechnical indices RMR and Q index have been imported into a 3D modelling package and contoured over proposed workings to provide the development planners with an idea of the ground conditions. This allows for more detailed planning and a decrease in risk of unplanned rock falls. These figures represent the weighted average of Rock Mass Rating and Q index for a two metre bolting horizon above a four metre working section.

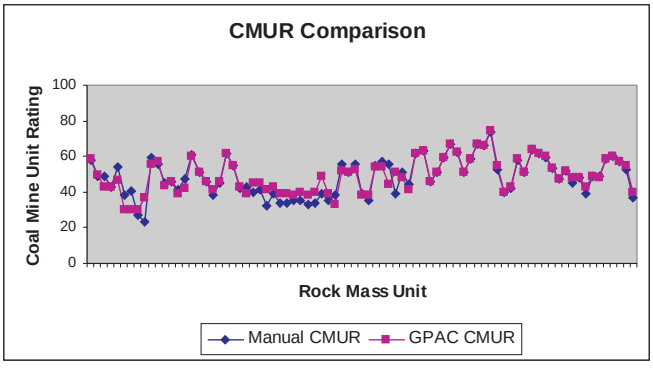

Figure 4: Coal Mine Unit Comparison

CONCLUSIONS

The GPAC geotechnical index calculations have been based on how they would be calculated manually. This makes the GPAC geotechnical index process easy to understand. The results from Newlands Northern Underground boreholes have shown that the manually calculated and GPAC calculated values show a strong correlation for RQD, RMR, and CMUR. GPAC standardises the methodology and provides more objective accurate values when compared to people calculating indices. The speed with which the

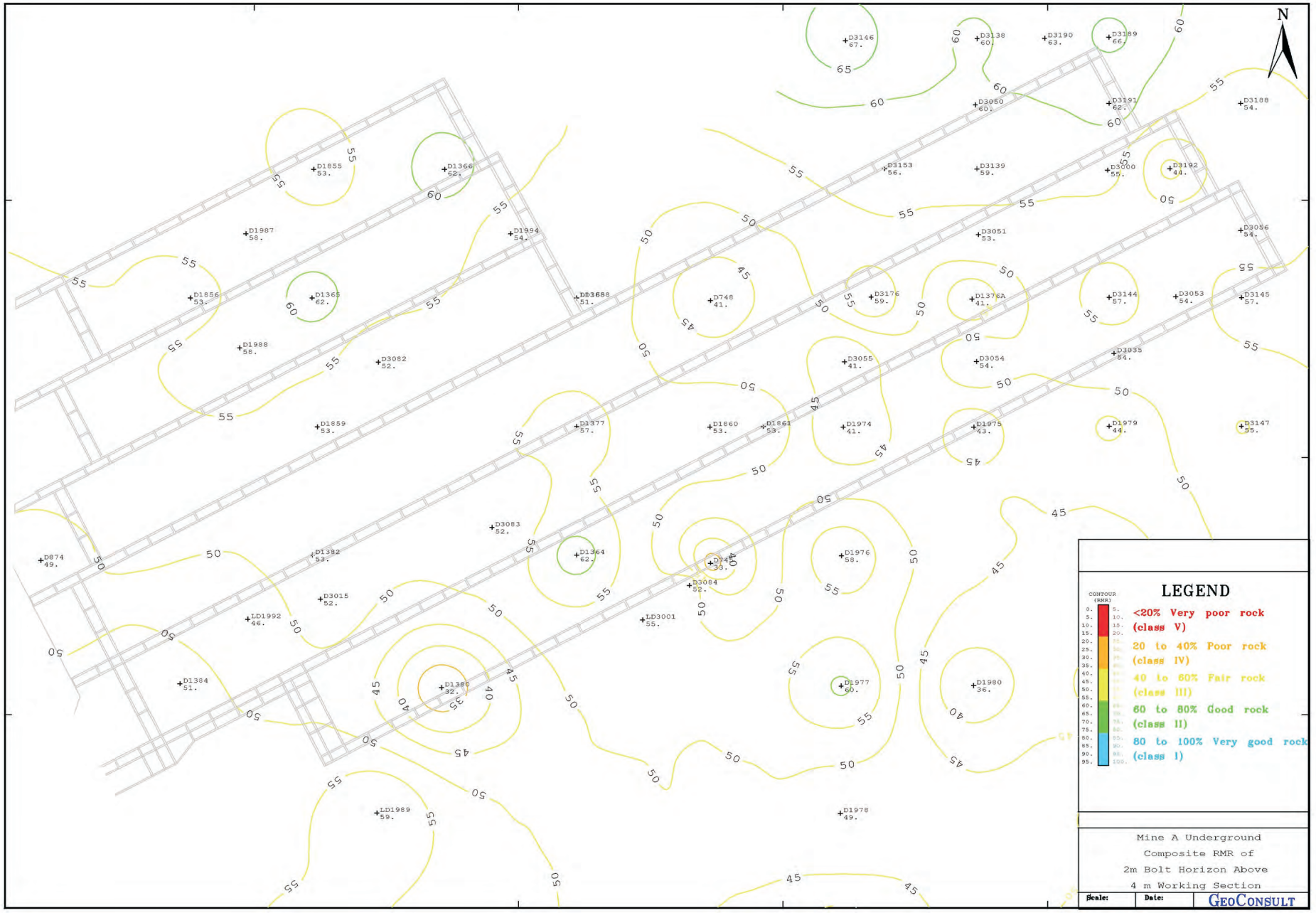

Figure 5: Contoured Rock Mass Rating values for a two metre primary bolt horizon, above a four metre working section at Newlands Northern Underground

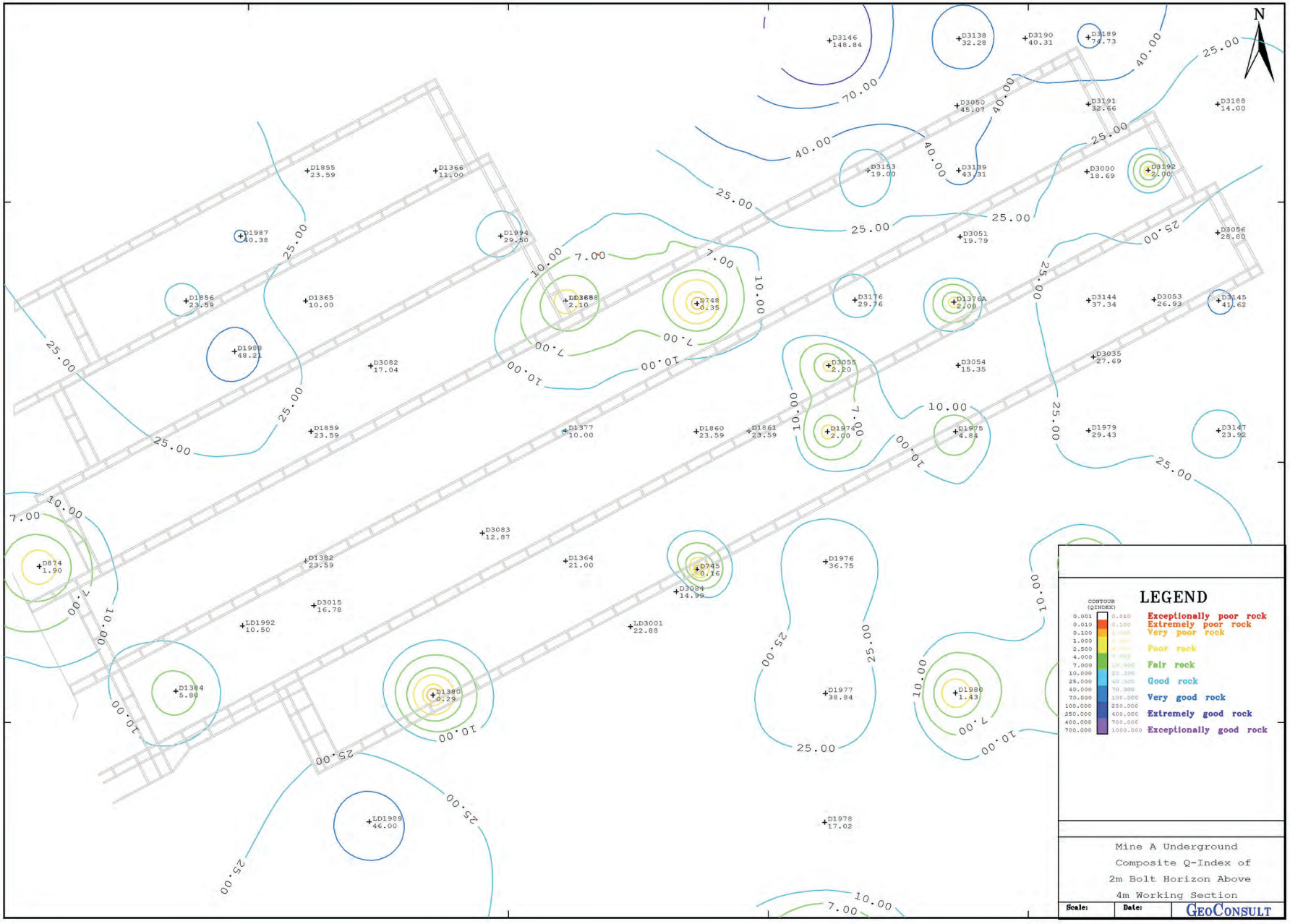

Figure 6: Contoured Tunnelling Quality Indices for a two metre primary bolt horizon, above a four metre working section, Newlands Northern Underground

software computes the indices provides not only time saving benefits but also increased accuracy.

The output from GPAC will provide development planners with data that is simple to acquire and model. The geotechnical indices can be contoured on proposed operational areas and demonstrate variable ground conditions and hence ground support requirements. The Indicies calculated in the case study were used comprehensively in mine planning and development preparation at Newlands Northern Underground.

We would like to thank Newlands Coal Project staff and management for the use of their data, support of the GPAC software and assistance in this study.

REFERENCES

AS 1726, 1993: *Australian Standard – Geotechnical Site Investigations*. Standards Australia.

BARTON, N., 1988: Rock Mass Classification and Tunnel Reinforcement Selection Using the Q-System. *In,* Kirkaldie, L., (Editor): *Rock Classification Systems for Engineering Purposes*, ASTM STP984, 60–88.

BIENIAWSKI, Z.T., 1988: The Rock Mass Rating (RMR) System (Geomechanics Classification) in Engineering Practice. *In,* Kirkaldie, L., (Editor): *Rock Classification Systems for Engineering Purposes*, ASTM STP984, 17–34.

DEERE, D.U., HENDRON, A.J., PATTON, F.D. & CORDING, E.J., 1967: Design of Surface and Near Surface Construction in Rock. *In,* Fairhurst, C., (Editor): *Failure and Breakage of Rock*, AIME, New York, 237–302.

MARK, C. & MOLINDA, G.M., 1996: Rating Coal Mine Roof Strength From Exploratory Core. *In*, Ozdemir, L. & others, (Editors): *Fifteenth International Conference on Ground Control in Mining*,Morgantown, WV, 415–428.

MOLINDA, G.M. & MARK, C., 1994: Coal Mine Roof Rating (CMRR). *In*, *A Practical Rock Mass Classification for Coal Mines,* Pittsburgh, PA: U.S. Department of the Interior, Bureau of Mines, RI 9387.

MOLINDA, G.M. & MARK, C., 2003: The Coal Mine Roof Rating in Mining Engineering Practice. *In*, *2003 Coal Operators Conference*, AusIMM, Illawarra, Australia, 50–61.

RILEY, M.W., 2000: A Review of Geotechnical Systems and Procedures used at Capcoal. Report by GeoConsult Pty Ltd, Brisbane.

SMYTH, W.D. & CLARE, D., 2002: Geological Report on Northern Underground Conceptual Plans and 5N Exploration. MIM Newlands Coal Project, April. 2002. GeoConsult Pty Ltd.

SMYTH, W.D., CLARE, D. & others, 2003: Geological Report on Northern Underground Stages 6 & 7N Exploration Structure & 3D Seismic Validation Drilling., MIM Newlands Coal Project, Feb. 2003. GeoConsult Pty Ltd.

SMYTH, W.D., CLARE, D. & others, 2003: Geological Hazard Zones Review Northern Underground Portal Dips, May 2003. GeoConsult Pty Ltd.

SMYTH, W.D., WILLIAMS, J. & CLARE, D., 2002: Geological & Geotechnical Site Investigation Newlands Northern Underground Vent Shaft Investigation, July–September 2002. GeoConsult Pty Ltd.

SMYTH, W.D., CLARE, D. & others, 2003: Geological Report on Northern Underground Conceptual Plans and 6 & 7N Exploration, MIM Newlands Coal Project, September. 2003. GeoConsult Pty Ltd.

Nicole Baldwin, Engineering Geologist, GeoConsult Pty Ltd
Warwick Smyth, Principal Consultant, GeoConsult Pty Ltd
07 38316122 geoconsult@geoconsult.com.au

David Noon

Case studies of slope stability radar used in coal mines

This paper presents case studies about how the Slope Stability Radar (SSR) system provided adequate warning to safeguard people and equipment prior to a highwall and low wall failure at two Australian coal mines. At Drayton mine, the SSR was able to provide the mine with sufficient warning to move the shovel and trucks away from the highwall, while personnel safely watched 50 000t of bulk material coming down from the wall. At Mount Owen mine, the SSR alarm allowed the mine to evacuate equipment and personnel four hours prior to a 30 000 000t low wall failure. These two case studies demonstrate how the SSR system is able to continuously monitor the stability of critical slopes, enabling greater mine productivity whilst maintaining the highest quality of safety.

INTRODUCTION

Ground instability in open cut mining operations is common, and mining can continue provided the wall does not collapse unexpectedly. Such risks can be virtually eliminated at the planning stage by reducing slope angles, but this carries a very high cost. Also, instabilities which develop whilst mining can lead to coal reserves being quarantined, representing a high cost. In spite of such safety measures, unexpected failures have occurred in the past.

These issues motivated the development of the slope stability radar (SSR). The SSR system can detect and alert movements of a wall with sub-millimetre precision, with continuity and broad area coverage, and without the need for mounted reflectors or equipment on the wall. In addition, the radar waves adequately penetrate through rain, dust and smoke to give reliable measurements, 24 hours a day.

SSR prototypes were tested under ACARP projects at Drayton, Moura, Callide, Tarong and Hunter Valley Operations coal mines from 1999–2002 (Reeves & others, 2000).

In 2003, GroundProbe® (http://www.groundprobe.com) was formed to provide SSR services to mine sites, and to date has provided services to numerous coal mines in Australia (Saraji, Goonyella Riverside, Burton, German Creek, Mount Owen, Liddell, Muswellbrook, Bengalla, Leigh Creek, and Bulga) and many of the large metalliferous mines in Australia and overseas.

To date, SSR units have detected and provided timely warning of over 50 rock falls ranging from just a few tonnes to gross failures of many millions of tonnes. See Noon (2003) for more details about the SSR technology.

This paper presents two case studies of the SSR providing sufficient warning for a highwall failure at Drayton and a low wall failure at Mount Owen.

Case Study 1: Drayton Coal Mine (NSW)

Drayton mine used the SSR system to continuously monitor an unstable highwall while coal was being extracted. Figure 1 displays the displacement measured by the SSR over three days in wall areas 1 and 2 of the photograph. Two small rock falls were measured (0310hrs on 16/11/04 and 1755hrs on 17/11/04) prior to the main highwall failure at 0930 hrs on 19/11/04.

Table 1 displays the five different alarm levels that were set by the mine geologist to warn the mine of the impending wall failure. Levels 1 to 4 sounded sequentially over the one hour period from 0730hrs to 0830hrs.

Table 1: Alarm Levels and Threshold Settings for Drayton

Alarm Level	Threshold	Period	Area on Wall
1	2mm	30min	$15m^2$
2	4mm	30min	$15m^2$
3	8mm	30min	$15m^2$
4	15mm	30min	$45m^2$
5 (Critical alarm)	20mm	30min	$60m^2$

Figure 2 is Figure 1 zoomed in to the last 4 hours prior to the main highwall failure. This figure shows the wall movement at the commencement of the shift (0730 hrs), the commencement of acceleration (0830hrs) and the start of the main highwall failure (0930hrs).

Figure 3 shows the Level 5 alarm being triggered at 0830hrs. The mine immediately moved the shovel and trucks away from the highwall and personnel watched as the 50 000t of bulk material came down from the face.

Figure 4 shows the photographs taken by the SSR on-board camera prior to (0800hrs) and after (1000hrs) the highwall failure. The mining equipment was moved away in sufficient time.

Case Study 2: Mount Owen Coal Mine (NSW)

Mount Owen was monitoring an unstable low wall using traditional methods for over twelve months. When the

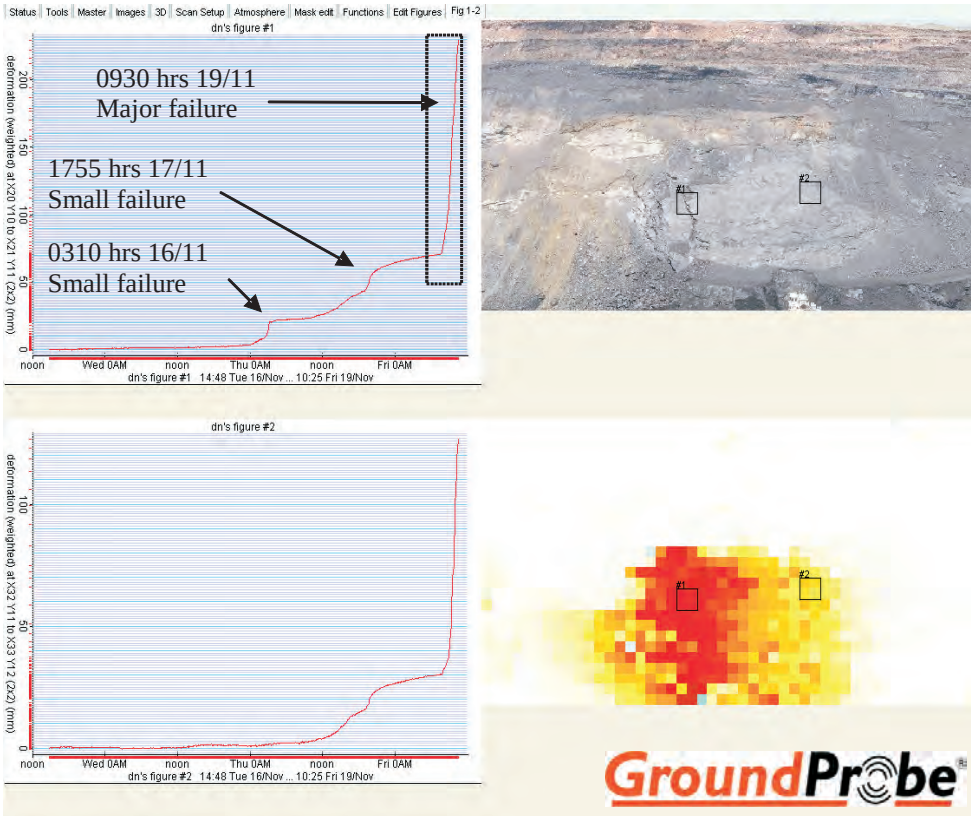

Figure 1: SSR display showing wall movements over three days prior to the main highwall failure at 0930 hrs. Two small rock falls were measured prior to the main highwall failure.

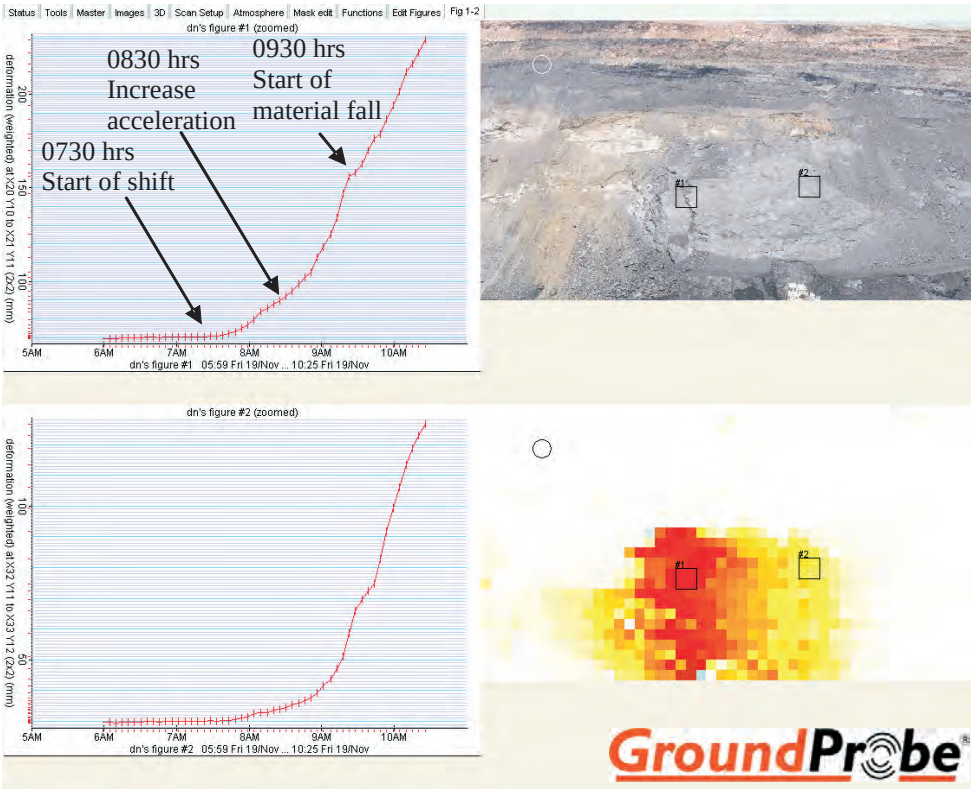

Figure 2: Same as Figure 1 except timescale is zoomed in to the 4 hours prior to the main highwall failure.

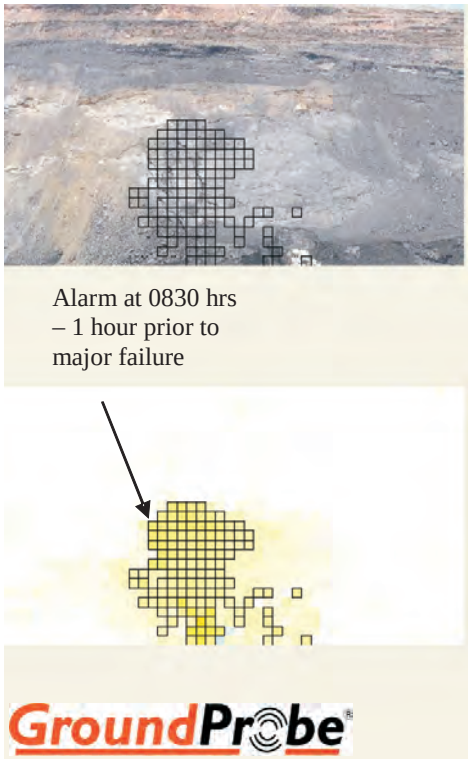

Figure 3: Pixels that triggered the Level 5 alarm (20mm over 30 minutes and over 60m^2 area) at 0830hrs. Each square pixel is approximately 9m^2 area on the wall.

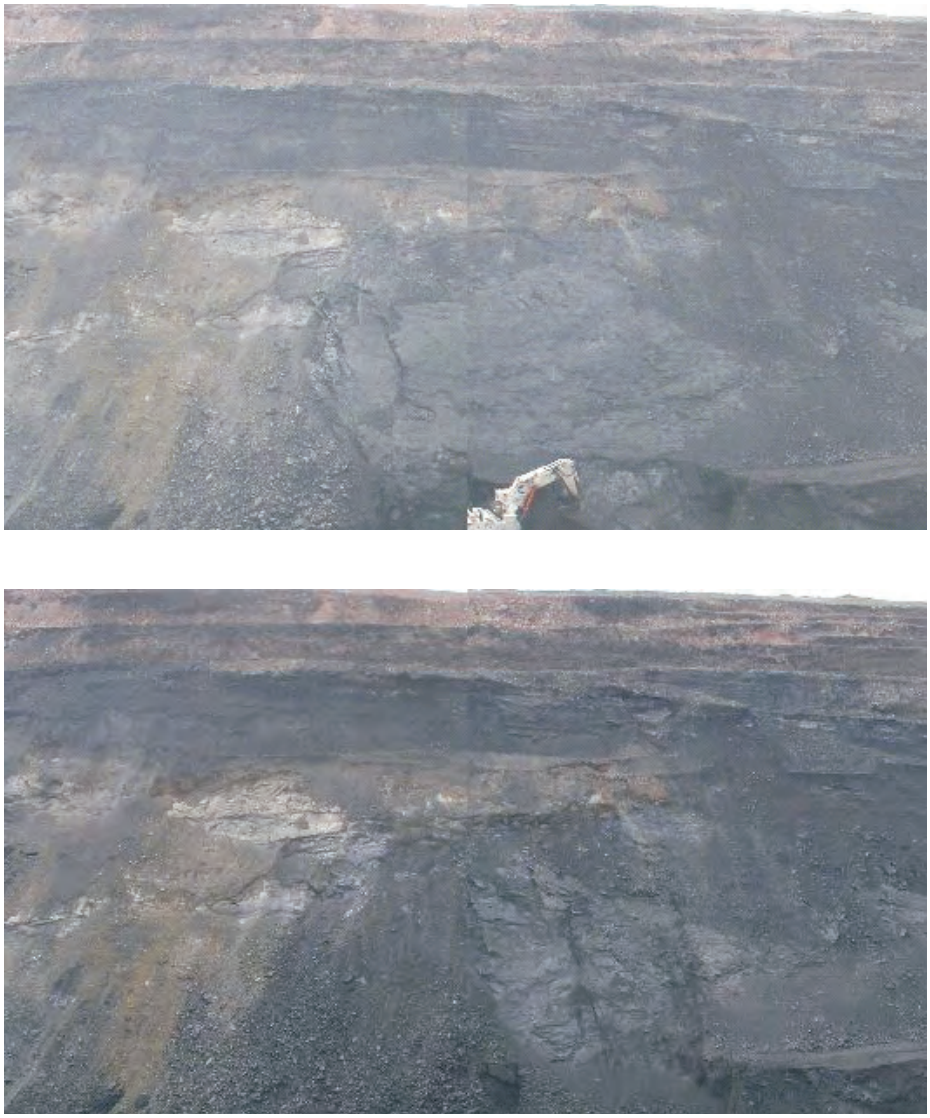

Figure 4: Photographs taken before (0800hrs) and after (1000hrs) the highwall failure on 19/11/04

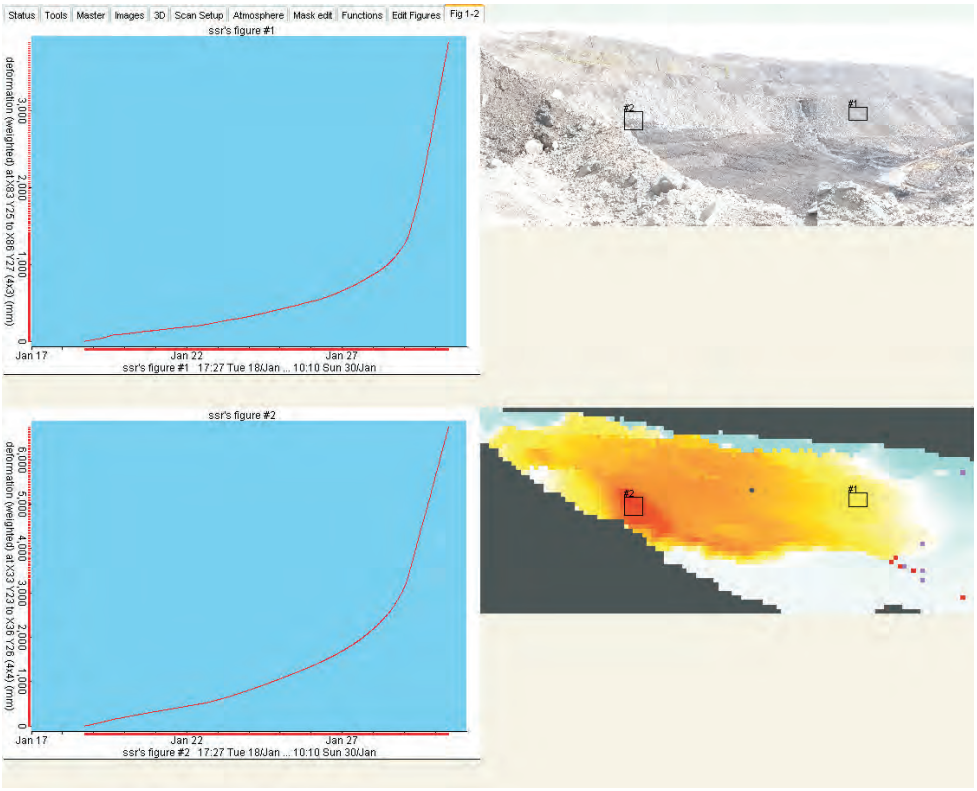

Figure 5: SSR display of the displacement measured over 13 days prior to the low wall failure

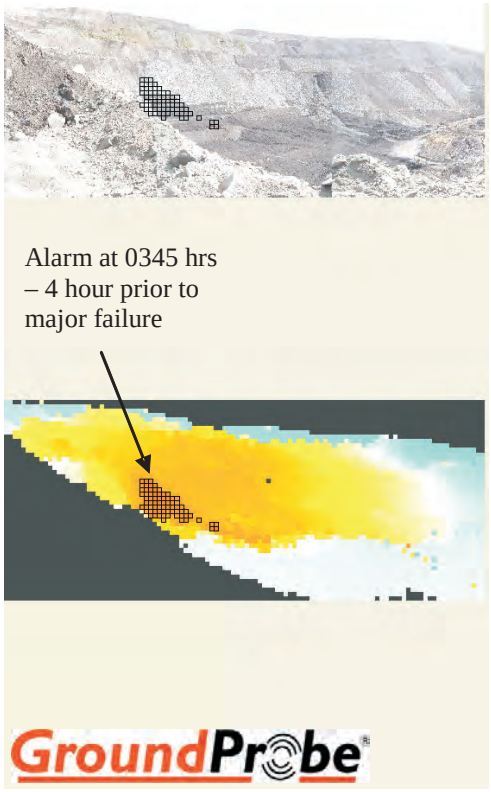

Figure 6: The triggered pixels at 0343hrs on 29/1/05

movement rates became excessive, the mine utilised the SSR system to continuously monitor the spoil while coal was being extracted from the pit floor.

Figure 5 displays the displacement measured by the SSR over 13 days in wall areas 1 and 2 of the photograph. One alarm level was set by the mine geologist at 70mm of movement over a 45 minute time period and over 1029m^2 of wall area.

Figure 6 displays the alarm sounding at 0343hrs on 29/1/05. The alarm sounded in the control room and mining equipment and personnel were evacuated in sufficient time prior to the failure occurring at 0740hrs on 29/1/05.

Figure 7 shows the photograph taken after the low wall failure. The slump area was approximately 1km long and 200m high. The low wall slumped as a single entity causing a 30m slump at the top and a heave of 10–15m on the pit floor. The mass of the slump was approximately 30 000 000t.

CONCLUSIONS

The SSR has intrinsically improved the safety management of coal mines by improving the available information on slope stability and thus allowing better decisions to be made. The technology overcomes the shortcomings of conventional geotechnical monitoring systems by providing extra warning time and greater coverage of the rock face. In conjunction with good management practices, the SSR system can dramatically reduce the risk of death, injury and equipment damage due to mine wall instability. Further, it gives confidence for mining to occur in areas that might otherwise be quarantined due to uncertainty over the extent of instability. These benefits translate to more assured productivity through quantifying and managing the risks associated with mining in pits which have potentially unstable walls.

Figure 7: The slump area was approx 1km long and 200m high. The low wall slumped as a single entity causing a 30m slump at the top and a heave of 10–15m on the pit floor. Approximate mass of the slump was 30Mt.

ACKNOWLEDGEMENTS

We thank Stuart Argent from Drayton Coal and Darren Pisters from Mount Owen Coal for the effective utilisation of the SSR units, and in defining the alarm settings and response.

REFERENCES

NOON, D., 2003: Slope stability radar for monitoring mine walls, Mining Risk Management Conference, Sydney, NSW, 9–12 September 2003, 1–12.

REEVES, B., NOON, D., STICKLEY, G. & LONGSTAFF, D., 2001: Slope stability radar for monitoring mine walls, *In* Beeston, J.W. (Editor): *Bowen Basin Symposium 2000 – The New Millennium – Geology*. Geological Society of Australia Inc. Coal Geology Group and the Bowen Basin Geologists Group, Rockhampton, October 2000, 139–142.

David Noon, GroundProbe Pty Ltd, 8 Hockings Street (PO Box 3934), South Brisbane, Qld 4101 Australia
Phone: 07 3010 8944, Fax: 07 3010 8988, Email: david.noon@groundprobe.com

Richard Campbell and Richard Mould

Geotechnical setting and constraints on hydraulic monitor operations at Spring Creek Mine, New Zealand

New Zealand's active tectonic setting results in young coal deposits which can be characterised as difficult in terms of geotechnical setting. Key parameters include; thick and structurally deformed seams, weak strata, and high stress.

The complex nature of the seams precludes the use of traditional high productivity mining methods such as longwall mining.

Hydraulic Monitor mining methods have been adopted in the Greymouth and Reefton Coalfields by Solid Energy New Zealand Ltd. This paper describes the geotechnical setting and constraints affecting the mining operation at Spring Creek Mine.

INTRODUCTION

Solid Energy operates Spring Creek Mine, on the West Coast of the South Island, 10km north-east of Greymouth. Figure 1 shows the location of Solid Energy's mining operations.

The operation utilises Hydraulic Mining methods that were proven to be a suitable high productivity, high recovery mining in similar structure and seam thickness environment at Strongman 2 Mine. Solid Energy closed Strongman 2 Mine in August 2003, Strongman 2 mined two 4–12m thick steeply (12–25°) dipping seams at a depth of 60–120m, under a thick 65–80MPa (UCS) sandstone roof.

The Spring Creek operation mines the 4–14m thick Main Upper and 8–30m thick Main Seam (combined Main Upper and Main Lower seams) at a depth of 200–370m. Typically, the strata above and below the mined seam is 15–60MPa (UCS) carbonaceous siltstone and fine sandstones.

The increase in working depth and decrease in strata strength has required a reassessment of the geotechnical controls (support mechanisms, extraction sequences etc) on the mining method.

HYDRAULIC MONITOR MINING

Hydraulic Mining utilises 300mm reducing to 200mm high pressure steel pipe lines to deliver water at a rate of between $6m^3$/min and $7m^3$/min to the monitor unit.

The water exits the monitor through a 24mm water cannon at a pressure of $175kg/cm^2$ (2500 PSI). Water is used for extraction, coal cutting and coal transportation via flumes to a dewatering plant, conveyor and slurry pump system.

Figure 1: Location Plan

Figure 2 is a simplified diagram of the Spring Creek operation.

The mining layout uses sublevels driven 20–25m apart at the base of the seam. Due to the steeply dipping nature of the deposit all development drivage is undertaken across the strike of the seam to minimise the grades of the sublevels and cut-throughs. Figure 3 illustrates the general layout of the Hydraulic Monitor extraction panels. Typical recovery is in excess of 75% of the seam thickness.

Maximum grades of 1:5 (11°), and minimum grades of 1:15 (3.8°) are planned, which suits both the development equipment and the requirement for gravity driven fluming of the coal slurry.

GEOLOGY

Spring Creek Mine is currently operating in the Main and Main Upper (MnU) seams of the Rewanui Coal Measures.

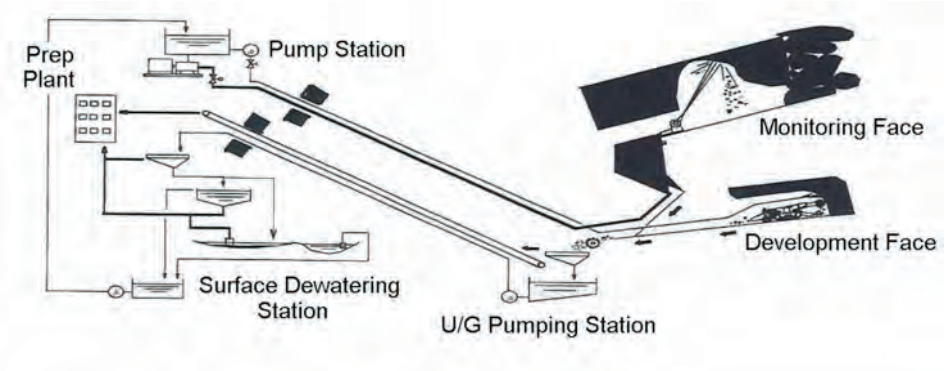

Figure 2: Simplified diagram of the Spring Creek operation

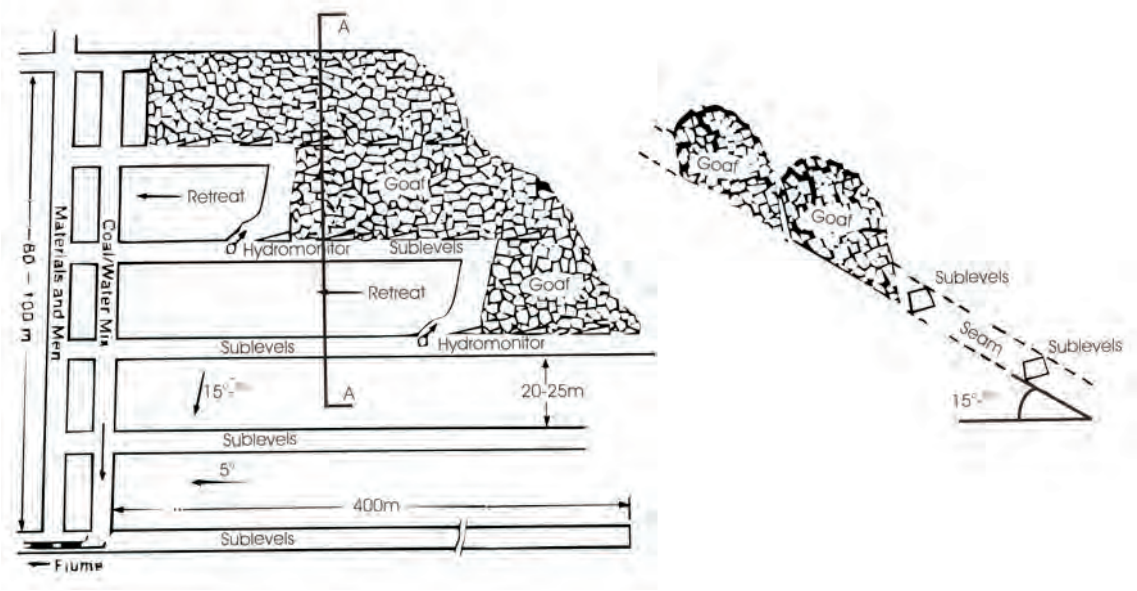

Figure 3: General layout of the Hydraulic Monitor extraction panels

Figure 4 shows the generalised stratigraphic column of the Greymouth Coalfield.

The target seams vary in rank across the lease area, from thermal, to semi-soft to high value coking and specialist coals.

Surface topography is characterised by steep hill and valley systems. The overburden is faulted and has a dip of ~10–15°. Mining has historically been undertaken in the Dunollie and Brunner Seams which are higher in the overburden sequence. Extraction of these seams has occurred in fault bound blocks which allowed outcrop adit access.

The seams dip generally to the WSW at moderate dips of between 10–20°. Depth of cover increases to the west, partially as a result of seam dip but also due to increasing topographic cover (Hall's Ridge). Depth of cover varies from ~200–370m.

Seam thickness is highly variable across relatively short distances, with Main seam thickness ranging between 8–30m, and Main Upper seam thickness ranging between 4–14m (over only 400m), although typically >7m.

The stratum immediately about the seam comprises coal bearing formations, interbedded siltstone, mudstone, sandstone and carbonaceous units. The floor strata has variable clay content and strength and can cause trafficability problems and flume road erosion.

New Zealand's active tectonic environment is manifest as a high level of macro and micro structural disturbance — from large scale faulting and folding to pervasive slickensides on bedding and coal seam contacts.

Structurally the deposit is characterised as being heavily faulted. Normal and high angle reverse faulting is common with fault off-sets typically ranging between 1–35m. The majority of structures strike north-north-east and are variable in throw along strike. Faults growing in throw from 3m to 12m over 20m of strike length are common.

The result being long narrow fault bound extraction panels developed between major structures as illustrated in Figure 5.

The nature of the surface terrain and the sensitive nature of the surface environment requiring expensive helicopter based drilling programmes has resulted in comparatively wide spaced borehole data for geotechnical characterisation.

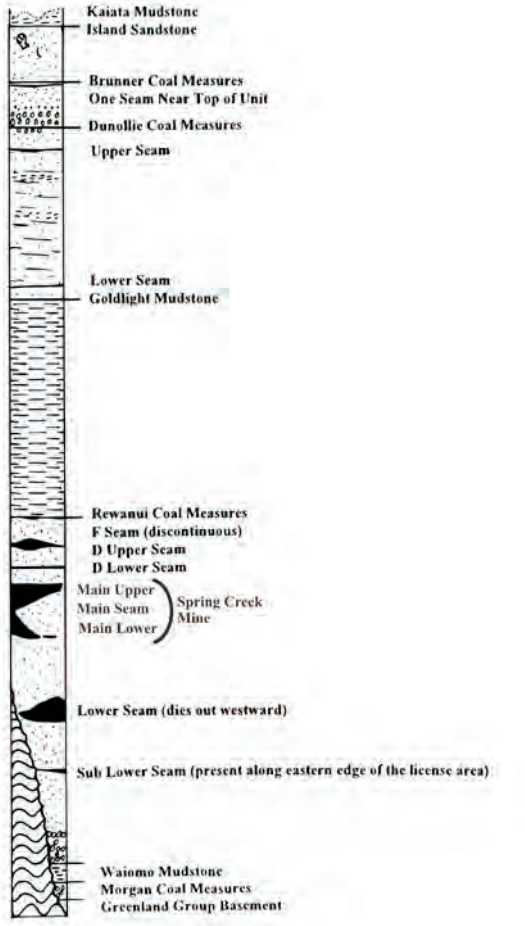

Figure 4: Generalised stratigraphic column of the Greymouth Coalfield

Structure presents the greatest risk to continuous development and high productivity extraction. To address this risk a 3D seismic survey is being run to target identification of faults with throws >5m.

GEOTECHNICAL CHARACTERISTICS

In mining terms, the Spring Creek operation is geotechnically complex making it difficult or unrealistic to predict the ground behaviour on the basis of past experience or empirical relationships obtained in other countries.

The main reasons for the non-applicability of empirical methods are the geological, structural and topographical environment, seam dip, panel layout parameters which are set by the extraction method, extraction sequence, seam thickness/ extraction height and depth.

Mine design requires site specific knowledge of the *in situ* mechanical properties of the rocks, the structure of the rock mass and *in situ* stresses as well as the geohydrological conditions in the zone of potential mining influence. A significant work programme is underway to quantify as many parameters as possible.

The current geotechnical design philosophy is based on the development of numerical models, by external consultants SCT Operations. The models are developed on the basis of detailed geotechnical testing of strata properties to assess the ground response characteristics to mining in this type of environment, along with detailed measurement of the strata response to reinforcement and mining induced loads. Measurement at another mine site suggests horizontal stress to be 1.5–2 times the vertical stress.

The horizontal stress regime, whilst not measured, has been characterised from observed roadway behaviour in the underground workings. Moderate to high levels of shear fracturing and guttering is evident in most underground roadways. Mapping of these features indicates a general ENE–WSW horizontal stress direction of a moderate to high magnitude.

Due to the requirement to mine across the strike of the seam to achieve the required flume grades, there is little room to lay out the mine in a favourable orientation to the horizontal stress direction. This is unlike what would traditionally be undertaken in a longwall or board and pillar operation.

Cleat direction can be variable, but is typically subperpendicular to the sublevels. At Strongman 2 cleat direction was found to have a significant effect on the hydraulic monitor cutting rates. The greater magnitudes of the vertical and horizontal stresses at Spring Creek have, however, reduced the affect of cleat and cleat direction on cutting rates compared to Strongman 2. Seam dip and the need to maintain flume gradients at Spring Creek are the overriding factors meaning monitor cutting directions may not always be optimal. The hydraulic monitor is however, designed to cut a 85° horizontal arc and approximately 50° vertically, allowing cutting across a large range in cleat direction.

GEOTECHNICAL MODELS

Due to the undeveloped nature of the coal deposit, geotechnical characterisation has had to occur in conjunction with the development phase of the mine.

Some of the key information gathered include UCS and staged triaxial testing of key units to determine the intact and residual strength characteristics of the strata. In addition a site specific sonic velocity to UCS relationship has been developed, typical results are illustrated in Figure 6. This information forms the basis of the numerical models.

Rock failure is based on Mohr-Coulomb criteria relevant to the confining conditions within the ground. Permeability in the horizontal and vertical planes is determined on the basis of the confining stress normal to the flow plane. Detailed models of the geology are necessary to obtain a satisfactory simulation of the rock failure mechanics. Definition of the rock intact and post failure strengths, stiffness, *in situ* stresses, permeability and bedding plane characteristics are key factors to be quantified.

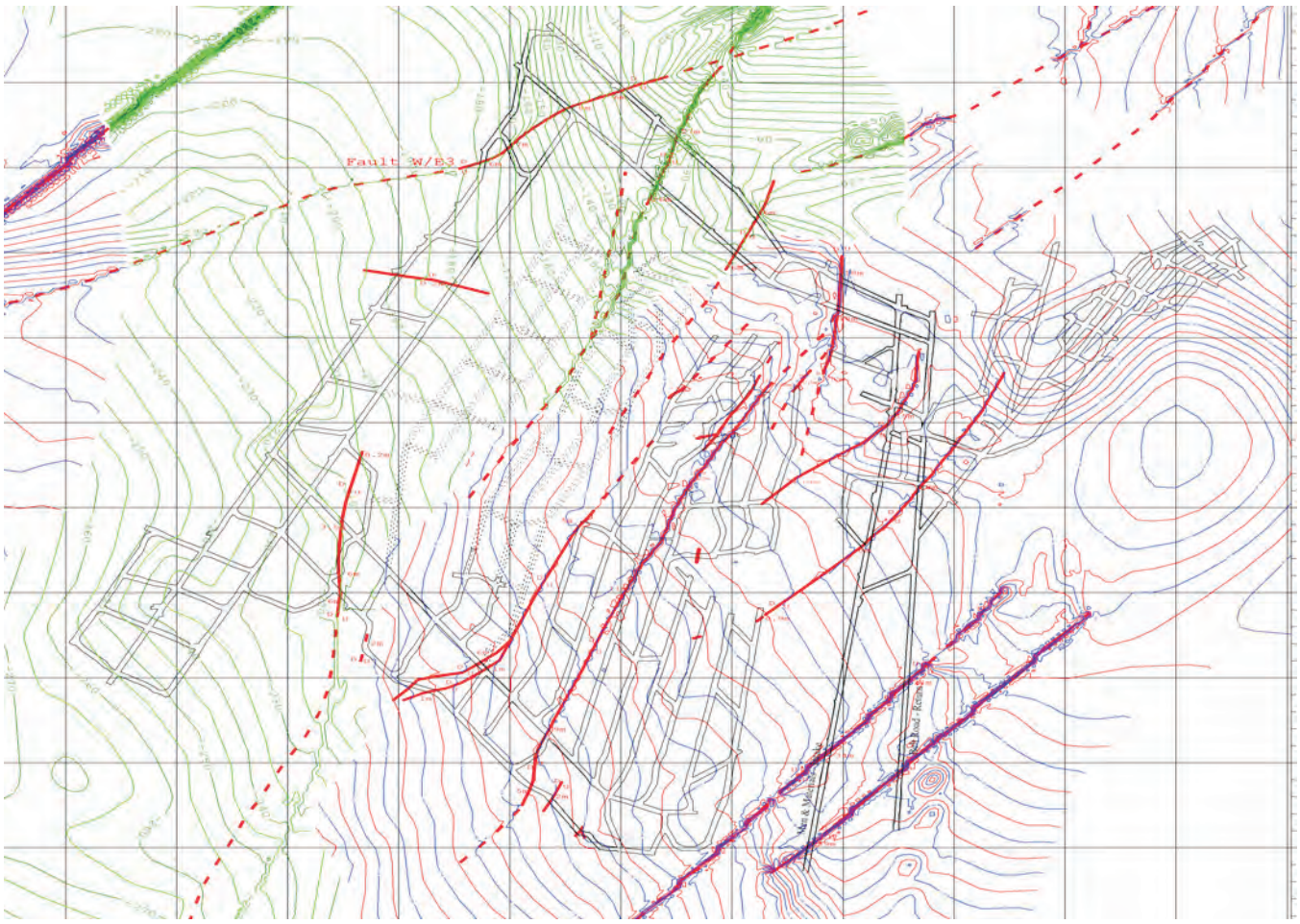

Figure 5: Layout of Spring Creek Mine

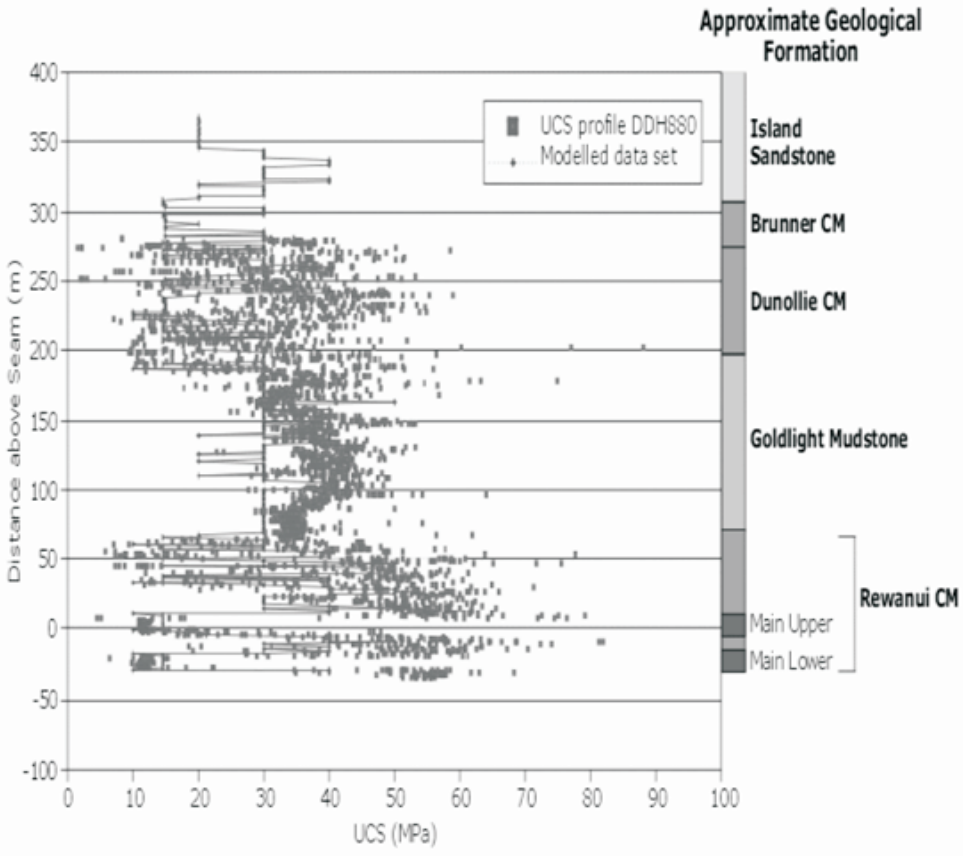

Figure 6: Strength profile for strata about the target seam

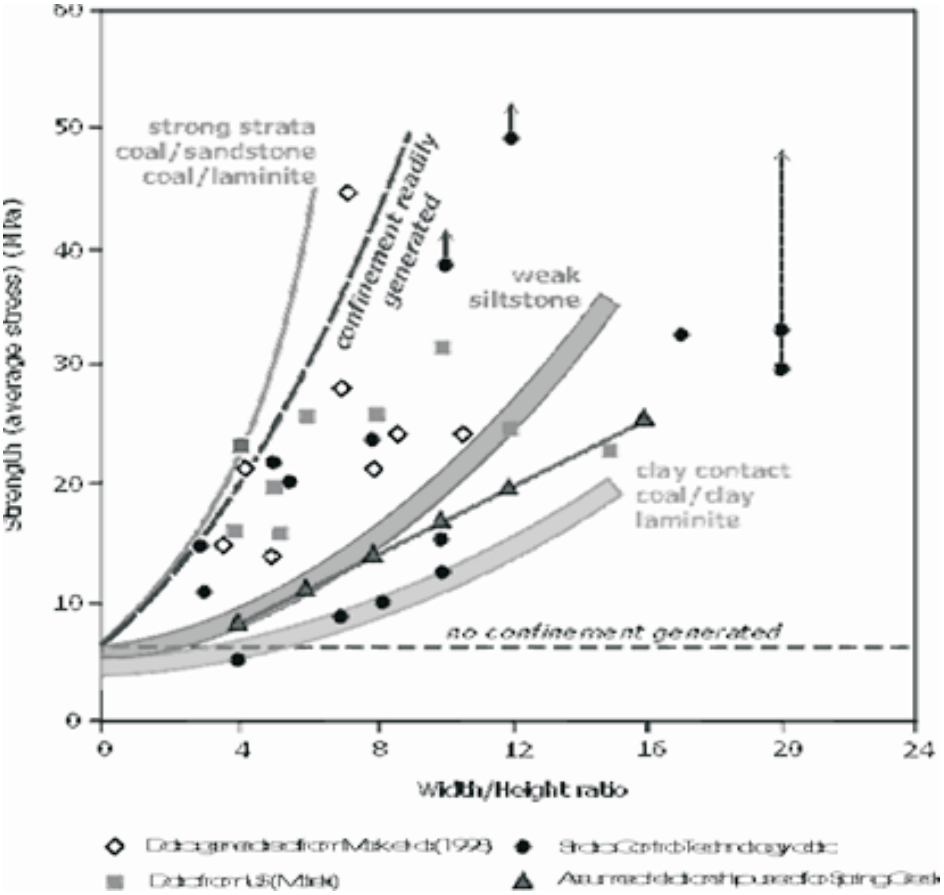

Figure 7: Coal strength pillar system for Spring Creek

The overall style of strata failure is characterised by shearing in low strength units (partings) or along weaker bedding contacts (slickenside surfaces), particularly adjacent to the top and bottom of the coal seam. This style of behaviour controls the caving process and the loading environment on the fenders.

The coal strength and pillar system is characterised as being weak, as shown in Figure 7.

MINING PARAMETERS

Key mine design parameters are fixed due to constraints relating to monitor extraction. These parameters include:

- 20–25m wide coal fenders, at 350m depth,
- wide extraction/goaf widths (ranging from 30–400m, and
- full seam extraction height of 8–28m.

Typically the mine design would be based on geotechnical controls, not the other way around. Hence the geotechnical design system and understanding has to accommodate difficult mining conditions, unconventional mining geometries and non-traditional design criteria standards.

The resulting mine layout and extraction system requires best practice and adaptive strata management systems.

To best predict and manage the behaviour of the strata during both the development and extraction phases 2D FLAC modelling undertaken by external consultants SCT Operations have been used (Gale, 2004; MacGregor, 2004). These models are currently being calibrated as more data comes to hand. Tools such as extensometers, tell tales installed every 20m, strain gauge bolts, pull tests etc are being used to gather the required data.

Models of the development and extraction phases have been undertaken. The key outputs have been an understanding of the style and magnitude of deformation about the headings (guttering, greater loading of up-dip rib etc), the effects of roof coal thickness and the required primary and secondary strata reinforcement on development and extraction respectively.

The numerical models have been used as the basis of trigger action response plans (TARPs), determining the reinforcement length, capacity and patterns. Typical outputs from the models are illustrated in Figure 8 and 9.

In addition to the roadway deformation modelling, assessments have been made of the extraction sequence on the undersized (this is terms of traditional bord and pillar or longwall pillars) fender stability. Figure 10 shows the extraction sequence modelled.

The modelling shows the system to represent a weak pillar environment, with significant yield of the fender and adjacent strata during extraction. However, the modelled

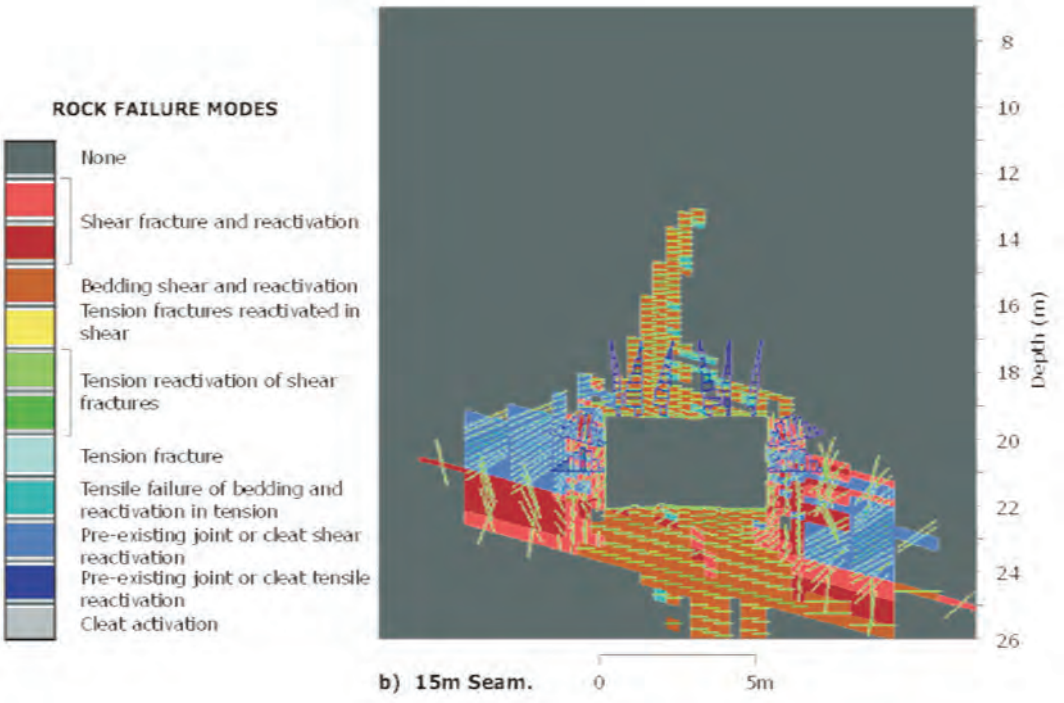

Figure 8: Modelled strata failure on development

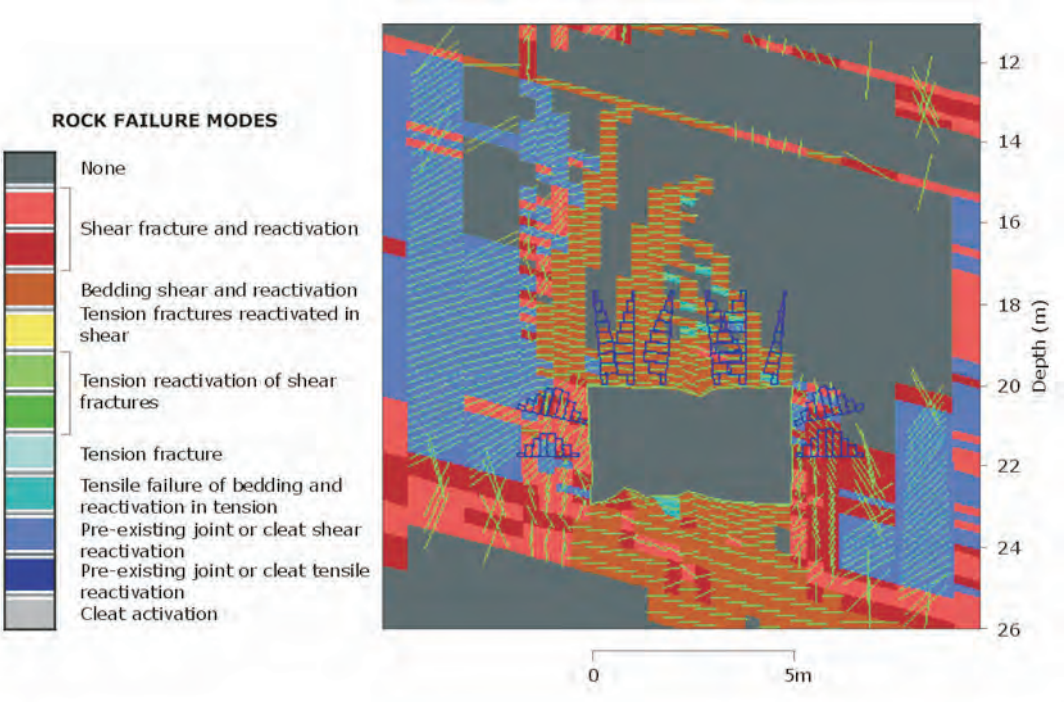

Figure 9: Modelled strata failure during extraction

20m fenders are able to gain strength above the unconfined strength of coal, with a peak strength in the order of 11–12MPa.

The fender is able to generate sufficient confinement during extraction to maintain its 11–12MPa strength. As such, and notwithstanding potential fault or other weakness planes in the fender, the potential for sudden pillar collapse is considered remote for the options assessed.

Whilst the modelling indicates the post-peak strength of the 20m fender to be maintained, the layout and sequencing of the extraction panels will be important for providing predictable goaf edge behaviour. To avoid premature goaf overriding, it is recommended that a solid abutment is maintained about the monitor location. The staggered offset of extraction panels provides the most secure extraction sequence.

GEOTECHNICAL MONITORING

As with all mining operations, geotechnical monitoring is used to gather data on the behaviour of the strata during all

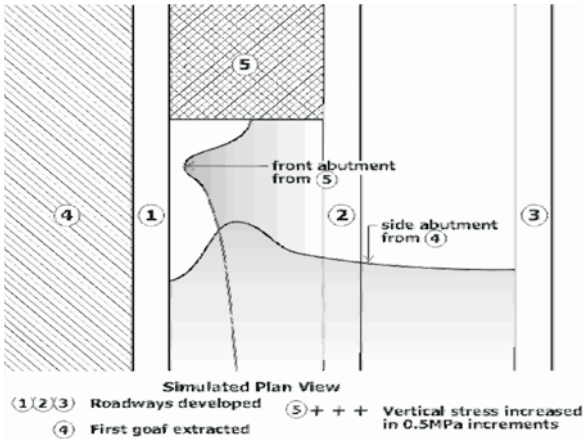

Figure 10: Modelled extraction sequence

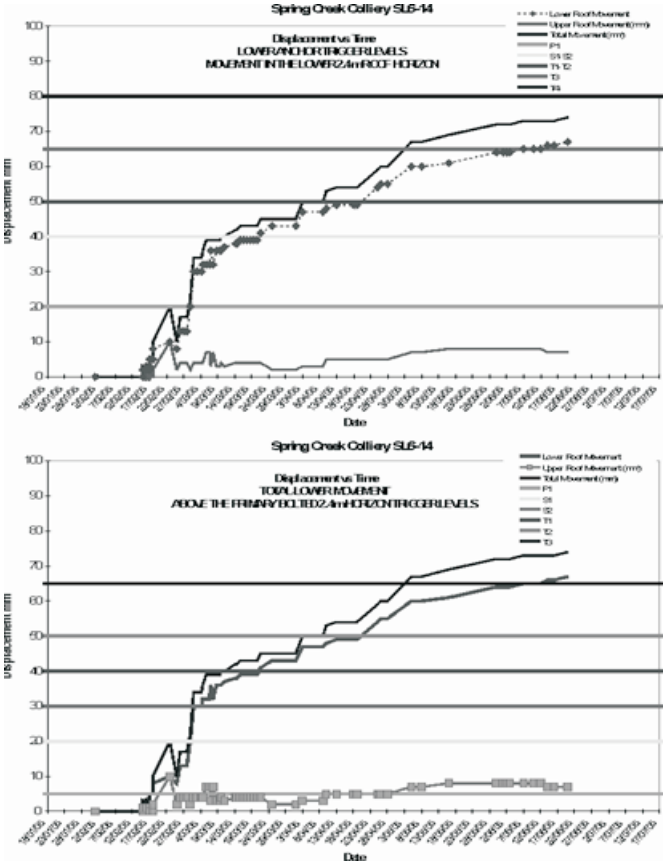

Figure 11: Tell tale monitoring data, and TARP trigger levels

phases of the operation. This data is used to check the design assumptions against the as-built behaviour, calibration of the numerical models, the performance of the reinforcement systems and for strata management in terms of TARPs.

Tell tales are installed every 20m of advance, with the deformation recorded being linked to the capacity/length of the reinforcement used. Figure 11 shows tell tale monitoring data, and TARP trigger levels.

Extensometers and strain gauge bolts are used routinely to:

- define the mechanics of strata deformation on development and extraction,

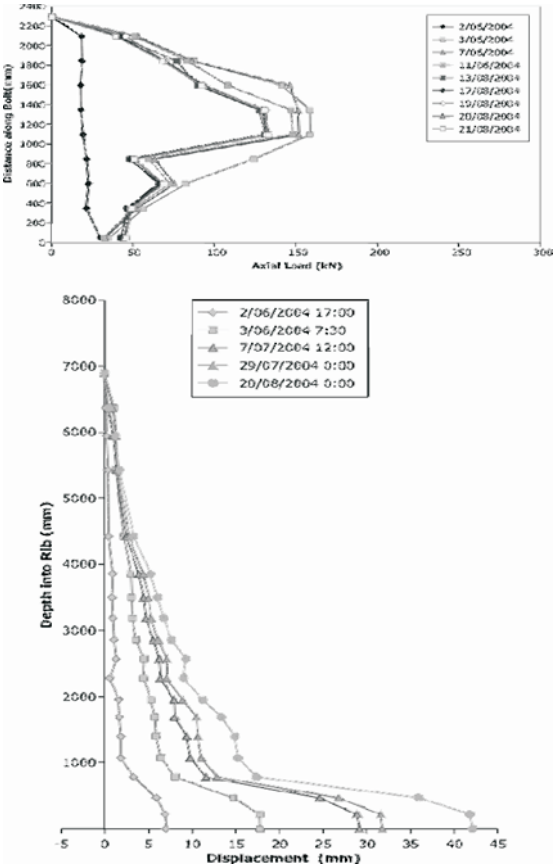

Figure 12: Instrumented bolt and extensometer data

- for the assessment of the appropriateness of the installed support elements, aimed at determining if the length and capacity of the current support system is adequate or could be further refined, and
- to quantify the timing, style and magnitude of load generation on the primary support system and the magnitudes of roof and rib deformation.

Figure 12 shows some instrumented bolt and extensometer data from Spring Creek Mine.

STRATA MANAGEMENT SYSTEM

The difficult mining conditions and unconventional mining geometries used at Spring Creek require best practice strata management systems, including both prescriptive and reactive strata reinforcement systems.

The basis of the strata management plan at Spring Creek is the Managers Support Rules, Roadway Development Standards and TARPS. The key to ensuring reaction to changes in conditions requires a high level of extraction and development operator awareness, an understanding of the geomechanical behaviour and anticipated conditions. Management must also accept the need to react rapidly to deterioration in mining conditions.

The operators, supervisors and line management have ownership of the strata management system. This is achieved by including all levels of the operation in the development of the standards and undertaking training of all personnel.

The reinforcement consumables used have been selected based on, capacity/length requirements equipment available (hand held bolters) and on ease of installation.

Routine use of geotechnical hazard plans for information transfer and characterisation of the as built conditions are playing a significant role in the management system.

CONCLUSIONS

Spring Creek Mine faces many geological and geotechnical challenges, as a result of the geological setting and the mining constraints on design.

The use of sound geotechnical design processes is providing an understanding of the expected behaviour, deformation levels, key risks and strata reinforcement requirements.

These best practice strata management systems being applied then allow SENZ to successfully mine the seams in a safe and economic manner.

ACKNOWLEDGEMENTS

The author would like to acknowledge and thank the management and crews of Spring Creek Mine for their willingness to undertake the geotechnical work, to take on board the recommendations, and to adopt the strata management systems in an enthusiastic manner.

Also the author would like to thank Solid Energy New Zealand Ltd for permission and encouragement to write this paper.

REFERENCES

GALE, W., 2004: Prediction of Caving and Surface Subsidence Characteristics for Spring Creek Mine. External consultants report SCT Operations Pty Ltd.

MACGREGOR, S., 2004: Assessment of Sub Level Cable Bolt Design. External consultants report SCT Operations Pty Ltd.

Richard Campbell, Geotechnical Engineer Spring Creek and Terrace Mines
Spring Creek Road, Dunollie via Greymouth, PO Box 24, Runanga, Westland, New Zealand
richard.campbell@solidenergy.co.nz Ph DD: +64 3 762 7964 Fax: +64 3 762 7712

Richard Mould, Senior Geotechnical Engineer
2 Show Place Addington, Christchurch New Zealand
richard.mould@solidenergy.co.nz

Darren Pisters

Development of generic guidelines for low wall instability management utilising the slope stability radar — case studies from the Hunter Valley and Bowen Basin

The greatest challenge in any low wall instability situation is knowing with confidence when a low wall dump is going to fail. With this critical information, management practices can follow, however if this information is unclear or not known there is potential for enormous implications to both safety and production. This knowledge is obviously a key to success in managing low wall instability issues.

Slope Stability Radar technology has been available to the mining industry for a number of years, however the setting of alarm trigger levels by mine geologists and geotechnical engineers still commonly remains a process of trial and error. This is easily understood, as each instability situation has different geological, geotechnical and mine design parameters. However, each time a false alarm is activated production is lost and the workforce can be affected by elevated levels of anxiety and/or complacency. This is clearly one of the main issues with managing low wall instability at present.

Evaluation of slope stability radar data from two case studies has determined that a potential key indicator for determining 'the point of failure' is not the rate of movement of a slope but the acceleration of the slope. The two cases presented in this paper indicate that at 3mm/hour/hour acceleration, failure can be considered imminent and it was considered at this point mine personnel should be evacuated from the affected area. This paper establishes a set of guidelines for setting slope stability radar alarms which may have the potential to be applied generically across most low wall instability circumstances. It is recommended that further slope stability radar case study data be evaluated to challenge, refine and support the guidelines presented.

INTRODUCTION

The development of a low wall management system was a requirement before a massive low wall failure occurred at the North Pit of the Mount Owen Complex in the Hunter Valley.

With an estimated volume in excess of 15 million BCM of spoil, the magnitude of this failure would easily place it as one of the largest to occur in Australia. With multiple low wall haul roads and dumps across the failure area, the potential impact to both safety and production was enormous.

The North Pit is the deepest and one of the most geologically challenging open cut coal operations in Australia and possibly the world. With depths in excess of 270m, the North Pit has required the development of considerable innovative techniques in its pursuit of 'digging deeper'.

GEOLOGICAL AND GEOTECHNICAL SETTING

The North Pit at the Mount Owen Complex mines 12 distinct seam groups from the Wittingham Coal Measures and the Wollombi Coal Measures of the Singleton Subgroup (Figure 1). Each seam group comprises multiple splits and varying thicknesses totalling up to 22 mineable coal sections within the pit shell (Frogley, 2003).

The North Pit has extreme and unusual geological conditions. It is located between two large regional thrust

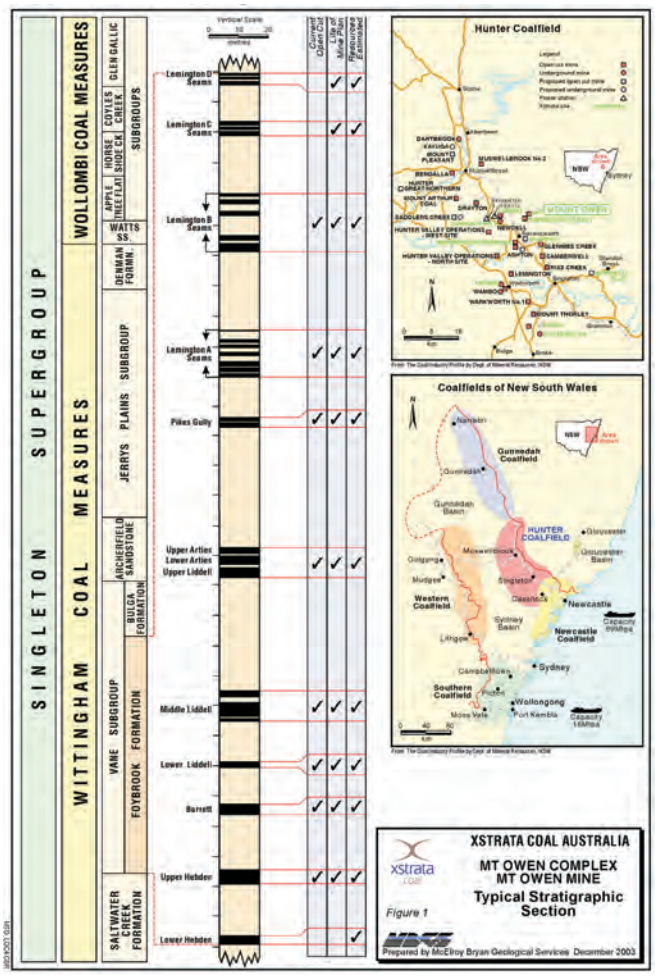

Figure 1: Stratigraphic Column Mount Owen Complex

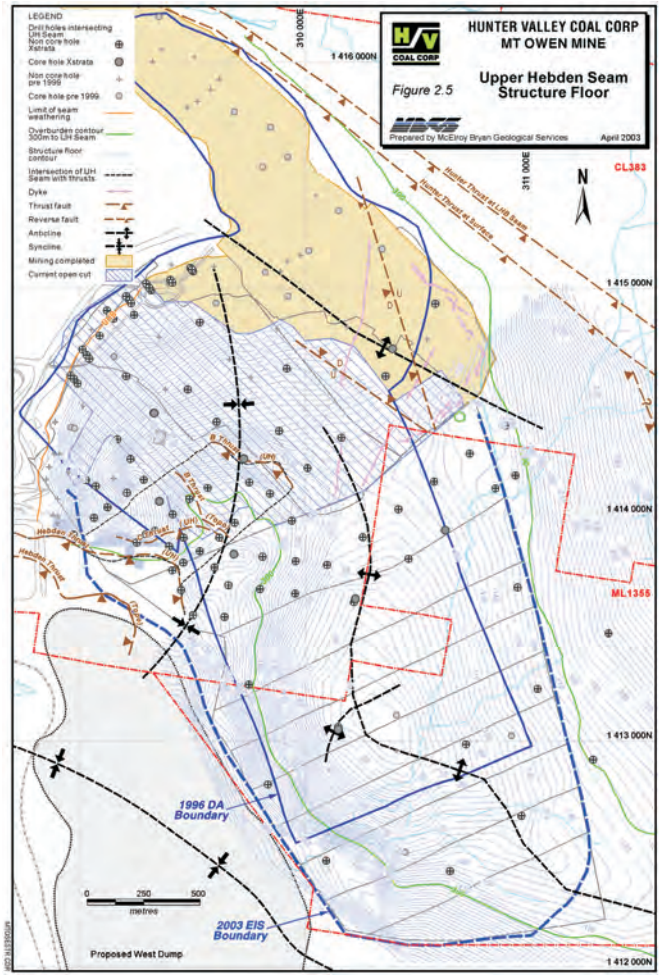

Figure 2: Geological Structure

faults, namely the Hunter Thrust to the North West and the Hebden Thrust to the South-East (Figure 2). Its coal seams dip at a steep angle of between 10-45 degrees (average 22 degrees) and are intensely faulted and folded. This unique geology presents a complex geotechnical environment unlike any other coal mine in Australia.

LOW WALL DUMP INSTABILITY

In June 2004, the main in-pit overburden dump had been identified as “failing” back into the pit. Cracks had developed around the perimeter of the dump in an area over 1000m wide and 220m high. The failure mechanism was principally along clay bands within the Lower Hebden Coal seam some 20m beneath the pit floor. A dolerite dyke and a seam roll/fault enabled a zone of weakness along two sides of the failure which ultimately enabled the failure to progress through the 20m of interburden between the Lower Hebden seam and the pit floor (Figure 3). Spoil material consisted of competent sandstones and siltstones with nominal material properties of c 30 KPa and q 28 degrees.

GPS survey stations monitored the slope in the 6 month lead-up to the failure. This data gave vital information on movement direction and the first indication of the onset of advanced failure. As the advanced failure period was

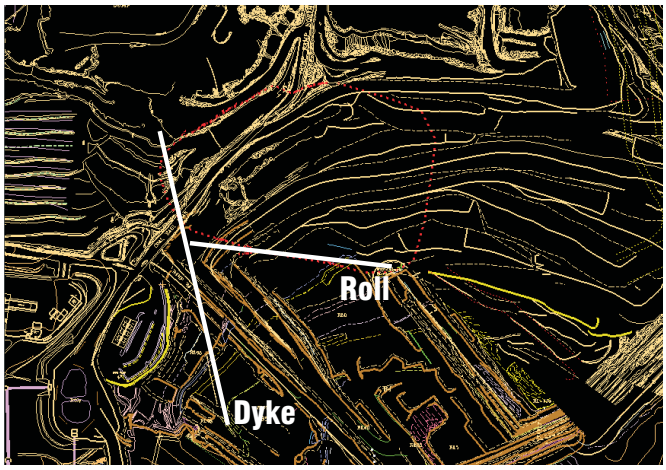

Figure 3: Failure Location

unknown, a management system that could accurately determine the “point of failure” was required in order to manage both the safety and productivity risks. At this point, the Slope Stability Radar monitoring system was commissioned on site.

SLOPE STABILITY RADAR (SSR)

The Slope Stability Radar System operates by scanning a slope from a stand off position and recording the reflected signal. The system operates continuously and slope movement is determined by the difference between subsequent scans. Correction algorithms are incorporated into the system, allowing for compensation for atmospheric changes and movement of mining equipment.

Once set up, the system can generally produce data for interpretation within 20 minutes. Data from the slope stability radar is presented in two formats. Firstly, a colour ‘rainbow’ plot of the slope representing total movement quickly enables the user to determine the extent of the failure and the area where the greatest movement is occurring. Secondly, time/displacement graphs can be selected at key locations to evaluate displacement rates.

Various options are available when setting the alarms within the system. This includes setting different alarm levels by an amount of movement, by an area of movement and by a time interval (20mm over 1000m^2 in 1 hour). This is often confusing and unclear when setting alarm levels and a process of trial and error generally occurs when setting the system up. This can lead to several instances of premature evacuation of the pit prior to failure.

LOW WALL MANAGEMENT SYSTEM

The Low wall management system developed by the Mount Owen Complex Management Team consisted of

- Risk Assessment,
- hiring of ‘Ground Probe’ radar,

- evaluation of radar data to develop guidelines for setting critical trigger levels,
- establishing an emergency response plan that included,
  - » TARP (Triggered Action Response Plan)
  - » Warning alarm in CHPP Control Room
  - » Activation of a Withdrawal Procedure
  - » Inspection Regime
  - » Continual Review
  - » Feedback sessions to employees.

The key aspect of the management system was the development of guidelines for setting critical trigger levels from radar data.

TRIGGER LEVELS

Every low wall instability situation will behave in a different manner as each will have different material types, different geological structure and different mine design parameters. Therefore, the concept of generic guidelines for setting trigger levels may be considered by some as not feasible.

The general concept behind setting generic levels is that once a low wall slope has moved around 200-300mm, material strengths within the slope have been reduced to a residual strength. This strength generally ranges between c = 0 KPa and q = 12°–18° for most sheared failure surfaces. Therefore, at this late stage of failure, low wall slopes approach a similar (but not the same) strength regime with the difference being the remaining diminishing intact geology at peak strength. With the assumption that the low wall slope is not under the influence of significant groundwater affects, the acceleration trend of a slope at the final stages of failure can be characterised and then guidelines from this trend can be applied to individual failure precursor conditions.

Before defining a trigger level, it is important to understand the failure mechanism of the slope. Low wall dumps generally have a long lead up time to failure and often failure is slow and manageable. This is true if the failure plane is within the spoil, however if the failure plane is deep seated, involves an *in situ* low wall buttress or any circumstance where intact geology is required to fail in order to complete the failure trajectory, the final onset of failure can be extremely rapid.

The first step in setting a trigger level is collecting and interpreting meaningful data from the SSR. This is done by identifying key failure daylighting locations where movement rate directly reflects the movement of the slope and is not affected by spoil 'skin' affects. These locations are generally where the movement indicated on the radar 'rainbow' plot is greatest (Figure 4 and 5), however the geologist/geotechnical engineer should determine the individual failure mechanism and field check.

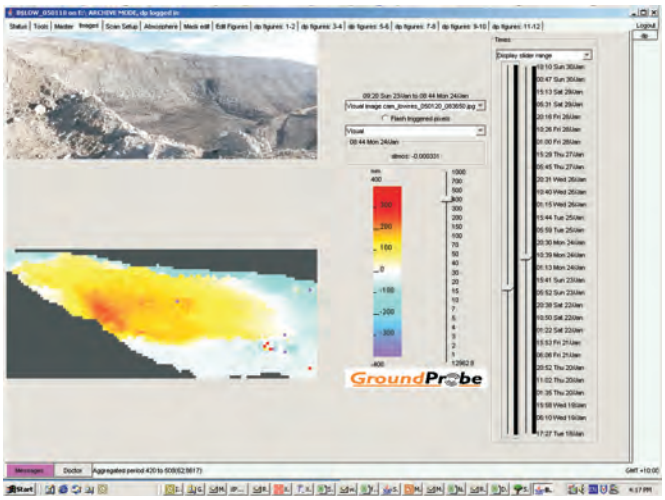

Figure 4: Ground Probe 'rainbow' plot showing location and amount of movement

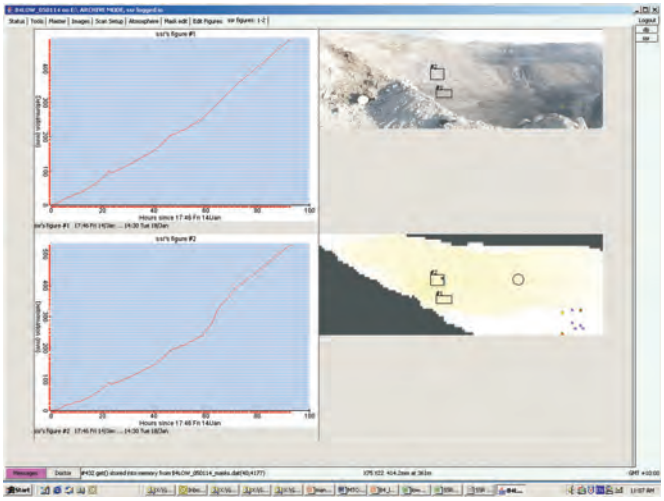

Figure 5: Determination of key monitoring locations on daylighting dominant failure surfaces

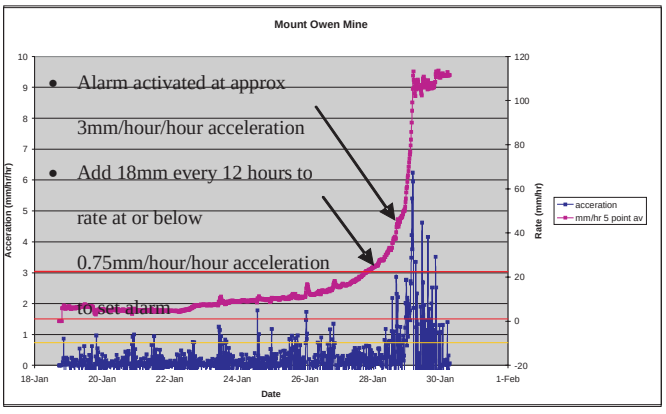

Figure 6: Mount Owen radar data-rate and acceleration vs. time

Once key monitoring locations have been established, data can be exported from the radar software and imported into excel to produce movement rate and acceleration graphs.

It is from this point the daily interpretation of the slope must be conducted. Figure 6 below is a graph of the Mount Owen radar data showing displacement rate and acceleration.

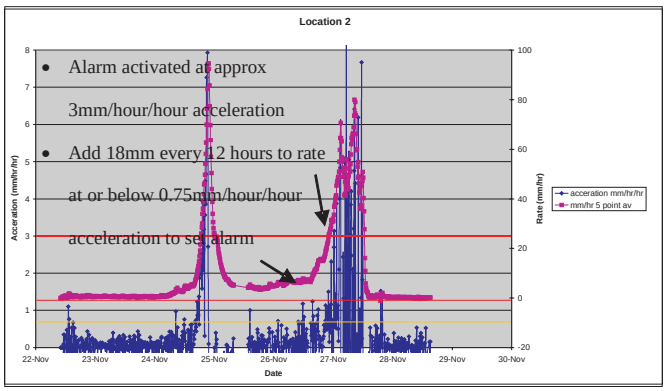

Figure 7: Bowen Basin case study site radar data-rate and acceleration vs. time

From the data, various jumps in acceleration can be seen before the final onset of failure. This can be interpreted as progressive failure of the slope as the rock mass continues to fail, allowing deeper penetration of water and shearing material to residual strength. Hence, the slope displays a continuous cycle of accelerating and decelerating as the failure cycle continues. At the final stages of failure, the onset can be seen at 0.75mm/hour/hour acceleration and imminent failure at 3mm/hour/hour acceleration. Precursor acceleration jumps breach the 1.5mm/hour/hour acceleration level, however it is not until sustained acceleration at the final stage breaches the 3mm/hour/hour trigger level.

The concept of a generic trigger level is essentially to set an alarm at the 3mm/hour/hour acceleration threshold rather than to a rate per hour of movement.

To do this, the alarm threshold (which currently is set on the radar as a rate) needs to be interpreted and adjusted on suggested 12 hourly intervals. If a sustained increase at rate of 1.5mm/hour over a 12 hour period is achieved, the rate of movement will increase by approximately 18mm (i.e. 12 * 1.5mm). Therefore if 18mm is added to the rate every 12 hours up to the point where 0.75mm/hour/hour acceleration is reached (marking the onset of failure), the alarm will be triggered at the corresponding rate when approximately the 3mm/hour/hour acceleration threshold is reached. At this point a window of 10.5 hours could be established from the trigger of an alarm to remove personnel and equipment from the failure area.

These guidelines are further supported by a second set of radar data from a Bowen Basin site with a completely different set of geotechnical circumstances and conditions. In this example the geotechnical conditions consist of shallow seam dips (<3 degrees) and weak weathered sediments and fissured clays (<20MPA) in a dragline box cut spoil dump.

The failure mechanism is a shallow seated failure occurring along the floor of coal horizon triggered by a subtle seam roll and coal production blasting. However, the trigger levels once set give a similar level of warning. Figure 7 shows the data from the slope stability radar from this case study.

Figure 8: Mt Owen–Low Wall Dump (Prior to Failure)

Figure 9: Mount Owen low wall post failure (in pit view)

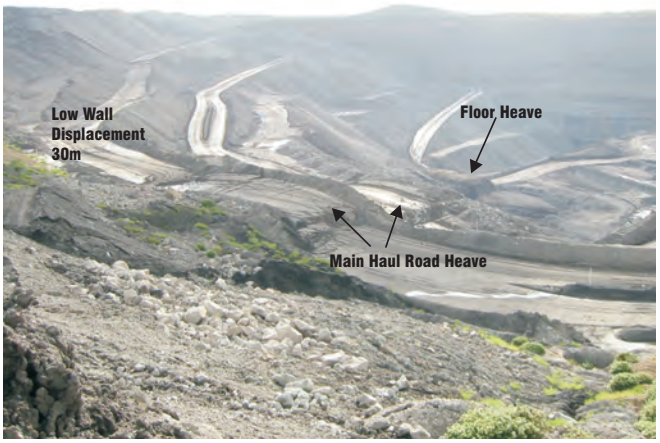

Figure 10: Mount Owen Low Wall Dump (Post Failure)

In this example the failure had a larger precursor condition before the main failure, however if 18mm (threshold of 1.5mm per hour increase over a 12 hour period) is added to the rate every 12 hours at or below the threshold level of 0.75mm/hour/hour acceleration, a 7 hour window to evacuate personnel and equipment could be established once an alarm had been initiated.

Figure 11: Mount Owen Low Wall Failure (view from B4 ramp)

Figure 12: Mount Owen Low Wall failure (view from 215RL dump)

Figure 13: B4 Low Wall Failure (view from B4 Highwall)

In both these examples, the alarm would have been activated at approximately the 3mm/hour/hour acceleration giving approximately 10.5 and 7 hours notice before failure. However, the equivalent rate per hour at 3mm/hour/hour acceleration is 45mm/hour at Mount Owen and 25mm/hour in the Bowen Basin example. This difference is characteristic of the different geological/geotechnical and mine design environments, and hence, by using an acceleration trend, a generic approach can be adopted.

STRATA MANAGEMENT PLAN

Every low wall instability situation must incorporate a strata management plan that defines clear responsibilities and actions for all personnel. A Triggered Action Response Plan (TARP) is commonly used in the mining industry to fulfil this requirement. The benefit of a TARP is the predefined thresholds as defined above can be incorporated into the plan.

An example of the Mount Owen Low wall TARP can be located in Appendix 1. The TARP consisted of 4 levels (green, yellow, orange and red). Each level includes visual, radar and survey monitoring data to determine the level of the TARP. Each level includes clear responsibilities and actions for all personnel on site.

MOUNT OWEN LOW WALL FAILURE

On Saturday the 29th January 2005, the Low-wall failed into the main pit area of Mt Owen. Management plans and early warning systems developed on site enabled operations to

continue up until approximately 5am that morning. At this point overburden haulage over the low wall dump ceased.

At approximately 7:40 am, the low wall failed.

Comments from members of the inspection team, who witnessed the failure unfold include;

"…There were few tell-tale signs when it failed, no rilling of material over the dump, no rapid opening of cracks, no dust, no noise, only minor trickling of material along the day-lighting surface of the failure."

"…Strange silence prior to failure… then I saw the ramp just raise 10m in the air at a rate of about 1m/second……."

"The whole event lasted no more than 10–15 seconds"

"…I have a new-found respect for spoil dumps…."

There were no injury to persons, no damage to equipment and minimal business interruption. On inspection by the Department of Primary Industries-Mineral Resources, the District Mines Inspector classified the event as a Low Potential Incident due to the successful implementation of the management plan in place.

Recently in NSW 3 major failures have occurred. These include Liddell, Muswellbrook Coal and Mount Owen. Of the three failures, Mount Owen was easily the largest and most extensive.

However, out of the three failures, Mount Owen is likely to have had the lowest risk to Safety and Production. The management system introduced at Mount Owen has clearly contributed to lowering the risk at this site. If the principles developed in determining critical trigger levels are identified to be representative of most low wall instability circumstances, then the OH &S and business benefits across not only the coal industry, but the mining industry as a whole, are immense.

CONCLUSIONS

The January 2005 dump failure at Mt Owen took the challenge of identifying the tell tale signs of pre-failure to a new level of understanding in the Australian Coal Mining Industry. Although the guidelines developed in this paper for setting critical alarm levels are based on only two case study data sets, the similarity of the warning period given the extreme differences in geological and geotechnical conditions is stunning. The author believes that as further radar data is collected, these guidelines can be challenged and refined into a more systematic approach for determining with confidence the 'point' of low wall failure.

REFERENCES

FROGLEY, S., 2003: Geological Review Mount Owen Report #189/8/2, in HVCC technical Library.

REEVES, B., NOON, D., STICKLEY, G. & LONGSTAFF, D., 2000: Slope Stability Radar for Monitoring mine walls. *In,* Beeston, J.W. (Editor): *Bowen Basin Symposium 2000 — The New Millennium — Geology*. Geological Society of Australia Inc. Coal Geology Group and the Bowen Basin Geologists Group, Rockhampton, October 2000, 139–142.

Appendix 1

MOUNT OWEN STRATA CONTROL PRINCIPAL HAZARD MANAGEMENT PLAN – B4 LOWWALL TRIGGER ACTION RESPONSE PLAN (TARP)

	L1 Green	L2 Yellow	L3 Orange	L4 Red
Low wall Conditions	Existence of minor long term cracks, AND/OR Existence of minor floor heave in B4 switch back area AND/OR Low wall monitoring is showing <10mm day convergence AND/OR Deceleration path in low wall monitoring over two weeks (at least 3 data sets required)	Opening of existing long term and development of new tensional cracks around low wall crest AND/OR Development of isolated floor heave in B4 switch back requiring infrequent road maintenance AND/OR Low wall monitoring showing greater than 0.25mm/hour and less than 0.75mm/ hour increase in rate over 12 hour period. AND/OR 4. Consistent acceleration path in GPS low wall monitoring showing over 1 week (at least 3 data set required)	Rapid opening and slumping of cracks around low wall crest or toe AND/OR Rapid onset of floor heave around switch back or UHB floor region AND/OR isolated spalling of low wall material AND/OR Low wall monitoring showing greater than 0.75mm/hour and less than 1.5mm/ hour increase in rate over 12 hour period. Rapid acceleration path in GPS low wall monitoring showing over 1 week (at least 3 data set required	Failure of low wall. AND/OR Imminent failure of low wall indicated by Rapid opening of cracks, floor heave, constant movement of spoil material. AND/OR 3. Low wall monitoring showing > 1.5mm/hour increase in rate over a 12 hour period.
Responses:				
Control Room			Contact O.C.E and Mine Geologist and notify an orange alarm level.	Contact O.C.E and Mine Geologist and notify a red alarm level.
Shift Supervisor	Produce to daily production plan	Monitor low wall conditions through the course of the shift. Report any noticeable change in conditions to the mine geologist / geotechnical engineer Report any change of conditions or change in TARP level to the next shift.	Communicate with workforce (MTO/WP/Workshop) an orange level has been reached. Closely Monitor low wall conditions through the course of the shift. Report any noticeable change in conditions to the mine geologist / geotechnical engineer. Report any change of conditions or change in TARP level to the next shift.	Communicate to workforce (MTO/WP/Workshop) a red alarm has been reached and withdraw personnel and equipment to a safe location. Secure area to prevent entry. Inspect area from outside the failure zone & report to Mine Superintendent and Mine Manager immediately Implement Recovery Plan once formulated (Risk Assessment required)
Mine Superintendent	Monitor production activities	Monitor production activities Communicate with Mine Geologist / Geotechnical Engineer.	Liaise with Shift Supervisor, assess situation & inspect as required Communicate with Mine Geologist / Geotechnical Engineer. Notify Mine Manager of the situation as appropriate	Inspect area from outside failure area and report to Mine Manager Implement recovery plan once formulated (Formal Risk Assessment Required).

Appendix (continued)

MOUNT OWEN STRATA CONTROL PRINCIPAL HAZARD MANAGEMENT PLAN – B4 LOWWALL TRIGGER ACTION RESPONSE PLAN (TARP)

	L1 Green	L2 Yellow	L3 Orange	L4 Red
Mine Geologist / Geotechnical Engineer	Continue routine monitoring and mapping	Conduct geotechnical inspections Determine what remedial action is required Determine whether additional monitoring is required Communicate with mine workers the location, nature and expected conditions associated with the failure.	Evaluate monitoring data and provide recommendation for TARP level advance. Conduct geotechnical inspections Determine what remedial action is required Determine whether additional monitoring is required	Inspect and formulate recovery plan (formal risk assessment required) Investigate & report to Mine Manager
Mine Manager		Monitor situation as required	Monitor situation as required	Agree on Recovery Plan Notify, Operations Manager, Mine Inspector Monitor situation as required
Mineworker	Produce to daily production plan	Become familiar with location of failure and monitor low wall conditions during the course of the shift. Report any significant change in low wall conditions to the shift supervisor. Produce to daily production plan	Elevate level of awareness and monitor low wall conditions during the course of the shift. Minimise 2 way chatter and provide feedback on low wall conditions.	Withdraw to safe location

John Simmons, Peter Simpson, Dennis McManus, Paul Maconochie and Philip Soole

Geotechnical design and performance of the Crinum East highwall trench excavation

INTRODUCTION

The Crinum East mining block is separated from the current Crinum (West) mine by a major fault zone. Crinum East mine is being developed as a punch longwall operation. The access for Maingates 3, 4 and 5 will be from the Gregory open cut mine final highwalls at Ramp 1 and Ramp 0 while Maingates 1 and 2 are accessed via a purpose-built trench. The Crinum East trench is aligned oblique to the Ramp 1 West highwall and parallel to the Ramp 3 East endwall (Figure 1).

To date the Gregory open cut highwalls have been generally stable, except for ravelling failures of Tertiary infill materials in palaeochannels in the Ramp 3 East area, and infrequent localised medium-scale wedge-block failures on adverse intersections with faults in Ramp 3 East and Ramp 3 West. Lowwall failures in Ramps 3 East and 1 East have occurred on weak bedding-parallel surfaces.

The proposed Crinum East trench is oriented with the north-west wall effectively updip, resulting in an apparent dip of about 3° across the trench towards the south-east wall. Updip wall stability was therefore of concern when geological and geotechnical investigations in 1999 and 2002 identified generally weak conditions just below the trench floor level.

In common with all open cut pit walls, slope design for Crinum East was based largely on experience and precedence. This paper describes assessments carried out in order to verify the long-term stability of the rock walls for the Crinum East project, particularly for the trench. These assessments consisted of:

- Stress-deformation analyses to identify mechanisms of movement and the potential for development of stress conditions that could lead to rock wall failure;
- Stability analyses to identify the likelihood of rock wall failure mechanisms;
- Prediction and verification of isolated rockfall hazards that were expected to develop as a consequence of rock wall exposure.

GEOLOGICAL AND GEOTECHNICAL INFORMATION

The Lilyvale (LV0) seam floor structure dips generally to the south at between 3° and 5°. Previous spoil dump lowwall instability in the Ramp 1 East and Ramp 3 East areas has

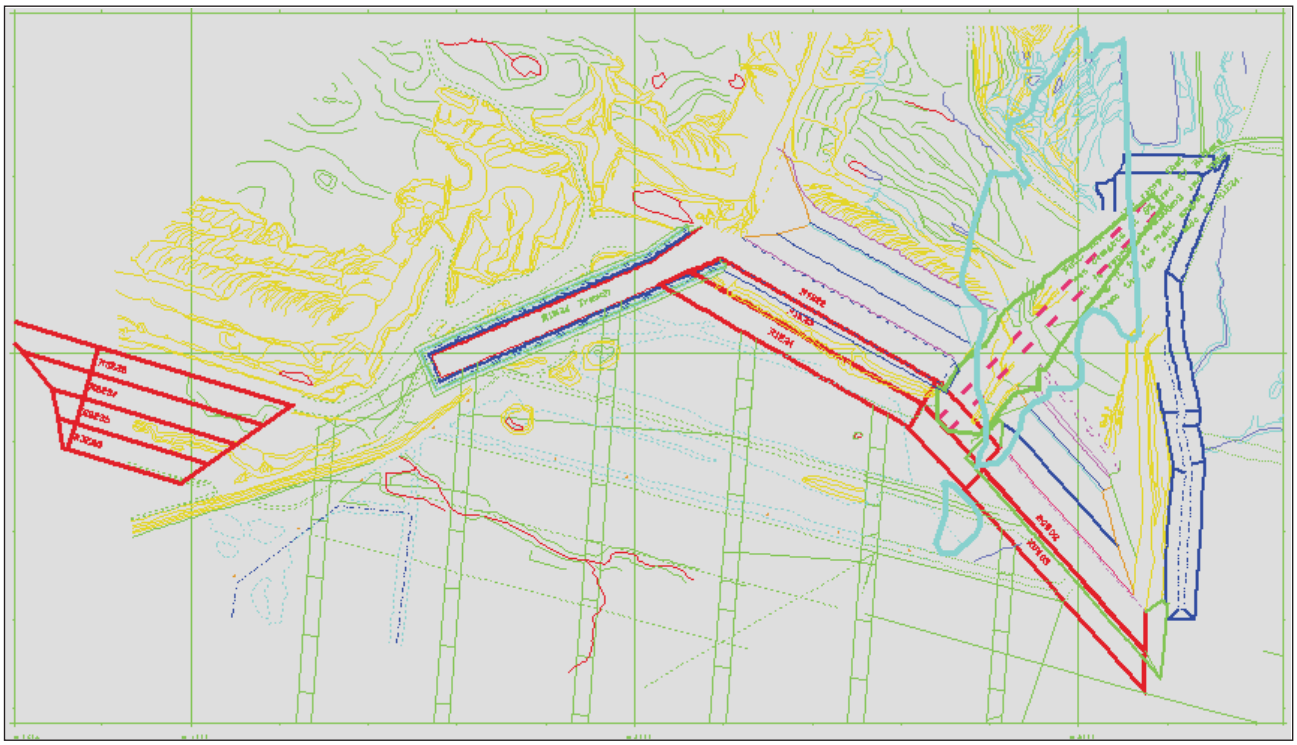

Figure 1: Layout plan view of Crinum East mining block and Gregory pit walls

Table 1: Summary overburden sequence profile for Crinum East Trench area

Unit	Description
Tertiary/modern	Typical thickness 1–2m, sometimes 5m. Mostly clayey sand sediments, some RS-CW basalt
Weathered (Permian) Corvus overburden	Typical depth to BUWE = 15m. CW-XW typically 4m, remainder DW-SW. Typical UCS = 0.6 (XW) – 2.0+MPa (DW-SW)
Fresh Corvus overburden	Typically lithic sandstone and interbedded siltstone-sandstone. Occasional sideritic bands. Typical UCS = 10–20MPa.
Corvus seam (CV0)	Typical depth at trench 44–45m. Low strength coal, typically 0.6m thick seam. Typically sheared and/or puggy band above, and sometimes below.
Corvus to Lilyvale interburden	Typical thickness 22 – 23m. Mostly sandstone, UCS = 5–10MPa, and siltstone or laminite intervals. Occasional 'ironstone' bands UCS = 40MPa, less than 2m thickness. Immediate 1–3m roof to Lilyvale seam has UCS = 2–5 MPa.
Lilyvale seam (LV0)	Typical depth at trench 66–68m. Low-medium strength coal, typically 3.2m thick seam. Low strength immediate roof, very low to low strength immediate floor. Minor stone bands within seam.
Lilyvale seam floor (LV0 to LV1)	Typical thickness 2.5 to 3m of muddy fine-grained sandstone. Immediate 1–2m floor to Lilyvale seam has UCS = 0.6 to 2 MPa, possibly sheared in places.
LV1 coal ply	Typical thickness 0.05m, typically coaly, but altered, sheared and/or puggy. Borehole 07035 has fault at about 50m depth and an additional coal interval 4m below LV1.
Lilyvale seam floor below LV1 ply	Variable thickness of sandstone and siltstone, expected UCS in range 6–20 MPa.

been associated with the low strength immediate LV0 floor rock plus weak seams and sheared surfaces associated with the minor LV1 coal ply at about 3m depth below the LV0 floor. About 18m above the LV0 roof is the Corvus (CV0) seam with associated puggy clay bands.

Geological investigations included four fully cored and seven partially cored boreholes along the initial trench alignment. An additional four partially cored boreholes were located on the revised proposed trench alignment. All holes were geophysically logged. Geological logs were reviewed in order to prepare a summary overburden sequence model. Graphic defect logs were reviewed to determine horizons and attitudes of weak units, shear surfaces, or core losses possibly related to weak or sheared ground conditions. Table 1 shows the summary overburden sequence for the trench and adjacent highwall areas.

Point Load Strength Index (PLSI) testing was undertaken on core from the original eleven holes. UCS-modulus and triaxial strength tests were undertaken on core from the additional four holes. Backanalysis of the Ramp 1 East lowwall failure in 1999 indicated that the effective shear strength of the weak floor material was about $\phi' = 15°$.

Groundwater level within the proposed trench area was not explicitly recorded with the geological information. From the reported difficulty in 'topping-up' boreholes for sonic logging, it is most likely that the groundwater level was generally within a few metres above the LV0 roof.

Hand mapping of highwall joint orientations was undertaken. More detailed defect mapping was undertaken using Sirovision for selected sections of the Ramp 3 East, Ramp 1 West and 1 East, and Ramp 0 West highwalls and endwalls and is described in more detail below.

TRENCH WALL DESIGN CONSIDERATIONS

The average depth of the trench was to be about 85m, and for operational reasons the trench width at LV0 floor level was set to 55m. The slope profile was initially set as steep as possible based on previous experience with 73° batters at Gregory and a previous BMA Coal longwall recovery excavation at Kenmare. Upper batters from natural surface to CV0 floor were set at 75°, with a 13m wide bench and then 75° batters to LV0 roof level. Consideration was also given to a single 75° batter from natural ground level to LV0 roof level, but this was not favoured based on the findings of the stability review.

To the east of the trench, the Ramp 1 East and Ramp 0 West highwalls were designed as normal Gregory strip highwalls with single presplit 73° batters to LV0 roof level. Slope profile transitions were therefore required to the benched trench profile. Because the trench walls intersect the open cut highwalls at an acute angle, lead-in sections of the trench walls were modified using joint orientation data to reduce the likelihood of corner failures.

Table 2: Interpreted defect set mean orientations

Set	Description	Dip	Dip.Dir	Cone.Angle	Weight
	SGRS hand-mapping 1999				
1 or 4	Lithological Joint	84	341	15	2
2	Lithological Joint	74	051	25	2
5	Fault-related fractures	45	322	15	2
B	Bedding	04	164	15	1
	BMA hand-mapping 1999				
1 or 4	Lithological Joint	87	149	20	1
3	Lithological Joint	86	239	25	1
	GTS SiroVision data 2003				
1 or 4	Lithological Joint	71	336	20	2
2	Lithological Joint	69	026	20	2
B	Bedding	04	170	15	2
	SGRS SV subset. 2003				
1 or 4	Lithological Joint	65	333	25	2
3	Lithological Joint	74	270	25	2

The Ramp 1 East and Ramp 0 West highwalls were excavated as an open cut dragline operation, whereas the trench contract walls were excavated by truck/shovel techniques under contract. The likely greater degree of blast damage and lower standard of wall cleanup of the dragline highwalls was expected to result in poorer stability conditions for highwall portals than for trench portals.

ROCK MASS DEFECT STRUCTURE ASSESSMENT

Sherwood Geotechnical and Research Services (SGRS) carried out limited hand mapping in the Ramp 3 East area during 1999. More extensive hand mapping was also carried out by BMA Coal during 1999 in the Ramp 3 East and Ramp 1 areas, but defect spatial locations were not recorded. Corelogs from 2002 provided dip but not dip direction information. Since the majority of the defect data to that date had limitations that were considered significant for design review, additional mapping of selected windows on all exposed highwalls adjacent to the trench was carried out during April 2003. The Sirovision system was used to acquire and process stereo models, and SiroJoint was used primarily by GeoTek Solutions (GTS) to map defect orientations, extent, and spatial location.

The SiroJoint system demarcates either surfaces or traces, to which a best-fit planar surface is mathematically fitted. The 'Quality' of the mathematical fit is expressed by a parameter that ranges from 0 (poorest) to 5 (best). The areas of demarcated surfaces are also computed, with the expectation that larger areas are more likely to be fitted accurately.

Table 2 shows the mean orientation data for the defect sets identified from all sources. The cone angle (half of a right cone apex angle) is the angular representation of one standard deviation about the mean pole position for each set. When the data from all sources was first compiled, there were obvious differences by method and by operator. For this reason, a few of the SiroVision models were also interpreted by SGRS and the resulting orientation data is also shown in Table 2. Taken together, this data indicated considerable variability of defect orientation by method and by operator.

With Sirovision, defect surface characteristics are assessed from 3D images created from stereo photos. Care is required not to include blast-induced fractures, as well as natural defects when interpreting. In addition, lighting conditions at the time of imaging can affect the quality of the 3D image for interpretation, with image regions of low contrast most likely to reduce the accuracy of fit. Table 2 shows significant differences between fits by two operators using Sirovision on the same models. Data differences were minimised by selecting only defects with Quality >2.5 and Area >3m^2.

Mean orientation data for all sets were weighted using the factors shown in Table 2 to take into account relative reliability of location, and a defect database was compiled using the DIPS code (Rocscience, 2002a). The true 3D relative proportions of defects within each set were estimated from selected stereomodels, taking into account confidence in judging natural defects versus possible blast fractures, raw data counts, and likely bias due to face orientation. From this process, a synthetic defect data set (Table 3) was generated for assessing whether structurally-controlled failure mechanisms were likely to develop on highwalls and trench walls. To make such analysis meaningful, the continuity (extent in horizontal and vertical directions) and persistence (nature of defect intersections) observations from the SGRS data set were assigned to the model sets, because all of the other data sets did not include continuity or persistence observations.

ROCK MATERIAL PROPERTIES

Average total densities (ie solids plus moisture) within the weathered and fresh zones were interpreted to be 2.20t/m^3

Table 3: Modelled defect data set parameters

Set	Description	Dip	Dip. Direction	Cone. Angle	Proportion
J1	Lithological Joint, dip to NNW	76	335	20	40%
J2	Lithological Joint, dip to NNE	72	039	20	27%
J3	Lithological Joint, dip to W	78	260	20	20%
F5	Fault-related fracture	45	322	10	3%
B	Bedding	04	170	02	10%

and 2.45t/m^3 respectively from geophysical logs. The mean and standard deviation of total density from laboratory tests were 2.30 and 0.09t/m^3 respectively, but consistency checks indicated some drying-back of core prior to testing. Total densities of 2.20t/m^3 and 2.40t/m^3 were therefore adopted for insitu weathered and fresh rock respectively.

Laboratory strength and stiffness testing included standard UCS, UCS with LVDT-based Young's modulus measurement, and UCS with strain gauges to measure Young's modulus and Poisson's ratio (Strata Testing Services, 2002). A large amount of Point Load Strength Index (PLSI) testing was carried out by BMA Coal. Triaxial shear strength tests were also undertaken using a staged technique on single specimens. Consistency checks indicated that most of the UCS and triaxial test specimens had experienced significant drying-back prior to testing.

Because of the generally low phreatic surface in the area of the proposed trench, and limitations experienced in topping-up boreholes with water, it was not possible to run sonic logs through the full overburden sequence. Where sonic log data was obtained, corresponding UCS data from laboratory tests were used to generate a site-specific sonic-UCS correlation. This was not successful due to the large scatter in the data. The following general sonic-UCS correlation determined by BMA Coal for similar range of rock materials was therefore adopted:

$$UCS\ (MPa) = 1178.e^{-0.041\Delta t}$$

where Δt = interval transit time (μs/ft) from sonic log.

Figure 2 shows a comparison of the Sonic-UCS and laboratory UCS profiles for corehole 7037. Generally there was very good agreement between correlations of PLSI and Sonic-UCS, provided that the UCS data was ignored for samples most noticeably affected by dry-back.

Laboratory values of Young's modulus (E) were determined by two techniques. In most cases the E values determined using LVDT's over the full specimen length were lower than E values determined using local strain gauges at the specimen midpoint. Rock material modulus values were used as a guide for selection of modulus values for the rock mass.

ROCK MASS STRENGTH AND STIFFNESS

For the purposes of design verification the entire rock mass profile was subdivided into the fewest possible material units as indicated in Table 1. The characteristic strength that was adopted for each unit was the 25th percentile UCS value for that unit. This approach virtually ignored the high strength of the sideritic intervals within the sequence, and possibly overestimated the low strength of some horizons, but was expected to result in a slight underestimate of overall stability.

For analysis and design purposes the Generalised Hoek-Brown (GHB) rock mass shear strength model was adopted. The RocLab code (Rocscience, 2003a) was used to determine GHB parameters for the overburden units. Table 4 is a summary of the input and output parameters relating to the GHB models. Where it was necessary to determine equivalent linear Mohr-Coulomb shear strength parameters, best fits to GHB strength envelopes were made using appropriate ranges of effective normal stress.

Rock mass stiffness is a function of lithology, strength, loading path, and amount of shear strain. It was considered to be more important to determine relative stiffness of different units of the rock mass, so that the overall pattern of deformation was reasonable even if the absolute magnitudes were not completely correct.

Stiffness in laboratory tests is measured at comparatively large shears strains, along stress paths very different from the unloading paths that occur during excavation. On this basis field stiffness would be much higher than indicated by laboratory tests. However core tests measure material rather than mass stiffness which is also affected by the presence of defects, particularly where joints open or are sheared because of the loading path. On this basis, mass stiffness should be less than material stiffness. Overall, it was considered reasonable to assign rock mass stiffness values similar to laboratory measurements. In locations where the primary

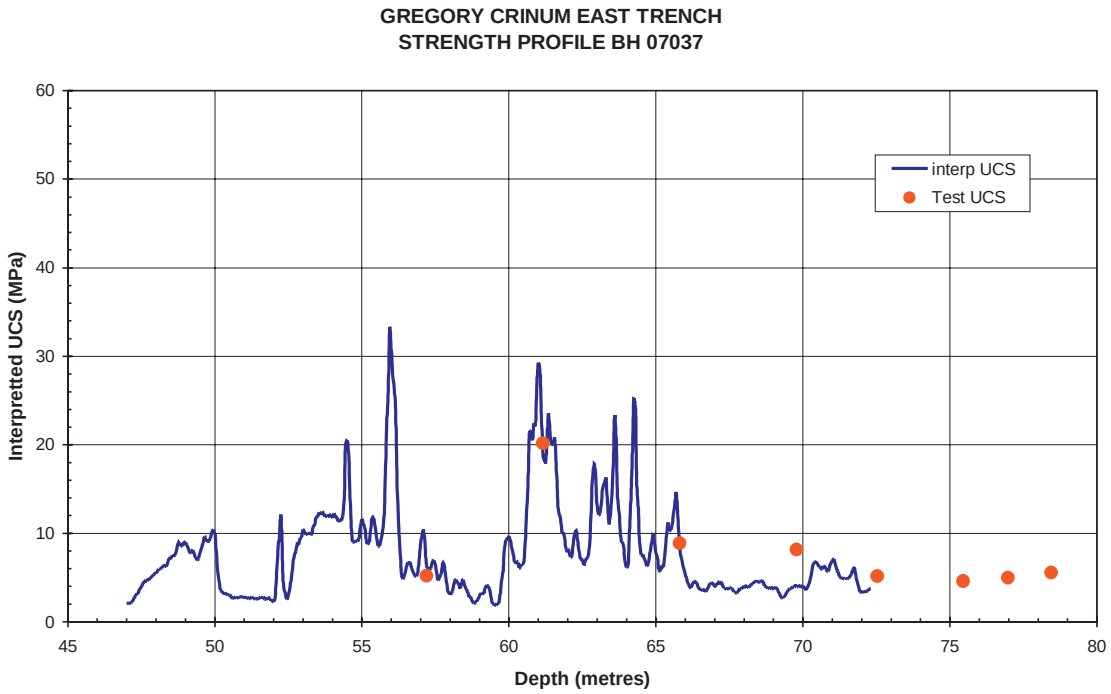

Figure 2: Example of Sonic-UCS and laboratory UCS profiles for borehole 07037

Table 4: Generalised Hoek-Brown (GHB) rock mass shear strength and stiffness parameters

Material	Input Parameters				GHB Strength & Stiffness Parameter Outputs					
	UCS (σ_{ci}, MPa)	GSI (Geological Strength Index)	m_i (mineralogy parameter)	D (Disturbance factor)	mb	s	a	E (MPa)	UTS (σ_t, MPa)	γ (MN/m^3)
Tertiary	0.60	22	16	0.0	0.987	0.0020	0.538	155	0.0	0.022
weathered Permian	2.0	60	18	0.7	1.999	0.0030	0.503	1640	-0.003	0.023
fresh Permian	4.0	70	18	0.7	3.463	0.0129	0.501	4100	-0.015	0.024
Coal	6.0	35	35	1.0	0.337	0.00002	0.516	520	0.0	0.015
Immediate LV0 Floor	2.0	80	5	0.7	1.666	0.0551	0.501	5170	-0.066	0.024

stress path was direct unloading, such as the exposure of floor by removal of overburden, stiffness was increased by a factor of 10. However, for direct unloading of coal, stiffness was reduced by a factor of 10 due to the softening effects of the fine-scale cleat structure of the seam plies. To simulate the effects of blasting, mass stiffness was reduced by a factor of 100.

Table 5 is a summary of the rock mass stiffness parameters that were adopted. Notably, the unit weights for all of the materials were chosen to be a constant value of 0.024MN/m^3. This was due to the limitation in the modelling code of assigning a single value of unit weight to represent variation on initial gravity stress with depth. From experience, this simplification does not have a significant influence on the results of analyses. Sensitivity analyses were undertaken to check for the effects of variations in stiffness on the computed stress and deformation states.

ROCK DEFECT SHEAR STRENGTH AND STIFFNESS

Defect surfaces were modelled as discontinuities with finite normal and shear stiffness. Initially defects are considered to be in the elastic or 'locked' condition, where very small normal and shear relative displacements occur of one side of the defect with respect to the other side. If the shear strength criterion for the defect is met or exceeded, additional relative shear deformation is modelled by reducing the effective shear stiffness until and if the surrounding mass comes to a state of equilibrium.

No data was available for shear strength of defects. Pre-sheared surfaces were assigned to the levels of the CV0 and LV1 seams. These seams were thin enough that they were modelled as a single defect rather than as a discrete

Table 5: Rock mass stiffness parameters adopted for deformation analyses

No.	Material	γ (MN/m^3)	UCS (MPa)	E (MPa)	ν (Poisson's Ratio)
1	Surface Soil & Tertiary	0.024	0.6	200	0.2
2	Shot Surface Soil & Tertiary	0.024	0.6	2	0.2
3	Weathered Permian	0.024	2.0	1600	0.2
4	Shot weathered Permian	0.024	2.0	16	0.2
5	Fresh Permian	0.024	4.0	4000	0.2
6	Shot fresh Permian	0.024	4.0	40	0.2
7	Coal	0.024	6.0	500	0.1
8	Shot & uncovered Coal	0.024	6.0	50	0.1
9	Immediate LV0 Floor	0.024	2.0	2000	0.2
10	Unloaded immediate LV0 Floor	0.024	2.0	20 000	0.2

Table 6: Rock defect shear strength and stiffness parameters adopted for deformation and stability analyses

No.	Defect Location	k_N (MPa/m)	k_S (MPa/m)	t (MPa)	c (MPa)	ϕ(deg)
1	CV0 seam/shear	250 000	100 000	0.001	0.0	15
2	LV0 roof	250 000	100 000	0.0	0.0	15
3	LV0 floor	250 000	100 000	0.0	0.0	15
4	LV1 seam/shear	250 000	100 000	0.001	0.0	18
5	'locked' defect	250 000	100 000	n/a	n/a	n/a

thickness of material. The roof and the floor of the LV0 seam were also considered to be pre-sheared, but were discretely modelled above and below the coal seam material.

Based on experience, it was assumed that weak sheared surfaces existed wherever core losses or clay material were logged, and that this material would be pre-sheared to a residual state with a friction angle of 15°. Other surfaces where shearing was logged or suspected based on corelog information were assumed to be at a residual state with a friction angle of 18°. Close inspection of the SiroVision models led to the conclusion that, it there had been any yield of defect surfaces in the Gregory open cut highwalls, the relative magnitude of slip was so small that it was not visually obvious.

There was no information available for either normal or shear stiffness of defect surfaces. The parameters assumed for analyses were values based on experience that were considered to be reasonable for such conditions. Table 6 is a summary of the rock defect stiffness and shear strength parameters that were adopted. Sensitivity analyses were undertaken to check for the effects of variations in stiffness on the computed stress and deformation states.

STRESS-DEFORMATION MODELLING OF TRENCH EXCAVATION

Based on previous experience with the Oaky North and Kenmare longwall recovery excavations, the stepped excavation profile was designed as a buttress to limit wall movements, and therefore to minimise loosening of the rock mass. The purpose of stress-deformation modelling was to identify mechanisms of deformation and zones of high shear strength mobilisation, and to determine whether such mechanisms or zones were likely to interact with adverse defect orientations to create conditions for both short-term and long-term instability of the trench walls.

The PHASE^2 finite element code (Rocscience, 2002b) was used for stress-deformation modelling. This code allows 2-D modelling of rock masses and discrete surfaces such as joints, under combinations of pre-existing ground stresses, excavation, and provision of backfilling or ground support.

The general deformation mechanism for the trench excavation was response to lateral unloading. The initial stress state of the rock mass is the controlling influence on such response, with the absolute magnitudes of deformations

Table 7: Summary of loading sequence used for deformation modelling

Step	Description
1	Start with initial 'at-rest' stress condition. 'Blast' upper section of CV0 overburden by removing slot and assigning 'blasted' stiffness parameters to affected layer. Results in heaving and lateral stress relief, but stress and deformation distributions in 'blasted' zone are ignored.
2	Excavate upper section of CV0 overburden. Creates stress relief: vertically in underlying material and laterally to upper trench walls. High shear stresses induced at corners of excavation zone.
3	'Blasting' of lower section of CV0 overburden by removing slot and assigning 'blasted' stiffness parameters to affected layer. Results in heaving and lateral stress relief; stress and deformation distributions in 'blasted' zone are ignored.
4	Excavate lower section of CV0 overburden. Creates stress relief: vertically in underlying material and laterally to middle trench walls. High shear stresses induced at corners of excavation zone.
5	'Blasting' of CV0 to LV0 interburden by removing slot and assigning 'blasted' stiffness parameters to affected layer. Results in heaving and lateral stress relief, but stress and deformation distributions in 'blasted' zone are ignored. Shear stresses induced in weak surfaces below LV0 floor.
6	Excavate CV0 to LV0 interburden. Creates stress relief to lower trench walls and to LV0 seam and weak floor. High shear stresses induced at corners of excavation zone, and along weak surfaces in LV0 floor.
7	Excavate LV0 coal. Creates stress relief and lateral deformation response of LV0 seam at updip and downdip walls of trench, and induces shear yielding of weak floor surfaces.

related to stiffness but the relative pattern of deformations related to the combinations of strength and stiffness at difference levels. The initial stress state was unknown, but in keeping with Bowen Basin experience the 'at-rest' coefficient K_0 was expected to be between 1.5 and 2.0. A K_0 value of 1.5 was chosen for the base case.

Excavation was simulated in seven steps, corresponding to blasting and overburden removal in two layers down to Corvus seam level, then blasting and overburden removal to expose the LV0 seam and finally LV0 seam removal. These loading steps are summarised in Table 7. Blasting of a layer was simulated by removing a thin slot at the centre, and by simultaneously assigning much lower stiffnesses to the layer. While modelling cannot not replicate all effects of blasting, the adopted process was considered to capture the principal effects of lateral stress relief and overall stiffness reduction while not removing material mass.

PHASE^2 is not a coupled poroelastic formulation, so it cannot simultaneously model the interactions of the rock material skeleton and groundwater response to excavation. However, it does have the facility to specify a groundwater state for each stage of analysis, in order to be able to calculate yielding in terms of effective stresses. For the purposes of this assessment, an initial groundwater level corresponding to the approximate level of the CV0 seam was chosen, and as excavation was taken below this depth the groundwater was modelled as a relatively steep drawn-down surface.

It was expected that, as excavation of the trench was taken down, yield would be induced in the weak bedding-parallel surfaces, and possibly also in highly stressed zones of the rock mass close to the corners of the excavation. The rock mass was simulated as initially elastic, but with the capability to model yield behaviour (plastic response) in most cases. Weak bedding-parallel surfaces were modelled as joints with initially elastic response but the capability to model yield behaviour in all cases.

The yield state in the rock mass was assessed using a Strength Factor (SF), calculated as the ratio of the actual shear strength available to the shear stress mobilised. SF is therefore equivalent to a localised safety factor against shear yield. SF was also calculated along the joints representing weak bedding-parallel surfaces.

The Hoek-Brown rock mass model was used as the base case to check for combinations of stiffness and strength conditions that might lead to more extreme stress of deformation states. Yield behaviour was allowed to occur but if overall equilibrium was achieved, the response would converge to a stable deformation state with appropriate stress redistribution. In none of the cases examined was there any hint of non-convergence indicating instability.

Figure 3 shows the SF state for the rock mass and for selected joints, for the final loading stages of the base-case model. SF plots for the other loading cases showed the same basic pattern.

Figure 4 is a view of the final excavation boundary showing the locations of selected points where the deformations were tracked for all of the analysed cases. In addition to these displacement points, the lengths of the yielded zones along selected joints were also tracked as an indicator of the extent of yielding. Figure 4 also includes a tabulation of the computed movements and extents of yielding for the maximum, average, and minimum movement conditions.

The wall deformations and yielded lengths were greater on the updip side of the trench than on the downdip side. This could be expected, given the component of dip out of the

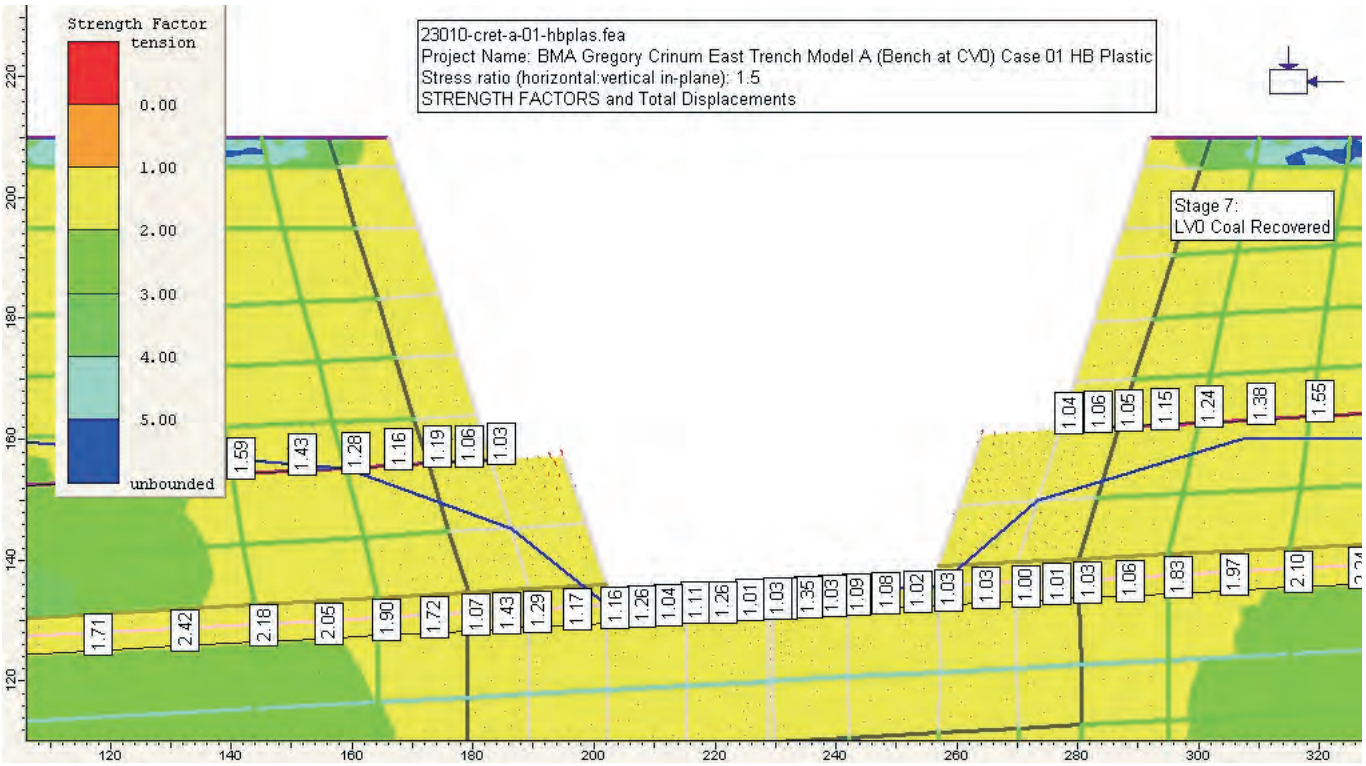

Figure 3: Strength Factors for Base Case, Load Step 7 (remove LV0 coal)

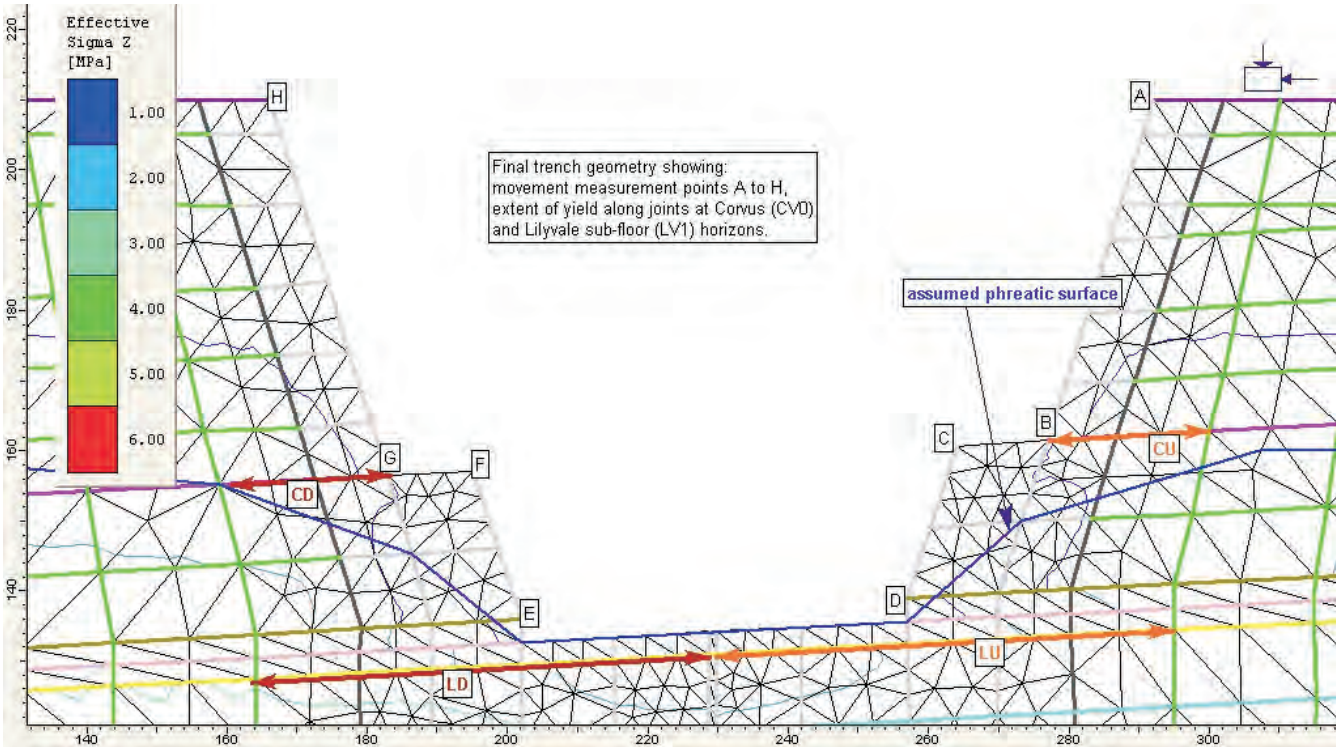

Case	Deformation (mm)								Yielded Length (m)			
	A	**B**	**C**	**D**	**E**	**F**	**G**	**H**	**CU**	**CD**	**LU**	**LD**
Max	63	83	96	84	81	93	67	54	80	71	88	85
Avg	**28**	**41**	**44**	**72**	**58**	**97**	**25**	**11**	**52**	**54**	**70**	**46**
Min	5	8	7	18	14	11	5	2	23	18	32	33

Figure 4: Trench geometry showing movement and yield locations and results

wall on the updip side. The maximum expected wall movement was predicted to be about 100mm for the base case, and under more extreme assumptions the movement was about 150mm. When the effect of unloading of large joints subparallel to the excavated batters was simulated, lateral deformations increased by a factor of about 2. The effects of the lateral stress condition area were very pronounced, with deformations for the low lateral stress condition being about 3 to 6 times smaller than for the high lateral stress condition.

Despite the significant extent of yielding along these surfaces, overall calculated deformations remained quite small. This indicated that the yield response was limited by the strength of the rock mass, with only limited yield propagation. Observations of the Ramp 3E and 1E highwalls confirm this interpretation. However, when the LV0 coal was removed, the actual response of the up-dip wall suggested that there was significant yield at the trench corners and within the weak zones of the immediate floor.

Potential rock mass sliding mechanisms were found to be similar in form to critical mechanisms identified in the stability analyses. While the strength mobilisation was locally very high, in overall terms the average SF value along a potential failure mechanism is relatively high indicating stable conditions.

EXCAVATED WALLS ROCK MASS STABILITY ASSESSMENT

Existing open cut highwalls were assessed to be adequately stable, with little evidence of long-term deterioration except for two circumstances:

- Deep Tertiary ‘palaeochannels’ with infillings of sediment and/or completely weathered basalt;
- Locations of structural disturbance, generally at and above Corvus seam level, involving combinations of bedding-parallel shears and faults or shears across bedding and adversely oriented to the highwall exposure.

With both of these circumstances, open cut experience had been that faces tend to ‘self-stabilise’ once oversteepened zones fall out or are dug out. Even in the Ramp 3E condition where weak floor conditions had resulted in lowwall failure, there had been no evidence of highwall instability. Neither condition was expected to occur within the trench excavation, but a deeply weathered zone of sediment and completely weathered basalt was identified in the Ramp 1E – Ramp 0W area.

Limit equilibrium stability assessments were made for the stepped trench wall profiles, up-dip and down-dip, and also for the non-stepped profiles of the adjacent open cut highwalls. These assessments took into account the rock mass strength and also the expected influence of groundwater conditions. Factors of Safety (FOS) were calculated using the Morgenstern-Price method for vertical slices, and the clipped-sine interslice force function, as implemented in the 2D limit-equilibrium stability analysis SLIDE (Rocscience, 2003b). Two types of potential instability mechanism were examined:

Mechanisms based on circular arcs, but incorporating composite surfaces formed of linear segments (weak bands at the base of the sequence, corresponding to the structural disturbance of the LV1 seam/shear) and vertical tension cracks of unlimited depth;

Non-circular surfaces following weak bedding-parallel surfaces and then extending steeply to ground level.

Two groundwater cases were considered. The likely case was based on a pre-mining piezometric level about 15m above the LV0 floor at the trench centreline, with the water level drawn down to an average profile of 3H : 1V by mining and the water pressure in the rock mass above the LV0 seam decoupled from the water pressure within the seam. The assumption of decoupling is considered reasonable, based on observations of rock wall exposures in Ramp 3E over the period 1999 to 2003. The worst case was based on a pre-mining piezometric level approximately 25m above the LV0 floor, with the water level drawn down to an average profile of 2.5H : 1V by mining and the water pressure in the rock mass above the LV0 seam fully coupled to the water pressure within the seam.

Table 8 is a summary of the minimum computed FOS values for the up-dip and down-dip walls, for the likely and worst-case groundwater cases and for both arc-crack and weak band mechanisms. Figure 5 shows the results for arc-crack mechanisms for the up-dip trench wall and the likely groundwater case, while Figure 6 shows the results for weak-band mechanisms for the down-dip face and the likely groundwater case.

The rock mass stability analyses for the likely groundwater condition gave minimum computed FOS values that were greater than 1.20, except for the critical full-face mechanism for the up-dip face where the minimum computed FOS was 1.15. On the up-dip face, drainage may be better than was assumed for these analyses, with a computed FOS value closer to 1.20. The computed FOS value of 1.15 is regarded as acceptable, provided that the wall is excavated to the expected standard. For the worst-case groundwater condition, no circumstances were identified where the computed FOS was less than 1.05.

Very small mechanisms at the immediate crests of the excavated walls had minimum computed FOS values of the order of 1.0, implying a relatively high probability of limited falls from the immediate crests. In practice, the uppermost 2–4m of the material exposed in the highwalls is likely to be hard soil or extremely low strength rock, susceptible to drying, loosening, and erosion and capable of generating isolated rockfalls. It was therefore recommended that the upper 2–4m of all excavated walls be chamfered to a 45°

Table 8: Summary Results of FOS Assessment for Trench Design Profile

Condition	Up-Dip Face		Down-Dip Face	
	arc-crack	weak band	arc-crack	weak band
Likely Groundwater Case:				
Full face mechanism	1.15	1.22	1.26	1.34
Upper batter only	1.26	1.29	1.26	1.24
Lower batter only	1.51	1.62	1.69	2.04
Worst Groundwater Case:				
Full face mechanism	1.05	1.06	1.13	1.20
Upper batter only	1.26	1.21	1.27	1.31
Lower batter only	1.25	2.06	1.47	1.54

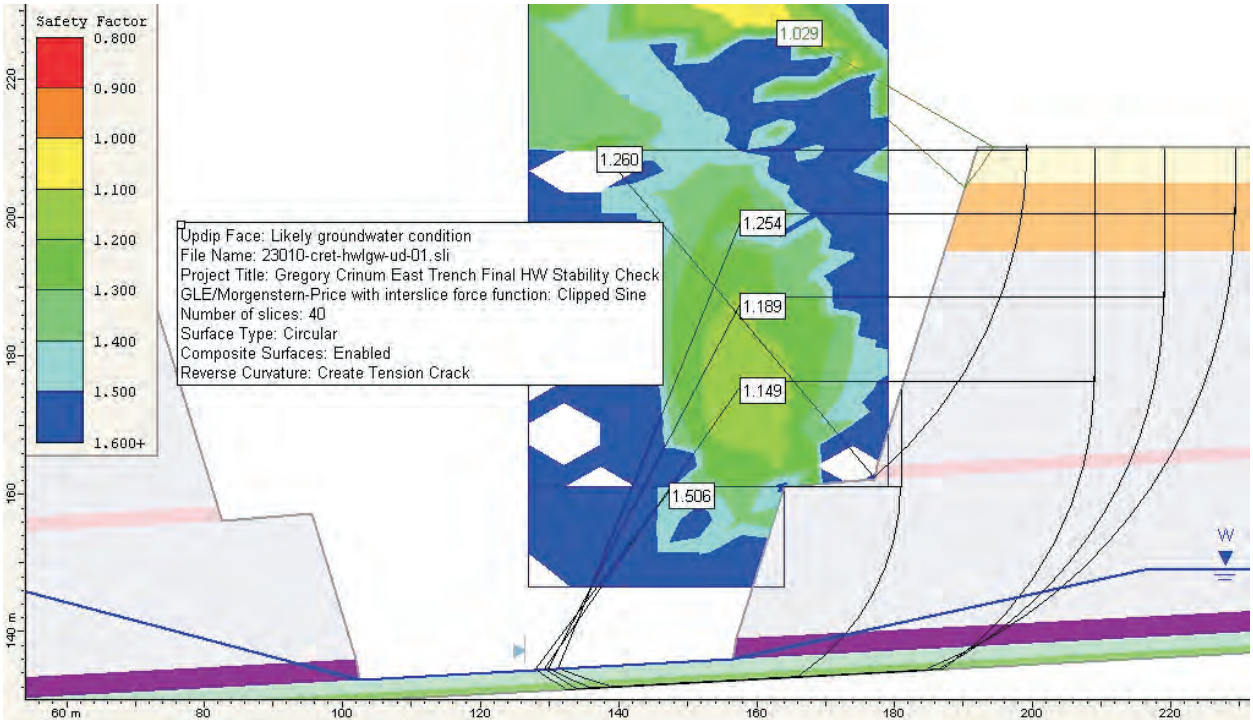

Figure 5: Up-dip wall, design profile, arc-crack mechanisms

batter to minimise the risk of post-excavation rockfalls from the crests of the walls.

STRUCTURALLY-CONTROLLED ROCK WALL INSTABILITY MECHANISMS

Kinematically possible mechanisms were assessed using the defect model described above and in Table 3. Records of joint continuity and persistence for each of the modelled sets were then used to determine whether significant volumes of unstable material were likely to form from possible mechanisms.

The structural model consists of three joints sets, and a hypothetic fault set based on 1999 observations in Ramp 3E that was thought to be linked to faulting that defines the corridor between the Crinum West and Crinum East mining areas.

For the up-dip trench wall (Figure 7) the only potential mechanism was toppling of the Joint4 set, which is expected to dip steeply into the up-dip batter faces. While Joint4 was expected to be laterally continuous for 20m or more, it was not expected to be persistent across major bedding partings. The risk of toppling was assessed to be low, provided that damage to the trench wall during blasting and excavation was minimised.

For the down-dip trench wall (Figure 8), Joint3 and Joint4 form potential wedges with an intersection dipping at between 40° and 50° out of the batter. The likelihood of such wedges creating significant instability was assessed to be very low, due to the limited persistence and continuity of Joint3. The majority of Joint4 structures are expected to be sub-parallel to the batter face, but some members may dip steeply into the batter and therefore create potential toppling conditions. The likelihood of this condition was assessed to be very low. If the Fault set does exist in the area of the trench, there is also the possibility of wedges formed by

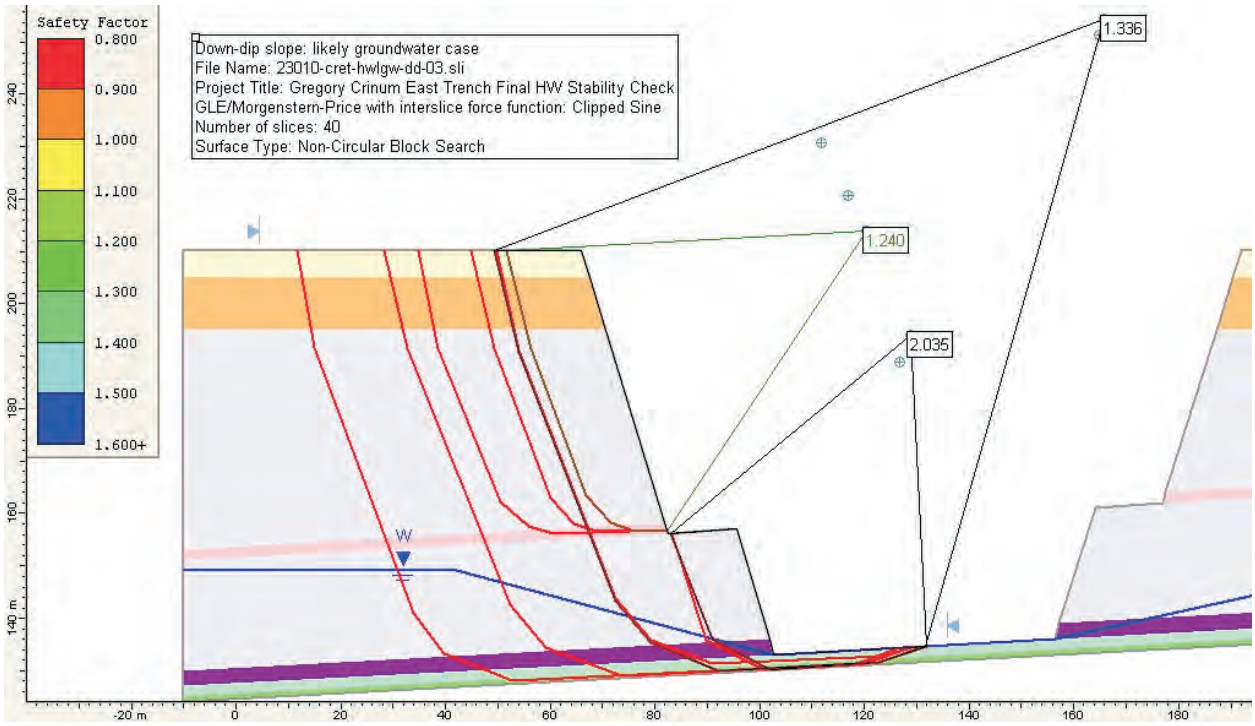

Figure 6: Down-dip wall, design profile, weak band mechanisms

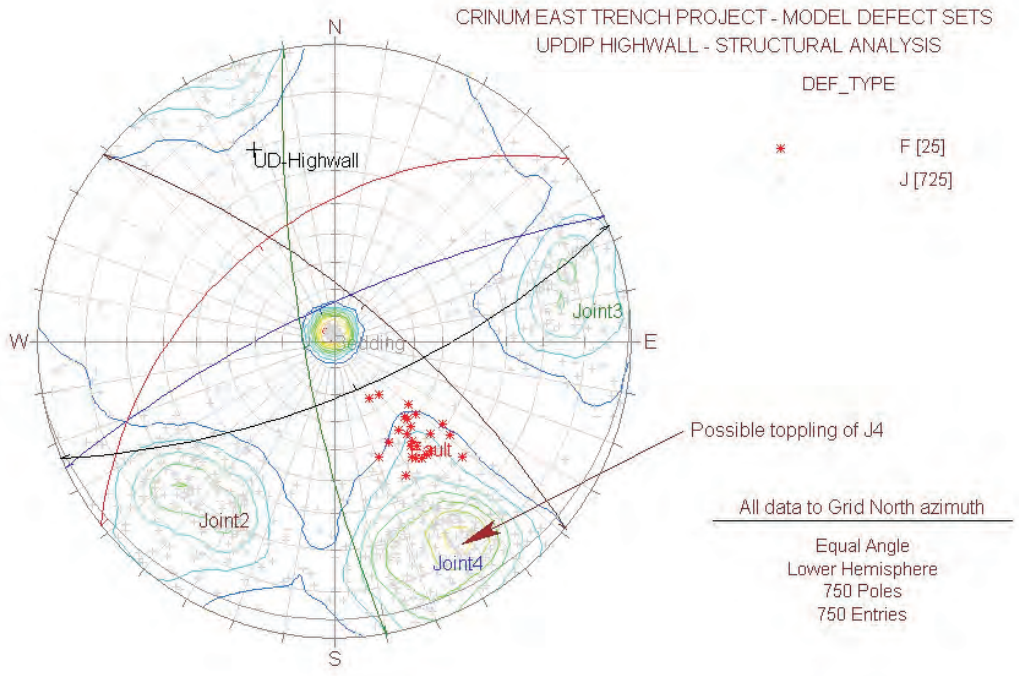

Figure 7: Stereoplot with potential instability mechanisms for up-dip wall of trench

intersections with Joint2 and with Joint3. Due to the expected limited persistence of these sets, wedges large enough to cause significant instability problems were not predicted or encountered.

Similar assessments were made for the SW endwall of the proposed trench, and also for the adjacent open cut highwalls. In all cases structurally-controlled mechanisms were expected to be relatively small and insignificant due to the limited continuity and persistence of the defects, provided that clean presplit faces were achieved with minimal blast damage behind the excavated faces.

TRENCH AND FINAL HIGHWALL CONSTRUCTION

The final open cut strips were mined progressively by dragline over the period from mid-2003 to mid-2004. The trench with its transitions to the final dragline highwalls was mined as a separate truck-shovel contract operation over the period from October 2003 to October 2004. After some initial difficulties in achieving smooth presplit walls, trench excavation proceeded without incident and resulted in clean and relatively smooth final faces (Figure 9). Localised hand mapping windows were carried out during the excavation to

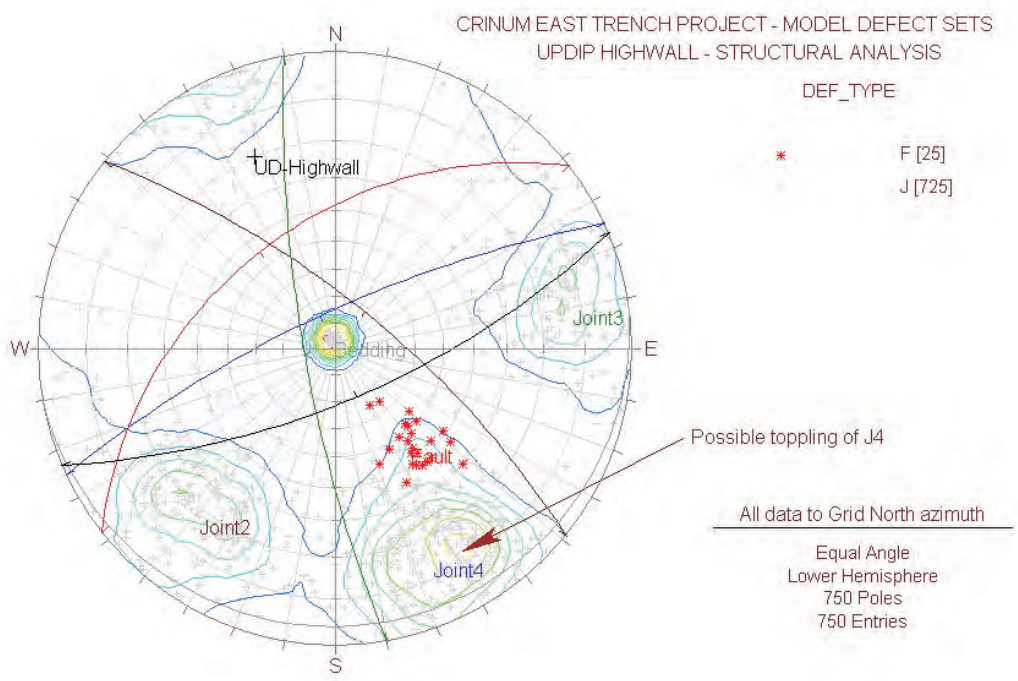

Figure 8: Stereoplot with potential instability mechanisms for up-dip wall of trench

Figure 9: View of down-dip wall of trench, May 2005

confirm the assumptions and concluions made during design regarding defect-controlled mechanisms.

During excavation, minor lipping was noted at the level of the weak bedding-parallel surfaces associated with the CV0 seam, but spalling was minimal and only initial movements were experienced. This was in keeping with the deformations predicted by the finite element modelling, and the magnitudes of displacements were within the tolerances for indicating stable conditions.

When the LV0 seam was mined the weak floor was exposed and a period of notable spalling of the up dip wall was initiated from the laminated, carbonaceous siltstone rock directly overlying the CV0 seam. This was interpreted by comparison to the finite element model predictions as the physical expression of yield propagation within the highly stressed corner zones of the trench. A very limited and stable heave zone was also observed in the Lilyvale seam floor at the same time of the up dip CV0 spalling. This was interpreted as confirmation of strength mobilisation within highly stressed weak zones during the final unloading path.

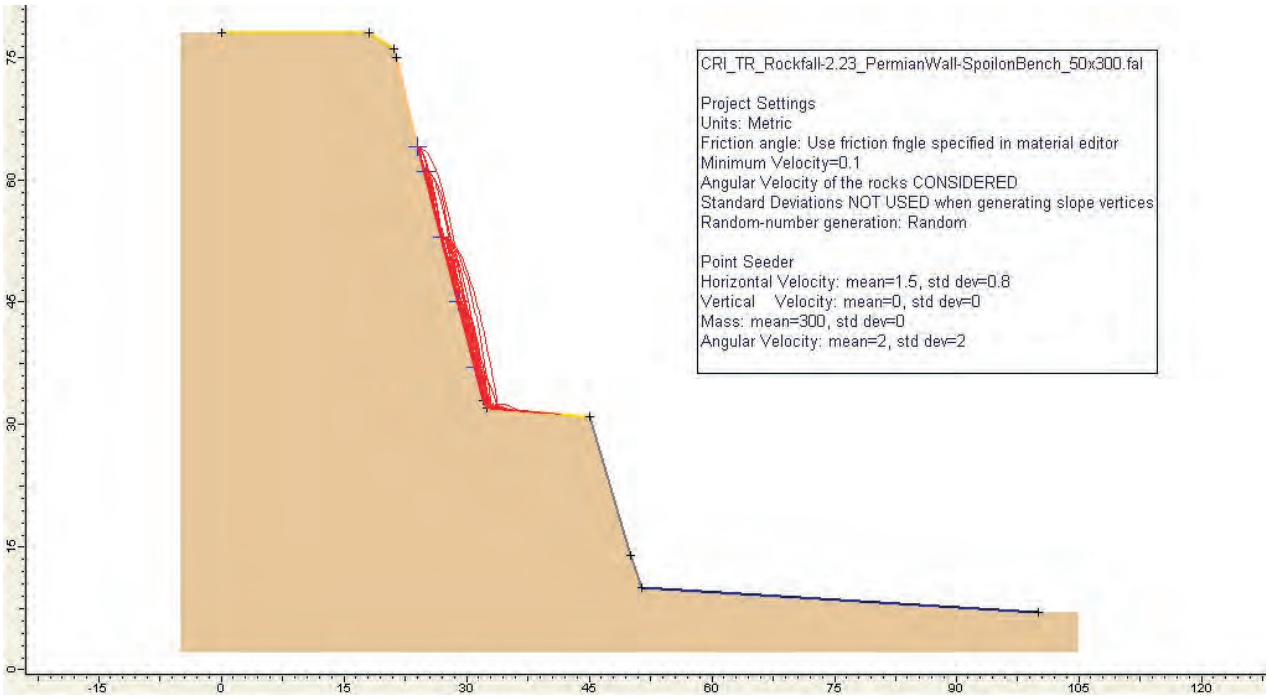

Figure 10: Example of rockfall simulation model for up-dip trench wall

Within the trench there was particular concern to minimise and control the risks of post-construction rockfalls. Several relatively small rocks fell in response to the first post-construction rainfall event, due to the inevitable removal by weathering and erosion of remnant loosened material. Sections of the trench walls adjacent to the initial punch longwall portals were scaled and meshed, and observations of fallen rocks were used to calibrate a rockfall simulation model (Figure 10 and Rocscience, 2001). This model has been remarkably successful for predicting the extent of individual rock movements, particularly in relation to rocks that fall onto the intermediate bench at CV0 floor level and then roll to the trench floor. The rockfall model was used to define stand-off zones from the trench walls with these areas now clearly barricaded and adopted into the safety management procedures of the Crinum East operation. Recently, the model has also been used to refine the zone of protection offered by the concrete portal structures.

During installation of rockfall mesh protection for the initial punch longwall access portals, some minor face bolting was undertaken to pin the mesh to the batter faces. In one location a significant 'crack' was observed and caused concern about face instability. Subsequent investigations showed that this was a superficial feature where a member of Joint4 (subparallel to the batter) had been slightly opened by weathering and erosion.

Subsequently the excavation faces have been exposed to several significant rainfall events, and there has been virtually no observable distress except for gullying and loosening of the extremely low strength material mainly in the chamfered sections near the crestlines. There have been no indications of destabilisation in any of the excavated faces, with minor continuing rockfall events as small blocks are loosened by weathering and erosion.

CONCLUSIONS

Deformation analyses indicated high levels of shear strength mobilisation within the weak materials in the immediate floor of the Lilyvale (LV0) seam. On the up-dip wall of the trench, the deformation analyses indicated that, despite this high strength mobilisation, wall movements were expected to be stable and in the order of 50mm to 150mm in response to excavation. Despite limited zones of localised yielding in the weak materials, there were no indications that overall stability of the trench walls was less than acceptable.

Defect structural analyses were undertaken for all of the final pit walls for the proposed punch longwall access entries. Some potential mechanisms were identified, but due to the limited continuity and persistence of the defects in question, no problems of structurally-controlled instability were predicted and none were encountered.

Limit equilibrium stability analyses were undertaken for the rock mass on the up-dip and down-dip sides of the proposed trench, as well as for the adjacent open cut highwalls. For the proposed excavated wall profiles, overall wall stability exceeded the acceptance criterion.

Based on the information reviewed and the results of the analyses undertaken, the benched design of the proposed trench is expected to function as intended. The existing highwalls in the adjacent open pit areas are unbenched and appear to be adequately stable and safe except in areas of deep palaeochannels or local disturbance by faulting. However rock wall movements are likely to be greater and the potential for localised rockfalls is therefore considered to be greater.

REFERENCES

ROCSCIENCE, 2001: ROCFALL. Computer code for simulation of falling and rolling rocks on slopes. Version 4. www.rocscience.com.

ROCSCIENCE, 2002a: DIPS. Computer code for rock mass defect data analysis and presentation, Version 5. www.rocscience.com.

ROCSCIENCE, 2002b: PHASE^2. Computer code for finite element modelling of stresses and deformations due to excavations in rock masses. Version 5. www.rocscience.com.

ROCSCIENCE, 2003a: RocLab v.1 Analysis of Rock Strength Data, incorporating Generalised Hoek-Brown rock mass shear strength criterion. www.rocscience.com.

ROCSCIENCE, 2003b: SLIDE. Computer code for limit equilibrium analysis of slope stability. Version 5. www.rocscience.com

.STRATA TESTING SERVICES, 2002: Crinum Trench Test Results for BH's 07035, 07036, 07037, & 07038, Sample Numbers L047-1 & L047-37. Report to BHP Billiton Mitsubishi Alliance, 14 November 2002.

John V Simmons, Sherwood Geotechnical and Research Services, (T) 07 3278 1060, (e) sgrs@bigpond.net.au

Peter J Simpson and Dennis A McManus, BMA Coal Pty Ltd Central Queensland Office, (T) 07 4968 8233, (e) Peter.J.Simpson@BHPBilliton.com, (e) Dennis.A.McManus@ BHPBilliton.com

A Paul Maconochie, GeoTek Solutions Pty Ltd, (T) 07 3720 1792, (e) gts@geoteksolutions.com

Philip Soole, CSIRO Exploration and Mining, (T) 07 3327 4413, (e) Philip.Soole@csiro.au

Abouna Saghafi, Stuart Day and John Carras

Gas properties of shallow Bowen Basin coal seams and gas leaks to the atmosphere

Data on gas content and other reservoir properties of shallow coals are scarce and to date have not yet been of interest to mine operators. This is changing rapidly, however, with increasing concern for greenhouse gas emissions from open cut mining. As part of two ACARP-funded studies measurements have been undertaken over the past 5 years of gas content and surface emissions from shallow coal seams of a number of open cut mines in the Bowen Basin. Results for one of the mines are reported here.

Emission rates were measured from uncovered exposed coal seam in mine pits. Surface emissions (CO_2 and CH_4) varied from 2.2 to 45.6mL/min/m^2 of coal surface. In terms of CO_2-equivalents this would be an emission of 26.4 to 349.2mg/min/m^2. In order to relate these emissions to the gas content of an exposed coal seam, coal samples from a blasted seam were collected and measured. The gas content of blasted coal varied from 0.5 to 1.1m^3/t with an average value of 0.7m^3/t. The seam gas was about 95% methane, with the remainder being CO_2, however, the gas emitted from the coal seam surface was rich in CO_2 (up to 55%). The measurement of surface emissions was carried out over two consecutive days to determine the time dependency of diffusion through coal surface. Surface emission rates were reduced on the second day of measurement and the emitted gas showed declining values of CO_2 content and increasing values of CH_4.

Coal samples were also obtained from exploration boreholes and *in situ* gas contents and diffusivity for these coals were measured. *In situ* gas contents of up to 1.5m^3/t were found for coals at depths of 40-45m and up to 5m^3/t for coals at depths of 120m. The gas diffusivity for coal was measured using a CSIRO-developed system. It was found that CO_2 diffuses in coal more rapidly than methane, with diffusivity values of order of 6.4 x$10^{-6}$$cm^2$/s compared to 3.5x$10^{-6}$$cm^2$/s for CH_4. The measured diffusivity values are consistent with the fact that the emitted gas was richer in CO_2 compared to the gas in coal and that the CO_2 in surface emitted gas reduced with time.

The data obtained in the course of these studies will assist in estimating gas emission volumes from coal seams in open cut mines. Data on the gas content of blasted coal together with seam surface emissions and gas diffusivity in coal will assist in estimating staged emissions from mine pits and standing highwalls.

INTRODUCTION

There are almost no published data on the gas content and reservoir properties of shallow coal seams in Australia. This is because the main driver for measuring coal seam reservoir properties has been either underground coal mine safety or, in the last decade, commercial methane production (CBM). However, with current concerns over the extent of greenhouse gas emissions from coal mining and in particular open cut mining, understanding the mechanisms of gas emissions from shallow coal seams has become of paramount importance.

During two recent projects funded by ACARP (Projects C9063 and C12072), measurements of surface emissions from uncovered coal seams and gas content from blasted coal were undertaken in a number of coal mines in the Bowen Basin. In one of the mines, core samples were also retrieved from exploration boreholes ahead of mining. These samples were measured for the *in situ* gas content and gas diffusivity properties.

In this paper, the results of measurements for one of these mines are presented.

METHODS

Three coal mines in the Northern and Southern Bowen Basin were studied. Numerous measurements of gas emissions from exposed coal seams were carried out in mines pits. Coal samples were collected in the pit after the coal seam had been blasted. Gas-tight canisters were used to seal and dispatch coal samples to the CSIRO gas laboratory for measurement of gas content and composition. In one of the mines, two exploration boreholes were drilled and cored. The *in situ* gas contents of all traversed coal seams were measured. The methods used in this study are presented in the following sections.

Surface emissions

Measurements of the emissions from exposed coal and inter-burden were made using a chamber technique developed at CSIRO (Carras & others, 2000). This technique involves placing a purpose-built chamber on the ground surface and measuring the concentration of CO_2 and CH_4 inside the chamber with continuous gas analysers located in an appropriately instrumented 4-WD vehicle. A steady stream of ambient air is drawn through the chamber to dilute the gas inside the chamber so that the concentrations of CO_2

Figure 1: Chamber method used for surface emissions; chamber on the left is connected to gas analysers and loggers which are installed in the 4WD on the right.

and CH_4 can be maintained within the dynamic ranges of the gas analysers. During the operation, the measured data from analysers are logged continuously on a laptop computer for further processing. The chamber in use during a measurement campaign is shown in Figure 1.

Gas content

Fresh coal samples were collected from in-pit or from exploration boreholes and were immediately sealed in gas-tight canisters to prevent any significant losses of desorbed gas. The coal canisters were made of stainless steel and were thoroughly leak-tested before deployment. Various size canisters were used; the largest canisters were 1m long and 65mm in diameter and could hold up to 3.0kg of coal (Figure 2). Coals were measured for the Q1 component in the field and for the Q_2 and Q_3 components in the laboratory. The CSIRO quick-crush method (Williams & others, 1992) was used to measure the Q_3 component.

Gas diffusivity in coal

A new innovative technique has been developed at CSIRO to measure the gas flux through a solid coal-disk prepared from core samples (Saghafi, 2001; 2003). Gas diffuses through solid coal under a concentration gradient. A schematic diagram of the apparatus used to measure diffusivity is presented in Figure 3.

Figure 2: CSIRO stainless steel canisters

SURFACE EMISSION RESULTS

Surface emission measurements were made at the mine pit, using the chamber technique. Surface emission

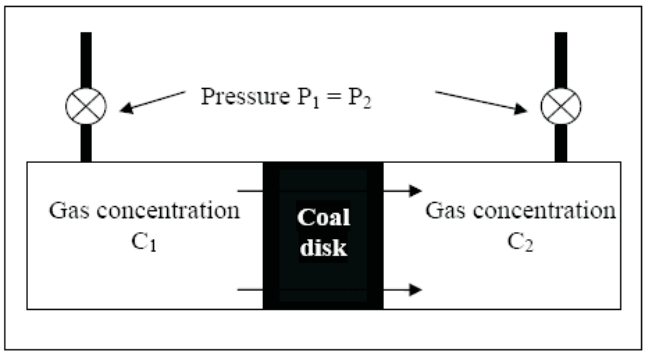

Figure 3: Schematic of CSIRO-developed measurement apparatus for gas diffusivity in solid coal

measurements were planned to be carried out soon after a coal seam was uncovered. The earliest opportunity arrived for Seam 1, where the measurements could take place on two consecutive days, 4 and 5 days after the uncovering of this seam.

Two consecutive days of measurement could give an indication of the change in the rate of gas diffusion with time for freshly uncovered coal seams. Seam 1 was 43–45m below the surface before the removal of the overburden. Surface emission measurements were made in various locations on the seam surface.

In Table 1, the results of measurement for 14 of the sites are presented. The measured emission rates show large scatter over these locations. As is seen, the average emission flux was 18.7mL/min/m^2 of coal surface on the first day, reducing to 12.3mL/min/m^2 on the second day. The CO_2 gas content decreased from 44% on the first day of measurement to 27% on the second day.

GAS CONTENT RESULTS

Residual gas content of blasted coals in the mine pit

Coal samples were collected from the blasted seam in Pit A, where surface emissions were measured. However, due to safety issues and mine production schedules, the gas content measurements could not be made on the same seam sections as those used to measure surface emissions. The gas content of blasted coal varied from 0.5 to 1m^3/t and analysis of the gas desorbed from the coal during crushing (Q_3 component of gas content) showed that the seam gas consisted mainly of methane (95% CH_4 and 5% CO_2).

The results of gas content measurements for 6 locations in this pit are presented in Table 2. A comparison of these data with elapsed times since blasting does not show any correlation. This is not to say that there is no relation between the volume of gas desorbed and time of desorption.

The gas content of coals depends on the overall length of the gas desorption for each individual sample, including the length of time the coal seam had been exposed before blasting. For example, in case of samples Loc_e and Loc_f in Table 2, these coals may have been uncovered for a much longer time before being blasted compared to other samples.

Table 1: Coal seam surface emissions measured at mine pit

Location ID	Time since coal uncovered (days)	CO_2 Flux (mL/min/m^2)	CH_4 Flux (mL/min/m^2)	Total Flux (mL/min/m^2)	CO_2 Equivalent (mg/min/m$_2$)	Gas composition $CH_4/[CH_4+CO_2]$
Loc2	4	0.0	3.1	3.1	36.6	1.00
Loc3	4	7.3	5.8	13.1	82.2	0.44
Loc4	4	19.2	26.4	45.6	349.2	0.58
Loc5	4	11.0	17.9	28.9	234.0	0.62
Loc6	4	6.6	13.8	20.4	176.4	0.68
Loc7	4	0.0	3.8	3.8	45.6	1.00
Loc8	4	0.0	16.1	16.1	192.0	1.00
Average day 4		**6.3**	**12.4**	**18.7**	**159.6**	**0.66**
Loc10	5	1.0	4.2	5.2	52.2	0.80
Loc11	5	14.6	22.9	37.5	298.8	0.60
Loc 12	5	0.0	5.3	5.3	62.4	1.00
Loc13	5	0.0	2.2	2.2	26.4	1.00
Loc14	5	0.0	5.0	5.0	60.0	1.00
Loc15	5	0.0	6.2	6.2	73.8	1.00
Loc16	5	0.0	6.7	6.7	80.4	1.00
Average day 5		**3.4**	**8.9**	**12.3**	**112.8**	**0.73**

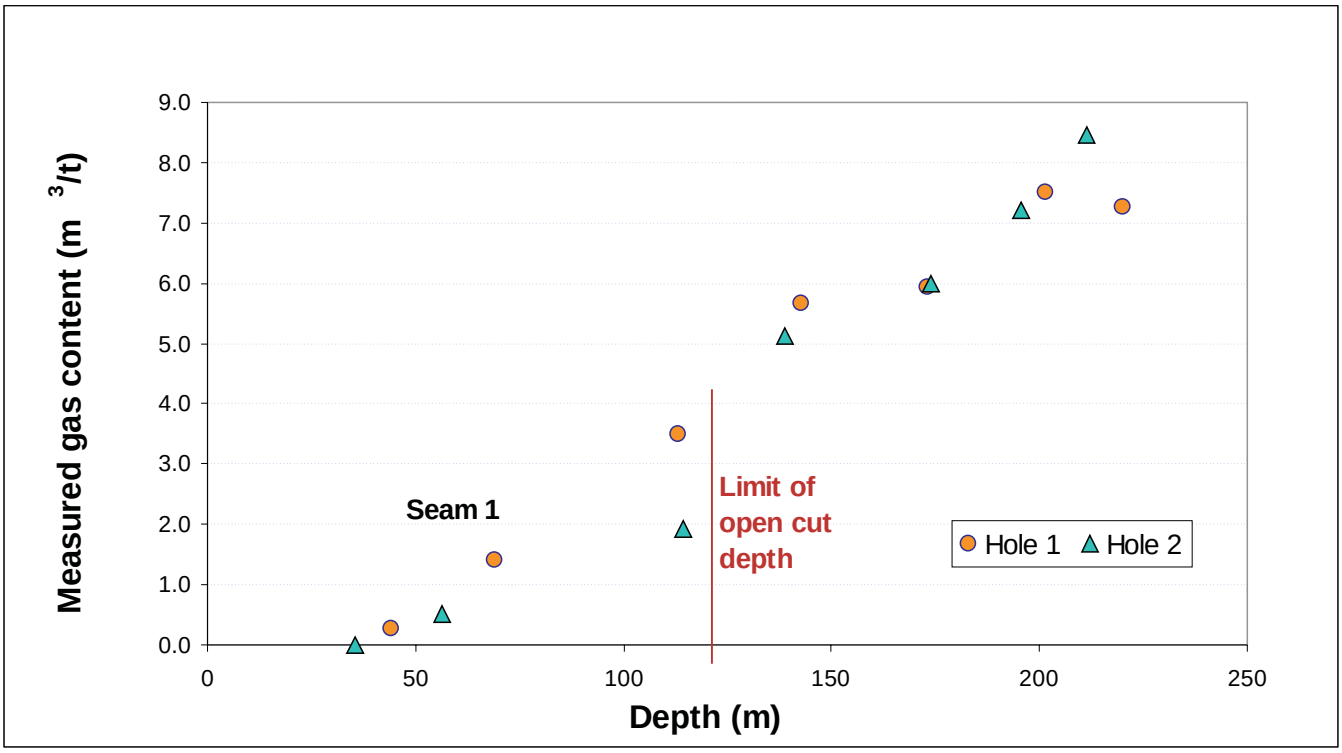

Figure 4: Gas content variation with depth from surface boreholes

Table 2: Gas content of blasted coals from mine pit

Sample ID	Time elapsed since seam blasted (days)	Gas content (m^3/t)	Gas composition $CH_4/[CO_2+CH_4]$
Loc_a	3.5	1.06	0.96
Loc_b	3.5	0.84	0.95
Loc_c	5.5	0.66	0.95
Loc_d	5.5	0.49	0.97
Loc_e	0.1	0.48	0.94
Loc_f	0.1	0.48	0.94
Average		**0.67**	**0.95**

Gas could have therefore been escaping for a longer time before the gas content was measured. The information on the length of time from uncovering of various sections of coal seam and the respective blasting time for these sections was not readily available, and mine staff suggested that seams may be exposed for periods ranging from a few days to many months before the coal is mined.

In situ gas content from exploration borehole

The *in situ* gas content of Seam 1 was not known at Pit A at the time of residual gas content and surface emission measurements. In a follow up study, two exploration boreholes were drilled in a greenfield area on the same mine lease. The boreholes were, however, about 7.5km away from Pit A. The borehole was drilled to a depth of about 210–220m and intersected Seam 1 at a depth of about 43–45m. In Pit A, the overburden height over Seam 1 was similar at Figure 2 — CSIRO stainless steel canisters Figure 2 — CSIRO stainless steel canisters 40–43m. Measurement of the gas content of coal core samples showed values of 1.3 to 1.5m^3/t for *in situ* gas content of Seam 1.

The measurement of gas contents for other seams showed that overall gas content increased with depth at that location. *In situ* gas contents of up to 5m^3/t were measured for various seams traversed to a depth of 120m (Figure 4).

Gas diffusivity measurement

For shallow coal seams with low gas content, the limiting emission rate is the diffusive flow, which is characterised by the diffusivity or diffusion coefficient. Using the CSIRO-developed system, coal samples from exploration boreholes were measured for their diffusivity to CO_2 and CH_4. The diffusivity values obtained were: 3.41 x $10^{-6}$$cm^2$/s for CH_4 and 6.37 x $10^{-6}$$cm^2$/s for CO_2.

DISCUSSION

The *in situ* and in-pit gas content data from coal seams can present valuable information on the overall level of gas release to the atmosphere during open cut mining. The surface emissions and diffusivity data indicate the speed of the gas release to the atmosphere.

The in-pit gas content of blasted coal from Pit A showed an average gas content of 0.7m^3/t while data from the surface

Table 3: Calculated emissions from exposed coal seam in mine pit; 1km x 60m coal surface is exposed

Based on data from Location	Annual gas flux (m^3/m^2)	Annual gas release from exposed coal seam (Mm^3)	Gas composition $CH_4/[CH_4+CO_2]$
Loc2	1.6	0.10	1.00
Loc3	6.9	0.41	0.44
Loc4	23.9	1.43	0.58
Loc5	15.1	0.91	0.62
Loc6	10.7	0.64	0.68
Loc7	2.0	0.12	1.00
Loc8	8.4	0.51	1.00
Average 1	**9.8**	**0.59**	**0.66**
Loc10	2.7	0.16	0.80
Loc11	19.6	1.18	0.60
Loc 12	2.8	0.17	1.00
Loc13	1.2	0.07	1.00
Loc14	2.6	0.16	1.00
Loc15	3.2	0.19	1.00
Loc16	3.5	0.21	1.00
Average 2	**6.4**	**0.39**	**0.73**

borehole averaged 1.4m^3/t. It can be estimated that 50% of gas is released during removal of the overburden and from the standing highwall, however, the boreholes were drilled at a distance of 7.5km from Pit A. Though the coal seam was intercepted by boreholes at a similar depth as in Pit A, the possibility of horizontal spatial variability still exists.

Surface emissions from the exposed coal showed a high degree of scatter (Table 1) but overall, in two consecutive days, it was higher for the first day (18.7mL/min/m^2) than for the second (12.3mL/min/m^2). The composition of emitted gas also showed an increase in CH_4 concentration with time, which is in agreement with the diffusivity values measured for CH_4 and CO_2 gases.

The measured surface emissions reported in Table 1 can be used to estimate the overall emissions from coal seams exposed to the atmosphere in mine pits. In this mine, the mined coal seams are usually exposed over a distance of 0.5 to 2km. Given the width of the pit of about 60m, if an average length of 1km is assumed, then a fresh coal surface of 0.06km^2 is exposed over the year. In Table 3, the annual emissions are calculated based on surface emission values measured at various locations in Pit A. It is assumed that fresh coal surface is continuously regenerated during mining operations. The data show that emissions from the exposed coal seam surface in a mine pit can vary from 0.1 to 0.9 x $10^6 m^3$ /y with an average emissions of 0.4 to 0.6 x 10^6 m^3/y.

CONCLUSIONS

Measurements of surface emissions from uncovered coal seams show large scatter, reflecting the non-homogeneity of surface emissions across a mine pit. The scatter is related to the local history of emissions as well as to the local coal reservoir properties. The measurements, however, showed that overall the emissions would reduce with time of exposure. Also, it was shown that the proportion of CO_2 emitted initially is higher than methane. This is consistent with the fact that laboratory-measured CO_2 diffusivity was higher than methane. The data obtained in the course of the project were used to estimate emissions from a typical mine, where a coal seam surface of up to 1km long and 60 m high was continuously exposed. It was found that, in such conditions, surface emissions from uncovered coal would range between 0.1 to 0.9 x 10^6 m^3 per year with an average of 0.4 to 0.6 x 10^6 m^3/y.

ACKNOWLEDGEMENTS

This work was funded by the Australian Coal Association Research Program as part of ACARP Project C9063 and C12072. We are sincerely grateful to the coal mining companies and their staff where the measurements were carried out in particular Ted Boulton, John Hoelle, Clark Davis, Bob Dunn, Pat Kelly and Jenny Reagan.

The authors would like also to thank Doug Roberts, Alfredo Quintanar and Robyn Fry of CSIRO Energy Technology for contributing to the field and laboratory measurements. Also thanks to CSIRO retirees David Williams and Tony Lagne for participating in the field measurement.

REFERENCES

CARRAS, J.N., DAY, S.J., SAGHAFI, A. & WILLIAMS, D.J., 2000: Measurement of greenhouse gas emissions from spontaneous combustion in open cut coal mines, CSIRO Energy Technology Investigation Report CET IR 333R, ACARP Project C8059 Final Report.

SAGHAFI, A., 2001: Coalbed gas reservoir characterisation and methane recovery in Australia, *In, Proceeding of the 2001 International CMM/CBM Investment and Technology Symposium*, November 7-8, Shanghai, China, 56-74.

SAGHAFI, A., 2003: Aspects of gas storage and flow properties of Australian coals, *In* the *Proceedings of the 2nd Annual Australian Coal Seam & Mine Methane Conference*, 19-20 February 2003, Brisbane, Australia.

WILLIAMS, D.J., SAGHAFI, A., DRUMMOND, D.B. & ROBERTS, D.B., 1992: Development of a new equipment for rapid determination of coal gas content, *In, Proceedings of Symposium on Coalbed Methane Research and Development in Australia*, Townsville, Australia, **4**, 21-30.

A.Saghafi, Abounda.saghafi@csiro.au; S. Day, stuart.day@csiro.au; J. Carras, john.carras@csiro.au
CSIRO Energy Technology, PO Box 330, Newcastle, NSW 2300, Australia

Peter Crosdale, Abouna Saghafi, Ray Williams and Eugene Yurakov

Inter-laboratory comparative CH_4 isotherm measurement on Australian coals

Unlike gas content measurement, there is currently no Australian standard for the measurement of gas adsorption isotherms. A preliminary study, funded by ACARP, comprising three Australian laboratories was carried out to compare the results of measurements of methane adsorption isotherm on a suite of coal samples from the Bowen and Sydney Basins. Participating laboratories were CSIRO Energy Technology, James Cook University and GeoGAS Pty Ltd.

Six coal cores were measured between the three laboratories. In addition to methane adsorption isotherms, the coals were measured for their gas content and composition. Proximate analysis was also performed on all coals. All the three laboratories used their own in-house developed gravimetric methods. For this comparison samples were analysed on an 'as received' basis.

Despite using the same analysis technique, isotherm results differed between the laboratories. The causes of the variation in the results were attributed to various factors including the differences in ash yield, moisture content and grain size distribution which showed substantial variations. Different coal-density vs ash yield relationships were also identified for the laboratories, which impacts on void volume calculations.

As a result of this study, all 3 laboratories have modified key procedures for adsorption isotherm measurement. It would now be highly desirable for a follow up study to assess the effectiveness of these modifications.

INTRODUCTION

Gas adsorption isotherms of coals are an essential input parameter for a variety of modelling purposes. They are used to predict gas drainage in underground coal mines, estimate gas reserves for coalbed methane, model production of coalbed methane wells and are becoming an important part of the evaluation of coalbeds for CO_2 sequestration. Worldwide, no standard exists for the experimental determination of high pressure gas adsorption isotherms on coals. Equipment is generally constructed in-house and analysis procedures and protocols are like-wise proprietary. Few inter-laboratory studies have been undertaken to evaluate the reproducibility of the isotherms.

Given the lack of national or international standard procedures, this study was a first attempt by Australian laboratories to assess the reproducibility of methane adsorption isotherms and to gain insights into factors which influence the reproducibility.

METHODS

Samples

Six coal core samples were selected from New South Wales and Queensland. Three cores were obtained from restricted areas within a single seam in the Rangal Coal Measures in the Northern Bowen Basin and similarly three cores from a single seam in the Newcastle Coal Measures in the Lower Hunter Valley. The coals are in similar stratigraphic positions being close to the Permian - Triassic boundary.

Coal characterisation

All 18 samples were characterised by proximate analysis according to Australian Standards by commercial laboratories. Crushed isotherm samples were analysed for particle size distribution in a Malvern Laser Particle Size Analyser. Moisture content of the samples was determined before and after analysis.

Adsorption isotherm analysis

Each of the 3 laboratories used a gravimetric technique. Apparatus was built in-house and, accordingly, details of design and precise operational parameters varies from laboratory to laboratory. However, some critical parameters were agreed to be standardised prior to analysis.

Coal samples were crushed and sieved to less than 0.212mm. The samples were run on an as received basis. Isotherm temperature was 30°C and results were reported at 20°C and 101.325kPa pressure. Seven point isotherms were run with pressures at approximately 250, 500, 1000, 1500, 2000, 3000 and a maximum 5000kPa.

An important variation between the labs occurred in the determination of the void (free) volume of the isotherm apparatus. One of the labs directly determined the void volume using helium, and subsequently calculated the density of the coal. Another lab took the apparent relative density of the coal and used this, along with the weight of the coal, to back-calculate the void volume. The remaining lab used a number of random lumps of coarser coal and evaluated their density in a helium pycnometer and used this helium density to back-calculate the void volume.

RESULTS AND DISCUSSION

The key aim of this project was to investigate the reproducibility of the methane adsorption isotherm. These reproducibility results are therefore discussed first and then other data is subsequently brought in to evaluate possible reasons for variations in the reproducibility.

Adsorption isotherm reproducibility

Adsorption isotherm parameters of Langmuir pressure (P_L) and Langmuir volume (V_L) were calculated for each sample on an as analysed and daf basis (Table 1). Visual assessment of the curves (Figure 1) indicated that the reproducibility between the labs was poor both for the as analysed and daf bases.

Rather than trying to plot all the isotherms together, the reproducibility was assessed as follows. The mean value of gas volume adsorbed was calculated for the 3 split samples from each core distributed to the 3 laboratories and the relative deviation from that mean was calculated for each lab. This was done for all 6 cores at pressures of 1MPa and 5MPa (Figure 2). A number of general trends can be observed. Laboratory 1 is consistently below average while Laboratory 2 is consistently above average and Laboratory 3 shows no trend about the average. This indicates systematic differences between the laboratories. Visual assessment indicates that the reproducibility is around ±20%.

Adsorption isotherm repeatability

Given the poor reproducibility of the isotherms and an indication of systematic differences between the laboratories, an assessment of the repeatability within a lab was made.

For each lab, the mean values for the 3 Queensland and the 3 New South Wales cores were calculated at 1MPa and at 5MPa. The percentage difference from this mean of each of the samples was then determined (Figure 3).

Note that this is not a true evaluation of the repeatability since the same sample was not used in multiple repeats. However, it is generally expected that similar samples from the same seam will give similar isotherms. If the results with a lab were markedly different between the 3 samples of each set, then a poor repeatability may be indicated. Given that for each sample set, each lab obtained similar results for each of the 3 samples it can be asserted that the repeatability is likely to be adequate, and probably around ±7%.

Data evaluation

As part of the data evaluation procedure, the relatively simple step of swapping all raw data between the labs was undertaken. Each lab has developed its own algorithms for calculating the adsorption and it was thought desirable to see if each lab could reproduce the isotherm of the other labs using the other labs' raw inputs. The result of this exercise

Table 1: Proximate analysis, Langmuir parameters and relative density determined of the samples studied

Sample No.	Lab No.	A (%, ar)	M (%, ar)	VM (%, ar)	FC (%, ar)	VM (%, daf)	PL (kPa abs)	VL (m^3/t, aa)	VL (m^3/t, daf)	RD (g/cc)
NSW001	1	9.2	2.1	29.5	59.2	33.3	1260	13.26	14.95	1.45
	2	10.3	2.5	31.0	56.2	35.6	2172	21.37	24.51	1.39
	3	9.0	2.0	31.0	58.0	34.8	2133	22.67	25.47	1.35
NSW002	1	15.6	2.0	25.7	56.7	31.2	1420	13.60	16.50	1.50
	2	14.5	2.5	27.6	55.4	33.3	1835	19.55	23.55	1.42
	3	15.5	1.8	28.8	53.9	34.8	1935	16.20	19.59	1.41
NSW003	1	18.2	1.8	29.8	50.2	37.3	1140	12.16	15.20	1.52
	2	17.7	2.5	29.8	50.0	37.3	1704	18.80	23.56	1.50
	3	19.1	1.9	28.6	50.4	36.2	2082	15.23	19.28	1.40
QLD001	1	25.1	3.0	25.6	46.3	35.6	1520	10.99	15.29	1.59
	2	26.6	3.4	25.5	44.5	36.4	1803	12.80	18.29	1.59
	3	25.7	2.9	25.0	46.4	35.0	2606	15.76	22.07	1.35
QLD002	1	14.2	3.6	27.6	54.6	33.6	1870	14.36	17.47	1.47
	2	11.0	4.1	27.4	57.5	32.3	1972	17.24	20.31	1.34
	3	11.4	3.3	26.7	58.6	31.3	1935	16.20	18.99	1.41
QLD003	1	9.3	3.8	30.4	56.5	35.0	1420	13.02	14.98	1.46
	2	10.5	3.8	31.7	54.0	37.0	2023	18.62	21.73	1.34
	3	10.0	3.7	31.3	55.0	36.3	2082	18.90	21.90	1.37

Isotherm testing was carried out at 30°C and results reported 20°C and 1atm pressure. The relative density of the coal was determined using a different technique in each laboratory. A = ash, M = Moisture, VM = volatile matter, FC = fixed carbon, PL = Langmuir pressure, VL = Langmuir volume, RD = relative density, ar = as received, daf = dry ash free, aa = as analysed.

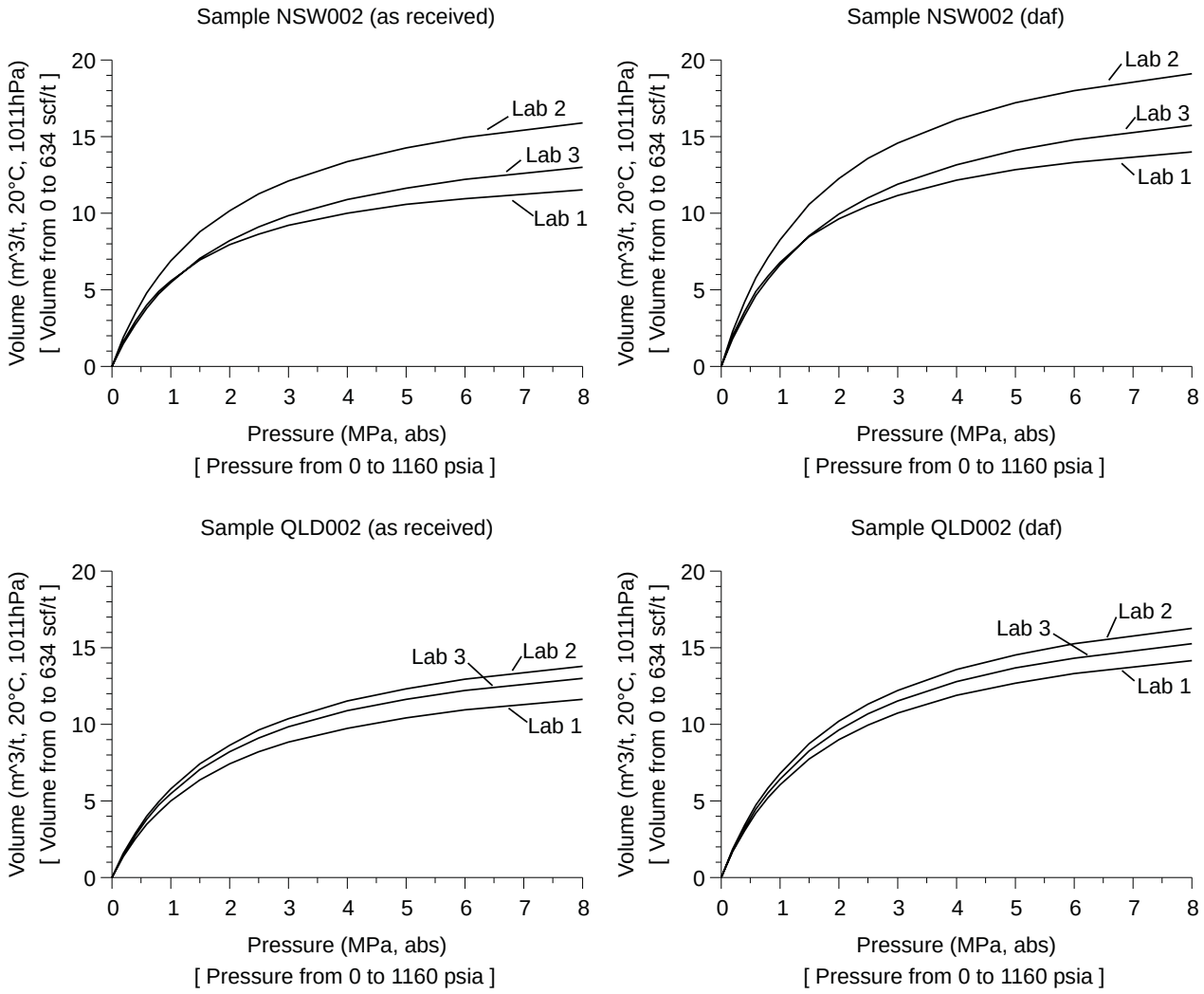

Figure 1: An example of the as analysed and daf isotherms for one New South Wales and one Queensland sample. Reproducibility between the 3 labs is quite poor.

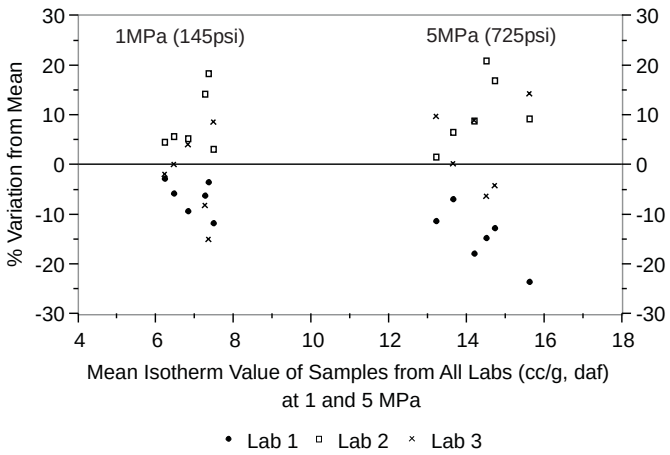

Figure 2: Reproducibility of all 18 isotherm samples at 1MPa and 5MPa

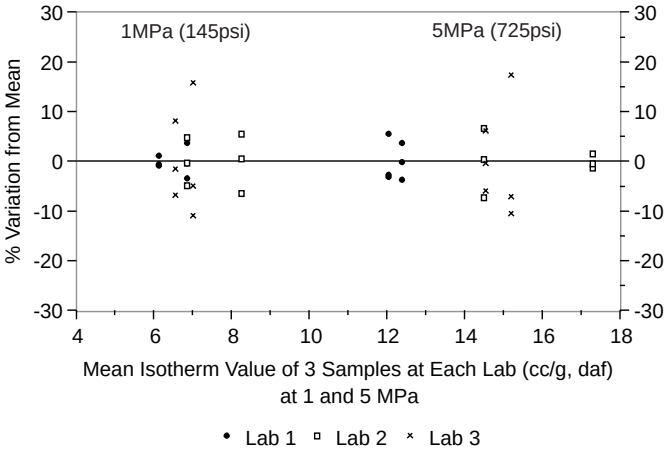

Figure 3: Repeatability of all 18 isotherm samples at 1MPa and 5MPa

proved to be satisfactory and no significant differences were found.

However, during this exercise it was observed that all 3 labs used a different value for the parameter of the density of adsorbed phase methane. These values were Lab 1 — 0.3196g/cc; Lab 2 — 0.6189g/cc and; Lab 3 — 0.415g/cc. Different values for the sorbed density of methane could account for up to 4.5% variation in the isotherm.

Sample characteristics

Proximate analysis data (Table 1; Figures 4 and 5) indicates that a variety of sampling problems occurred. Large variations in ash yield were found in samples from the same core, up to 4.2% for samples from QLD002. Moisture variations (ash free) of up to 0.9% were recorded for the

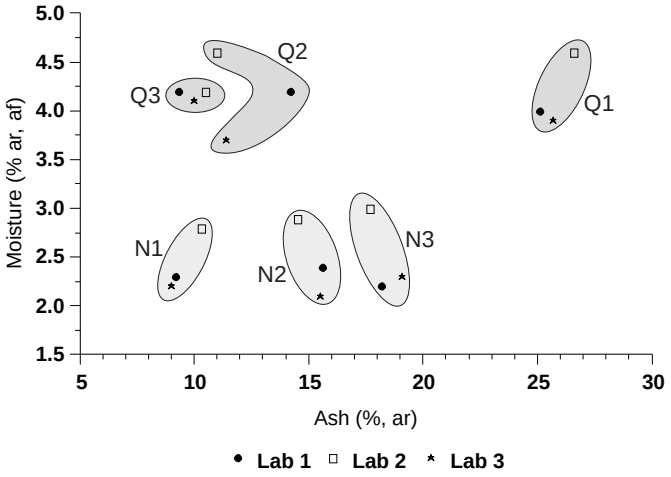

Figure 4: Variation in ash and moisture between the 18 samples. Q1 = sample QLD001 etc and N1 = sample NSW001 etc.

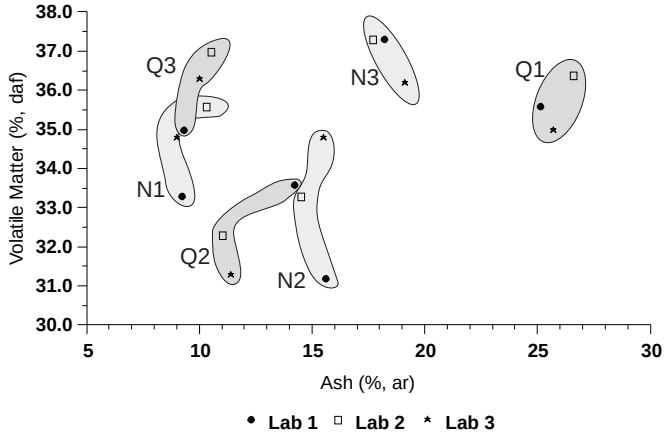

Figure 5: Variation in volatile matter and ash between the 18 samples. Q1 = sample QLD001 etc and N1 = sample NSW001 etc.

same sample. The moisture contents of the samples at laboratory 2 were consistently higher than those at laboratories 1 and 3.

Volatile matter (daf) (Figure 5) showed similar discrepancies between sample splits. Variation of up to 3.6% was found for samples from the same core. Coal type variation is clearly indicated between the sample splits. Vitrinite-rich and inertinite-rich coals have been shown to have different adsorption characteristics. Detailed enquiry indicated that rather than homogenising the core and then splitting for distribution, sequential vertical sections of the core were distributed to the labs.

Moisture content of the coal was determined both before and after the adsorption isotherm (Figure 6). Since moisture content of the coal affects the adsorption of methane, it was desired to be sure that the moisture content had not fundamentally changed during the isotherm procedure. Both the absolute and relative change in values of coal moisture before and after measurement are plotted (Figure 6). The percentage data suggests a slight loss of moisture since most, but not all, values are negative. However, a 5% loss (the maximum) at a moisture content of 4.5% is an absolute loss of 0.2% moisture and close to the repeatability limit.

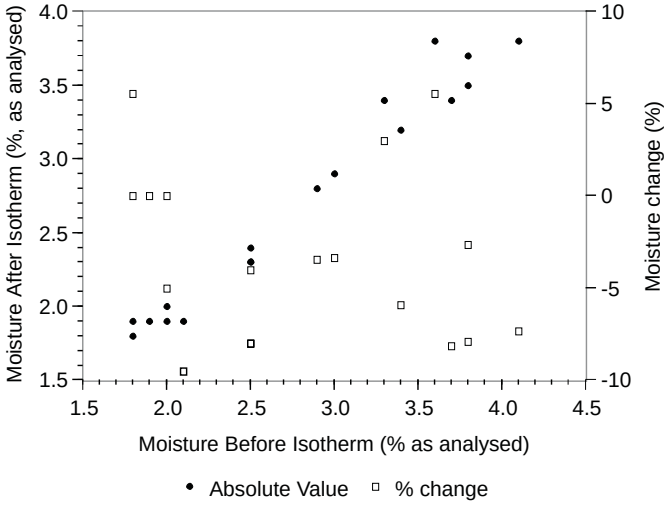

Figure 6: Moisture content of the coal before and after adsorption isotherm analysis

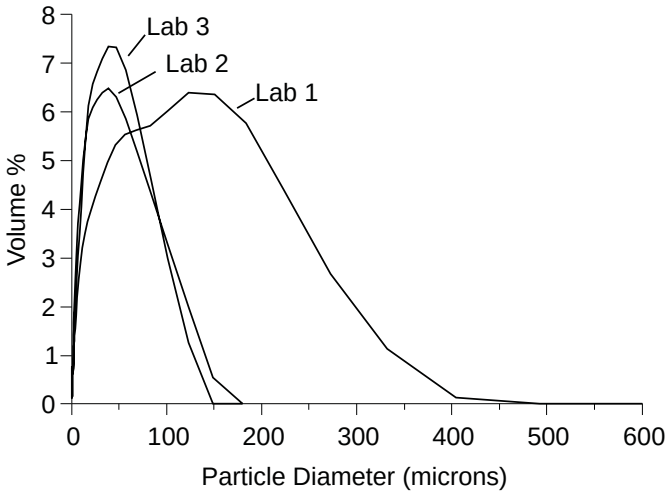

Figure 7: Variation in mean particle size distribution between the 3 labs

Particle size distribution of the crushed and sieved isotherm samples was also undertaken (Figure 7). All laboratories sieved the coals at 0.212mm. The laser particle sizer data indicates that laboratory 1 had a significant fraction of the coal exceeding this sieve aperture. However, this data can also be interpreted to mean that laboratory 1 produced thin, needle-like particles by its crushing procedure. While influence of particle shape on the adsorption isotherm is unknown, it should be noted that laboratory 1 produced systematically lower isotherm results than the other 2 laboratories.

Void volume determination

Determination of the void (or free) volume of the adsorption apparatus is an essential part of the procedure. Each of the three laboratories used a different analytical technique. One laboratory directly determined the void volume using helium — the mass of coal and its volume then being known, its density can be calculated. The other two laboratories used independently determined density data — the coal density being known and its mass allows calculation of the void volume.

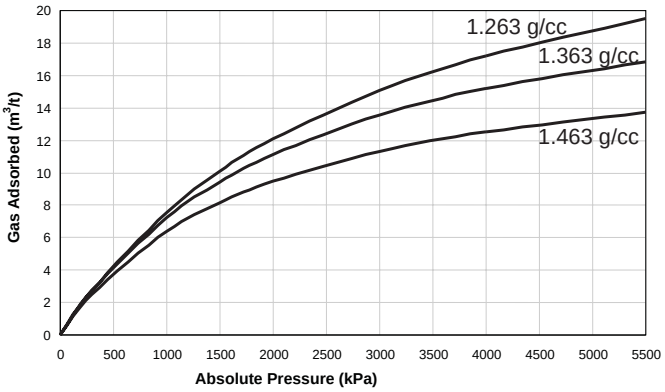

Figure 8: A family of methane adsorption isotherms calculated using the same input data but varying the density used for the coal. The density of the coal is used to calculate the dead (free) volume of the apparatus.

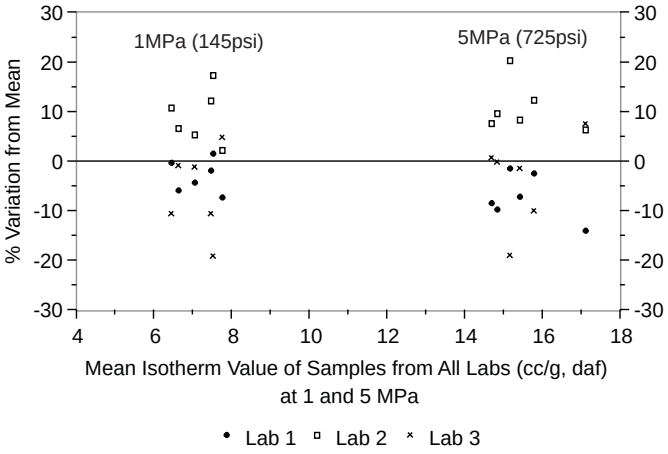

Figure 9: Reproducibility of all 18 isotherm samples at 1MPa and 5MPa. In this case, ash yield data has been used to estimate coal density, and hence the dead volume. All 3 labs used the same ash-density relationship. A marked improvement in the reproducibility is observed.

The void volumes between each laboratory cannot be directly compared since they depends on individual apparatus and precise amount of coal used in each analysis. However, the density values can be directly compared as they are a ratio of these two variables. Comparison of density and ash yield values indicated that laboratory 1 had consistently higher density values than the other laboratories. A sensitivity study of the effects of coal density on the calculation of the methane adsorption isotherm (Figure 8) shows that small changes in the coal density value used in the calculation algorithms has a marked effect on the calculated adsorbed volume. For example (Figure 8) a change of ±0.1g/cc on coal of density 1.363g/cc (i.e. ±7%) resulted in a change of adsorbed gas volume at 5500kPa of +16% (1.263g/cc) and -18% (1.463g/cc) compared to the 1.363g/cc value. The respective Langmuir parameters were P_L = 2967kPa, V_L = 30.00cc/g (1.263g/cc); P_L = 2396kPa, V_L = 23.51cc/g (1.363g/cc) and; P_L = 1907kPa, V_L = 18.49cc/g (1.463g/cc).

A large data set of apparent relative density versus ash yield was used to give a laboratory-wide consistent base line. The ash yield of the 18 isotherm samples was then used to calculate a coal density. This coal density was then used to re-calculate all 18 isotherms and the reproducibility re-assessed (Figure 9). Similar to the initial evaluation, laboratory 2 data was consistently above the mean but both laboratories 1 and 3 data were now consistently below the mean. However, now the variation about the mean has greatly improved from around ±20% to around ±12%.

It is clear that accurate determination of the void volume is a crucial procedure in obtaining reproducible isotherm results.

CONCLUSIONS

Reproducibility of methane adsorption isotherms is affected by a great variety of factors. Detailed evaluation in this study was hampered by sample heterogeneity and factors such as coal type and sample freshness may have played a role in the discrepancies observed.

Different calculation procedures used in the individual laboratories was shown to play no role in isotherm variation.

However, it is clear from this study that void volume determination is a key factor. The use of uniform criteria to calculate the void volume improved the reproducibility from around ±20% to around ±12%.

The use of different values for density of sorbed methane may have also influenced the isotherms by up to 4.5%.

The role of particle shape and distribution might also be important and needs to be further investigated.

Following this work, each of the laboratories has reassessed a number of key inputs, especially for void volume determination and particle size distribution. New round robin analyses now need to be conducted to assess the efficacy of these adjustments.

ACKNOWLEDGEMENTS

This work was funded by the Australian Coal Association Research Programme as part of ACARP Project C1000 Improved Application of Gas Reservoir Parameters.

Part of this work was undertaken by Peter Crosdale while at James Cook University, Coalseam Gas Research Institute. The use of facilities and resources is gratefully acknowledged.

Peter Crosdale, Energy Resources Consulting Pty Ltd, PO Box 54, Coorparoo, Qld 4151, Australia, peter.crosdale@energyrc.com.au
Abouna Saghafi, CSIRO Energy Technology, PO Box 330, Newcastle, NSW 2300, Australia, Abouna.saghafi@csiro.au
Ray Williams, GeoGAS Systems Pty Ltd, PO Box 342, Wollongong, NSW 2520, Australia, rayjwilliams@geogas.com.au
Eugene Yurakov, GeoGAS Systems Pty Ltd, PO Box 342, Wollongong, NSW 2520, Australia, eyurakov@geogas.com.au

Paul Bannerman, Peter Crosdale and Raphael Wüst

Controls on distribution and origin of gases at Oaky Creek

Mine gases at Oaky Creek range in content up to 15m^3/t and in composition from 100% CH_4 to 88% CO_2 Gas content generally increases from nil at outcrop to 15m^3/t at a depth of 260m. However, complex distribution patterns exist which are superimposed on this general relationship of increasing gas content with increasing depth. Gas composition normally exceeds 95% CH_4 but locally exceeds 50% CO_2.

Gas distribution was initially investigated at a metre scale in individual bore cores. Two or three seam sections were normally available from gas desorption bombs. Total gas content and composition was compared to brightness logs, coal quality data and roof lithologies. The top and base of the seam showed a small depletion in gas content which was correlated to the presence of dull coal. Higher gas contents in the middle section was related to bright coal and probably increased vitrinite content. Cross-sections showed that these trends were consistent over wide areas. Gas composition was homogenous throughout individual seam sections.

Lateral variability in gas content was investigated in relation to depth, structure, coal composition and coal quality. A general pattern of increasing gas content was found with increasing depth. Structural elements (faults and folds) also strongly influenced gas content. Faulting appears to be responsible for depletion of total gas content, where zones of greatest undersaturation correlate to zones of most intense faulting. Gas content is also relatively depleted around domes and anticlines. In structurally similar areas, gas content exhibits a pod-like distribution which appears to be related to vitrinite content: higher gas being associated with higher vitrinite content.

Stable isotope studies indicated a bacterial origin for the methane and a magmatic origin for the carbon dioxide.

INTRODUCTION

Gas storage and release by coal is controlled by many factors including rank, composition (maceral and mineral composition, ash yield), moisture content, temperature, pressure (burial depth), porosity and stress (Joubert & others, 1973; Kim, 1977; Rightmire, 1984; Levine, 1992; Lamberson & Bustin, 1993; Crosdale & Beamish, 1994; Busch & others, 2003), type of secondary mineralisation, permeability (fracture development) (Crosdale & others, 1998), size of coal particles (Yalçin & Durucan, 1991), surface area of coal (Lama & Bodziony, 1996), depositional systems and coal distribution, tectonic and structural setting, basin hydrodynamics (Faiz, 1996; Scott, 2002).

This study assesses how some of these factors influence the distribution of gases at Oaky Creek Coal mine.

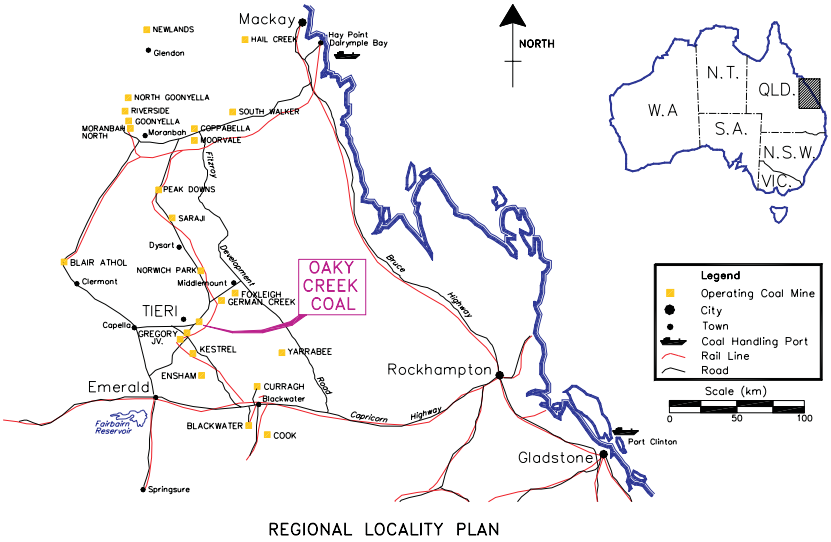

REGIONAL LOCALITY PLAN

Figure 1: Regional map displaying the locality of the Oaky Creek Coal mine site

The Oaky Creek Coal mine site is located in central Queensland (Figure 1) within the Bowen Basin. The study area of approximately 175km^2 encompassed the Oaky Creek Coal Pty Ltd (Xstrata Coal Queensland) mining, mining development and exploration leases ML1832, ML70241, MDL163 and EPC713. Open cut operations commenced in late 1982 with underground operations commencing in late 1990. The original open cut and the present underground operations target the German Creek coal seam of the German Creek Coal Measures. Present open cut operations mine the Aquila coal seam, along with the minor Pleaides coal seams, situated ~110m higher up in the sequence.

The German Creek Seam is a medium-volatile bituminous coal, with an average R_{Vmax} of 1.4%. It is generally a medium low ash (<20%), medium volatile matter (<25%) and very low sulphur (<0.05%) coal, which along with its high rank, makes it ideal for coking purposes.

The main gases found at Oaky Creek Coal are methane (CH_4) and carbon dioxide (CO_2), although small amounts of many other gases are also found e.g. higher hydrocarbons (ethane, propane), nitrogen, hydrogen sulphide, helium and carbon monoxide.

Regional geology

The Bowen Basin is a significant structural element within the eastern part of the Tasman Orogenic Zone. It is recognised as the northern continuation of the composite Bowen–Gunnedah-Sydney Basin (Totterdell & others, 1995), which developed in the hinterland of the New England Orogeny (Murray & others, 1987). The Bowen Basin lies on the boundary between Palaeozoic deposits of the Lachlan Fold Belt (and equivalent aged units) to the west, and of extensive Permian and Triassic igneous rocks of the New England Fold Belt to the east (Mallett & Russell, 1992). The Bowen Basin is partially overlain by Jurassic-Cretaceous sediments of the Surat Basin, and itself overlies a basement of Silurian, Devonian and Carboniferous magmatic or marine sedimentary rocks and Early Palaeozoic metamorphic rocks of the Anakie Metamorphics.

Site geology

The German Creek Seam is the lowest, but most important, member of the German Creek Coal Measures (Figure 2), which also contain the Pleaides 1, 2 and 3 Seams, the Aquila Seam, Tieri 1 and 2 Seams and Corvus 1, 2 and Middle Seams. The German Creek Seam ranges in thickness from over 5m in the north-east to less than 1m in the south and south-east, thinning through a series of floor and roof splits. The floor splits are labelled sequentially from the base as A, B, C and D. The roof splits are labelled F and G and they occur in the southwestern portion of the lease. Split lines tend to trend northeast or easterly.

Roof rock of the German Creek Seam is generally a fine to medium grained sandstone with a vertical extent of up to

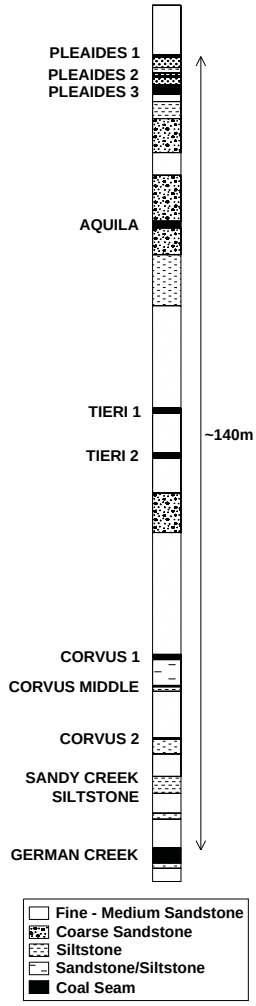

Figure 2: Generalised stratigraphic column depicting the German Creek Coal Measures.

15m and contains a variable amount of interlaminated siltstone. Sandstone composition is predominantly volcano-lithic and quartz, with minor amounts of mica and feldspar. Siltstone laminae are more common in the immediate 1m of roof. The floor lithology has a similar composition to that of the roof, except it generally has increased amounts of interbedded siltstone. Minor amounts of marine-derived carbonate and pyrite are also found in the roof and floor sediments of the German Creek Seam.

Folding and faulting is complex as a result of its position at the juncture between the Capella Block and the Comet Ridge. North of the Oaky Creek area, the German Creek Seam and equivalents dip eastward at around 4–5°, while to the south-west they dip to the south. Oaky Creek Mine exhibits both aspects of these trends. These two dip directions are separated by a syncline that trends south (in the north) to south-west (in the south). Prominent domes also occur in the north of Oaky North Mine and in the Sandy Creek area, locally known as the Aquila High.

Faulting can be categorized into two faults sets, one trending NNW and the other NE. NNW trending faults predominate

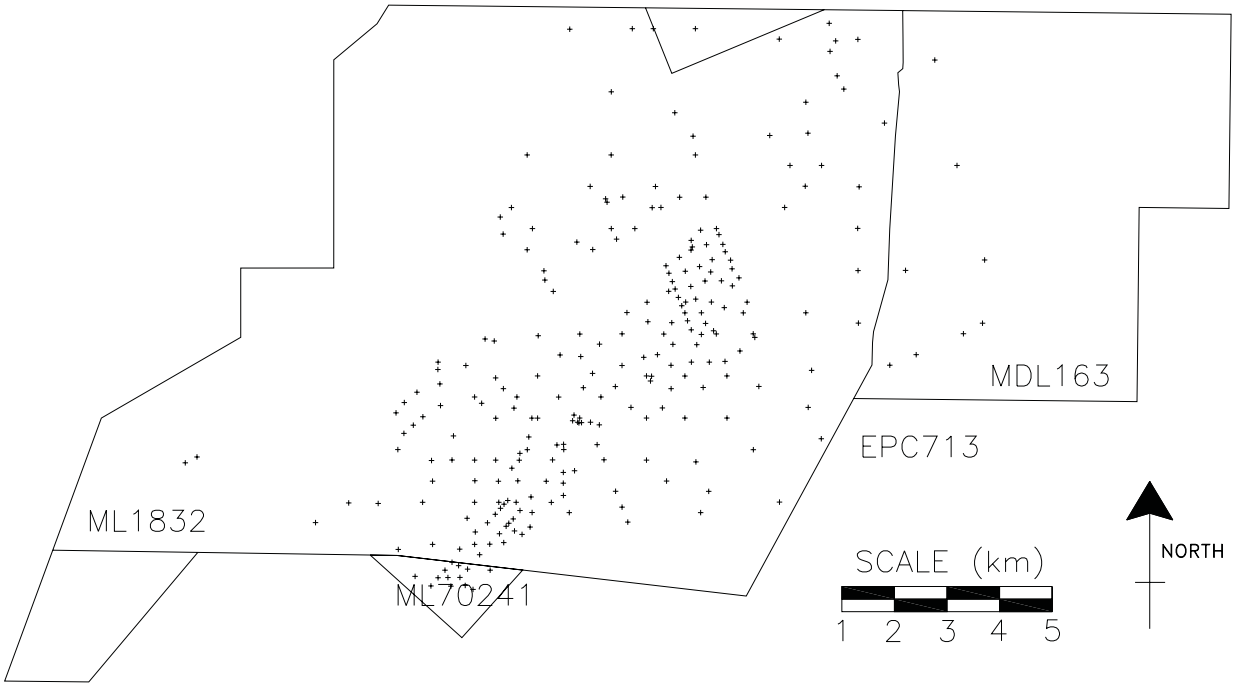

Figure 3: Locations of the specific gas test boreholes across Oaky Creek Coal utilised in the study.

and are mostly normal but some thrusts occur. Length ranges from <100m for small individual faults and up to 6km for large complex fault systems with spacings of generally less than 500m. The thrust faults are likely to be reactivated earlier normal faults. NE trending faults are less common and are nearly all thrust faults with less than 3m throw, except in the southernmost lease area where normal faults with this orientation have been identified by 3D seismic survey. Length is usually less than 500m and they occur in narrow (~600m) but widely spaced (4km) zones.

The distribution of gas content and composition in the German Creek coal seam across the Oaky Creek Coal mine site does follow a more regional, albeit weak correlation with depth of cover. Gas contents are extremely low (<1m^3/t) in the shallow areas down dip of the German Creek open cut pits, the northern Oaky North panels and on the Aquila High. In some mines this transition zone can contain high H_2S as a function of the biogenic reduction of sulphate in groundwater, with concomitant methane oxidation. However, Oaky Creek is relatively H_2S free with only a few localised zones encountered around the northern blocks of the Oaky No.1 underground operation.

Gas contents increase downdip, exceeding 5m^3/t at 160m to 180m, and are up to 15m^3/t in the east of the lease where the seam is deepest. Gas content is low over the Aquila High dome where the German Creek seam is closer to the surface (suggesting gas escape), but tend to 'pool' moatlike in the synforms around the dome. The coal seam gas across the study area is predominantly CH_4, but the percentage of CO_2 increases with depth from about 160m. CO_2 distribution and is more associated with the southeastern side of the Aquila High dome.

METHODS

Boreholes and samples

This investigation used all of the available specific gas test boreholes (~150) (Figure 3) and all specific coal quality holes (~150). Vertical gas variation investigations were limited to those 96 boreholes which also had proximate analysis data. These 96 holes were also used in conjunction with the isotherm results to determine the relative degree of saturation across the mine site. Additionally, all available mine data was used to generate cross-sections and lateral distribution maps.

Each borehole contained a number of separate splits, depended on the size of the seam at the place of testing. The number of splits per borehole ranged from 2 to 4, with the majority containing 3. Splits were labelled as Top, Middle or Bottom for ease of identification. If there were more than 3 splits then multiple Middle samples were allocated, if there were less than 3 then only Top and Bottom were allocated. The total number of splits in the study is 242.

Data treatment as different scales

Small and large scale variations in gas content and composition were investigated. Within individual boreholes, gas parameters were averaged and weighted for thickness to obtain a mean for the whole seam. Values for each split were

compared to the whole seam mean such that an assessment of vertical variations on a metre scale could be obtained.

A number of cross-sections were then constructed of closely spaced, neighbouring holes to check for lateral continuity and variability on a 10s to 100s metre scale. Included in these cross sections were gas content, gas composition, density log, volatile matter, ash yield, roof / floor lithology and brightness profiles.

Finally, variability on a 100s m to 10s km scale was assessed using contour maps, superimposed with other relevant information such as structure.

Total gas content

For gas content testing, the seam was separated into splits which could be placed into the gas testing canisters. The average length of the splits was 0.78m, but ranged from 0.76m to 0.80m. Portions of the coal seam that were less than 0.20m in length were omitted from gas testing as dead volume of the canister became too large for accurate readings.

Total gas content (Q_T) of a coal seam is given by the sum of the lost gas (Q_1) plus the desorbed gas (Q_2) plus the residual gas (Q_3). Q_1 testing was conducted as per Australian Standard AS3986-1999 by both the field geologist and GeoGAS Pty Ltd (Mackay). The Q_2 and Q_3 tests were conducted as per Australian Standard AS3980-1999 by GeoGAS Pty Ltd. The Fast Desorption method (AS 3980-1999) was employed in the determination of the gas content for each of the borehole samples. The Q_T data, along with gas composition data, received from GeoGAS (Mackay) was expressed either in terms of 'sample ash' or '15% ash', and was subsequently converted into a dry ash free basis at 1013hPa (1 atmosphere) and 20°C.

Proximate analysis

The proximate analysis for each of the 'split' samples was conducted as per Australian Standard AS1038.3-2000 by Casco Pty Ltd (Mackay). Volatile matter, moisture content and ash yield were determined, with fixed carbon being calculated as the difference with 100. The proximate analysis data was converted to a dry ash free basis.

Gas composition

Gas composition was determined on all desorption samples by GeoGAS Pty Ltd using standard gas chromatographic techniques.

Gas isotopes

Gas isotope analysis was conducted at the CSIRO Petroleum Laboratories in North Ryde, NSW. The gas sample was introduced into a sample loop at atmospheric pressure for preparatory gas chromatography with four packed columns being employed to separate the gases for the 20 minute run. To allow complete conversion of the collected hydrocarbons to carbon dioxide and water the separated gas components were then passed through a copper oxide furnace with a pulse of oxygen. These components were then separated cryogenically using liquid nitrogen and a shush bath of dry ice/acetone, with the stable isotopic composition of the collected carbon dioxide being determined by an isotopic ratio mass spectrometer. The exact analytical method and apparatus used is stated in the CSIRO Petroleum report produced for Oaky Creek Coal Pty. Ltd. (Stalker & others, 2004). The CSIRO standard (in-house) has been related to the NGS#1 and NGS#2 international standards, with the CSIRO carbonate reference being calibrated to NBS#19 (IAEA international standard defining VPDB, Vienna PeeDee Belemnite) (Stalker & others, 2004).

Adsorption isotherm analysis

Three coal samples underwent isotherm analysis. A gravimetric method was used to measure the high pressure CH_4 and CO_2 sorption isotherms. The total mass of gas adsorbed is defined by the difference between the mass of the sample with and without gas. Analysis was carried out at the Coalseam Gas Research Institute, James Cook University, using their standard procedures on -0.212mm, equilibrium-moist coal.

Maceral analysis

Maceral analysis was conducted on the adsorption isotherm samples. Twenty grams of coal was removed prior to the isotherm analysis for maceral analysis. The analysis was conducted as per Australian Standard AS2856.2-1998. The sampling method used 40 evenly spaced 'spoonfuls' of crushed coal across the whole sample, with each 'spoonful' being approximately 0.5g.

METRE-SCALE VARIATION OF GAS COMPOSITION AND CONTENT

Gas content and vertical variation

Factors investigated in relation to the vertical variation of the gas content in the seam included volatile matter content, ash yield, relative density, coal lithotype and immediate roof lithology. Fine crushing during gas testing precluded petrographic examination. However, several coal quality boreholes adjacent to gas test boreholes provided some information on the influence of maceral composition. Gas content herein refers to the total gas content ($CH_4 + CO_2$, m^3/t) unless otherwise stated.

In each borehole, the mean gas content was derived using a weighted for thickness average of all the splits. The percent difference away from this average was then determined for each split (Figure 4). Generally, the top (Figure 4 'A') and

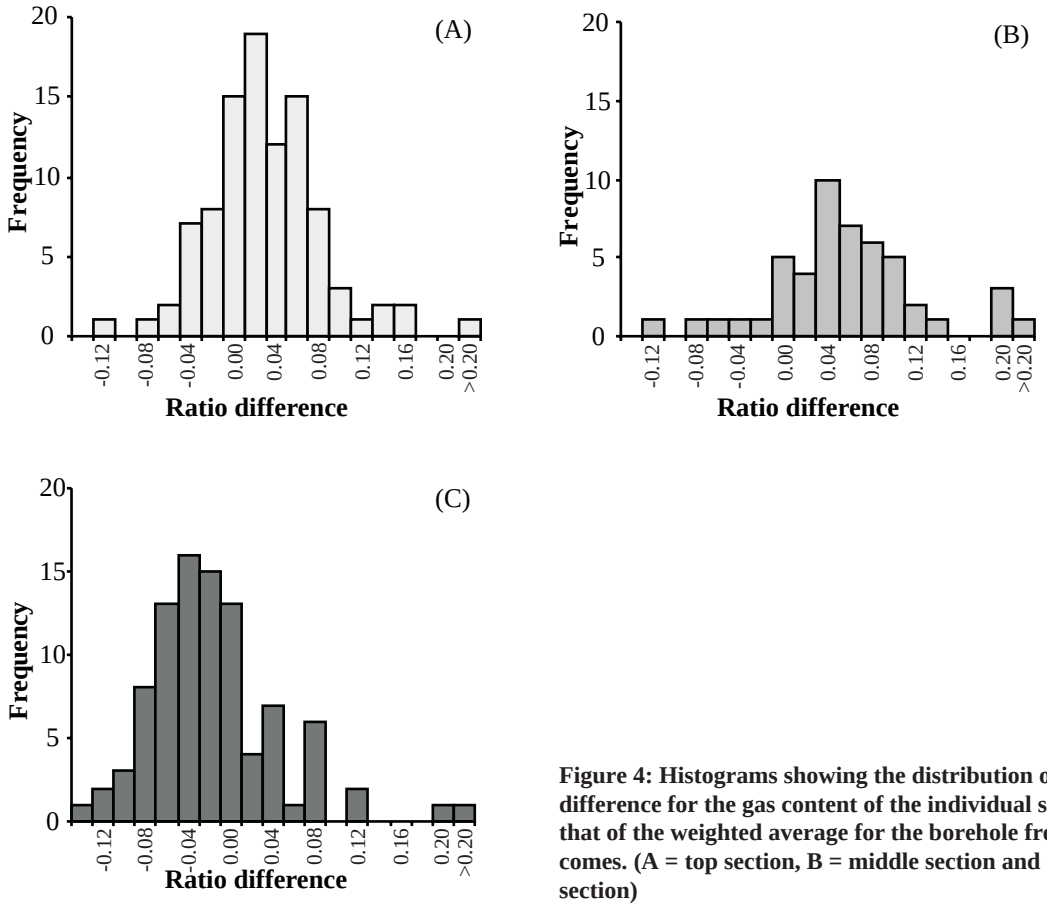

Figure 4: Histograms showing the distribution of the ratio difference for the gas content of the individual samples with that of the weighted average for the borehole from which it comes. (A = top section, B = middle section and C = bottom section)

middle (Figure 4 'B') samples have higher gas content (positively skewed) than the weighted average, while the bottom sample (Figure 4 'C') is less than the mean (negatively skewed). The middle sample also had higher gas content than the top sample on average. This gas content pattern of intermediate in the uppermost split, highest in the middle split and lowest in the bottom split was consistently repeated in most holes.

Immediate roof lithology was examined to determine if the vertical variation observed may be influenced by the sealing properties of the roof strata. An impermeable roof could trap upwards migrating gas, leading to depletion in the lower portions of the seam. Immediate roof data was separated into two main types, either sandstone or siltstone. The percent difference of the top split from the borehole average was plotted against the total borehole gas content for each roof rock type. No relationship of roof rock to gas content within the uppermost split was indicated.

Comparison of volatile matter content (daf) with total gas content (daf) shows a broad increase in the total gas content with a decrease in volatile matter. Additionally, the top seam section tends to have higher volatile matter content (daf) than the basal section of the seam, a trend also reflected in the gas content. Volatile matter is related to both coal type (petrographic composition) and rank (degree of coalification) as well as being influenced by inorganic constituents. Coal rank is known to vary across the site as shown by independent vitrinite reflectance data. Similarly, coal type varies significantly within individual holes as indicated by lithotype logs.

Ash yield (from proximate analysis) showed no obvious relationship with total gas content. Ash yield relates to the mineral matter contained within the coal, which generally plays the part of an inert diluent (Laxminarayana & Crosdale, 1999), and thereby reducing the storage capacity. Relative density of the individual splits was used as a check on the findings of the ash yield data.

The density data also show no obvious relationships with the total gas content of a particular split sample, confirming the findings from the ash yield. It is interesting to note that the middle samples usually have lower ash yield than the top and bottom sample sets, both of which in turn show a large degree of scatter. This may be due to a more homogeneous composition of the middle seam section, containing less non-coal bands.

Petrographic correlations to vertical gas content trends could not be directly established due to the methodology of the gas content testing procedure. The petrology or coal composition was therefore investigated from specific quality boreholes that were situated near gas test boreholes. Only quality and gas boreholes that were within 100m of each other were utilised in order to maintain some horizontal integrity, even though depositional trends could still vary over these distances and in turn affect the observations. Four pairs of boreholes were investigated.

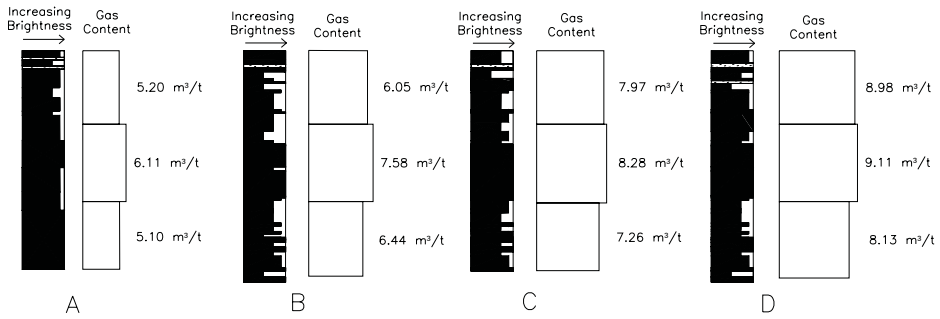

Figure 5: Cross-section of neighbouring gas test and quality boreholes

The analysis of the four borehole pairs shows that the middle portion of the seam is dominated by bright coal (vitrinite-rich) (Figure 5), whereas the top and bottom sections of the seam contain bands that are duller. Dull coal types may be mineral-rich, inertinite-rich or liptinite-rich, and require petrographic analysis for determination. The top section of the seam often contains small stone bands (siltstone/carbonaceous mudstone) and has higher density on the density logs. Comparison of brightness and total gas content indicated that the middle sample often contains slightly higher gas content which could be attributed to the petrographic composition. Integration of volatile matter (daf), ash yield and lithotype logs suggests that:

1. The bottom section of the seam is inertinite dominated, giving low volatile matter (daf), dull lithotypes and high ash yield, where mineral matter is deposited in primary phyteral porosity,

2. the middle section of the seam is vitrinite (telinite B large plant parts representing twigs, roots, etc) dominated, giving intermediate volatile matter (daf), bright lithotypes and low ash yield, and

3. the upper section of the seam is vitrinite (desmocollinite —B fragment plant parts cemented with high volatile matter organic gels) dominated, giving higher volatile matter (daf) and associated with detrital mineral matter giving dull coals, stone bands and high ash yield.

However, detailed petrographic analysis is required to confirm this. Petrographic properties of coals strongly influence coal quality and possibly also gas content. Bright (vitrinite-rich) coals generally have a greater methane adsorption capacity than dull (inertinite-rich) coals due to their different physical characteristics (i.e. pore space) (Crosdale & Beamish, 1993).

Gas Content and Lateral Persistence

Lateral persistence of these vertical variations was investigated by comparing two separate cross-sections, one from Oaky North and one from Oaky No. 1. The cross-section for Oaky North was taken across the main synclinal feature that traverses across most of the southern longwall blocks in an NE–SW orientation. The Oaky No. 1 section was taken along another synclinal feature that crosses the Sandy Creek longwall blocks in an ENE B WSW orientation. Each of the cross-sections included the roof lithology immediately above the top of the coal seam, as well as the density, total gas content, ash yield and volatile matter for the respective seam section samples. Due to seam thickness decreasing to the south, some boreholes had only 2 samples.

The cross-sections showed that the majority of trends previously observed are laterally persistent i.e. the middle seam section tends to have higher gas content than the adjacent samples; the middle portion of the seam tends to have intermediate volatile matter and lower density. The ash yield for the Oaky North middle sections is similar to the formerly noted trend, being lower than the surrounding top and bottom splits. The lower sections from Oaky No.1 do not follow this observation, with the ash yields often very similar and in some cases higher than their adjacent counterparts.

A separate and important observation to arise from the analysis of these two sections traversing individual synclines is the relationship between the total gas content and the position of borehole relative to the base of the syncline. Faiz (1996) noted that for the Sydney Basin the highest accumulation of methane is in the base of synclinal structures. This is not observed at Oaky Creek, with the higher gas values being part way up the southern limbs.

Gas composition and vertical variation

Gas composition refers to the $CH_4/(CH_4 + CO_2)$ ratio for each individual split and is expressed in terms of %. The

majority of the samples (~66%) had CH_4 ratios exceeding 95%. To assess if the CH_4 or CO_2 occurred preferentially in the top, middle or bottom of the seam, weighted average gas composition of the seam was first calculated. The difference of each sample from the mean was determined.

Little or no vertical variation in gas composition is observed as most samples are located around the 0% difference point. The majority of all individual gas samples (~77%) have the same gas composition as that of the weighted average for the same borehole. The range of any variation is ±0.06% which encompasses 99.98% of all the splits, with only 6 samples (0.02%) falling outside this range. This indicates no preferential separation or distribution of the adsorbed gas (CH_4 or CO_2) within the coal matrix across the vertical coal sequences.

The observed lack vertical compositional variation may be related to:

- The factors which affect gas content do not influence gas composition.
- The observed compositional distribution is related to the sampling technique and resolution.
- The seam may not be thick enough for any differential distribution to occur.
- The petrology or chemical composition of the coal within the vertical section is so similar that there is no preferential separation or accumulation of the gas.
- There has been sufficient time for the seam to arrive at a compositional equilibrium either due to tectonic activity or a regional geochemical event.

MINE SITE VARIATION IN GAS COMPOSITION, CONTENT AND DISTRIBUTION

Several factors that contribute to variation in gas content were investigated, including depth, coal rank, coal composition, ash yield, moisture content, and relation to structure. The gas composition was also investigated over some of these parameters to see if any relationship existed. The results of the isotherm analysis were compared to previous analyses collected in 2000 and 2003 (GeoGAS Reports), to determine if there were any areas of greater under or over saturation.

Depth and gas content

The depth of cover has a large effect on gas retention capacity of coal as the depth of cover is directly proportional to the hydrostatic pressure and the gas content is maintained by the hydrostatic head of water on the seam. Generally, a positive correlation exists between gas content and depth (Figure 6), which shows that the gas storage capacity of coal progressively increases with increasing hydrostatic pressure (Kim, 1977; Scott, 2002).

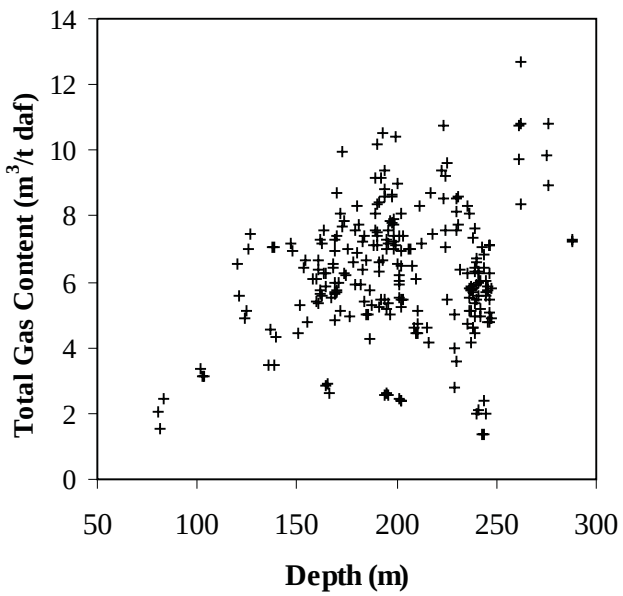

Figure 6: The relationship of the total gas content (m^3/t) of the German Creek coal seam with respect to depth (m) as observed across the Oaky Creek Coal mine lease

At Oaky Creek a similar trend, albeit not truly correlative, of increasing depth increasing total gas content is observed (Figure 6). The relationship is however, not strictly definitive as there are a number of low content boreholes at depth.

Areal distribution of the total gas content with respect to depth to top of coal (Figure 7) shows a number of key features. Highest gas contents are to the east of the area, where the seam is at its deepest, (Fig 7 'C') but areas of higher gas content also occur through the middle region of the study area (Figure 7 'B'). Gas in region 'B' has a pod-like distribution and this area is dominated by a syncline that originates from the north. A zone of low gas content in the south of the study area (Figure 7 'A') occurs around the Aquila High, which is a dome-like feature. The region of low gas content along the western side of the study region (Figure 7 'D') is related to the proximity of the coal seam to the abandoned open cut pits and the shallowness of the seam to the surface. This zone of low gas content extends into the seam due to permeation and diffusion of the gas into the atmosphere.

Gas composition

The gas composition of the coal seam gas was investigated relative to depth (Figure 8). Two trends emerge with respect to the CO_2 content within the coal, one of decreasing CO_2 with increasing depth (Figure 8 'A') and the other of increasing CO_2 with increasing depth (Figure 8 'B'). These opposing trends are related to the Aquila High, which is a dome-like structure occurring at a depth of about 120m in the German Creek seam. The relative decrease in the CO_2 content with increasing depth (Figure 8 'A') is found downdip of the Aquila High and is away from the inferred CO_2 source, while the increase in CO_2 content with increasing depth is also found downdip of the Aquila High,

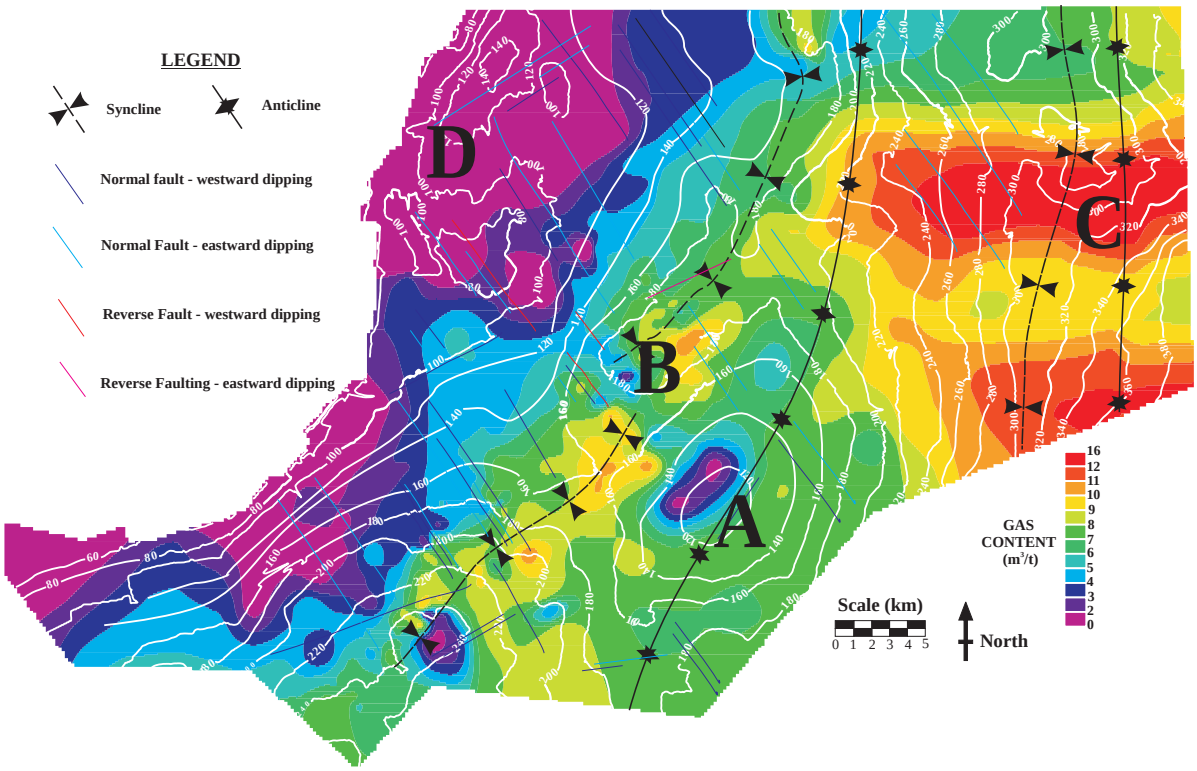

Figure 7: Plan map of the Oaky Creek Coal study area displaying the total gas contents (m^3/t) [colour contours] and the depth to top of coal contours (m) [line contours] and the structural setting (i.e. depth of seam, folding and faulting). (A = Aquila High; B = Syncline; C = Eastern deep area; D = Western shallow area)

but it is towards the inferred CO_2 source (Figure 8 'B'). Faiz (1996) noted that for the Sydney Basin the relative CO_2 proportion increased with decreasing depth, and speculated that the increase in CO_2 was related to the temperature regime which inhibited bacterial CO_2 reduction to methane as depth increased. This observation is also apparent for the Oaky Creek mine site.

Areal distribution of CH_4 shows highest values of >7m^3/t in the east and central areas, and lowest values of <4m^3/t in the west and around the Aquila High. In general the CH_4 distribution is related to the depth of the seam. High levels of CH_4 occur in the seam at depth levels greater than 160m. These regions also correspond to the syncline through the middle of the study region and where the seam dips downwards in the east.

The CO_2 distribution shows a much simpler pattern than the CH_4 distribution. Most CO_2 occurs around the south-eastern side of the Aquila High dome. The observed CO_2 distribution is therefore partly related to the depth of the coal seam but probably more the result of some igneous intrusions to the south of the study area. The distribution pattern of CO_2 suggests up-dip migration from a deeper source.

Coal rank

Coal rank is often considered to be the main parameter affecting methane sorption capacity and a relationship of increasing capacity to increasing rank has been previously established (Kim, 1977; Levy & others, 1997; Scott, 2002). This can be explained by the increasing proportion of micropores in the pore structure, but it is highly variable due to geological heterogeneities (Scott, 2002).

Comparison of total gas content to mean maximum reflectance (% R_{Vmax}) showed only a poor relationship. A

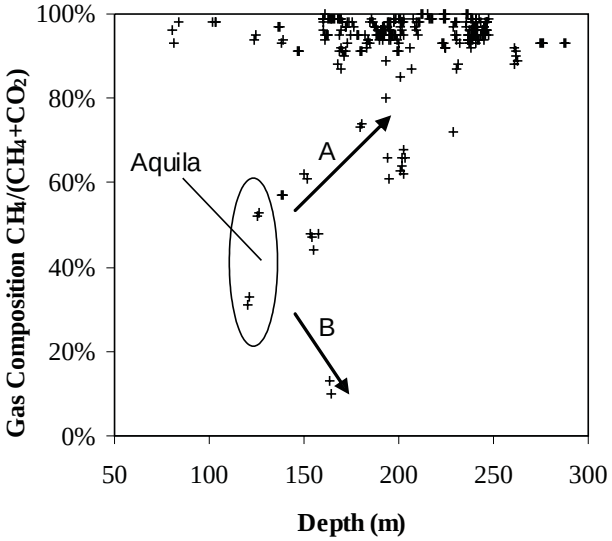

Figure 8: The relationship of the gas composition [$CH_4/(CH_4 + CO_2)$ %] of the German Creek coal seam with respect to depth (m) as observed across the Oaky Creek Coal mine site. The Aquila High has been highlighted with the two opposing CO_2 trends: (A) decreasing CO_2 with increasing depth, and (B) increasing CO_2 with increasing depth

zone of elevated vitrinite reflectance in the east (R_{Vmax} > 1.4%) broadly corresponded to higher gas contents. This eastern zone also corresponds to the deepest coals. For the western part of the site, no relationship was observed and gas content trends are orthogonal to the reflectance trends. Therefore while coal rank may affect adsorption capacity, it is not the definitive parameter corresponding to the observed gas content distribution.

Coal composition

The influence of the maceral composition of coal on methane sorption capacity is poorly understood (Laxminarayana & Crosdale, 1999). Many workers have indicated that coal type influences the methane sorption (e.g. Levine, 1992, 1993; Busch & others, 2003). Many studies have demonstrated that bright (vitrinite-rich) coals have a greater methane adsorption capacity than dull (inertinite-rich), rank-equivalent coals (Crosdale & Beamish, 1994; Lamberson & Bustin, 1993; Levine & others, 1993; Crosdale & others, 1998; Laxminarayana & Crosdale, 1999).

Vertical variation investigations (Figure 5) showed the middle section of the seam had a higher proportion of bright coal horizons and in turn contained higher amounts of the gas, relative to the adjacent sections. Therefore the lateral distribution of vitrinite content was investigated to see if it had any bearing on the overall gas content trend. An increase in the relative amount of vitrinite may be expected to be seen in the middle and towards the east of the study region to coincide with the increase in gas content. Unfortunately, in general, there appears to be no relationship between the total vitrinite content and total gas content.

However, some regions of high vitrinite content in the middle of the study region (synclinal zone ‘B’ of Figure 7) do correlate with areas of higher gas content. Both vitrinite and gas contents have a pod-like distribution through this area where the pods broadly, but not always precisely, correspond. Here, depth range is also relatively narrow at between 160m and 200m.

A decrease was observed in the overall vitrinite percentage to the east, which in turn does not correlate with the overall gas trend. Generally, the high gas content areas are seen to correspond with areas of lower vitrinite content. The higher vitrinite zones are actually in the west where the total gas content is at its lowest. The vitrinite content can still have an influence on the gas content but other factors are influencing the gas content/composition to a greater degree.

Ash yield

Ash yield (mineral matter content) usually correlates strongly to methane adsorption capacity, with increasing ash yield related to a reduction in the methane adsorption capacity of the coal (Laxminarayana & Crosdale, 1999). A linear decrease in adsorption capacity with increasing ash yield indicates that the ash (mineral matter) acts as a simple diluent, thereby reducing the storage capacity (Laxminarayana & Crosdale, 1999).

Ash yield was therefore investigated to see if it had any bearing on gas content trends. Vertical variation analysis did not reveal an obvious trend with respect to ash yield and gas content. However, it was found that the brighter coal horizons did yield consistently lower ash values. Ash yield (based on whole seam section averages) ranges from 14–20% across the study region. No overall trend was found relating an increase in total gas content with a decrease in ash yield. This observation could result from the large size of the data set and the relatively narrow range of ash values.

Moisture content

Moisture content of coals has a marked effect on gas adsorption capacity. However, because moisture content varies with coal rank and composition, and methane adsorption also changes with these variables, it is difficult to isolate the effects of moisture content (Scott, 2002). In general, the capacity of a coal to adsorb methane may increase with coal rank but is reduced with an increase in moisture content (Joubert & others., 1973; Yalçin and Durucan, 1991; Levine & others., 1993; Levy & others., 1997). Water and methane are both sorbates and compete with each other for some sorption sites in the coal structure; therefore any moisture may block access to the microporosity.

Isograds of moisture content showed high variability the mine site, ranging from 0.8–2.4%. Higher moisture contents were in the west and generally decreased eastwards. The eastern-central section contained the lowest moisture values, ranging from 0.8–1.2%. The eastern area ranged from 1.0–1.4%. However, no obvious relationship exists between the moisture content and the total gas content.

Structural setting

Tectonic and structural setting of a basin during deposition will control the distribution and geometry of coal beds in the basin and may influence the lateral variability of macerals. Post-depositional tectonic and structural setting will control the location and geometry of folds and faults that may strongly influence the recharge of meteoric water, and consequently, the generation of biogenic gases (Scott, 2002). Uplift and basinal cooling will also have an effect and results in undersaturation in the coals with respect to methane and also possible degassing of coal beds (Scott, 2002). Faiz (1996) found that CH_4 is the dominant gas in structural lows (i.e. synclines), whereas the proportion of CO_2 increases towards structural highs and near some faults in the southern Sydney Basin sequence. Furthermore, at a given location the proportion of CO_2 in the gas increases with decreasing depth (Faiz, 1996).

The structural setting of the coal seam (Figure 6) was investigated to see if it had any bearing on the gas content

trend of the mine site. As previously stated, the total gas content increased with increasing depth, however there are areas where the seam is not at its deepest but relatively high values are recorded. Faiz (1996) observed that CH_4 was dominant in the base of synclines, but this relationship is not exactly observed in the study area where regions of higher gas content were found to be actually part way up the southern limbs of the synclinal structures. However, the CO_2 proportion was found to increase around the structural high (Aquila High).

The German Creek coal seam thins from the northwest towards the south and east of the study area. In the northwest the seam is at thicknesses of >4.5m and gradually thins towards <1.4m at the edge of the southern and eastern mining lease boundaries. Isolated zones of thinning coincide with the base of the syncline in the northern half of the region. Hence the thickness of the coal seam has no bearing on the total amount of gas stored within it, as the gas content increases to the east and in the vicinity of the syncline.

Relative seam saturation

Relative saturation of the German Creek coal seam was interpreted from isotherm data. The isotherm analysis, and resultant Langmuir equation, provides information on the maximum amount of CH_4 that can be stored within the coal at a particular depth. Example results from 3 samples are tabulated along with the actual measured CH_4 content (Table 1).

Using mean values of the Langmuir co-efficients, degree of relative saturation was determined for all samples and the maximum possible gas content was plotted against the actual measured gas content (Figure 9). It is concluded that the German Creek coal seam across the Oaky Creek Coal mine site is undersaturated with respect to CH_4. On average, the degree of the undersaturation is approximately 55% of the maximum quantity potentially able to be stored at a given depth.

Areally, the undersaturation of the coal seam with respect to CH_4, ranges from 30–100% (Figure 10) with the higher undersaturation levels are recorded in the south-west and in the vicinity of the Aquila High (Figure 10 'A'). The areas of lesser undersaturation are documented in the central

Table 1: Resultant data from the 3 samples that underwent the isotherm analysis. Displayed are their respective depths, maximum CH_4 content (m^3/t) and the actual measured CH_4 content (m^3/t). Maximum CH_4 content (m^3/t) based on resultant Langmuir coefficients: P_L = 1.34MPa, V_L = 25.60cm^3/g.

Borehole	Depth (m)	Maximum CH_4 content (m^3/t)	Actual CH_4 content (m^3/t)
C11193	173.44	14.30	5.93
C11245	176.28	14.40	7.18
C11246	175.02	14.35	5.99

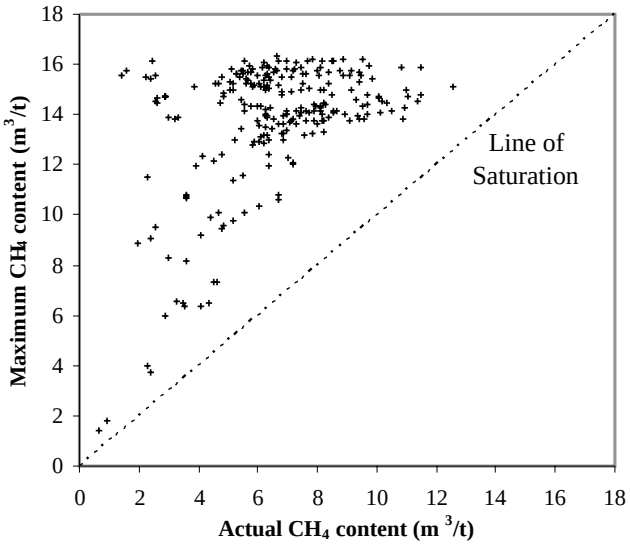

Figure 9: Plot of relative saturation of the German Creek coal seam as displayed by the relationship between the actual gas content (measured) and the possible maximum gas content (determined by isotherm analysis)

(Figure 10 'B') and eastern regions (Fig 10 'C'). The observed undersaturation of CH_4 around the Aquila High correlates with the high CO_2 levels previously noted.

An interesting observation was the north–western region (Figure 10 'D_a') which exhibited an undersaturation to a lesser degree than the areas to the immediate south (Figure 10 'D_b') and east. The area to the south is of similar depth and proximity to the open cut pits, while the area to the east is of greater depth. Therefore, depth is not the sole explanation as to the observed undersaturation.

Faulting was investigated to determine if it has any relation to the observed undersaturation scenario (Figure 10). The faulting can be categorized into two faults sets, one trending north-north-west and the other north-east. NNW trending faults are the most common and they range in length between <100m for small individual faults and up to 6km for large complex fault systems. The faults are predominantly normal faults, but some are thrust faults. NE trending faults are less profuse and occur in narrow (~600m) but widely spaced (4km) zones. Nearly all of the faults are to the west of the syncline where they have been located from mapping underground and further correlated with 3D seismic and borehole interpretation.

The majority of the faults are predominantly located over areas of increased undersaturation (Figure 10). Therefore the faulting can be assumed to be related to the observed undersaturation in that the fault planes, with associated shearing and jointing, would provide migration pathways for the gas to escape. Furthermore, the faults could also provide pathways for the infiltration of meteoric waters into the coal seam.

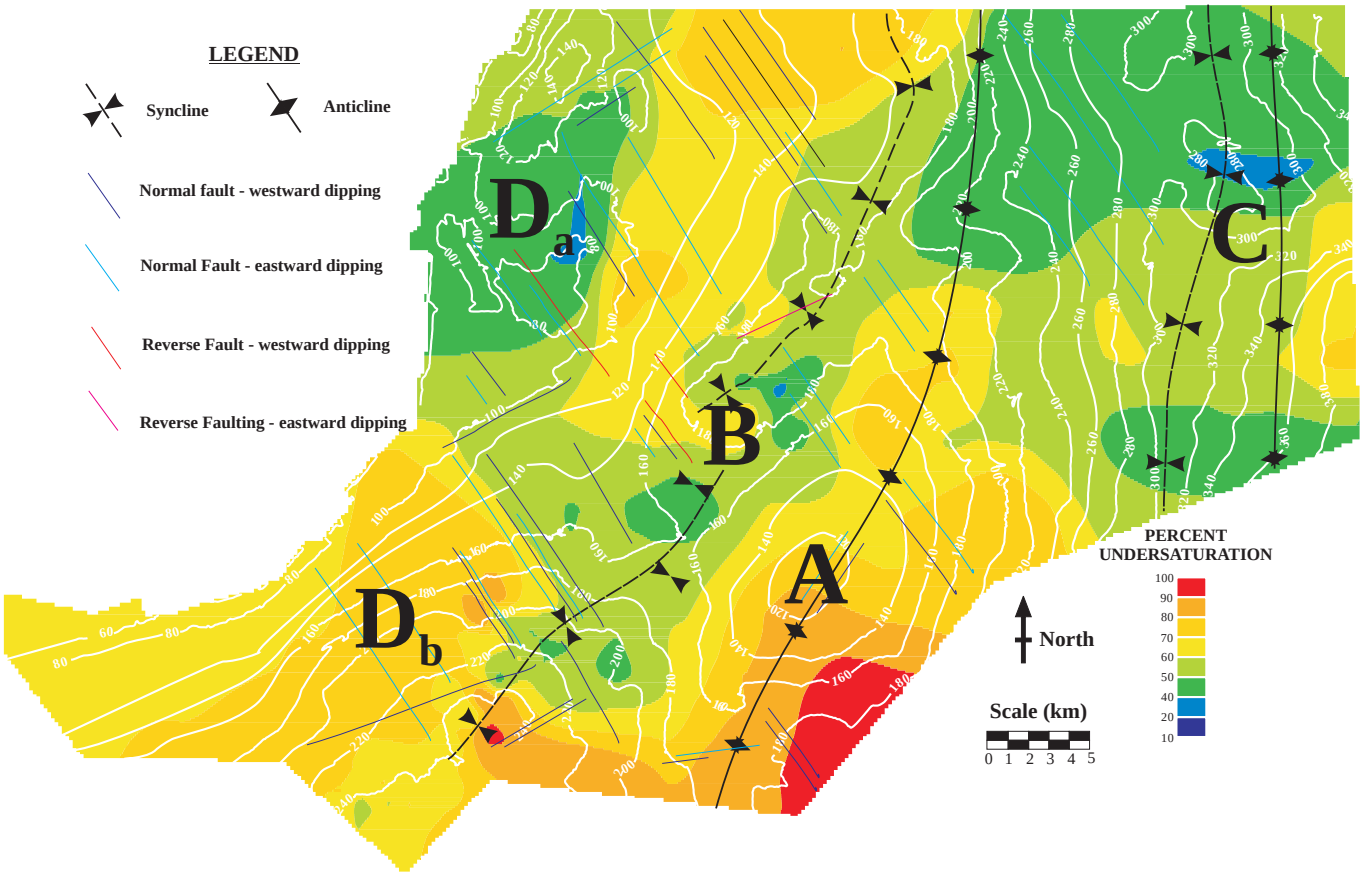

Figure 10: Plan map of the study region showing the relationship of the relative degree of saturation (with respect to CH_4) [coloured contours] with the depth of the seam and structural setting. (A = Aquila High; B = Syncline; C = Eastern deep area; D_a and D_b = Western shallow areas)

GAS ORIGINS

Carbon and oxygen isotopes were determined in methane and carbon dioxide in order to constrain possible origins for these gases. Five gas samples were obtained from dedicated cores taken for gas desorption (Table 2). Isotope samples were taken from the middle section of the seam.

Carbon isotopes for methane range from −65.9‰ to −80.2‰ VPDB (Table 2) and are highly depleted in ^{13}C. The ranges of $ä^{13}C_{CH4}$ values are at the lower end of the observed range for the Bowen and Sydney Basins and overlap with that shown for microbial methane (Figure 11). Methane very much enriched in ^{12}C occurs by microbial action kinetic isotope fractionations on the organic material by methanogenic bacteria, with typical $ä^{13}C$–values between −110‰ and −50‰ (Hoefs, 1997). Thermogenically derived CH_4 exhibits higher $ä^{13}C$ values.

The high percentage of methane in the majority of the standard gas test samples suggests almost complete reduction of any (thermogenic) CO_2 present. The $ä^{13}C$ of the residual dissolved CO_2 becomes isotopically heavier as isotopically light CO_2 is removed for CH_4 formation (Rice & Claypool,

Table 2: Oaky Creek Coal gas isotope samples and results, along with the in-house CSIRO standards. (Standards are quoted at ±0.2‰, n.d. = not determined due to insufficient recovery.

Sample No.	Sample Depth (m)		‰ VPDB $ä^{13}C_{Methane}$	‰ VPDB $ä^{13}C_{CO2}$	‰ SMOW $ä^{18}O_{CO2}$
	From	To			
C11476-7	200.83	201.62	-65.9	n.d.	n.d.
C11477-7	169.41	170.21	-75.7	n.d.	n.d.
C11478-8	203.21	203.96	-74.4	n.d.	n.d.
C11479-9	202.48	203.24	-67.2	-7.6	1.0
C11480-9	128.53	129.32	-80.2	-4.5	4.9
In-house Standard			-38.4	-9.4	-12.5
			-38.3	-9.3	-12.8
Average value of the in-house standard			-38.6		

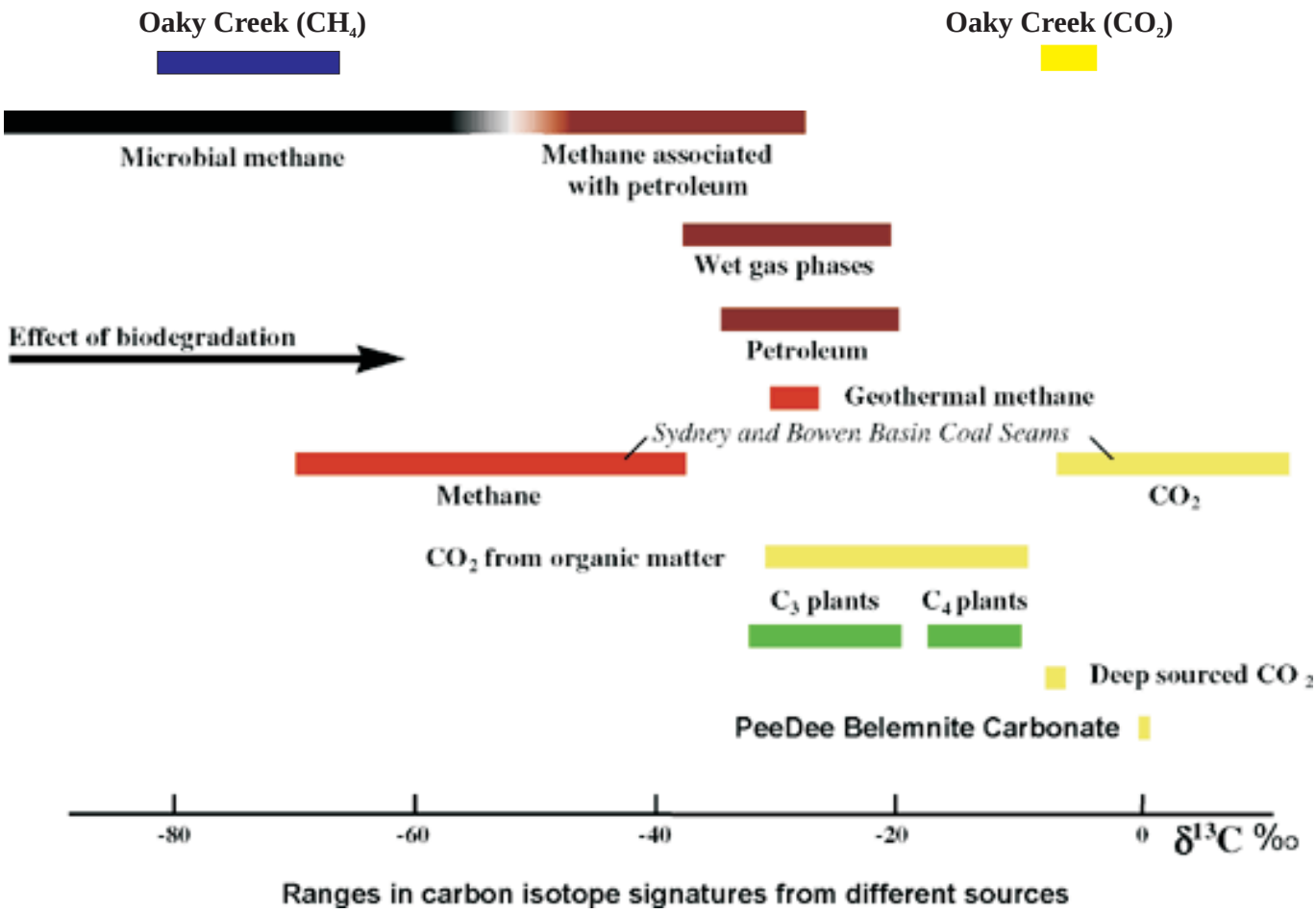

Figure 11: Generalised ranges of carbon isotope signatures for particular coalbed gases and the range of recorded values for Oaky Creek. Diagram based on Taylor (1978) and Hoefs (1997)

1981). Isotopic analysis of the (thermogenic) CO_2 component should result in range near that of the coal (~ -23‰).

Carbon dioxide recovery was sufficient in only two of the five samples for analysis and hence the $ä^{13}C_{CO2}$ and $ä^{18}O_{CO2}$ results are slightly under correlated. The $ä^{13}C_{CO2}$ values for the two samples are −7.6 and −4.5‰ VPDB and are on the lower end of the spectrum observed for Bowen and Sydney Basin coal seams (Figure 11). They correlate somewhat with deep sourced igneous-related CO_2, which usually has a range of −7±2‰ (Smith & Pallaser, 1996).

In the area where there is a high percentage of CO_2, there is almost no methane, therefore it is suggested that intruding igneous-related CO_2 has displaced the residual methane (Smith & Pallaser, 1996). This accounts for the observed $ä^{13}C_{CO2}$ values. According to Ahmed & Smith (2001) the interpreted transient nature of CO_2 reduction may account for the presence of apparently inert magmatic CO_2 ($ä^{13}C_{CO2}$ = −7±2‰) which may have migrated into the seam after reducing conditions had terminated. Changes of isotopic composition of coal seam CO_2 with increasing CO_2 content (observed in the south Sydney Basin) is consistent with seam invasion by CO_2 of constant isotopic composition from an external source (Smith & Pallaser, 1996).

On the basis of the total isotopic and compositional evidence, a biogenic origin for the CH_4 via the reduction of coal-associated CO_2 (Smith & Pallaser, 1996; Ahmed & Smith, 2001) has been proposed. The proposition that CH_4 ($ä^{13}C$ = −55±10‰) resulting largely from biogenic reduction of CO_2, requires a large source or sources of essentially pure CO_2 with an isotopic composition similar to that of the coal ($ä^{13}C$ = −23‰) (Ahmed & Smith, 2001). Aliphatic and aromatic hydrocarbons degrade to CO_2 by way of microbial oxidation and decarboxylation reactions and this is the process by which the initial CO_2 was produced.

The introduction of this CO_2 into the highly reducing methanogen-rich environment in undisturbed coal results in a rapid, possibly instantaneous reduction of CO_2 with $ä^{13}C$ values approximating -55‰ and +5‰, respectively (Smith & Pallaser, 1996). The absence of CO_2 with $ä^{13}C$ values close to that of the coal suggests CO_2 to be present transiently, prior to conversion to CH_4. The interpreted transient nature of CO_2 reduction may be accounted for by the presence of apparently inert magmatic CO_2 which may have migrated into the seam after reducing conditions had terminated.

By investigating the $ä^{18}O$, the type of magmatic body from which the gas originated may possibly be determined. The

$ä^{18}O_{CO2}$ values for the two samples are 1‰ and 4.9‰ SMOW. These values were then compared to the typical ranges of $ä^{18}O$ values for plutonic and igneous rocks (Taylor, 1978). Volcanic rocks possess lower $ä^{18}O$ values than those of standard plutonic rocks. However, some crustal contamination must have occurred which has decreased the original $ä^{18}O$ values to those exhibited at Oaky Creek. For example, interaction with groundwater that has low $ä^{18}O$ (i.e. <0‰) the value will decrease the observed $ä^{18}O$ value (Taylor, 1978).

CONCLUSIONS

Metre-scale vertical variation

Significant variations were found in gas content of sequential seam samples from single boreholes. The middle section of the seam generally contained the highest gas contents, the top section an intermediate gas content and bottom sections the lowest gas content. Highest gas contents were found to be related to bright-coal horizons and the lowest gas contents correlated to the lowest volatile matter, dullest sections. Detailed petrographic analysis was unable to be performed due to sampling restrictions and these general relationships could not be further investigated. However, it is postulated that the middle section of the seam is vitrinite (telocollinite)-rich, the upper section is vitrinite (desmocollinite)-rich and the lower section is inertinite-rich. Ash yield and relative density showed no strong relationship to gas content of serial samples. Roof lithology was found to play no important role in vertical variability within the seam.

These observed trends in coal characteristics are mostly due to depositional processes during seam formation. It is therefore seen that primary depositional characteristics of the coals may influence gas contents.

No vertical variation was found with respect to gas composition. It is postulated that the processes which affect gas content variation are not selective with respect to gas composition.

Lateral persistence of metre-scale vertical variations

The generalised vertical trends in gas content, gas composition and coal properties could be traced over 100s to 1000s of metres. This is consistent with coal depositional models and confirms the influence of primary depositional characteristics over some of the gas storage properties of the seam.

Mine-site scale variations

Depth and gas content

Total gas content generally increased with increasing depth. Lowest concentrations of gas were observed along the western edge of the study area adjacent to the old open cut pits. Seam depth and gas content then both increased to the east and south, with maximum values of ~360m depth and ~15m^3/t methane. Total gas content also influenced by structural features where elevated values were associated with the southern limb of a north-south/south-west orientated syncline through the centre of the study area. A pod like distribution of gas content was also associated with this syncline.

Gas composition

Gas composition generally exceeded 95% CH_4. An exception occurred around the south-eastern side of the Aquila High, where gas composition can exceed 95% CO_2. This specific structure, in turn, has relatively low gas content, possibly indicating that uplift and fracturing of the above strata have provided routes of escape. Distribution patterns of the CO_2 suggested upward migration from a deeper source.

Coal rank

Vitrinite reflectance (% R_{Vmax}) across the Oaky Creek study region ranged from 1.09–1.62%, increasing from the south-west towards the northeast. Some correlation of increasing rank and increasing gas content was observed in the east. However, in general, correlations of rank and gas content were poor, especially when influenced by structural feature such as the central syncline.

Coal composition

Vitrinite content was investigated and may be locally important, especially in the synclinal zone where samples are at similar depth in a similar structural setting. Here there are pod-like occurrences of high gas content associated with pod-like occurrences of higher vitrinite percentage. Lower gas content also more or less correlates with low vitrinite percentage.

Ash yield

Ash yield ranged from 14–20% and trend was found relating an increase in total gas content with a decrease in ash yield. This observation could result from the large size of the data set and the relatively narrow range of ash values.

Moisture content

Moisture within the coal seam can compete for adsorption sites with the CH_4, but no direct relationship was observed. Moisture ranged from 0.8–2.4% but no definitive higher moisture zones corresponded with lower gas contents.

Structural setting

Higher gas contents were observed to the east, where the seam is deepest, and in the general region of the synclinal feature through the middle of the mine site. The syncline originates from the north and appears to split into two

separate structures. The first terminates in the middle of the Oaky North southern blocks after altering its strike from North–South to North-east–South-west. The second syncline continues in a North–South orientation then deviates also to a North-east–South-west orientation when it approaches the Aquila High dome structure. The compressional event(s) that produced the observed syncline(s) and anticlines are also responsible for the production of jointing, tensile fracturing and cracking of the overlying strata.

It is hypothesised that gas is lost over the anticlines due to fracturing during deformation. Significant gas depletion of the coal seam reservoir can occur over geological time. In the case of coals occurring at shallow depths, leakage to the surface via tensile cracks associated with uplift and unloading is common. Equally, where the reservoir permeability is high, up-dip leakage along the seam could be anticipated. The association with synclines, then, is one of retention under higher reservoir pressures, potentially with tighter fractures. This compression of the strata overlying the seam in the syncline has produced a relatively impermeable barrier and, in conjunction with higher hydrostatic pressure at the base of a syncline could result in the observed increased gas content in those areas.

Relative seam saturation

The German Creek coal seam across the Oaky Creek Coal mine site was ascertained to be on average 55% undersaturated with respect to methane. Zones where undersaturation of the seam is highest are around the Aquila High, in the south-west and the central north. Relative CH_4 undersaturation around the Aquila High is explained by the high CO_2 contents in this region. Other regions of lower undersaturation corresponds with the area of the centrally located syncline and to the east —– both of which contain elevated gas contents and are generally at greater depth than the rest of the mine site.

Increased faulting generally corresponds with the zones of increased undersaturation; especially in the south-west where there are several large fault zones occur. Shearing and jointing associated with the faulting could have provided pathways for upward migration of the gas into the overlying strata. These same faults may also have provided pathways for the infiltration of meteoric waters downwards. Therefore the structural setting of the mine site, both the folding and faulting could be related to the observed relative undersaturation of the German Creek coal seam, as well as the maintained moisture content within the coal seam.

Origin of the gases

The $\ddot{a}^{13}C$ and $\ddot{a}^{18}O$ isotope values of methane and carbon dioxide were analysed to determine the origin of the coal seam gases. Results showed that the CH_4 is predominantly of biogenic origin, as indicated by its light isotopic composition (−65.9 to −80.2‰ VPDB). The CH_4 was most probably produced by way of CO_2 reduction, which in turn was formed due to the degradation of aliphatic and aromatic hydrocarbons.

The CO_2 within the seam in the southern areas was indicated to be of igneous origin as it was isotopically heavier (−4.5 and −7.6‰ VPDB) than standard coal-derived CO_2 (~ −23‰). The invasive CO_2 is probably from a mantle-derived igneous body that has had some interaction with groundwater to reduce it from the typical $\ddot{a}^{18}O$ range of +5.7±0.2‰ SMOW. The magmatic CO_2 is regarded as being inert and this is displayed by it presumably only displacing the CH_4 from its present location.

Another important outcome from the analysis is that the CO_2 present around the Aquila High is of igneous origin and has migrate up-dip from some source post biogenic methane production (i.e. after CO_2 reduction).

ACKNOWLEDGEMENTS

We would like to thank Oaky Creek Coal Pty Ltd for providing funding and time off, for Paul Bannerman, to undertake the study, as it was initially performed as part of the Honours thesis submitted by Paul Bannerman in 2004.

We would also like to thank James Cook University, who allowed us to use the University facilities, in particular those of the Coal Seam Research Institute, to perform the isotherm analyses.

REFERENCES

AHMED, M. & SMITH, J.W., 2001: Biogenic methane generation in the degradation of eastern Australian Permian coals. *Organic Geochemistry*, **32**, 809–816.

AUSTRALIAN STANDARD AS1038.3-2000: Coal and coke – analysis and testing, Part 3: Proximate analysis of higher rank coal. Standards Australia, North Sydney.

AUSTRALIAN STANDARD AS2856.2-1998: Coal petrography, Part 2: Maceral analysis. Standards Australia, North Sydney.

AUSTRALIAN STANDARD AS3986-1999: Guide to the determination of gas content of coal – Direct desorption method. Standards Australia, North Sydney.

BUSCH, A., KROOSS, B.M., GENSTERBLUM, Y., VAN BERGEN, F.& PAGNIER, H.J.M., 2003: High-pressure adsorption of methane, carbon dioxide and their mixtures on coals with a special focus on the preferential sorption behaviour. *Journal of Geochemical Exploration*, **78-79**, 671–674.

CROSDALE, P.J.& BEAMISH, B.B., 1993: Maceral effects on methane sorption by coal. *Proceedings of New Developments in Geology Symposium*, Brisbane, 95–98.

CROSDALE, P.J.& BEAMISH, B.B., 1994: Methane sorption studies at South Bulli (NSW) and Central (Qld) collieries using a high pressure microbalance. *Proceedings of the 28th Newcastle Symposium on Advances in the Study of the Sydney Basin*. The University of Newcastle, Newcastle, 118–125.

CROSDALE, P.J., BEAMISH, B.B.& VALIX, M., 1998: Coalbed methane sorption related to coal composition. *International Journal of Coal Geology*, **35**, 147–158.

FAIZ, M.M., AZIZ, A.I., HUTTON, A.C.& JONES, B.G., 1992: Porosity and gas sorption capacity of some eastern Australian coals in relation to coal rank and composition. *Symposium on Coalbed Methane Research and Development - Volume 4*. James Cook University, Townsville, 19–21 November 1992, 9–30.

FAIZ, M.M., 1996: Gaseous hydrocarbons in the southern Sydney Basin. *Proceedings of the 30th Newcastle Symposium,* "*Advances in the Study of the Sydney Basin*", The University of Newcastle, 175–182.

HOEFS, J., 1997. *Stable Isotope Geochemistry – 3rd completely revised and enlarged edition*. Berlin, New York, Springer-Verlag.

JOUBERT, J.I., GREIN, C.T.& BIENSTOCK, D., 1973: Sorption of methane on moist coal. *Fuel*, **52**, 181–185.

KIM, A.G., 1977: Estimating the methane content of bituminous coalbeds from adsorption data. USBM Reports of Investigation RI 8245.

LAMA, R.D.& BODZIONY, J., 1996: Outburst of Gas, Coal and Rock in Underground Coal Mines. Westonprint, Kiama, NSW, Australia.

LAMBERSON, M N.& BUSTIN, R M., 1993: Coalbed methane characteristics of Gates Formation coals, northern British Columbia: effect of maceral composition. *AAPG Bulletin*, **77**, 2062–2076.

LAXMINARAYANA, C.& CROSDALE, P.J., 1999: Role of coal type and rank on methane sorption characteristics of Bowen Basin, Australian coals. *International Journal of Coal Geology*, **40**, 309–325.

LEVINE, J.R., 1992: Influences of coal composition on coal seam reservoir quality: a review. *Symposium on Coalbed Methane Research and Development - Volume 1*. James Cook University, Townsville, 19–21 November 1992, i–xxviii.

LEVINE, J.R., 1993: Coalification: the evolution of coal as source rock and reservoir. *In* Law, B.E.& Rice, D.D. (Editors): *Hydrocarbons from coal*. American Association of Petroleum Geologists, AAPG Studies in Geology, No. 38, 39–77.

LEVY, J.H., DAY, S.J.& KILLINGLEY, J.S., 1997: Methane capacities of Bowen Basin coals related to coal properties. *Fuel*, **76**, 813–819.

MALLETT, C.W.& RUSSELL, N.J., 1992: The Thermal History of the Bowen-Gunnedah-Sydney Basins. *Coalbed Methane Symposium – Volume 1*. Townsville, 19–21 November 1992, 75–79.

MURRAY, C.G., FERGUSSON, C.L., FLOOD, P.G., WHITAKER, W.G.& KORSCH, R.J., 1987: Plate tectonic model for the Carboniferous evolution of the New England Fold Belt. *Australian Journal of Earth Science*, **34**, 213–236.

RICE, D.D.& CLAYPOOL, G.E., 1981: Generation, accumulation and resource potential of biogenic gas. *American Association of Petroleum Geologists Bulletin*, **65**, 5–25.

RIGHTMIRE, C.T., 1984: Coalbed methane resources. *In: Coalbed Methane Resources of the United States*. *American Association of Petroleum Geologists, AAPG Studies in Geology* **17**, 1–13.

SCOTT, A.R., 2002: Hydrogeologic factors affecting gas content distribution in coal beds. *International Journal of Coal Geology*, **50**, 363–387.

SMITH, J.W.& PALLASER, R.J., 1996: Microbial origin of Australian coalbed methane. *AAPG Bulletin*, **80**, 891–897.

STALKER, L., PRASAD, P.S.& SMITH, J.K., 2004: Stable carbon and oxygen isotope analysis of gas samples from Oaky Creek coal mine. CSIRO Petroleum Confidential Report No. 04-045.

TAYLOR, H.P., Jr., 1978: Oxygen and hydrogen isotope studies of plutonic granitic rocks. *Earth and Planetary Science Letters*, **38**, 177–210.

TOTTERDELL, J.M., BARKER, A.T., WELLS, A..& HOFFMANN, K.L., 1995: Basin phases and sequence stratigraphy of the Bowen Basin. *In* Follington, I.W., Beeston, J.W., Hamilton, L.H. (Editors): *Proceedings of the Bowen Basin Symposium 1995*. Geological Society of Australia, Coal Geology Group, Mackay, 247–256.

YALÇIN, E.& DURUCAN, S., 1991: Methane capacities of Zonguldak coals and the factors affecting methane adsorption. *Mining Science and Technology*, **13**, 215–222.

Paul Bannerman, Oaky North Mine, PO Box 1, Tieri, Qld 4709, ph. (07) 4984 7134; fax (07) 4984 7160; mailto:pbannerman@xstratacoal.com.au

Peter J. Crosdale, Energy Resources Consulting Pty Ltd, PO Box 54, Coorparoo, Qld 4151, ph. (07) 3394 3011; fax (07) 3394 3088; mailto:peter.crosdale@energyrc.com.au

Raphael Wüst, School of Earth Sciences, James Cook University, Townsville, Qld 4811, ph. (07) 4781 4627; fax (07) 4725 1501; mailto:raphael.wust@jcu.edu.au

GEOLOGY OF THE CALLIDE BASIN

GEOLOGICAL SETTING

The Callide Mine coalfield covers an area of about 18,000ha and is located within a north-west to south-east trending synclinal basin 22.5km long by 8km wide (Biggs & others, 1989). This basin is called the "Callide Basin" and the term for the coal-bearing sequence "Callide Coal Measures" was first used by Jensen (1923). In the southern half of the Callide Basin, present open-cut mining operations are located in the Dunn Creek, Trap Gully and The Hut areas which, when combined together, are called "Southern Area". Boundary Hill is located in the north-west of the basin. All mining areas are linked by, connecting roads and the operations are integrated to form Callide Mine.

PHYSIOGRAPHY AND DRAINAGE

There are marked topographical contrasts between areas of Tertiary sediments to the west of the Callide Basin, and the Mesozoic and Palaeozoic rocks to the east. Areas underlain by granitic intrusions or covered by Tertiary sediments have subdued and undulating topography (Figure 1).

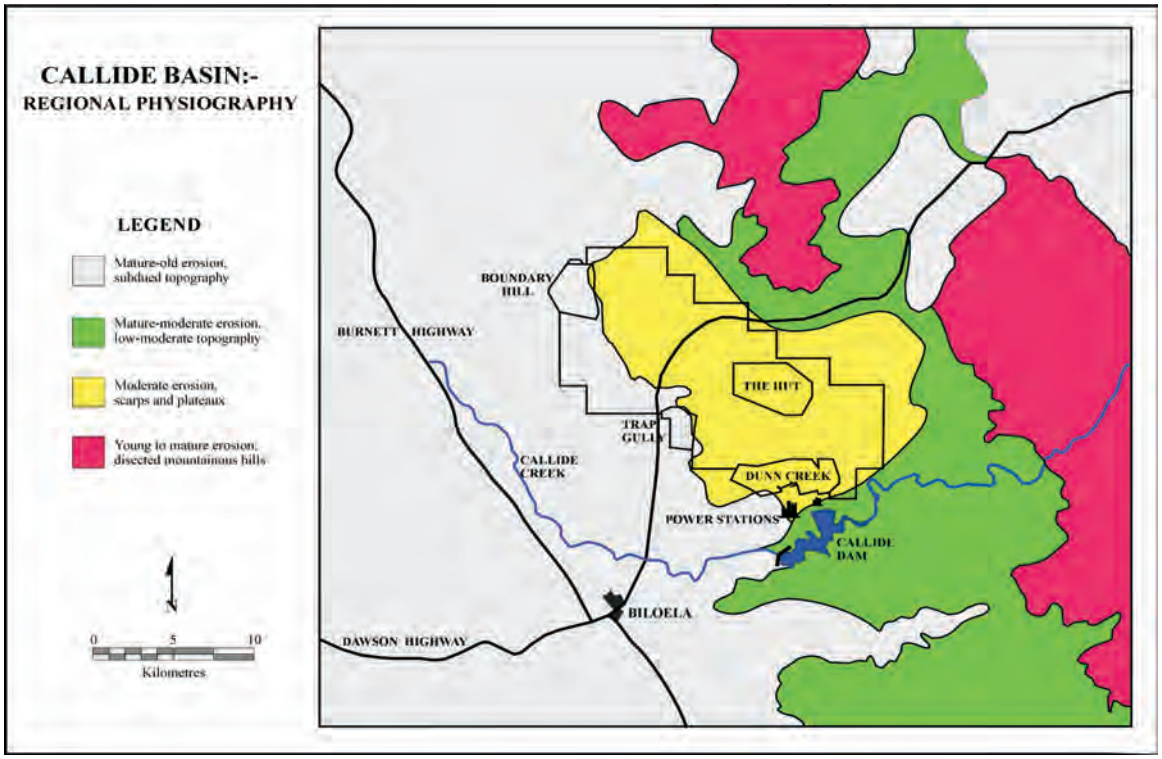

Figure 1: Regional physiography (after Biggs & others, 1989)

The subtropical climate, with high summer temperatures coupled with moderate rainfall, has prompted decomposition and subsequent deposition of surficial material cover over much of the basin. The major stream systems drain south-westerly and often scour flat-topped, low ridges of Tertiary laterite in the north-west of the basin.

Topography becomes progressively higher towards the east and is dominated by escarpments and incised plateaux up to 520m (eg. Mount Murchison, midway between Dunn Creek and Trap Gully area). Mesozoic sandstones and siltstones support sparse dendritic drainage and form prominent scarps that delineate the basin from Palaeozoic strata to the east. Beyond the eastern margin of the basin the topography within the Palaeozoic sequence varies to 700m, with strike ridges common. Well defined rugged and dissected terrain is associated with some radial drainage patterns upon intrusives of the Mount Gerard Complex, in the extreme north-west. Occasional remnants of Tertiary sheet basalts form elongate mesas of moderate relief within the basin (Biggs & others, 1989).

TRIASSIC CALLIDE COAL MEASURES

The Triassic Callide Coal Measures form a grossly fining upward megasequence with thick conglomerate sequences at the base passing upward somewhat abruptly into coal-bearing, fine-grained clastic rocks. Initial deposition of the course, clastic basal conglomerates occurred within an alluvial fan environment. Subsequently, a fluvio-lacustrine/braided-stream environment developed and the thick coal seam sequence was formed (Jorgensen, 1997).

The Callide Seam Member consists of a number of discrete seams that, when coalesced, ranges from approximately 4m up to 32m in thickness. This seam member is mined where it is close enough to the surface to be economically extracted. Currently, the coalesced thicknesses of coal being mined is 22m at Boundary Hill, 12m at Trap Gully, 10m at The Hut, and 16m at Dunn Creek. The thickest coalesced coal sequence occurs at Kilburnie (32m).

The coal seams are characterised by a high-ash top which grades into thick sub-bituminous, mainly dull, coal. Thicker, lenticular, vitrinitic pods are widely-spaced and only minor bright bands are common.

JURASSIC PRECIPICE SANDSTONE

The thick, laterally-extensive, quartzose, fluviatile, 'sheet' sandstones of the Precipice Sandstone were deposited over the Callide Coal Measures by a braided river system in the Early Jurassic. These sandstones are typically ~95% silica and were deposited *in situ* with minimal clay binding matrix.

TERTIARY SEDIMENT-ATION AND VOLCANISM

The Callide Basin sequence was tilted down to the south-west during the Tertiary, exposing and eroding the eastern margins and subsequently burying the western margins under Tertiary sediments of the Tertiary Biloela Basin. Much of the western margin has been drag-folded up and exhibits strata with dips of 55–75°. This drag folding only occurs within a narrow corridor and dips decrease to the typical 5–10° within approximately 50–100m laterally from the western margin (Figures 2 and 3). Drag folding along the margin in the south at Dunn Creek (Figure 4) is much less pronounced.

Volcanic activity, exhibited by basalt flows that blanket much of the eastern area, accompanied the tilting. Basalt dykes and stocks also intruded the Callide Coal Measures at Boundary Hill, Kilburnie and The Hut. Narrow, breccia dykes also intersect the coal seam and overlying sediments at Trap Gully. These dykes appear to have originated from Tertiary intrusive material contacting aquifers in the basal conglomerates below the coal seams and the ensuing vented steam/gas has provided the mechanism for emplacement.

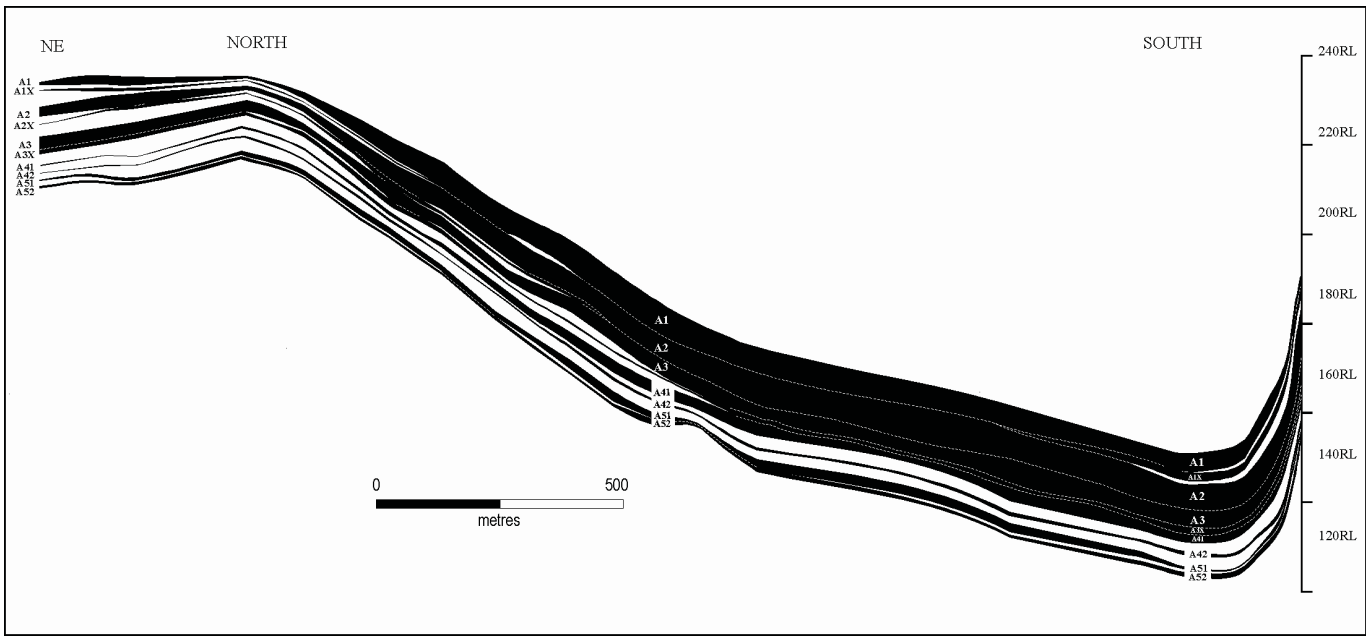

Figure 2: Schematic Seam Splitting/Coalescing and Structure at Boundary Hill Mine

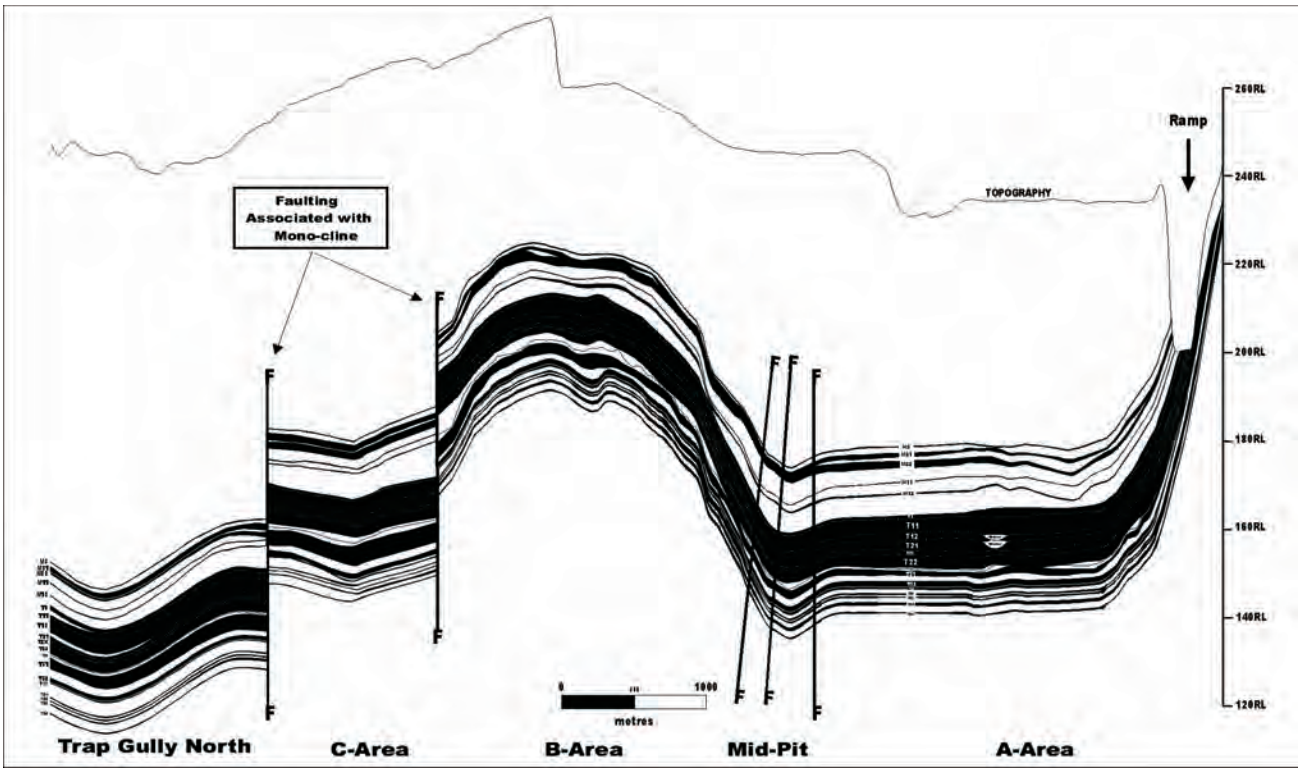

Figure 3: Schematic Seam Splitting/Coalescing and Structure at Trap Gully

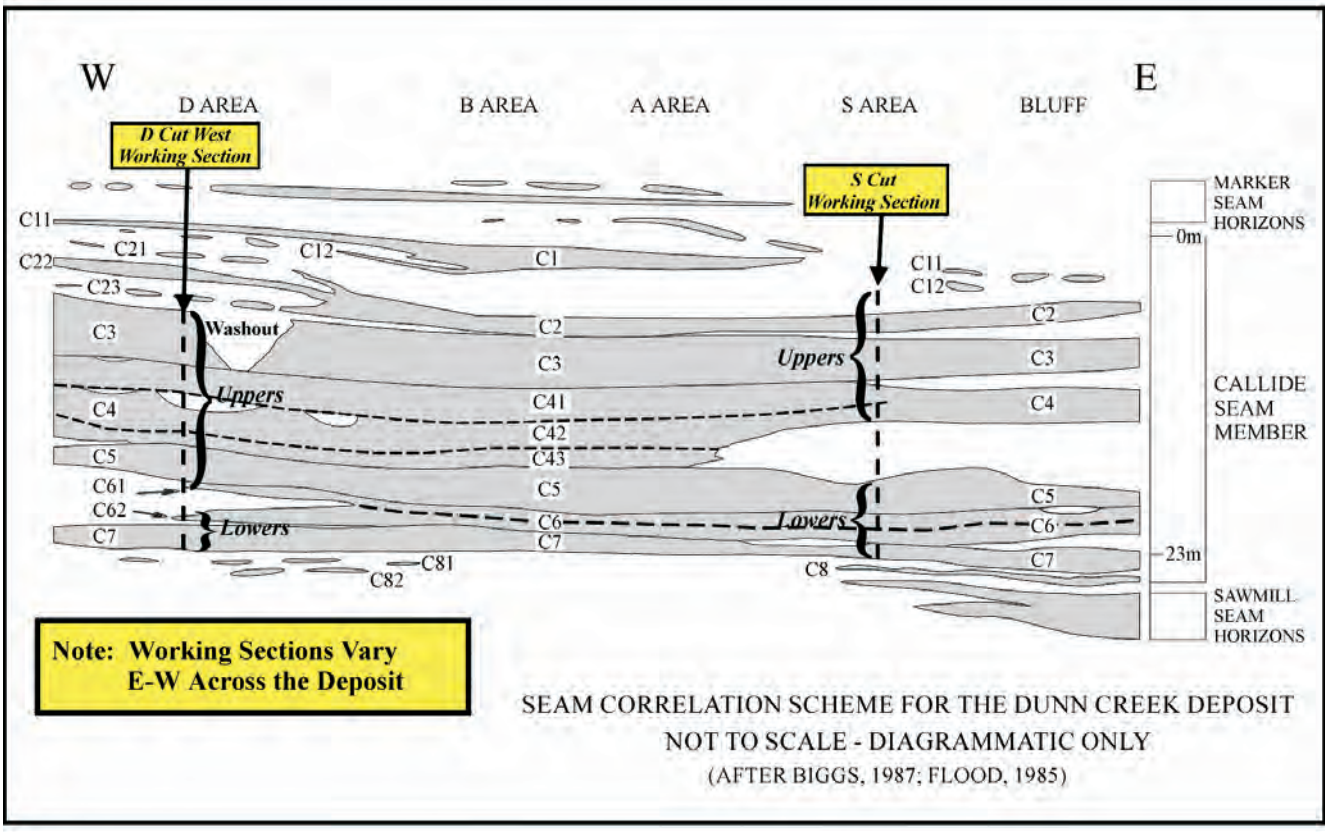

Figure 4: Schematic Seam Splitting/Coalescing at Dunn Creek

Basalts and indurated Tertiary sediments are generally not problematic for mining, although they do require different approaches in blasting and digging. The weathered basalts are beneficial in that they are a source of topsoil for rehabilitation purposes.

Considerable thicknesses (up to 150m) of clay-rich Tertiary sediments exist in the Kilburnie area and these will need careful consideration in any mining process applied there.

QUATERNARY EROSION AND SEDIMENTATION

The geomorphology of the Precipice Sandstone terrain has precluded thick soil development. Only skeletal, sandy soils (up to 10cm thick) are found on most of the dissected plateau of this terrain.

Pebble-boulder conglomerates and sands form the alluvium within creek and gully beds. Deep weathering of basalt flows has formed the gilgai black, cracking-clay soils within some areas of the Callide Basin and within most of the Biloela Basin to the west (Biggs & others, 1989).

Figure 5 shows the typical stratigraphic column for the Mesozoic sediments of the Callide Basin. Figure 6 shows typical a) north-west to south-east, and b) west to east cross-sections through the Callide Basin. Figure 7 shows the regional tectonic setting of the Callide Basin and its relationship to other surrounding geological elements.

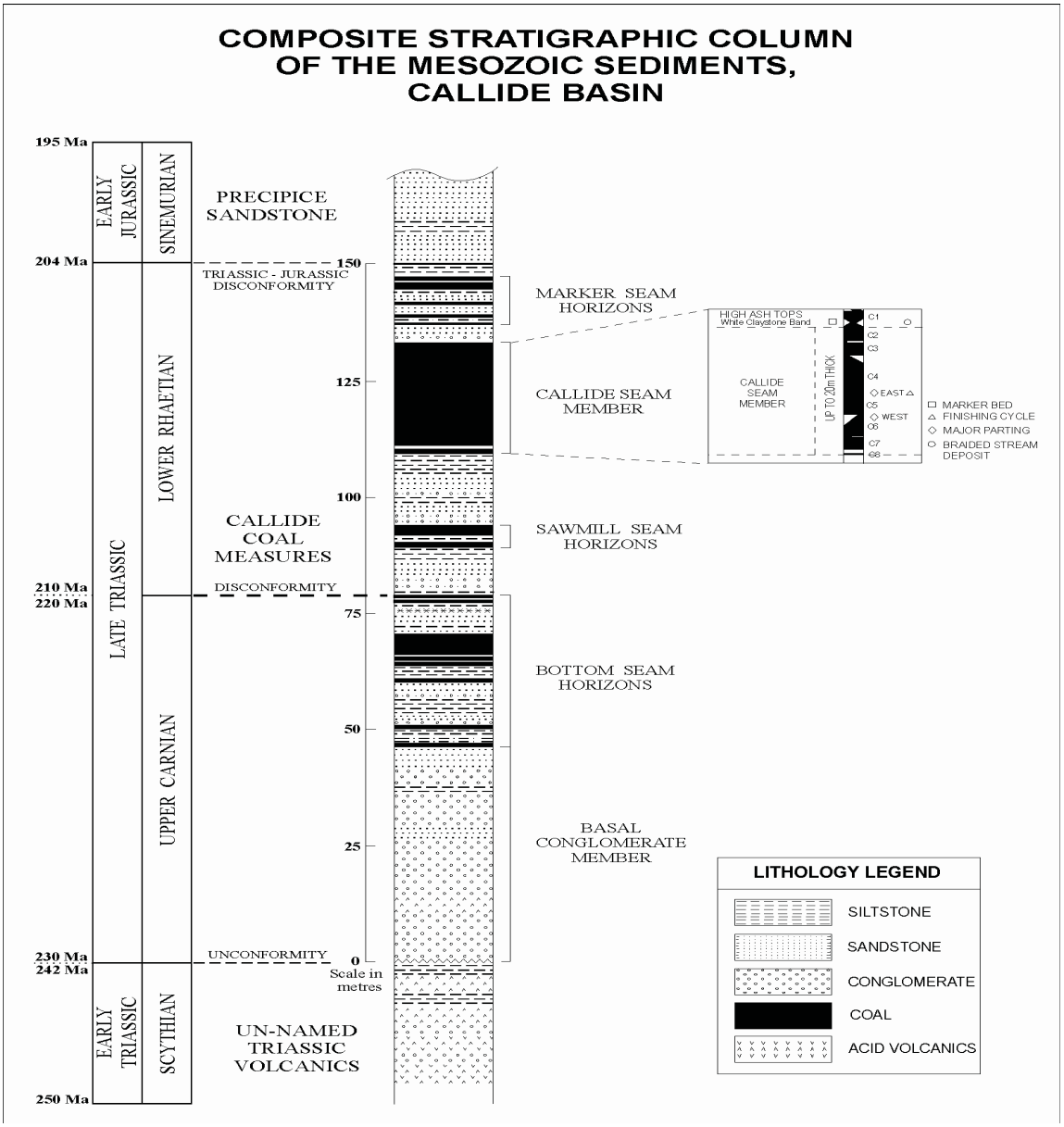

Figure 5: Stratigraphic Column

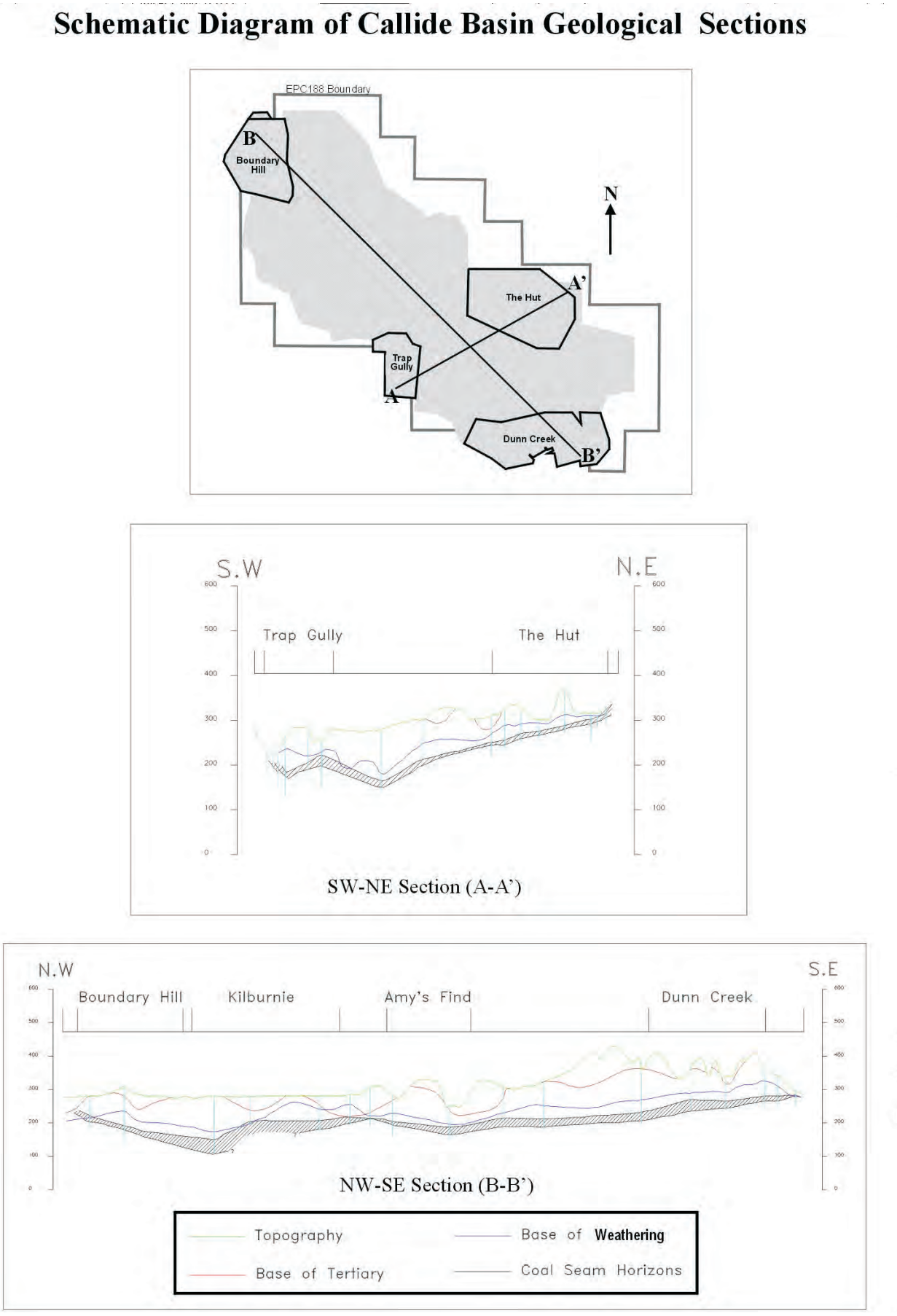

Figure 6: Cross Sections of the Callide Basin

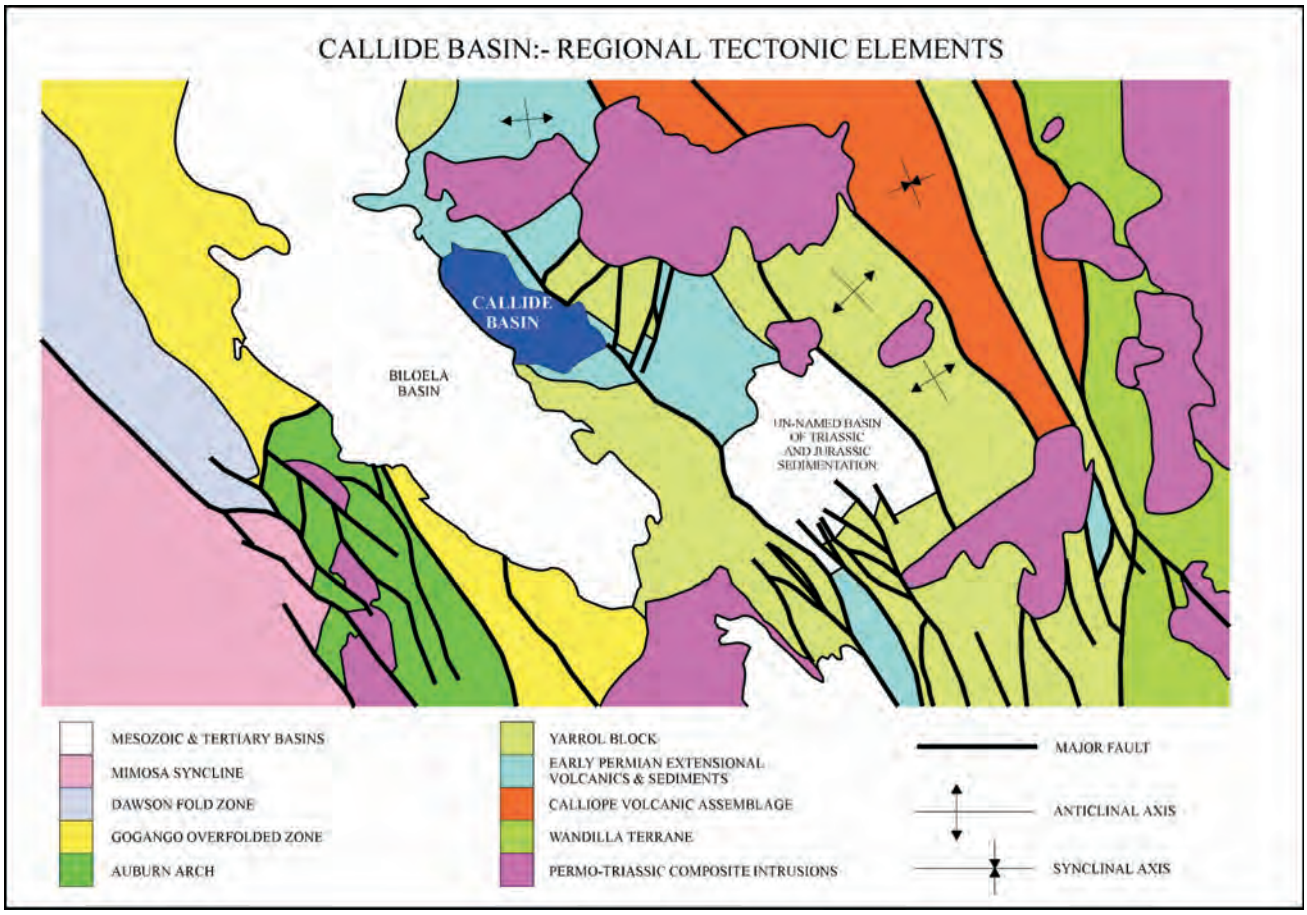

Figure 7: Callide Basin Regional Tectonic Elements

COAL SUBCROP (LOXLINE)

The coal seam comes close to the surface at many locations along the Callide Basin margin. In these locations, the coal oxidises to clays down to the base of weathering and, then, fresh coal occurs below this boundary. The limit-of-oxidation line (loxline) is that line which marks the boundary between fresh coal and oxidised coal on the deposit margins. Because of the resistivity contrast that exists between fresh and oxidised coal, the loxline has been an excellent target for the TSIM VLF-EM technique (Nichols, 1996).

In subcrop areas, differential weathering of the coal seams produces an undulating profile. Unweathered, competent coal can be replaced by weathered, sooty, clayey coal within a very short lateral distance. Following top of coal clean-up, (i.e. after the weathered material has been removed), the upper surface often resembles a moonscape.

FAULTS

Both normal and reverse faulting occurs within the Callide Basin. Normal faulting tends to be high angle (>45°, typically 60–75°) whereas reverse faulting tends to be low angle (<45°, typically 30°). Vertical displacements on faults within the mine areas very from approximately 0.3m up to 20m.

The shear zone along the fault planes in the overburden tends to be very narrow and is usually exhibited by a clean, sharp break (Figure 8). Crush zones in coal can be either narrow or wide.

In many cases, post-depositional faulting is accommodated in the coal seam which seems to have ‘absorbed’ the vertical displacement. Consequently, the vertical displacement at the top of the main seam may be quite obvious. The fault angle can change within the thick coal seams (even becoming horizontal in some cases and sliding along the top of the coal seam), leaving no evidence of vertical displacement at the base of the seam.

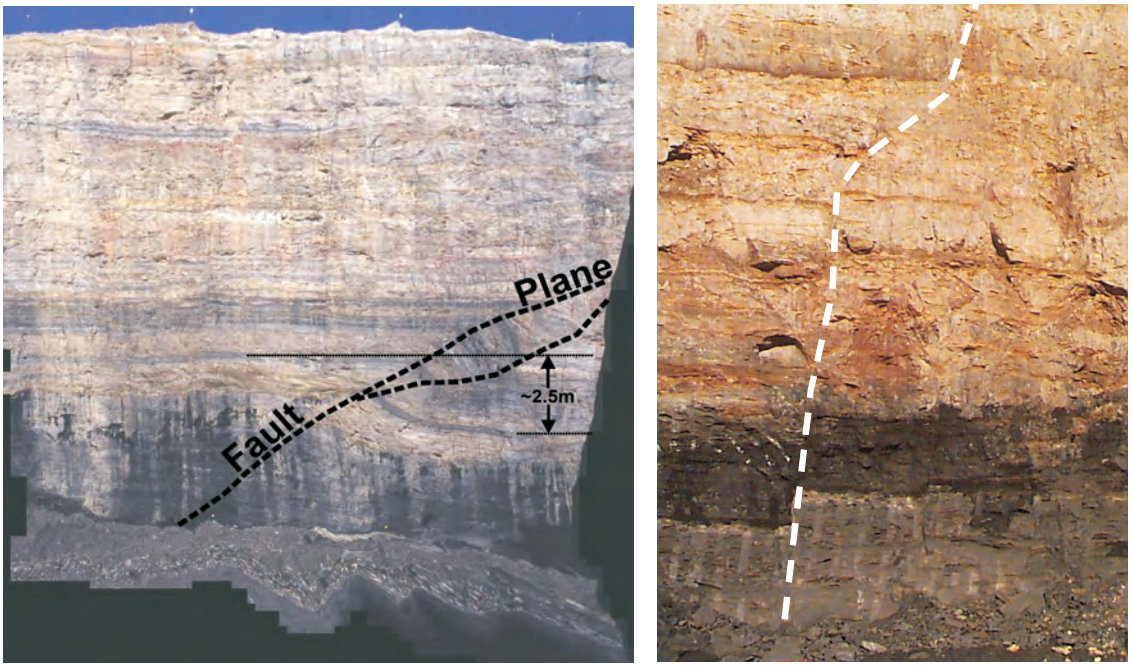

Figure 8: Trap Gully Thrust Fault (left) and Boundary Hill Normal Fault (right)

Voids in the shear zones can be either air or water filled. Where they are air-filled, the shear zone becomes more resistive than the surrounding rock. Conversely, where the voids are water-filled, the shear zone becomes less resistive than the surrounding rock. In either case, the shear zone offers a reasonable target for resistivity and electromagnetic geophysical techniques.

TERTIARY BASALT-DOLERITE INTRUSIVES

Tertiary intrusions (mainly basalt/dolerite) cut vertically across the coal seams and, in many cases, have flowed out onto the palaeosurface or down palaeogullies. Most of these surface flows have been deeply weathered to red clay and soil. The central dykes and stocks that have been encountered so far have consisted of fresh basaltic/doleritic material.

Consequently, because of the basalt's magnetite content and conductivity, these dykes and stocks are excellent targets for magnetic and EM geophysical techniques.

Several large stocks are known to exist within existing and proposed mining areas. Plugs have been encountered in-pit and mined through at Boundary Hill. Boundary Hill itself was a doleritic/basaltic stock cylindrical in form and approximately 100m in diameter. Additionally, a large (130m wide x 150m long) in-pit stock was mined past in Strip 6 at Boundary Hill. Sub-vertical stringer dykes that cut across Triassic and Jurassic sediments are up to 0.3m wide and emanate in a north-west direction from these intrusions. In general, there is only a narrow (~1–2m) coked zone around these intrusives but they do cause elevated pyrite content which, in turn, has caused up to 4.9% sulphur in product coal.

At Kilburnie, a large plug (approximately 400m x 200m) is known to exist from ground-borne and airborne geophysics (Figure 9). Drilling into this plug encountered clay/weathered basalt for 25m and then solid, fresh basalt down to 164m where the rock became too hard to drill. Sill-like intrusives with elevated pyrite content were encountered in the coal seam in a hole to the south of this large plug.

At The Hut, two plugs that were detected in airborne geophysics (Figure 9) have been verified by ground-borne geophysical surveys (Nichols & Wilson, 2000). The Hut Crater plug is 360m in diameter and intrudes the coal bearing horizons down dip of the mining pits. Another plug (300m x 150m) sits off the end of the current Eastern Hillside pit area and outside The Hut mine lease boundary. Some sill intrusives have been intersected in boreholes to the north-west of the mined-out Northern Valley pits.

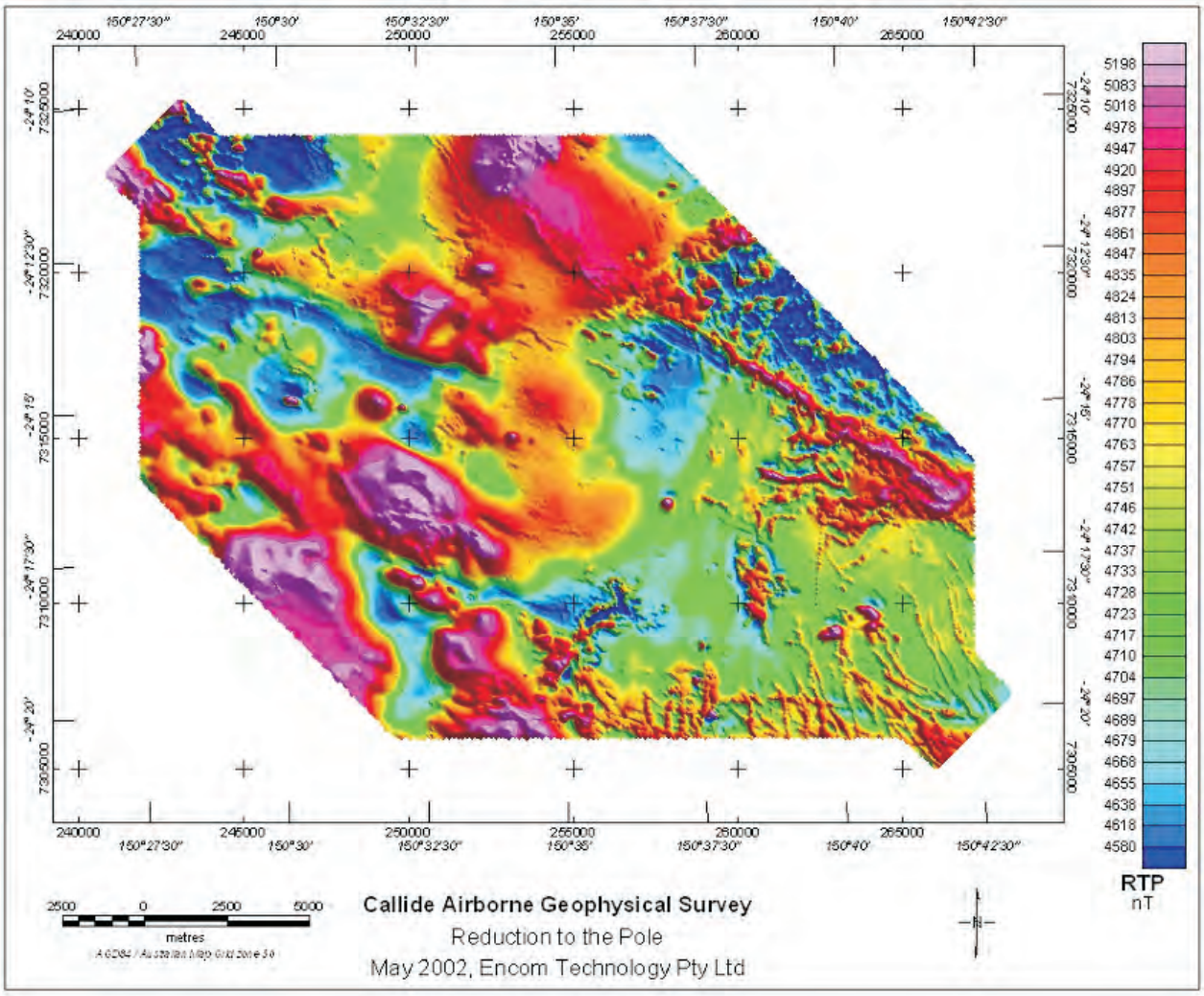

Figure 9: Callide Basin Regional Airborne Geophysics (TMI RTP)

BRECCIA DYKES

Breccia dykes (Figure 10) have been encountered in Trap Gully B Area and the Trap Gully A Area ramp.

The dykes have been mainly composed of soft, highly weathered, kaolinitic material. Amongst the remnant brecciated angular clasts are some remnant rounded clasts that appear to have originated from basal conglomerates.

The dykes are post-depositional (probably Tertiary) and appear to have originated from intrusive material (basalt/dolerite) punching up through the lower basement conglomerates (Devonian Kroombit beds) below the Callide Coal Measures. These intrusions have probably contacted an aquifer below the Callide Coal Measures and the ensuing vented steam/gas has provided the explosive, fluid mechanism for pneumatolytic/hydrothermal dyke emplacement.

Because the dykes are thin (<1m thick) and localised, they do not form a target for normal exploration drilling and have not been detected by this method in the past. Also, it is unlikely that they would present a signature that could be readily detected by ground-borne geophysical methods.

SEAM WORKING SECTION ROOF/FLOOR

The immediate roof of the main coal working section is comprised of fine-grained, carbonaceous siltstones of the Callide Coal Measures. These siltstones are commonly massive and vary in strength (ranging from 5–60MPa). Apart from in weathered subcrop areas, they are competent and do not pose problems for mining or highwall stability.

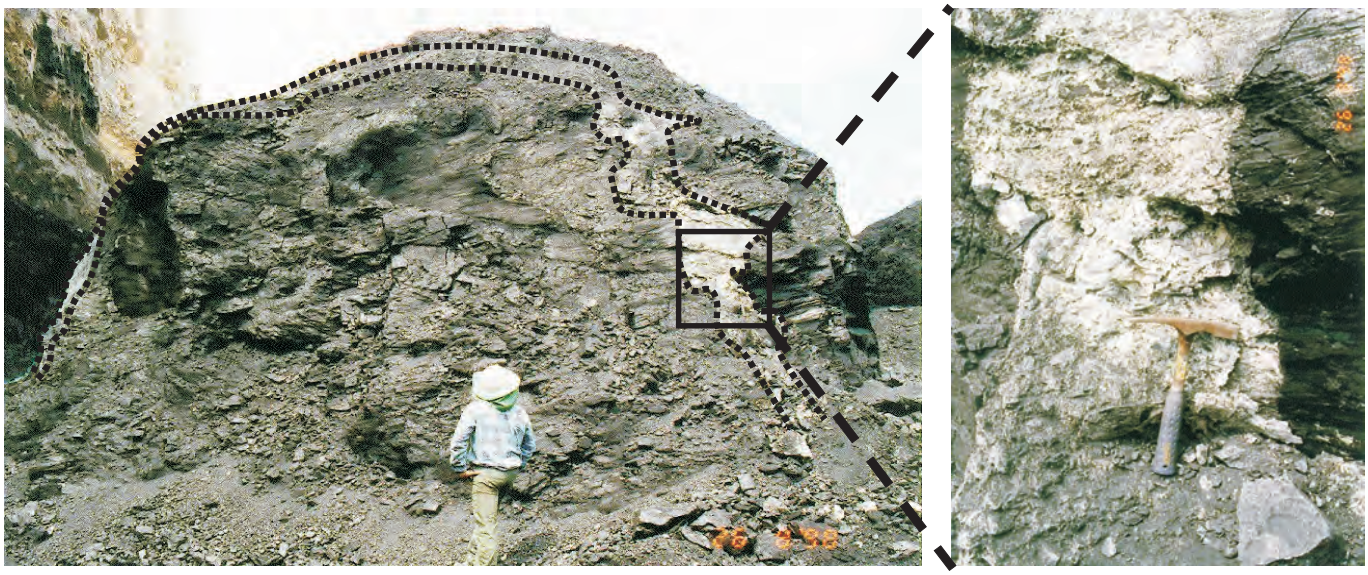

Figure 10: Trap Gully A Ramp — Breccia Dyke

The floor of the main working section consists of similar rock types to the roof. In several areas (especially where it is saturated), the higher clay content in bands within the first 10m below the floor poses problems for low-wall stability. In these areas, the floor is usually blasted to provide a frictional base to prevent low-wall failure into the pit.

OVERBURDEN/ INTERBURDEN

Primarily, the overburden sequence consists of the quartzose Precipice Sandstone (previously described) and the upper argillaceous and arenaceous sediments of the Callide Coal Measures. In most areas, there are vertical sections of varying thickness within the Precipice Sandstone where the binding matrix has since been eroded and sequences of loose, unconsolidated 'sugar sands' have formed. The sand grains within these 'sugar sands' are commonly held together only by quartz overgrowths. The 'sugar sands' are consolidated enough to prevent free-digging by excavator, yet pieces can be readily broken off by hand.

Upon exposure, these unconsolidated sands erode readily to masses of pure white sand. They are problematic in blasting and absorb a proportion of the blast energy. This impedes rock fragmentation.

Interburden consists of the argillaceous/carbonaceous siltstones of the Callide Coal Measures. These siltstones are usually very competent and are not problematic in mining.

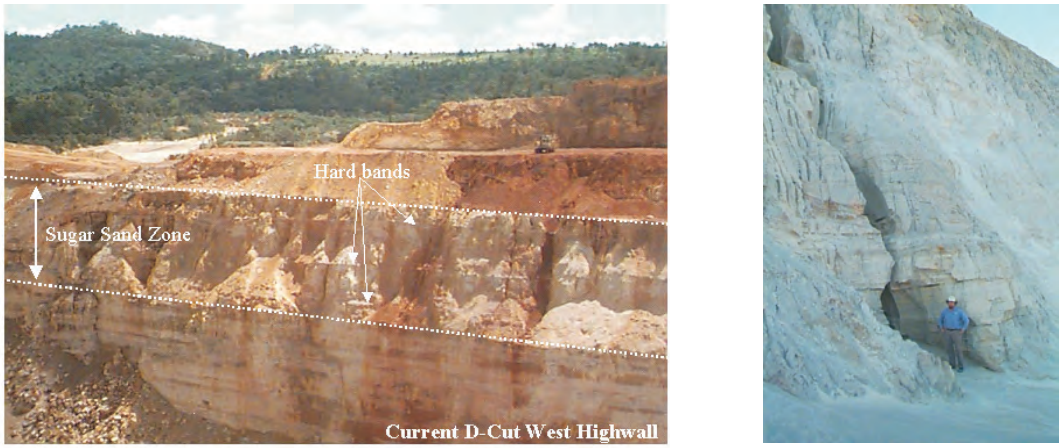

Figure 11: Unconsolidated 'sugar sands' in the Precipice Sandstone

As mentioned previously in this section, the more problematic horizons exist in the underburden.

AQUIFERS

The major aquifer horizons exist in the extremely porous Precipice Sandstone. At Dunn Creek and The Hut, in-pit flows are minimal ranging up to 8 000L/hr. Flows at Boundary Hill and Trap Gully are more problematic being around 23 000–30 000L/hr at both sites.

The highest volume flows within the Callide Basin occur at Kilburnie. In the northern Kilburnie area, flows range between 500–28 000L/hr with flows tending to increase from north-west to the south and south-east. In the southern Kilburnie area, water flows greater than 67 000L/hr have been encountered and artesian flows have occurred from 2 exploration boreholes.

Contribution of water flows from the Tertiary horizons and Callide Coal Measures is minimal.

Water quality tests show that the water conductivity ranges between 700–5000 micro-siemens per centimetre (averaging around 1200 micro-siemens per centimetre). In general, it is not potable or suitable for irrigation, but it is suitable for watering stock.

COAL QUALITY

Callide produces a sub-bituminous, very sub-hydrous, low rank, steaming coal with good combustion properties, primarily for domestic power generation. Raw steaming coal is supplied to five separate customers, CS Energy Callide B Power Station and CPM Callide C Power Station (adjacent to the mine site); Queensland Alumina (QAL), Comalco Alumina Refinery (CAR) and Gladstone (GPS) Power Station (these latter three customers

Table 1: Callide Mine typical coal quality parameters

	Boundary Hill	Callide
Proximate Analysis (%ad)		
Moisture	11.0	8.5
Ash	14.9	18.3
Volatile Matter	24.8	24.2
Fixed Carbon	49.5	49.2
Total Moisture (%)	19.0	15.5
Equilibrium Moisture (%)	15.0	11.5
Calorific Value (MJ/kg ad)	21.92	22.00
Ultimate Analysis (%ad)		
Carbon	74.16	77.68
Hydrogen	3.15	4.03
Nitrogen	1.07	1.08
Sulphur	0.38	0.24
Oxygen	20.66	16.74
Total	99.42	99.77
Sulphur (%ad)		
Pyritic	0.20	0.12
Sulphate	0.02	0.06
Organic	0.07	0.06
Total	0.29	0.24
Relative Density (ad)	1.50	1.55

Table 1 (continued)

	Boundary Hill	Callide
Hardgrove Grindability	89	85
Abrasion Index (mg/kg)	3	7
Ash Fusion Temperature (Reducing Atmosphere)		
Deformation	1320	1330
Spherical	1440	1460
Hemispherical	1460	1490
Flow	1510	1530
Petrographic Analysis (% by volume)		
Vitrinite	30.9	23.7
Liptinite	3.8	1.1
Inertinite	55.5	68.4
Mineral Matter	9.8	6.8
Total	100	100
Mean maximum vitrinite reflectance ($R_v$max)	0.54	0.52
Ash Analysis (%)		
SiO_2	38.44	47.32
Al_2O_3	33.13	30.99
Fe_2O_3	15.67	14.95
TiO_2	1.99	1.80
Mn_3O_4	0.44	0.29
CaO	3.52	1.53
MgO	1.99	1.07
Na_2O	0.34	0.16
K_2O	0.15	0.13
P_2O_5	0.86	0.14
SO_3	2.66	0.93
BaO	0.35	0.04
Loss On Ignition	0.46	1.81
Total	100	100
Minor Constituents (db)		
Phosphorus (%)	0.012	0.020
Chlorine (%)	0.015	0.010
Fluorine (mg/kg)	0.099	
Arsenic (mg/g)	2.550	0.800
Boron (mg/kg)	17.040	
Cadmium (mg/kg)	0.110	
Mercury (mg/kg)	0.017	
Caking & Coking Properties		
Crucible Swell Number	0	0

are in Gladstone). In addition to the domestic supplies, Callide coal has been exported as a blend product to power utilities in Asia.

In general, seam splitting is increasing and quality deteriorates down-dip. The coal has variable total moisture, raw ash, ash fusion properties and iron oxide in ash values. There is a general rank increase from north to south across the basin. Higher total moisture values at Boundary Hill/Kilburnie are offset by lower ash values. Conversely lower total moisture values are offset by higher ash content in the south at Dunn Creek.

Callide product coal can be characterised as follows:

- medium ash, sub-bituminous, Ro (max) = 0.52
- anomalously low vm (daf) for carbon and vitrinite content (34%, 77%, 30%)
- sub-hydrous, non-caking
- anomalously high hgi (85–90) for rank
- high oxygen in coal matter
- coal ash low in silica and variable in iron (Biggs, 1996)
- high carbon char reactivity.

General coal quality parameters are shown in Table 1.

REFERENCES

BIGGS, M.S., BROADLEY,, R., CRAWFORD, E. & CARR, G., 1989: Summary of the Geology and Mining Operations of the Dunn Creek, Trap Gully and Hut Deposits, Callide Coal Measures Basin, Central Queensland. Callide Coalfields report.

BIGGS, M.S., BROADLEY, R., CRAWFORD, E. & SCOTT, M., 1989: Summary of the Geology and Mining Operation of the Boundary Hill Mine, Callide Coal Measures Basin, Central Queensland. Callide Coalfields report.

BIGGS, M.S., 1996: The Distribution and Significance of Iron Minerals in the Callide Coal Measures, East Central Queensland. MSc (App) Thesis, Queensland University of Technology (School of Geology) Brisbane.

JENSEN, H.I., 1923: Some Notes on the Permo-Carboniferous and Overlying Systems in Central Queensland. *In: Proceedings of the Linnean Society of New South Wales*, **48**, 154–158.

JORGENSEN, P.J., 1997: An Integrated Analysis of the Callide Basin, East-Central Queensland. PhD Thesis, The University of Queensland (Department of Earth Sciences) Brisbane.

NICHOLS, W.J.F., 1995: Location of Coal Subcrop at Callide Coalfields Using the TSIM Geophysical Method. *In* Follington, I., Beeston, J.W. & Hamilton, L., (Editors): *Bowen Basin Symposium 1995*, Geological Society of Australia Inc. Coal Geology Group and the Bowen Basin Geologists Group 1995, 257–263.

NICHOLS, W.J.F., 2001: Surface and Borehole Geophysical Analysis of Structures Within the Callide Basin, Eastern Central Queensland. MSc (App) Thesis, Central Queensland University (James Goldston Faculty of Engineering and Physical Systems).

NICHOLS, W.J.F. &WILSON, G.A., 2000: Applications of Multiple Geophysical Techniques for the Identification of a Suspected Intrusion at Callide Coalfields. *In* Beeston, J.W. (Editor): *Bowen Basin Symposium 2000 - The New Millenium - Geology*, Geological Society of Australia Inc. Coal Geology Group and the Bowen Basin Geologists Group, Rockhampton, October 2000, 335–342.

CODRILLA DEPOSIT

LOCATION AND TENEMENT DETAILS

The Codrilla Deposit is located in the Late Permian Rangal Coal Measures which occur in the eastern half of EPC 676 held by Moorvale Coal Pty Ltd. It is situated wholly on freehold land situated astride the Fitzroy Developmental Road approximately 25km south of its junction with the Peak Downs Highway in Central Queensland, and less than 30km from the Peak Downs rail line. The company's Moorvale Mine is 25km to the north-west (Figure 1). Either way, rail distance to the Dalrymple Bay Coal Terminal is of the order of 140–150kms.

EXPLORATION HISTORY

Prior to the grant of EPC 676, only sporadic exploration had been undertaken. The earliest reported company exploration was a reconnaissance survey of the Isaacs River region by Consolidated Zinc (Whitcher, 1960 CR1153). Published quarter million scale mapping of the day (Olgers, 1969; Malone, 1970) showed Triassic and undifferentiated Permian outcropping amidst widespread Cainozoic cover to the south east of the Daunia region. Coal exploration drilling was conducted by the Utah Development Corporation (UDCL) as part of AP 6C in the 1960s and 1970s. Holes to the north of Mt Coxendean bottomed in the Rewan Formation (CRs 3118, 4797, 5094) and cross-sections in CR3118 depict undeformed seams of the Rangal Coal Measures dipping east beneath Rewan Formation at the eastern ends of drill lines. Departmental hole Killarney NS 5 was spudded in Rewan Formation to the east of Iffley HS in the far south of EPC 676 in 1979–1980 and intersected coal seams from 811m, bottoming in a 34m thick coked coal seam at 916.52m (Matheson, 1990). Shallow anthracitic coals were intersected in a scout hole by Bellambi Coal in 1968 on Old Bombandy station (CR 2644). In the late 1980s, White Industries Ltd explored the arcuate outcrop of Moranbah, Fort Cooper and Rangal Coal Measures around the domed Bundarra Intrusive Complex south of the Peak Downs Highway as part of ATP's 436C & 445C (CRs 20858, 21262, 22350). WIL's focus was the anthracitic coals of the extremely deformed and intruded Moranbah Coal Measures, and drill traverses rarely extended upsection into the Rangal Coal Measures.

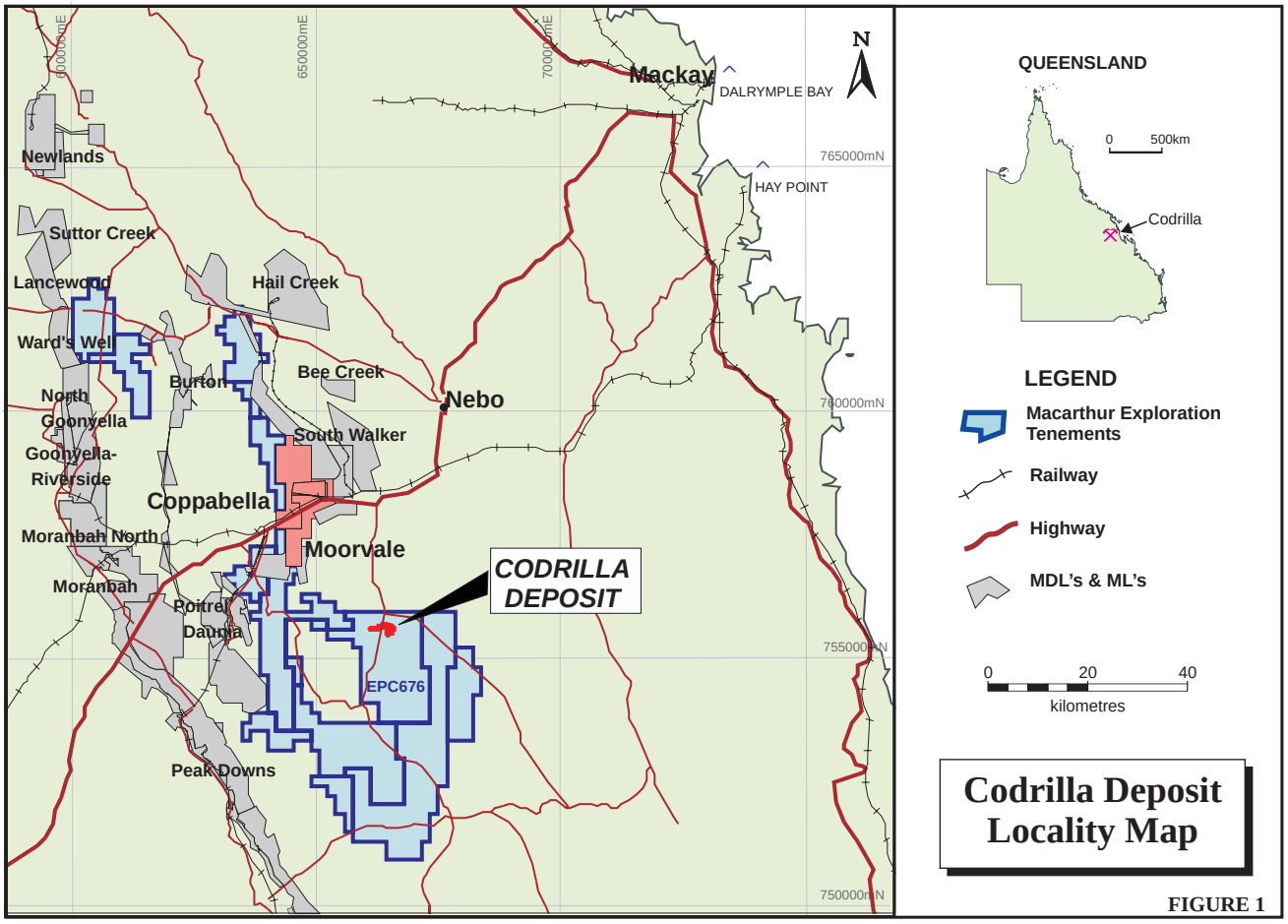

FIGURE 1

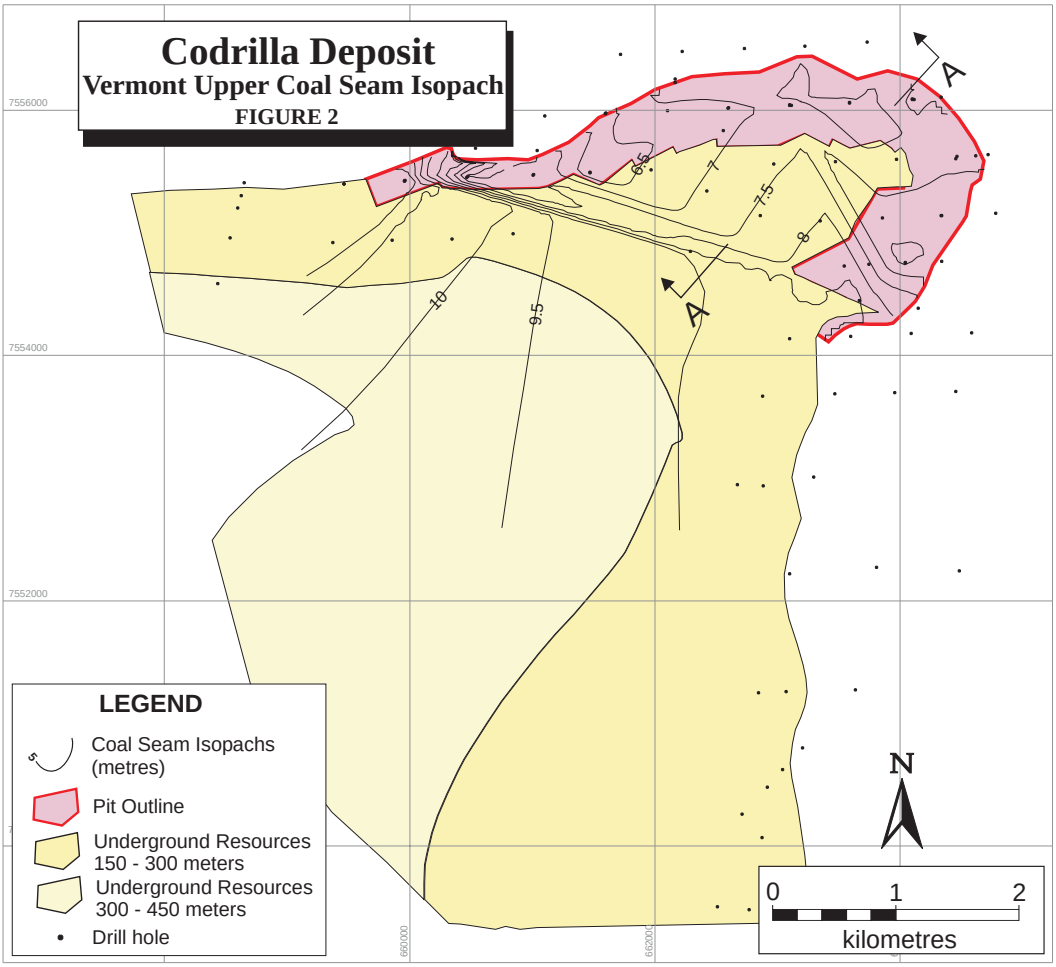

During the late 1980s, the Department compiled the 1:500 000 Bowen Basin map (Queensland Government Printer, 1988), including UDCL, TDM and WIL data but depicting the Rangal Coal Measures as faulted out against a large regional thrust in the region of EPC 676.

By 1996, Lance Grimstone & Associates Pty Ltd had compiled enough evidence to support the theory that a large synclinal feature existed to the south of the Bundara intrusive complex, and the region was one of a number of targets recommended to Macarthur Coal Pty Ltd in 1997–1998. The prospectivity of EPC 676 was enhanced when exploration drilling on neighbouring EPC 649 established the western margin of the syncline beneath Mt Coxendean. Photomapped trends of bedding from the projected outcrop zones along the eastern flank of the proposed syncline were used to define initial areas for investigation. Targeted Mini-SOSIE seismic surveys commenced on EPC 676 in July, 1998 and provided immediate proof of the existence of the major syncline. Drilling and geophysical signatures were used to correlate the principal, flat lying, seismic reflectors with Leichhardt and Vermont Seams of the Rangal Coal Measures being explored on EPC 649 further west.

Follow-up drilling targeted the projected crop of these two seams where they reached commercial thickness on Codrilla Station in the northeast of EPC 676. Detailed core drilling and testing was conducted on a 500m grid spacing designed to provide sufficient data for geological modelling and the definition of Measured open cut resources. To date, some 11576.67m of drilling has been completed in 70 holes including 192.08m of 100mm core and 70.68m of 63mm core, the larger core size adopted to maximise core recovery. Drill hole locations are shown in Figure 2. Holes with coal intersections were geophysically logged and used as pilot holes for subsequent core holes.

GEOLOGY

The Codrilla Deposit occurs on the eastern flank of this large regional synclinal feature (informally named the Coxendean Sub-basin) at the point where its northward extend has been disrupted by doming caused by intrusions related to the Bundara Intrusive Complex. The coal seams are cupped into a gentle syncline dipping southwest, forming a U-shaped

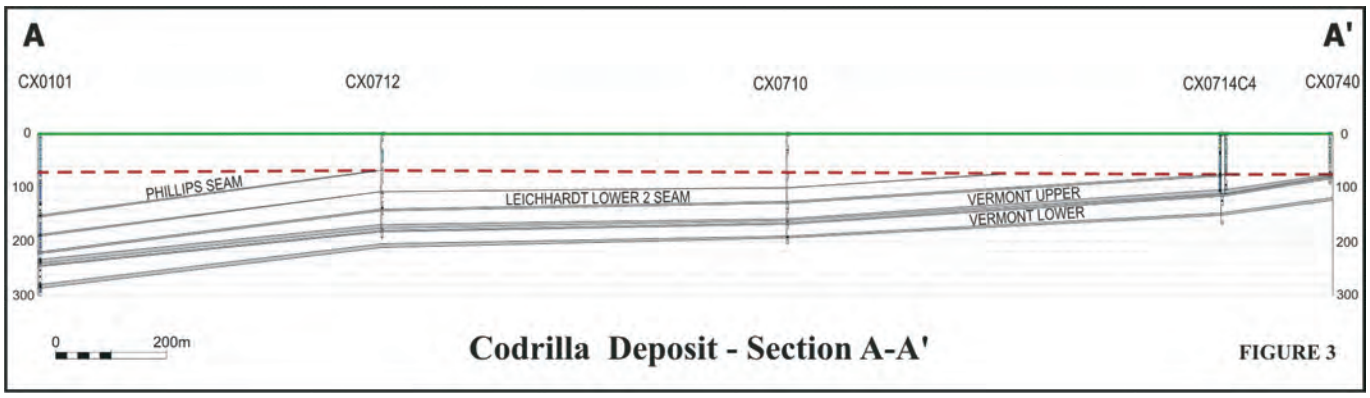

crop zone and a compact deposit. Up to four Permo-Triassic units have been intersected during drilling at Codrilla (Figure 3).

The **Moranbah Coal Measures (MCM)** consists of labile sandstone, siltstone, mudstone and coal seams. Although extensively mined on the western margin of the Bowen Basin, the unit is as yet unworked on the eastern flank of the Bowen Basin where its thickness is thought to be of the order of 400–450m. Numerous thin bright coal seams with apparent thickness ranging from 0.18–2.15m have been intersected in holes to the east of the Codrilla deposit. These seams are believed to lie within the MCM, although seam stratigraphy is still uncertain as both the MCM and overlying **Fort Cooper Coal Measures (FCCM)** are highly deformed and intruded with local dips up to 70° from verticality logs. The FCCM are estimated to be approximately 350m to 400m thick in the region to the east of Codrilla. The formation consists of labile sandstones and siltstones, and thick seams of interbedded coal, carbonaceous mudstone and tuffaceous claystone. Coal seams typically contain high percentages of inherent ash and have no export potential. The best developed seam is the Girrah Seam, which can be up to 25m thick of interbanded coal, tuffs and carbonaceous mudstone, with the stone bands >50% of the seam. The Vermont Lower Seam (VL) ranges from 1.0–5.4m thick, generally heavily banded with dirt, and in places, splitting into the Vermont Lower 1 (VL1) and Vermont Lower 2 (VL2).

The **Yarrabee Tuff Bed (YTB)** is regarded as the top of the FCCM (Matheson, 1990). At Codrilla, it comprises up to 1m of brown, tuffaceous claystone within the Vermont Seam and characterised by its high natural gamma response. The overlying **Rangal Coal Measures (RCM)** comprise 140–195m of light grey, lithic sandstones (commonly siderite cemented) interbanded with layers of siltstone, mudstone, minor carbonaceous shale and low to moderate ash coal seams. Two coal seams reach economic thickness at Codrilla. The Vermont Upper Seam (VU) is a clean, bright, unbanded seam which averages 7.5m within the Deposit (Figure 4). The Leichhardt Lower 2 Seam (LL2) ply averages 1.75m comprises of interbanded dull and bright coal with no significant stone bands. Other minor splits of the Leichhardt Seam occur intermittently, ranging in thickness to 1.4m of dull, but generally clean coal.

The **Rewan Group**, which conformably overlies the RCM, comprises distinctive greenish-grey labile sandstones and siltstones, and mottled red and green mudstones, but no coal. The unit is at least 730m thick in Killarney NS5 and devoid of coal. The boundary with the underlying RCM is taken at the top of the uppermost carbonaceous bed, or at the colour change from the greenish-grey sediments of the Rewan Group, to the grey sandstones and siltstones of the RCM.

The Permo-Triassic sediments are unconformably overlain by a thin veneer of **unconsolidated Tertiary and Quaternary sediments** comprising mainly clays, fine to coarse-grained sands and gravel, and which can cause borehole instability problems. Strongly lithified silcrete and ferricrete layers mark buried paleo-landsurfaces. Some of the clays are highly slaking. **Deep weathering** of the Rewan Group in particular, has been mistaken as Tertiary in earlier drilling.

Coal Ply Stratigraphy of the Leichhardt Lower 2 and Vermont Upper Seams at Codrilla

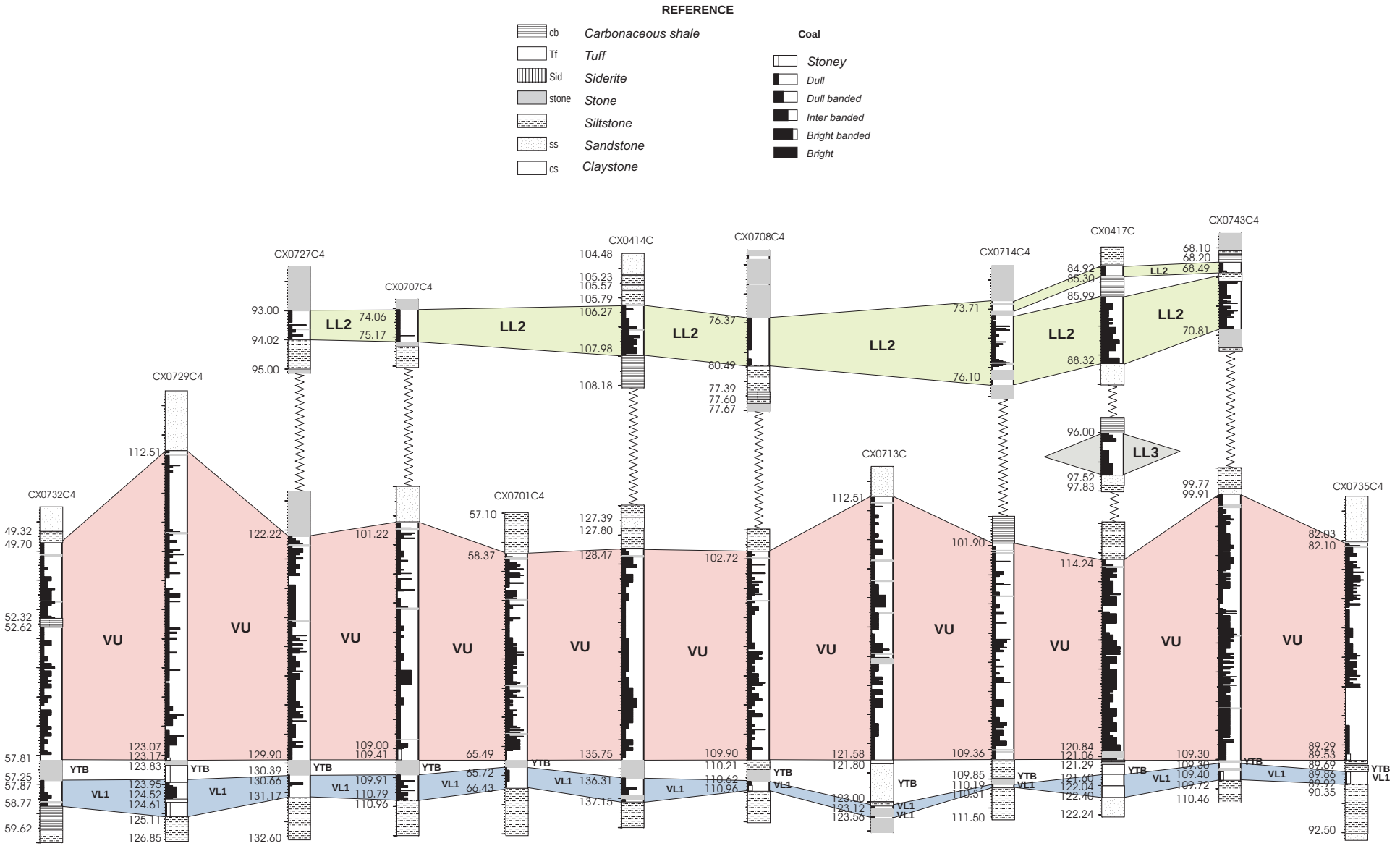

FIGURE 4

No intrusions have been intersected in the targeted seams within the Codrilla Deposit. However, igneous bodies form major topographic highs to the north and some dykes can be expected, as has been the case at Coppabella.

COAL QUALITY

The coal quality of the compact U-shaped Codrilla Deposit has been established by some 18 slimcores (100mm) completed on a 500m grid across the likely mine area. Line of oxidation (LOX) drilling and large core drilling for preparation plant design have not yet been undertaken. Slimcores were sampled on a ply x ply basis and tested at ACIRL for raw coal properties. Ply samples were combined into appropriate working section samples for subsequent washability analysis and clean coal testing of selected washed coal fractions for their PC1 or thermal properties.

The Codrilla Deposit is well suited to preparation of a low sulphur PCI product in the ash range 8.5% to 10% (ad), similar to that produced at Coppabella and South Walker Creek. The high rank will be attractive to many PCI users, and the high specific energy is favourable for coke replacement ratio. An export quality thermal coal 13% – 14% ash (ad) can also be produced, although blending with higher volatile coals would be required for certain power stations and cement industry applications. Product specifications are yet to be finalised, but typical air dried product quality of the principal seams is tabulated below:

	8.5% PCI		**10% PCI**		**THERMAL COAL**	
	LL2	**VU**	**LL2**	**VU**	**LL2**	**VU**
Average Thickness (m)	1.75	7.50	1.75	7.50	1.75	7.50
Inherent Moisture (wt %)	1.0	1.6	1.1	1.6	1.2	1.6
Ash (wt %)	8.5	8.5	10.0	10.0	14.0	13.1
Volatile Matter (wt %)	13.8	13.3	13.5	13.2	13.0	13.5
Specific Energy (MJ/kg)	32.64	32.21	32.00	31.58	30.31	30.26
Total Sulphur (wt %)	0.58	0.38	0.58	0.37	0.62	0.43
CSN	>1.5	>0.5	>1	>0.5	<0.5	<0.5
Phosphorus (wt %)	0.105	0.094	0.132	0.107	nd	nd
Vitrinite %	nd	41.2	48.3	40.4	nd	nd
Vitrinite Reflectance $R^{o}max$	1.87	1.84	1.81	1.85	nd	nd
AFT (IDT red °C)	nd	nd	1354	1374	1345	1354

COAL RESOURCES

Large inferred *in situ* resources of bituminous coal occur at depths greater than 55m and at dips less than 10°. Detailed resource assessment is confined to the potential open cut resources which occur in a flat lying synclinal feature astride the Fitzroy Beef Development Road. A comprehensive geological database was compiled from all company drill holes on a 500m grid and cross-sections along each traverse were generated at 1:2000 scale. As topography is extremely flat, surveyed collar elevations were used to generate topographic contours, enhanced with ground survey points at 100m intervals along drill traverses. An accurate deposit model for mine planning was generated in VULCAN. Crop lines were generated from the intersection of structure contours on the roof of each working section with base of weathering, and/or the 1:2000 cross-sections.

Table 1: Resource status — Codrilla

Status	**Seam**	**Ave Thickness metres**	**50–100m depth M tonnes**	**100–150m depth M tonnes**	**150–180m depth M tonnes**	**Total M tonnes**
Measured	Leichhardt Lower 2	2.2	3.5	5.1	-	8.6
	Vermont Upper	7.1	11.1	21.8	-	32.9
Subtotal			**14.6**	**26.9**	-	**41.5**
Indicated	Leichhardt Lower 2	2.0	-	3.1	-	3.1
	Vermont Upper	7.2	-	-	14.8	14.8
Subtotal			-	**3.1**	**14.8**	**17.9**
Total			**14.6**	**30.0**	**14.8**	**59.4**

To assist with a preliminary assessment of the Codrilla deposit's potential as a satellite mining operation to the Moorvale Mine, *in situ* mining block resources were generated as in Table 1.

No attempt has been made to quantify the large underground resources downdip or the open cut potential alongstrike.

MINING DEVELOPMENT

Codrilla, will yield a low ash, low volatile, export quality PCI coal of similar quality to that being produced from Coppabella or South Walker Creek. Codrilla has potential as a future satellite pit for the Moorvale mine being developed further north, and detailed drilling and testing has raised the confidence of the potential open cut resources to Measured Status. Further upside exists to extend the resource base, both downdip and along strike.

Internal evaluations have indicated that the resource has a number of favourable features for mining development:

- thick seam, compact size
- close to existing infrastructure (rail, roads, towns, port)
- some overburden can be dug unshot with assistance from dozer ripping
- gentle topography
- construction materials exist nearby.

Once markets for the coal are secured, it is envisaged that conventional strip mining by hydraulic excavator/truck and/or dragline will be employed for the bulk of the resources. Should the open cut resource be extended beyond its current limits into steeper dipping seams alongstrike, terrace mining techniques may be employed. Geotechnical assessment of the site conditions has yet to be undertaken.

REFERENCES

ANON, 1966: Blackwater report on areas relinquished from AP6C effective 1/12/66. CR 2429

ANON, 1968: Geological reports on 3 areas of AP3C relinquished as from 31.12.67. TDM Pty Ltd. CR 2479.

ANON, 1969: Report on areas to be relinquished from AP67C, Utah Development Company. CR 3118.

ANON, 1973: Report on areas relinquished from AP67C, Utah Development Company. CR 4797.

ANON, 1989: AP448C. Final progress report on operations for 6 months ending 13/9/89. Sedgman & Associates Pty Ltd. CR 20858.

ANON, 1989: AP436C Harrybrandt. First relinquishment Report. Tonford Pty Ltd, submitted by White Industries (Qld) Pty Ltd. CR 21262.

ANON, 1990: AP436C (Harrybrandt) AP445C (Oxford Downs) Combined relinquishment report by White Mining Ltd, prepared by Sedgman & Associates Pty Ltd. CR 22350.

BUZACOTT, R., 1980: AP3C Report on final area relinquishment. TDM Pty Ltd. CR 7937.

DASH, P.H., 1986: Shallow coal resources of the Annandale area, north Bowen Basin. GSQ Record 1985/24.

ELDRIDGE, B., 1974: Final geological report for areas relinquished, Blackwater - Goonyella area. CR 5094.

MALLETT, C.W., HAMMOND, R.L., LEACH, J.H.J., ENEVER, J.R. & MENGEL, C., 1988: Bowen Basin – Stress, Structure and Mining Conditions Assessment for Mine Planning, NERDDC Project No.901. Final Report. CSIRO Division of Geomechanics.

MATHESON, SG. 1990. Coal geology & exploration in the Rangal Coal Measures, North Bowen Basin, Winchester - South Poitrel coal field, Daunia, Suttor Creek, Broadmeadow:- Wotonga, Mavis Downs, Moranbah. *Queensland Geology* **1**.

QUINN G, 1982. Report on area relinquished. Final report AP292C. TDM Coal Pty Ltd (Rangals). CR 10729

FREITAG CREEK DEPOSIT

LOCATION AND TENEMENT DETAILS

The Freitag Creek deposit is located within in the Late Permian Bandanna Formation which outcrops within EPC 786 held by Macarthur Exploration Pty Ltd. It is situated wholly upon freehold land some 40km south of Springsure in Central Queensland and some 25km west of Xstrata Coal Qld's Rolleston Mine and the Bauhina Branch Line being constructed to service it (Figure 1).

EPC 786 is the northernmost of a group of tenements comprising the West Rolleston Project Area which stretches some fifty kilometres to the south over the Bandanna Formation crop line.

EXPLORATION HISTORY

Coal has been known from the Rolleston area to the east of EPC 786 for quite some time. Brigalow Mines, MIM and thence Xstrata conducted exploration drilling at their Meteor Park deposit at Rolleston for the past thirty years. Oil and gas exploration (seismic and drilling) was carried out throughout the 1960s to 1980s in the Denison Trough to the east. Departmental drilling along the eastern limb of the Serecold Anticline to the south (Anderson, 1974a, 1974b) confirmed the presence of shallow, thick, low ash coal seams of rank similar to Rolleston coal first reported by Jensen (1921). Departmental drilling at Buckland some 30 to 40km further west of EPC 786, also demonstrated that coal development within the Bandanna Formation deteriorated westward across the Springsure Shelf away from the Merivale Fault which forms the western boundary of the Denison Trough (Anderson, QGMJ 1976). Figure 2 is modified after Dixon & Bauer (1982) to illustrate the sedimentary and structural relationships across the Merivale Fault evident in the seismic data.

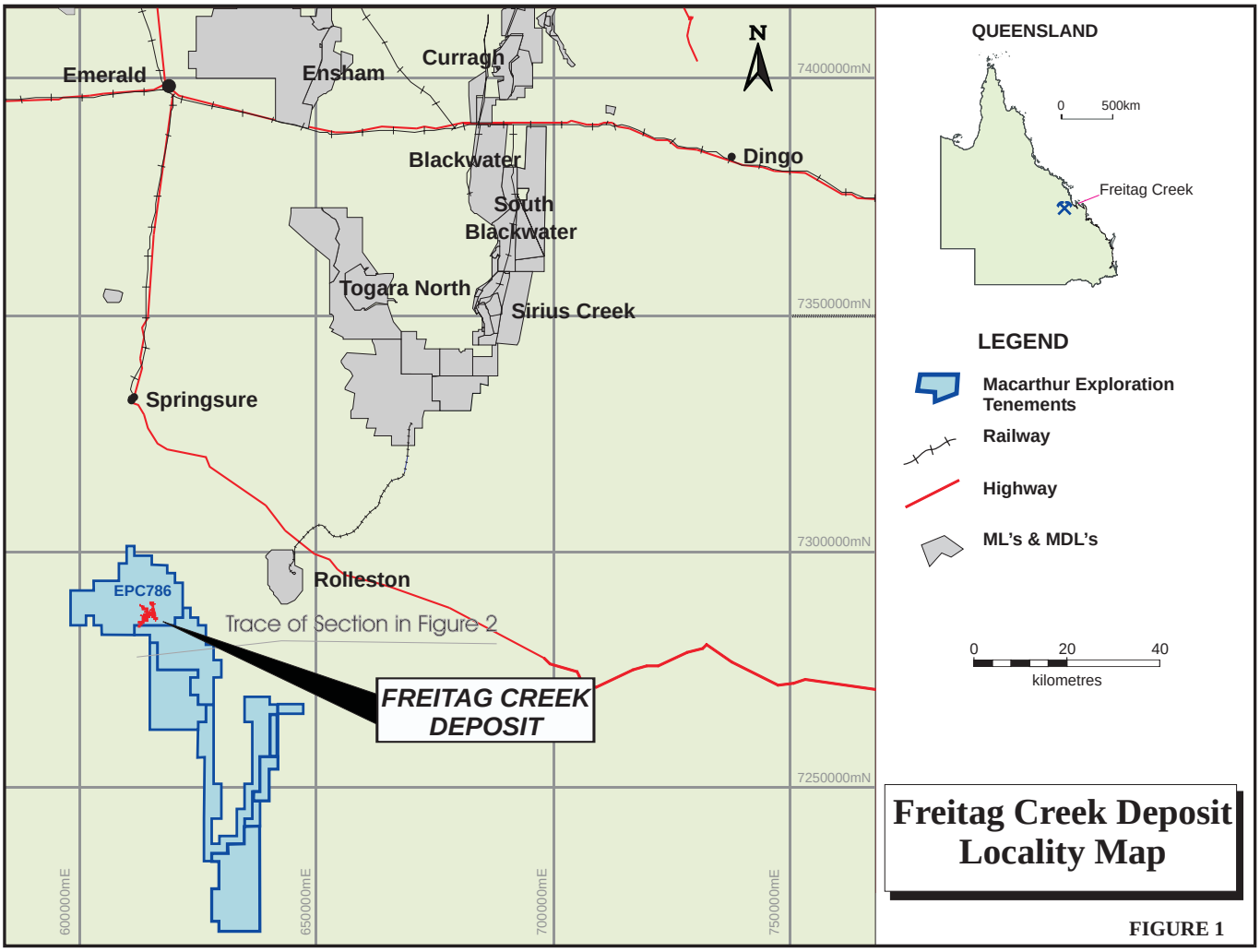

FIGURE 1

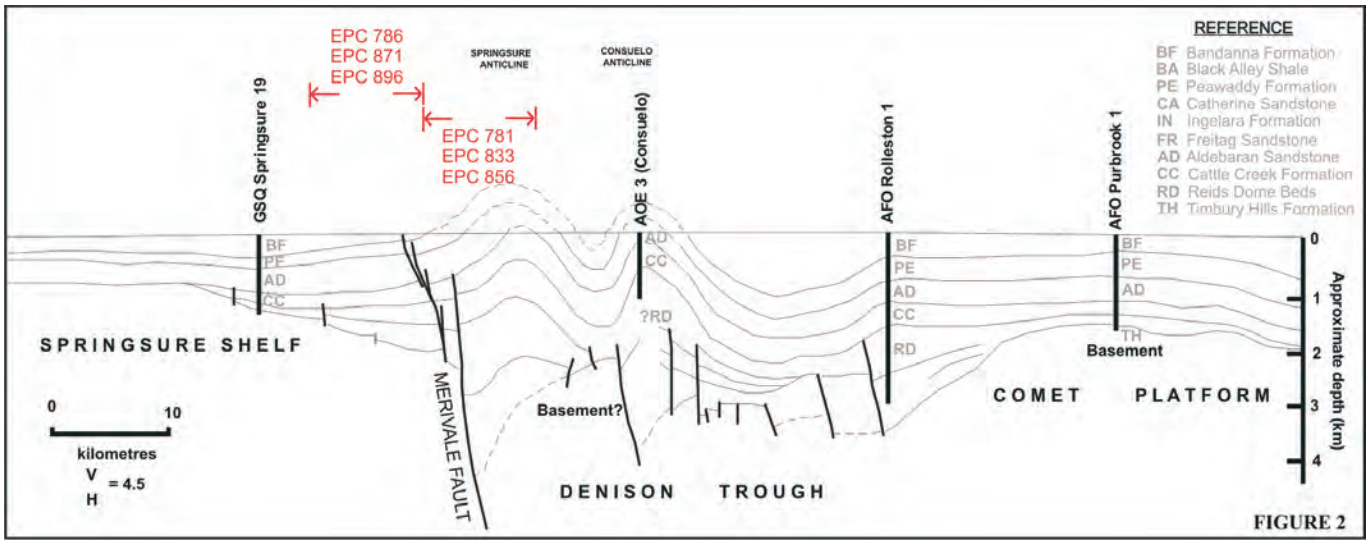

FIGURE 2

Departmental and petroleum exploration drilling in and around EPC 786 has, for the large part, been spudded in sediments below the upper Bandanna Formation (eg Asteroid 1, Meteor 1 and GSQ Springsure 10 to the east, GSQ Springsure 11 and 12, and Penjobe 1 to the west). Only GSQ Springsure 19 to the southwest, and Mount Ogg 1 in the south-east, intersected the prospective upper Bandanna Formation. Thin seams <1m were recorded in the former and a number of seams to 1.9m thick in the latter.

Magnum Resources Pty Ltd explored for coal to the north of the Freitag Creek Deposit (Rasmus, 1992). Although scout drilling confirmed the presence of the lowermost Bandanna Formation, it failed to intersect the coal bearing upper Bandanna Formation. Rasmus reported that 3 coal seams were known to outcrop over a 20m interval in Freitag Creek some 5km to the south of their EPC 510, but the area was never applied for and the ground was relinquished.

Prior to Macarthur Exploration acquiring EPC 786 no exploration had been undertaken in the Freitag Creek area. It was reasoned that any discovery in the south-west Bowen Basin could benefit from new infrastructure being considered for a proposed new mine at Rolleston.

A number of coal seam outcrops were mapped within the tenement, all of which confirmed as belonging to the Bandanna Formation, by comparison with the type section exposed on the company's tenements further south at Oil Shale Gully (Anderson, 1974b).

Scout drilling commenced in July 2003 and met with early success with the intersection of shallow seams of mineable thickness and quality and the drilling program was accelerated, including the necessary cultural heritage and environmental approvals. A regional database of seam intersections was compiled from all previous drilling and updated with MacEx drill hole data as it became available. Structure contours constructed from this database were compared with topographic contours to guide the drilling program. Initially, the topography was derived from AUSLIG 20 metre contours, but as the project advanced, new aerial photography was acquired and accurate topographic contours generated.

A drilling program to lift the Indicated Resources to Measured status was completed in February 2005. Due to the dissected terrain, a grid drilling approach was not possible and the drilling layout was extended to give sufficient coverage for geological modelling at Measured and Indicated resource status throughout this initial area whilst exploration of the surrounding region continued.

To date, some 6369.25m of drilling has been completed within the Freitag Creek deposit in 84 holes including 981.53m of HQ core (Figure 3). A further 31 (2934m) holes have been drilled within EPC 786 but are out of the measured resource area. Holes with coal intersections were geophysically logged and used as pilot holes for subsequent core holes.

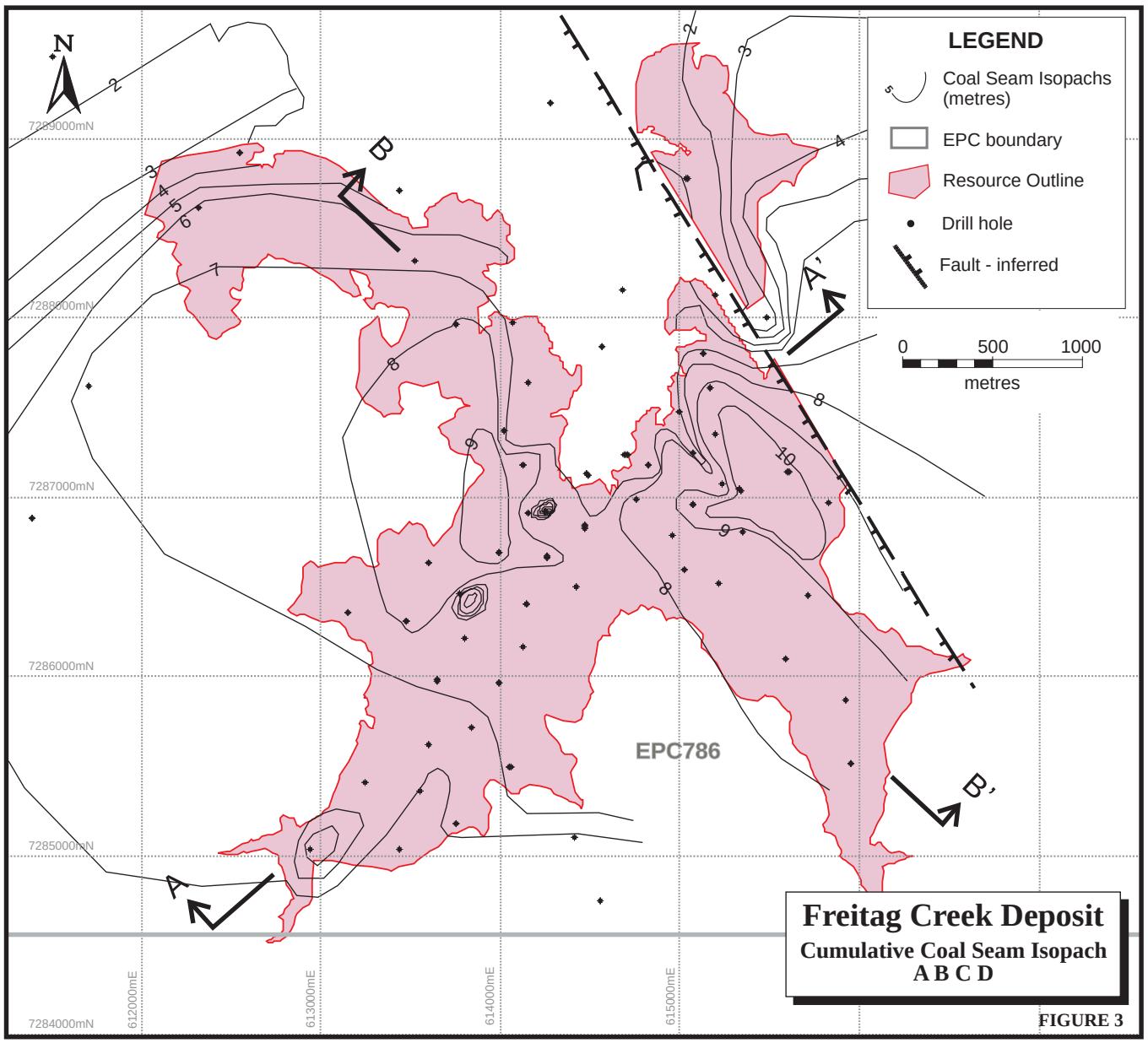

FIGURE 3

GEOLOGY

The Freitag Creek Deposit is now understood to be located on the Springsure Shelf west of the Springsure Anticline, along whose western flank is thought to be the surface expression of the Merivale Fault, traditionally regarded as the western edge of the Denison Trough and the Southern Bowen Basin.

The Merivale fault was active from the Early Permian, attracting thick sedimentary deposits within the downthrown Denison Trough. These sediments included coal measures, commencing with the Reids Dome Beds and culminating with the Bandanna Formation. The principal stratigraphic units intersected in drilling at Freitag Creek include the Upper Permian Peawaddy Formation, Black Alley Shale and Bandanna Formation, and the Triassic Rewan Group (Figure 4).

The **Peawaddy Formation** is known from numerous Departmental drillholes in the vicinity of EPC 786. It can be up to 260m thick and consist of lithic sandstones, carbonaceous siltstone and shales. At the top of the sequence lies a lenticular coquinite bed (Mantuan Productus Bed). One hole intersected the upper part of the formation and a 3m thick lithic sandstone unit containing abundant shelly material has been tentatively correlated as the Mantuan Productus Bed.

The **Black Alley Shale** consists of dark shales and bentonitic, tuffaceous clays and is presumed to be disconformable on the Peawaddy Formation. Unit thickness is in the order

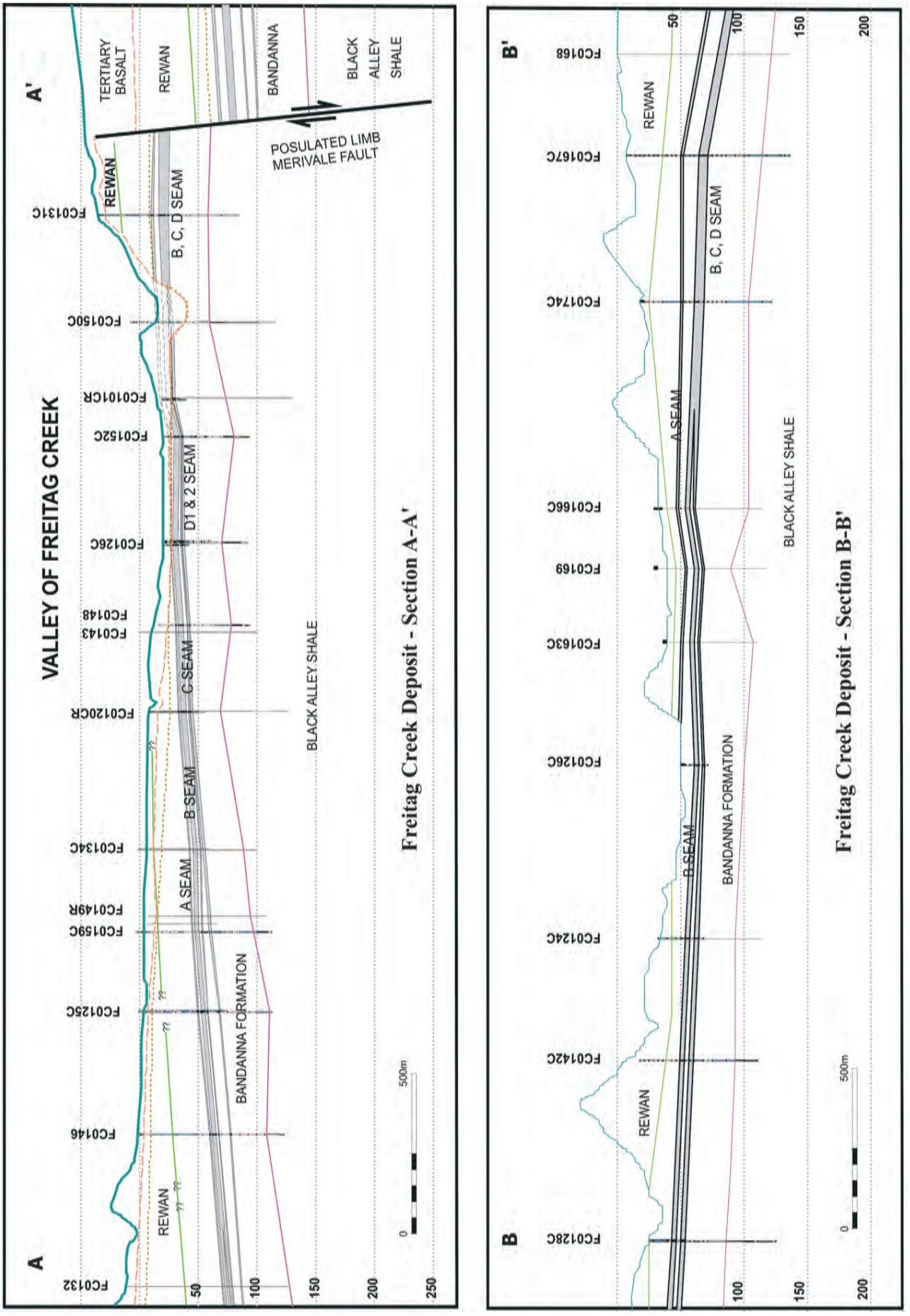
A
A'
VALLEY OF FREITAG CREEK
TERTIARY BASALT
REWAN
BANDANNA
BLACK ALLEY SHALE
POSULATED LIMB MERIVALE FAULT
B, C, D SEAM
D1 & 2 SEAM
C SEAM
B SEAM
A SEAM
BANDANNA FORMATION
BLACK ALLEY SHALE
Freitag Creek Deposit - Section A-A'
500m
B
B'
Freitag Creek Deposit - Section B-B'

FIGURE 4

of 100m. Wherever possible, a drill hole at each site has been terminated within the Black Alley Shale for stratigraphic control and to help assist in seam identification. Although no coal seams are present in the Black Alley Shale, it is regarded by Andersen (1974), perhaps together with the lower section of the Bandanna Formation, as the lateral equivalent of the Burngrove Formation identified in the Blackwater area.

The **Bandanna Formation** is correlative to the Rangal Coal Measures and Baralaba Coal Measures and forms perhaps the most widespread and consistent of the coal measures known in the Bowen Basin (Mallett, 1983; Matheson, 1990). Normally some 120–140m thick, drill hole data suggests that the formation thickness in Freitag Creek is less than 100m, probably between 80m to 90m. The unit comprises dominantly labile sandstone with lesser amounts of siltstone, mudstone and minor carbonaceous shale. Humic and sapropelic coal seams occur in the upper part of the formation (Andersen, 1974). Sandstone units within the formation have a very high clay content which can cause difficulties when coring. The lower boundary of the Bandanna Formation is taken as being at the top of the first tuffaceous interval of the Black Alley Shale.

Four seams have been regularly intersected at Freitag Creek, namely A, B, C, and D seams (Figure 5). Typically, 7.5m of coal occurs in A to D Seam over a 13.7m interval. The BCD seams approach near-coalescence in the east, where the cumulative coal can be 10m over a 14m interval. The BC and CD partings both gradually increase away from this zone of near-coalescence to the south-west, to around 5m and 10m respectively. In the north-east, the D Seam splits locally into D1 and D2. The AB seams approach near-coalescence to the north-west and the AB parting gradually increases to 13m in the south-east.

The uppermost seam, A Seam, ranges up to 3.45m in thickness in the Freitag Creek deposit and is high in inherent ash, often grading into carbonaceous shale at the floor. It was possibly developed on a levee bank. The upper portion of the seam (average 1.45m thick) consists of cleaner coal.

The best developed seam in the Freitag Creek deposit is the B Seam which averages 4.13m and is consistently clean. The C Seam averages just under 1m in the Freitag Creek deposit area, and is also consistently clean. For considerable part of the deposit it is coalesced or at near coalesence with the underlying D Seam, another consistently clean seam, which averages 1.54m in the deposit area.

Away from the deposit area to the west, all four seams deteriorate in thickness and quality. Beneath the escarpment to the east, the seam geometry is little understood, but it is suspected to be eventually downthrown into the Merivale Fault system, or a correlative of it. Until further drilling resolves this region, the deposit model is artificially bounded by a notional fault.

Proximal to this notional fault system, the conditions appeared ideal for seam coalesence, and the BCD Seam represents at least 6.5m of low ash coal above which the A Seam provides an additional 1.5m of high ash coal, and at shallow depths conducive to open cut extraction. Structural interpretation and exploration drilling suggest that the Bandanna Formation strikes roughly east–west in the deposit area and dips to the south at between 2–40°. Drilling and mapping have defined what appear to be quite narrow, localised linear zones of faulting with bedding dips up to 30°.

The Triassic **Rewan Formation** appears to conformably overly the Bandanna Formation. It comprises distinctively greenish-grey coloured labile sandstones, siltstones and mottled red and green mudstones. Few holes have intersected the Rewan Formation in Freitag Creek, and only the lower section. The boundary with the underlying Bandanna Formation is difficult to discern with any accuracy, but has been taken at the colour change to the grey sandstones and siltstones of the Bandanna Formation.

The deposit lies beneath a juvenile landform at the headwaters of the region's drainage system, which involves multiple **Tertiary** basalt flows, from fresh to deeply weathered, and intervening Tertiary sediments, which have been heavily dissected by later Quaternary

Coal Ply Stratigraphy of A, B, C, D1 & D2 Seams at Frietag Creek

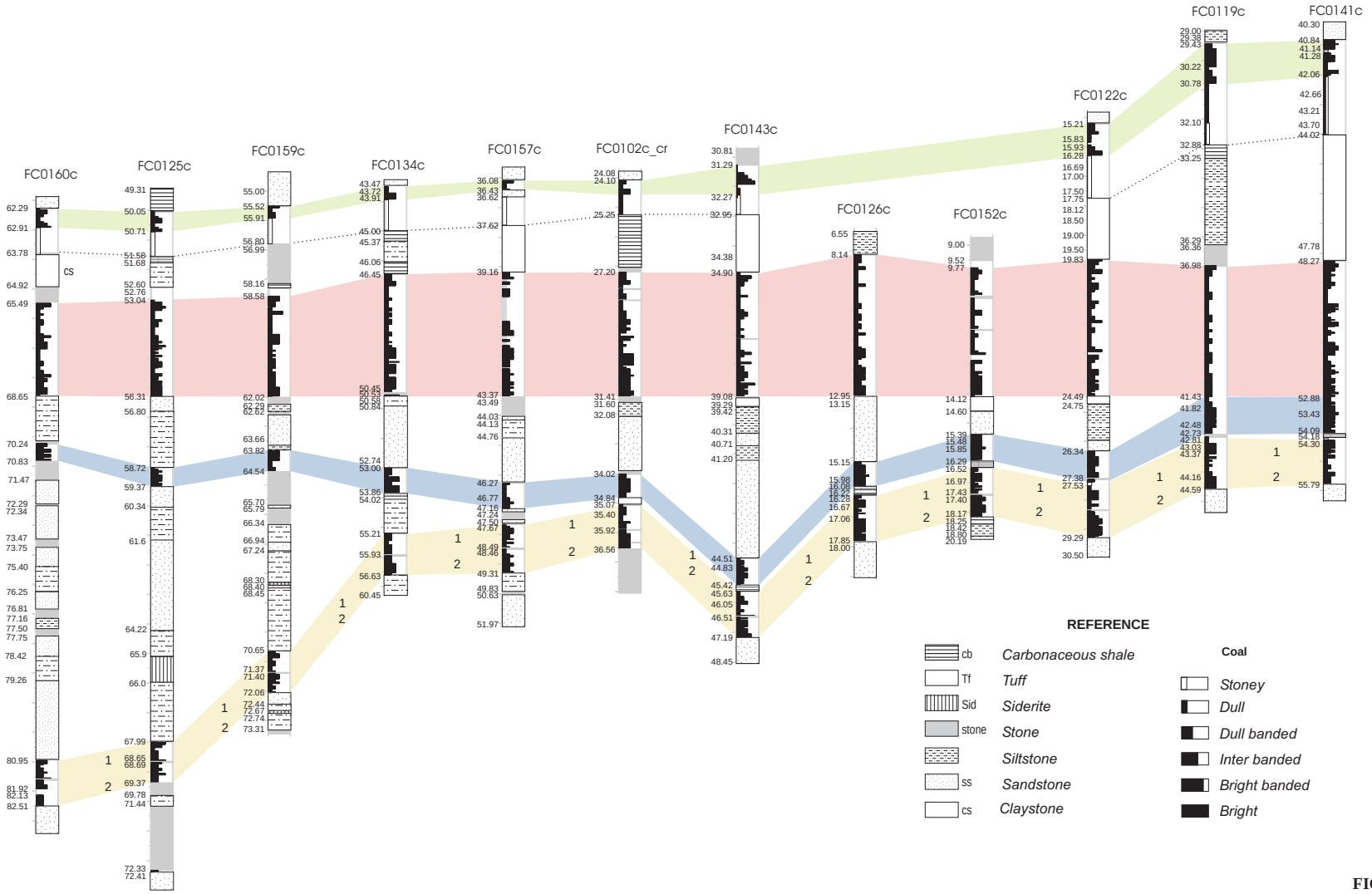

FIGURE 5

erosion. The result is an intermix of depths of weathering depending upon location within the juvenile landscape. The lighter, more erodable weathered materials have been stripped from the Tertiary sequence, particularly the weathered boulder basalt profiles, leaving behind Quaternary colluvial and alluvial lag gravels to carpet the valley floor and slopes. On the valley floor these Quaternary gravels can rest on fresh **Permian**, including coal seams at very shallow depths. Indeed, coal outcrops can appear remarkably unweathered.

The Deposit is located well south of the significant **intrusions** which form the major topographic highs to the north around Springsure and no intrusions have been intersected within the deposit to date. Seams in outcrop can appear locally 'burnt' where cut by a basalt flow.

COAL QUALITY

All slimcore samples from Freitag Creek were tested at either ACIRL's Ipswich or Emerald laboratories. Raw coal ply analyses from each of the four seams A to D were compared with seam brightness profiles in order to devise the raw coal and F1.60 washed coal composites to prepare for final testing. At the time of writing, the testing of washed coal composites was approximately 50% complete.

On a dry ash free basis, the coal is similar to Rolleston coal. However, it would be classified as sub-bituminous A (ASTM) based on vitrinite reflectance, thereby slightly lower in rank than Rolleston. The air dried (to equilibrated moisture) raw and washed coal quality of the A and BCD seams is summarised below which appears comparable with that reported from the Bandanna Formation across the southwest Bowen Basin.

	Raw Coal		**F1.60 Coal**		**Raw BCD+**
	A	**BCD**	**A**	**BCD**	**F1.60 A**
Inherent Moisture (wt %)	9.3	10.8	9.2	10.2	10.5
Ash (wt %)	25.3	10.9	16.8	7.6	12.0
Volatile Matter (wt %)	26.3	30.6	29.1	32.0	30.3
Specific Energy (MJ/kg)	19.5	24.13	21.50	24.58	23.75
Total Sulphur (wt %)	0.35	0.40	0.30	0.32	0.38
Fe+Ca in Ash (wt %)	12.9	20.6	11.4	14.1	18.83
AFT (IDT red oC)	1283	1188	1289	1192	1205
Chlorine (wt %)	0.01	0.02	nd	na	na
Vitrinite %	31.7	52.9	nd	na	na
Vitrinite Reflectance $R^{o}max$	0.44	0.43	nd	na	na

A raw coal blend of A, B C and D Seams appears ideally suited to domestic power generation and a raw coal blend of DCD may prove suitable for export, especially if enhanced by partial washing of the coarse fraction. Combustion behaviour is yet to be evaluated but already it can be noted that the ash fusion properties will require careful monitoring. Positive quality features include low fuel ratio, (good combustion properties), low sulphur, low chlorine and moderate Hardgrove Grindability Index.

COAL RESOURCES

Topographic contours at 1–2m accuracy were derived from new low level aerial photography acquired by the company to assist resource assessment. There is sufficient analytical coverage for declaration of *in situ* Measured, Indicated and Inferred Resources of raw coal as follows:

Measured Resources	43.5Mt
Indicated Resources	15.5Mt
Inferred Resources	21.6Mt
TOTAL	80.6Mt

MINING DEVELOPMENT

Preliminary internal evaluations have indicated that the resource has a number of favourable features for mining development:

- thick seam development
- compact size

- a very low strip ratio box cut
- no anticipated ground stability problems
- domestic and export market potential
- construction materials exist onsite.

This work has also identified issues that will need to be addressed including coal preparation, transport infrastructure and drainage control. It is envisaged that conventional mining by hydraulic excavator/truck will be employed for the bulk of the resources. Geotechnical assessment of the site conditions has not been been undertaken. Baseline environmental studies are underway as part of the preparation of an EMOS leading to the early grant of a mining lease for a contract open cut mining operation to commence once markets are secured.

REFERENCES

ACIRL Reports of MacEx slimcores

ANDERSON, J.C., 1974a: Departmental Coal Drilling, Consuelo Programme, South-West Bowen Basin. *Queensland Government Mining Journal*, **Aug 1974**, 273–275.

ANDERSON, J.A., 1974b: Departmental Coal Drilling, Consuelo Programme, South-West Bowen Basin. GSQ Record 1974/13.

ANDERSON, J.C., 1976: Coal Evaluation of the Bandanna Formation, Western Springsure Shelf. *Queensland Government Mining Journal*, **May 1976**, 201–203.

ANDERSON, J.C. & LEBLANG, G.M., 1975: Rolleston-Springsure District. *In Economic Geology of Australia and Papua New Guinea: Volume 2 Coal*. AusIMM monograph series, 106.

DIXON, O. & BAUER, J.A., 1982: Southern Denison Trough – Interpretation of Seismic Data from the Rolleston Area. *Queensland Government Mining Journal*, **Mar 1982**, 122–131.

DRAPER, J.J., & GREEN, P.M., 1983: Stratigraphic Drilling Report – GSQ Eddystone 4 and 5. *Queensland Government Mining Journal*, **Aug 1983**, 308–317.

GRAY, A.R.G., 1976: Stratigraphic relationships of Late Palaeozoic Sediments Between Springsure and Jericho. *Queensland Government Mining Journal*, **April 1976**, 147–163.

GRAY, A.R.G., 1980: Stratigraphic relationships of Permian Strata in the Southern Denison Trough. *Queensland Government Mining Journal*, **Feb 1980**, 110–130.

GREEN, P.M., 1982: Stratigraphic Drilling Report – GSQ Springsure 19. *Queensland Government Mining Journal*, **Oct 1982**, 457–463.

JENSEN, H.I., 1921: The Geology and Mineral Resources of the Carnarvon District. Condensed preliminary report. *Queensland Government Mining Journal*, **Oct 1921**, 401–407.

RASMUS, P.L., 1992: EPC 510 Rainworth. Final Report. Prepared for Magnum Resources Pty Ltd by Earth Resources Australia Pty Ltd. ERA Report A/345. Held by the Queensland Department of Natural Resources and Mines as CR23230.

REID, J.H., 1930: The Geology of the Springsure District, Parts 1 and 2. *Queensland Government Mining Journal*, **Mar 1930**, 87–99, and **Apr 1930**, 149–157.

Other Company reports on open file at NR&M library:
CR27; CR667; CR1992; CR6369; CR7999; CR16508; CR16706; CR23567; CR26888; CR26910

OLIVE DOWNS DEPOSIT

LOCATION AND TENEMENT DETAILS

The Olive Downs Deposit is located in the Late Permian Rangal Coal Measures which occur along a 25km strike length in the southern half of EPC 649 held by Moorvale Coal Pty Ltd. It is situated wholly on freehold land to the east of CQCA's Daunia Deposit in Central Queensland. The northern end of the Deposit is approximately 20km south of the township of Coppabella on the Peak Downs Highway (Figure 1). The Peak Downs rail line approaches to within 8km in the west, and rail distance to the Dalrymple Bay Coal Terminal is of the order of 150kms. Access from Mackay is by the sealed Peak Downs Highway and unsealed Council roads. The Deposit lies within three freehold properties, namely Olive Downs, Iffley and Vermont Park Stations, with current mine planning confined to the Olive Downs property.

The Isaac River divides the Deposit into two, with some 9km of strike length to the north and 16km to the south, extending into EPC 850. The Deposit extends downdip to the east into EPCs 676 and 721.

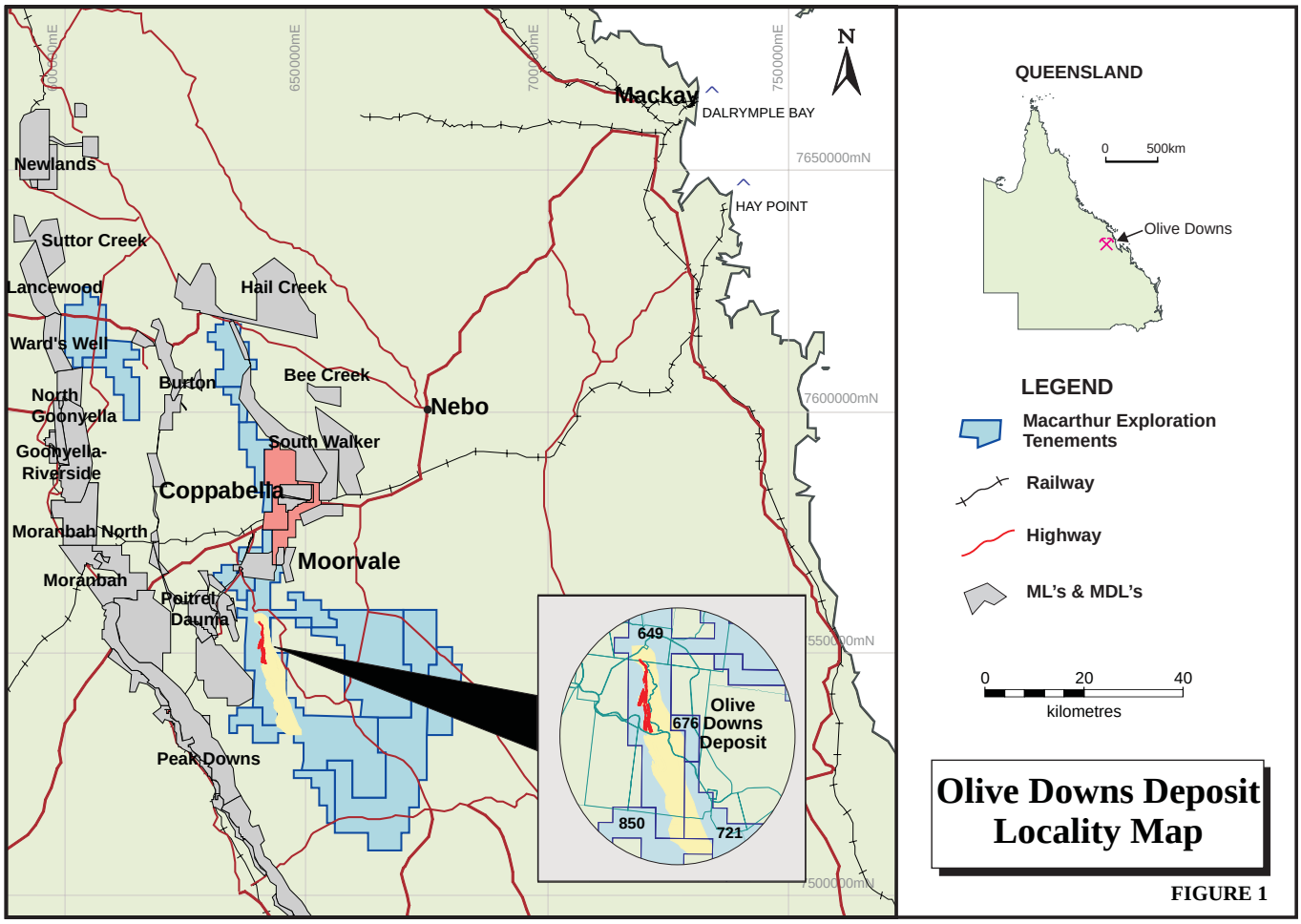

FIGURE 1

EXPLORATION HISTORY

The nearest relevant Departmental exploration occurred at Lake Vermont North to the south (Sorby & Matheson, 1983; Sorby, 1986: Matheson, 1986, Dixon & Sorby, 1988) and at Annandale to the north (Dash, 1986).

The area was first held by Utah Development Company Limited under Authority to Prospect 6C and 67C.

UDCL's drilling intersected both the Leichhardt and Vermont Seams within the Olive Downs area, but a combination of poor drilling conditions, structural uncertainty and market conditions discouraged further exploration and the ground was dropped in 1974 (CRs 2429, 2479, 3118, 4797; Eldridge, 1974). Of the areas retained by UDCL, their Daunia Deposit (UDCL, 1985) is adjacent to the western margin of the Olive Downs Deposit. The Olive

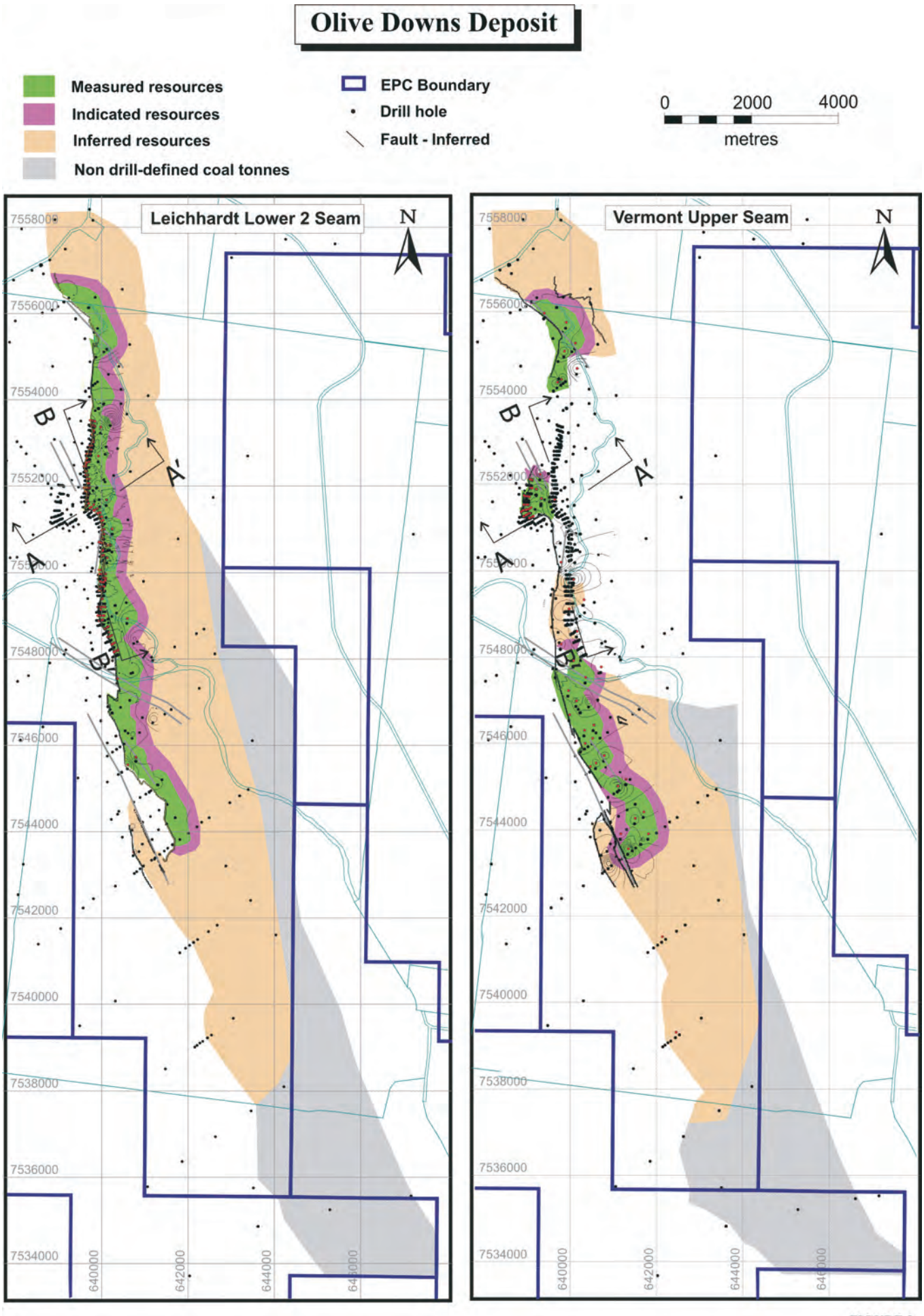
Olive Downs Deposit
Measured resources
Indicated resources
Inferred resources
Non drill-defined coal tonnes
EPC Boundary
Drill hole
Fault - Inferred
0
2000
4000
metres
Leichhardt Lower 2 Seam
Vermont Upper Seam
N
A
A'
B
B'
7558000
7556000
7554000
7552000
7550000
7548000
7546000
7544000
7542000
7540000
7538000
7536000
7534000
640000
642000
644000
646000

FIGURE 2

Downs region was also reviewed by others such as BP Petroleum (CR7000).

The Moorvale to Olive Downs region was one of a number of areas recommended to Macarthur Coal Pty Ltd by Lance Grimstone & Associates Pty Ltd and EPC 649 was secured on its behalf in October, 1997. Scout drilling commenced in March 1998, and met with early success. Follow-up exploration at Olive Downs was put on hold whilst activity at its other discovery nearby at Moorvale was accelerated. Exploration at Olive Downs recommenced in mid-1999 when a grid system of drill traverses was established across the shallow crop zone.

North of the Isaac River, detailed slimcore drilling and testing on a 500m grid has raised open cut resources to Measured Status along a 7km strike length where the lateral continuity of the Leichhardt Lower Seam was demonstrated. Exploitation of the Vermont Upper Seam north of the Isaac River is limited by intrusion to discreet areas of non-heat-affected coal. Initial open cut pits were defined and additional drilling was carried out for structural control, line of oxidation (LOX) definition and large diameter core drilling to support initial mine development planning (Figure 2).

South of the Isaac River, detailed grid drilling has extended the definition of open cut resources of both seams for part of the strike length in EPC 649, although exploitation of the Vermont Upper Seam will again be restricted by localised intrusive activity. Widespaced grid drilling has demonstrated lateral continuity of the Leichhardt Lower seam and Vermont Upper seam further south still and into the adjacent EPC 850.

To date, some 48 927.04m of drilling has been completed in 625 holes including 1925.97m of HMLC, HQ and 200mm core. Drill hole locations are shown in Figure 2. All holes intersecting coal were geophysically logged and used as pilot holes for subsequent core holes.

GEOLOGY

The Olive Downs Deposit is now understood to be located along a north–south strike on the western flank of a major synclinal feature informally named the Coxendean Sub-basin, where seismic evidence has shown that Upper Permian strata dip eastwards beneath thick Triassic. Three major Permo-Triassic units have been intersected in drilling, namely the Upper Permian Fort Cooper Coal Measures, the Upper Permian Rangal Coal Measures and the Triassic Rewan Group (Figure 3).

Although the complete section has not been intersected, the **Fort Cooper Coal Measures** are estimated to be approximately 350m thick and consist of labile sandstones and siltstones and thick seams of interbedded coal, carbonaceous mudstone and tuffaceous claystone. These rocks were often hard to penetrate and appear silicified, perhaps by fluid flow generated by igneous activity. Coal seams within the Fort Cooper Coal Measures contain high ash coals heavily banded with tuffs. The Yarrabee Tuff Bed (YTB), a basin-wide tuffaceous horizon with a characteristically high natural gamma response, is taken as the upper boundary of the formation (Matheson, 1990). At Olive Downs, the YTB generally overlies the Vermont Lower Seam (VL) which can be up to 6m thick and generally high in ash, composed of thin dull and bright banded coal plies interbedded with tuffaceous mudstone. Occasionally, it is at near-coalescence with the overlying Vermont Upper Seam.

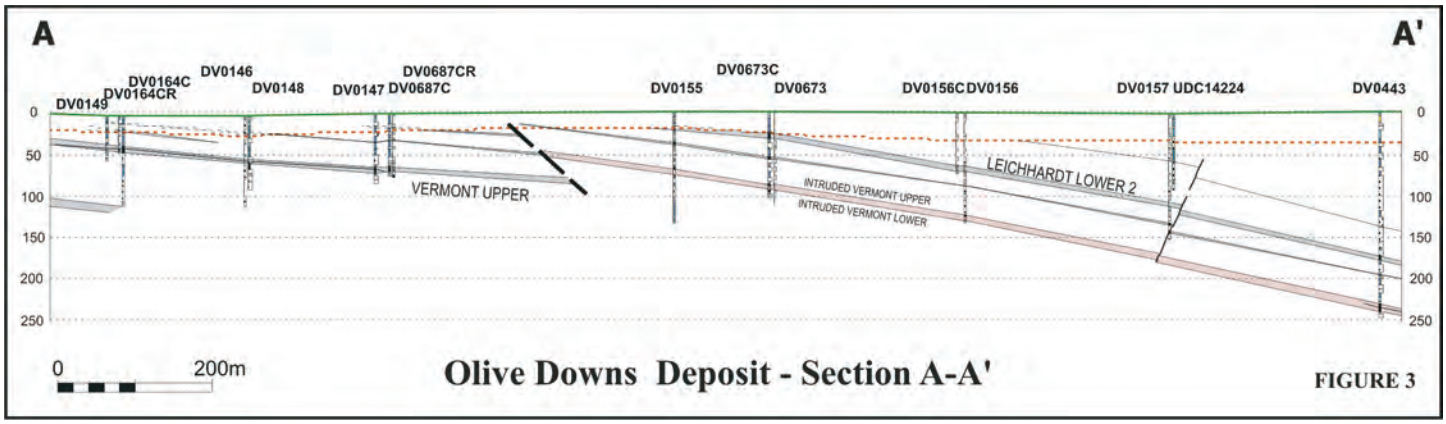

Olive Downs Deposit - Section A-A'

FIGURE 3

The **Rangal Coal Measures** immediately overlie the YTB and the Fort Cooper Coal Measures. They range from 90–195m thick and comprise dominantly lithic labile sandstone with banded siltstone, mudstone, minor carbonaceous shale and coal. The formation is the most widespread and consistent of the coal measures in the Bowen Basin (Mallett & others, 1983; Matheson, 1990). Carbonate infilling on fractures is common within the sandstone units at Olive Downs.

A number of seams have been intersected at Olive Downs North, some of which are depicted in Figure 4. The Leichhardt Upper Seam averages 1.58m of high ash, primarily dull coal. Where intersected, the Leichhardt Lower 1 Seam (LL1) averages 1.77m of dull coal, brighter to the base, and occurs some 10–15m above the Leichhardt Lower 2 Seam. The Leichhardt Lower 2 Seam (LL2) occurs towards the middle of the formation, and is easily the most consistent ply, laterally continuous throughout the Deposit. Slimcores at 500m centres show it to average 4.0m of dull and bright coal, brighter towards the base, and to be generally devoid of stone bands. The roof of the seam is usually silty mudstone with a sharp boundary. The Leichhardt Lower 3 Seam (LL3) averages 1.55m of interbanded carbonaceous shale with bright coal bands, which occurs 5–10m beneath the Leichhardt Lower 2 Seam.

The Vermont Upper Seam (VU) averages 3.2m thick and occurs towards the base of the Measures, some 30m to 40m below the Leichhardt Lower 2 Seam and is generally composed of a dull banded upper ply (VU1) with a bright banded lower ply (VU2). Although it can be the highest quality seam within the Deposit, it can be compromised by intrusions and variously heat affected.

The Triassic **Rewan Formation** conformably overlies the Rangal Coal Measures and is devoid of coal. It comprises distinctively greenish-grey coloured labile sandstones, siltstones and mottled red and green mudstones.

For much of the Deposit north of the Isaacs River, only a thin veneer of **Tertiary and/or Quaternary** sediments overlies the Permian and Triassic strata. However, south of the confluence of the Isaac River and North Creek, Tertiary/Quaternary alluvial sediments thicken substantially. Similarly, the **depth of weathering** gradually increases from 25m to >70m in the far south of the Deposit.

Photomapped trends of Permo-Triassic bedding and faulting have been correlated with aeromagnetic, seismic and drill hole data. Major fault systems originally defined by CQCA drilling at Daunia such as the New Chum, West Daunia and East Daunia faults can be traced southward through the Olive Downs region (BHP Coal, 1995). Direct evidence of minor faulting was observed during the drilling programs and close spaced faults have been interpreted from cross-sections.

Significant **intrusions** form the major topographic highs to the north and northeast of the Deposit. The extent of sub-surface intrusive activity was therefore detected by low level aeromagnetic data, including a possible feeder dyke north of the Isaac River. Intrusive activity is thought to decrease southwards away from the intrusions in the north. Rank decreases southwards accordingly. The underlying Fort Cooper Coal Measures are heavily intruded. In contrast, the Rangal Coal Measures are less so, activity ceasing upwards at the Vermont Seam horizon. Only in the immediate vicinity of the feeder dyke is the Leichhardt Lower in any way heat affected.

COAL QUALITY

Coal quality data at Olive Downs has been established from some 82 slimcore sites along a 25km strike length, including 1 Departmental and 2 UDCL slimcores. The principal seam, **LL2,** has been tested in 46 of these, and the **VU** Seam in 43. The lesser seams show promising results, but have yet to be tested in sufficient boreholes or detail (ie the LL1 in 13 holes, the LL3 in 23 holes to date). HQ slimcores were sampled on a ply x ply basis and tested at ACIRL for raw coal properties. Ply samples were combined into working section samples for subsequent washability analysis and clean coal testing of selected washed coal fractions for their coking, PCI or thermal properties.

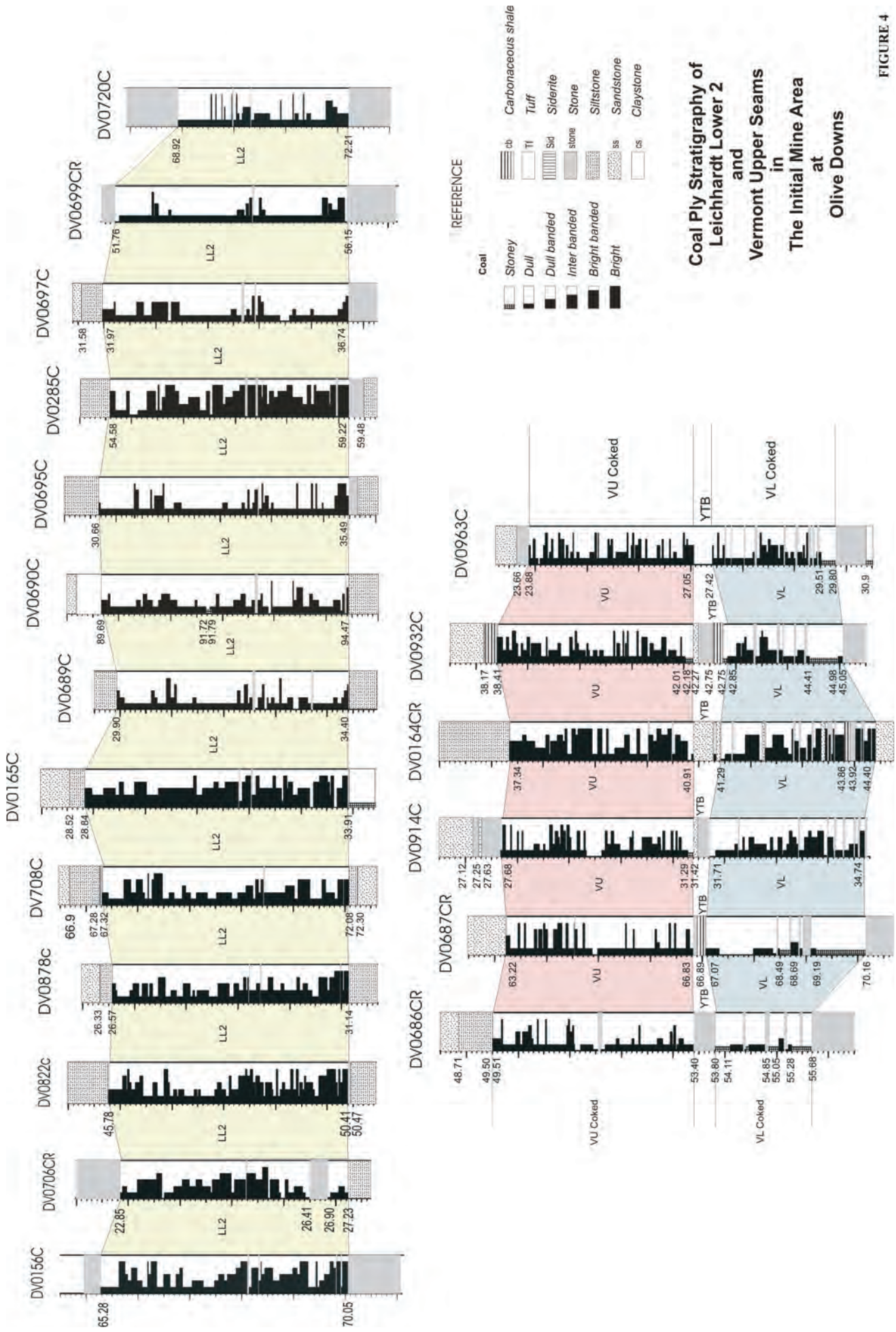
Coal Ply Stratigraphy of Leichhardt Lower 2 and Vermont Upper Seams in The Initial Mine Area at Olive Downs
REFERENCE
Coal
Stoney
Dull
Dull banded
Inter banded
Bright banded
Bright
cb Carbonaceous shale
Tf Tuff
Sid Siderite
stone Stone
Siltstone
ss Sandstone
cs Claystone
DV0156C
DV0706CR
DV0822c
DV0878c
DV708C
DV0165C
DV0689C
DV0690C
DV0695C
DV0285C
DV0697C
DV0699CR
DV0720C
DV0686CR
DV0687CR
DV0914C
DV0164CR
DV0932C
DV0963C
LL2
VU
VL
YTB
VU Coked
VL Coked

FIGURE 4

A range of coal fractions may be produced from Olive Downs coal, including coking coal, weak coking coal, PCI coal, thermal coal, and ultra high volatile coal. Two 200mm diameter borecores were taken in the proposed initial mine area north of the river to provide larger samples for liberation, size analysis, detailed washability, froth flotation and coke oven testwork, and for process simulation studies to assist in the design of the optimum preparation process. Product specifications are yet to be finalised, but average air dried product qualities of the 30 working sections of the principal **LL2** Seam within the initial mine area are summarised below:

	10% PCI	**8.5% S/COKING**	**7% COKING**
Inherent Moisture (wt %)	1.3	1.3	1.4
Ash (wt %)	10.0	8.5	7.0
Volatile Matter (wt %)	18.7	19.0	19.4
Specific Energy (MJ/kg	31.78	32.39	33.08
Total Sulphur (wt %)	0.4	0.39	0.39
CSN	>2.5	>3.5	>5.5
Max Fluidity (dd/min)	19	24	46
Phosphorus (wt %)	0.074	0.058	0.058
Vitrinite %	39.3	41.6	47.2
Vitrinite Reflectance R^{o}_{max}	1.41–1.35	1.41-1.34	1.41–1.29

Froth flotation was not undertaken on the slimcores, and large core testing shows a much improved coking coal quality. In places, raw LL2 coal could be produced as high energy, **export thermal coal**.

Similar specifications can be produced from some 15 working sections of the Vermont Upper seam in the initial mine area. Elsewhere, moderate yields of a medium ash ultra low volatile product may be derived from the heat affected areas of the Vermont Upper Seam. The Vermont Lower Seam resources consist of high ash thermal domestic grade coal only.

Average phosphorus levels for the coking fractions from Olive Downs are generally within normal specifications, but phosphorus content of the seams in the Rangal Coal Measures in this region is known to be variable. Localised high fault and dyke frequencies are anticipated and as a consequence, coking properties will need constant management during mining.

COAL RESOURCES

Resource estimates were brought into line with the 2004 JORC Code. The modelled area was extended downdip to 450m depth and alongstrike to capture additional data. Provisional revised drill defined JORC Code resource estimates of LL2 and VU Seams to 450 metres depth comprise:

- 56.4Mt of Measured Resource of which 42.3Mt are at less than 100m depth
- 34.1Mt of Indicated Resource of which 8Mt are at less than 100m depth
- 306Mt of Inferred Resource of which 26Mt are at less than 100m depth. The calculations also reveal the potential availability of comparable additional tonnage from 300m to 450m depth which is, as yet, not appropriately drill defined.

The interaction of the major fault lines and the crop line south of the Isaac River has not been fully appraised, and further resources may exist in downthrown fault blocks to the west of the currently defined crop line. In addition, further resources of non-heat-affected VU Seam coal may still be uncovered by closer spaced drilling. Thick, high ash Vermont Lower and Girrah Seams which occur beneath the target seams have not been evaluated at this time.

MINING DEVELOPMENT

Conceptual mine development planning has examined the Olive Downs Area north of the Isaac River as a satellite mining operation for the Moorvale Mine. The resource has a number of favourable features for mining development:

- reasonably thick, high quality seams close to the surface
- no anticipated ground stability or water problems
- close to existing company mine infrastructure (washplant, rail loadout)
- gentle topography
- multi-product market potential
- construction materials exist nearby.

Although initial extraction would be by traditional truck and shovel methods, the moderately steep dips point to the eventual employment of terrace mining techniques in places. Geotechnical assessment of the site conditions for the early years of mining has been undertaken. The potential for partial inundation from the Isaac River has been reviewed and baseline environmental studies are underway as part of the preparation of an EMOS leading to the early grant of a mining lease for a contract open cut mining operation to commence once markets are secured.

REFERENCES

ANON, 1966: Blackwater report on areas relinquished from AP6C effective 1/12/66. Held by the Department of Natural Resources and Mines as CR2429.

ANON, 1969: Report on areas to be relinquished from AP67C, Utah Development Company. Held by the Department of Natural Resources and Mines as CR3118.

ANON, 1973: Report on areas relinquished from AP67C, Utah Development Company. Held by the Department of Natural Resources and Mines as CR4797.

ANON, 1989: AP448C. Final progress report on operations for 6 months ending 13/9/89. Sedgman & Associates Pty Ltd. Held by the Department of Natural Resources and Mines as CR20858.

BHP AUSTRALIA COAL PTY LTD, 1995: The Daunia Coal Deposit, *In*, Follington, I.L., Beeston, J.W. & Hamilton, L.H., 1995: *Proceedings of the Bowen Basin Symposium 1995*, Bowen Basin Geologists Group and Geological Society of Australia Inc. Coal Geology Group, Mackay, 275–282.

BP AUSTRALIA LTD, 1979: An assessment of the Rangal Coal Measures between Middlemount and Olive Downs, Central North Bowen Basin, Queensland. Held by the Department of Natural Resources and Mines as CR7000.

DASH, P.H., 1986: Shallow coal resources of the Annandale area, north Bowen Basin. Geological Survey of Queensland Record 1985/24.

DIXON, O. & SORBY, LA., 1988: Shallow seismic reflection survey at Lake Vermont, North Central Bowen Basin. Geological Survey of Queensland Record 1988/03.

ELDRIDGE B, 1974: Final geological report for areas relinquished, Blackwater - Goonyella area. Held by the Department of Natural Resources and Mines as CR5094.

MACARTHUR COAL LTD, 2005: Annual Report to June 2005.

MALLETT, C.W., HAMMOND. R.L., LEACH, J.H.J., ENEVER, J.R. & MENGEL, C., 1988: Bowen Basin – Stress, Structure and Mining Conditions Assessment for Mine Planning, NERDDC Project No.901, Final Report, CSIRO Division of Geomechanics.

MATHESON, S.G., 1986: Exploration of the Rangal Coal Measures, Vermont North area, North of Central Bowen Basin. Geological Survey of Queensland Record 1986/19.

MATHESON, S.G., 1990: Coal Geology and Exploration in the Rangal Coal Measures, North Bowen Basin, *Queensland Geology* **1**.

SORBY, L.A., 1986: Investigation of Geological structure at Lake Vermont, North Central Bowen Basin. Geological Survey of Queensland Record 1986/29.

SORBY, L.A. & MATHESON, S.G., 1983: Stage 2 drilling programme, Lake Vermont, North Central Bowen Basin. Geological Survey of Queensland Record 1983/16.

UTAH DEVELOPMENT COMPANY LTD, 1985: The Daunia Coal Deposit. Bowen Basin Coal Symposium, *Geological Society of Australia, Abstracts*, **No 17**.

THE PICARDY COAL DEPOSIT

LOCATION

The Picardy Coal Deposit is located approximately 200km south-south-west of the Central Queensland city of Mackay and 15km east of Norwich Park Mine (Figure 1).

TENURE

Exploration Permit for Coal No. 718 (Picardy), originally covering 300 sub-blocks was granted to the Central Queensland Coal Associates Joint Venture (CQCA) for a term of five years on 26th September 2000. CQCA acquired the EPC to explore for resources of shallow coal east of Norwich Park Mine in the Rangal Coal Measures (RCM). Under the terms and conditions of the EPC, 150 sub-blocks were relinquished in 2002 and a further 75 sub-blocks were relinquished in 2003. The remaining 75 sub-blocks were held in 2004 and 2005, see Figure 2. 15 sub-blocks will be relinquished in September 2005 and a renewal application has been submitted to retain 60 sub-blocks for another 3 years while a Mineral Development License or a Mining Lease is applied for over the most prospective coal resources.

EXPLORATION

Prior to the grant of EPC 718, exploration had been undertaken in the area by:

- Utah Development Company during assessment of ATP 6C in the 1960s;
- Anglo American – Kaiser Steel Joint Venture in ATP 98C;
- BHP in ATP 65C;
- German Creek Mine in ATP 315C;
- DME during reconnaissance drilling programs between 1972 and 1986;
- Australian Coal Enterprises in EPC 611 during 1996 and 1997.

EPC 718 was explored using a variety of techniques including photogeology, drilling and surface geophysics. During the first 3 years of tenure 149km of 2D mini-SOSIE reflection seismic were recorded along sixteen regional traverses. Prominent reflectors identified on the seismic sections were subsequently tested by drilling. Over the last 5 years 396 holes (55 101m including 23 cored quality holes) have been drilled. The purpose of these drilling programmes was to:

- complement the seismic lines,
- define coal oxidation limits,
- delineate resources, and
- indicate structural issues with faults and seam intrusions.

To help delineate intrusions further, both a down hole magnetic survey and a ground magnetics survey were also undertaken.

GEOLOGY

Regional Geology

The Picardy deposit is located on the eastern margin of the Bowen Basin in the “Bee Creek Syncline” and is characterised by north easterly dips and some compressional structural deformation. The EPC is bound by two major thrust faults, the Jellinbah Fault along the western side and the Foxleigh Fault on the eastern side (Figure 3).

Stratigraphy

The stratigraphic sequence in EPC 718 is summarised in Figure 4. In general, over much of the area, the Permo-Triassic sediments are overlain by Tertiary sediments and Recent alluvium. The alluvial sediments comprise light coloured clays, clayey sands and sands, with grit and gravel beds near the base of the sequence. The Tertiary cover in the centre of the EPC is thin (generally <10m) and thickens to the north and south to >50m.

Figure 1: Location map

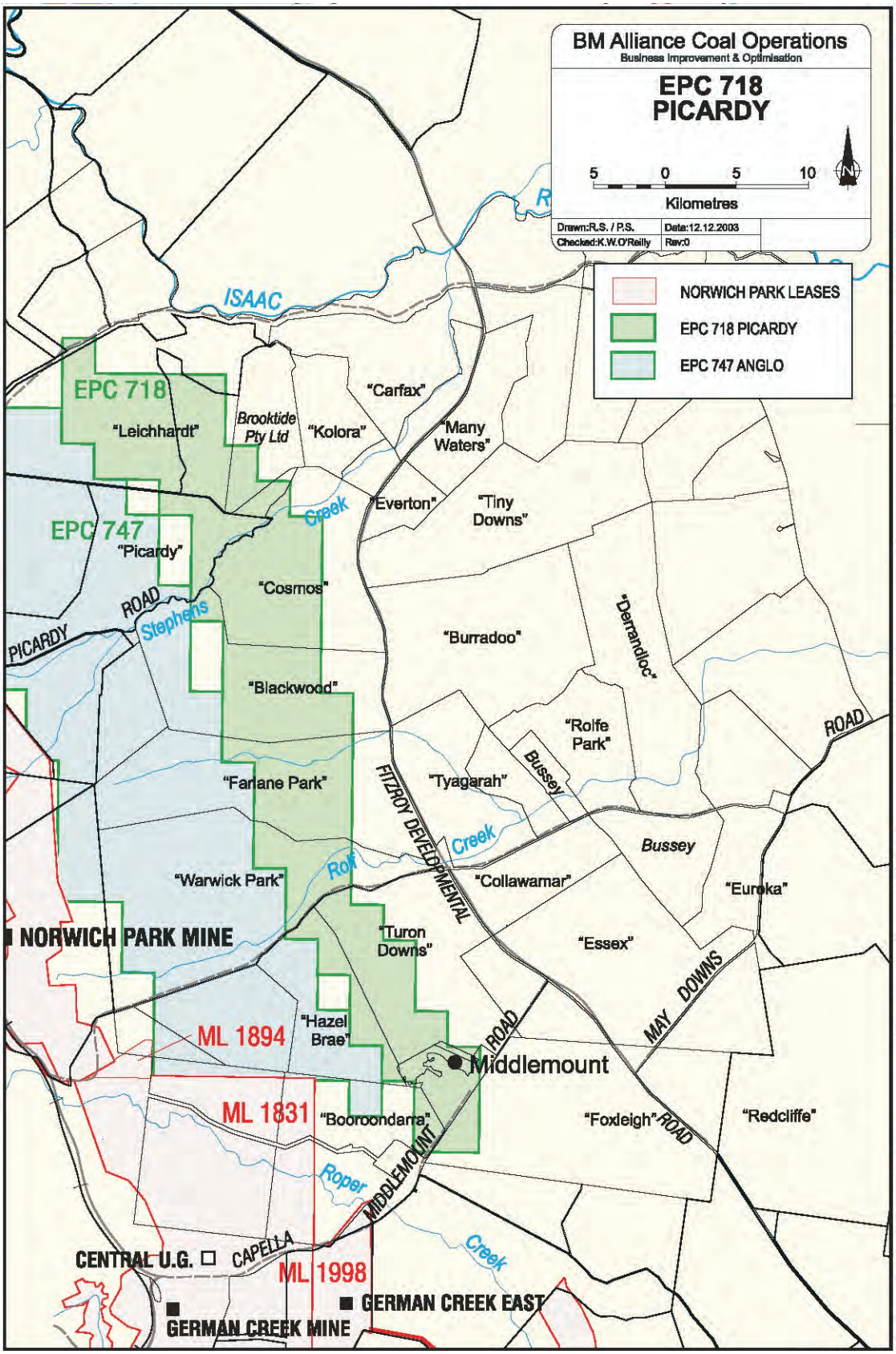

Figure 2: Tenement map

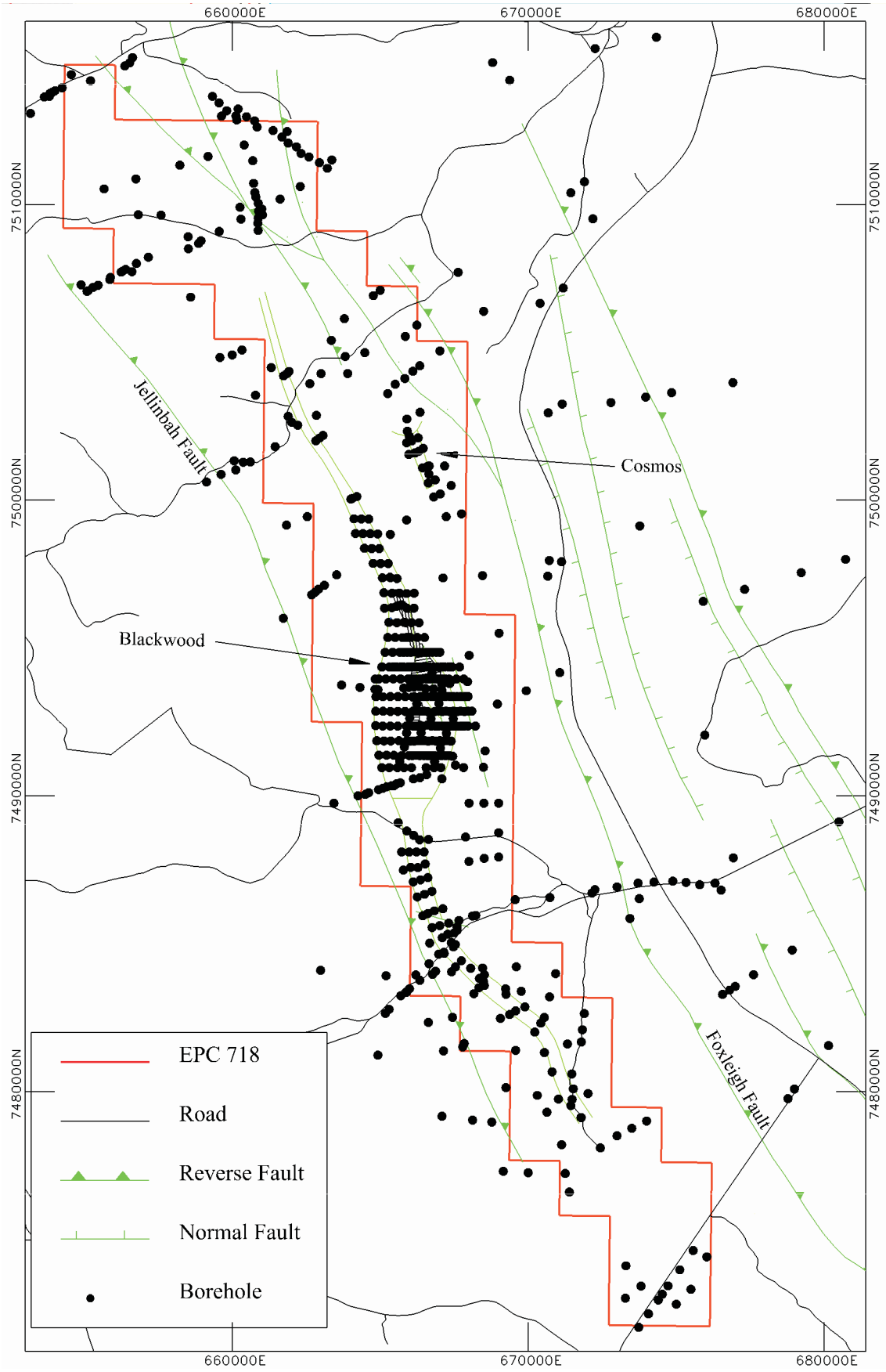

Figure 3: Structural map

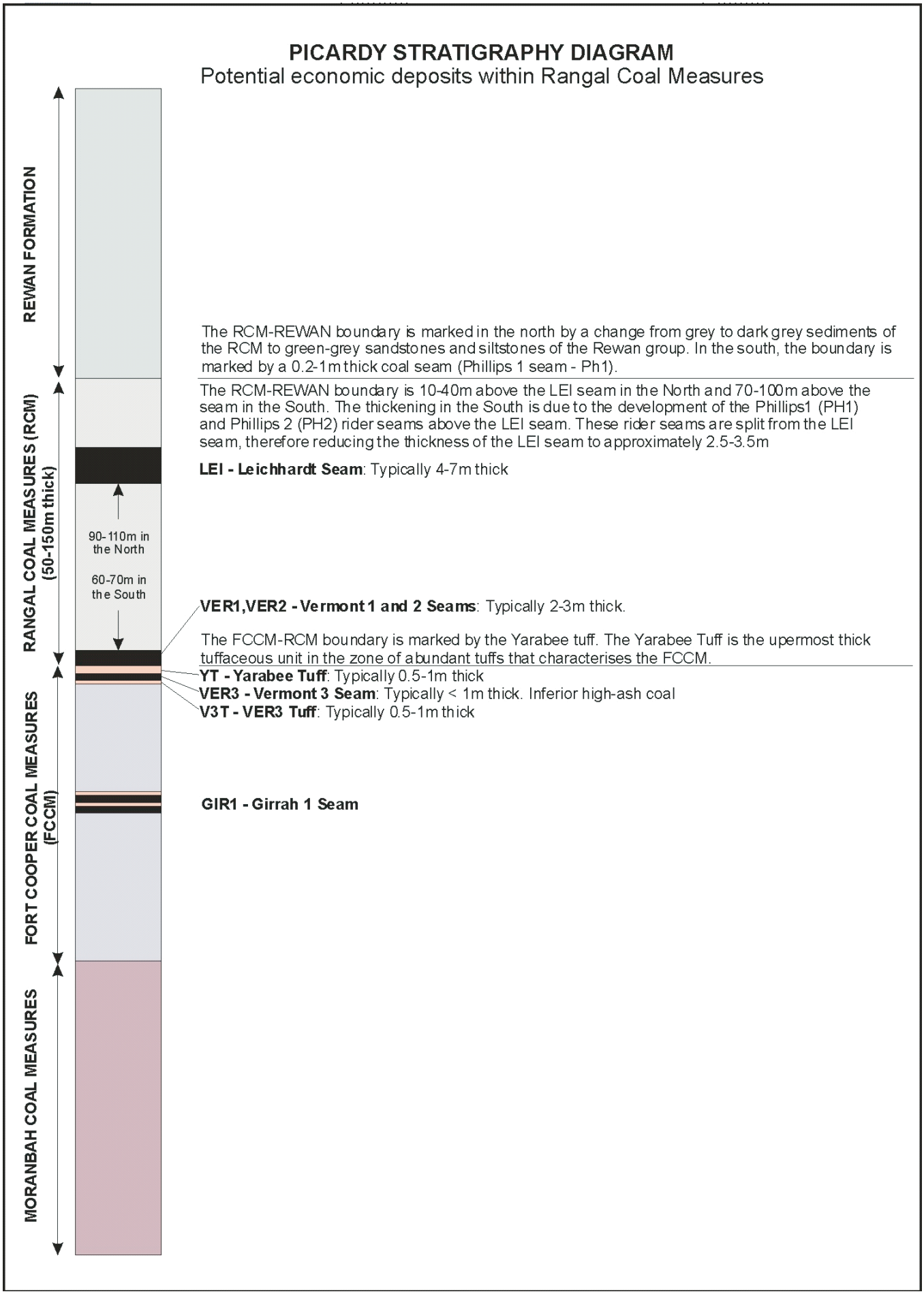

Figure 4: Stratigraphy

Depth of weathering averages 42m below topography and is typically 10–30m below the base of the Tertiary cover. In the north and south of the EPC weathering is around 50m deep but it tends to be shallower in the central region with a minimum of 14m.

The Permo-Triassic sequence comprises, from youngest to oldest, the Rewan Formation, the Rangal Coal Measures (RCM) and the Fort Cooper Coal Measures (FCCM). The potentially economic coal seams are confined to the RCM. The FCCM have a vertical thickness of approximately 400m and crop over the east and west of the Jellinbah Fault. The seams of the FCCM are typically thick, tuff-banded horizons containing numerous thin, high inherent ash coal plies.

The Rewan Group sediments were deposited in a fluvial floodplain environment and comprise green sandstones and siltstones, and red and green mudstones. The basal formation of the Rewan Group, the Sagittarius Sandstone, conformably overlies the RCM. The RCM comprises grey sandstones and siltstones with minor mudstones and two potentially commercial coal seams, the 3–6m thick Leichhardt seam and the 2–3m thick Vermont Upper seam.

The Vermont Upper seam directly overlies the Yarrabee Tuff Bed (YT), a basin-wide unit that marks the last major ash-fall event in the Permian sediments of the Bowen Basin. In Picardy, the YT is typically a 0.5–1.0m thick, grey to brownish-grey, tuffaceous mudstone. The boundary between the RCM and the FCCM is placed at the top of the YT.

Structure

Structure is dominated by the north-north-west trending Jellinbah and Foxleigh thrust faults, which are located 6km to 8km apart (Figure 3).

Between the Jellinbah and Foxleigh Faults at the southern end of the deposit, sediments of the FCCM and the overlying RCM dip gently east at approximately 10°; but are dragged up against the Foxleigh Fault. Further north, the sediments have been folded into a series of broad anticlines and synclines with a north northwest strike and a gentle plunge to the south. The RCM subcrop along the steeply dipping eastern limb of one of these anticline; but subcrop again to the east across the crest of a second anticlinal/domal structure. The dip at the western subcrop of the RCM can be very steep in some places (up to 35°), as interpreted from seismic sections. In the centre of the EPC there is a zone of reverse faulting which has raised the Leichhardt and Vermont seams close to the surface.

Intrusives

A number of holes have intersected feldspar porphyry (monzonites) and basaltic intrusives of Cretaceous to Tertiary which have intruded coal seams. The northern end of the EPC has zones of narrow intrusions which are indicative of dykes. Over other part of the EPC there are sills intruding coal seams which extend over 12km in strike length. The Vermont seam has been extensively intruded and coked by magmatic fluids, probably derived from the Middlemount Intrusive Complex, which crops to the west of Middlemount Township.

COAL SEAMS

There are four main coal seams in the RCM and upper FCCM at Picardy, the Phillips, Leichhardt, Vermont and Girrah Upper seam. Numerous other seams have been intersected within the FCCM that underlie the RCM. However, the FCCM seams are heavily stone-banded and have no economic potential. Figure 5 shows a schematic cross section from west to east across the EPC.

At the northern end of the EPC and across the crest of the Picardy Anticline, the Phillips and Leichhardt seams are separated by less than 1m of mudstone. The Phillips seam is 0.5m thick and the Leichhardt seam is 5m to 6m thick. In the southern part of the EPC the Phillips Lower seam splits away from the Leichhardt seam and reduces the Leichhardt seam thickness to 2.5–3.5m. The Leichhardt seam is a clean, dull coal that displays sharp roof and floor contacts and a uniform profile in geophysical logs. The interburden between the

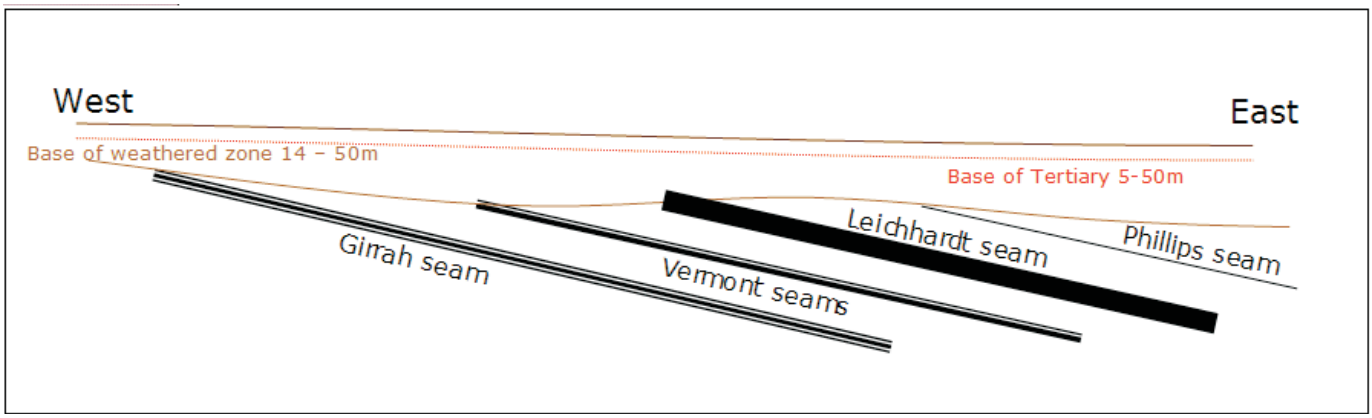

Figure 5: Schematic cross-section

Phillips and Leichhardt seams thickens progressively from north to south, up to 90m near Middlemount.

The Vermont seam splits into the 2–3m thick Vermont Upper seam and the Vermont Lower seam and is separated by the Yarrabee Tuff. Over most of the EPC, the Vermont Upper seam can be further subdivided into a low-ash upper ply and a higher ash lower ply. In some parts of the EPC the Vermont Lower seam thickens and improves to be of equivalent quality to the Vermont Upper seam.

The Yarrabee Tuff (YT) is a basin-wide unit that marks the last major ash-fall in the Permian sediments of the Bowen Basin. In Picardy, the YT is typically a 0.5m to 1m thick, grey to brownish-grey tuffaceous mudstone. The boundary between the RCM and the FCCM is located at the top of the YT.

The Vermont Lower seam is located directly below the YT. The seam usually comprises less than 1m of inferior, high-ash coal, but in some areas, there is an additional development of up to 3m of coaly and carbonaceous material. A tuffaceous unit occurs within 1m below the base of the normal Vermont Lower seam.

The Girrah Upper seam, which has split from the main Girrah seam throughout Picardy, comprises four bands; roof tuff, coal band, tuff and shaly coal. The four units are recognisable as the upper units of the thick Girrah seam that occurs elsewhere in the northern Bowen Basin. The Girrah seam has no economic potential, but has a distinct geophysical profile and has proved invaluable in stratigraphic correlation throughout Picardy.

Table 1: Raw coal analysis

Seam	Phillips	Leichhardt	Vermont Upper 1	Vermont Upper 2	Vermont Lower
Thickness (m)	0.80	4.20	1.06	1.29	0.93
Inherent Moisture (%adb)	1.5	1.5	1.1	1.4	1.3
Ash (%adb)	42.0	14.8	18.6	23.5	38.6
Volatile Matter (%adb)	13.9	12.5	13.0	11.4	12.8
Fixed Carbon (%adb)	42.7	71.3	67.3	63.6	47.3
Sulphur (%)	0.15	0.41	1.16	0.37	0.24
Chlorine (%)	0.03	0.06	0.05	0.05	0.05
Phosphorous (%)	0.027	0.075	0.213	0.123	0.101
Specific Energy (Kcal/kg)	4314	6991	6771	6359	4745
Note: The Phillips seam includes interburden material					

Potentially economic resources in Picardy are restricted to the Leichhardt and Vermont Upper seams of the RCM.

COAL QUALITY

Indicative coal quality for the most prospective seams can be seen in Table 1.

CONCEPTUAL MINE STUDY

Within the Picardy EPC two potentially economic targets have been defined, the Blackwood and Cosmos deposits. A Resource Development Plan has been prepared for Blackwood (Figure 6). This area was the focus of an exploration drilling program from July 2003 to February 2004 to generate sufficient geological data for evaluation. The Cosmos deposit is approximately 3km north-east of the Blackwood deposit and will be investigated once drilling in the area is completed.

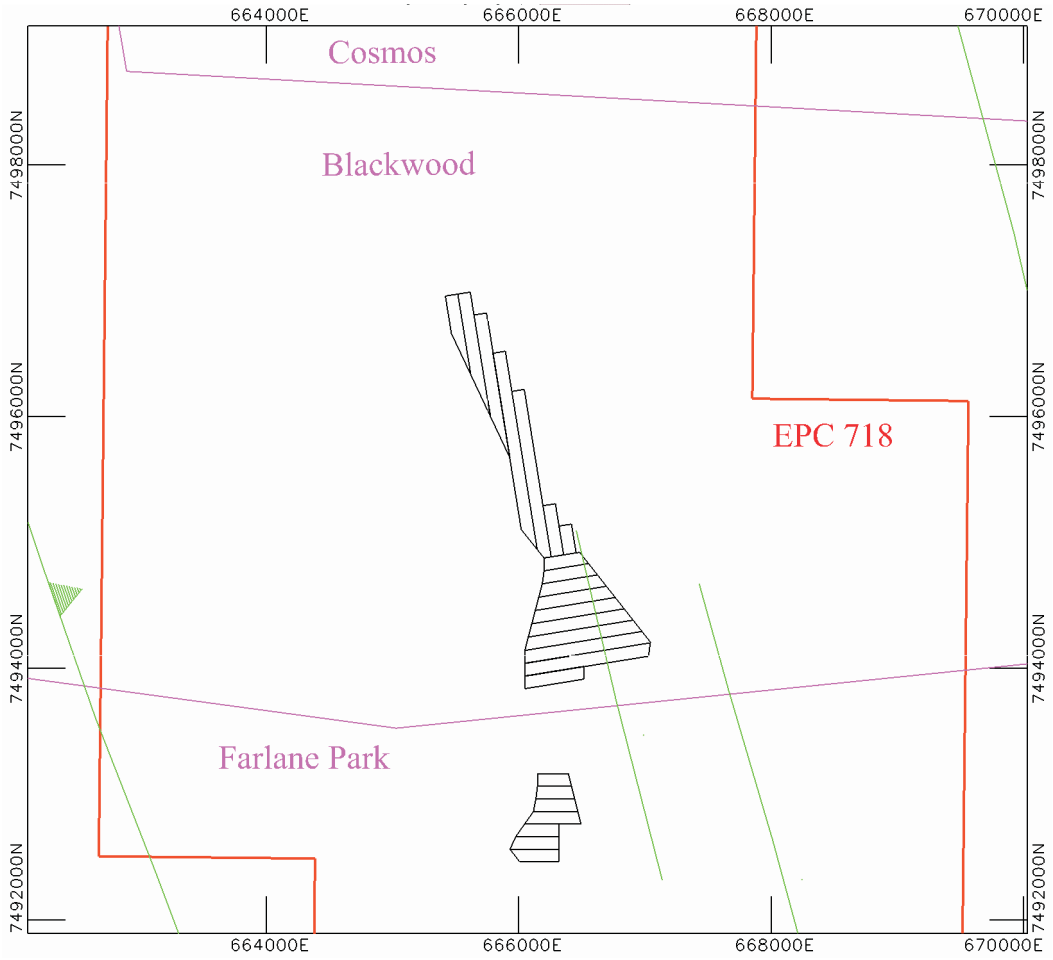

Figure 6: Concept pit design for Blackwood

The Blackwood deposit is characterised by steep dips in the north, disturbed by a series of reverse faults in the central area. The western side of the deposit is oxidised and an intrusion in the southern sector has coked some of the coal. In the south-east of this deposit there is also some complex faulting. The Leichhardt seam was the target seam with thickness ranging from 4m to 7m. The Vermont seam occurs below the Leichhardt seam at a depth of about 90m and has potential economic value towards the subcrop areas. It has a thickness of 2–3m, but due to a lack of infill drilling it was not included in the study.

Reserves of 8.0 million product tonnes have been defined and the economic strip ratio is 8 to 1. A truck and shovel operation is the planned stripping method due to its flexibility and capacity to effectively maximise the recovery of the potentially sheared and dipping coal seam.

FUTURE PROSPECTS

Further work is planned to investigate complex geological structures to the north of the EPC as well as locate any potential economic targets in the south of the EPC. More drilling is needed to define the potentially economic Cosmos area as well as collect seam quality information. The Blackwood area has had some more recent drilling in 2005 which will needed to be evaluated in an updated concept mining to determine whether it should move to a prefeasibility level.

REFERENCES

CLARETE, G., 2004: Picardy Resource Development Plan – Business Planning & Optimisation/Geological Services August 2004. Confidential report to BMA Coal Operations.

FRATER, D., 2004: EPC 718 – Picardy, Report for the 12 Months ending 25 September 2004. Statutory Report (Closed File) to the Qld Dept of Natural Resources and Mines.

O'REILLY, K.W., 2000: EPC 718 – Picardy, Data evaluation and Target Generation Report. Confidential report to BMA Coal Operations.

O'REILLY, K.W., 2001: EPC 718 – Picardy, Report for the 12 Months ending 25 September 2001.Statutory Report (Closed File) to the Qld Dept of Natural Resources and Mines.

O'REILLY, K.W., 2002: EPC 718 – Picardy, Report for the 12 Months ending 25 September 2002. Statutory Report (Closed File) to the Qld Dept of Natural Resources and Mines.

O'REILLY, K.W., 2003a: EPC 718 – Picardy, Report for the 12 Months ending 25 September 2003. Statutory Report (Closed File) to the Qld Dept of Natural Resources and Mines.

O'REILLY, K.W., 2003b: EPC 718 – Picardy, Report for the 12 Months ending 25 September 2003. Statutory Report (Closed File) to the Qld Dept of Natural Resources and Mines.

Aaron Donelan, BHP Billiton Mitsubishi Alliance (BMA)

THE RIDGELAND COAL DEPOSIT

LOCATION

The Ridgeland coal deposit is located some 20 to 25km north-east of Injune and 120km north of Roma in southern Queensland (Figure 1). Roma is approximately 400km west of Brisbane.

Nearest railhead to Gladstone is Theodore, 200km to the east, with Gladstone a further 240km distant. Should the inland rail from Gladstone be extended to pass through Taroom in the future, an additional 110km of track would be needed to reach Ridgeland.

TENURE

Exploration Permit for Coal (EPC) 851 Ridgeland of 107 Sub-blocks was granted to the BHP Billiton Mitsubishi Alliance (BMA) for a period of two years from 16 March 2004.

EXPLORATION

The existence of thick coal seams at relatively shallow depth has been known at Ridgeland since the drilling of oil well OSL Hutton Creek 2 over the period 1935 to 1938 (Crespin, 1945). Coal intersections comprised:

- 7.6m at 274.3m
- 2.7m at 334.1m
- 10.1m at 407.5m
- 1.5m at 469.4m.

In 1975–76 the government drilled a stratigraphic bore, GSQ Taroom 11/11A, to further investigate these coal occurrences (Heywood, 1977). The bore intersected Surat Basin sediments to 109m, Permian Peawaddy Formation to 126m, Ingelara Formation to 270m and Reids Dome beds to total depth. Thick coal seams were noted in the Reids Dome beds, including a 5.1m seam at 298.7m depth and a 12.5m seam at 426.5m. Four seams greater than one metre occurred between 290 and 490m depth.

Analyses of the two thicker seams showed the coal to be high volatile bituminous in rank (Ro max 0.60–0.85%) and low in raw ash (10.5–13.9% ad) (Johnston, 1077). With CSN's of 1.5 to 4, a high energy by-pass thermal coal or a weak coking coal could be possible products.

EPC 279 Arcadia was granted to Otter Exploration NL for a two year period from 27 December 1979. Target for exploration was coal within the Hutton Sandstone, Walloon Coal Measures and Evergreen Formation of the Surat Basin sequence, as well as coal within the Permian Reids Dome beds. Hole AR-1 was completed 10km south-east of GSQ Taroom 11/11A in an attempt to trace the thick coal seams found in OSL Hutton Creek 2 and GSQ Taroom 11/11A (Bichard, 1981). The hole penetrated Precipice Sandstone to 74m, then Ingelara Formation, before entering Devonian basement metasediments of the Timbery Hills Formation.

To aid in the understanding of geological structure over the 10km strip, a high resolution Mini-Sosie seismic survey was commissioned. Approximately 18km of seismic was acquired over eight overlapping lines (Birchard, 1982). A number of reflectors were apparent in some areas (see Figure 2), but the seams within OSL Hutton Creek 2 and Taroom 11/11A presented poorly. An interpretation at the time put the more prominent reflectors in the Triassic and Jurassic. Nonetheless, hole AR-10 was drilled targeting a group of strong reflectors some 4km south of Taroom 11/11A.

Hole AR-10 intersected around 10m of poor quality coal over a 22m interval from 164m depth within what was believed to be the Boxvale Sandstone Member of the Evergreen Formation. The hole terminated at 194m in supposed Moolayember Formation.

A more recent review of regional structure, reinterpretation of the Otter seismic profiles and a reassessment of strata found in holes AR-1 and AR-10, led to the conclusion that the

Figure 1: Locality Map

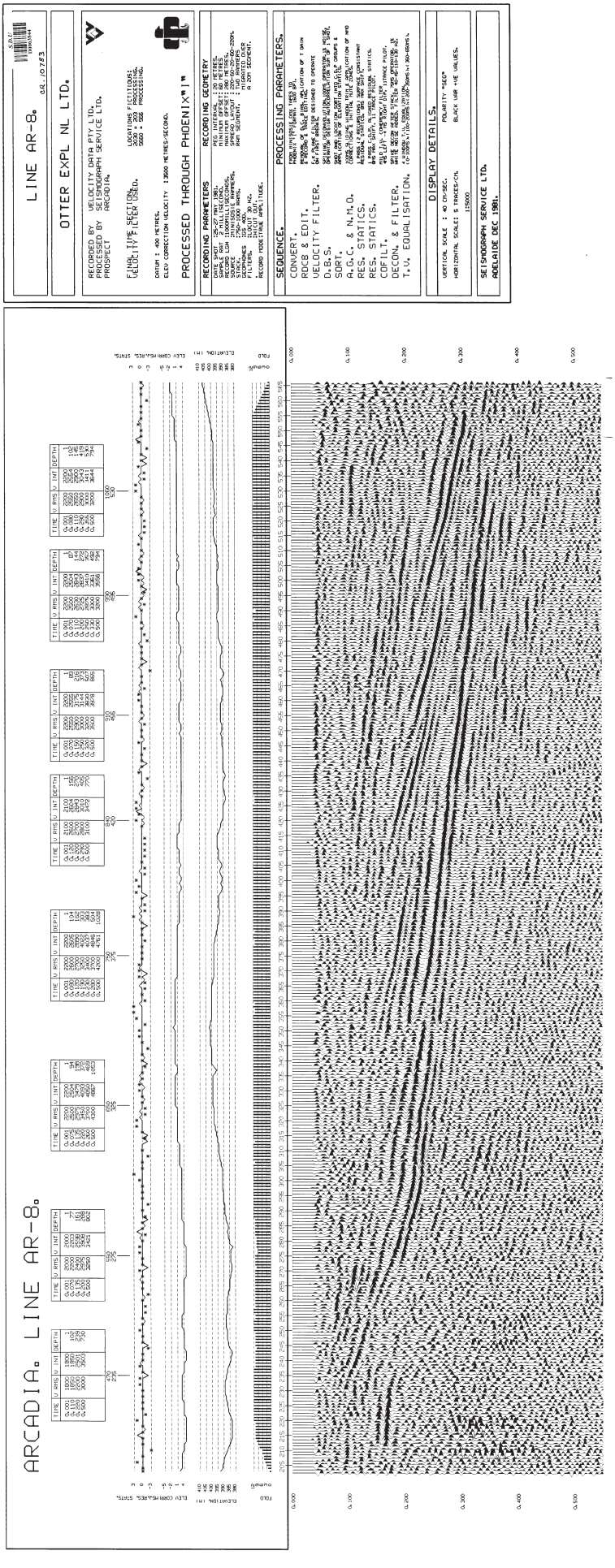

Figure 2: Otter Seismic Section AR-8

package of thicker seams in the Reids Dome beds can in fact be traced at relatively shallow depth across the 10km distance from OSL Hutton Creek 2/Taroom 11/11A, preserved within a thrust block below Surat Basin cover. It was believed potential existed for a large open cut coal deposit of several hundred million tonnes. Shallowest coal could be expected beneath surface exposures of Precipice Sandstone, the basal unit of the Surat Basin, which is typically 70 to 90m thick. An application was subsequently lodged for a new EPC at Ridgeland.

Exploration during the first year of tenure of EPC 851 involved a compilation of previous exploration data, especially seismic surveys, a photogeological study and the drilling of ten open holes and one part cored hole, the latter for coal quality determination. The photogeological interpretation and drill hole locations are shown in Figure 3.

The results confirmed, through palynology, that the coal-bearing strata were Reids Dome beds, and showed that thick coal seams can be traced to the south-east, reaching a maximum combined coal thickness of 41.1m (Figure 4), but that coal quality had deteriorated away from OSL Hutton Creek 2/Taroom 11/11A.

GEOLOGY

Regionally, Ridgeland is located at the northern margin of the Surat Basin, with the Jurassic sequence gradually thickening southwards, masking sediments of the underlying Bowen Basin. The Bowen Basin sediments lie within the Denison Trough near its transition to the Comet Platform in the east and the Roma Shelf in the south.

The Hutton-Wallumbilla flexure zone is the current surface expression, through minor late stage adjustment, of a much more significant west-vergent thrust that dislocated the Bowen Basin sequence in the Late Triassic. A throw of 1.0 to 1.5km is indicated. The Triassic and Permian succession on the upthrust block was eroded immediately adjacent to the thrust prior to deposition of the Surat Basin. Dips within the Permian strata at Ridgeland are to the north-east, with angles of about 15º in the Reids Dome beds.

The stratigraphy of the Ridgeland area is summarised in Table 1.

Table 1: Ridgeland Stratigraphic Summary

Age	Basin Sequence	Formation
Jurassic	Surat	Birkhead Formation
		Hutton Sandstone
		Evergreen Formation
		Precipice Sandstone
Early Triassic	Bowen	Rewan Formation
Late Permian		Bandanna Formation
		Peawaddy Formation
		Ingelara Formation
Early Permian		Reids Dome beds
Devonian	Basement	Timbery Hills Formation

The Devonian Timbery Hills Formation, a unit of hard, silicified quartzose sandstone with lesser interbedded siltstone, occurs as basement to the Bowen Basin sequence in the Ridgeland area.

The Reids Dome beds, the major target of current exploration, is a thick sequence of siltstone, sandstone, mudstone, carbonaceous shale, coal, conglomerate and ironstone, in excess of 900m thick in GSQ Taroom 11/11A. The unit was deposited in generally half-graben rift features at the base of the Bowen Basin sequence within the Denison

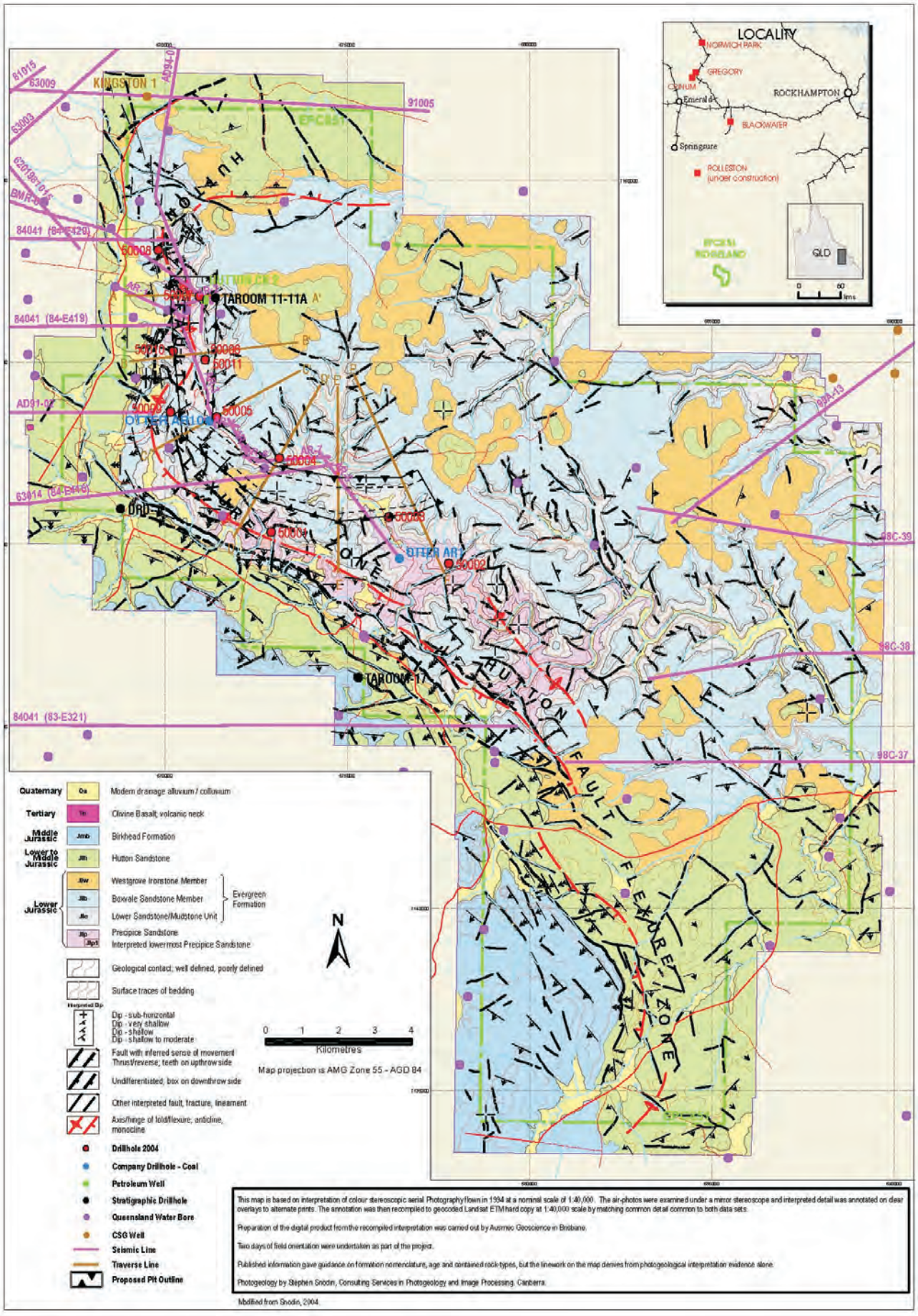

Figure 3: Geology and Hole Locations

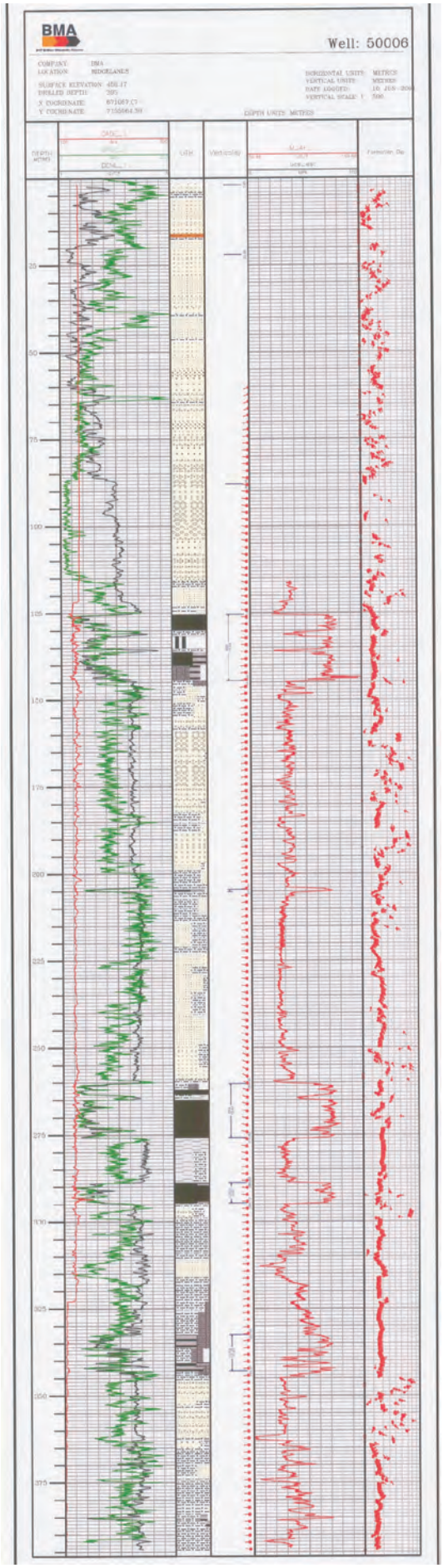

Figure 4: Graphic Log and Geophysics for Hole RDG 50006

Trough. Rapid seam thickness changes and splitting are characteristic, and thick seams have developed locally.

The Ingelara Formation at Ridgeland unconformably overlies the Reids Dome beds and consists of around 140m of siltstone, mudstone, shale, sandstone, minor coquinite, tuff and conglomerate. The more usual Early Permian succession above Reids Dome beds, the Cattle Creek Formation, Aldebaran Sandstone and Freitag Formation, are not present at Ridgeland.

The Peawaddy Formation in GSQ Taroom 11/11A is only 17m thick. It appeared conformable on Ingelara Formation, but its top was eroded and is now overlain directly by the Precipice Sandstone. It is represented by a light grey green very fine sandstone.

The Precipice Sandstone is the basal unit of the Surat Basin, mostly 70 to 90m thick, and comprises mainly medium to coarse quartzose sandstone with minor silty mudstone. It is a major aquifer.

The Evergreen Formation is around 150m thick, and comprises a sandstone–mudstone base, overlain by the 'Boxvale Sandstone Member', a scarp-forming subunit, and the Westgrove Ironstone Member. It is conformable on Precipice Sandstone.

COAL SEAMS

The results of recent drilling confirm that thick coal seams extend within Reids Dome beds at moderately shallow depths to the south-east over a distance of 10km away from the site of OSL Hutton Creek 2 and Taroom 11/11A. The thick seams are contained within a 200m stratigraphic interval, and dips of around 15º are indicated. Closest approach to surface varies from 100 to 150m.

Cumulative coal seam thicknesses at the site of the oil well and stratigraphic hole, and at successive sites at approximately 2km spacings to the south and then east are:

- 21.6m in GSQ Taroom 11/11A
- 41.1m in RDG 50006/50011
- 36.4m in RDG 50005
- 31.6m in RDG 50004.

Four main coal horizons are recognised, in down-hole order named Airlie, Binnaway, Coolah and Dunnedoo seams.

The coal seams thicken away from OSL Hutton Creek 2 and Taroom 11/11A, but also deteriorate, with the inclusion of multiple partings.

Gas testing on one hole showed that the coal seams contain very little coal seam gas.

COAL QUALITY

At GSQ Taroom 11/11A, a raw, high energy thermal coal could be produced full seam from the two main seams that were analysed. A high yield, high volatile semi-soft could also be expected.

Preliminary results from RDG 50011, the only other hole so far analysed, show deteriorated seams but greater cumulative seam thickness. A 9% ash high volatile semi-soft coking coal may be obtainable at 50% yield by selective mining of the better coal plies, being a combined working section of around 25–30m. Alternatively, a high-energy export thermal coal at 15% ash may be won from the full coal thickness, but again yield would only be around 50%.

Indicative properties of a potential semi-soft product could be CSN 3, volatile matter 36% air dried (ad), sulphur 0.90% ad, phosphorus 0.050% dry basis, vitrinite 70%, Ro max 0.60–0.80%, ash basicity index 0.11. Fresh samples have yet to be tested for plastic properties.

An export thermal product would have around 36% ad volatile matter, moisture 3.5% ad, sulphur 0.85% ad, calorific value 6,500 kcal/kg ad, nitrogen 2.0%, HGI 50 and an ash fusion temperature of 1500ºC initial deformation, reducing atmosphere.

RESOURCES

Coal resources that may be amenable to open cut mining have been estimated on the basis of recent drilling, old petroleum and stratigraphic wells and seismic lines. Down-dip limit for potential open cut coal was taken as 15:1 vertical clean coal strip ratio (bcm/t) for a potential semi-soft product. Open cut coal resources to an inferred level of confidence are estimated to be 203Mt.

REFERENCES

BICHARD, A.N., 1981: Authority to Prospect 279C Arcadia, Six Monthly Report for the Period Ended 26th June, 1981. Held by the Queensland Department of Natural Resources and Mines as CR9505.

BICHARD, A.N., 1982: Authority to Prospect 279C Arcadia, Six Monthly Report for the Period Ended 26th December, 1981. Held by the Queensland Department of Natural Resources and Mines as CR10783.

CRESPIN, I., 1945: The Hutton Creek Bore, Queensland. *BMR Report* **1945/14**.

HEYWOOD, P.B., 1977: Stratigraphic Drilling Report — GSQ Taroom 11-11A. *Queensland Government Mining Journal*, **78**, 624–629.

JOHNSTON, B.K., 1977: Petrological Study of Coal Seams in GSQ Taroom 11-11A. *Queensland Government Mining Journal*, **78**, 630–633.

SNODIN, S., 2004: Photogeological Interpretation of the Ridgeland area, Queensland, for BM Alliance Coal Operation Pty Ltd. BMA Library Consultants Report.

R.N. Cranstoun, Cranstoun Geological Pty Ltd

Nick Gordon and Elliot Tembo

The roof strength index — a simple index to one possible mode of roof collapse

Depending on the rock strength, the bedding and joint structure, and the imposed horizontal stresses, a coal mine roof can fail and collapse by a range of mechanisms — delamination, joint bounded block collapse or overall compressive failure. In the Bowen Basin coal measures, comparatively low roof strengths at shallow depth, result in some longwall operations being particularly exposed to overall compressive failure. In this failure mode, mining induced fractures can extend above the height of the primary roof bolting and can define large volumes of rock that can only be supported with either standing or long-tendon support.

This paper presents a simple way of identifying this overall compressive hazard in exploration programs so as to allow adequate planning of ground support. It is emphasised that this compressive failure mode is only one of several failure modes that need to be assessed in a strata hazard management plan.

FAILURE OF INTACT ROCK AND ROCK MASSES

Common practice in examining strata failure around coal mine roadways is to use numerical codes to determine the redistribution of stresses around an opening and to compare these stresses with the strength of the rocks. Most commonly, the Mohr-Coulomb failure criterion is employed. When laboratory strength values are used, failure around roadways is often not indicated. It is common practice to reduce the laboratory unconfined compressive strength values by 50–60% so as to better represent the strength of the rock mass.

The strength of rock masses continues to receive attention, with the most recent development being the formalisation of a method to assess the strength of rock masses based on the laboratory strength and the Geological Strength Index (Hoek & Brown, 1997). An important point to note is the direction by the authors not to use it for problems where the geometric scale of the problem is similar to the spacing of the discontinuities — it is contended that this embargo includes the coal mine roof problem.

Workers in Canada (Martin & others, 1999) have proposed an approach estimating the height of roof falls developed above excavations on the assumption that the rock behaves in a brittle fashion. Their work has indicated that the use of the Hoek-Brown and Mohr-Coulomb compressive failure criteria can be misleading for situations where failure develops in a brittle fashion. They recommend the use of 'brittle' rock parameters in the Hoek-Brown criterion — m = 0, s = 0.11. One of their case studies included sedimentary strata similar to coal measures, and it is contended that such parameters may also be used for coal mine applications.

Figure 1 is reproduced from their paper. This shows the height of brittle failure as a function of the shape of flat topped roadways and the ratio of the far-field major principal horizontal stress to the UCS of the rock; the height of failure is normalised to the roadway width.

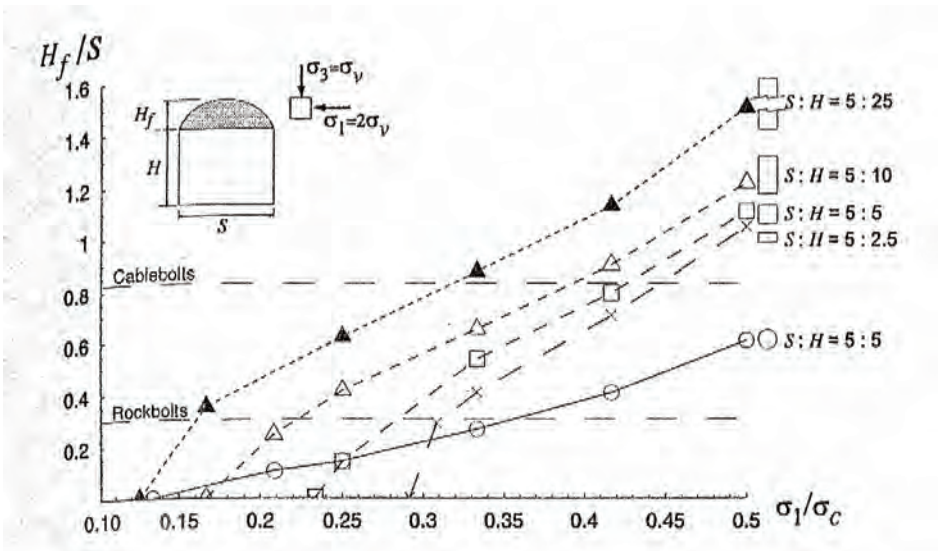

Figure 1: The relationship between failure height and the stress/strength ratio in homogeneous brittle rock (Martin & others, 1999)

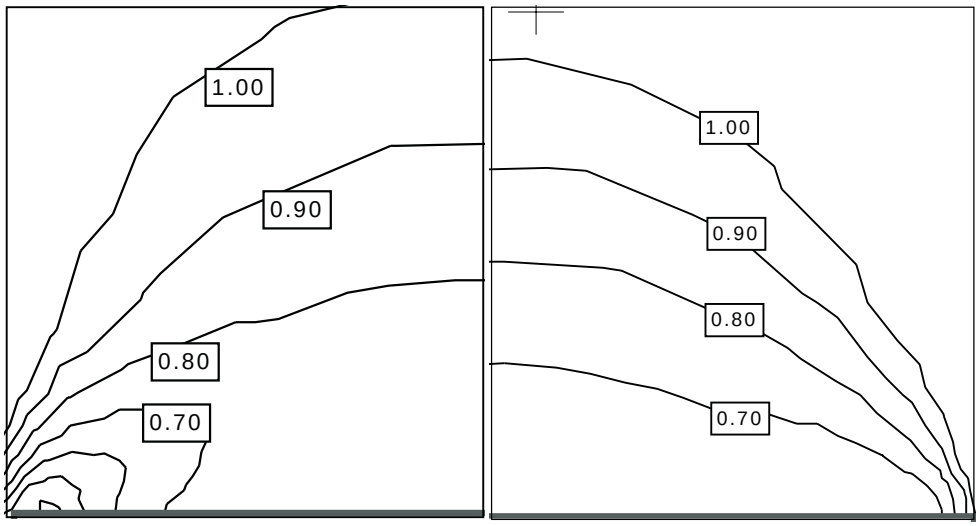

Figure 2: Comparison of failure zones defined by the strength factor between brittle parameters and reduced Mohr-Coulomb parameters.

As an example, we have modelled a roadway around a typical coal mine roadway — 10MPa isotropic material, 4.8m wide and 3.3m high roadway, depth of 200m and a horizontal stress being twice the vertical. A Phase2 analysis using the brittle rock parameters (m = 0, s = 0.11) reproduces the shape and location of 'guttering' better than a Mohr-Coulomb criterion. It is noted that to achieve a similar magnitude of strength factors around the roadway, the unconfined compressive strength had to be reduced to 2.8MPa (Figure 2).

Using the same approach as Martin & others (1999), it is possible to determine a relationship between the height of failure above the modelled roadway and the ratio of the unconfined compressive strength and the far field horizontal stress (Figure 3). There are slightly different curves for different horizontal to vertical stress ratios. Note that the height of failure goes above typical bolt lengths at ratios less than about 3.

From a ground support perspective, the height of failure can be used to determine the capacity and length of long tendon support.

ROOF STRENGTH INDEX

From inspection of Figure 3, it is readily apparent that the ratio of the unconfined compressive strength to the far field horizontal stresses resolved into the plane of the excavation ($UCS/ó_h$) is of fundamental importance to roof support planning.

An index of roof performance can be derived from the estimated strength of the roof and the estimated horizontal

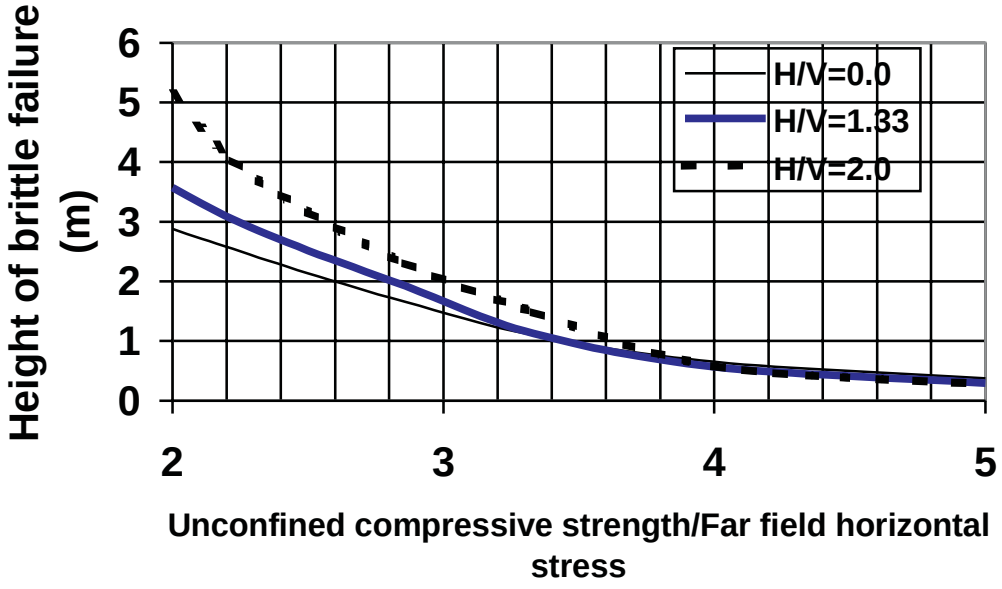

Figure 3: Onset and height of failure as a function of unconfined compressive strength and far-field horizontal stress.

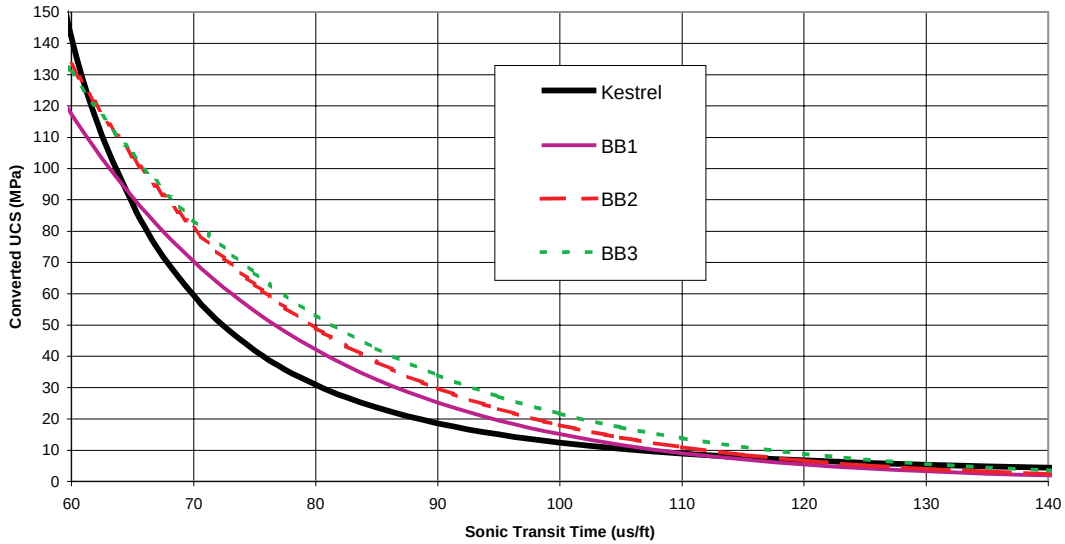

Figure 4: Comparison of the Kestrel sonic velocity/strength regression compared with 3 alternative equations used in Bowen Basin Mines

stress applied to the roof. Whilst the UCS is fixed, the magnitude of the horizontal stress acting across a roadway can vary, depending on the alignment of the roadway with respect to the horizontal stress field.

Consider the relationship:

$RPI = UCS/ó_h = RSI/SCF$

RPI = Roof Performance Index = $UCS/ó_h$
RSI = Roof Strength Index = $UCS/ó_v$
SCF = stress concentration factor = $ó_h/ó_v$

A SCF can be calculated for development as well as for retreat. In Australian coal measures, *in situ* stress measurements consistently show that the principal horizontal stress is about 1.5–2.5 times the vertical stress. Furthermore, it is known that there is a concentration of stresses around a retreating longwall face, and this is quoted as a change with respect to the *in situ* horizontal stress. Thus all the horizontal stresses that develop around a roadway can be related by some combination of multiples of the vertical stresses.

It can be readily appreciated that:

$SCF = K_h * K_o * K_l$

K_h = ratio of initial horizontal to vertical stress (typically in the range of 1.5-2.5),
K_o = factor to account for orientation of the roadway to the principal horizontal stress direction (development), and
K_l = longwall stress concentration factor.

It is not clear from the work of Matthews & others (1992) and subsequent workers if the stress concentration factor reported by them includes the resolution of the stresses across the roadway (is it K_l or K_l*K_o in the terminology of this paper). It will be assumed that it is simply the magnitude of the major principal horizontal stress, and hence needs to be resolved across the roadway — the problem being that the direction of the stress is not known.

It is assumed that around the retreating longwall there are similar changes in the vertical stress magnitudes so that the ratio of the vertical to horizontal stress remains similar. The validity of this assumption is not known, and is one reason why calibration to site conditions is required.

From Figure 3 the following provisional interpretations of the Roof Performance Index are proposed:

- RPI > 3.5 — roof performance controlled by bedding spacings
- 2.8< RPI <3.5 — primary roof bolting needed to build thick beams – bolt anchorage above brittle failure
- RPI < 2.8 — compressive failure of roof above the bolted horizon - secondary support required.

APPLICATION

The Roof Strength Index can be estimated from standard geophysical logs of sonic and density. The sonic velocity log is converted to an indicated rock strength log using published or site-specific relationships. Note that for this application, the quality of the sonic velocity/rock strength becomes particularly important. Sonic log derived estimates of strength can vary by up to 100 % depending on the regression used (Figure 4) and may represent the greatest level of uncertainties in the RSI process. The vertical stress is estimated from the depth and an average density of the overlying strata from the density log.

The Stress Concentration Factor will vary from site to site and may require a high level of geotechnical expertise to

determine a value from first principles. For a current operation with some history of roof instability, the actual value of the SCF is not critical, as a back analysis will readily show what value of the RSI is critical.

The use of sonic-derived roof strength for hazard mapping in the Bowen Basin has been published (Gordon, 2000, 2002). This continues to work well on a panel basis, where large changes in horizontal and vertical stress usually do not occur. The simple conversion of the roof strength to RSI provides greater insight into the fundamental mechanism and allows consideration of the impact of changes in mining direction or the mining in new areas, where depths are significantly different.

CALIBRATION STUDY — KESTREL

Kestrel is currently longwalling the German Creek Seam in the 300 series area at depths between 200 and 310m. Previous extraction occurred in the 100 and 200 series areas at similar depths of cover (Figure 5).

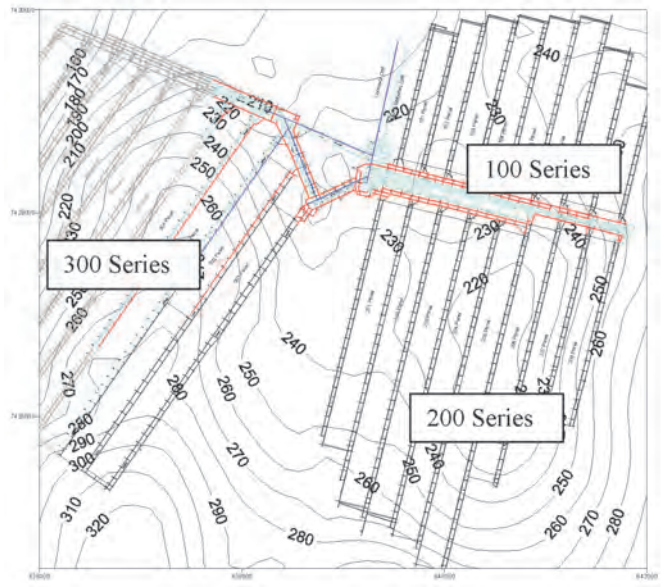

Figure 5: Depth of Cover

Measurements across the lease in conjunction with underground observations indicate the principal horizontal stress is in the range of 35–40° (SCT Operations, 2001) with K_h values of 1.2 for the minor principal horizontal stress and 1.6 for the major principal horizontal stress. With this information the stress concentration factor can be calculated for development and longwall extraction for the three mining areas, as tabulated in Table 1.

The distribution of the primary roof strength as derived from the sonic velocity over the first 2m of roof, is shown in Figure 6. Mining has been carried out at a range of values from <15MPa to >35MPa. The strengths have been determined using the Kestrel site correlation of:

$$UCS = 0.3196 * e^{(0.0012 * \text{sonic velocity (m/sec)})} \ MPa$$

Utilising this strength data and depth of cover (converted to vertical stress with reference to the density log) the Roof Strength Index can be calculated, as shown in Figure 7.

Figure 7 highlights areas of likely poor roof performance in the 100 series panels with RSI values mostly less than 2.5. From Table 1 the threshold value for the onset of compressive failure is 4.5. Many areas of the 100 series Maingates were heavily supported with secondary cables on advance, as shown in Plate 1.

For the 200 series panels, the roof strengths were higher and the stress concentration factors are lower because the orientation and retreat direction was such that the minor horizontal stress was concentrated in the Maingate corner. RSI values are mostly greater than 3.5. The theoretical threshold value is 3.9 on development and 7.5 on retreat. Secondary support was not needed on development (Plate 2) and only the outbye areas of these blocks where the RSI decreases towards 3.5 was secondary cabling required near the maingate/face area.

The 300 series layout seeks to minimise the horizontal stress concentrations in the roadways. Most of the area has Roof Strength Index values of greater than 3.0. The threshold values for the roof strength index on development are 3.6.

Table 1: Theoretical Stress Concentration Factors

	100 Series	200 Series	300 Series (LW302 -)
Component acting on Maingate	Major	Minor	Major
Horizontal/vertical ratio K_h (minor/major)	1.2/1.6	1.2/1.6	1.2/1.6
Angle of gates to principal horizontal stress	30	30	10
Resolved horizontal stress/vertical stress $K_h * K_o$ = SCF (development)	1.5	1.3	1.2
Minimum RSI for development (RPI=3)	4.5	3.9	3.6
Matthews Stress Concentration Factor	1.7–2.1	1.7–2.1	1.5–1.7
SCF (longwall retreat)	2.8	2.5	1.9
Average minimum RSI for retreat (RPI=3)	8.4	7.5	5.8

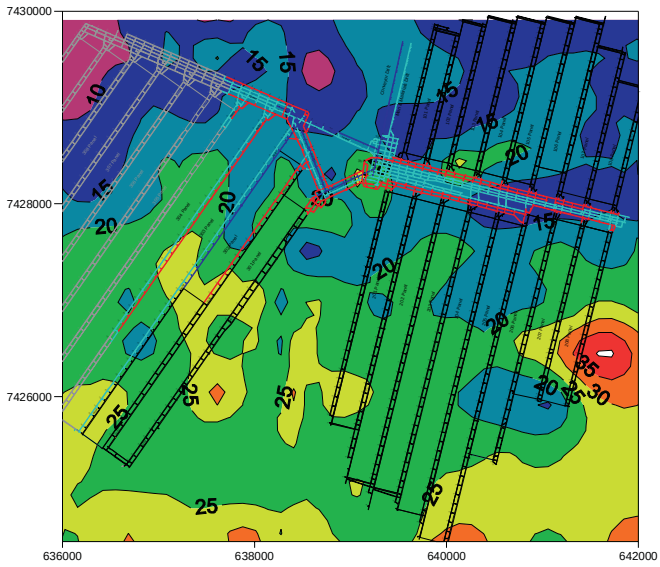

Figure 6: Primary Roof Strength

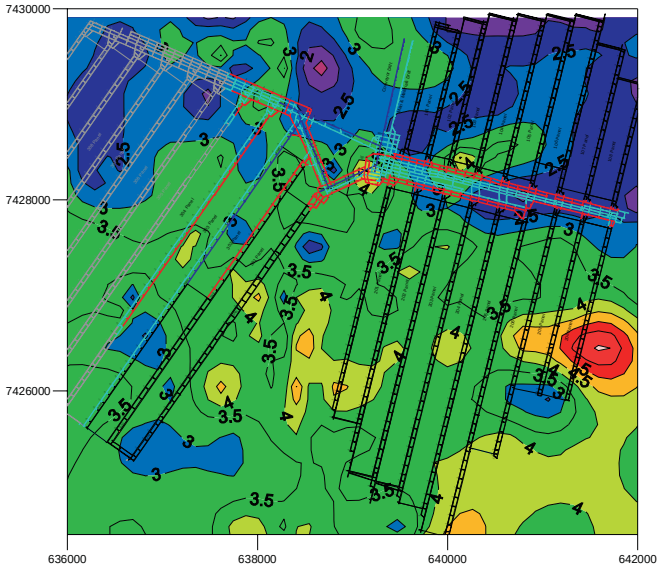

Figure 7: Roof Strength Index

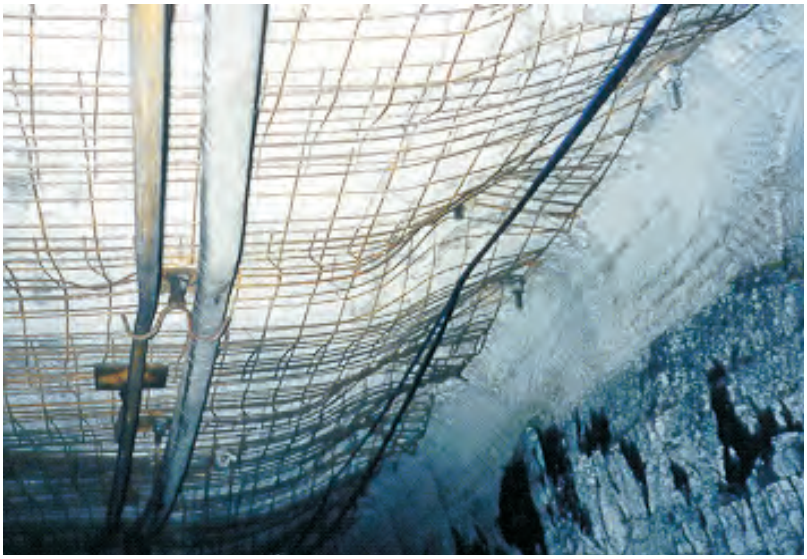

Plate 1: 100 Series Maingate (RSI <2.5, RPI<1.67 on development)

Plate 2: 200 Series Maingate (RSI > 4, RPI>3.1 on development)

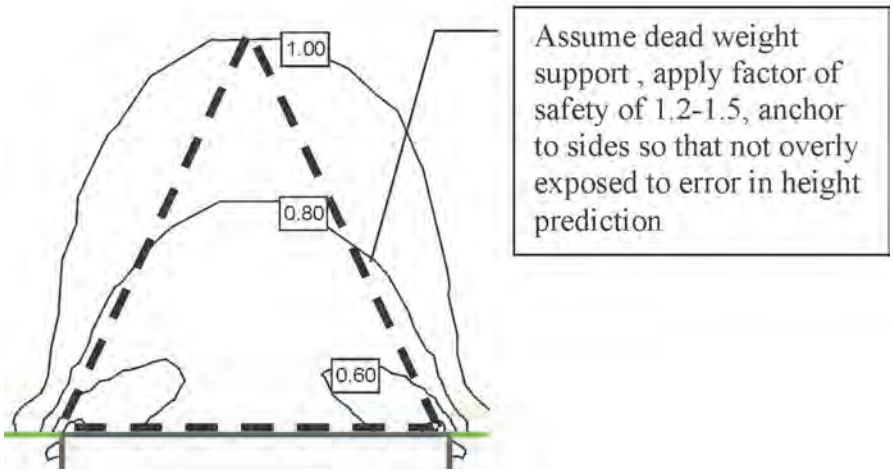

Figure 8: Shape of failure zone for a UCS/horizontal stress ratio of 2.0 showing possible fall wedge and design approach for long tendon support

No cables are required on advance, except in some of the cutthroughs. During the initial retreat of LW301 there was a maingate fall in an area where the RSI was approximately = 3.0. Kestrel now routinely installs cables prior to retreat in all maingates of the 300 series.

CONCLUSIONS

Roof Strength Index is a simple index that can be readily calculated and plotted. It should be included in all geophysical logging, and plotted as plans as input to support design. In-mine calibration to determine threshold values should be conducted as soon as possible. It is encouraging that there is reasonable agreement between the critical RSI values observed on development and those which can be derived from geotechnical principles — this should allow it to be used for hazard assessments in feasibility studies. Closer attention to the regression procedures used for the sonic log/strength relationship is required.

There is not good agreement between the index and the use of secondary support at the maingate corner. It is not known why this discrepancy exists — it suggests that the Matthews stress factors are too high — perhaps they represent a peak transient stress in a direction sub parallel to the gateroads.

Figure 3 suggests that the brittle parameters can also be used to estimate the height of falls and hence the length and capacity of cable supports. This has not yet been calibrated and is one of the objectives of the ACARP project run by University of Wollongong and Seedsman Geotechnics. Certainly, Martin & others (1999) argued that the brittle parameters gave a good estimate of the location and height of falls, even though the shape was not well represented. If this is the case for coal measures, then the RSI can be used as input into the design of secondary support (Figure 8).

Finally, it is stressed that brittle compressive failure is only one failure mode of coal mine roofs. For single seam operations with stone roof, delamination of thinly bedded strata, due to an insufficient density of bolts to resist shear, must be considered for roofs with a RPI greater than 3.

ACKNOWLEDGEMENTS

Ross Seedsman is thanked for introducing the concepts discussed in this paper to Nick Gordon whilst he was working at Kestrel. The authors wish to thank Kestrel Coal for their permission to allow the publication of this case study.

REFERENCES

MATTHEWS, S.M., NEMCIK, J.A. & GALE, W.J., 1992: Horizontal stress control in underground coal mines. *11th International Conference in Ground Control in Mining,* University of Wollongong, NSW, 289–296.

GORDON, N.G., 2000: Strata characterisation at Kestrel Mine. *Bowen Basin Symposium 2000*, 125–132.

GORDON, N.G., 2002: The development of hazard plans at Kestrel Mine. *AUSIMM 2002 Coal Operators Conference*, 159–168.

HOEK, E. & BROWN, E.T., 1997: Practical estimates of rock mass strength . *International Journal of Rock Mechanics, Mining Science & Geomechanics, Abstracts*, **34**(8), 1165–1186.

MARTIN, C.D., KAISER, P.K. & McCREATH, D.R., 1999: Hoek-Brown parameters for predicting the depth of failure around tunnels. *Canadian Geotechnical Journal*, **36**, 136–151.

SCT OPERATIONS, 2001: Kestrel western area geotechnical study.

SGPL, 2003: Estimation of mining conditions in the updip areas of the 300 series Panels. Report No. Kest2003-02.

N. Gordon, Seedsman Geotechnics Pty Ltd
E. Tembo, Kestrel Coal Pty Ltd

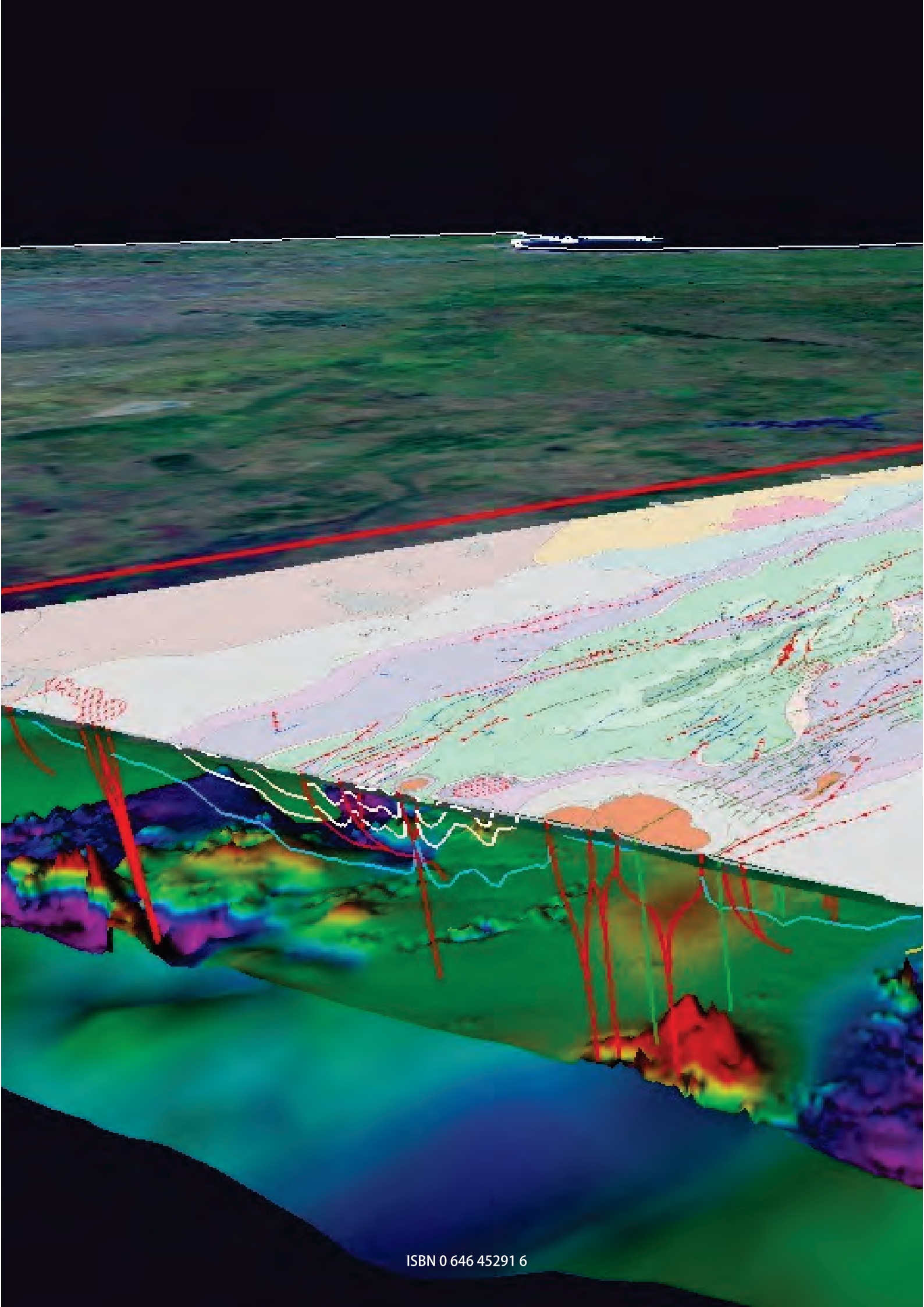

ISBN 0 646 45291 6